

This document was produced
by scanning the original publication.

Ce document est le produit d'une
numérisation par balayage
de la publication originale.



**GEOLOGICAL SURVEY OF CANADA
COMMISSION GÉOLOGIQUE DU CANADA**

**PAPER/ÉTUDE
92-1A**

**CURRENT RESEARCH, PART A
CORDILLERA AND PACIFIC MARGIN**

**RECHERCHES EN COURS, PARTIE A
CORDILLÈRE ET MARGE DU PACIFIQUE**



Energy, Mines and
Resources Canada

Énergie, Mines et
Ressources Canada

Canada

THE ENERGY OF OUR RESOURCES - THE POWER OF OUR IDEAS

L'ÉNERGIE DE NOS RESSOURCES - NOTRE FORCE CRÉATRICE

NOTICE TO LIBRARIANS AND INDEXERS

The Geological Survey's Current Research series contains many reports comparable in scope and subject matter to those appearing in scientific journals and other serials. Most contributions to Current Research include an abstract and bibliographic citation. It is hoped that these will assist you in cataloguing and indexing these reports and that this will result in a still wider dissemination of the results of the Geological Survey's research activities.

AVIS AUX BIBLIOTHÉCAIRES ET PRÉPARATEURS D'INDEX

La série Recherches en cours de la Commission géologique contient plusieurs rapports dont la portée et la nature sont comparables à ceux qui paraissent dans les revues scientifiques et autres périodiques. La plupart des articles publiés dans Recherches en cours sont accompagnés d'un résumé et d'une bibliographie, ce qui vous permettra, on l'espère, de cataloguer et d'indexer ces rapports, d'où une meilleure diffusion des résultats de recherche de la Commission géologique.

GEOLOGICAL SURVEY OF CANADA
COMMISSION GÉOLOGIQUE DU CANADA

PAPER / ÉTUDE
92-1A

CURRENT RESEARCH, PART A
CORDILLERA AND PACIFIC MARGIN

RECHERCHES EN COURS, PARTIE A
CORDILÈRE ET MARGE DU PACIFIQUE

1992

© Minister of Supply and Services Canada 1992

Available in Canada through

authorized bookstore agents and other bookstores

or by mail from

Canada Communication Group — Publishing
Ottawa, Canada K1A 0S9

and from

Geological Survey of Canada offices:

601 Booth Street
Ottawa, Canada K1A 0E8

3303-33rd Street N.W.,
Calgary, Alberta T2L 2A7

100 West Pender Street,
Vancouver, B.C. V6B 1R8

A deposit copy of this publication is also available for
reference in public libraries across Canada

Cat. No. M44-92/1A
ISBN 0-660-57062-9

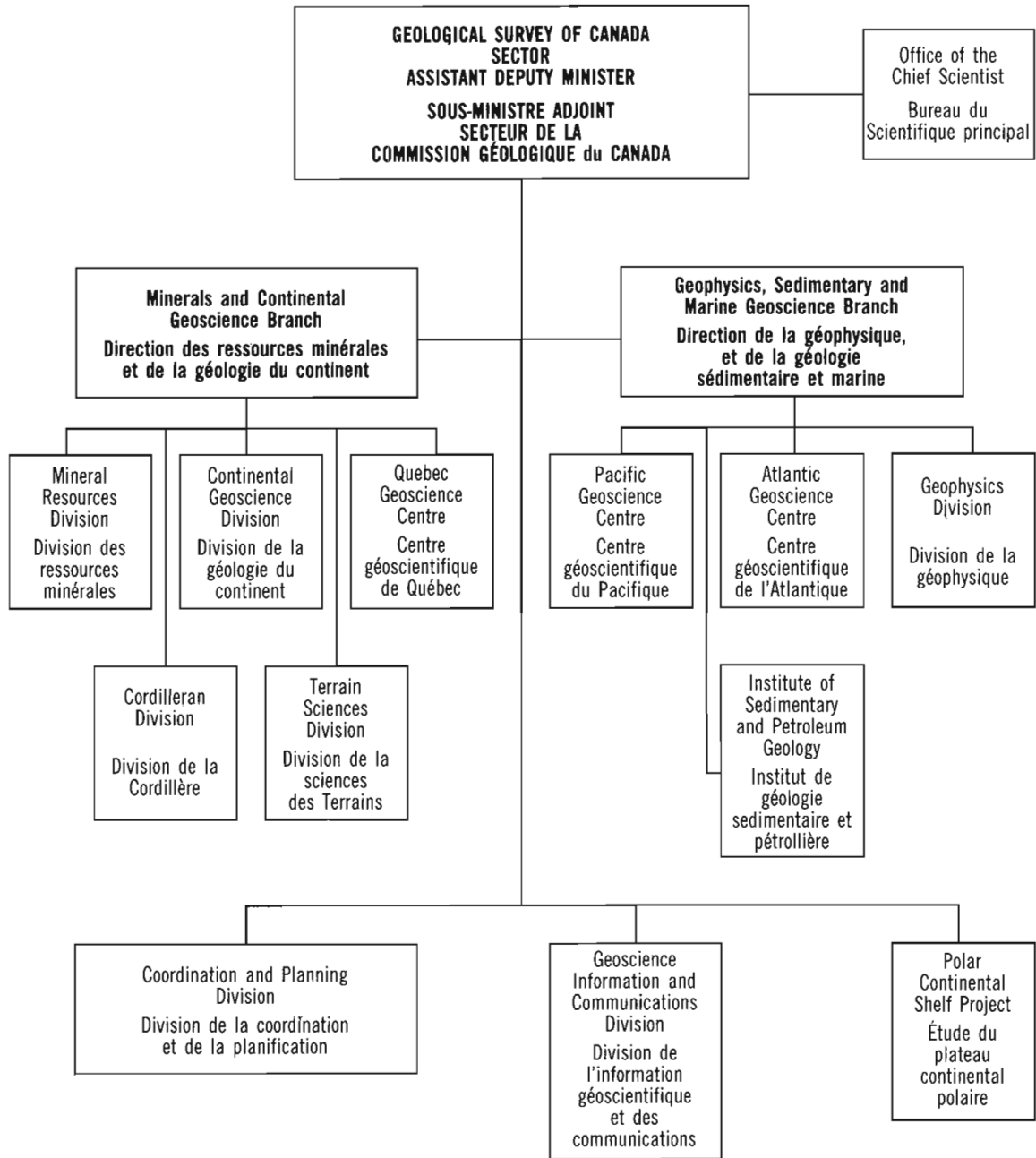
Price subject to change without notice

Cover description

Mount Logan was named after Sir William Logan, the first Director of the Geological Survey of Canada, has a peak elevation in excess of 5951 m, and is one of the largest mountain massifs in the world. The main mass is composed of grey Jurassic and Cretaceous granitic rock which intrudes Wrangellia, whereas the lower southwestern slopes are underlain by sedimentary strata of the Cretaceous Valdez Group of the Chugach Terrane. Separating these two rock types is the Border Ranges Fault, clearly shown as the sharp change from grey to dark brown colours. Photo by C.J. Yorath. KGS 2262

Description de la photo couverture

Le mont Logan, qui s'élève à plus de 5 951 m d'altitude, est le plus haut sommet au Canada, et le deuxième en Amérique du Nord. Nommé d'après Sir William Logan, qui fut le premier directeur de la Commission géologique du Canada, le mont Logan forme aussi un des plus imposants édifices montagneux dans le monde. Son corps principal se compose de roches granitiques grises du Jurassique et du Crétacé qui recourent la Wrangellie, tandis que son versant sud-ouest renferme dans sa partie inférieure des strates sédimentaires appartenant au Groupe de Valdez (Crétacé) du terrane de Chugach. Ces deux lithologies sont séparées par la faille de Border Ranges, qui se reconnaît aisément sur la photo à un brusque changement de couleur du gris au brun foncé. Photo : C.J. Yorath. KGS 2262



Separates

A limited number of separates of the papers that appear in this volume are available by direct request to the individual authors. The addresses of the Geological Survey of Canada offices follow:

601 Booth Street
OTTAWA, Ontario
K1A 0E8
(FAX: 613-996-9990)

Institute of Sedimentary and Petroleum Geology
3303-33rd Street N.W.
CALGARY, Alberta
T2L 2A7
(FAX: 403-292-5377)

Cordilleran Division
100 West Pender Street
VANCOUVER, B.C.
V6B 1R8
(FAX: 604-666-1124)

Pacific Geoscience Centre
P.O. Box 6000
9860 Saanich Road
SIDNEY, B.C.
V8L 4B2
(Fax: 604-363-6565)

Atlantic Geoscience Centre
Bedford Institute of Oceanography
P.O. Box 1006
DARTMOUTH, N.S.
B2Y 4A2
(FAX: 902-426-2256)

Québec Geoscience Centre
2700, rue Einstein
C.P. 7500
Ste-Foy (Québec)
G1V 4C7
(FAX: 418-654-2615)

When no location accompanies an author's name in the title of a paper, the Ottawa address should be used.

Tirés à part

On peut obtenir un nombre limité de «tirés à part» des articles qui paraissent dans cette publication en s'adressant directement à chaque auteur. Les adresses des différents bureaux de la Commission géologique du Canada sont les suivantes:

601, rue Booth
OTTAWA, Ontario
K1A 0E8
(facsimilé : 613-996-9990)

Institut de géologie sédimentaire et pétrolière
3303-33rd St. N.W.,
CALGARY, Alberta
T2L 2A7
(facsimilé : 403-292-5377)

Division de la Cordillère
100 West Pender Street
VANCOUVER, British Columbia
V6B 1R8
(facsimilé : 604-666-1124)

Centre géoscientifique du Pacifique
P.O. Box 6000
9860 Saanich Road
SIDNEY, British Columbia
V8L 4B2
(facsimilé : 604-363-6565)

Centre géoscientifique de l'Atlantique
Institut océanographique Bedford
B.P. 1006
DARTMOUTH, Nova Scotia
B2Y 4A2
(facsimilé : 902-426-2256)

Centre géoscientifique de Québec
2700, rue Einstein
C.P. 7500
Ste-Foy (Québec)
G1V 4C7
(facsimilé : 418-654-2615)

Lorsque l'adresse de l'auteur ne figure pas sous le titre d'un document, on doit alors utiliser l'adresse d'Ottawa.

CONTENTS

1	J.B. PERCIVAL, A. MUDROCH, G.E.M. HALL, and C.E. DUNN Geochemical studies in the Howe Sound drainage basin, British Columbia
13	P.S. MUSTARD and G.E. ROUSE Tertiary Georgia Basin, British Columbia and Washington State: a view from the other side
25	L.C. STRUIK Further reconnaissance observations in the Pine Pass southwest map area, British Columbia
33	L.E. JACKSON, Jr. and W. STEVENS A recent eruptive history of Volcano Mountain, Yukon Territory
41	P.H. THOMPSON The Winter Lake – Lac de Gras regional mapping project, central Slave Province, District of Mackenzie, Northwest Territories
47	J.J. CARRIÈRE and D.F. SANGSTER Preliminary studies of fluid inclusions in sphalerite, quartz, and dolomite from Gayna River MVT deposit, Northwest Territories
55	B.S. HART Side-scan sonar observations of Point Grey dump site, Strait of Georgia, British Columbia
63	J.L. CROWLEY, R.L. BROWN, and S.E. CROWLEY Reinterpretation of the Clachnacudainn terrane and Standfast Creek fault, southern Omineca Belt, British Columbia
71	J.J. VOGL and P.S. SIMONY The southern tail of the Nelson Batholith, southeast British Columbia: structure and emplacement
77	C.A. EVENCHICK Bowser Basin facies and map units in southwest Toodoggone map area, British Columbia
85	C. LOWE, D. SEEMANN, and C.A. EVENCHICK A preliminary investigation of potential field data from north-central British Columbia
95	R.A. COISH and J.M. JOURNEAY The Crevasse Crag Volcanic Complex, southwestern British Columbia: structural control on the geochemistry of arc magmas
105	P.B. READ Geology of parts of Riske Creek and Alkali Lake areas, British Columbia
113	P. van der HEYDEN and S. METCALFE Geology of the Piltz Peak plutonic complex, northwestern Churn Creek map area, British Columbia
121	D. BROWN and K. McCLAY Structure of the Vangorda Pb-Zn-Ag deposit, Anvil Range, Yukon Territory
129	C.J. HICKSON An update on the Chilcotin-Nechako Project and mapping in the Taseko Lakes area, west-central British Columbia
137	R.M. FRIEDMAN and P. van der HEYDEN Late Permian U-Pb dates for the Farwell and Northern Mt. Lytton plutonic bodies, Intermontane Belt, British Columbia

- 145 C.J. GREIG
Fieldwork in the Oweegee and Snowslide ranges and Kinskuch Lake area, northwestern British Columbia
- 157 M. COLPRON and R.A. PRICE
Preliminary results on the stratigraphy and structure of the Lardeau Group in the Illecillewaet synclinorium, western Selkirk Mountains, British Columbia
- 163 C.F. ROOTS and D.C. MURPHY
New developments in the geology of Mayo map area, Yukon Territory
- 173 K.M. DAWSON
Progress report on the project in comparative metallogenesis and tectonics of the U.S.S.R. Far East, Alaska and the Canadian Cordillera
- 179 K.V. ROSS, K.M. DAWSON, C.I. GODWIN and L. BOND
Major lithologies of the Ajax West pit, an alkalic copper-gold porphyry deposit, Kamloops, British Columbia
- 185 J.J. CLAGUE and S.G. EVANS
A self-arresting moraine dam failure, St. Elias Mountains, British Columbia
- 189 A. PLOUFFE
Quaternary stratigraphy and history of central British Columbia
- 195 A. BLAIS
Holocene sediments from Saanich Inlet, British Columbia and their neotectonic implications
- 199 L.D. CURRIE
Metamorphic rocks in the Tagish Lake area, northern Coast Mountains, British Columbia: a possible link between Stikinia and parts of Yukon-Tanana Terrane
- 209 J.A. O'BRIEN, G.E. GEHRELS, and J.W.H. MONGER
U-Pb geochronology of plutonic clasts from conglomerates in the Ladner and Jackass Mountain groups and the Peninsula Formation, southwestern British Columbia
- 215 J.M. JOURNEY and B.R. NORTHCOTE
Tectonic assemblages of the Eastern Coast Belt, southwest British Columbia
- 225 J.M. JOURNEY, C. SANDERS, J.-H. Van-KONIJNENBURG and M. JAASMA
Fault systems of the Eastern Coast Belt, southwest British Columbia
- 237 B.E. BROSTER and D.H. HUNTLEY
Quaternary stratigraphy in the east-central Taseko Lakes area, British Columbia
- 243 J.B. MAHONEY
Middle Jurassic stratigraphy of the Lillooet area, south-central British Columbia
- 249 J.B. MAHONEY, C.J. HICKSON, P. van der HEYDEN, and J.A. HUNT
The Late Albian-Early Cenomanian Silverquick conglomerate, Gang Ranch area: evidence for active basin tectonism
- 261 R.M. FRIEDMAN, T.M. TYSON, and J.M. JOURNEY
U-Pb age of the Mt. Mason Pluton in the Cairn Needle area, southern Coast Belt, British Columbia
- 267 S.A. GAREAU
Report on fieldwork in the southern Big Salmon metamorphic complex, Teslin map area, Yukon Territory

279	S.P. GORDEY Geological fieldwork in Teslin map area, southern Yukon Territory
287	R.A. STEVENS Regional geology, fabric, and structure of the Teslin suture zone in northwest Teslin map area, Yukon Territory
297	T.A. HARMS Stratigraphy of the southern Thirtymile Range, Teslin map area, southern Yukon Territory
303	W.C. McCLELLAND Permian and older rocks of the southwestern Iskut River map area, northwestern British Columbia
309	S. PORTER Elbow Mountain crystalline complex, Iskut River map area, northwestern British Columbia
315	M.H. GUNNING Carboniferous limestone, Iskut River region, northwest British Columbia
323	J.R. HENDERSON, R.V. KIRKHAM, M.N. HENDERSON, J.G. PAYNE, T.O. WRIGHT, and R.L. WRIGHT Stratigraphy and structure of the Sulphurets area, British Columbia
333	G. NADARAJU and P.L. SMITH Jurassic biochronology in the Iskut River map area, British Columbia: a progress report
337	J.W. HAGGART Highlights of the 1991 geological field program, Queen Charlotte Islands, British Columbia/ Points saillants du programme de travaux géologiques sur le terrain dans les îles de la Reine-Charlotte en Colombie-Britannique
343	J.G. SOUTHER Geology of central Lyell Island, Queen Charlotte Islands, British Columbia
351	M. SANBORN-BARRIE Geology of the Darwin Sound area, Queen Charlotte Islands, British Columbia
361	J.W. HAGGART Progress in Jurassic and Cretaceous stratigraphy, Queen Charlotte Islands, British Columbia
367	C.A. GAMBA Lithofacies of the late Early to early Late Cretaceous Queen Charlotte Group, Queen Charlotte Islands, British Columbia
377	Author Index

Geochemical studies in the Howe Sound drainage basin, British Columbia

J.B. Percival, A. Mudroch¹, G.E.M. Hall, and C.E. Dunn
Mineral Resources Division

Percival, J.B., Mudroch, A., Hall, G.E.M., and Dunn, C.E., 1992: Geochemical studies in the Howe Sound drainage basin, British Columbia; in Current Research, Part A; Geological Survey of Canada, Paper 92-1A, p. 1-11.

Abstract

*A reconnaissance geochemical survey was conducted in Howe Sound to identify sources and dispersion of natural and anthropogenic inorganic constituents. Waters from creeks draining into the Sound, near-shore bottom sediments, and seaweed (rockweed, *Fucus gardneri*) were collected. A more detailed study focused on the drainage around the abandoned Britannia Cu mine.*

All sample media contain anomalous levels of Cu and Zn in the vicinity of the Britannia mine site. Rockweed was not found on shores within 3 km of Britannia Beach, presumably due to metal poisoning. Concentrations of 44 ppm Cu and 26 ppm Zn in waters emanating from the mine portals at Britannia are reduced significantly to about 300 ppb at the mouth of Britannia Creek by dilution and co-precipitation with amorphous Fe-oxides. With the exception of Britannia, creeks flowing into Howe Sound contain low concentrations of the elements (e.g., As, Ni, Pb) determined.

Résumé

*Une étude géochimique de reconnaissance a été réalisée dans la baie Howe pour identifier les sources et la dispersion des constituants inorganiques naturels et anthropiques. On a recueilli des échantillons d'eau dans les ruisseaux se jetant dans la baie Howe, des sédiments littoraux et des varechs (*Fucus gardneri*). Une autre étude plus détaillée a porté sur les eaux de drainage autour de la mine de cuivre abandonnée Britannia.*

Tous les échantillons provenant du voisinage de la mine contenaient des concentrations anormales de Cu et de Zn. On n'a pas trouvé de varechs sur les rives, à moins de trois km de la plage Britannia, du fait probablement d'un empoisonnement des algues par ces métaux. Les concentrations de 44 ppm en Cu et de 26 ppm en Zn dans les eaux provenant des entrées de galerie de la mine Britannia diminuent considérablement pour atteindre 300 ppb à l'embouchure du ruisseau Britannia par suite d'une dilution et d'une coprécipitation sur des oxydes de Fe amorphes. À l'exception du ruisseau Britannia, les ruisseaux se jetant dans la baie Howe contiennent de faibles concentrations des éléments analysés (par ex. As, Ni, Pb).

¹ National Water Research Institute, Environment Canada, Burlington, Ontario

INTRODUCTION

Howe Sound, located in the southwest Coast Belt immediately north of Vancouver, is a 42 km long fjord divided into two basins by a 35-70 m deep sill (Syvitski, 1979) that trends northwest from Porteau Cove on the eastern shore, north of Anvil Island (Fig. 1). The northern basin is 17 km long, averages 3 km wide (Syvitski, 1979) and has a maximum depth of 290 m (Fisheries and Oceans, 1989). The southern basin, bounded by Georgia Strait to the south, is populated by several islands.

In July 1991 reconnaissance geochemical surveys were conducted in the Howe Sound drainage basin to identify sources and map dispersion of natural and anthropogenic inorganic constituents. These surveys form part of a newly-established multidisciplinary program to examine the physical, biological, and chemical attributes and processes that characterize the Sound. Industrial activity within the drainage basin includes two pulp and paper mills, a chemical plant, and an abandoned copper mine (Britannia). In addition, the area is used by recreational boaters and supports a sport and commercial fishing industry.

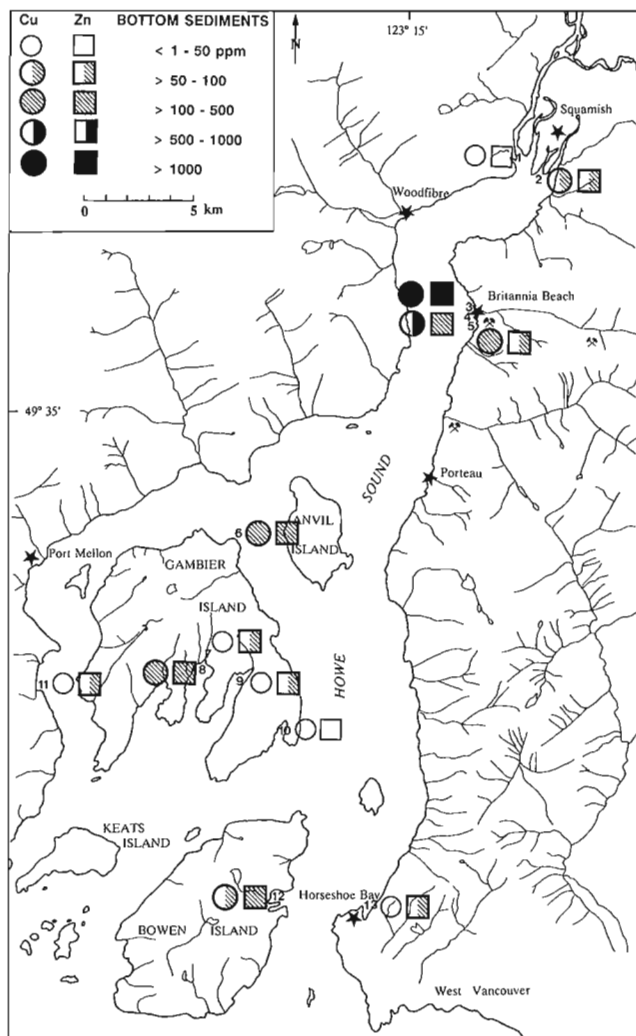


Figure 1. Concentrations of Cu and Zn (in ppm) in bottom sediments in the Howe Sound drainage basin.

The reconnaissance surveys involved the collection of several sample types: surface waters from the mouths of creeks and rivers draining the eastern side of the Sound, and a few at depth within some bays; near-shore bottom sediments from several bays; and seaweed from rocks along shorelines within the Sound. In addition, creek waters, acid mine waters, and mineral precipitates were collected from the Britannia mine site for detailed study. In this paper emphasis is placed on the distribution of Cu and Zn, as these metals were mined at Britannia and show greater regional variation than other elements in the drainage basin.

REGIONAL GEOLOGY

The southwest Coast Belt has been subdivided into three north-northwest-trending tracts: the Sechelt, Howe Sound, and Squamish River (Monger, 1991). The southern part of the Howe Sound drainage basin lies within the Sechelt tract which is composed of Lower and Middle Jurassic interbedded clastic sediments and volcanic rocks of the Bowen Island Group, with minor metabasalt and marble. Monger (1991) indicates that these stratified rocks form a series of north-northwest-trending pendants within Late Jurassic and Early Cretaceous granitic plutons. The northern part of the drainage basin is underlain by the Howe Sound tract, consisting of Lower Cretaceous volcanic and sedimentary rocks of the Gambier Group and Early Cretaceous felsic plutons (Monger, 1991). The Gambier Group comprises a lower volcanic complex, a middle sedimentary interval, and an upper volcanic complex (Roddick, 1965; Lynch, 1991) which hosts the Britannia Cu-Zn-Pb-Ag-Au orebodies.

SAMPLE COLLECTION AND METHODS

Two water samples were collected at each site: one 250-mL volume for cation determination and one 125-mL volume for anion determination and pH. The Nalgene bottles (LPE) were used as purchased, that is, not acid-washed, but were rinsed repeatedly with the sample prior to capping. Experience at the GSC has demonstrated that contamination from these bottles at the ppb level for elements such as Cu, Ni, Pb, and Zn is insignificant. Electrical conductivity and pH were determined in the field using a Myron L digital pH/conductivity meter (Model DCH 4). Upon delivery to the GSC laboratory, within a week of collection, the waters were filtered through 0.45 μ m Millipore filter paper (type HAWP) and the 250-mL samples were acidified with Ultrex nitric acid to a concentration of 0.1%.

The major elements Ca, Mg, Na, and K were determined in the acidified sample by air-acetylene flame atomic absorption spectrometry (FAAS) after making the samples 0.1% in Cs (as an ionization buffer) and 0.1% in La (as a releasing agent). The elements Fe, Mn, Cd, Co, Cu, Ni, Pb, and Zn were also determined on the acidified portion by FAAS using an air-acetylene flame. Calibration standards were made in deionised water containing identical concentrations of acid and buffers. Arsenic, Bi and Sb were determined by hydride generation quartz tube AAS using NaBH_4 as reducing agent. The elements were pre-reduced to

their lower valency states (i.e., V to III) by addition of 5% KI and ascorbic acid. Water analyses that are incomplete at this time include the determination of: the anions (F, Cl, Br, NO₃, SO₄, and PO₄) by ion chromatography; alkalinity; and dissolved organic carbon.

Sediment samples of 100-200 g were collected by a petite Ponar grab sampler (sampled sediment area 15 x 15 cm) and placed into plastic bags which were sealed and shipped to the laboratory. All samples were freeze dried and pulverized using an automatic grinder equipped with an agate dish. The analyses represent, therefore, whole sediment composition, and not any particular size fraction.

Precipitates or coatings on pebbles were collected from stream and mine waters in the Britannia area. The pebbles were cleansed using an ultrasonic bath and the material liberated was concentrated by centrifugation and freeze dried.

Major elements in sediments were determined by DC plasma emission spectrometry following lithium borate fusion, and trace elements were determined by inductively coupled plasma emission spectrometry (ICP-ES) following sediment digestion with aqua regia. Analysis was carried out

at Bondar-Clegg & Company Ltd. (Ottawa, Ontario). A split of each sediment sample was used for particle size analysis, heavy mineral separation, and carbonate analysis (Leco determination). Bulk mineralogy of sediments and precipitates was determined using X-ray diffraction analysis of oriented, air-dried mounts. Samples were run on a Philips PW1710 diffractometer using Cu K α radiation with a Ni filter at operating conditions of 50 kV and 30 mA.

Seaweed samples were collected at intervals of approximately 5 km during periods of medium to low tides. About 100-200 g of seaweed were plucked from the rocks at each of the 36 sites selected within the 300 km² study area. The only stretch of shoreline devoid of seaweed extends southward for 3 km from a point 1.5 km north of Britannia Beach.

The basal holdfasts were removed with pruning snips, and any biota (mostly mussels, *Mytilus spp.*) were picked off the seaweed blades. Samples were placed in 'ziploc-type' plastic bags while at sea, and later placed into cloth bags to facilitate drying. Partially dried samples were ignited for 24 hours in aluminum trays in a pottery kiln at a temperature of 470°C.

Table 1. Major, minor, and trace element concentrations in bottom sediments from Howe Sound. Site numbers correspond to those on Figure 1.

Site	1	2	3	4	5	6	7	8	9	10	11	12	13
"Whole rock" analysis (LiBO ₂ fusion + ICP-ES), values in %													
SiO ₂	65.89	55.98	55.75	54.52	28.34	46.14	61.80	37.27	60.05	61.56	52.68	58.55	60.00
TiO ₂	0.36	0.66	0.54	0.61	0.23	0.59	0.51	0.50	0.42	0.42	0.32	0.47	0.48
Al ₂ O ₃	15.93	15.77	12.95	13.93	58.86	13.36	16.17	10.39	14.15	14.52	11.89	14.54	15.24
Fe ₂ O ₃	3.29	6.28	9.33	7.22	2.82	5.98	5.33	4.98	3.96	3.37	3.07	4.85	5.06
MnO	0.07	0.12	0.12	0.12	0.05	0.11	0.09	0.07	0.07	0.06	0.06	0.07	0.09
MgO	1.55	3.02	3.94	3.12	2.23	3.17	2.32	2.78	1.89	1.71	1.74	2.28	2.25
CaO	4.45	4.87	2.44	3.31	2.38	7.85	4.04	2.51	4.22	4.25	5.21	4.25	5.20
Na ₂ O	4.43	4.34	2.53	3.49	1.51	3.69	3.87	4.85	4.29	4.30	4.50	4.06	4.14
K ₂ O	1.67	1.93	1.93	1.66	0.93	1.89	1.55	1.43	1.25	1.22	1.51	1.63	1.60
P ₂ O ₅	0.15	0.25	0.10	0.13	0.13	0.25	0.14	0.29	0.16	0.17	0.12	0.23	0.17
LOI	0.79	5.40	9.00	11.04	1.67	15.41	2.21	33.43	8.15	8.33	16.96	7.92	3.23
"Total"	98.57	98.61	98.64	99.15	99.15	98.44	98.03	98.50	98.62	99.92	98.05	98.85	97.46
Trace element analysis (aqua regia digestion + ICP-ES), values in ppm													
As	5	13	46	29	5	22	16	33	16	10	9	17	11
Ag	ND	ND	1.4	0.5	0.2	ND	ND	0.4	ND	ND	ND	ND	ND
Ba	51	177	165	257	594	288	43	127	46	48	35	98	63
Cd	ND	ND	7.5	2.7	7.7	0.8	1.0	3.2	0.7	0.4	0.3	1.0	1.1
Co	4	12	16	17	13	17	11	13	7	5	4	15	9
Cr	9	21	29	41	9	24	16	41	14	15	13	27	16
Cu	12	64	1752	721	149	116	24	138	30	26	30	58	24
La	4	7	7	7	2	11	2	10	4	4	4	9	4
Mo	ND	ND	7	3	ND	2	ND	19	3	2	7	1	2
Ni	6	15	18	28	7	23	12	33	11	10	9	25	11
Pb	10	14	117	65	23	14	14	35	16	16	13	35	29
Sb	7	12	15	14	8	17	10	12	8	7	7	9	8
Sr	49	98	78	92	51	311	42	141	61	89	107	122	70
V	33	73	67	74	26	87	46	71	31	26	32	55	46
Y	3	6	11	11	3	10	4	10	5	4	4	8	5
Zn	32	97	1501	308	86	288	74	199	53	48	66	101	63
ND — Not detected													

Ash portions weighing 0.5-1 g were transferred into plastic vials and submitted for multi-element instrumental neutron activation analysis (INAA) at Activation Laboratories Ltd., Ancaster, Ontario. In addition, an ash split of similar size was submitted for analysis by ICP-ES at Min-En Laboratories, Vancouver, in order to obtain data for elements of interest that are not readily determined by INAA, notably the base metals. Several elements were determined by both techniques.

SEDIMENT STUDY (A. Mudroch)

Introduction

Thirteen sediment samples were collected from near-shore sites in the Sound (Fig. 1). The number of sediment samples was limited by the great depth of water, the nature of the bottom sediments (commonly coarse sand, pebbles, and bark fragments) and the type of sampling device. Samples were taken to: (i) examine the nature and possible source of the materials sedimenting in the bays; and (ii) determine their geochemical signature and identify natural background versus point source contamination.

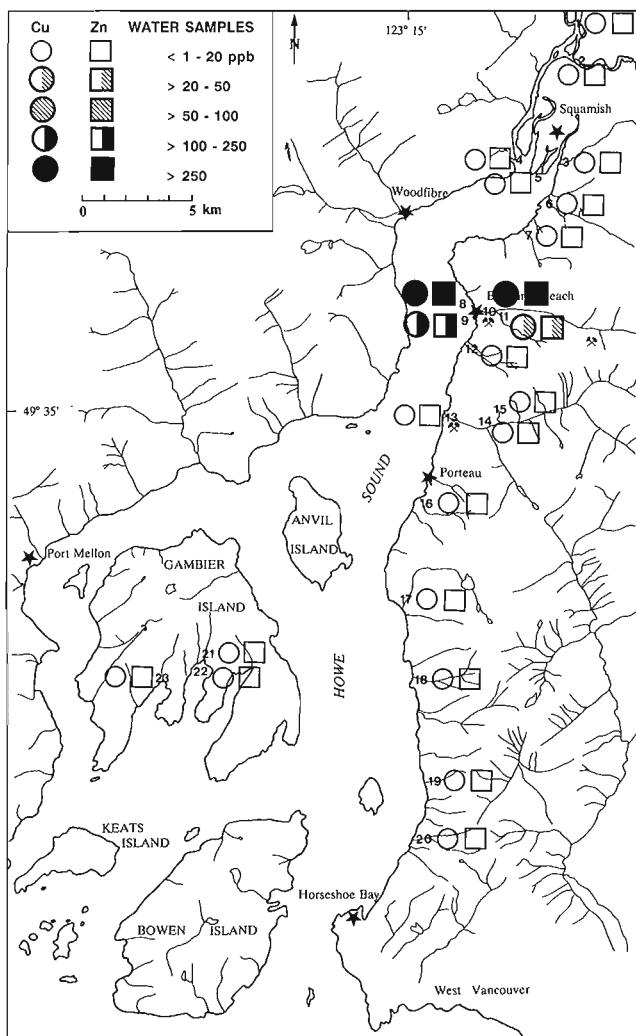


Figure 2. Concentrations of Cu and Zn (in ppb) in surface waters from stream mouths and bays in Howe Sound.

Table 2. Analyses of water samples from the Howe Sound drainage basin. Values for Ca, Mg, Na, and K are in ppm, and for Fe and Mn in ppb. Electrical conductivity (COND.) measurements are in $\mu\text{S}/\text{cm}$. Site numbers correspond to those on Figure 2.

Site No.	pH	Cond.	Ca	Mg	Na	K	Fe	Mn
1	8.1	20	2.29	0.25	0.74	0.52	139	10
2	6.6	1060	3.54	0.36	0.94	0.26	40	ND
3	6.8	19	2.14	0.23	0.67	0.19	34	10
4	6.5	24	2.10	0.51	2.93	0.54	51	22
5	6.3	3400	25.6	75	630	24.3	64	13
5-10m	5.9	49400	313	1020	7800	360	ND	18
5-20m	5.7	21400	335	1080	8325	375	ND	17
6	6.5	9	1.14	0.09	0.35	0.11	10	ND
7	6.3	7	0.74	0.09	0.33	0.11	22	ND
8	5.3	521	7.45	10	76	2.97	113	48
9	5.7	2560	20.0	52	450	17	26	37
10	5.8	39	4.13	0.67	0.52	0.11	68	53
11	5.4	8	12.3	0.60	1.14	0.18	36	ND
12	6.2	25	2.93	0.28	0.93	0.24	ND	ND
13	6.0	17	2.18	0.21	0.58	0.14	ND	ND
14	7.1	25	2.46	0.50	2.04	0.35	ND	ND
15	6.7	29	3.20	0.50	1.32	0.36	ND	ND
16	6.0	9	0.90	0.16	0.43	0.16	ND	ND
17	5.9	17	1.89	0.16	0.61	0.14	26	10
18	5.8	29	2.91	0.38	1.15	0.11	ND	ND
19	5.9	52	7.52	0.51	1.29	0.39	ND	ND
20	6.3	12	1.22	0.16	0.70	0.11	28	ND
21	6.0	465	10.6	8.25	63	2.65	ND	ND
22	7.4	19300	123	390	3045	119	ND	ND
22-10m	7.2	34600	244	780	6075	270	ND	15
22-20m	7.1	41400	309	990	7665	330	ND	13
22-50m	6.9	45800	342	1110	8460	375	ND	13
23	5.7	74	8.00	1.08	3.81	0.27	ND	ND

ND — Not detected, at levels below: 20 ppb for Fe and 10 ppb for Mn

Results and discussion

Results of the chemical analyses of the sediment samples are listed in Table 1 with Cu and Zn values plotted in Figure 1. Concentrations of Cu and Zn range from 12 to 1750 ppm and 32 to 1500 ppm ($\mu\text{g}/\text{g}$), respectively. The highest values occur in the two most northerly Britannia Beach samples (sites 3 and 4) and reflect the presence of Britannia mine tailings in recent (post 1974) sediments, and probably the continuous input of these metals from the mine site. In the southern basin two sites (6 and 8) are slightly richer in Cu and Zn than the other sites probably because these two samples contained a substantially higher component of clay-sized particles providing greater surface area for metal adsorption. Zinc concentrations are generally higher than Cu, reflecting the greater natural abundance of Zn.

Barium and cadmium concentrations appear to mirror Cu and Zn levels in the sediments, and Pb and Sb levels are generally higher at Britannia Beach than elsewhere. Most other trace elements represent background values. The sediments are composed of quartz, feldspar, chlorite, mica, and amphibole reflecting the mineralogy of the source rocks. Syvitski and Macdonald (1982) have shown that the presence of mica indicates a Squamish River sediment source whereas chlorite is derived from the Fraser River.

WATER STUDY (G.E.M. Hall)

Introduction

A total of 44 water samples were collected, 20 focusing on the drainage in the area of the Britannia Cu mine as it was anticipated that this source would provide the major contribution of inorganic pollutants to the Sound. The regional sites (23 in number) of the water survey are shown

in Figure 2. Samples were collected at various depths (e.g., surface, 10m, 20m) at sites 5 and 22 to examine the effect of mixing river or creek outflow with seawater. Surface waters in the Sound have low salinity due to the high influx of fresh waters from the surrounding mountains. This vertical stratification of the waters has a significant effect on the vertical profile of the water chemistry.

Results and discussion

Analyses of the drainage basin waters are shown in Table 2 for Ca, Mg, Na, K, Fe, and Mn; Table 3 lists values for trace elements determined to date. Not shown in Table 3 are data for Cd, Ni, and Pb as concentrations of these elements in all waters were less than detection limits of 2, 10, and 20 ppb, respectively. Concentrations of Cu and Zn are shown in Figure 2. With respect to the data in Table 2, the high levels of major cations and, hence, conductivity in samples taken at the Squamish River harbour mouth (sites 5, 5-10m, and 5-20m; see Fig. 2 for location), Britannia Creek side channel (site 9) and Gambier Island (sites 21, 22, 22-10m, 22-20m, and 22-50m) are due to mixing with seawater. The influence of the Britannia mine is seen in the

Table 3. Trace element analyses (in ppb) of water samples from the Howe Sound drainage basin. Site numbers correspond to those of Figure 2.

Site No.	As	Bi	Cu	Sb	Zn
1	ND	0.1	ND	ND	ND
2	ND	0.1	ND	ND	ND
3	ND	ND	9	0.3	3
4	0.1	ND	ND	ND	3
5	0.5	ND	ND	ND	6
5-10m	1.0	ND	21	0.1	26
5-20m	1.1	ND	7	4.33	26
6	0.2	ND	ND	ND	ND
7	ND	0.2	ND	0.1	3
8	ND	ND	378	ND	323
9	ND	0.1	192	0.2	214
10	0.1	ND	276	ND	267
11	ND	ND	30	ND	24
12	0.1	ND	ND	ND	ND
13	ND	ND	11	0.2	7
14	ND	0.1	ND	0.1	4
15	0.1	0.1	ND	0.1	2
16	ND	ND	ND	0.1	2
17	0.1	ND	ND	0.1	ND
18	0.1	ND	5	ND	ND
19	0.2	ND	6	ND	ND
20	ND	0.2	ND	ND	3
21	0.1	0.1	ND	ND	ND
22	ND	0.3	7	ND	5
22-10m	0.9	ND	ND	0.2	5
22-20m	1.1	0.1	ND	0.1	ND
22-50m	1.1	0.1	ND	0.1	4
23	ND	0.3	ND	ND	ND

ND — Not detected, at levels below: 20 ppb for Fe and 10 ppb for Mn

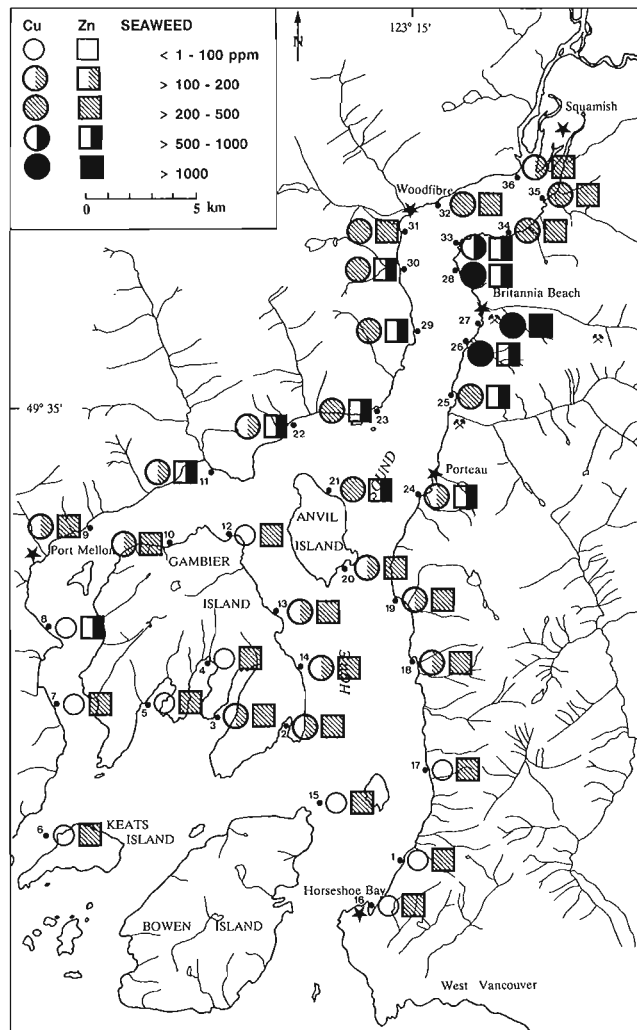


Figure 3. Concentrations of Cu and Zn (in ppm) in the ash of common rockweed (*Fucus gardneri*) from the shores of Howe Sound.

more acidic pH levels at sites 8 to 10 and in the elevated contents of major cations due to acid leaching. Iron and Mn concentrations show little variation throughout the Sound and are in the low ppb ($\mu\text{g/L}$) range.

With reference to Table 3, the waters in the Sound contain insignificant amounts of Bi and Sb, at or near the analytical method detection limit of 0.1 ppb. The high value of 4.33 ppb of Sb at site 5-20m (Table 3) was confirmed by re-analysis but the source is perplexing as the values above and below in this water column are low. Although values for As are also at or near the detection limit of 0.1 ppb for most samples, they approach 1 ppb with depth due to the influence of more saline waters (sites 5, 5-10m, 5-20m, 22, 22-10m, 22-20m, and 22-50m). Arsenic is certified at 1.65 ppb in the seawater reference material, NASS-2 (Certificate of Analysis for NASS-2, National Research Council of Canada, 1986). The only significant levels of Cu and Zn in the drainage basin waters occur, not surprisingly, in samples taken at the mouth of Britannia Creek where they rise to a few hundred ppb (sites 8 to 10; Fig. 2).

SEAWEED STUDY (C.E. Dunn)

Introduction

A few studies have investigated the use of seaweed (macro-algae) chemistry in mineral prospecting and environmental monitoring (Black and Mitchell, 1952; Bryan, 1969; Fuge and James, 1974; Asmund et al., 1975; Sharp and Bolviken, 1979). Certain seaweed species are enriched in Pb and Zn near deposits of galena and sphalerite on the coast of Greenland (Bollnberg and Cooke, 1985).

Recent studies along the coast of western Canada have documented the chemistry of several seaweed species and have shown that of the three types (brown, red, and green), the brown seaweeds generally accumulate the most metals (Dunn, 1990). During the summer of 1990 these studies were pursued near Bamfield (west coast of Vancouver Island), from which it became apparent that the species *Fucus gardneri* (common rockweed) is one of the more abundant and metal sensitive of the brown seaweeds (unpublished data).

Table 4. Analyses of the ash of common rockweed (*Fucus gardneri*) from the shores of Howe Sound. Cu, Zn, Ni, and Pb determined by ICP-ES (aqua regia digestion); Fe, U, Ba, and As by INAA. Site numbers correspond to those of Figure 3.

Site No.	Cu	Zn	Fe	U	Ba	As	Ni	Pb
1	69	231	800	4	180	10	22	5
2	102	355	1300	5	280	19	27	<2
3	106	220	900	5	290	8	30	<2
4	69	337	600	4	200	22	34	<2
5	75	356	700	4	180	16	32	6
6	58	217	1300	4	170	17	23	4
7	68	493	1600	4	190	28	27	<2
8	79	507	2000	6	240	23	22	2
9	160	432	1400	6	180	14	15	2
10	132	462	1200	4	220	12	26	4
11	105	551	700	6	150	20	29	8
12	79	240	1800	5	210	14	9	14
13	152	422	1600	5	190	19	21	5
14	143	420	3900	5	190	7	29	8
15	72	323	1000	3	140	14	28	5
16	67	346	900	4	<20	19	36	10
17	64	306	500	4	150	19	25	9
18	102	351	900	4	210	21	29	4
19	129	406	800	4	190	17	19	3
20	119	410	1000	5	150	21	16	<2
21	220	595	2600	7	410	19	15	<2
22	193	821	3400	6	340	14	24	<2
23	202	783	5000	6	310	16	20	3
24	181	544	1200	5	190	10	17	4
25	346	878	2300	5	280	18	18	8
26	2304	525	4100	11	510	7	6	<2
27	1438	1543	5000	8	380	9	7	3
28	3211	700	3100	15	600	7	2	<2
29	220	559	3600	5	430	19	11	3
30	235	539	3500	11	700	12	12	<2
31	228	246	3300	10	920	11	1	<2
32	258	312	2400	8	760	19	2	<2
33	581	890	3400	6	400	17	6	3
34	237	333	11000	10	1000	20	4	<2
35	227	308	3200	11	1200	26	1	<2
36	180	496	2600	9	940	18	2	<2

ND — Not detected, at levels below: 20 ppb for Fe and 10 ppb for Mn

Rockweed (or wrack), as described by Scagel (1967), is an erect, flattened, cartilaginous plant, up to 50 cm high, that is olive green to yellowish green. It has repeated dichotomous branching that starts 2-5 cm above a basal discoid holdfast. The tips have swollen yellowish receptacles. This common seaweed clings to rocks in the intertidal zone. It occurs in abundance along the shores of Howe Sound and the islands

Table 5. Major element analyses of water samples from the Britannia Cu mine area. Values for Ca, Mg, Na, and K are in ppm, and for Fe and Mn in ppb. Electrical conductivity (COND.) measurements are in $\mu\text{S}/\text{cm}$. Site numbers correspond to those on Figure 4.

SITE NO.	pH	COND.	Ca	Mg	Na	K	Fe	Mn
1	6.3	468	79.1	9.00	3.27	0.16	ND	ND
2	6.6	83	14.2	0.52	1.72	0.11	ND	ND
3	7.5	7	0.93	0.11	0.27	0.14	ND	ND
4	6.3	106	15.2	1.23	1.41	0.18	ND	103
5	5.1	106	15.3	1.23	1.35	0.15	ND	106
6	2.4	1730	160	46.1	3.15	0.42	16125	2940
7	2.3	1730	162	46.5	3.18	0.42	12025	2784
8	2.7	904	82.1	21.7	2.21	0.33	1479	1398
9	3.7	70	78.3	20.8	2.17	0.28	2150	1300
10	4.5	74	6.61	1.51	0.48	0.12	140	101
11	6.0	85	4.17	0.85	0.38	0.06	155	59
12	5.8	690	12.3	0.60	1.14	0.18	36	ND
13	4.2	1950	380	64.3	7.79	1.10	215	3940
14	4.3	2130	418	71.6	8.20	1.23	176	4544
15	4.6	2190	421	71.6	8.23	1.23	3184	4545
16	3.8	592	33	11.2	2.64	1.44	4312	820
17	5.7	51	7.93	0.33	0.63	3.00	ND	ND
18	5.8	1200	4.13	0.67	0.52	0.11	68	53
19	5.3	2560	20.1	52.5	450	17.2	26	37
20	5.7	523	7.45	10.1	76.1	2.97	113	48

ND - Not detected, at levels below: 20 ppb for Fe and 10 ppb for Mn.

Table 6. Trace elements (ppb) in water samples from the Britannia Cu mine area. Site numbers correspond to Figure 4.

SITE NO.	As	Bi	Cd	Cu	Ni	Pb	Sb	Zn
1	0.1	ND	ND	20	ND	ND	0.4	10
2	0.3	ND	-	ND	-	-	0.1	5
3	0.1	ND	-	5	-	-	0.2	3
4	0.2	0.2	4	127	54	ND	ND	551
5	1.0	ND	4	94	62	ND	ND	559
6	0.5	0.1	163	43950	48	39	ND	26450
7	0.3	0.1	164	29975	57	ND	0.1	26425
8	0.1	ND	76	19850	31	20	0.1	12250
9	0.1	ND	75	19100	30	36	0.3	11913
10	0.5	0.2	3	1172	ND	ND	ND	790
11	0.1	ND	2	647	15	ND	0.2	388
12	ND	ND	3	30	ND	ND	ND	24
13	ND	ND	106	12675	55	106	ND	22463
14	0.3	0.1	119	14750	68	89	0.1	24975
15	0.3	0.2	119	10825	57	67	0.4	24875
16	0.3	0.1	20	6700	29	188	ND	4600
17	ND	0.1	ND	35	ND	ND	ND	39
18	0.1	ND	ND	276	ND	ND	ND	267
19	ND	0.1	ND	192	ND	ND	0.2	214
20	ND	ND	ND	378	ND	29	ND	323

ND - Not detected, at levels below: 0.1 ppb for As, Bi, Sb; 2 ppb for Cd, Zn; 5 ppb for Cu; 10 ppb for Ni; and 20 ppb for Pb.

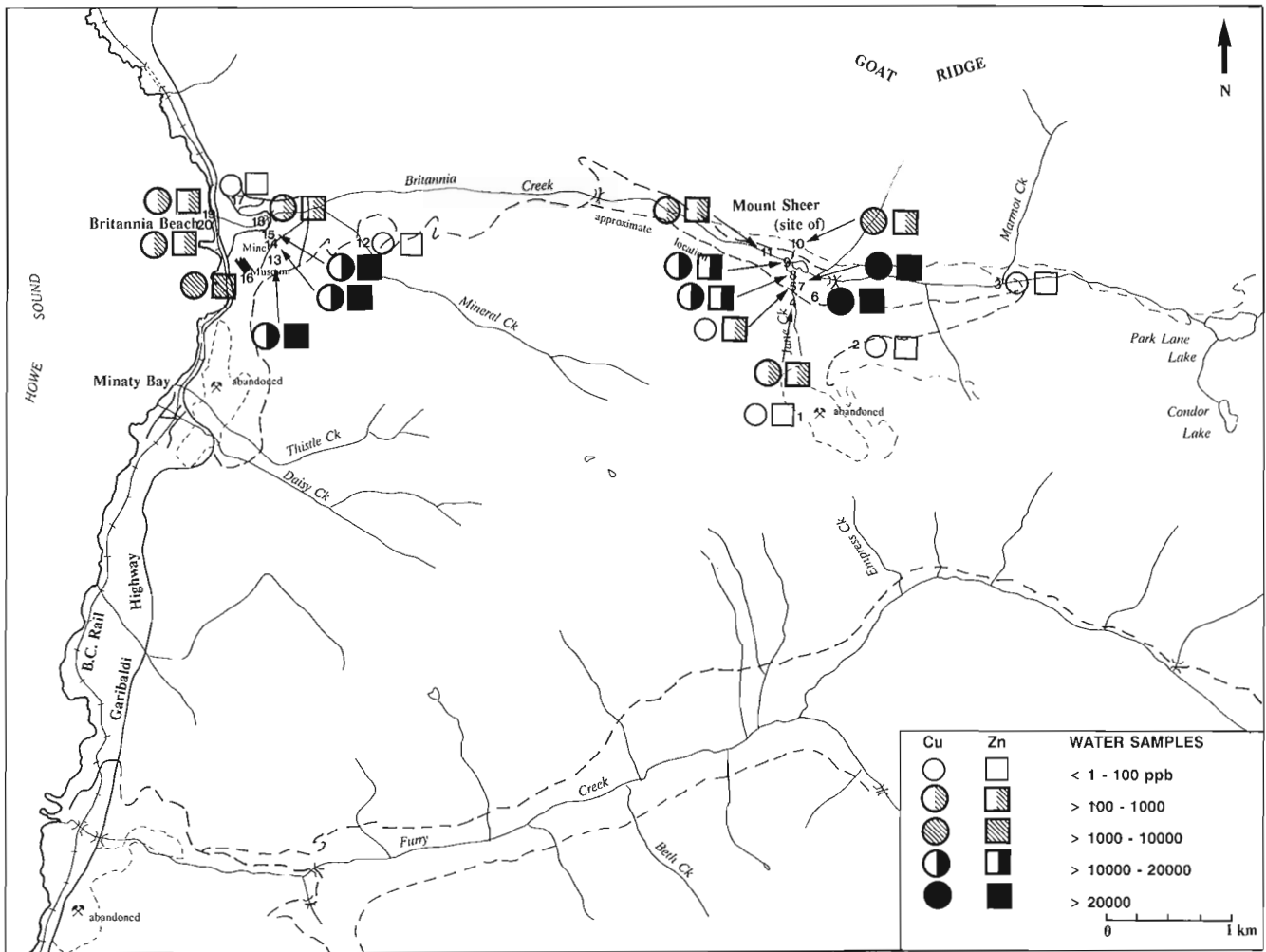


Figure 4. Concentrations of Cu and Zn (in ppb) in water samples collected in the detailed study of the Britannia Mine drainage.

within the Sound. It is, in fact, the only seaweed at most locations because of its high tolerance to the relatively low salinity of the Howe Sound waters.

Results and discussion

An earlier study showed that the ash yield from rockweed is approximately 30% (Dunn, 1990). Data presented here are all quoted as element concentrations in ashed tissue (Table 4). Figure 3 shows the concentrations of Cu and Zn to be more enriched at the north end of the Sound than farther to the south. Of particular note is the pattern of Cu distribution: in the south near Bowen Island concentrations are generally 60-70 ppm Cu, whereas near Britannia Beach they locally exceed 3000 ppm Cu. Similarly, Zn levels are up to 1543 ppm near Britannia Beach, and mostly 300-400 ppm in the south basin. Dispersion of these elements from the mineralized rocks in this area is evident; some elements have been transported northward and some toward the south as far as Anvil Island. Uranium levels are highest at the north end of the Sound, and are presumably derived from the plutonic rocks which characteristically have higher U content than volcanogenic and sedimentary rocks of the type that

dominate the southern half of the Sound. In addition, levels of Fe and Ba are higher in the north than the south. Conversely, As, Pb, and Ni concentrations are lowest in samples from the Britannia area (sites 26, 27, 28). The low As and Pb levels are probably due to their precipitation on pebbles and rocks (see Table 7) or adsorption on to clay minerals, thereby removing them from the waters draining into the Sound in this area. The higher Ni content of samples in the southern basin reflects the relatively mafic composition of the local volcanic and sedimentary rocks. Data for Bi and Sb are not shown in Table 4 since, like the waters, their concentrations are close to, or below, their detection limits of 2 ppm Bi (by ICP-ES) and 0.1 Sb (by INAA).

BRITANNIA MINE SITE STUDY (J.B. Percival)

Introduction

Mineralization at the Britannia mine site (Britannia Beach, Fig. 1) was discovered more than a century ago. The deposits occur as volcanogenic Cu-Zn massive sulphide orebodies that

Table 7. Major, minor, and trace element concentrations in precipitates - Britannia mine area.

	1	2	3	4	5	6	7	8	9	10A	10B	11
"Whole rock" analysis (LiBO ₂ fusion + ICP-ES), values in %												
SiO ₂	5.23	17.51	21.20	12.30	17.55	38.50	0.55	1.77	8.24	57.16	62.90	12.50
TiO ₂	0.09	0.08	0.09	0.19	0.28	0.08	0.04	0.06	0.14	0.72	0.52	0.01
Al ₂ O ₃	5.01	29.05	34.45	3.95	4.70	28.40	2.20	1.13	7.15	17.20	14.25	21.18
Fe ₂ O ₃	54.16	1.14	2.10	35.70	42.00	2.20	58.82	56.80	41.60	8.30	6.50	3.04
MnO	0.20	0.07	0.04	0.65	1.16	0.30	0.01	0.01	0.03	0.53	0.40	0.05
MgO	0.20	0.30	0.38	0.65	0.61	0.92	0.04	0.13	0.57	2.83	2.10	0.11
CaO	0.15	0.76	0.41	1.44	0.61	0.92	0.04	0.12	0.77	3.06	6.47	1.45
Na ₂ O	0.20	0.25	0.36	1.16	0.63	1.48	0.02	0.08	0.38	4.30	2.55	0.02
K ₂ O	0.17	0.19	0.19	0.53	0.58	0.95	0.02	0.05	0.15	2.51	0.95	0.03
P ₂ O ₅	0.32	ND	ND	ND	0.09	ND	ND	ND	ND	0.21	0.11	ND
LOI	33.00			24.62	32.01		37.60	37.74		0.93	1.82	31.31
Total	98.55	49.35	59.22	80.58	99.65	72.86	100.37	97.89	59.03	97.75	98.57	80.70
Trace element analysis (aqua regia digestion + ICP-ES), values in ppm												
As	143	56	132	149	172	32	69	22	46	27	31	35
Ag	2.2	0.3	10.5	3.3	2.92	4.62	1.2	1.1	1.4	0.4	0.8	0.3
Ba	15	108	30	43	165	128	5	9	20	458	190	34
Bi	5	43	49	231	ND	13	ND	ND	ND	ND	5	210
Cd	2.1	12.8	7.7	8.3	4.2	13.2	3.2	5.4	4.8	0.6	1.7	17.9
Co	ND	11	10	14	2	3	ND	ND	2	13	11	ND
Cr	108	39	357	45	23	72	7	19	32	21	17	23
Cu	1876	19733	17602	13.1%*	1565	17333	607	3759	5323	98	165	12.3%*
La	5	23	75	ND	3	67	6	5	9	6	6	33
Mo	46	7	6	5	7	1	11	24	55	7	18	8
Mn	108	788	346	323	349	194	31	29	163	2892	2070	315
Ni	68	55	238	55	22	48	2	1	28	21	15	14
Pb	128	226	576	227	169	480	ND	80	419	108	118	1572
Sb	91	82	83	96	12	33	ND	ND	20	17	15	99
Sn	61	47	ND	72	57	ND	64	63	64	ND	ND	47
Sr	3	43	7	5	12	13	1	2	16	59	124	76
Te	50	51	43	110	12	20	10	ND	16	ND	ND	89
V	1	16	14	25	26	5	1	9	74	99	71	1
W	ND	ND	ND	53	ND	ND	ND	ND	ND	ND	ND	35
Y	5	53	273	4	2	189	2	2	10	13	13	48
Zn	95	3027	2397	393	297	3991	60	31	177	180	388	9890
* estimated value												
ND - Not detected												

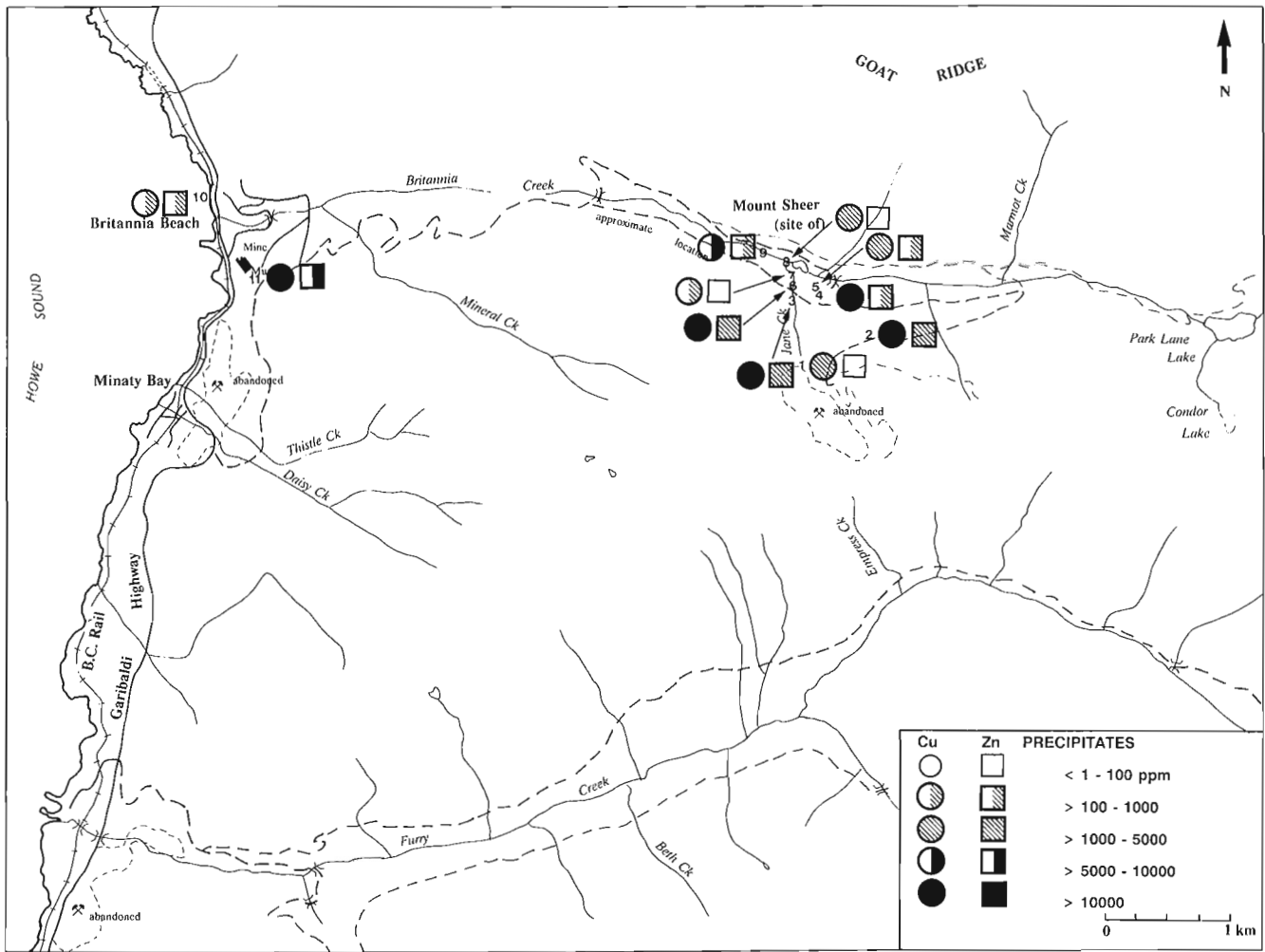
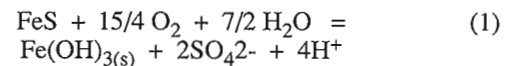


Figure 5. Concentrations of Cu and Zn (in ppm) in the precipitates collected in the detailed study of the Britannia Mine area.

were deposited by hydrothermal and exhalative solutions. They were emplaced into the Britannia shear zone, which is a northwest-trending zone of flattening (Payne et al., 1980; Lynch, 1991). Copper was first reported in 1888 by Forbes, and in 1898 Oliver Furry staked five claims (Ebbutt, 1935). Underground and open pit production began in 1905 by the Britannia Mining and Smelting Company and continued until 1963, when the Anaconda Mining Company operated the mine until closure in 1974. About 50 million tonnes of ore grading 1.1% Cu, 0.65% Zn, 6.8 g/tonne Ag, and 0.68 g/tonne Au were produced (Payne et al., 1980).

During the mining operations, mine waters from the 2200 and 4100 levels (sites 6-7 and 13-15, respectively in Fig. 4) flowed through two Cu precipitation plants which contained scrap metal (tin and iron). This process reduced the amount of dissolved Cu discharged to receiving waters. Currently, acidic mine waters exiting from the 2200 and 4100 levels supply high concentrations of Cu and other metals to nearby surface waters. The acidic water results from the oxidation of

pyrite by O_2 and is characterized by low pH, high SO_4^{2-} in solution, and the presence of a yellowish-red precipitate of amorphous Fe-oxide (limonite) (Eq. 1).



The low pH results in leaching of metals in the mine workings and their concomitant transport to receiving waters though their concentrations in solution may be reduced by co-precipitation or sorption with limonite.

Results and discussion

Results from the water analyses are shown in Tables 5 and 6. Copper and Zn data are plotted separately in Figure 4. The highest metal and lowest pH values occur in waters emanating from the mine portals at the 2200 (site 6) and 4100 (site 13) levels and in the mine museum tunnel (site 16). The lowest concentrations occur in waters above and slightly east of the open pit area (sites 1 and 2), in Britannia Creek near

Marmot Creek (site 3), in Mineral Creek (site 12), and in the town drinking water (site 17). All other samples show elevated levels of Cu and Zn. All samples have low to non-detectable As, Bi, and Sb, and Cd appears to follow the Zn trend. The acidic mine waters have elevated levels of the major elements, especially Fe and Mn (sites 6 to 9 and 13 to 16).

The effects of dilution by receiving waters is readily observed at the Mount Sheer site. Water emanating from the 2200 level portal (site 6) is highly acidic and carries high concentrations of dissolved metals. Over a short distance (<10 m) the Cu concentration drops from 43 950 to 29 975 ppb (site 7). When the mine water mixes with Jane Creek (site 8) the concentration of Cu decreases again, down to 19 850 ppb. The Cu level is stable until the combined waters mix with Britannia Creek (site 10). At this point, a major decrease from over 19 000 ppb to 1170 ppb indicates strong dilution by the larger creek.

The decrease in dissolved metal loadings may also reflect co-precipitation or sorption of metals by amorphous Fe-oxides (limonite; yellowish red) or Al oxides (white) that occur ubiquitously in the stream bed as coatings or precipitates on pebbles. Chemical data for the precipitates are shown in Table 7 and those for Cu and Zn are plotted in Figure 5. Zinc concentrations correspond to high Al₂O₃ values; elevated Cu levels are associated with both high Fe₂O₃ and Al₂O₃ concentrations. Levels of the other trace elements are highly variable, ranging from nondetectable to more than 1000 ppm (e.g., Pb). Major element concentrations, other than those of Al₂O₃ and Fe₂O₃, are very low. These samples may contain trace amounts of clay (kaolinite or chlorite), quartz, and feldspar but are dominated by the amorphous oxides.

Although there is a natural decrease in the loadings of the metals from the Britannia mine to the Sound, the data show that levels of metals entering Howe Sound are elevated relative to the background values. The concentrations of Cu and Zn emanating from Britannia Creek are within the drinking water guidelines (Cu <1 ppm; Zn <5 ppm, Canadian Water Quality Guidelines, 1987) but exceed safe limits for freshwater aquatic life (Cu, <2-4 ppb; Zn <30 ppb; Canadian Water Quality Guidelines, 1987). Also, Britannia Creek experiences high flows in the spring and fall as well as periodic flooding (last event was August 29-30, 1991). During these events, it is highly probable that the precipitates would be flushed out and released or deposited in Howe Sound. It is clear that the Britannia mine area needs periodic sampling to monitor seasonal and temporal changes in water and sediment quality.

SUMMARY

Reconnaissance geochemical studies of the Howe Sound drainage basin involved the collection and analysis of near-shore bottom sediments, stream waters, waters at several depths from within the Sound, and the brown seaweed known as rockweed (*Fucus gardneri*). A more detailed study was conducted around the abandoned Britannia Cu mine to examine local variations in stream water

chemistry, and the precipitates on rock surfaces. This study places emphasis on the distribution of Cu and Zn in and around the Sound, because of the significant influence of the Britannia area from where these metals were mined.

High levels of Cu and Zn were found in all sample media from the vicinity of the mine; no seaweed grows on the shores either side of Britannia for a total distance of 3 km presumably because of metal poisoning. In the southern basin Zn concentrations in sediments and seaweeds are higher than those of Cu in accord with the relative crustal abundances of these metals.

Except near Britannia Beach, waters of the Sound contain low concentrations of most of the elements determined, although major cations are enriched at the north end. Surface waters have low salinity due to the influx of fresh waters from the surrounding mountains, and concentrations of some elements (e.g., As) increase with depth and increasing salinity. The rockweed appears to be a sensitive indicator of the chemistry of the environment exhibiting enrichment of Cu, Zn, Fe, U, and Ba in the north basin.

Waters flowing from the mine portals are acidic and contain high concentrations of dissolved metals, and the study demonstrates clearly the dilution effect by receiving waters, frequently associated with co-precipitation of metals with the Fe or Al oxides that coat pebbles in the stream beds. Periodic flooding probably flushes the precipitates into the Sound, resulting in temporal variations in the chemistry of the Howe Sound waters, sediments, seaweeds, and biota. Consequently, monitoring of these media is required in order to establish long term patterns of chemical variability.

ACKNOWLEDGMENTS

We are grateful to Ken Hill (Environment Canada) and Bob Turner (GSC, Vancouver) for their assistance in the field. Ken Hill from Westwater Research Centre (U.B.C.) kindly loaned the Boston whaler boat used for sampling in the Sound. Special thanks to S. Phaneuf for X-ray diffraction analysis of precipitates and sediments, J. Vaive and G. Gauthier for AA analysis of water samples, M. Wyergangs for determining physical properties of sediments and heavy mineral and clay-size separations, and to M.L. Wilson for preparation of the tables.

REFERENCES

- Asmund, G., Bollnberg, H.J., and Bondam, J.
1975: Continued environmental studies in the Qaumarujuk and Adfardikavsa fjords, Maarmorilik, Umanak district, West Greenland; Geological Survey of Greenland, Report 80, p. 53-61.
- Black, W.A.P. and Mitchell, R.I.
1952: Trace elements in the common brown algae and in sea water; Journal of the Marine Biologists Association U.K., v. 30, p. 575-584.
- Bollnberg, H.J. and Cooke, H.R., Jr.
1985: Use of seaweed and slope sediments in fjord prospecting for lead-zinc deposits near Maarmorilik, West Greenland; Journal of Geochemical Exploration, v. 23, p. 253-263.
- Bryan, G.
1969: The absorption of zinc and other metals by the brown seaweed *Laminaria digitata*; Journal of the Marine Biologists Association, U.K., v. 49, p. 225-243.

Canadian Water Quality Guidelines

1987: Canadian Council of Resource and Environment Ministers, Environment Canada, Ottawa, Ontario, Canada.

Dunn, C.E.

1990: Results of a biogeochemical orientation study on seaweed in the Strait of Georgia, British Columbia; in *Current Research, Part E*; Geological Survey of Canada, Paper 90-1E, p. 347-350.

Ebbutt, F.

1935: Relationship of structure to ore deposition at the Britannia mine; Canadian Institute of Mining and Metallurgy Transactions, v. 38, p. 123-133.

Fisheries and Oceans

1989: Howe Sound, British Columbia, Chart No. 3526, Canadian Hydrographic Service, Minister of Fisheries and Oceans, Ottawa, Ontario, Canada.

Fuge, R. and James, K.H.

1974: Trace element concentrations in *Fucus* from the Bristol Channel; *Marine Pollution Bulletin*, v. 5, p. 9-12.

Lynch, J.V.G.

1991: Georgia Basin Project: stratigraphy and structure of Gambier Group rocks in the Howe Sound-Mamquam River area, southwest Coast Belt, British Columbia; in *Current Research, Part A*; Geological Survey of Canada, Paper 91-1A, p. 49-57.

Monger, J.W.H.

1991: Georgia Basin Project: structural evolution of parts of southern Insular and southwestern Coast belts, British Columbia; in *Current Research, Part A*; Geological Survey of Canada, Paper 91-1A, p. 219-228.

Payne, J.G., Bratt, J.A., and Stone, B.G.

1980: Deformed Mesozoic volcanogenic Cu-Zn sulfide deposits in the Britannia district, British Columbia; *Economic Geology*, v. 75, p. 700-721.

Roddick, J.A.

1965: Vancouver North, Coquitlam and Pitt Lake map-areas, British Columbia; Geological Survey of Canada, Memoir 335, 276 p.

Scagel, R.F.

1967: Guide to common seaweeds of British Columbia; British Columbia Provincial Museum, Department of Recreation and Conservation, Handbook No. 27.

Sharp, W.E. and Bolviken, B.

1979: Brown algae: a sampling medium for prospecting fjords; *Proceedings, 7th International Geochemical Exploration Symposium, 1978*, Golden, Colorado; Association of Exploration Geochemists, Rexdale, Ontario, p. 347-356.

Syvitski, J.P.M.

1979: Flocculation, agglomeration, and zooplankton pelletization of suspended sediment in a fjord receiving glacial meltwater; in *Fjord Oceanography*, (ed.) H.J. Freeland, D.M. Farmer and C.D. Levings; Plenum Press, New York and London, p. 615-623.

Syvitski, J.P.M. and Macdonald, R.D.

1982: Sediment character and provenance in a complex fjord; Howe Sound, British Columbia; *Canadian Journal of Earth Sciences*, v. 19, p. 1025-1044.

Geological Survey of Canada Project 890043

Tertiary Georgia Basin, British Columbia and Washington State: a view from the other side¹

Peter S. Mustard and Glenn E. Rouse²
Cordilleran Division, Vancouver

Mustard, P.S. and Rouse, G.E., 1992: Tertiary Georgia Basin, British Columbia and Washington State: a view from the other side; *in* Current Research, Part A; Geological Survey of Canada, Paper 92-1A, p. 13-23.

Abstract

Tertiary Georgia Basin comprises Paleocene to Recent strata, mainly preserved on mainland Washington State and in the Vancouver area of British Columbia. Several islands in southern Georgia Strait contain Tertiary strata. Tumbo Island rocks, previously believed to be late Cretaceous, contain Paleocene palynomorphs. Most rocks of the Sucia Island chain also contain Paleocene pollen, allowing correlation with Tumbo Island and with lower Chuckanut Formation on the mainland. Deposition occurred in a braided stream to lower alluvial fan system, flanked by marshes with abundant fungal and fern components, and low areas supporting angiosperms and conifers. Conglomerate clast types and paleocurrents indicate a west or northwest source. These paleocurrent and provenance patterns and the source-proximal sedimentation suggest these deposits formed near the early Tertiary basin western margin. This implies the early basin was entirely continental, reducing the probability of significant oil generation due to the lack of marine source rocks.

Résumé

Le bassin de Georgia du Tertiaire comprend des couches remontant jusqu'au Paléocène, principalement conservées sur le continent, dans l'État de Washington et dans la région de Vancouver (Colombie-Britannique). Plusieurs îles dans le sud du détroit de Georgia contiennent des couches tertiaires. Les roches de l'île Tumbo, que l'on avait au préalable datées du Crétacé supérieur, recèlent des palynomorphes paléocènes. La plupart des roches de la chaîne de l'île Sucia contiennent elles aussi du pollen paléocène, d'où une corrélation entre l'île Tumbo et la base de la formation de Chuckanut sur le continent. La sédimentation a eu lieu dans un milieu allant de cours d'eau anastomosés à cône alluvial inférieur, flanqué de marais où abondaient champignons et fougères et de basses terres où croissaient angiospermes et conifères. Les types de clastes des conglomérats et les paléocourants indiquent une source dans l'ouest ou le nord-ouest. Ces configurations de paléocourants et de provenance ainsi qu'une sédimentation proche de la source révèlent que ces sédiments se sont déposés près de la bordure occidentale du bassin datant du Tertiaire inférieur. Il ressort de ce qui précède que le bassin était à l'origine entièrement constitué de sédiments continentaux, réduisant la probabilité d'une formation importante de pétrole étant donné l'absence de roches mères marines.

¹ Contribution to Frontier Geoscience Program

² PCI Palynox Consulting Inc., 2134 West 53rd Avenue, Vancouver, British Columbia V6P 1L6

INTRODUCTION

The Georgia Basin is a northwest-oriented structural and topographic depression encompassing Georgia Strait, eastern Vancouver Island, the Fraser River lowlands of southwest British Columbia, and the northwest mainland of Washington State. Sedimentary rocks of the Georgia Basin comprise two main packages: the Upper Cretaceous Nanaimo Group, exposed mainly on eastern Vancouver Island and the Gulf Islands of Georgia Strait, and a superimposed Tertiary basin mostly preserved in the Vancouver area and northwest Washington (Fig. 1). The Tertiary part of Georgia Basin, termed Whatcom or Bellingham Basin by some authors (e.g., Miller and Misch, 1963; Hopkins, 1968) has recently been the target for renewed hydrocarbon exploration, with three wells drilled in 1991.

Prior studies of Tertiary Georgia Basin have concentrated on the mainland exposures. These have been interpreted as entirely terrestrial, with paleocurrent indicators and provenance data supporting an origin from Coast Belt or Cascade sources to the north or east of present exposures (Kerr, 1942; Miller and Misch, 1963; Johnson, 1982, 1984). Several islands in Georgia Strait contain rocks which were originally mapped as part of the upper Cretaceous Nanaimo Group, but which have more recently been considered to be

Tertiary age. This study documents the geology of these islands, presenting new palynological data confirming a Paleocene age for these rocks. The preserved lithofacies provide evidence of a terrestrial fluvial environment of deposition, and paleocurrent and provenance data indicate that the sediments derive from sources to the west or northwest. The Tertiary rocks of these islands probably formed near the original western margin of the Tertiary basin, indicating that the Tertiary part of Georgia Basin was continental with the exception of marginal marine middle Miocene rocks documented by Rouse et al. (1990). The lack of evidence for pre-Miocene marine facies in this basin decreases the likelihood of good source rocks for hydrocarbon, particularly oil, generation.

REGIONAL GEOLOGY

The Georgia Basin overlies three different basement entities: Wrangellia on Vancouver Island; the Coast Belt on the mainland of British Columbia; and the Cascade terrane in northwest Washington State (Fig. 1 and Monger, 1990). A mid- to late Cretaceous southwest-vergent thrust system is preserved at the southern margin of the Georgia Basin (Brandon et al., 1988) and in the eastern Coast Belt, mainly east of Harrison Lake (Journeay, 1990). The basin has also

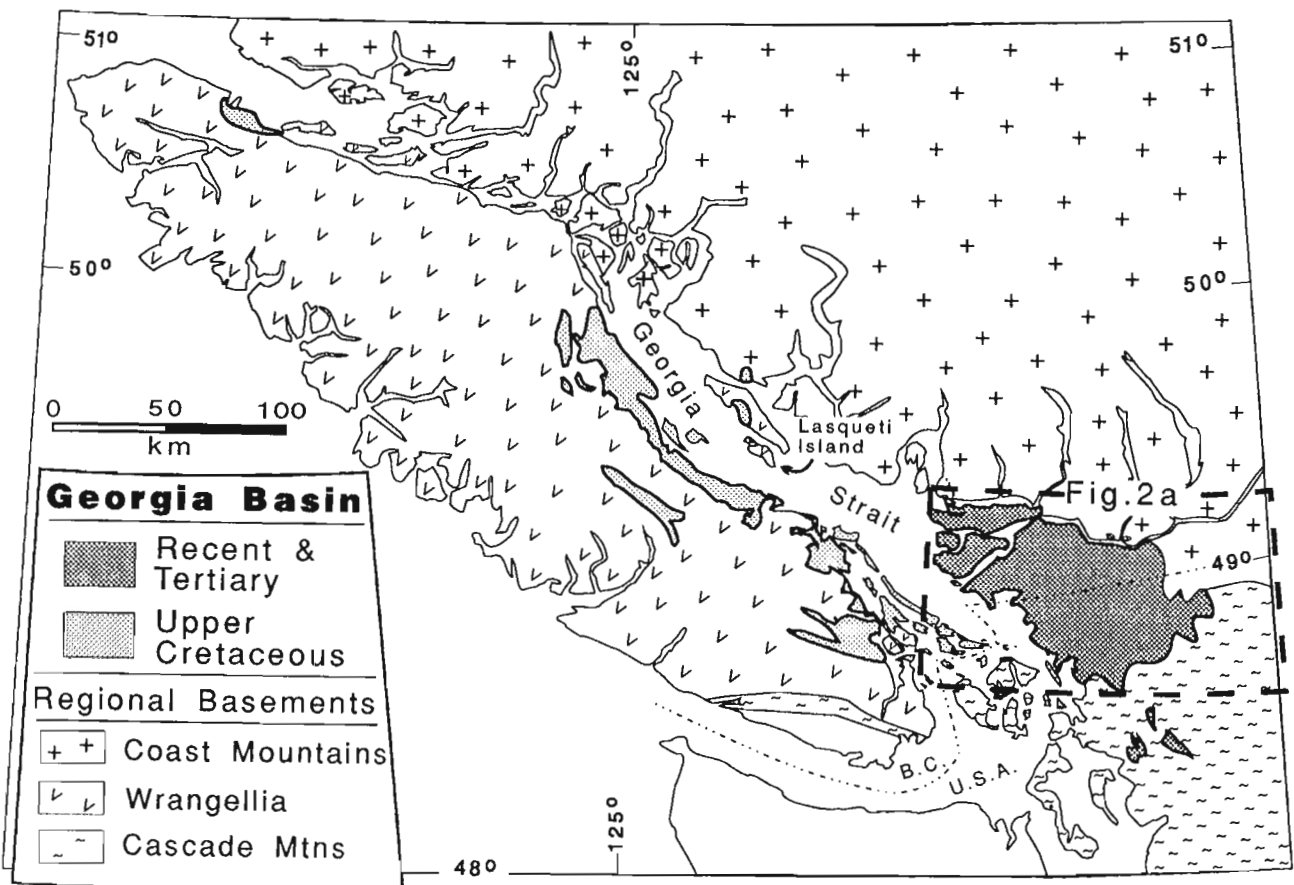


Figure 1. Regional setting of the Georgia Basin (modified from Monger, 1990). The area shown in Figure 2A is outlined.

been affected by early Tertiary compression, which resulted in southwest-directed thrusting in the Nanaimo Group (England, 1990; England and Calon, 1991) and possibly caused northwest plunging folds in the Chuckanut Formation (Johnson, 1982, 1984). Younger (Miocene?) northeast-trending faults and folds are evident on gravity and seismic profiles of the Fraser River lowlands. These are probably the subsurface expression of Tertiary structures preserved in the Coast and Cascade mountains to the east and north (Monger, 1990).

TERTIARY GEORGIA BASIN

The Tertiary rocks of the Georgia Basin are predominantly exposed in the lower Fraser Valley and northwest Washington (Fig. 1, 2A). The main stratigraphic components are nonmarine clastics of the Paleocene-Eocene Chuckanut Formation of Washington State, the partly equivalent upper Burrard and Kitsilano formations of the Vancouver area, the upper Eocene to Oligocene age Huntingdon Formation, and younger (mostly Miocene) sedimentary rocks known from subsurface drilling and rare surface exposures. Upper Cretaceous rocks occur disconformably beneath the Tertiary

strata at Burrard Inlet in Vancouver (Blunden, 1971; Rouse et al., 1975) and in the western Fraser River delta subsurface (Hopkins, 1968).

The upper part of the Burrard Formation (the Ferguson Point Formation of Blunden, 1971) and the overlying Kitsilano Formation are Paleocene-Eocene fluvial clastic rocks derived from the east or northeast. In Washington, upper Paleocene and Eocene rocks of the Chuckanut Formation have been studied in detail by Johnson (1982, 1984). The Chuckanut Formation comprises as much as 6 km of nonmarine conglomerate, sandstone, mudstone, and minor coal. Deposition occurred in meandering and braided fluvial deposystems in which alluvial fan deposits accumulated close to syndepositional normal faults. Paleocurrent trends and conglomerate clast compositions demonstrate derivation from local Coast Mountain or Cascade sources north and east of the basin. The Huntingdon Formation is a late Eocene to Oligocene succession of terrestrial clastic rocks up to 500 m thick that unconformably overlies the Chuckanut Formation east of Bellingham and Cascade or Coast Belt metavolcanic rocks in the upper Fraser River valley and Sumas, Washington areas (Kerr, 1942; Miller and Misch, 1963). In the upper Fraser Valley, the Huntingdon Formation

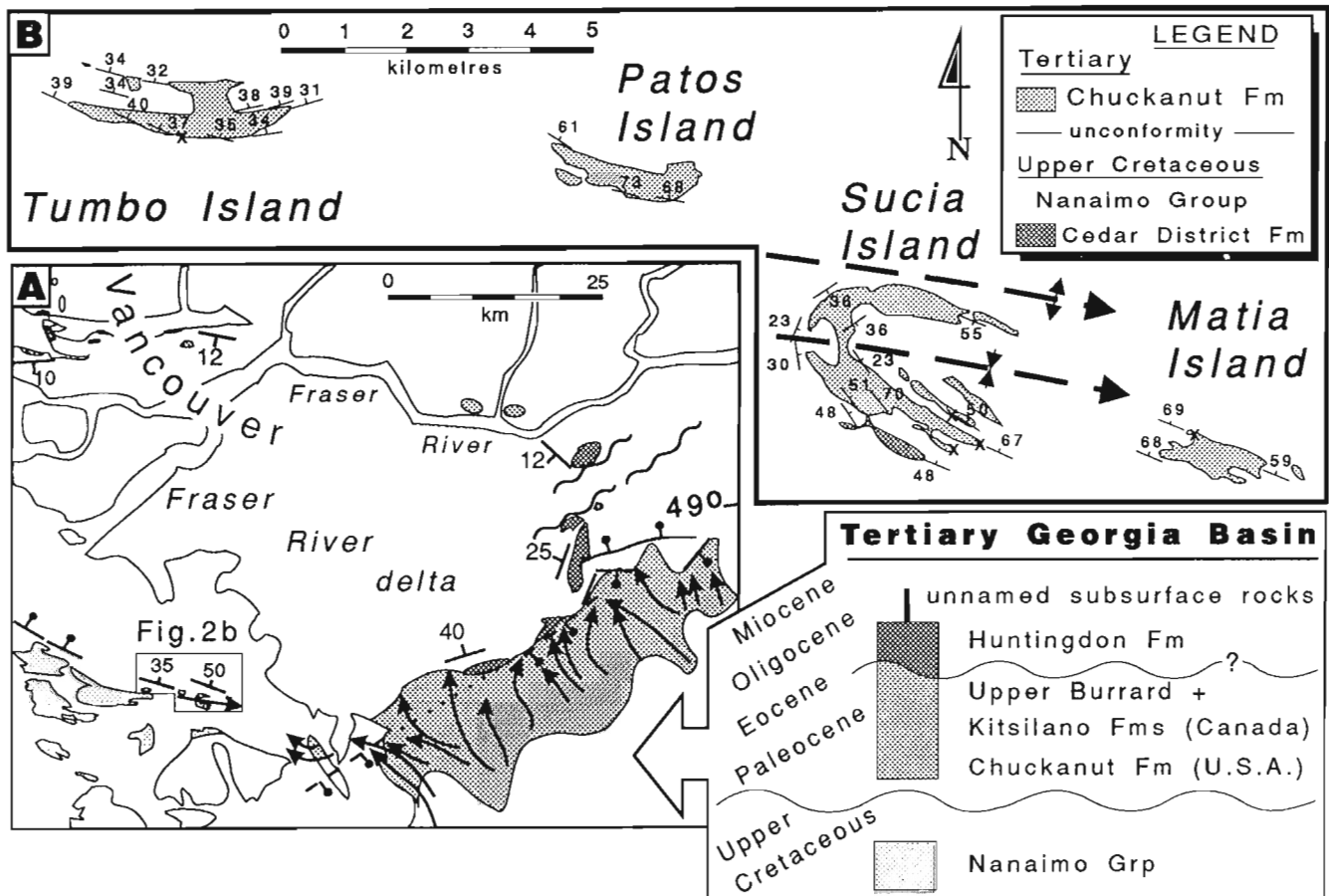


Figure 2. A. Tertiary Georgia Basin and simplified stratigraphic nomenclature. A small outlier of Paleocene sedimentary rocks on Lasqueti Island (Fig. 1) is also part of the Tertiary basin. **B.** Geology of the Tertiary and associated rocks of Tumbo Island, B.C., and the Sucia Island chain, northwest Washington State. Palynology sample sites are indicated by X.

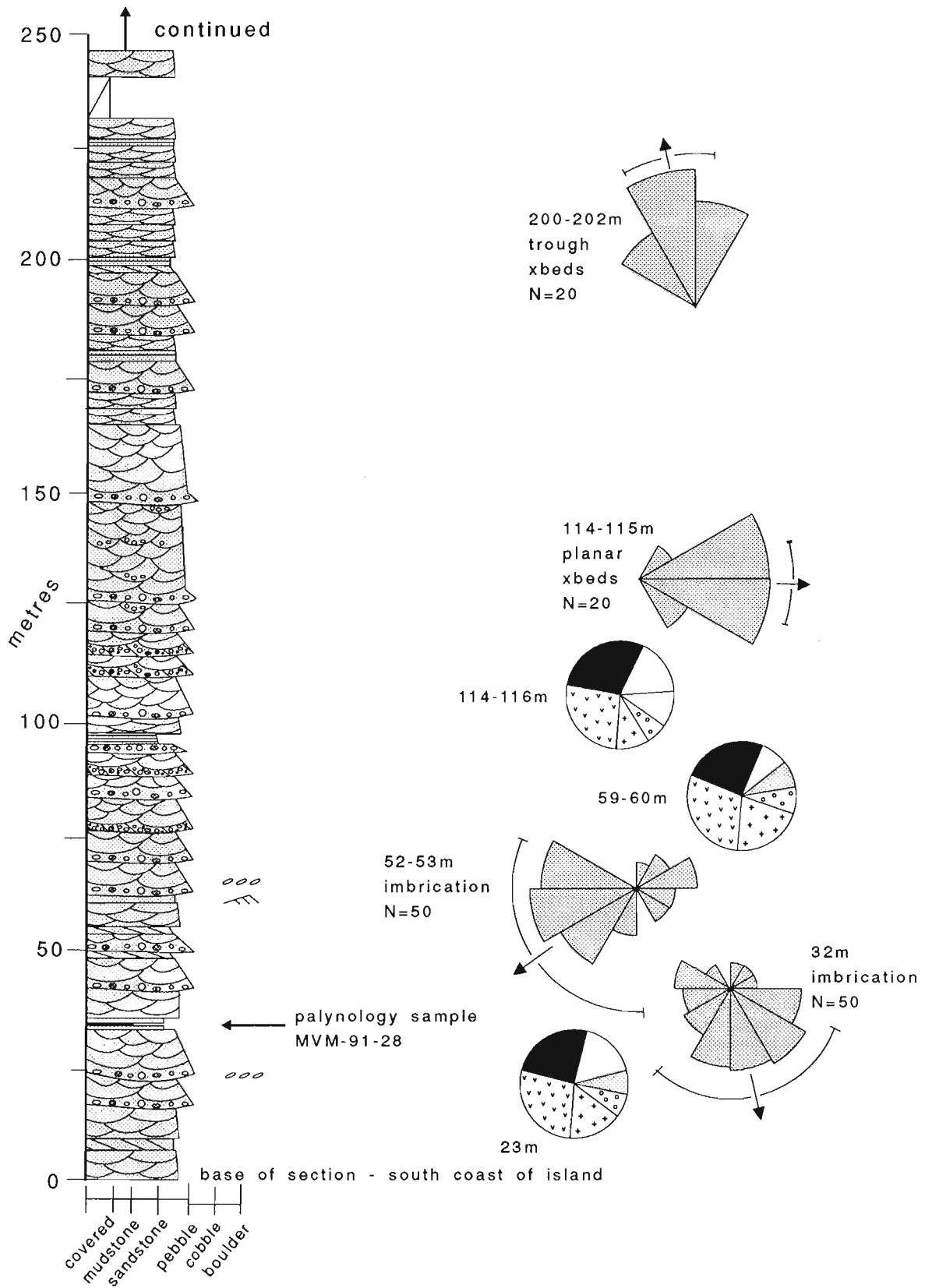


Figure 3. Composite measured stratigraphic section from Tumbo Island. Pie graphs summarize conglomerate clast compositions of individual beds (100 clasts/graph). See Figure 5 for clast type legend. Rose histograms display paleocurrent data (see Figure 4 for legend and scale). The section was measured using a Jacobs Staff on continuous coastal exposures of Tumbo Island (see inset map) with several strike-parallel offsets required to obtain a continuous section.

Stratigraphic Section - Tumbo Island

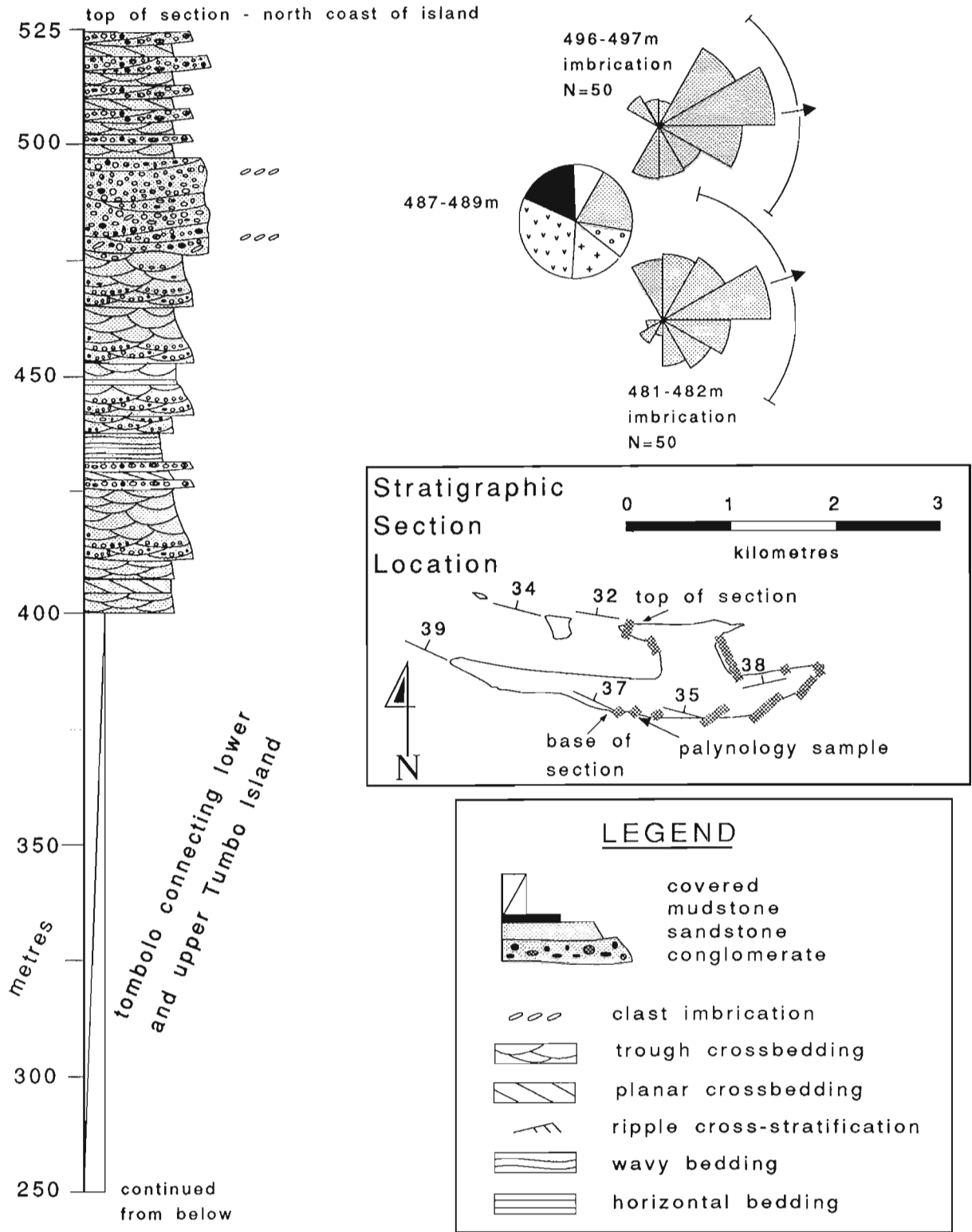


Figure 3 (cont.)

comprises several coarsening-upward megasequences (100 m scale) interpreted as the product of repeated progradation of lower alluvial fan facies over braided stream and floodplain facies. Paleocurrents and clast compositions indicate derivation from the Cascades to the east and southeast (Mustard, unpublished data).

Miocene and younger sedimentary rocks of greater Vancouver and northwest Washington are known mainly from hydrocarbon exploration drilling where as much as 1200 m of Miocene sandstone and mudstone have been intercepted (Hopkins, 1968; Rouse et al., 1990). These rocks have been interpreted as terrestrial, mainly fluvial deposits, although marginal marine siltstone and mudstone are also present (Rouse et al., 1990). The absence of outcrop and lack of detailed subsurface data preclude complete interpretation of these younger rocks.

Tertiary Georgia Basin rocks of the Gulf and San Juan islands

Several islands in Georgia Strait contain strata now known to be part of Tertiary Georgia Basin. An isolated occurrence of Paleocene rocks on Lasqueti Island was described in detail in Mustard and Rouse (1991). The other Paleocene rocks occur on the most northerly San Juan islands (Sucia, Matia and Patos islands, hereafter termed the Sucia chain) and on Tumbo Island of the Canadian Gulf Islands (Fig. 2).

The rocks of the Sucia chain were originally correlated with the Campanian age Cedar District and De Courcy formations of the Nanaimo Group (Janbaz, 1972; Ward, 1973, 1976, 1978; Pacht, 1980, 1984). Paleontological evidence for these correlations exists only on Sucia Island, where the lowest strata contain abundant marine fossils of mid-Campanian age suggesting correlation with the Cedar District Formation (Ward, 1978). A subtle, but distinct unconformity separates these lower marine mudstones and sandstones from up to 700 m of nonmarine sandstone and conglomerate which make up the majority of the Sucia chain (Fig. 2B). These nonmarine rocks have not yielded macrofossils and previous to this study have not been examined for microfossils. Johnson (1982, 1984) suggested, on the basis of lithological similarity, that the nonmarine rocks were part of the middle Eocene age Padden Member of the Chuckanut Group. Johnson interpreted fission track ages of detrital zircons to indicate a late Paleocene or younger age for the sandstone (Johnson, 1982, 1984).

The rocks of Tumbo Island (Fig. 2B) were originally correlated with the Maastrichtian age Gabriola Formation of the upper Nanaimo Group (Muller and Jeletzky, 1970; Sturdavant, 1975; Muller, 1980). England and Hiscott (1991, in press) re-examined the Tumbo Island beds and interpreted them as fluvial deposits, in contrast to the submarine fan deposits of the upper Nanaimo Group. England and Hiscott suggested the Tumbo Island beds are Tertiary in age, based on their nonmarine character, similarity to the Sucia Island and mainland Chuckanut Group strata and on an inferred low angle unconformity between these strata and the upper Nanaimo Group of the other outer Gulf Islands.

Lithofacies description

The Tertiary rocks of Tumbo Island and the Sucia chain are very similar, dominated by sandstone which has a brown to tan weathering colour and a light yellow-brown fresh colour. The preserved thickness of Tertiary strata on both islands is about 500 m (Fig. 3 and Janbaz, 1972). The top of the unit is not exposed and the base is exposed only on Sucia Island where the Tertiary rocks disconformably overlie the Campanian age Cedar District Formation of the Nanaimo Group. The unit coarsens upward with conglomerate much more abundant in the upper part of the Tumbo Island succession and slightly more abundant in the upper part of the Sucia Island succession. The sandstone occurs in laterally overlapping and vertically stacked fining-upward sequences generally 1 to 5 m thick, rarely up to 10 m thick (Fig. 3). The sandstone is generally a medium- to coarse-grained lithic arenite with abundant broken carbonaceous plant debris and rare carbonaceous and partly silicified logs. The best preserved fining-upward sequences (e.g., 190-200 m in Fig. 3) show an upward change from a pebble-rich base (locally imbricated) with abundant mudstone ripups in some beds, to complexly overlapping trough crossbedded sandstone, commonly pebbly in the lower part, to planar crossbedded sandstone, capped by wavy (rarely rippled) horizontal thin beds of medium- or fine-grained sandstone and very rare mudstone laminae. This ideal sequence is generally not preserved because the bedsets occur as deeply channelized lenses which laterally overlap and display extensive lateral and vertical cut outs. Several metres of erosion into underlying sequences can be demonstrated in many places. Consequently the upper parts of sequences are in most places not preserved and only the basal pebble-rich layer and trough crossbedded sandstone is present.

Pebble-cobble conglomerate forms <10% of the succession and in most places occurs as a discontinuous basal component of fining-upward sequences or as small pebble layers at the base of individual trough crossbeds. The upper part of the succession on Tumbo Island contains >50% conglomerate, including overlapping and stacked beds each >50 cm thick which form laterally extensive composite units up to 15 m thick (Fig. 3, 480-495 m). These thicker beds are framework-supported and moderately sorted, with pebbles and <30% cobbles up to 15 cm diameter in a matrix of medium- to very coarse-grained lithic arenite. The thick beds are generally massive with poor normal grading. Bed contacts are curved and eroded into underlying sandstone at least several tens of centimetres. Most of the upper conglomerates (above 495 m in Fig. 3) occur as lenses <1 m thick and 10-30 m long with curved, channelized bases. These lenses are moderately to well-stratified with normal graded internal beds 3-10 cm thick of pebble conglomerate grading up to coarse-grained arenite. Both the conglomerate and sandstone commonly display trough or planar crossbedding. The upper, conglomerate-rich part of the Tumbo Island succession is separated from the lower sandstone-dominated part by a 150 m thick covered interval. The covered interval is a tombolo of glacial material and recent sand and gravel which connects the two parts of the island. The depression, now filled by the tombolo, was most likely shaped by Quaternary

glaciation. England and Hiscott (1991, in press) inferred that this covered interval represents a recessive fine-grained member. Similar, but thinner covered intervals on Sucia Island form some of the smaller bays and Janbaz (1972) inferred a similar recessive lithology. However, medium- to coarse-grained sandstone can be traced around the heads of most the small bays on Sucia Island, suggesting the topography does not reflect recessive versus resistant weathering rock types. It more likely reflects the importance of the last glacial event in shaping the topographic features of the islands in Georgia Strait.

Paleocurrents were measured from pebble imbrication, planar crossbeds and rarely trough crossbeds where three-dimensional exposure was sufficient to allow definition of trough long axes and the sense of downcutting. A wide variance in paleoflow directions is apparent with most indicators suggesting flow ranged from northeast to southeast (Fig. 4). This general trend is also apparent in the orientation of the major channelized lenses.

Conglomerate clast compositions were studied by identifying 100 clasts from a single bed at thirteen sites (Fig. 5A,B). The most abundant clast type is black chert commonly containing deformed milky white quartz veinlets. Aphanitic green-grey volcanic clasts are slightly less common, followed by subequal amounts of white chert

(rarely quartzite), red chert (including jasper), felsic intrusives and sedimentary clasts, the latter mostly massive, fine- to medium-grained arkosic sandstone.

Lithofacies interpretation

The lithofacies and sedimentary structures of the islands are consistent with the nonmarine, mostly braided river interpretation of England and Hiscott (1991, in press) and Johnson (1984). The overall coarsening upward trend suggests progradation of an upper braidplain or lower alluvial fan deposystem. The wide variance of paleocurrent indicators and overall radial pattern is typical of lower alluvial fan braided stream deposition (Rust and Koster, 1984). The abundant black and red chert and mafic volcanic clasts are all compositions common on the San Juan islands to the southwest, which probably originally extended farther north (Brandon et al., 1988). The sandstone clasts are identical to sandstone of the upper Nanaimo Group preserved northwest of the islands. The disconformity on Sucia Island between the Tertiary rocks and middle Campanian strata of the underlying Nanaimo Group suggests that a thick section of upper Nanaimo Group strata (upper Campanian and Maastrichtian age) has been eroded. England and Hiscott (1991) estimated the thickness of eroded Nanaimo Group at 1.5 km, based on the thickness of upper Nanaimo Group preserved in islands to the north and missing at Sucia Island.

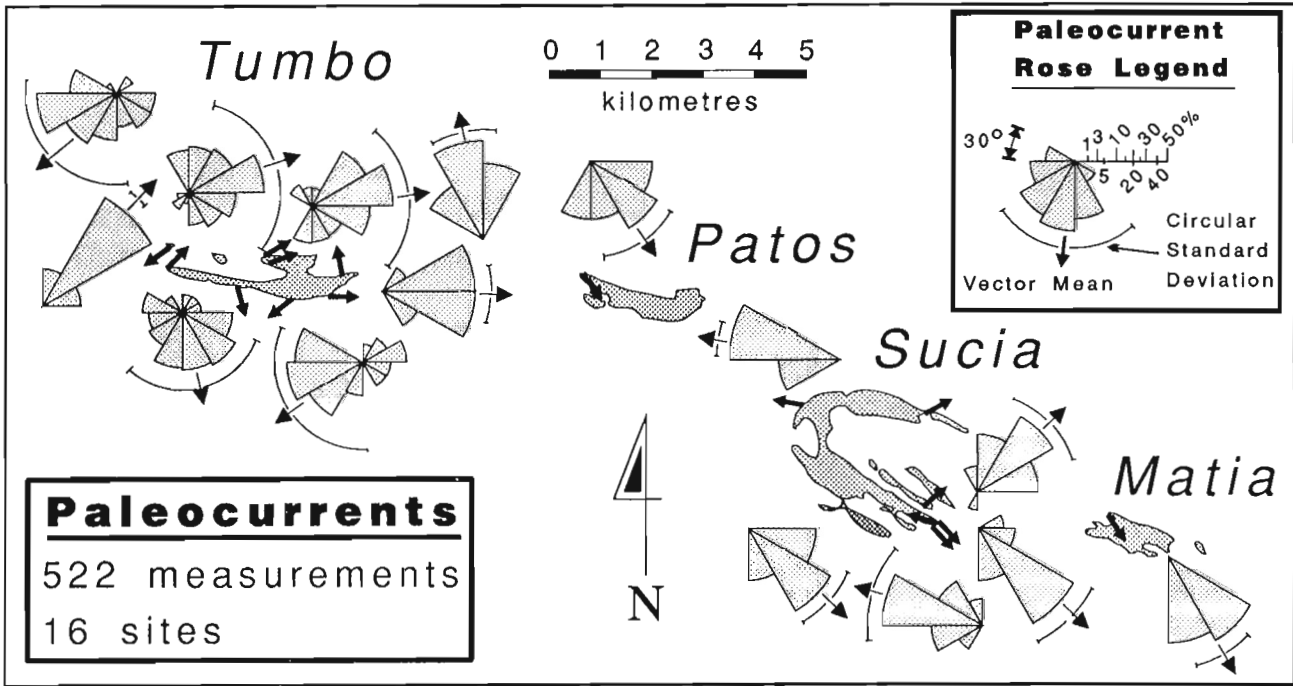


Figure 4. Summary diagram of paleocurrent data. Measurements have been corrected for fold plunge and bed-tilt. Paleocurrent measurement sites are located on each island with an arrow which is also the vector mean. Current roses for each site are shown near each locality and the same spatial grouping of the sites has generally been maintained. Current roses are plotted using a nonlinear scale as advocated by Nemeč (1988). Only sites with Rayleigh significance test values less than 0.05 were used for paleocurrent analysis (method of Curray, 1956). Circular standard deviation was calculated using the method of Krause and Geijer (1987).

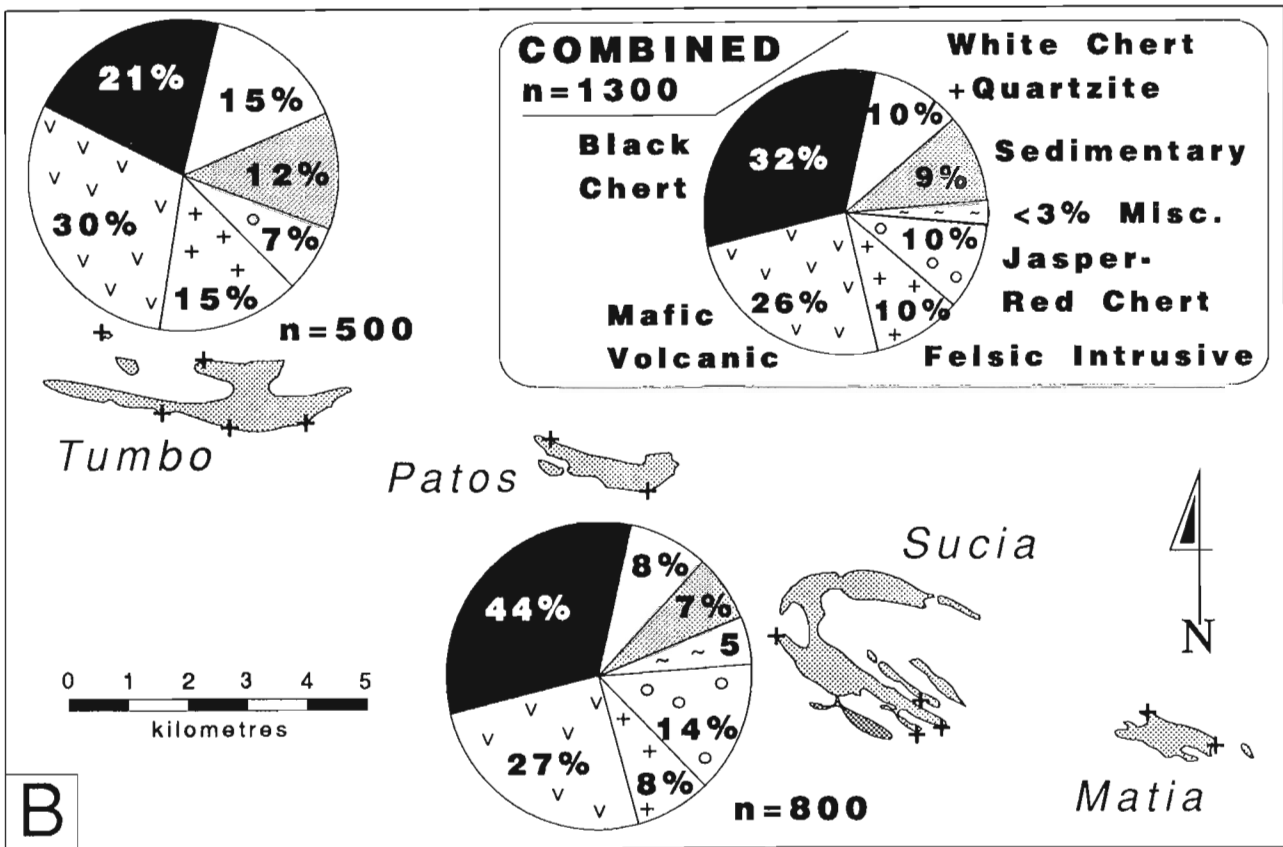
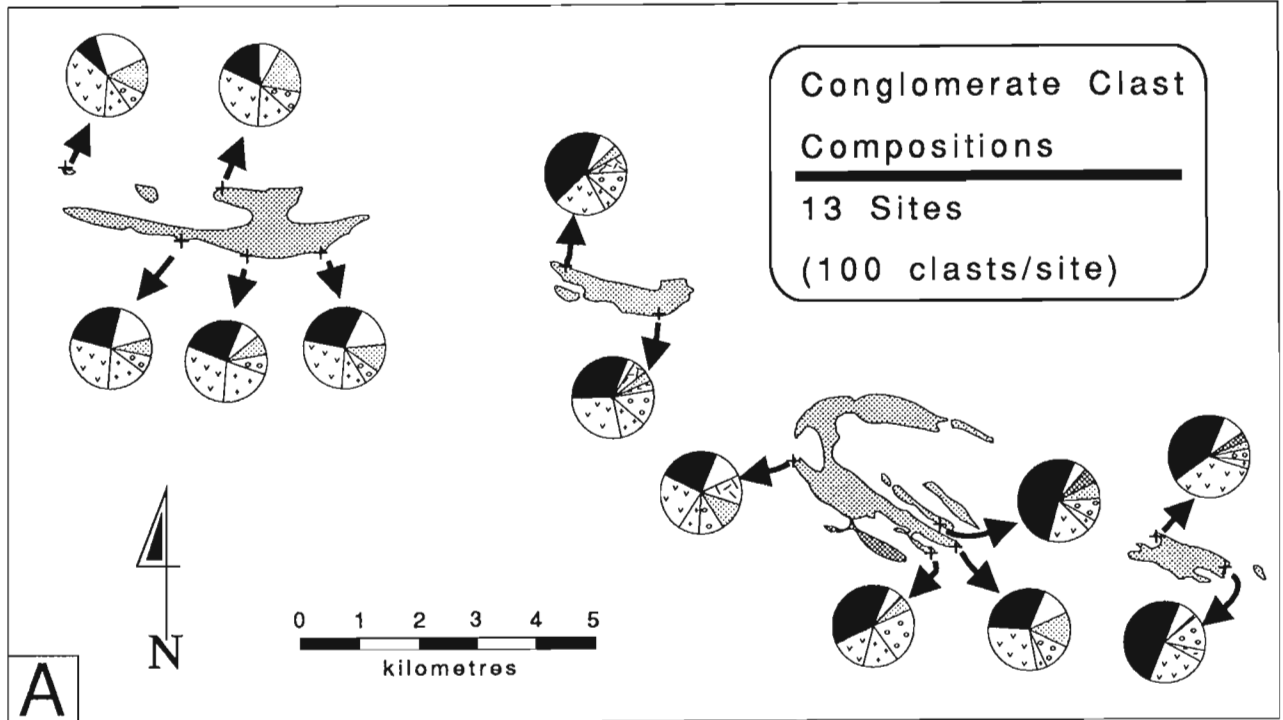


Figure 5. Conglomerate clast compositions. **A.** Individual sites, each located on the island by a cross. **B.** Sites combined in terms of Tumbo Island (5 sites) and the Sucia chain (8 sites) with all thirteen sites combined in the inset. Clast counts were conducted by identifying all clasts encountered on a random line to a total of one hundred per site.

Palynology

Reasonably well preserved and representative palynoassemblages were recovered from samples collected on the Sucia chain (Table 1, Fig. 2B) and Tumbo Island (Table 2, Fig. 2B). Both assemblages are dominated by fungal spores, with fewer angiosperm pollen and fern spores. Both are correlated with those from other rock units previously assigned to the late Paleocene, particularly those from the Arctic and Rocky Mountain foothills regions (Rouse, 1977), and from Lasqueti Island (Mustard and Rouse, 1991). Diagnostic species include *Multicellaesporites irregularis*, *M. "giganteus"*, *Inapertisporites elongatus*, *Staphlosporites allomorphus*, *Brachysporisporites cotalis*, *B. catinus*, *Callimothallus pertusus*, and *Dicellaesporites laevis* among the fungal spores (and reproductive units). Diagnostic angiosperm pollen are *Subtriporopollenites-A* (= pre-*Tilia*), *Rhoipites cryptoporus*, and *Paraalnipollenites alterniporus*. These species occur in assemblages immediately below the Eocene containing the earliest true *Tilia* pollen, ie. *Tilia vesicipites* and *Tilia crassipites*. The angiosperm pollen *Rhoipites cryptoporus*, first described by Srivastava (1972) from the Paleocene in Alabama, is a diagnostic middle and late Paleocene palynomorph from Arctic and western Canada (Rouse, 1977). It also occurs in the late Paleocene beds at Third Beach, Stanley Park, Vancouver (Blunden, 1971) and in late Paleocene beds about 15 m above the base of the Chuckanut Formation on the shore of Lake Samish at Bellingham, Washington (Rouse, unpublished data).

Table 1. Palynomorphs from Sucia Island (3 samples) and Matia Island (1 sample). Sample localities are shown in Figure 2B.

<u>Fungal Spores</u>	<u>Conifer Spores</u>
<i>Multicellaesporites irregularis</i>	<i>Pinus haploxylon</i> -type
<i>M. capsularis</i>	<i>P. diploxylon</i> -type
<i>M. "giganteus"</i>	<i>Picea grandivescipites</i>
<i>M. sacciformis</i>	<i>Tsuga igniculus</i> - type
<i>M. pandus</i>	<i>Cupressacites hiatipites</i>
<i>Callimothallus pertusus</i>	
<i>Tricellaesporites semicircularis</i>	<u>Angiosperm Pollen</u>
<i>Dicellaesporites fusiformis</i>	<i>Subtriporopollenites-A</i>
<i>D. laevis</i>	(=pre- <i>Tillia</i>)
<i>D. appendiculatis</i>	<i>Rhoipites cryptoporus</i>
<i>Staphlosporites conoideus</i>	<i>Arecipites columellus</i>
<i>S. allomorphus</i>	<i>Ericipites ericius</i>
<i>Brachysporisporites cotalis</i>	<i>Myricipites dubius</i>
<i>B. opimus</i>	<i>Alnus vera</i>
<i>B. catinus</i>	<i>Fraxinopollenites variabilis</i>
<i>Striadiporites sanctae-barbarae</i>	<i>Momipites rotundus</i>
<i>Inapertisporites vittatus</i>	cf. <i>Carya veripites</i>
<i>I. elongatus</i>	
	<u>Fern Spores</u>
	<i>Deltoidospora diaphana</i>
	<i>Anemia poolensis</i>
	<i>Osmunda irregulites</i>
	<i>Bullasporis</i> sp.

Table 2. Palynomorphs from Tumbo Island, British Columbia. Sample localities are shown in Figure 2B.

<u>Fungal Spores</u>	<u>Angiosperm Pollen</u>
<i>Multicellaesporites pandus</i>	<i>Paraalnipollenites alterniporus</i>
<i>M. "giganteus"</i>	<i>Pachysandra</i> sp.
<i>Brachysporisporites cotalis</i>	<i>Liliacidites</i> sp.
<i>B. catinus</i>	
<i>Callimothallus pertusus</i>	<u>Fern Spores</u>
<i>Staphlosporites allomorphus</i>	<i>Anemia poolensis</i>
<i>Inapertisporites elongatus</i>	<i>Osmunda irregulites</i>
<i>Dicellaesporites punctatus</i>	<i>Laevigatosporites discordatus</i>
" <i>Circulosporites</i> " sp.	<i>L. albertensis</i>
	Polypodiaceae - forma 1.
<u>Conifer Spores</u>	<i>Bullasporis</i> sp.
<i>Picea grandivescipites</i>	<i>Cicatricosisporites intersectus</i>
<i>Pinus haploxylon</i> -type	<i>Azolla</i> sp. - massula
<i>P. diploxylon</i> -type	
	<u>Algal Cysts</u>
	<i>Michrystridium</i> sp.
	<i>Schizosporis texus</i>
	<i>Lejeunia hyalina</i>

DISCUSSION

The occurrence of Paleocene beds on the Sucia chain and Tumbo Island provides a key link in reconstruction of the extent and depositional environment of the early Tertiary Georgia Basin. Terrestrial Paleocene strata are now documented from Lasqueti Island in the north, English Bay in Vancouver, probably in outcrops near Haney in the Fraser Valley (Rouse, unpublished data) and in the southeast from the lowest Chuckanut Formation in the Samish Bay – Lake Samish areas of Washington State.

The presence of terrestrial Paleocene rocks on Tumbo and Sucia islands provides further evidence that the initial (Paleocene-early Eocene) Tertiary Georgia Basin was entirely continental (first suggested by Johnson, 1982 with respect to the Chuckanut Formation). There is no evidence for a marine component to the basin. The late Paleocene sandstone and conglomerate described from Lasqueti Island are terrestrial and appear to have been deposited near a northern margin of the basin, with paleocurrents suggesting southerly flow (Mustard and Rouse, 1991; Mustard, unpublished data). The late Paleocene-early Eocene part of the Chuckanut Formation on the Washington State mainland is composed entirely of terrestrial fluvial and lower alluvial fan facies with paleocurrents demonstrating west or southwest flow from the eastern margin of the basin (the Bellingham Bay Member of Johnson, 1982, 1984). The terrestrial fluvial facies of Tumbo Island and the Sucia chain demonstrate a strong component of east or southeast flow. The immature and conglomeratic nature of the lithofacies and the abundance of conglomerate clasts of probable local derivation suggest these rocks were deposited close to the western margin of the basin in this area. Thus on at least three sides the basin appears to have been intracontinental with separation of only a few tens of kilometres between these areas. There is no constraint on the southern margin to the Tertiary Georgia Basin.

The possibility that Tertiary Georgia Basin was entirely continental during at least Paleocene and early Eocene time has several implications for hydrocarbon exploration. A lack of marine organic matter (alginite and exinite, the Type I and II kerogens of many source rock classifications, e.g., Tissot and Welte, 1984) reduces the likelihood of significant oil generation, even if optimal thermal maturity was reached and migration into the abundant fluvial sandstone reservoirs had occurred. Thus hydrocarbons in the Tertiary Georgia Basin are likely to be gas derived from terrestrial organic matter (mostly Type III kerogen). Coupled with the low thermal maturity reported from well data (Bustin, 1990; Mustard and Rouse, 1991) the hydrocarbon potential of Tertiary Georgia Basin appears to be low.

ACKNOWLEDGMENTS

We thank Bertrand Groulx who provided cheerful and competent field assistance, and Jane Broatch for very able lab processing and editorial assistance. Permission to examine the geology of the Washington State part of Georgia Basin was kindly given by the Washington State Department of Natural Resources, Division of Geology and Earth Resources. Bill Lingley, Pat Pringle and Tim Walsh of this division are specifically thanked for their help and for useful discussions on Chuckanut Formation geology, as is Sam Johnson (U.S.G.S., Denver). Research in the Sucia Island Marine State Park was conducted under the terms of a research permit granted by the Washington State Parks and Recreation Commission. David W. Heiser of this agency is thanked for facilitating the granting of this permit. Research on Tumbo Island was done with the generous permission of the owner, Mr. Richard Hojohn.

REFERENCES

- Blunden, R.H.**
1971: Vancouver's downtown (coal) peninsula urban geology; B.Sc. thesis, University of British Columbia, Vancouver, 45 p.
- Brandon, M.T., Cowan, D.S., and Vance, J.A.**
1988: The Late Cretaceous San Juan thrust system, San Juan Islands, Washington; Geological Society of America, Special Paper 221, 81 p.
- Bustin, R.M.**
1990: Stratigraphy, sedimentology, and petroleum source rock potential of the Georgia Basin, southwest British Columbia and northwest Washington State; in Current Research, Part F, Geological Survey of Canada, Paper 90-1F, p. 103-108.
- Curray, J.R.**
1956: The analysis of two-dimensional orientation data; Journal of Geology, v. 64, p. 117-131.
- England, T.D.J.**
1990: Late Cretaceous to Paleogene evolution of the Georgia Basin, southwestern British Columbia; Ph.D. thesis, Memorial University of Newfoundland, St. John's, 481 p.
- England, T.D.J. and Calon, T.J.**
1991: The Cowichan fold and thrust system, Vancouver Island, southwestern British Columbia; Geological Society of America Bulletin, v. 103, p. 336-362.
- England, T.D.J. and Hiscott, R.N.**
1991: Upper Nanaimo Group and younger strata, outer Gulf Islands, southwestern British Columbia; in Current Research, Part E, Geological Survey of Canada, Paper 91-1E, p. 117-125.
- England, T.D.J. and Hiscott, R.N. (cont.)**
in press: Lithostratigraphy and sedimentology of the upper Nanaimo Group (Upper Cretaceous) and possible Paleogene sedimentary rocks, outer Gulf Islands, southwestern British Columbia; Canadian Journal of Earth Sciences.
- Hopkins, W.S.**
1968: Subsurface Miocene rocks, British Columbia-Washington; Geological Society of America, Bulletin, v. 79, p. 763-768.
- Janbaz, J.E. Jr.**
1972: Petrology of the Upper Cretaceous strata of Sucia Island, San Juan County, Washington; M.Sc. thesis, Washington State University, Pullman, 104 p.
- Johnson, S.Y.**
1982: Stratigraphy, sedimentology, and tectonic setting of the Eocene Chuckanut Formation, Northwest Washington; Ph.D. thesis, University of Washington, Seattle, 222 p.
1984: Stratigraphy, age, and paleogeography of the Eocene Chuckanut formation, northwest Washington; Canadian Journal of Earth Sciences, v. 21, p. 92-106.
- Journeay, J.M.**
1990: A progress report on the structural and tectonic framework of the southern Coast Belt, British Columbia; in Current Research, Part E, Geological Survey of Canada, Paper 90-1E, p. 183-195.
- Kerr, S.A.**
1942: The Tertiary sediments of Sumas Mountain; M.A. thesis, University of British Columbia, Vancouver, 48 p.
- Krause, R.G.F. and Geijer, T.A.M.**
1987: An improved method for calculating the standard deviation and variance of paleocurrent data; Journal of Sedimentary Petrology, v. 57, p. 779-780.
- Miller, G.M. and Misch, P.**
1963: Early Eocene angular unconformity at western front of northern Cascades; American Association of Petroleum Geologists Bulletin, v. 47, p. 163-194.
- Monger, J.W.H.**
1990: Georgia Basin: regional setting and adjacent Coast Mountains geology, British Columbia; in Current Research, Part F, Geological Survey of Canada, Paper 90-1F, p. 95-102.
- Muller, J.E.**
1980: Geology of Victoria (1:100 000); Geological Survey of Canada, Map 1553A.
- Muller, J.E. and Jeletzky, J.A.**
1970: Geology of the upper Cretaceous Nanaimo Group, Vancouver Island and Gulf Islands, British Columbia; Geological Survey of Canada, Paper 69-25, 77 p.
- Mustard, P.S. and Rouse, G.E.**
1991: Sedimentary outliers of the eastern Georgia Basin margin, British Columbia; in Current Research, Part A, Geological Survey of Canada, Paper 91-1A, p. 229-240.
- Nemec, W.**
1988: The shape of the rose; Sedimentary Geology, v. 59, p. 149-152.
- Pacht, J.A.**
1980: Sedimentology and petrology of the Late Cretaceous Nanaimo Group in the Nanaimo Basin, Washington and British Columbia: implications for Late Cretaceous tectonics; Ph.D. thesis, Ohio State University, Columbus, 368 p.
1984: Petrologic evolution and paleogeography of the Late Cretaceous Nanaimo Basin, Washington and British Columbia: implications for Cretaceous tectonics; Geological Society of America Bulletin, v. 95, p. 766-778.
- Rouse, G.E.**
1977: Paleogene palynomorph ranges in western and northern Canada; in Contributions of Stratigraphic Palynology, Vol. 1, Cenozoic Palynology; American Association of Stratigraphic Palynologists, Contribution Series 5A, p. 48-65.
- Rouse, G.E., Lesack, K.A., and White, J.M.**
1990: Palynology of Cretaceous and Tertiary strata of Georgia Basin, southwestern British Columbia; in Current Research, Part F, Geological Survey of Canada, Paper 90-1F, p. 109-113.
- Rouse, G.E., Mathews, W.H., and Blunden, R.H.**
1975: The Lions Gate Member: a new late Cretaceous sedimentary subdivision in the Vancouver area of British Columbia; Canadian Journal of Earth Sciences, v. 12, p. 464-471.

Rust, B.R. and Koster, E.H.

1984: Coarse alluvial deposits; in *Facies Models*, (ed.) R.G. Walker; Geoscience Canada, Reprint Series 1, p. 53-70.

Srivastava, S.K.

1972: Some spores and pollen from the Paleocene Oak Hill Member of the Naheola Formation, Alabama (U.S.A.); *Reviews of Paleobotany and Palynology*, v. 14, p. 217-285.

Sturdavant, C.D.

1975: Sedimentary environments and structure of the Cretaceous rocks of Satuma and Tumbo Islands, British Columbia; M.Sc. thesis, Oregon State University, Corvallis, 195 p.

Tissot, B.P. and Welte, D.H.

1984: *Petroleum Formation and Occurrence*, 2nd Edition; Springer-Verlag, New York, 699 p.

Ward, P.D.

1973: Stratigraphy of Upper Cretaceous rocks on Orcas, Waldron, and Sucia Islands; M.Sc. thesis, University of Washington, Seattle.

1976: Stratigraphy, paleoecology and functional morphology of heteromorph ammonites of the Upper Cretaceous Nanaimo Group, British Columbia and Washington; Ph.D. thesis, McMaster University, Hamilton, 189 p.

1978: Revisions to the stratigraphy and biochronology of the Upper Cretaceous Nanaimo Group, British Columbia and Washington State; *Canadian Journal of Earth Science*, v. 15, p. 405-423.

Geological Survey of Canada Project 890038

Further reconnaissance observations in the Pine Pass southwest map area, British Columbia

L.C. Struik
Cordilleran Division, Vancouver

Struik, L.C., 1992: Further reconnaissance observations in the Pine Pass southwest map area, British Columbia; in Current Research, Part A; Geological Survey of Canada, Paper 92-1A, p. 25-31.

Abstract

Lower Cambrian quartzite and Cambrian carbonate typical of the Rocky Mountains to the east underlie the low ridges north of Nation River. Basalt and sedimentary rocks previously mapped as upper Paleozoic may be entirely Triassic and part of the Takla Group. Sequences of calcsilicate and marble have been mapped in the predominantly orthogneiss and quartzofeldspathic paragneiss of the Wolverine Metamorphic Complex.

Résumé

Le quartzite du Cambrien inférieur et le carbonate cambrien, typiques des montagnes Rocheuses à l'est, reposent au-dessous des crêtes de bas niveaux situées au nord de la rivière Nation. Les roches basaltiques et sédimentaires antérieurement cartographiées comme des roches du Paléozoïque supérieur pourraient être entièrement triasiques et faire partie du groupe de Takla. Les séquences de silicates calciques et de marbre ont été cartographiées dans l'orthogneiss et le paragneiss quartzo-feldspathique dominants du complexe métamorphique de Wolverine.

INTRODUCTION

This report elaborates on last year's preliminary reports of geological mapping in southwestern Pine Pass map area (93O/SW, west of the Northern Rocky Mountain Trench and south of Williston Lake, Figure 1; Struik and Northcote, 1991; Northcote, 1991). The mapping has focused on increasing the detail of the previous Geological Survey of Canada 1:250 000 geology map (Muller, 1961), and particularly on understanding the regional context of the geology. The area is of interest for its mineral potential, and for its regional tectonic significance. Triassic-Jurassic basalt and plutons of the Takla Group host the Mount Milligan copper-gold camp at the western border of the map area and those same rocks occupy much of Pine Pass southwest map area. A wide zone of dextral strike-slip faults transects the area, and includes a high-grade metamorphic complex (Fig. 1).

Rocks and structures of Pine Pass southwest map area can be divided into two domains separated by the McLeod Lake Fault (Fig. 2, 3). East of the fault the rock consists of Precambrian shelf clastics and Paleozoic platform carbonates. West of the fault, the rock consists of off-shelf

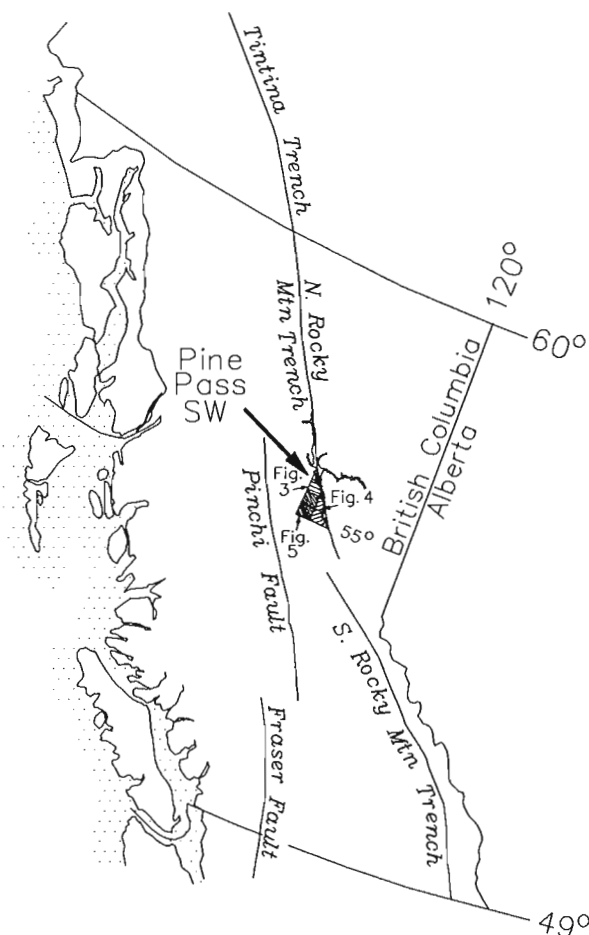


Figure 1. Location of Pine Pass southwest map area in British Columbia.

clastics and volcanics, and mafic intrusions. Folds and thrusts dominate the structures east of the McLeod Lake Fault, and dextral strike-slip and extension faults dominate the structures southwest of the fault. The strike-slip and extension faults are superimposed on older folds and thrusts (Fig. 3, 4, 5).

EAST OF MCLEOD LAKE FAULT

Most of the rock characteristic of the Rocky Mountains lies along a narrow zone between Williston Lake and the McLeod Lake Fault. Most of the exposure of these Precambrian and Cambrian sedimentary rocks is at Mt. Chingee (described by Struik and Northcote, 1991), and immediately north of the Nation River (units A, B, and C of Fig. 2, 3, 4). The Nation River locality consists of muddy dark grey quartzite like that of the late Precambrian, orthoquartzite typical of the Early Cambrian, and limestone and silty limestone characteristic of the Cambrian (see McMechan, 1985 for detailed descriptions of these rocks from the east side of Williston Lake). Fossil sponges have been sampled from limestone localities near the orthoquartzite sequence. The sequence outlines several broad asymmetric folds and is cut by northwest trending shear zones. Along Williston Lake the orthoquartzite is permeated with shear zones.

WEST OF MCLEOD LAKE FAULT

West of the McLeod Lake Fault, the rocks can be described as three assemblages: probable Cambrian through middle Paleozoic clastics and minor basalt, Triassic and Lower Jurassic island arc volcanics and clastics of the Takla Group, and Mesozoic and Tertiary granitic and metamorphic rocks of the Wolverine Complex (Fig. 2, 3, 4, 5). Struik and Northcote (1991) have outlined the units of these three assemblages. Some additions and changes to that outline will be made here for the Takla Group and Wolverine Complex.

Takla Group

The Takla Group is exposed throughout the southern and western parts of the map area. It includes rocks assigned by Struik and Northcote (1991) to the upper Paleozoic Philip Creek succession. The age of the Philip Creek succession is still uncertain, however some conodont fragments from limestone in the succession may be Triassic (M.J. Orchard, pers. comm., 1991). Takla Group can be divided into 4 successions and a pyroxenite body (unit N, Fig. 2). The successions are the Tabor Mountain of mainly sedimentary rocks (unit L, Fig. 2), the Philip Creek of volcanoclastics (unit K, Fig. 2) and limestone (unit J, Fig. 2), unnamed basalt agglomerate and tuff (unit M, Fig. 2), and unnamed maroon basalt (unit O, Fig. 2).

Tabor Mountain succession (L) consists of basalt-derived greywacke, siltite, argillite, slate, phyllite and dark grey limestone. Reference sections for these rocks are exposed along McLeod River below Warhorse Lake south of Pine Pass map area (Struik, 1989), and at Tabor Mountain east of Prince George.

Philip Creek succession (K) consists of mainly volcanoclastic basalt, limestone and basalt tuff, with minor diorite and gabbro intrusions. The coarse-grained basalt consists of augite-porphry breccia and agglomerate fragments in a pyroxene-plagioclase sand. Volcanoclastic rock consists of pyroxene-plagioclase greywacke and minor dark grey siltite, argillite, and conglomerate. Laterally the volcanoclastics grade into pyroclastic debris flows. Bedding styles range from graded laminates to thick (1 m) beds stacked in bundles up to 10 m thick. Local synsedimentary slump features are rare.

Basalt tuff of the succession, varies from cherty to coarse grained. Black and olive cherty tuff beds are thin (0.5-4 cm) and mostly separated by films of phyllite or slate. Lapilli tuff beds range from thin to thick. They locally have lenses with a brown weathering calcareous matrix. The fragmental basalt is intruded by diorite sills and dykes throughout the map area.

Microporphyrific diorite intrudes pyroclastic basalt, black siliceous argillite and micaceous quartzite. Locally, it is foliated, like parts of the Scovil diorite (Northcote, 1991), but mostly it is undeformed. It consists of primary plagioclase (50-70%), pyroxene and hornblende, and secondary hornblende, actinolite, epidote, chlorite and calcite. Although included with the Takla Group the diorite may actually be part of the Scovil diorite suite.

The limestone (J) is grey, weathers light grey and can have abundant poorly preserved macrofossils, mostly crinoid ossicles. North of Philip Lakes it is gradational with pyroxene-plagioclase sand and silt, where they are interbedded on a 2-5 cm scale. Generally the limestone is massive and featureless; this is probably due to tectonism and recrystallization. South of the Nation River the limestone unit is involved in several regional open folds.

The basalt agglomerate and tuff unit (M) has all the characteristics of the Chuchi Lake Formation as described by Nelson et al. (1991) for the area around the Mount Milligan copper-gold deposit to the west.

Maroon and red basalt agglomerate and breccia (O) near Munro Lake consists of augite porphyry and feldspar porphyry fragments in 20-80% matrix of augite-feldspar tuff. Laterally the red basalt is mixed with olive and dark-grey basalt agglomerate and breccia. Augite phenocrysts occupy 3-20% of the fragments and range in size from 1-10 mm. Feldspar phenocrysts occupy up to 25% of the fragments and range in size from 0.5-35 mm; the larger crystals show zoning.

Wolverine Metamorphic Complex

Metamorphic rocks of the Wolverine Complex generally are quartzofeldspathic gneiss, amphibolite, calcsilicate, granite pegmatite, granodiorite, schist, marble and minor quartzite at

WEST OF MCLEOD LAKE FAULT

TERTIARY

V basalt

U biotite granite

LIGNITE PLUTON

T biotite granite

CRETACEOUS AND TERTIARY

WOLVERINE COMPLEX (P-S)

S granite pegmatite

R foliated granodiorite

Q quartzofeldspathic gneiss, schist, granite pegmatite

P amphibolite, calcsilicate, marble, paragneiss, schist

TRIASSIC AND LOWER JURASSIC

TAKLA GROUP (J-O)

O red fragmental basalt

N pyroxenite

M fragmental augite porphyry basalt, limestone

Tabor Mtn succession

L phyllite, greywacke, limestone

Philip Ck succession (J-K)

K volcanoclastic basalt, diorite

J limestone

CARBONIFEROUS OR PERMIAN

H diorite

G Scovil Diorite

ORDOVICIAN(?) TO

LOWER CARBONIFEROUS

EARN GROUP AND (?)

ROAD RIVER GROUPS (E-F)

F micaceous quartzite, tuff, phyllite, marble

E siltite, phyllite, conglomerate quartzite, limestone, basalt

LOWER CAMBRIAN

ATAN GROUP

D quartzite, limestone, marble

EAST OF MCLEOD LAKE FAULT

CAMBRIAN

KECHIKA GROUP AND

SKOKI FORMATION

C limestone, dolostone, phyllite

LOWER CAMBRIAN

GOG GROUP

B Bq: quartzite, slate, siltstone

BI: limestone, dolostone

PRECAMBRIAN

MISINCHINKA GROUP

A quartzite, slate, siltstone conglomerate

Legend

- Contacts (approx. & assum.) ———
- Faults (approx. & assum.) ———
- Anticline, asymmetric to hook ———
- Syncline, asymmetric to hook ———

Figure 2. Legend for the preliminary geology maps of Pine Pass southwest map area of Figures 3, 4 and 5.



Figure 3. Geology of parts of the 93O/12, and 93O/11 map areas at approximately 1:250 000 scale (see Figure 2 for the legend).

sillimanite grade metamorphism. Locally, amphibolite, grit, schist and marble have staurolite-kyanite assemblages. Foliated granodiorite and granite intrude and are deformed with the paragneiss. Cursory descriptions of these rocks are given by Struik and Northcote (1991).

Calcsilicate and marble units have been mapped near Mount Bisson (Fig. 3) during the 1991 field season. They are separated by granodiorite orthogneiss, leucocratic biotite granite and minor paragneiss and orthoquartzite.

STRUCTURAL GEOLOGY

The structural style described for Pine Pass southwest map area by Struik and Northcote (1991) contains most of the elements seen during the 1991 field season. These elements include regional northwest and north-northwest trending dextral strike-slip faults, northeast and east-northeast trending extension faults, and isoclinal to open folds that affect all the sedimentary, volcanic and metamorphic rocks and many of the plutonic rocks of the area.

The Takla Group and parts of the Earn, Road River and Atan groups are separated from the Wolverine Metamorphic Complex across shallowly dipping extension faults and steeply dipping strike-slip faults (Struik and Northcote, 1991). The extension fault zones are manifest in the sedimentary rocks by semi-ductile and some brittle shear fabric, and in the metamorphic rocks by ductile shear zones hundreds of metres thick. The extension fabric in the sedimentary and metamorphic rocks is superimposed on regional and outcrop scale folds, and on metamorphic minerals such as chlorite, biotite, garnet, and kyanite. Sillimanite and kyanite appear to have grown before and possibly during the crustal extension.

DISCUSSION

Struik and Northcote (1991) speculated that the Philip Creek succession of fragmental basalt, diorite sills and dykes, and limestone may be upper Paleozoic and represent an eastern continental margin rift facies equivalent to a western marginal basin rift floor facies of the Slide Mountain Group. Three limestone samples from unit J (Fig. 2) have yielded a

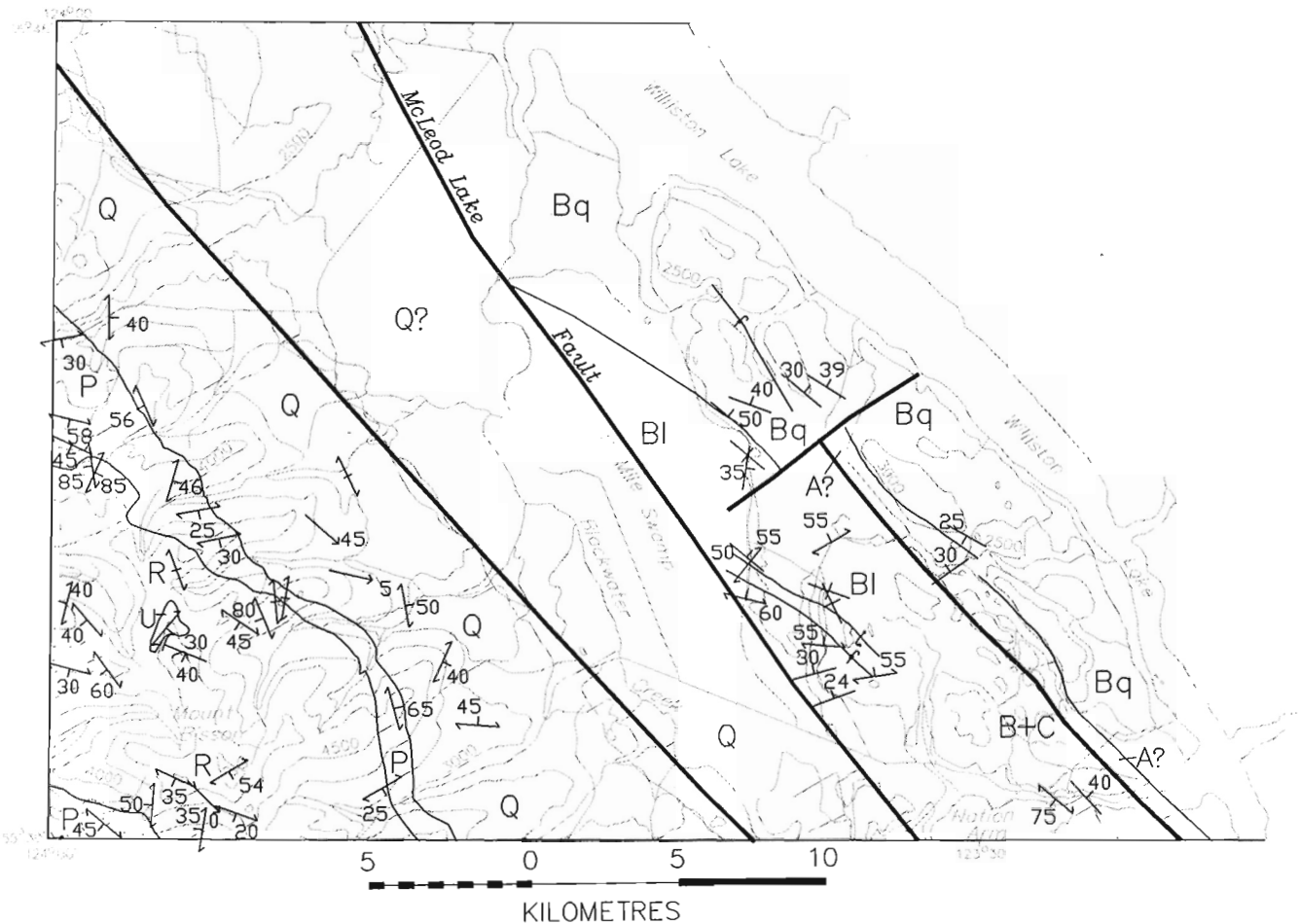


Figure 4. Geology of the 930/3 and parts of the 930/2 map areas at approximately 1:250 000 scale (see Figure 2 for the legend).

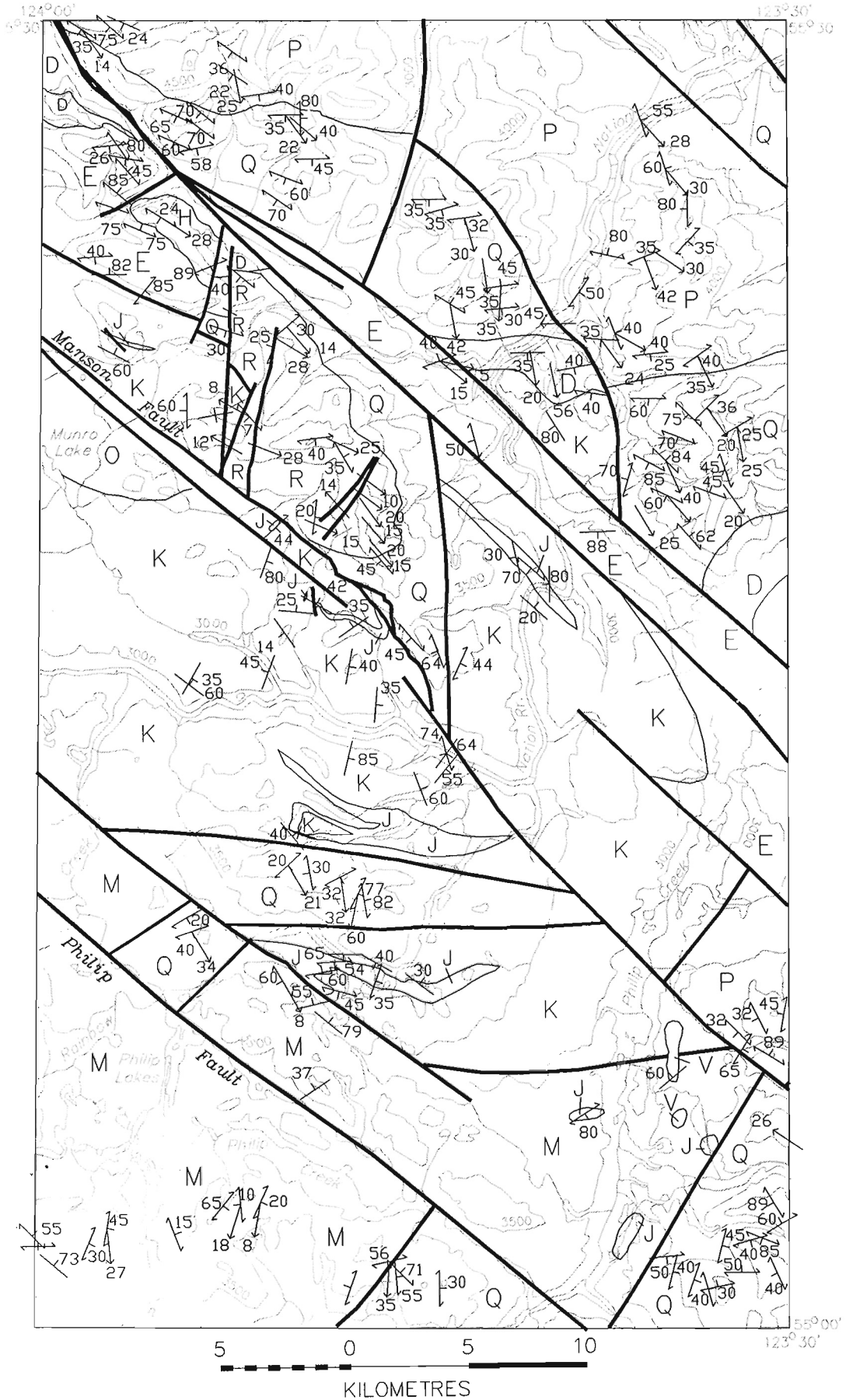


Figure 5. Geology of the 93O/5 and 93O/4 map areas at approximately 1:250 000 scale (see Figure 2 for the legend).

single conodont fragment each and each of these may be Triassic (M.J. Orchard, pers. comm., 1991). It is conceivable that the Philip Creek succession with its dominance of volcanoclastic and transitional pyroclastic basalt, and its limestone may be a facies of the Triassic Takla Group island arc suite. If so, Slide Mountain Group or any other upper Paleozoic oceanic facies is absent in Pine Pass map area, contrary to Muller (1961) and Struik and Northcote (1991).

REFERENCES

McMechan, M.E.

1985: Stratigraphy and structure, Mount Selwyn map area, Rocky Mountains, northeastern British Columbia; Geological Survey of Canada, Paper 85-28.

Muller, J.E.

1961: Geology, Pine Pass, British Columbia; Geological Survey of Canada, Map 11-1961.

Nelson, J., Bellfontaine, K., Green, K., and MacLean, M.

1991: Regional geological mapping near the Mount Milligan Copper-gold deposit (93K/16, 93N/1); in Geological Fieldwork 1990, British Columbia Ministry of Energy, Mines and Petroleum Resources, Paper 1991-1, p. 89-110.

Northcote, B.K.

1991: Petrography and tectonics of the Scovil diorite, southwest Pine Pass map area, British Columbia; in Current Research, Part A; Geological Survey of Canada, Paper 91-1A, p. 241-244.

Struik, L.C.

1989: Regional geology of the McLeod Lake map area, British Columbia; in Current Research, Part E; Geological Survey of Canada, Paper 89-1E, p. 109-114.

Struik, L.C. and Northcote, B.K.

1991: Pine Pass map area, southwest of the Northern Rocky Mountain Trench, British Columbia; in Current Research, Part A; Geological Survey of Canada, Paper 91-1A, p. 285-291.

Geological Survey of Canada Project 870060

A recent eruptive history of Volcano Mountain, Yukon Territory

Lionel E. Jackson, Jr. and Wayne Stevens¹
Terrain Sciences, Vancouver

Jackson, L.E., Jr. and Stevens, W., 1992: A recent eruptive history of Volcano Mountain, Yukon Territory; in Current Research, Part A; Geological Survey of Canada, Paper 92-1A, p. 33-39.

Abstract

The most recent eruptions of Volcano Mountain are no younger than mid-Holocene and could be early Holocene or older. The latest events erupted lava flows and pyroclastic ejecta from a central crater and lava flows from breakouts low on the flanks of the mountain. These were accompanied by collapse of the crater rim on the east and west sides of the mountain.

Résumé

Les plus récentes éruptions du mont Volcano datent tout au plus du milieu de l'Holocène et pourraient même remonter au début de l'Holocène ou même plus tôt. Lors des dernières éruptions, les coulées de lave et les projections volcaniques provenaient d'un cratère central et des laves s'épanchaient également de fissures sur les flancs de la montagne. L'effondrement du bord du cratère a accompagné ces phénomènes sur les côtés est et ouest de la montagne.

¹ Department of Geography, University of Victoria, Victoria, British Columbia

INTRODUCTION

Volcano Mountain¹ is a sparsely vegetated cinder cone 17 km north of the confluence of Yukon and Pelly rivers in central Yukon (Fig. 1 and 2). It is the youngest eruptive centre within the Selkirk volcanics, a complex of valley-filling basalts and hyaloclastites ranging in composition between alkaline olivine basalt, olivine nephelinite, and basanite (Francis and Ludden, 1990). These were erupted predominantly during the early Pleistocene or late Pliocene partly beneath glacial ice during one of the pre-Reid glaciations (Francis and Ludden, 1990; Jackson et al., 1990). The apparent freshness of the cinder cone and largely unvegetated basalt flows within the crater and along the south flank have suggested to geologists since the late 19th Century that its last eruptions may have been geologically recent. An investigation aimed

at establishing an eruptive history of the mountain was carried out during the 1989 field season. This report describes the results of this investigation.

SETTING

Volcano Mountain rises to 1239 m and has a relief of up to 540 m above the surrounding valley bottoms (Fig. 2-4). The uppermost 210 m of the mountain is a cinder cone sparsely vegetated by grasses, low herbaceous plants, lichens, and scattered, stunted trees. It is cut from northeast to southwest by a V-shaped notch which bisects the crater. The walls of the crater are marked by scarps and scars created by landsliding of the crater walls. The crater is floored by a sparsely vegetated lava flow which is broken into a jumble of pinnacles and trenches (Fig. 5). The walls of the crater are

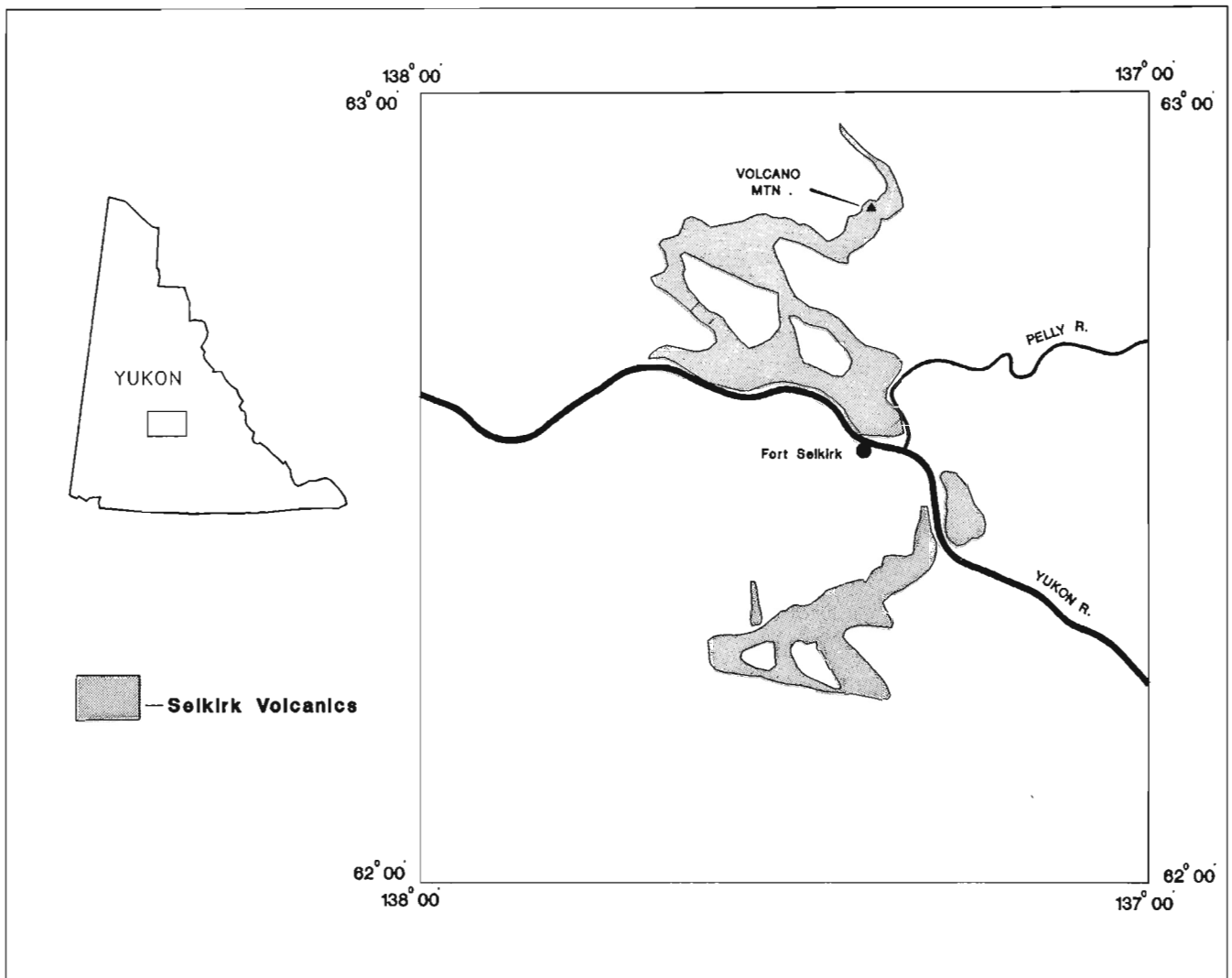


Figure 1. Location of Volcano Mountain and the Selkirk Volcanics (stipple pattern).

¹ The aboriginal (Northern Tutchone) name for Volcano Mountain, according to Harry Baum, an elder of the Selkirk First Nation interviewed in 1988, is Nelruna. This was transcribed into phonetic spelling by Ruth Gotthardt.

locally continuously vegetated by spruce and dwarf birch. Lava flows erupted from the summits and flanks extend down the valley of Grand Valley Creek to the north and into the Black Creek drainage basin to the south. The composition of the cone and flows is olivine nephelinite (Francis and Ludden, 1990).

Immediately to the west is a low and rounded hill with scattered exposures of stratified and gently dipping basaltic lava flows and ash beds. This feature appears to be the erosional remnant of an older volcano which preceded Volcano Mountain (Fig. 3, AVM).

Exclusive of the cone, crater lava flow, and breakout flows on the southwest flank of the mountain (Fig. 3, PV, 2N and 2Sa and 2Sb, respectively), the massif is heavily forested or is mantled by a thick turfy mat of moss and foliose lichen with a dwarf birch overstory. Although dendrochronological sampling and study dated the oldest tree growing on the crater lava flow (Fig. 3 and 4, 2N) at approximately 300 a, the flow substantially predates this vegetative cover as it becomes partly forested and covered by moss and foliose lichen turfy mat where it exits the northeast side of the crater and continues down the northeast side of the mountain. The flows on the southwest flank of the mountain have a thin and discontinuous covering of crustose and foliose lichens, low herbaceous woody plants, and scattered spruce and pine trees.

PREVIOUS WORK

The first reference to what is now known as Volcano Mountain was by Hayes (1892) who noted, during his traverse of upper Yukon River and Saint Elias Mountains, the existence of a "symmetrical cone" ten miles north of Fort Selkirk (p. 150). McConnell (1903) climbed the mountain and described the most recent lava flow within the main crater and remarked at the freshness of the basalt and cinder cone. Bostock (1936) further described the geomorphology of Volcano Mountain and its recent lava flows. He also introduced the name "Selkirk volcanics" for all the fresh

volcanics in the Fort Selkirk area. Tempelman-Kluit (1984) remapped the geology of the Carmacks map area and subdivided lava flows from Volcano Mountain by relative age. Francis and Ludden (1990) investigated the petrology and magmatic evolution of the Selkirk volcanics and further defined the limits of this formation.

LATEST ERUPTIONS

The most recent eruptions of Volcano Mountain have been characterized by pyroclastic eruptions and lava flows from the main crater, lava flows issuing from breakouts along the west and east sides and lava flows from a small satellite crater on the south margin of the summit (Fig. 3 and 4).

Crater and northeast breakout eruptions

The most recent lava flows and ejecta on the northeast margin of Volcano Mountain were erupted from breakouts low on the flank of the mountain and the central crater during at least two separate eruptions. The period of time separating these eruptions is not known. Initially, lava flowed 8 km down the valley of Grand Valley Creek (Fig. 3 and 4, 1N). This is the most extensive identifiable flow from Volcano Mountain. Assuming a minimal average thickness of 4 m, it represents at least $1 \times 10^7 \text{ m}^3$. It is not clear whether this flow was erupted as a breakout or from the central crater because the flow is buried by a complex of younger basalt flows and blocks of former crater wall near the base of the mountain. The crater fragments flowed into place when the northeast crater rim collapsed and remnants were rafted along in a combination landslide and lava flow (Fig. 3 and 4, NLS). Assuming that the unfailed cone had a regular surface, this failure involved approximately $1.5 \times 10^7 \text{ m}^3$ of cone rim. Dimensions of individual blocks of the former crater rim reach the size of small apartment buildings. Collapse of the crater rim was followed by the eruption of at least $1.2 \times 10^6 \text{ m}^3$ of lava from the central crater (Fig. 3 and 4, 2N) which flowed 2.5 km down the east side of the mountain and partly buried the

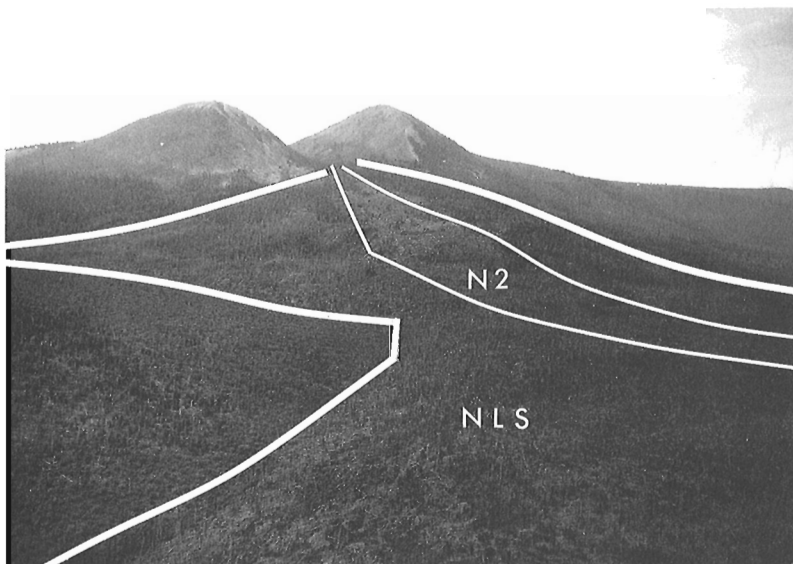


Figure 2. The northeast face of Volcano Mountain. The V-shaped cleft marks the source of the large combined landslide and lava flow (NLS).

collapsed crater rim debris. When this last eruption terminated, magma drained from beneath a solidified crust within the crater causing it to collapse into a jumble of pinnacles and trenches previously noted (Fig. 5). At some point during these eruptions, a lapilli blanket was erupted over the valley of Grand Valley Creek and likely over a large adjacent area. In the area of Caitlin Pond (Fig. 3, CP, and 4), the blanket is locally more than 0.5 m thick; permafrost within the blanket prevented excavation to its base.

Latest eruptions along the southwest margin of Volcano Mountain

A succession of lava flows have issued from breakouts along the western base of Volcano Mountain and the small satellite crater at its southern margin. The contrasting density of forest cover or lack of forest cover on these flows suggests that they represent two or three distinct eruptions although the period of time separating them is unknown. The two most

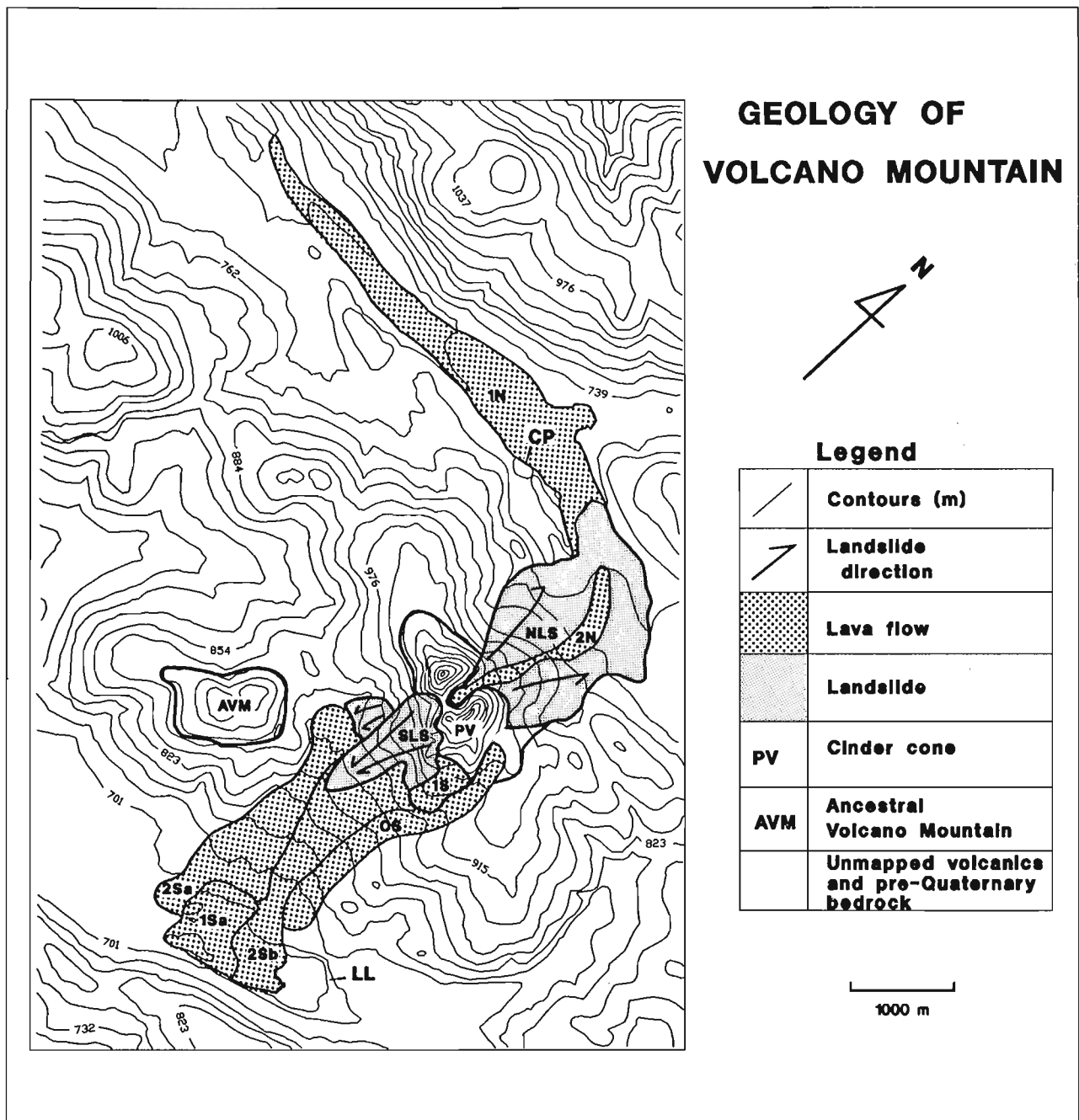


Figure 3. Volcano Mountain, most recent identifiable lava flows, and related volcanics. On the southwest side, lava flows decrease in age in the series OS, 1S, 2Sa, 2Sb. The latter two are probably of the same age. On the north side, 1N predates 2N. PV denotes the largely unvegetated cinder cone. AVM denotes the remains of a volcano which was ancestral to Volcano Mountain.

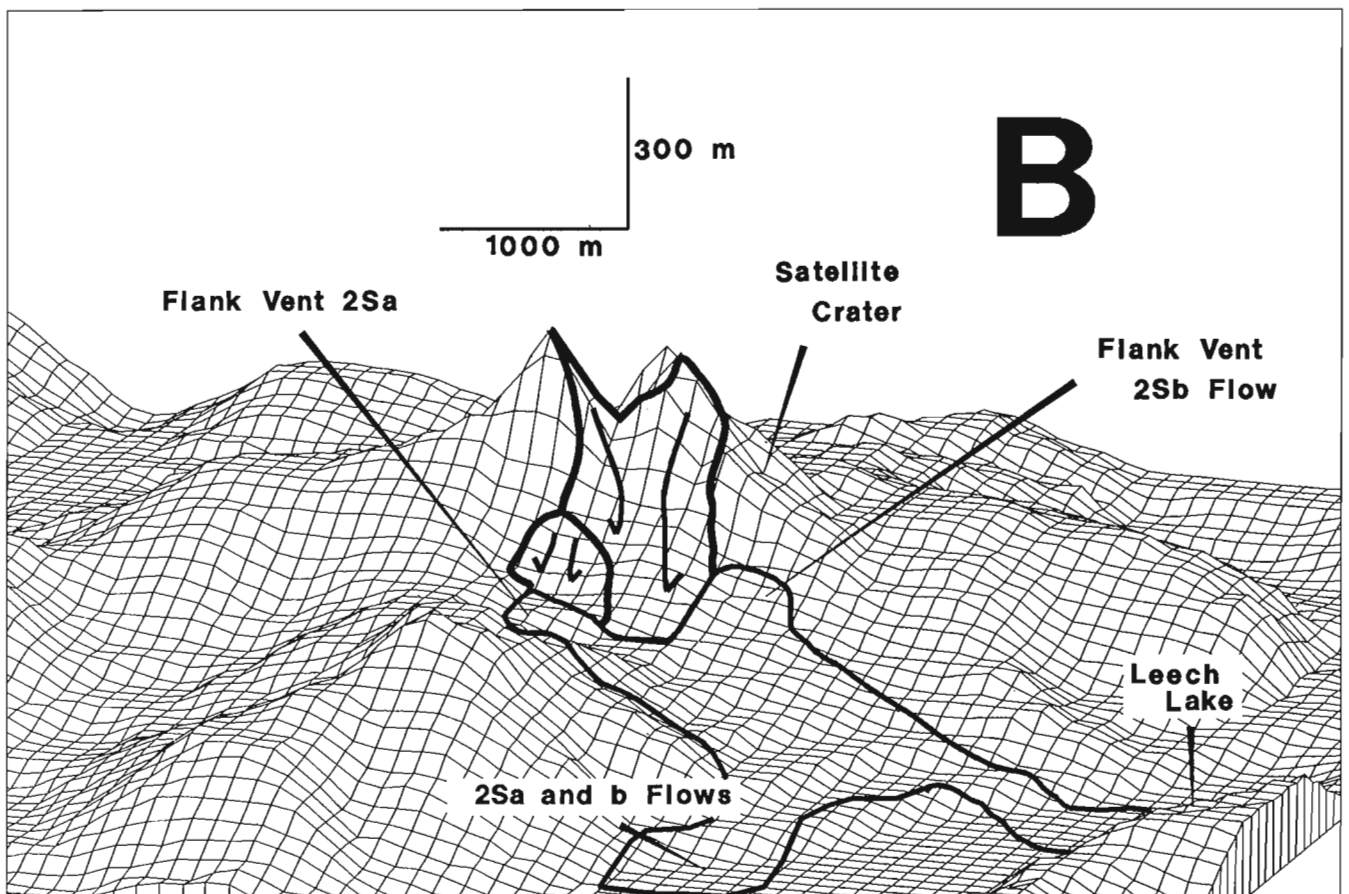
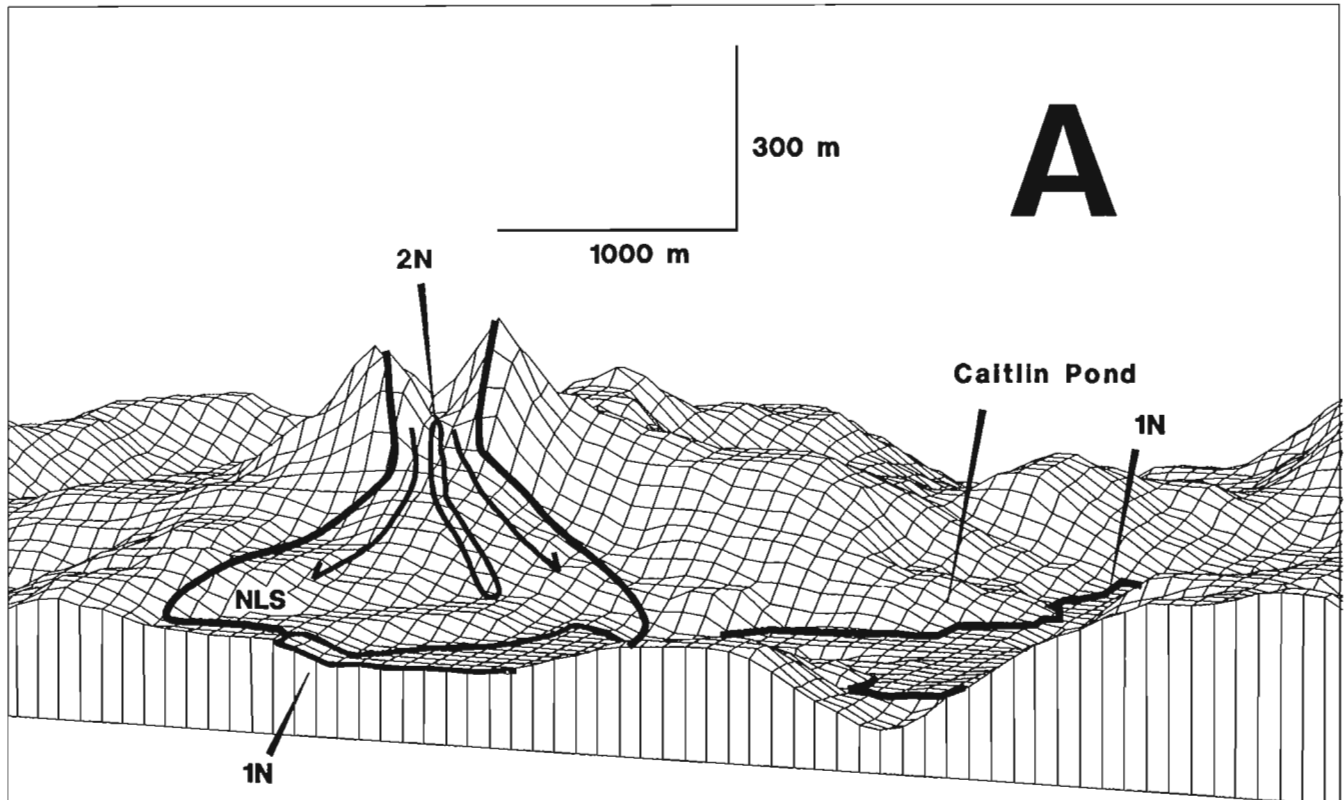


Figure 4. Computer-generated perspective views of Volcano Mountain from the northeast (A) and southwest (B), showing most recent lava flows NLS, 2Sa and 2Sb, 1N, 2N, eruptive vents and related landslides triggered by eruptions.

recent flows (Fig. 3 and 4, 2Sa and 2Sb) extend 3 km from the base of the mountain and a conservative estimate of their volume, assuming a average thickness of 3 m is approximately $8 \times 10^6 \text{ m}^3$. They partly bury older flows 1S and 0S (Fig. 3 and 4). The breakout of 2Sa and 2Sb was combined with and may have triggered the landsliding that removed the eastern margin of the crater rim (SLS, Fig. 3 and 4). This failure, along with the collapse of the eastern margin of the crater rim, produced the contemporary V-notched profile of the mountain (Fig. 2). A conservative estimate of the volume of this failure, assuming a regular surface on the unfailed cone, is $7 \times 10^6 \text{ m}^3$.

RELATIVE AND LIMITING AGES OF THE MOST RECENT ERUPTIONS

Based on the relatively sparse vegetative cover on 2N and 2Sa and 2Sb, and the lack of a lapilli blanket on these flows, it is reasonable to suggest that they date from the same eruptive

episode or were at least closely spaced in time. There is no way, given the limited data at hand, to presently correlate older eruptive and landslide units between the northeast and southwest side of the mountain. Future mapping of the extent of the blanket of lapilli that covers lava flows in the valley of Grand Valley Creek would further clarify the chronological relationships between events on the two sides of Volcano Mountain.

Lava flows from both the northeast and southwest sides of Volcano Mountain have dammed small lakes, two of which are informally called Caitlin Pond and Leech Lake (Fig. 3, CP and LL, respectively). Two cores from different locations were obtained from the bottoms of each lake by Les Cwynar of the University of New Brunswick during field operations. Approximately 6.5 m and 0.6 m of sediment, almost entirely gyttja, was recovered from Caitlin Pond and Leech Lake, respectively. Although numerous inorganic laminae were found within the cores, all proved to be quartzose silt likely of eolian origin. Both cores terminated

Figure 5. Views of lava flows in the main crater: **A.** View from the southwest side of the crater. **B.** Pinnacles formed by the collapse of solidified crust of the lava flow following drainage of the underlying magma.



in quartzose silt or sand. One isolated piece of lapilli was found near the base of one of the Caitlin Pond cores. This likely was washed into the pond from the lapilli blanket that covers the surface of the adjacent basalt flow.

Radiocarbon ages were determined on gyttja at the base of the deepest core from Caitlin Pond – 7350 ± 90 BP (GSC-4984) – and both cores from Leech Lake – 3210 ± 70 BP (GSC-5143) and 4210 ± 90 BP (GSC-5141). These ages indicate that Caitlin Pond and Leech Lake were ponded by the adjacent lava flows prior to ca. 7300 BP and ca. 4200 BP. Based upon the absence of any pyroclastic material in lake bottom sediments from both north and south sides of Volcano Mountain, it appears unlikely that there have been eruptions of any kind since Leech Lake was dammed in the middle Holocene and perhaps since Caitlin Pond was dammed in the early Holocene.

ACKNOWLEDGMENTS

The senior author gratefully acknowledges assistance in the field by Les Cwynar and his support crew, Brent Ward, Jamie Isobe and Ruth Gotthardt. The hospitality of Hugh and Glen Bradley of Pelly Ranch and the expert helicopter piloting of Spring Harrison all contributed greatly to the success of this investigation. The senior author's interest in the eruptive

history of Volcano Mountain was stimulated by oral accounts of Selkirk First Nation elders Tommy McGinty and Harry Baum. This paper was improved by a constructive review provided by Cathie Hickson.

REFERENCES

- Bostock, H.S.**
1936: Carmacks District, Yukon; Geological Survey of Canada, Memoir 189, 67 p.
- Francis, D. and Ludden, J.**
1990: The mantle source of olivine nephelinite, basanite and alkaline olivine basalt at Fort Selkirk, Yukon, Canada; *Journal of Petrology*, v. 31, p. 371-400.
- Hayes, C.W.**
1892: An expedition through the Yukon District; *National Geographic Magazine*, v. 4, p. 117-162.
- Jackson, L.E. Jr., Barendregt, R., Irving, E. and Ward, B.**
1990: Magnetostratigraphy of early to middle Pleistocene basalts and sediments, Fort Selkirk area, Yukon Territory; in *Current Research, Part E*, Geological Survey of Canada Paper 90-1E, p. 277-286.
- McConnell, R.G.**
1903: The Macmillan River, Yukon; in *Summary report 1902* by R. Bell; Geological Survey of Canada, Summary Report, p. 22a- 38a.
- Tempelman-Kluit, D.J.**
1984: Geology, Laberge (105E) and Carmacks (115I), Yukon Territory; Geological Survey of Canada Open File 1101, scale 1:250 000.

Geological Survey of Canada Project 800001

The Winter Lake – Lac de Gras regional mapping project, central Slave Province, District of Mackenzie, Northwest Territories

Peter H. Thompson
Continental Geoscience Division

Thompson, Peter H., 1992: *The Winter Lake – Lac de Gras regional mapping project, central Slave Province, District of Mackenzie, Northwest Territories; in Current Research, Part A; Geological Survey of Canada, Paper 92-1A, p. 41-46.*

Abstract

Located 250 km north of Yellowknife, the map area (10 800 km²) includes parts of the three volcano-sedimentary domains (Point Lake-Contwoyto Lake, Yellowknife-Beaulieu River and Lac de Gras-Courageous Lake) that have produced most of the mineral wealth of the Slave Province. A reconnaissance this summer expanded the area of known supracrustal rocks, found structural and stratigraphic evidence of potential granitoid basement, confirmed the lack of mappable contact aureoles around major "plutons" in the Lac de Gras domain, and documented interlayering of potential basement and supracrustal rocks that is tentatively attributed to thrusting during main phase deformation.

A better understanding of the origin, evolution and economic potential of the region will be obtained during the next three field seasons with a combination of 1:250 000 scale mapping, detailed mapping of the Courageous Lake volcanic belt and the western supracrustal domain, and topical studies in geochronology, metallogeny, petrology, and geophysics.

Résumé

Situé à 250 km au nord de Yellowknife, la région cartographiée (10 800 km²) comprend des portions des trois domaines volcano-sédimentaires (Point Lake-Contwoyto Lake, Yellowknife-Beaulieu River et Lac de Gras-Courageous Lake) qui ont généré la majeure partie de la richesse minérale de la province des Esclaves. Un levé de reconnaissance effectué cet été a permis d'élargir la superficie de roches supracrustales connues, de découvrir les indices structuraux et stratigraphiques de la présence possible d'un socle granitoïde, de confirmer l'absence d'aureoles de contact pouvant être cartographiées autour de grands «plutons» dans le domaine de Lac de Gras, et de décrire l'interstratification de roches appartenant peut-être au socle et de roches supracrustales, que l'on attribue provisoirement à un charriage survenu pendant la principale phase de déformation.

On parviendra à une meilleure compréhension de l'origine, de l'évolution et du potentiel économique de la région pendant les trois prochaines saisons d'études de terrain, en combinant la cartographie à l'échelle de 1/250 000, la cartographie détaillée de la zone volcanique de Courageous Lake et du domaine supracrustal occidental, et les études de thèmes en rapport avec la géochronologie, la métallogénie, la pétrologie et la géophysique.

INTRODUCTION

A 1:250,000 scale mapping project that will cover 10,800 km² during the next three field seasons has been initiated. The objective is to better understand the origin, evolution and economic potential of the region by upgrading the bedrock geology of the east half of the Winter Lake (NTS 86A) and west half of the Lac de Gras (76D) map areas.

Located 250 km north of Yellowknife (Figure 1), the area includes parts of the Point Lake – Contwoyto Lake, Yellowknife – Beaulieu River, and Lac de Gras – Courageous Lake supracrustal domains. The richest gold mines in the Slave Province have been found in one or other of these volcano-sedimentary sequences, and significant massive sulphide deposits occur north of Point Lake. The project will provide an opportunity to compare and contrast the rock types, mineral deposits, and history of deformation, magmatism and metamorphism in all three domains. As presently defined, the volcano-sedimentary elements are separated by relatively poorly-known gneissic, migmatitic and massive granitoid rocks that underlie about sixty percent of the area. These rocks are part of the extensive "pink areas" in the Slave Province that, until recently, have received relatively little attention even though they are a key part of any reconstruction of the tectonic evolution of the Slave Province. As a result, they are *terra incognita* as far as mineral potential is concerned. A principal objective of this project is to redress this imbalance. As bedrock mapping proceeds, it would be useful to upgrade knowledge of surficial geology in the Winter Lake – Lac de Gras area. This information is important for mineral exploration, for planning and constructing roads and for study of the environmental impact of development.

The project began this summer with a three week reconnaissance on "Noname" Lake, Lake Providence, and Courageous Lake (Figure 1). Field work combined brief visits to previously-mapped outcrops with regular traverses that represent the start of systematic mapping. Information collected was stored and processed using a combination of FIELDLOG (Brodaric and Fyon, 1989) and AUTOCAD. Preliminary work also began on several of the special studies that will be linked, scientifically and logistically, to the regional mapping project. Specifically, samples were collected for paleomagnetism of basic dykes, for geochronology and for a gravity and aeromagnetic study aimed at determining the three dimensional shape of supracrustal and plutonic units.

RESULTS

The reconnaissance confirmed the importance of the Winter Lake – Lac de Gras area with respect to several fundamental aspects of Slave Province geology. These include: a) occurrence of sialic basement to the Yellowknife Supergroup supracrustal rocks; b) extension of economically important metasedimentary and metavolcanic rocks into high grade gneissic and migmatitic terranes; c) heat source for regional metamorphism; d) role of thrusting and transcurrent shear zones; e) metallogeny of gold and base metals. Bearing in

mind the preliminary nature of the work so far, this report summarizes the implications of some of the observations made this summer.

The provisional outline of litho-structural domains (Figure 1) is derived from earlier regional mapping of the west (Fraser, 1958, 1969) and east (Folinsbee, 1949) halves of the area. The subdivision is determined by the predominant rock types in each domain. Homogeneous plutons have not been singled out. The western supracrustal belt is the southern extension of the Point Lake – Contwoyto Lake supracrustal succession and the eastern metasedimentary rocks are part of the extensive Lac de Gras supracrustal domain. The northern limit of metasedimentary rocks continuous with the Yellowknife supracrustal domain and the northern end of the Beaulieu River metavolcanic belt occur in the southwest corner of the map area. The northern metasedimentary migmatite domain is more of a composite element than the others. It is a transitional domain in that the high grade metasedimentary rocks link the Point Lake – Contwoyto Lake and Lac de Gras supracrustal domains. Furthermore, the occurrence of bodies of granitoid complex make the northern domain transitional between the main mass of granitoid complex to the south and the major Point Lake – Contwoyto Lake supracrustal domain to north of the map area.

1) Rock Types and Stratigraphy

In the northern domain (Figure 1), migmatite and gneiss in Fraser's (1969) Unit 4 and in Folinsbee's (1949) Unit 5 were found to be derived from both sedimentary and plutonic protoliths. The distinction is important for two reasons. First, the metamorphic transformation of supracrustal rocks to migmatite or gneiss does not necessarily reduce their economic potential. Therefore, the area of interest for mineral exploration can be extended into high grade terrains (e.g., gold-bearing, Lupin-type iron formation in the sillimanite and migmatite zones in northeastern Slave (Thompson et al., 1986)). Secondly, granitoid rocks can be transformed as well to migmatite or gneiss by anatexis, injection of melt, and metamorphic segregation before, during, or after main phase deformation. Such rocks form the crystalline basement to supracrustal rocks in, for example, the Alpine, Cordilleran and Wopmay Orogens. Distinction of metasedimentary and granitoid protoliths in gneissic and migmatitic terranes may be a key element in determining the distribution of sialic basement to the Yellowknife Supergroup in the Slave Province.

In his compilation of Slave Province geology (McGlynn, 1977) included a large part of the granitoid complex underlying the western half of the map area in a unit identified as "potential" or "in part" basement. East of Noname Lake volcanic belt, most of the granitoid complex is distinctly heterogeneous. From one outcrop to the next and commonly within a single outcrop, structures vary from massive to foliated to migmatitic granitoid and gneiss while various modal combinations of biotite, quartz, plagioclase, and potassium feldspar range from granite to granodiorite. Hornblende-bearing tonalitic or dioritic phases are less common.

East of the west arm of Courageous Lake (Figure 1), metamorphosed gabbro dykes with chilled margins cut across granitoid complex to form metagabbro sills in the mafic metavolcanics (Moore, 1956). Interpreted by Dillon-Leitch (1981) as related to volcanic magmatism, the metagabbro indicates the granitoid rocks are older than the volcanic belt. Reconnaissance structural and stratigraphic data (see below) are consistent with McGlynn's attribution but further

mapping and detailed geochronology are required to determine how much of the granitoid complex is basement to the Yellowknife Supergroup.

Thinly-layered, greenish-grey- to black-weathering amphibolitic gneiss a few tens of metres thick was found in the northern metasedimentary migmatite domain. Not shown on Folinsbee's map, the gneiss occurs between pelitic

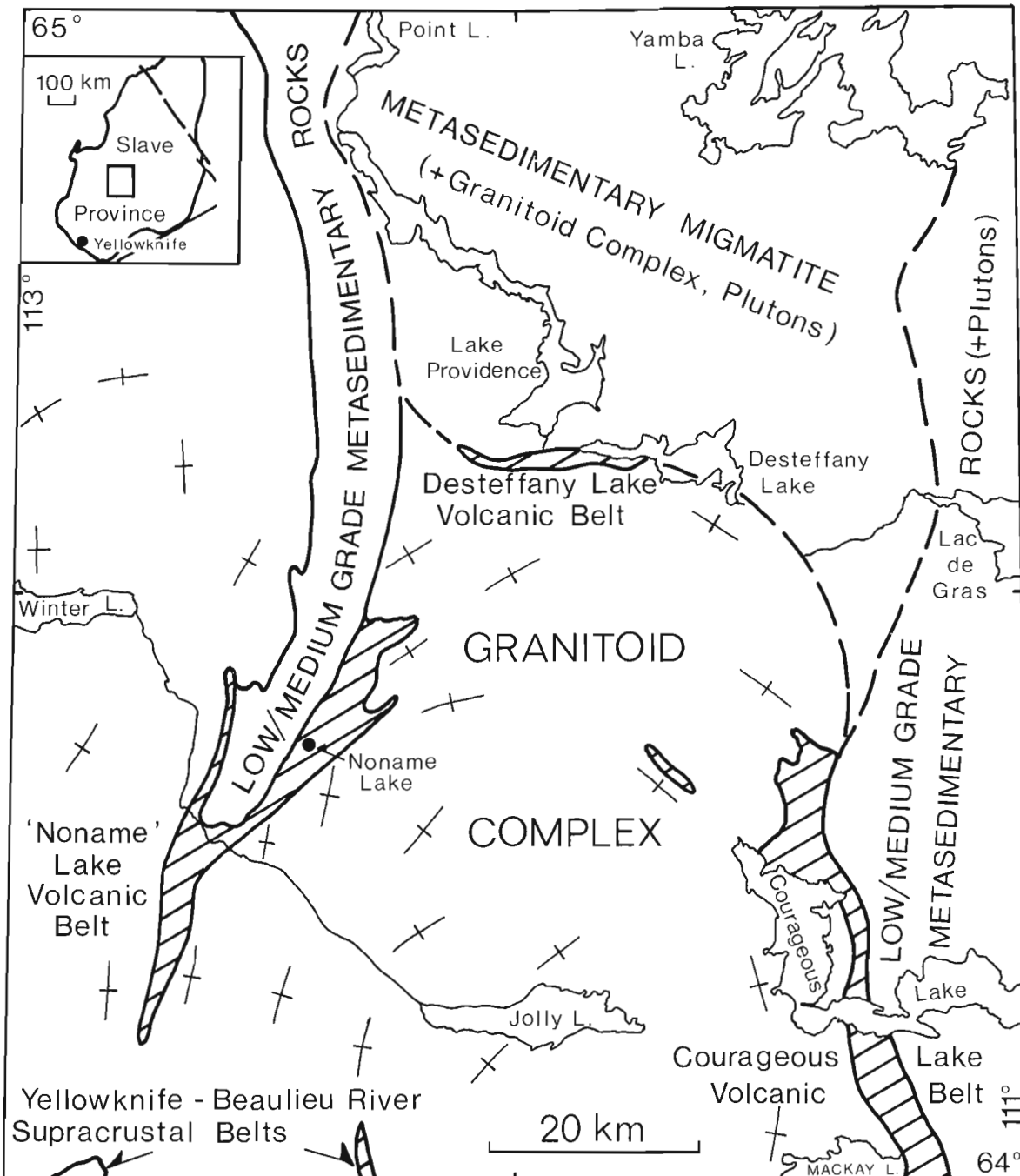


Figure 1. Provisional lithostructural elements of the Winter Lake – Lac de Gras map area. The subdivisions reflect the dominant lithology in each domain. Note that parts of the Point Lake – Contwoyto Lake, Lac de Gras, and Yellowknife – Beaulieu River volcano-sedimentary successions are present.

metasedimentary rocks and foliated, migmatitic granitoid and quartzofeldspathic gneiss that resemble the rocks in the granitoid complex to the south (Figure 1). Both amphibolitic gneiss and metasedimentary rocks are considered to be part of the Yellowknife Supergroup. Walking up the gently northward-dipping structural section, the kilometre scale sequence consists of granitoid complex, amphibolitic gneiss, metasedimentary rocks, amphibolitic gneiss, granitoid complex, metasedimentary rocks, amphibolitic gneiss, mylonitic quartzofeldspathic rocks and foliated granitoid. The "stratigraphy" and rock types are strikingly similar to that mapped in the eastern (west of Healey Lake, Henderson et al., 1982; Henderson and Thompson, 1982) and northeastern (east of Bathurst Inlet; Thompson et al., 1986; Thompson, 1986) Slave Province where a thin metavolcanic unit separates metamorphosed Yellowknife sedimentary rocks from granitoid migmatites considered to be, at least in part, basement to the supracrustal rocks.

There are marked differences between the Noname Lake and Courageous Lake volcanic belts. Metavolcanic rocks in the western belt are basic to intermediate in composition and are commonly pillowed. Volcaniclastic units are prominent. Felsic rocks were not observed and Fraser (1969) did not mention them. The volcanic rocks are intimately associated with sills of metagabbro that were considered by Fraser to be related genetically to volcanism. At the western contact of the metavolcanic rocks with metasedimentary rocks, the metavolcanic rocks are interlayered with a spectacular volcanic and plutonic pebble metaconglomerate (Fraser, 1969; Rice et al., 1990). Within the volcanic succession east of the conglomerate, two zones (600 and 300 metres thick) of quartz-rich and pelitic metasedimentary rocks were found that are similar to those included in the Beniah Formation (Covello et al., 1988; Roscoe et al., 1989) 100 km to the south. The eastern contact with the granitoid complex was covered where traversed but the nearest exposed supracrustal rocks are relatively highly strained.

In contrast, felsic volcaniclastic rocks and flows and quartz-feldspar porphyry are a major component of the Courageous Lake volcanic belt (Folinsbee and Moore, 1950; Moore, 1956; Dillon-Leitch, 1981). Within the volcanic pile metasedimentary rocks are limited to a thin pelitic unit a few metres thick and granitoid pebble-bearing metaconglomerate is restricted to a single outcrop (Dillon-Leitch, 1981). Metamorphosed synvolcanic gabbro dykes described above indicate the granitoid complex to the west is older than the Courageous Lake volcanic belt (Moore, 1956).

2) Metamorphism

The widespread occurrence of andalusite, sillimanite, cordierite at medium grade, and an abundance of metasedimentary migmatite with cordierite in the leucosome indicate that low-pressure, greenschist to upper amphibolite facies conditions of regional metamorphism were attained. Porphyroblasts of cordierite and andalusite overgrowing the principal foliation, sillimanite lineations, minor folds cut by anatectic leucosome that itself has been folded and sheared document the overlap in time of metamorphism and

deformation. Limited distribution of garnet is typical of the generally iron-poor compositions of metasedimentary rocks in the Slave Province (Thompson, 1978). On the other hand, at two localities in the Noname Lake volcanic belt, the abundance of garnet in metasedimentary rocks interlayered with mafic metavolcanics indicates the occurrence of more iron-rich compositions in this association.

At one locality within the easternmost of the two sedimentary sequences in the Noname Lake volcanic belt, metamorphic grade jumps from upper greenschist to upper amphibolite facies across a 100 metre wide covered interval. Neither of the two outcrops is strongly deformed. The sudden increase in grade occurs across the strike of the layering and principal foliation in the belt. West of Lake Providence (Figure 1), there appears to be a larger scale telescoping of metamorphic grade between the lower grade rocks in the north-trending supracrustal belt and the metasedimentary migmatites of the northern domain to the east. Unusually steep or discontinuous metamorphic gradients in the area will be studied in considerable detail because they may be the result of tectonic breaks along major syn- to post-metamorphic shear zones.

Metamorphic field relations in the Winter Lake – Lac de Gras area indicate the abundant granitoid rocks are probably not the principal source of heat for regional metamorphism. For example, in the eastern supracrustal domain (Figure 1), the cordierite isograd cuts across contacts between granitoid and metasedimentary rocks (*see* Folinsbee, 1949; Dillon-Leitch, 1981). Furthermore, the prominent plutons north of Courageous Lake in eastern metasedimentary domain that lack mappable metamorphic aureoles in adjacent greenschist grade phyllite and metagreywacke (Folinsbee, 1949) were found to be themselves metamorphosed and variably-deformed. The decrease in metamorphic grade southward across the northern metasedimentary domain and Desteffany Lake volcanic belt (Figure 1) is consistent with the granitoid complex being basement, or at least pre-metamorphic, but not consistent with it being a major source of heat. Finally, if the granitoid complex, the predominant unit in the western half of the map area, was a major source of heat, it is surprising that only greenschist grade conditions were attained in the central part of the Noname metavolcanic belt. Metamorphic data in the map area indicates that a significant proportion of the granitoid rocks may be older than the metamorphism and, therefore, contrary to Folinsbee's (1949) suggestion they are not likely to be a major source of heat during regional metamorphism. The map area will provide an opportunity to test an alternative hypothesis that both granitoid magmatism and low pressure metamorphism are the product of moderate overthickening of previously thinned sialic crust and associated sedimentary rocks (Thompson, 1989).

3) Structure

Three lines of structural evidence suggest sialic basement may be a component of the granitoid complex. At the regional scale (Figure 1), the occurrence of the major volcanic belts along the contact between granitoid complex and

metasedimentary rocks is similar to the situation elsewhere in the Slave Province where granitoid basement to the Yellowknife Supergroup has been confirmed by geochronology (Frith et al., 1977; Henderson, 1985; Easton, 1985). Secondly, the angular discordance between gneissic layering and foliations in the granitoid complex and the stratigraphy and principal foliation in adjacent supracrustal rocks may be only a major structural discontinuity but the discordance is consistent also with a basement/cover relationship and a longer, more complex history in the granitoid complex. The discordance is 20 degrees with respect to the underlying Noname volcanic belt and 90 degrees with respect to underlying amphibolitic gneiss and metasedimentary rocks east of Lake Providence. Thirdly, refolded, kilometre-scale interlayering of granitoid complex, amphibolitic gneiss and metasedimentary rocks near Lake Providence implies all three units existed before main phases of crustal thickening began. This is consistent with granitoid complex as basement to the supracrustal sequence or as an early (synvolcanic?) intrusive phase. Clearly, while the existence of basement is not yet proven, it remains a distinct possibility.

The role of thrusting in the deformation history of the Slave Province remains controversial in part because repetition of the stratigraphy is difficult to prove in the absence of continuous and extensive marker horizons like quartzite or marble. The repetition of the "stratigraphy" (granitoid complex-amphibolitic gneiss-metasedimentary rocks) near Lake Providence is, therefore, very interesting. If thrusting is responsible for the moderately-dipping structural sequence there, the process may also be a factor elsewhere in the area, for example, in the origin of the interlayering of mafic metavolcanic rocks, metagabbro and low grade metasedimentary sequences within the Noname Lake volcanic belt.

There is abundant evidence of shear strain in the Winter Lake – Lac de Gras area. Narrow zones of grain-size reduction parallel straight contacts within and along the boundaries of supracrustal belts. Metamorphic grade in the zones ranges from greenschist to middle amphibolite facies. Sheared-off leucosomes cutting shear zones that displace older leucosomes indicate shearing occurred at the highest grade as well. Telescoping of metamorphic gradients in the western half of the area may be the result of thrusting, extensional faulting, transcurrent shear, or some combination of these processes. Straight topographic lineaments like the one along the southeast boundary of the Noname Lake volcanic belt and some narrow linear aeromagnetic anomalies are candidates for late brittle faults.

4) Economic Geology

The distribution of supracrustal rocks with potential economic interest has been extended and differences between supracrustal domains documented. While knowledge of such differences may eliminate a domain with respect to one kind of exploration target, it may be very favourable for another target. For example, does the absence of significant discoveries in the Noname Lake volcanic belt mean the rocks

are barren or, given the clear lithologic differences with respect to the Courageous Lake volcanic belt, has just one of several potential exploration targets been eliminated? The metasedimentary rocks in the northern and eastern domains (Figure 1) appear to be more arenaceous and less pelitic than the Yellowknife Supergroup metasedimentary rocks east of Bathurst Inlet that contain Lupin-type gold-bearing iron formation (Thompson et al., 1986; Thompson, 1986). Is the apparent absence of iron formation in the Winter Lake – Lac de Gras area a reflection of a sedimentary depositional environment that favoured a different kind of ore deposition? Are there favourable areas within the northern and southern parts of the Courageous Lake belt that may be expected to contain gold deposits similar to those in the central part? What is the potential for the discovery of base and/or precious metal synvolcanic ores? These are the kinds of questions that this project with its combination of regional mapping and metallogenic studies is designed to answer.

ACKNOWLEDGMENTS

At different times, Boyan Brodaric, Mike Villeneuve, and Cathy Langill provided enthusiastic and very competent assistance in the field while teaching me about their respective areas of expertise: computers, geochronology, and mountaineering. Expediting by Jason Chillibeck and split charters arranged with Martin Irving (Geology Office of GNWT) were much appreciated. Bill Padgham's (DIAND) recommendation that we include a large chunk of the "pink area" underlain by gneissic and granitoid rocks in this project was a very good idea. The report has benefited from critical commentary by Tony Davidson, Janet King, and John B. Henderson.

REFERENCES

- Brodaric, B. and Fyon, J.A.**
1989: OGS FIELDLOG: a microcomputer-based methodology to store, process and display map-related data; Ontario Geological Survey, Open File Report 5709, 73 p. and 1 magnetic diskette.
- Covello, L., Roscoe, S.M., Donaldson, J.A., Roach, D., and Fyson, W.K.**
1988: Archean quartz arenite and ultramafic rocks at Beniah Lake, Slave Structural Province, Northwest Territories; in *Current Research, Part C*, Geological Survey of Canada, Paper 88-1C, p. 223-232.
- Dillon-Leitch, H.C.H.**
1981: Volcanic stratigraphy, structure and metamorphism in the Courageous-Mackay Lake Greenstone Belt, Slave Province, Northwest Territories; MSc thesis, University of Ottawa, Canada, 169 p.
- Easton, M.E.**
1985: The nature and significance of Pre-Yellowknife Supergroup rocks in the Point Lake area, Slave Structural Province, Canada; in *Evolution of Archean Supracrustal Sequences*, Eds., Ayres, L.D., Thurston, P.C., Card, K.D., and Weber, W., Geological Association of Canada Special Paper 28, p. 153-167.
- Folinsbee, R.E.**
1949: Lac de Gras, District of Mackenzie, Northwest Territories; Geological Survey of Canada, Map 977A.
- Folinsbee, R.E. and Moore, J.C.**
1950: Matthews Lake, Northwest Territories; Geological Survey of Canada, Paper 50-4.
- Fraser, J.A.**
1958: Fort Enterprise, Northwest Territories; Geological Survey of Canada, Map 16-1958.

- 1969: Winter Lake, District of Mackenzie; Geological Survey of Canada, Map 1219A.
- Frith, R., Frith, R.A., and Doig, R.**
 1977: The geochronology of the granitic rocks along the Bear-Slave Structural Province boundary, northwestern Canadian Shield; Canadian Journal of Earth Sciences, v. 14, p. 1356-1373.
- Henderson, J.B.**
 1985: Geology of the Yellowknife – Hearne Lake Area, District of Mackenzie: a segment across an Archean basin; Geological Survey of Canada, Memoir 414, 135 p.
- Henderson, J.B. and Thompson, P.H.**
 1982: Geology of Healey Lake map area (1:125,000 scale map and marginal notes); Geological Survey of Canada, Open File 860.
- Henderson, J.B., Thompson, P.H., and James, D.T.**
 1982: The Healey Lake map area and the Thelon Front Problem, District of Mackenzie; in Current Research, Part A, Geological Survey of Canada, Paper 82-1A, p. 191-195.
- McGlynn, J.C.**
 1977: Geology of the Slave Province; Geological Survey of Canada, Open File 445 (1:1,000,000 map and legend).
- Moore, J.C.**
 1956: Courageous Lake – Matthews Lakes area, District of Mackenzie, Northwest Territories; Geological Survey of Canada, Memoir 283, 52 p.
- Rice, R.J., Long, D.G.F., Fyson, W.F., and Roscoe, S.M.**
 1990: Sedimentological evaluation of three Archean metaquartzite- and conglomerate-bearing sequences in the Slave Province, N.W.T.
- Roscoe, S.M., Stuble, M., and Roach, D.**
 1989: Archean quartz arenites and pyritic paleoplacers in the Beaulieu River supracrustal belt, Slave Structural Province, N.W.T.; in Current Research, Part C, Geological Survey of Canada, Paper 89-1C, p. 199-214.
- Thompson, P.H.**
 1978: Archean regional metamorphism in the Slave Province: a new perspective on some old rocks; in Metamorphism of the Canadian Shield, Eds., J.A. Fraser and W.W. Heywood, Geological Survey of Canada Paper 78-10, p. 85-102.
 1986: Geology of Tinney Hills – Overby Lake (west half) map areas (1:125,000 scale map and marginal notes); Geological Survey of Canada, Open File 1316.
 1989: Moderate overthickening of thinned sialic crust and the origin of granitic magmatism and regional metamorphism in low-pressure/high-temperature terranes; Geology, v. 17, p. 520-523.
- Thompson, P.H., Culshaw, N., Buchanan, J.R., and Manojlovic, P.**
 1986: Geology of the Slave Province and Thelon Tectonic Zone in the Tinney Hills – Overby Lake (west half) map area, District of Mackenzie; in Current Research, Part A, Geological Survey of Canada, Paper 86-1A, p. 275-289.

Geological Survey of Canada Project 870008NM

Preliminary studies of fluid inclusions in sphalerite, quartz, and dolomite from Gayna River MVT deposit, Northwest Territories

J.J. Carrière and D.F. Sangster
Mineral Resources Division

Carrière, J.J. and Sangster, D.F., 1992: Preliminary studies of fluid inclusions in sphalerite, quartz, and dolomite from Gayna River MVT deposit, Northwest Territories; in *Current Research, Part A*; Geological Survey of Canada, Paper 92-1A, p. 47-53.

Abstract

Preliminary fluid inclusion and petrographic studies were conducted on sphalerite, authigenic quartz and dolomite in breccias from the Host Unit of the Little Dal Group. In sphalerite, the average homogenization temperature found was 186°C for primary and pseudosecondary inclusions and 161°C for secondary inclusions, with salinities ranging from 16 to more than 23 equivalent weight % NaCl. In quartz, the average homogenization temperature was 192°C with salinities similar to those for sphalerite. Six primary fluid inclusions in dolomite gave an average Th of 173°C; no salinity data were obtained for inclusions in dolomite. Temperatures of first recognized liquid + ice + vapour were all less than -25°C, indicating the presence of salt(s) other than NaCl. In cathodoluminescence, crystalline (saddle) dolomite was zoned, vein dolomite was uniformly dull, and interstitial dolomite varied between uniform dull and uniform bright to mottled. Microprobe analyses supported the presence of three types of dolomite.

Résumé

Des analyses préliminaires portant sur les inclusions et la pétrographie d'échantillons de sphalérite, de quartz et de dolomite authigènes prélevés dans des brèches de l'unité encaissante du groupe de Little Dal ont été réalisées. Dans la sphalérite, la température d'homogénéisation moyenne est de 186°C pour les inclusions primaires et pseudosecondaires et de 161°C pour les inclusions secondaires; les salinités se situent entre 16 et plus de 23% en poids équivalent de NaCl. Dans le quartz, la température d'homogénéisation moyenne s'élève à 192°C et la salinité atteint des valeurs semblables à celles de la sphalérite. Six inclusions fluides primaires dans la dolomite donnent une température moyenne de 173°C; aucune donnée n'a été recueillie sur les inclusions contenues dans la dolomite. Les premières températures relevées pour l'ensemble liquide + glace + vapeur sont toutes inférieures à -25°C, indiquant la présence de sel(s) autre(s) que NaCl. La cathodoluminescence a révélé que la dolomite à cristaux en selle est zonée, que la dolomite veinée est uniformément mate et que la dolomite interstitielle varie d'uniformément mate et uniformément brillante à bigarrée. Les analyses à la microsonde ont confirmé la présence de ces trois types de dolomite.

INTRODUCTION

Fluid inclusion microthermometry and cathodoluminescence (CL) of the Gayna River zinc-lead deposit is part of a longer term research project to investigate the thermal history and relative timing of carbonate-hosted zinc-lead deposits of the Mackenzie Platform of northern British Columbia, western Northwest Territories, and eastern Yukon. This report presents results of a preliminary study of fluid inclusions in sphalerite, quartz, and dolomite conducted to determine the minimum formational temperature of the deposit and the salinity of the mineralizing fluid(s), and CL of the dolomite cement.

DEPOSIT GEOLOGY

The Gayna River zinc-lead deposit (Fig. 1), in western Northwest Territories (64°56'N, 130°41'W; 106B/15), is a Mississippi Valley-type (MVT) deposit which occurs in the Proterozoic Little Dal Group. Discovered in 1974, the deposit contains reserves of 50 million short tons (approximately 45 million tonnes) of 4.7% zinc and 0.3% lead (Hewton, 1982).

The host rocks are platform carbonates of the Helikian Little Dal Group, Mackenzie Mountains Supergroup. Zinc and lead sulphides occur in most units of the Group but are concentrated in secondary breccias in dolostones of the Host Unit. Secondary breccias are interpreted to have formed by a variety of processes including faulting, solution-collapse, and recrystallization. These processes have resulted in different secondary breccia

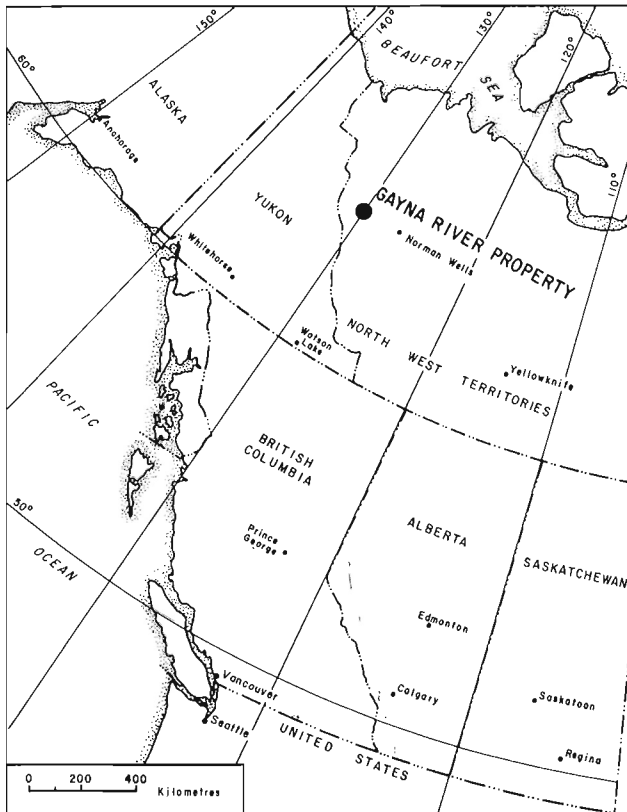


Figure 1. Location of Gayna River deposit (Hewton, 1982).

types, including such forms as mosaic and rubble, distinguished mainly by differing associations of the cement and fragments. The mosaic breccia shows little or no rotation and very little displacement of the dolostone fragments. The rubble breccia shows marked rotation and displacement of the dolostone fragments leaving large gaps which are filled with ore and gangue minerals (Hewton, 1982).

MATERIALS STUDIED

Samples were selected from twenty-six hand specimens in existing GSC collections. Sample SP3389 is from the mosaic breccia, and the remaining samples are from the rubble breccia. The samples consist of dolostone fragments, varying widely in shape and size, and cemented by sphalerite, dolomite, and quartz (Fig. 2). Galena, pyrite, calcite, barite, and smithsonite are minor constituents of the cement. In some of the samples the cement is mainly sphalerite with minor quartz. The sphalerite ranges from pale buff to brilliant yellow, orange and red, and forms euhedral to subhedral crystals up to 0.5 cm in diameter.

PETROGRAPHY

Preliminary petrographic studies were conducted on six fluid inclusion plates and two polished thin sections. Dolostone, dolomite, sphalerite, quartz, galena, pyrite, calcite, and smithsonite were observed in thin section.

Petrographic and cathodoluminescence work (CL) indicated the presence of three textural and compositional types of dolomite: 1) saddle dolomite distinguished by curved crystal faces and radiating extinction pattern in polarized light and zoning in CL light; 2) vein dolomite distinguished by uniform dull luminescence; and 3) interstitial dolomite distinguished by straight crystal faces and uniform extinction and, in CL light, variation from uniform dull to uniform bright to mottled. The paragenetic sequence interpreted from the CL study showed dolostone followed by zoned dolomite, quartz, and sphalerite.

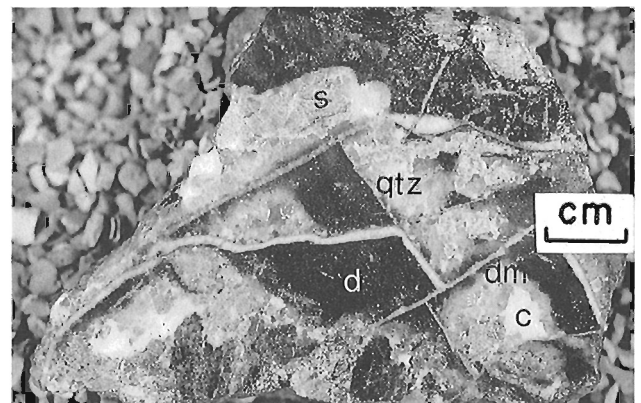


Figure 2. Sample SP3409, an example of secondary breccia, consisting of angular dolostone fragments (d) with sharp boundaries cemented by a thin layer of white, coarsely crystalline, sparry dolomite (dm), sphalerite (s), calcite (c), and quartz (qtz).

A microprobe traverse was conducted across a zoned (saddle) dolomite crystal. The luminescence-compositional relationships observed for the saddle dolomite at Gayna River are comparable to those compiled by Marshall (1988, Fig. 7.13) where $MnCO_3$ (mole %) is plotted against $FeCO_3$ (mole %). The plot shows that commonly CL intensity increases with increasing $MnCO_3/FeCO_3$ ratio. These preliminary results from Gayna River suggest that luminescent signatures may ultimately be used to correlate dolomites between deposits in Mackenzie Platform. A composite drawing (Fig. 3) illustrates the luminescent signature present, and the supporting microprobe data.

The fluid inclusions observed were all two phase: liquid plus vapour. Three modes of occurrence of fluid inclusions were present: in randomly distributed clusters, in healed fractures within crystals, and in healed fractures across crystals. These modes of occurrence were interpreted as corresponding to primary, pseudosecondary, and secondary inclusions according to the criteria of Roedder (1976). Inclusions were quite abundant and many had irregular

shapes, although negative crystal shaped inclusions were common. Inclusions ranged in size from 5 to 40 μm . Vapour bubbles were small, occupying approximately 5 volume per cent of the inclusions. The inclusions found in the random, three-dimensional distribution (cluster) in a sample of a yellow sphalerite zone, adjacent to an inclusion-free white sphalerite zone (Fig. 4) were interpreted as primary (Roedder, 1981, p. 136). The size and shape of inclusions along healed fractures tended to be uniform, whereas size and shape varied among isolated inclusions and those contained in clusters. Planar groups of very thin, flat inclusions, showing evidence of necking (Fig. 5), or inclusions in healed fractures (i.e. those that do not terminate within the crystal) were interpreted as secondary (Roedder, 1981, p. 137).

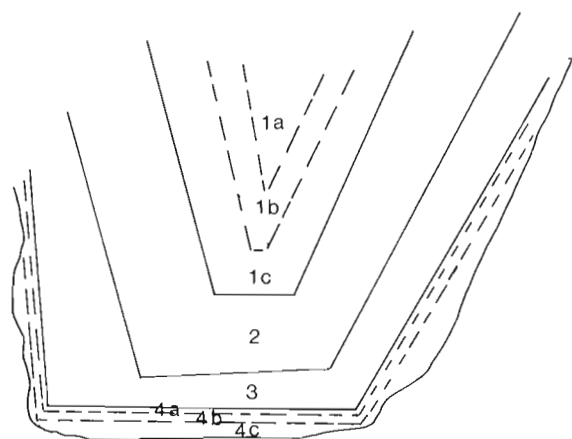
HOMOGENIZATION TEMPERATURES

Using a Linkam TH600 heating/freezing stage, homogenization temperatures (T_h) were determined on 71 inclusions in sphalerite (Fig. 6) and 67 inclusions in quartz (Fig. 7). The stage was calibrated both before and after measurements using SYN FLINC synthetic Calibrations Standards and four compounds of known melting points ranging from -56.6° to $200^\circ C$. The accuracy was considered to be about $1.3^\circ C$. The poor optical quality of many inclusions and the rapid movement of the tiny bubbles near homogenization limited the precision to about $2^\circ C$. Temperature determinations were repeated on most inclusions and results were duplicated to within $2^\circ C$. All inclusions homogenized to the liquid phase (i.e. by the expansion of the liquid to eliminate the bubble).

The homogenization temperatures determined for primary inclusions fell within the range of those for pseudosecondary inclusions. This supported the premise that both primary and pseudosecondary inclusions were early-formed with respect to crystal growth.

Homogenization temperatures provide a minimum estimate of temperature of formation. The temperature of entrapment of the fluid inclusion is derived by adding a pressure correction to the temperature of homogenization. Since the timing (and hence the depth) of mineralization at Gayna River is not known, no corrections were made to the determined temperatures but, at these moderately low temperatures and high salinities, such corrections would be small, even at 5 km depth (Roedder, 1984).

Table 1 summarizes the fluid inclusion data for sphalerite. Primary and pseudosecondary fluid inclusions in sphalerite have homogenization temperatures in the range of 156° to $231^\circ C$ with a mean of $186^\circ C$ (Fig. 6). Secondary fluid inclusions in sphalerite have homogenization temperatures in the range of 134° to $176^\circ C$ with a mean of $161^\circ C$. Since the homogenization temperatures of the secondary inclusions are only slightly lower than for primary and pseudosecondary inclusions and the salinities are comparable, it would seem likely that the secondary inclusions represent a continuum in hydrothermal activity. Inclusions in the same sphalerite crystal commonly show a wide range of formation temperatures (as much as 69° , and averaging 29°), which could indicate rapidly fluctuating depositional conditions or extremely slow growth rates.



Point on Traverse	Mole %			Luminescence Intensity	Zone
	$FeCO_3$	$MnCO_3$	$MnCO_3/FeCO_3$		
1.	.07	.15	2.14	Bright	4c
2.	.52	.07	0.13	Bright or dull	4b
3.	.68	.15	0.22	Bright	4a
4.	.47	.02	0.04	Dull	3
5.	.00	.02	0	Non-luminescent	3
6.	.00	.00	0	Non-luminescent	3
7.	.27	.02	0.07	Dull	3
8.	.85	.08	0.09	Bright	2
9.	.88	.13	0.15	Bright	2
10.	2.55	.15	0.06	Dull	1

Figure 3. Composite drawing illustrating luminescent signature found in Gayna River saddle dolomite with supporting microprobe data. Zones 1a, 1b, and 1c are not distinguished in this data set.



Figure 4a. Photomicrograph of cluster of primary fluid inclusions confined to growth zone defined by yellow sphalerite adjacent to inclusion-free white sphalerite.

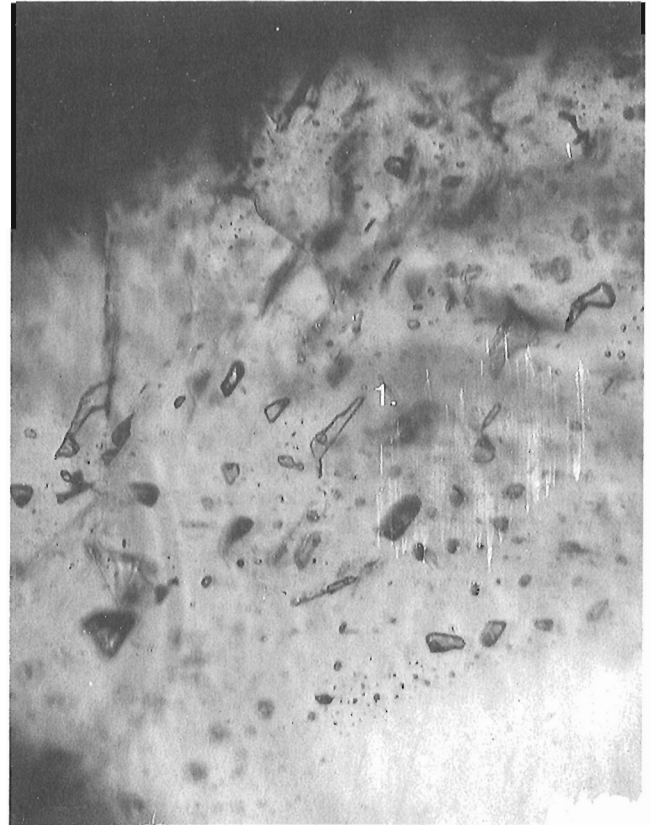


Figure 4b. Detail of 4a. showing primary inclusions in yellow colour-zoned sphalerite crystal. Inclusion No. 1 is 30 μm long.

Table 2 summarizes the fluid inclusion data for quartz. Primary and pseudosecondary fluid inclusions in quartz have homogenization temperatures in the range of 139° to 243°C with a mean of 192°C. Inclusions in the same quartz crystal show an even wider range of formation temperatures (as much as 75°, and averaging 60°C). The possibility that inclusions were stretched during the post depositional history of the deposit is discussed below.

Six primary inclusions in dolomite have homogenization temperatures in the range of 153° to 195°C and a mean of 173°C.

ICE MELTING TEMPERATURES

Inclusions were cooled to -70 to -80°C with most inclusions freezing around -65°C. The first appearance of liquid upon heating was difficult to see due mainly to the small size of the inclusions. The temperature of first recognized liquid + ice + vapour in 13 inclusions in sphalerite and 16 inclusions in quartz were all lower than -25°C. These temperatures represent maximum values for the eutectic temperatures. Because the eutectic temperature of the H₂O-NaCl system is -21.2°, initial melting temperatures lower than this indicate the presence of other salts, probably CaCl₂.

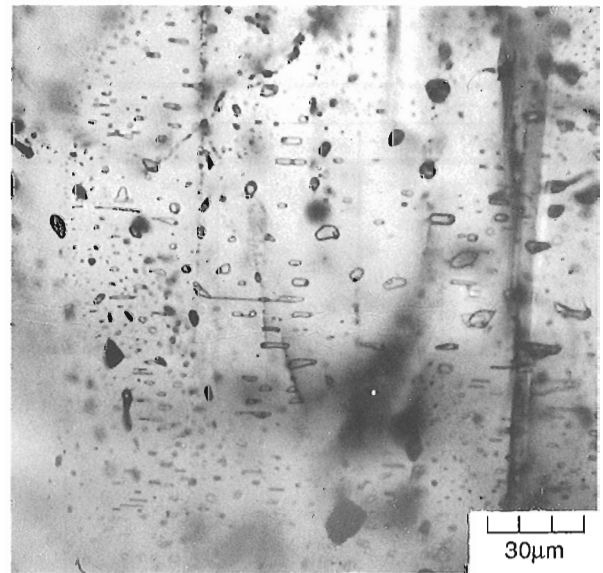


Figure 5. Photomicrograph showing plane of thin, flat secondary inclusions in sphalerite. Note inclusion in central part of photo in the process of necking down.

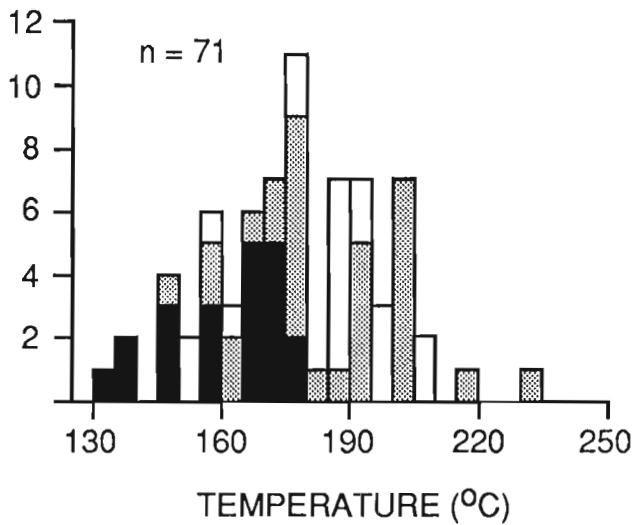


Figure 6. Homogenization temperatures of inclusions in sphalerite. Primary inclusions are unshaded, pseudosecondary are shaded, and secondary are black.

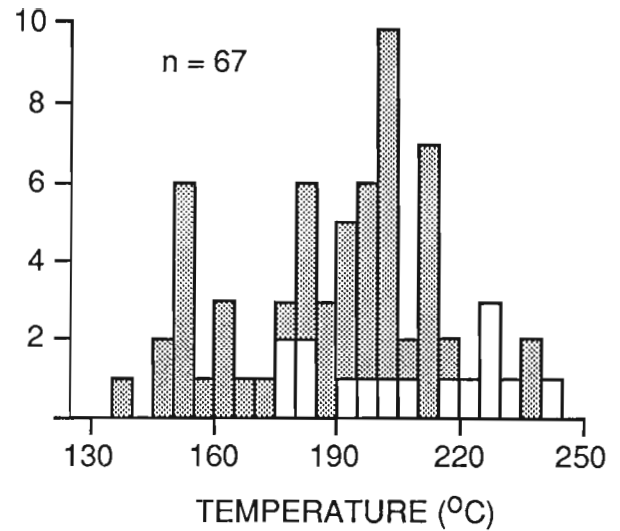


Figure 7. Homogenization temperatures for inclusions in quartz. Primary inclusions are unshaded, pseudosecondary are shaded, and secondary are black.

Table 1. Summary of data for fluid inclusions in sphalerite

HOMOGENIZATION TEMPERATURES (Th)				MELTING TEMPERATURES (Tm)		
Sample No.	No. of inclusions	Range (°C)	Avg. (°C)	No. of inclusions	Range (°C)	Avg. (°C)
PRIMARY FLUIDS						
SP 3389	7	157-177	168	6	-12 to -21	-16
SP 3389A	6	156-191	180	1	-15	-15
SP 3406	21	162-231	200	18	-14 to -23	-17
SP 3408A	4	157-201	176	4	-20 to -22	-21
SP 3409	9	150-191	177	13	-12 to -18	-15
SP 3409B	3	188-189	189	3	-20 to -22	-21
Summary	50	156-231	186	45	-12 to -23	-17
SECONDARY FLUIDS						
SP 3389	4	149-176	163	1	-19	-19
SP 3389A	7	158-172	165	1	-17	-17
SP 3408A	5	134-149	141	5	-21.2 to -21.5	-21.4
SP 3409	5	171-175	173			
Summary	21	134-176	161	7	-17 to -21.5	-20

Table 2. Summary of data for primary and pseudosecondary fluid inclusions in quartz

HOMOGENIZATION TEMPERATURES (Th)				MELTING TEMPERATURES (Tm)		
Sample No.	No. of Inclusions	Range (°C)	Avg. (°C)	No. of inclusions	Range (°C)	Avg. (°C)
SP 3408A	42	119-236	191	41	-10 to -24	-16
SP 3409B	25	139-243	193	14	-10 to -16	-13
Summary	67	139-243	192	55	-10 to -24	-15

Ice melting temperatures were determined for 53 inclusions in sphalerite and 55 inclusions in quartz. The ice melting temperature of primary and pseudosecondary inclusions ranged from -12°C to -24°C in sphalerite with a mean of -17°C; in quartz, the range was from -10° to -24°C with a mean of -15°C. Ice in secondary inclusions in sphalerite melted in the range of -12° to -24°C with a mean of -20°C. This suggested that the mineralizing fluid was a brine containing 16 to greater than 23 equivalent weight per cent of NaCl (Potter et al., 1978).

Homogenization temperatures versus salinity plots for sphalerite (Fig. 8) are similar to those for quartz (Fig. 9); the only significant difference being that primary inclusions in quartz are slightly higher temperature and lower salinity than those in sphalerite. These results indicate that sphalerite and quartz were deposited under similar temperature conditions and by fluid(s) of similar salinity.

SUMMARY

Homogenization temperatures obtained from primary and pseudosecondary inclusions in sphalerite in this study averaged 186°C; ice melting temperatures averaged -17°C. Homogenization temperatures obtained from secondary inclusions in sphalerite averaged 161°C; ice melting temperatures averaged -20°C. Homogenization temperatures obtained for primary and pseudosecondary fluid inclusions in quartz averaged 192°C; ice melting temperatures averaged -15°C. The six homogenization temperatures in dolomite averaged 173°C.

DISCUSSION

Sphalerites in North American MVT deposits yield Th determinations ranging from 50 to 190°C with a mode of approximately 100-110°C and ice melting temperatures ranging from -9° to -30°C and averaging -19°C (Roedder, 1976). In the present study the average sphalerite Th of 186°C is in the upper end of this range and significantly above the mode. It is important first to assess if these high homogenization temperatures reflect high minimum temperatures of formation of the deposit or if they result from other processes such as stretching.

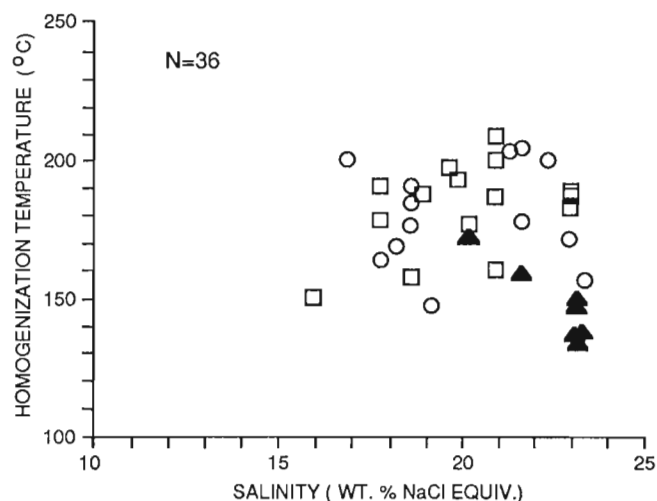


Figure 8. Homogenization temperature versus equivalent weight % NaCl for fluid inclusions in sphalerite. Primary inclusions are open squares, pseudosecondary are open circles, and secondary are solid triangles.

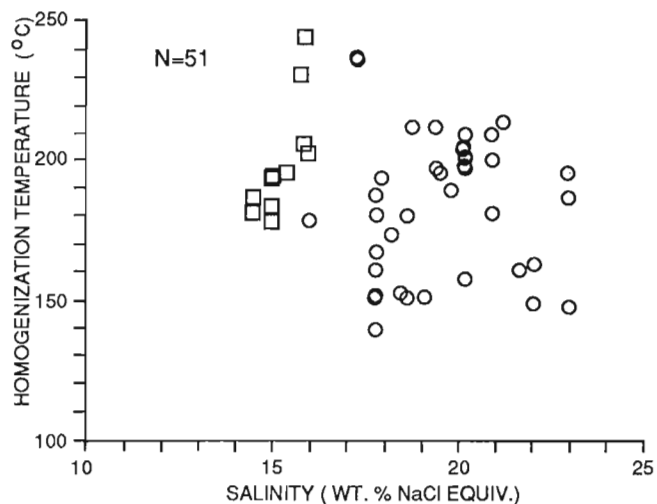


Figure 9. Homogenization temperature versus equivalent weight % NaCl for fluid inclusions in quartz. Primary inclusions are open squares, pseudosecondary are open circles.

Stretching of fluid inclusions can result in measured homogenization temperatures being considerably higher than the actual trapping temperatures. Stretching can result from the rocks being previously heated above the original homogenization temperature of the inclusions contained within them. This overheating could be a result of accidental overheating during sample preparation, during the actual heating runs, or due to natural overheating sometime after formation of the sphalerite.

Overheating during sample preparation was not considered likely as the samples were prepared under controlled conditions which allowed a maximum temperature of 125°C during preparation. The possibility of overheating during actual heating runs was examined carefully. The maximum and minimum homogenization temperatures determined for inclusions in each chip were recorded. Th ranges were all less than 36°C, except for one chip which was heated 69°C above the lowest Th in that chip. According to experiments reported by Bodnar and Bethke (1984), inclusions in sphalerite overheated by less than approximately 40°C rarely showed an increase in Th greater than 1.0°C. As the temperature of overheating was increased beyond 40°C, however, a greater percentage of the inclusions stretched, although several did not stretch when overheated by 100°C. Stretching is also related to bubble diameter. The majority of inclusions examined from Gayna River had vapour bubbles ranging in size from 2.0 to 4.0 µm. The amount of overheating required to initiate stretching of inclusions with vapour bubbles of this size range was from 58°C to 77°C (Bodnar and Bethke, 1984). Since maximum overheating, with one exception, was less than 40°C, it is unlikely that the high Th determined in this study are a result of stretching of fluid inclusions by overheating during sample runs.

Natural stretching in fluid inclusions due to overheating during burial would require depths in excess of 6 km (at a thermal gradient of 30°/km). Because the age of mineralization is not known, post-ore burial depths cannot be evaluated. Thus, although natural overheating may explain the high Th, exceptional burial depths would be required.

A final factor which could lead to erroneously high homogenization temperatures is leakage which can be aggravated by the presence of methane (Hanor, 1980). No evidence of leakage or presence of methane was found in this study.

Another aspect which deserves discussion is the range of homogenization temperatures within individual crystals which could be caused by leakage. Because leakage and stretching have been concluded to be unlikely in this study,

the wide Th range, as much as 69° within a single sphalerite crystal and up to 75° within a single quartz crystal, cannot be fully explained within the scope of this study.

In conclusion, it has been shown by the study of fluid inclusions that sphalerite, quartz, and saddle dolomite have similar microthermometric characteristics, and by petrography and cathodoluminescence that they are closely related paragenetically, and also that an identifiable luminescent signature is present. The unusually high temperatures of the ore-forming fluid indicated by the inclusions in Gayna River sphalerite are concluded to be real. These temperatures could simply represent deep circulating formation waters, or signal the presence of abnormally high regional geothermal gradients during sphalerite deposition.

ACKNOWLEDGMENTS

François Robert (GSC) kindly reviewed the manuscript and made many useful suggestions. John Stirling (GSC, Mineralogy Section) provided the microprobe analyses. Sections were prepared by Vancouver Petrographics Ltd.

REFERENCES

- Bodnar, R.J. and Bethke, P.M.**
1984: Systematics of Stretching of Fluid Inclusions: Fluorite and Sphalerite at 1 Atmosphere Confining Pressure; *Economic Geology*, v. 79, p. 141-151.
- Hanor, J.S.**
1980: Dissolved methane in sedimentary brines: potential effect on the PVT properties of fluid inclusions; *Economic Geology*, v. 75, p. 603-609.
- Hewton, R.S.**
1982: Gayna River: A Proterozoic Mississippi Valley-type Zn-Pb deposit; in *Precambrian Sulphide Deposits*, H.S. Robinson Memorial Volume, (ed.) R.W. Hutchinson, C.D. Spence, and J.M. Franklin; Geological Association of Canada, Special Paper 25, p. 667-700.
- Marshall, J.D.**
1988: Cathodoluminescence of geological materials; Unwin Hyman, Boston, 146 p.
- Potter, R.W., Clynne, M.A., and Brown, D.L.**
1978: Freezing point depression of aqueous sodium chloride solutions; *Economic Geology*, v. 73, p. 284-285.
- Roedder, E.**
1976: Fluid-inclusion evidence of the genesis of ores in sedimentary and volcanic rocks; in *Handbook of strata-bound and stratiform ore deposits*, v. 2, (ed.) K.H. Wolf, p. 56-110.
1981: Origin of fluid inclusions and changes that occur after trapping; in *Short Course Handbook; Fluid inclusions: applications to petrology*, (ed.) L.S. Hollister and M.L. Crawford; Mineralogical Association of Canada, Calgary, May 1981, p. 101-137.
1984: Fluid Inclusions; *Mineralogical Society of America, Reviews in mineralogy*, v. 12, 644 p.

Side-scan sonar observations of Point Grey dump site, Strait of Georgia, British Columbia

B.S. Hart
Pacific Geoscience Centre, Sidney

Hart, B.S., 1992: Side-scan sonar observations of Point Grey dump site, Strait of Georgia, British Columbia; in Current Research, Part A; Geological Survey of Canada, Paper 92-1A, p. 55-61.

Abstract

Side-scan sonar imagery of the sea floor of the Strait of Georgia near Vancouver readily detects evidence of anthropogenic material dumped at the Point Grey offshore disposal site because its acoustic characteristics contrast markedly with those of the ambient prodelta (> 200m) mud. Dumped material consists primarily of sandy dredge spoils from harbours and waterways, and excavation material from lower mainland sites. Despite efforts to monitor dumping activities, it appears that disposal may be continuing outside the limits of the dump site, potentially conflicting with bottom fishing activities in some areas. Repeat side-scan sonar coverages would allow patterns and rates of disposal outside the spoil zone to be determined, essential information in assessing the need for enhanced disposal monitoring programs.

Résumé

Les images recueillies par sonar à balayage latéral du fond océanique dans le détroit de Georgia près de Vancouver donnent des indices évidents d'accumulations anthropiques à la décharge extracôtière de la pointe Grey, où les données acoustiques contrastent nettement avec celles produites par la boue prodeltaïque environnante (> 200m). Les matériaux jetés sont surtout composés de déblais de sable dragués dans des ports et des canaux et de déblais d'excavation provenant des basses terres continentales. Malgré les mesures prises pour surveiller les activités de déversement, il semblerait qu'elles se poursuivent à l'extérieur des limites de la décharge, entrant peut-être en conflit avec la pêche des poissons de grand fond dans certaines zones. En effectuant plusieurs levés par sonar à balayage latéral, il serait possible de déterminer les modes et les vitesses de déversement à l'extérieur de la zone de déblais et de recueillir des données pour évaluer la nécessité d'améliorer les programmes de surveillance d'élimination des déchets.

INTRODUCTION

Part of the Geological Survey of Canada's mandate in Marine Environmental Geoscience entails the monitoring of coastal processes and Man's activities in the coastal zone as they pertain to changes in the physical and chemical environment. Particularly when the zones are in proximity to large urban centres, where coastal activities are varied and often conflict, such information may be a critical component when planning for, or adjusting to environmental changes.

The delta of the Fraser River and adjacent Strait of Georgia (Fig. 1) are typical of such regions. Adjacent to the rapidly growing urban centre of the Vancouver area, the waters and substrates of the strait here are host to a variety of activities which include (but are not restricted to) navigation (commercial and recreational), fishing, sewage disposal, offshore dumping, and power/telephone transmission between the mainland and Vancouver Island via underwater cables.

Marine geophysical surveying by the Geological Survey of Canada, conducted as part of a program aimed at assessing the offshore hazards potential and effects of anthropogenic activities in the central Strait of Georgia (Hart et al., 1991), crossed the Point Grey offshore dump site (Fig. 1). This site was established by the Ministry of Transportation in 1968

seaward of the North Arm of the Fraser River in about 210 m water depth. This is the most frequently used offshore dump site in the Pacific Region, with over 3×10^6 m³ of material dumped as of early 1987 (Sullivan, 1987). Summaries of dumping activities and monitoring programs at the Point Grey dump site include those prepared by Packman (1980) and Sullivan (1987).

Commercial fisheries in this area harvest at least 10 species of fish (including the bottom-dwelling sole and grey cod), and the seafloor of the neighbouring delta slope along Point Grey and Sturgeon Bank is the site of trawling for 6 species of shrimp (Hoos, 1977). Clearly, given the presence of the dump site, there is conflict potential between fishing and dumping activities, and monitoring of the geographic range of each is essential. In this paper, the nature and geographic distribution of offshore dumping in this area will be presented. These results are based on side-scan sonar imagery of the sea floor, and illustrate the potential of this type of surveying to monitoring programs of offshore dump sites.

METHODS

The results presented here are based on two surveys conducted by the Geological Survey of Canada in February and May of 1991 on board the CSS Tully and CSS Parizeau respectively. Data collected on these cruises included high resolution seismic profiles (Huntec Deep Tow Seismic boomer system), 100 kHz side-scan sonar imagery (Klein 595 recorder with correction for slant range distortion), 12 kHz echo sounding profiles and piston and vibrocores. Navigation was performed using both GPS and Loran-C. Selective availability was off for both cruises, so that GPS locations are theoretically precise to within 20 m. Some preliminary results from the delta slope are reported by Hart et al. (1991). Sonographs collected in the vicinity of the Point Grey dump site (Fig. 1) from both cruises will form the primary database for this report.

IDENTIFICATION OF DUMPING ACTIVITIES AT POINT GREY

Side-scan sonar images of undisturbed portions of the lower Fraser delta slope and prodelta regions indicate that these areas are characterized by flat, featureless sea floor consisting of mud. The interpretation of substrate type is confirmed by earlier grab sampling of the sea floor throughout the central Strait of Georgia (Pharo and Barnes, 1976). However, south of the Point Grey dump site, in deep water offshore from Sturgeon Bank and between the Fraser Ridge and McCall Bank (Fig. 1), surveying revealed the previously undetected presence of a pockmark field (Figs. 2, 3a). These depressions are gas escape features which in this area vary from a few to over 80 m in diameter, and range up to 4 m deep. They are scattered over the otherwise undisturbed sea floor of this part of the prodelta region and, despite their proximity to the Point Grey disposal site, are considered to be a natural phenomenon (Hovland and Judd, 1988).

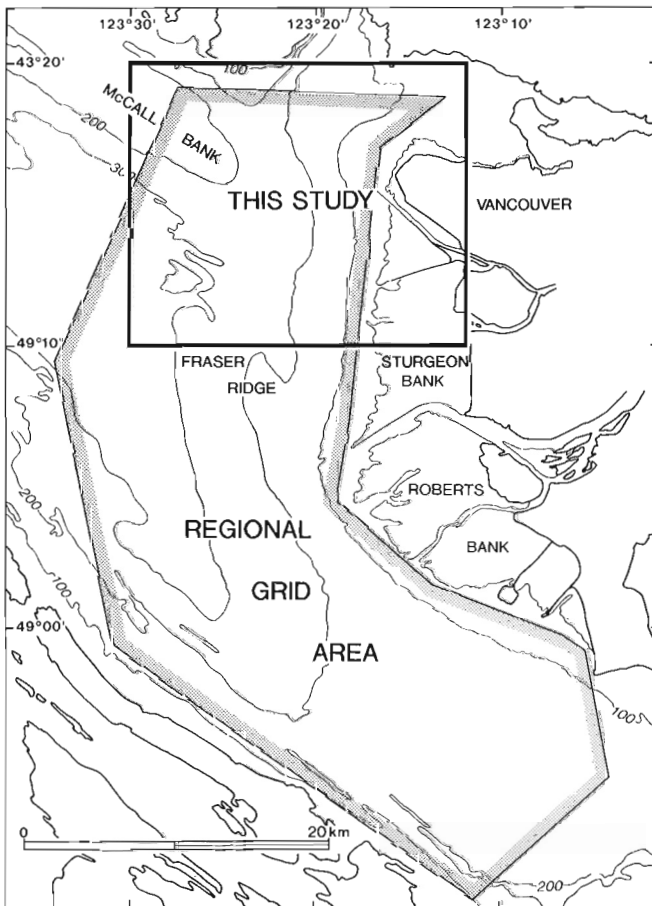


Figure 1. Location of study area.

In contrast to the homogeneous substrates observed over most deep water portions of the central strait, side-scan sonographs of the sea floor in the vicinity of the Point Grey dump site contain abundant evidence of anthropogenic disturbance (Figs. 2, 3). Perhaps the most prominent of these are circular to irregular dark patches many metres in diameter (Figs. 3b-d), of which two end member types can be recognized. The first consists of large patches many tens of metres in diameter. These patches tend to be somewhat irregular in outline, but occasionally a radial "splay" pattern can be observed (Fig. 3b) which suggests outward dispersal of material from a central source. The second type consists of linear or curvilinear successions of dark patches, each typically 15 to 20 m in diameter (Fig. 3c). Discrete patches (both types) are observable outside the dump site, but within the dump site itself the sea floor is almost completely covered by patches (Figs. 2,3d). In general, the patches close to or in the dump site tend to be quite dark on the sonographs, whereas a high proportion of patches outside the spoil zone appears as a lighter grey tone.

The patches are clearly surface features, as corresponding high resolution seismic records indicate that they do not represent surface exposure of otherwise buried "hard" substrates such as till; they are not associated with significant (greater than 1 or 2 m) sea floor mounds. The strong returns are suggestive of highly backscattering material such as sand, or material less porous than the surrounding sea floor (D'Olier, 1979). Repeat grab sampling using a grid centred on the dump site in 1975 and 1978 indicates that the sea floor in this region had very high sand contents (up to 55%) compared to the surrounding sea floor (less than 1%), and that the proportion of sand had increased in the 3 years between surveys (Packman, 1980; Fig. 4). The patches are thus interpreted as representing sandy dredge spoils deposited on the muddy sea floor.

Truitt (1988) described the behaviour of dumped material descending through the water column and indicated that its behaviour is a function of the initial mechanical properties of the sediment and their subsequent alteration by dredging operations. Sand was observed with piles of wood waste during submersible dives in 1978 (Packman, 1980), indicating that the piles of dumped material retained their integrity (i.e. were partly cohesive) while falling through the water column. The curvilinear trends of the 15 to 20 m patches are suggestive of repetitive spoil dumping (e.g. by bulldozer) from a moving barge; this is a common practice for disposal of dredgeate which has been dumped into a barge from a clamshell dredging operation (Levings, 1982). The larger patches probably represent disposal of larger quantities of sediment from self-emptying (bottom-opening) barges, the usual discharge method for hopper dredges (Levings, 1982). Both types of dumping operations occur at the Point Grey dump site (e.g. MacNeill, 1976). The radial pattern observed on some sonographs (e.g. Fig. 3b) appears to represent the effects of an outward density surge produced by the descending jet of dumped material as it impacts on the sea floor (Truitt, 1988).

Other types of anthropogenic refuse are also visible on the sonographs. These consist of generally unidentifiable, irregularly shaped side-scan "targets", typically several meters in length (Fig. 3d). Some of the targets can be found within craters which can be over 10 m in diameter (Fig. 3d). Submersible observations of the sea floor described by Packman (1980) indicate that concrete blocks and pipes, hardpan, miscellaneous rubble, cable, tires and other types of debris have been dumped in this area. Some of these items (presumably concrete blocks) must have been big enough to generate impact craters upon contact with the sea floor.

Sunken logs are also abundant in this area (e.g. Fig. 3d). One possible source for them are the booming grounds along the North Arm of the Fraser River. It should be noted that although these areas represent in essence an anthropogenic source of logs, Johnston (1921) indicated that logs have been retrieved from the sea floor in this area since the early part of this century. Thus it appears that natural processes must contribute an unknown proportion of the logs found on the sea floor at this locality.

The activity of bottom trawlers is also detectable with side-scan sonar imagery. Trawler marks are visible as curvilinear parallel grooves on the sea floor, typically 20-30 m apart; they have been detected on McCall Bank and Sturgeon Bank (Figs. 1, 2) and in two locations were observed to coincide with the location of dredge spoil tracks (Fig. 5). Trawler marks were not seen in proximity to "hard" debris such as concrete blocks or logs. Johnston (1921) noted that

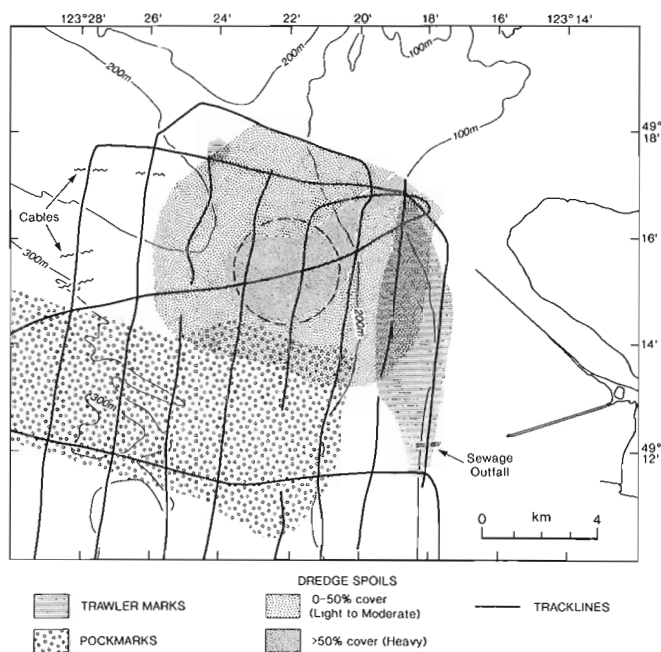


Figure 2. Sea floor features in vicinity of Point Grey dump site detected with side-scan sonar imagery. Dredge spoil cover is densest within limits of dump site (dashed circle), and in a corridor connecting the dump site and Vancouver Harbour. Zone of dredge spoil cover partially overlaps with zone of trawler marks, and pockmark field.

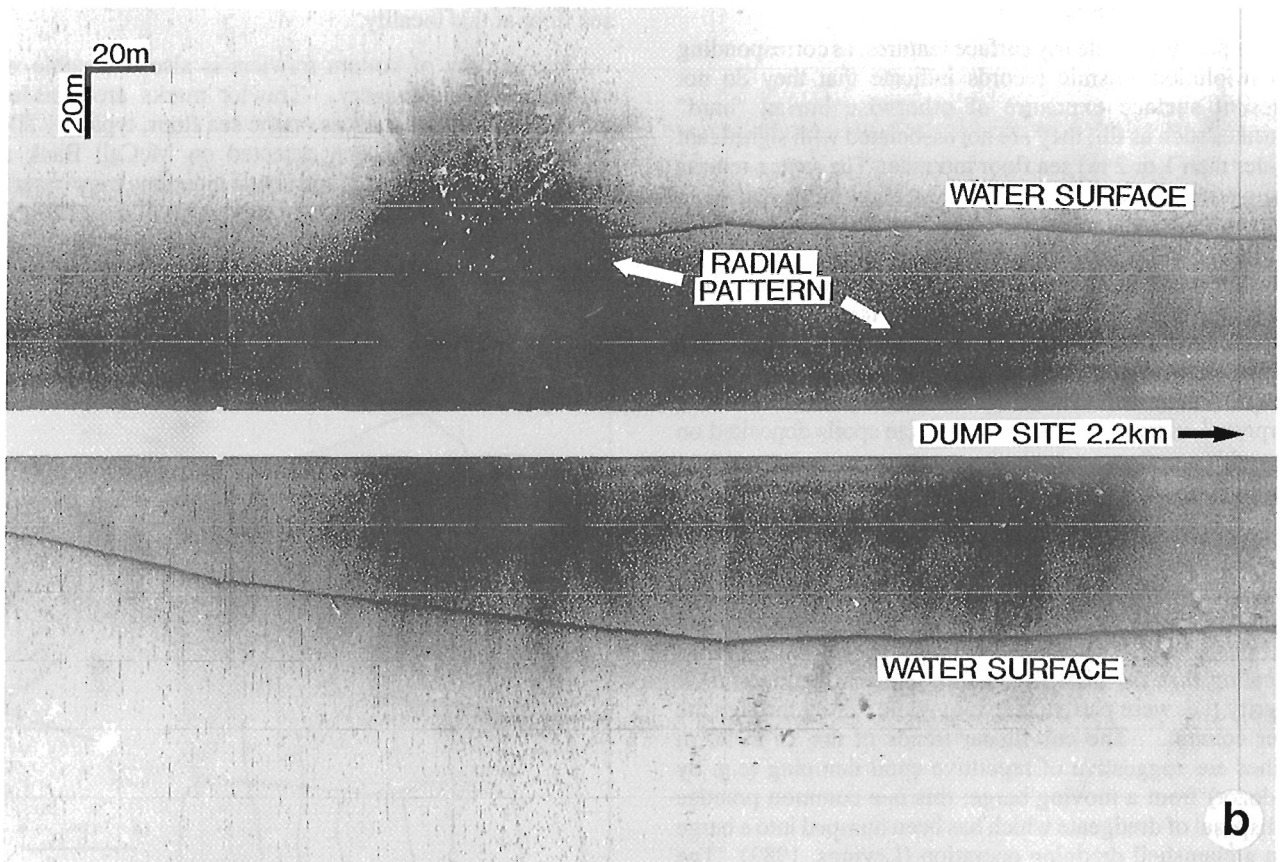
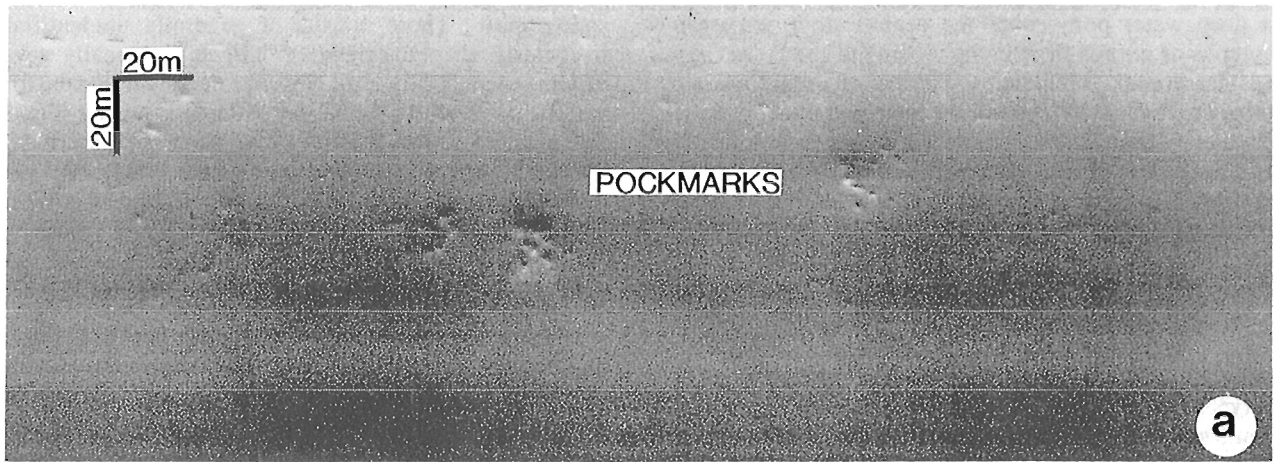
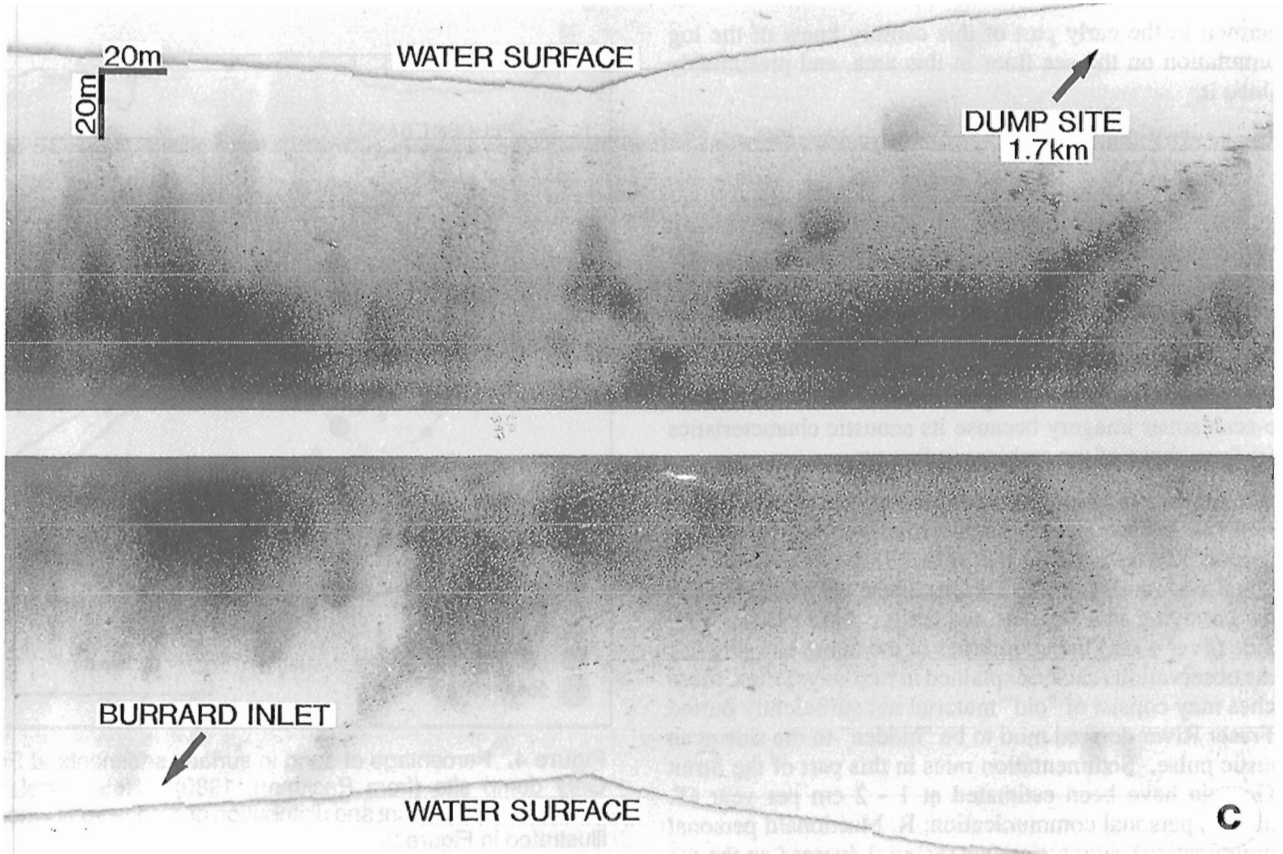


Figure 3. Side-scan sonographs of features on sea floor near Point Grey dump site. **a)** Pockmarks, gas escape depressions on sea floor between Fraser Ridge and McCall Bank. Diameters of some depressions exceeds 80 m. **b)** Dark patches several tens of metres in diameter showing radial splay pattern interpreted to represent outward density/momentum surge of dredged material produced upon impact with sea floor. **c)** Linear arrays of smaller dark patches interpreted to have been produced by repeated dumping of dredge material from a moving source. Orientation of spoil patches suggests dumping *en route* between Vancouver Harbour and Point Grey dump site. **d)** Heavy cover of sea floor in dump site by dredge spoil patches, sunken logs, and unidentifiable refuse.



fishermen in the early part of this century knew of the log accumulation on the sea floor in this area, and presumably avoided it.

DISCUSSION

Disposal of dredged material in deep water provides a convenient means of eliminating that sediment from coastal waterways. The dumped material is permanently removed from the shallow water sediment transport system, and hence cannot return to infill nearshore waterways - a problem common to shallow water dump sites (e.g. Levings, 1982). In the present case, the dumped material is detectable via side-scan sonar imagery because its acoustic characteristics differ from those of the ambient sediments.

Monitoring of dumping activities at this site has been carried out by the Vessel Traffic Management Service of Transport Canada since the mid-1980's (D. Brothers, personal communication). Despite these efforts, side-scan sonar surveying in 1991 detected dredge spoil patches well outside (over 4 km) the boundaries of the dump site (Fig. 2). These observations can be explained in two ways. First, these patches may consist of "old" material not sufficiently buried by Fraser River derived mud to be "hidden" to the side-scan acoustic pulse. Sedimentation rates in this part of the Strait of Georgia have been estimated at 1 - 2 cm per year (T. Hamilton, personal communication; R. Macdonald personal communication), suggesting that material dumped on the sea floor should be buried by 6 to 12 cm of mud in 6 years.

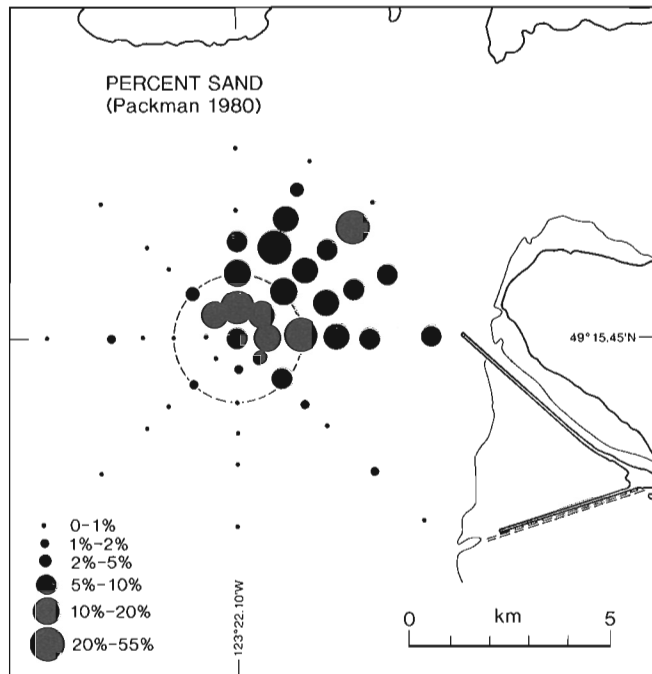


Figure 4. Percentage of sand in surface sediments at Point Grey dump site (from Packman, 1980). Note correlation between sand content and distribution of dredge spoil patches illustrated in Figure 2.

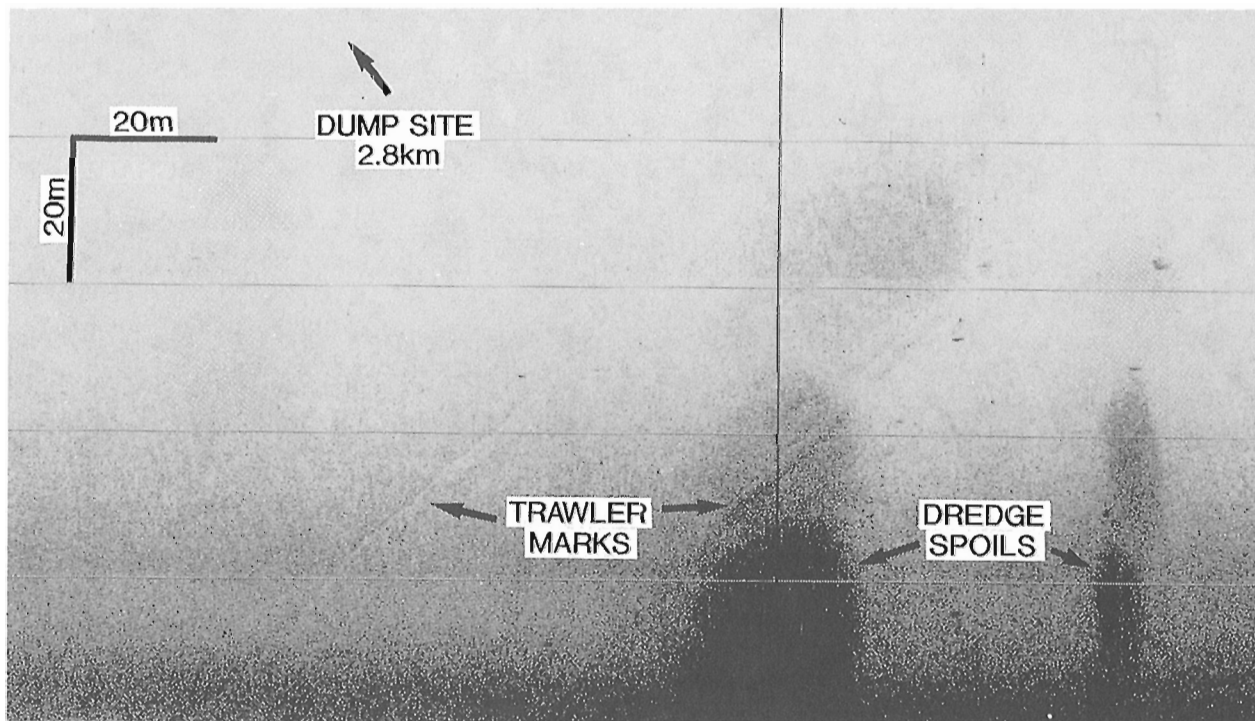


Figure 5. Coincidence of trawler marks and dredge spoil patches, McCall Bank.

The second alternative is that dumping continues outside of the established dump site. If, in a general way, the darkness of the dredge spoil patch on the sea floor represents its "freshness" (older patches being progressively buried by acoustically "softer" mud), then it does seem probable that many of the lighter grey spoil patches identified outside the dump site boundaries consist of "relict" dredge material, probably dumped before initiation of the mid-1980's monitoring program. Darker patches are still abundant in some areas, suggesting that dumping outside the spoil zone has not been completely curtailed.

Although the hydrographic charts clearly delineate the dumping site, there is a potential conflict due to the close proximity of fishing operations (e.g. Figs. 2,5) and the physical presence of the dredgeate; establishing which of the above possibilities is most likely becomes a critical issue. Repeat surveys of this area could resolve this question by detecting (or not) the presence of new dredge spoil patches. These results would be of use in establishing the need for focusing or intensifying monitoring of dumping activities.

Previous studies of the chemistry of bottom sediments at this site have experienced poor reproducibility of results between successive surveys. Sullivan (1987) suggested that this may be due to "heterogeneity of sediments at the dump site, changes in analytical procedures, contamination of samples after or during collection, or a combination of these variables". The results presented here indicate that the sea floor in this area is characterised by dredge spoil patches with diameters of tens of metres. Repeat sampling of exactly the same portion of the sea floor is unlikely, given the accuracy of most conventional navigation systems, and a 30 m diameter patch of contaminated sediments sampled on one survey could go undetected on subsequent visits to that site. This indicates that some of the poor reproducibility described by Sullivan can be explained by sediment heterogeneity on the sea floor.

SUMMARY

Side-scan sonar imagery of the sea floor near the Point Grey dump site readily detects dumped material since the acoustic characteristics of the spoils contrast with those of the ambient prodelta sediments. Despite current efforts to monitor waste disposal in this area, it appears probable that some dumping of dredged material continues outside the designated limits of the spoil zone, although the evidence suggests that such activities have decreased. Repeat side-scan sonar surveys of the sea floor here would be useful in evaluating the need for enhancing monitoring efforts. Similar surveys of other disposal sites could provide a means of quickly assessing the nature of dumping activities there, and act as a base for the establishment of chemical or biological studies of those areas.

ACKNOWLEDGMENTS

I thank the officers and crew of the C.S.S. Tully and C.S.S. Parizeau and the scientific staff of cruises PGC Cruises 91-01 and 91-04 for their efforts. My understanding of dumping operations has benefited from discussions with Duane Brothers (Environment Canada) and Robie Macdonald (Fisheries and Oceans). Vaughn Barrie and Duane Brothers are thanked for their helpful reviews.

REFERENCES

- D'Olier, B.**
1979: Side-scan sonar and reflection seismic profiling; in *Estuarine Hydrography and Sedimentation* (ed. by K.R. Dyer), Cambridge University Press, New York, p. 57-86.
- Hart, B.S., Barrie, J.V., Currie, R.G., Luternauer, J.L., Prior, D.B. and Macdonald, R.D.**
1991: High resolution seismic and side-scan sonar mapping of the Fraser Delta front and adjacent Strait of Georgia, British Columbia; in *Current Research, Part E; Geological Survey of Canada, Paper 91-1E*, p. 19-23.
- Hoos, R.A.W.**
1977: Environmental assessment of an ocean dumpsite in the Strait of Georgia, B.C.; Environmental Protection Service, Report No. EPS-5-PR-77-2, 31 p.
- Hovland, M. and Judd, A.G.**
1988: Seabed Pockmarks and seepages; Graham and Trotman, Boston, 293 p.
- Johnston, W.A.**
1921: Sedimentation of the Fraser River Delta; Geological Survey of Canada Memoir 125, 46 p.
- Levings, C.D.**
1982: The ecological consequences of dredging and dredge spoil disposal in Canadian waters; National Research Council Canada Report 18130, 142 p.
- MacNeill, M.**
1976: Study of dispersion of dumped materials in Georgia Strait (Point Grey); Dobrocky Seatech Ltd. Report to Ocean Chemistry, Institute of Ocean Sciences, 58 p.
- Packman, G.**
1980: An environmental assessment of the Point Grey ocean disposal area in the Strait of Georgia, British Columbia; Environmental Protection Service (Pacific) Regional Program Report 80-3, 79 p.
- Pharo, C.H. and Barnes, W.C.**
1976: Distribution of surficial sediments of the central and southern Strait of Georgia, British Columbia; Canadian Journal of Earth Sciences, v. 13, p. 684-696.
- Sullivan, D.L.**
1987: Compilation and assessment of research, monitoring and dumping information for active dump sites on the British Columbia and Yukon coasts from 1979 to 1987; Department of Environment, Pacific Region Ocean Dumping Advisory Committee, Report 87-02.
- Truitt, C.L.**
1988: Dredged Material Behaviour during open water disposal; Journal of Coastal Research, v. 4, p. 389-397.

Geological Survey of Canada Project 890052

Reinterpretation of the Clachnacudainn terrane and Standfast Creek fault, southern Omineca Belt, British Columbia

James L. Crowley¹, Richard L. Brown¹, and Stephen E. Crowley²
Cordilleran Division, Vancouver

Crowley, J.L., Brown, R.L., and Crowley, S.E., 1992: Reinterpretation of the Clachnacudainn terrane and Standfast Creek fault, southern Omineca Belt, British Columbia; in *Current Research, Part A; Geological Survey of Canada, Paper 92-1A*, p. 63-70.

Abstract

Stratigraphic, structural, and metamorphic evidence from recent fieldwork indicates that the Clachnacudainn terrane is an integral part of the Selkirk allochthon. Major isoclinal folds in the lower Paleozoic Hamill Group, Badshot Formation, and Lardeau Group extend throughout the terrane and into the overlying allochthon. Regional metamorphic isograds are not appressed or omitted across the Standfast Creek fault (the upper boundary of the terrane). These observations suggest that the fault is an insignificant tectonic feature that is attributable to fold limb attenuation and/or local brittle displacement on a scale of metres. The Clachnacudainn terrane therefore cannot be a distinct terrane or a high grade salient of the Shuswap metamorphic complex that was denuded in the Eocene. The relatively large volume of late- to post-tectonic plutonism in the Clachnacudainn igneous complex is the main aspect that distinguishes the terrane from the remainder of the allochthon.

Résumé

Des données stratigraphiques, structurales et métamorphiques recueillies récemment sur le terrain indiquent que le terrane de Clachnacudainn fait partie intégrante de l'allochtone de Selkirk. D'importants plis isoclinaux dans la partie inférieure du groupe de Hamill du Paléozoïque, dans la formation de Badshot et du groupe de Lardeau, affectent tout le terrane et même l'allochtone sus-jacent. Les isogrades métamorphiques régionaux ne sont ni trop proches ni omis à travers la faille du ruisseau Standfast (la limite supérieure du terrane). Ces observations révèlent que la faille est un élément tectonique important attribuable à une atténuation des flancs des plis et (ou) à un déplacement cassant local d'échelle métrique. Le terrane de Clachnacudainn ne peut pas, par conséquent, être un terrane distinct ou une saillie à degré de métamorphisme élevé du complexe métamorphique de Shuswap dénudé durant l'Éocène. Le plutonisme de tectonisme tardif à postérieur et relativement volumineux observé dans le complexe ignée de Clachnacudainn est le principal élément qui distingue le terrane du reste de l'allochtone.

¹ Department of Earth Sciences, Carleton University and Ottawa-Carleton Geoscience Centre, Ottawa, Ontario K1S 5B6

² Department of Geology, Amherst College, Amherst, Massachusetts U.S.A. 01002

INTRODUCTION

The Clachnacudainn terrane has been considered to be one of three slices of the Selkirk allochthon in the southern Canadian Cordillera (Fig. 1; Brown and Lane, 1988). Selkirk allochthon metasediments include Upper Proterozoic and lower Paleozoic North American continental margin deposits and more distal, possibly marginal-basin sediments of the Kootenay suspect terrane. At the latitude of the Clachnacudainn terrane, the Selkirk allochthon is separated from the underlying Monashee complex by the east-dipping compressional Monashee décollement and the superposed shear zone of the extensional Columbia River fault (Brown and Lane, 1988). The allochthon was displaced at least 80 km eastward onto the North American foreland on the mylonitic shear zone of the Monashee décollement possibly starting in the Jurassic (Read and Brown, 1981), with latest motion occurring in the Late Cretaceous and Paleocene (Journeay, 1986; Journeay and Brown, 1986; Parrish et al., 1988; Carr, 1990). Further east-directed displacement of the allochthon occurred on the Columbia River fault in the Eocene (Read and Brown, 1981; Parrish et al., 1988).

The Clachnacudainn terrane has been interpreted as a distinct part of the Selkirk allochthon, thought to differ profoundly in structural, metamorphic, and lithological aspects from the overlying Illecillewaet and Goldstream slices. These interpretations suggest the Clachnacudainn terrane is one or more of the following: i) a separate deeper tectonic level, termed the infrastructure (Thompson, 1972; Sears, 1979); ii) a high grade salient of the Shuswap metamorphic complex that is juxtaposed against the considerably lower grade overlying slices (Price et al., 1981); iii) a suspect terrane that was driven eastward as a wedge beneath the allochthon, thereby delaminating the crust (Price, 1986); iv) a structural horse accreted to the hanging wall of the Monashee décollement during initial stages of development of a duplex within the Monashee complex (Brown and Lane, 1988); v) part of the middle crust that was denuded and rapidly cooled during Eocene ductile extension (Parrish et al., 1988). The upper boundary of the terrane, the Standfast Creek fault, has therefore been interpreted as the zone of accommodation between the terrane and the rest of the allochthon. Hypotheses about motion along the Standfast Creek fault were derived to fit the different interpretations of the Clachnacudainn terrane. These hypotheses (outlined by Crowley et al., 1991), include, among others, early east-directed thrusting (Brown and Lane, 1988), west-directed thrusting (Price, 1986), and Eocene ductile extension (Parrish et al., 1988).

The initial goal of this study was to determine the timing, amount, and direction of motion on the Standfast Creek fault. After fieldwork in 1990, Crowley et al. (1991) suggested that the fault had a complex displacement history and that major motion on the ductile portion of the fault was not required by the data but could not be ruled out. Since it was realized that understanding the fault would require studying more than just the fault zone itself, fieldwork this past summer was carried out over most of the footwall (Clachnacudainn terrane) and the adjacent hanging wall (Illecillewaet slice). A reinterpretation of the Clachnacudainn terrane is offered

based on new evidence from the recent fieldwork concerning its stratigraphy, vergence of major folds, metamorphism, the Clachnacudainn igneous complex, and the Standfast Creek fault.

STRATIGRAPHY

Illecillewaet slice

Lithologies in the Illecillewaet slice are more readily correlated than those in the Clachnacudainn terrane because the fossiliferous marble of the lower Middle Cambrian Badshot Formation forms a marker horizon (Thompson, 1972). The Badshot marble is conformably underlain by the light green calcareous phyllite and minor pelite of the Mohican Formation of the Eocambrian Hamill Group, and

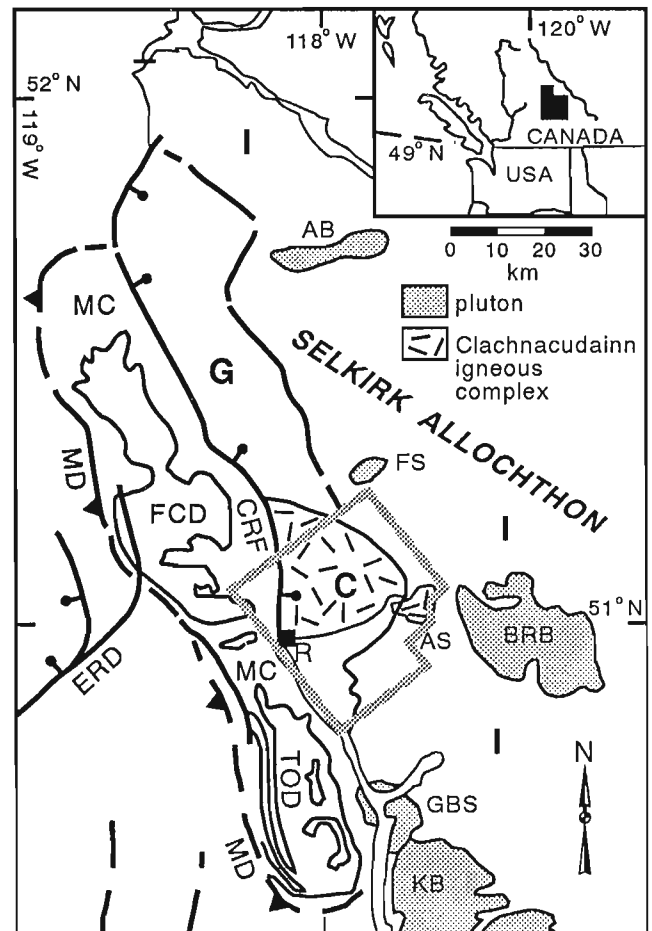


Figure 1. Major tectonic features of the northern Selkirk Mountains, modified from Brown and Lane (1988). Selkirk allochthon is composed of Clachnacudainn terrane (C), Goldstream slice (G), and Illecillewaet slice (I). Features in the Monashee complex (MC) are Frenchman Cap dome (FCD) and Thor-Odin dome (TOD). Faults are Columbia River fault (CRF) and Eagle River detachment (ERD). Plutons are Adamant batholith (AB), Albert stock (AS), Battle Range batholith (BRB), Fang stock (FS), Galena Bay stock (GBS), and Kuskanax batholith (KB). Area outlined by the grey box is shown in more detail in Figure 2.

that by the clean, massive tan quartzite of the Marsh Adams and Mount Gainer formations of the Hamill Group. The Badshot marble is conformably overlain by the typically dark blue to black graphitic phyllite correlated with the Index Formation of the lower Paleozoic Lardeau Group. The siliceous marbles in the Albert Peak and Albert Canyon areas are correlated with the Lade Peak Formation of the Lardeau Group (Zwanzig, 1973; Sears, 1979).

Clachnacudainn terrane

Read and Thompson (1980) recognized that Clachnacudainn terrane stratigraphy may be correlative with that in the overlying Selkirk allochthon and suggested that the terrane is composed of mostly inverted Lardeau Group. Our work is in general agreement with their lithological interpretation (Fig. 2). Clean tan quartzite, micaceous quartzite, and garnet-biotite schist at the head of the East Twin and West Twin creeks is correlated with the Marsh Adams, Mount Gainer, and Mohican formations of the Hamill Group; the adjacent marble is most likely Badshot. Dark blue to black graphitic phyllite with minor marble that directly underlies the Badshot marble in the hanging wall of the Standfast Creek fault in the Ghost Peak area is readily correlated with the Index Formation. The graphitic phyllite is underlain by more siliceous rocks within the Lardeau Group. The section of interlayered dark blue phyllite, chloritic phyllite, micaceous quartzite, quartzite, amphibolite, and marble that underlies the Badshot Formation on the ridges south of Mount LaForme and north of West Woolsey Creek also resembles parts of the Lardeau Group. The siliceous Lardeau is conformably underlain by an amphibolite-marble \pm chloritic phyllite package that is continuous for nearly the entire north-south length of the Clachnacudainn terrane. This package is correlated with the Jowett Formation of the Lardeau Group. The marble-amphibolite package is underlain by light green and purple siliceous phyllite, micaceous quartzite, and metaconglomerate of the Broadview Formation. These units are folded into complex isoclines within the Clachnacudainn terrane.

Discussion of stratigraphy

Crowley et al. (1991) tentatively correlated most of the Clachnacudainn terrane with the Horsethief Creek Group based on an amphibolite package (thought to be equivalent to the semipelite amphibolite unit) that is overlain by a marble-bearing lithology higher in the terrane (thought to be middle marble member). During recent fieldwork this section was studied in more detail, and we now consider that Read and Thompson's (1980) correlation of terrane stratigraphy with Lardeau Group is correct. The amphibolite is everywhere intimately interbedded with marble and calc-silicate, forming a package that resembles more closely the Jowett Formation rather than the semipelite amphibolite unit of the Horsethief Creek Group. The marble-bearing sequence that occurs higher in the terrane is interlayered with dark blue to black graphitic phyllite that strongly resembles the Index Formation rather than the middle marble member of the Horsethief Creek Group.

VERGENCE OF THE MAJOR FOLDS

Thompson (1972) mapped two recumbent isoclines with amplitudes approaching 6.5 km in the base of the Illecillewaet slice and concluded that they have an easterly sense of vergence. Our mapping of minor folds and stratigraphy across these isoclines indicates that these folds are more likely west-verging structures (Fig. 2).

Akolkolex anticline

Recent mapping of the change of vergence of minor folds across the Akolkolex anticline in the well-exposed cirque at the head of the southernmost tributary of Standfast Creek indicates that the anticline is southwest-verging. These minor folds are thought to be parasitic to the major fold because they have the same geometry and orientation as the larger structure. Observed to the southeast, down the shallow plunge of the hinge line, the minor folds in the upper limb of the anticline are Z-shaped, those in the core are M-shaped, and those in the overturned limb are S-shaped. Bedding-cleavage relationships in the Hamill quartzite also require a southwest-verging fold. These observations, along with the fact that the structure has an easterly-dipping axial surface with Hamill quartzite exposed in the core, requires that the Akolkolex anticline is a southwest-verging antiformal anticline in this location.

Thompson (1972) mapped the Akolkolex anticline as a northeast-verging synformal structure, based on a closure in a cliff face east of lower Standfast Creek (Thompson, 1972, Plate 4-5) and on asymmetric isoclinal folds in a cliff face east of upper West Twin Creek (Thompson, 1972, Plate 4-6). In our view these data are ambiguous concerning the vergence of the Akolkolex anticline. In the former location, the trend of the fold hinge line is nearly parallel to the cliff face; a slightly more southerly hinge line trend than that inferred by Thompson (1972) would imply a southwest-verging anticline. In the latter location, it is not known whether the asymmetrical folds occur in the upper or lower limb of the structure; a fold axial surface within the thick section of Mohican Formation in the lower portion of the cliff would imply a southwest-verging anticline. The Badshot Formation is not observed at this locality in the inferred overturned limb, but this is a common attribute of the overturned limb of the Akolkolex anticline (Thompson, 1972).

A southwest-verging sheath fold geometry (a canoe-shaped, doubly plunging fold) would reconcile our minor fold observations with Thompson's (1972) observations, and would also account for the apparent closure of the anticline to the south, northeast of McCrae Peak. Although Thompson (1972) did not map a closure in the McCrae Peak area, the width of the Hamill Group in the core is drastically reduced, suggesting that the anticline tightens and may close in the poorly exposed ground south of Thompson's (1972) map area. Given the available data, the Akolkolex anticline is therefore tentatively interpreted as a west-verging antichlinal sheath fold. More study is clearly

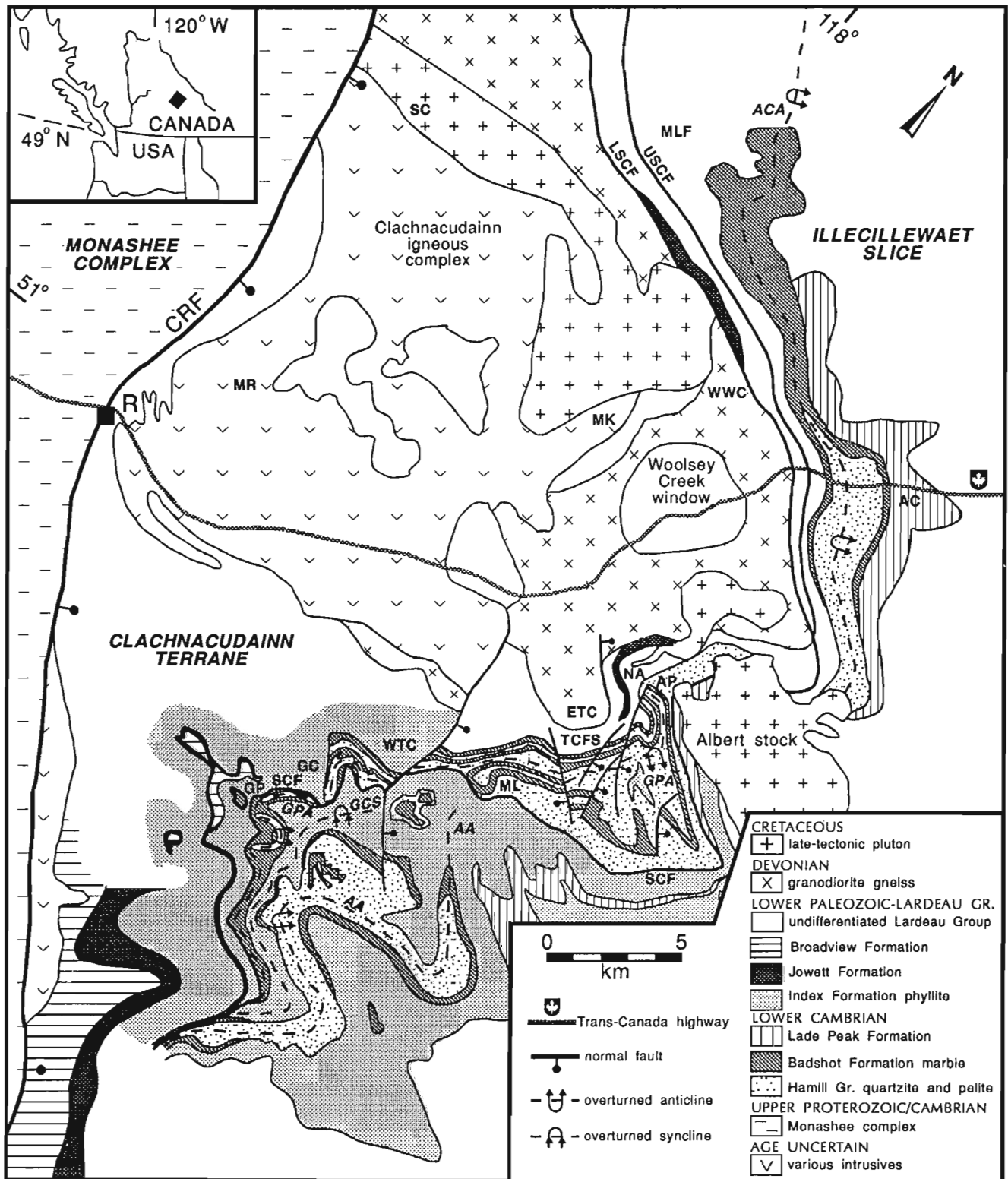


Figure 2. The Clachnacudainn terrane and adjacent Illecillewaet slice, based on data from Thompson (1972), Zwanzig (1973), Sears (1979), Price (1986), and this study. Faults are Standfast Creek fault (SCF), lower Standfast Creek fault (LSCF), upper Standfast Creek fault (USCF), Twin creeks fault system (TCFS), and Columbia River fault (CRF). Other geological features are Albert Canyon anticline (ACA), Akolkolex anticline (AA), Greeley Creek syncline (GCS), and Ghost Peak anticline (GPA). Geographical features are Albert Canyon (AC), Ghost Peak (GP), Greeley Creek (GC), Mount LaForme (MLF), Mount Klotz (MK), Mount Llewellyn (ML), Albert Peak (AP), North Albert Peak (NA), Mount Revelstoke (MR), West Twin Creek (WTC), East Twin Creek (ETC), West Woolsey Creek (WWC), Sale Creek (SC), and Revelstoke (R).

needed in this area to determine if the structure closes in the south and if the minor folds record the rotation of the sheath fold hinge line.

Ghost Peak anticline

Thompson (1972) mapped the antiformal Drimmie Creek syncline beneath the Akolkolex anticline as a northeast-verging structure based on stratigraphy. This structure directly overlies the Standfast Creek fault mapped by Thompson (1972). We agree with Thompson (1972, Plate 4-7) that the structure closes to the west within Ghost Peak, an erosional remnant of the thickened hinge zone cored by Badshot marble (Fig. 3). We also agree that the axial surface is outlined directly southeast of Ghost Peak by a thin band of clastic rock sandwiched between the Badshot marble in the upper and lower limbs. The vergence of the isocline depends on the correlation of this clastic rock in the core. Thompson (1972) correlated it with the Index Formation of the Lardeau Group, thereby requiring the structure to be a syncline. We, however, correlate it with the Hamill Group, thereby requiring the structure to be an anticline. This correlation is based on the predominance of thick-bedded, noncalcareous, clean quartzite that bears a strong resemblance to Hamill in the core of the Akolkolex anticline. The minor garnet-bearing pelitic and calcareous interlayers are more readily correlated with the Mohican Formation than the Index Formation. The dark blue to black graphitic phyllite that typifies the Index Formation in contact with the underlying Badshot marble in nearby localities (Fig. 4) is entirely absent from this section. The Index Formation comprises quartzite, but it occurs higher in the formation and is not seen adjacent

to the Badshot marble in the study area. Hamill quartzite and Mohican phyllite are also exposed in the core of this isocline in the cliffs directly east of Ghost Peak (shown in Plate 4-7 of Thompson, 1972). In order to avoid confusion, we name this west-verging antiformal anticline the Ghost Peak anticline, since the peak prominently displays the thickened hinge zone (Fig. 3).

Since the dark blue to black phyllite beneath Ghost Peak is correlatable with the Index Formation, as first suggested by Read and Thompson (1980), then the Index in the hanging wall of the Standfast Creek fault is traceable over the Ghost Peak anticline into the footwall. The Ghost Peak anticline is therefore responsible for inverting the Lardeau Group beneath Ghost Peak.

We suggest that the Ghost Peak anticline continues northeast of Ghost Peak through Mount Llewelyn into the Albert Peak area. Over this interval, recumbent isoclinal folds in the Clachnacudainn terrane involve up to seven marble layers separated by micaceous quartzite, clean quartzite, garnet-biotite schist, and black graphitic phyllite. Read and Thompson (1980) correlated the marble with the Badshot Formation and the siliceous clastics with Hamill. The black graphitic phyllite is probably Index in the core of an appressed west-verging syncline noted by Thompson (1972). Thompson (1972) also found stratigraphic evidence for a west-verging anticline at the head of Standfast Creek. Thompson (1972), however, did not find stratigraphic evidence within the clastics for folds repeating all the layers, and Sears (1979) found no evidence of folding. The high variability in clastic lithology both along and across strike may be responsible for the obscurity.



Figure 3. South face of Ghost Peak, an erosional remnant of the thickened hinge zone of the Ghost Peak anticline composed of Badshot marble. Index Formation dark blue graphitic phyllite is separated from the overlying Badshot marble by a brittle normal fault that overprints a ductile shear zone with minor displacement. These faults occur at the Standfast Creek fault mapped by Thompson (1972).



Figure 4. Contact zone between the Badshot Formation marble and Index Formation dark blue graphitic phyllite, east of the head of Drimmie Creek along the overturned limb of the Akolkolex anticline. The clasts of marble within the phyllite are interpreted to represent a stratigraphic rather than tectonic contact.

The Albert stock intrudes the anticline in the vicinity of Albert Peak. North of Albert Peak, this same structure may continue as the Albert Canyon anticline, a west-verging isocline that is cored by Hamill with attenuated Badshot marble in the limbs (Zwanzig, 1973). From the Albert Peak area northward, the Lade Peak Formation occurs in the upright limb between the Badshot and Index formations (Zwanzig, 1973; Sears, 1979). The Albert Canyon anticline continues north of the Trans-Canada Highway to the Mount LaForme area.

Greeley Creek syncline

The intervening syncline cored by the Index Formation between the Ghost Peak anticline and Akolkolex anticline is named the Greeley Creek syncline, based on the creek that flows north from the core of the structure.

Folds within the Clachnacudainn terrane

At least one recumbent west-verging anticline-syncline pair occurs in the Clachnacudainn terrane beneath Ghost Peak. The amphibolite-marble package in the Jowett Formation and the dark blue graphitic phyllite in the Index Formation serve as marker units that outline these folds. Thick vegetation on the slopes above the Columbia River make these interpretations considerably more conjectural than interpretations of structures exposed in the alpine to the east.

Discussion of west-verging folds

West-verging large-scale isoclines, such as the Albert Canyon anticline (Zwanzig, 1973) and the Carnes nappe (Brown and Lane, 1988), are major structures within the Selkirk allochthon. If reinterpretation of Thompson's (1972) northeast-verging folds as west-verging structures that continue into the Clachnacudainn terrane is confirmed, then structural style in the terrane is similar to that in the rest of the Selkirk allochthon.

The vergence of minor folds changes across the axial surface of the Akolkolex anticline. It is suggested that these minor folds are local second phase structures that are parasitic to the Akolkolex anticline. It is suggested that the Ghost Peak anticline is a first phase fold in the overturned limb of the Akolkolex anticline based on an absence of a minor fold vergence change.

METAMORPHISM

The assertion by Price et al. (1981) that the Standfast Creek fault severely appressed or omitted metamorphic isograds was used to support a model of Eocene ductile denudation and rapid cooling of the Clachnacudainn terrane (Parrish et al., 1988).

The supposed dramatic increase in regional metamorphic grade across the Standfast Creek fault has not been documented and no evidence for it was found in this study. Garnet-bearing schists are the highest grade rocks

documented by Gilman (1972) in the footwall metasediments within the Woolsey Creek window. Zwanzig (1973) mapped garnet and staurolite in both the footwall and hanging wall. Sears (1979) documented a maximum of garnet grade of regional metamorphism in the footwall. Thompson (1972) documented a narrow zone of sillimanite- and kyanite-bearing schist within and directly above the gneiss, leucogranite, and diorite that occur structurally more than 2 km below the fault. This study has documented kyanite- and staurolite-bearing schist at the base of the Clachnacudainn terrane south of the Trans-Canada Highway, garnet-bearing schist throughout the terrane south of the highway and in pelite in the hanging wall, and sillimanite- and andalusite-bearing schist in metasedimentary screens within undeformed granitoids in the Clachnacudainn Range. The screens within the granodiorite gneiss do not contain sillimanite or kyanite (Gilman, 1972; Zwanzig, 1973), possibly because of retrogression during later thermal events or because of a low alumina content.

The sillimanite- and andalusite-bearing schist in the Clachnacudainn Range is invariably engulfed by intrusives that are possibly coeval with the Albert stock. The sillimanite and andalusite isograds associated with the contact aureole of the Albert stock postdate the Standfast Creek fault, all penetrative ductile structures, and regional metamorphic isograds (Sears, 1979). Based on field study and textural relationships in thin section, we consider the sillimanite in the Clachnacudainn Range to be also of contact metamorphic origin.

Discussion of metamorphism

Upon distinguishing between contact and regional metamorphism, it is clear that isograds are not appressed or omitted across the upper boundary of the Clachnacudainn terrane. This evidence is in agreement with the stratigraphic relationships that require little or no motion along the Standfast Creek fault.

Parrish et al. (1988) inferred Eocene-age tectonic denudation and rapid cooling of the Clachnacudainn terrane based on sharp thermal and geochronological contrasts across the Standfast Creek fault. These contrasts consist of 45-60 Ma K-Ar mica cooling ages in the footwall juxtaposed against generally older than 100 Ma K-Ar ages in the hanging wall. All the footwall sample localities (Parrish et al., 1988, Fig. 1) are from the Clachnacudainn Range, which is heavily intruded by multiple igneous phases. The leucogranite phase, a sample of which from Mount Revelstoke is dated as 70 Ma by U-Pb zircon method (R.R. Parrish, pers. comm., 1991), could be the heat source that is responsible for the Eocene footwall ages. The K-Ar mica cooling dates from the Clachnacudainn Range are possibly recording young intrusions in the footwall, and therefore do not require the hypothesis of ductile denudation and rapid cooling of the terrane. A K-Ar mica cooling age traverse across the Standfast Creek fault beginning in the intrusive-free southern portion of the terrane would be considerably more conclusive. A P-T study currently underway should also provide more evidence on Clachnacudainn terrane metamorphic conditions.

CLACHNACUDAINN IGNEOUS COMPLEX

The Clachnacudainn salient of the Shuswap metamorphic complex was originally termed by Wheeler (1965) to only include the great variety of granitic rocks with metasediment screens that occur northeast of Revelstoke in the Clachnacudainn Range. The Clachnacudainn salient subsequently came to include the metasediments in the southern half of the Clachnacudainn terrane. We propose the term Clachnacudainn igneous complex for the multiple intrusive phases that occur mainly within the Clachnacudainn Range but also in the Albert Peak area and at the base of the terrane south of Revelstoke. The undeformed intrusives in the complex have contact metamorphosed the metasedimentary screens to sillimanite grade. The Albert stock, which straddles the border between the Clachnacudainn and Illecillewaet slices, is the only body that has been studied and named (Sears, 1979). Therefore, the following description is based on sparse data.

Description

The complex contains three deformed, one partly deformed, and at least seven intrusive phases that postdate the majority of the ductile deformation. The only dated deformed body is hornblende-biotite granodiorite gneiss that is dated by U-Pb zircon method as Devonian (R.R. Parrish, unpub. data, reported in Price et al., 1981). Price et al. (1981) and Crowley et al. (1991) suggested that the gneiss is a recrystallized mylonite related to the Standfast Creek fault. However, identical looking fabric in hornblende-biotite gneiss at the base of the Clachnacudainn terrane suggests that the gneissosity is unrelated to the Standfast Creek fault. The other deformed intrusives are leucogranite and a large volume

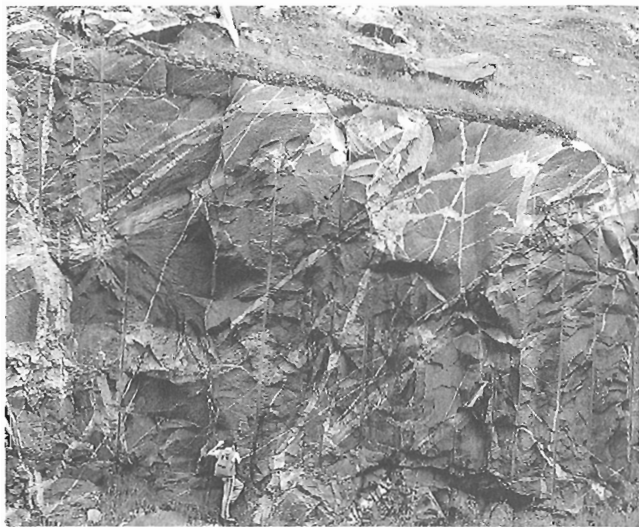


Figure 5. Southwest-verging folds (view is to southeast) of leucogranite dykes within Devonian granodiorite gneiss, 2 km west of Albert Canyon station along the railroad. The fabric within the gneiss is axial planar to the southwest-verging folds and is overprinted by a second generation of leucogranite dykes. The geologist in bottom centre of photo is the scale.

of variably foliated, blue, fine grained diorite. The leucogranite postdates the diorite and Devonian granodiorite gneiss and is deformed by west-verging folds (Fig. 5). The partly deformed body is a K-feldspar megacrystic granite that is mylonitized at the base of the Clachnacudainn terrane by the Monashee décollement (Brown and Murphy, 1982). A sample of this megacrystic granite from near Sale Creek is dated as mid-Cretaceous by U-Pb zircon method (R.L. Armstrong, unpub. data; R.R. Parrish, pers. comm., 1990). This body is undeformed where it crosscuts the Devonian granodiorite gneiss and is postdated by an undeformed granitoid and diorite plutons to the southeast.

The largest volume intrusive that postdates the ductile deformation is hornblende biotite quartz monzonite that occurs in the Albert stock and on the ridge north of West Woolsey Creek. Hornblende from the Albert stock gives a K-Ar date of 100 Ma (reported in Price et al., 1981). U-Pb zircon age of the quartz monzonite phase of the Albert stock is forthcoming. Other plutons that postdate ductile deformation are composed of muscovite biotite granite and dark green hornblende diorite. Phases that postdate the voluminous plutons include fine grained granite, leucogranite, and pegmatite. A slightly foliated leucogranite sampled from the top of Mount Revelstoke is dated as 70 Ma by U-Pb zircon method (R.R. Parrish, pers. comm., 1991). These intrusives that postdate the majority of the ductile deformation are deformed by late brittle deformation. The minor basalt and andesite dykes that comprise the youngest phase in the Clachnacudainn igneous complex appear to postdate the brittle deformation.

STANDFAST CREEK FAULT

Displacement along the Standfast Creek fault south of the Trans-Canada Highway, as mapped by Thompson (1972) and Sears (1979), must be minimal according to stratigraphic constraints. In the Ghost Peak area, the Standfast Creek fault juxtaposes Badshot marble in the hanging wall against Index graphitic phyllite in the footwall, with minor shearing between the two along the overturned limb of the Ghost Peak anticline (Fig. 3). At the head of Standfast Creek, graphitic Index phyllite in the hanging wall is juxtaposed against Hamill quartzite and schist in the footwall. The Standfast Creek fault attenuated the Badshot marble along this section. In the Albert Peak area, the Lade Peak Formation, a possible facies of the Badshot marble, is juxtaposed against Hamill quartzite. Minor shearing along the attenuated, overturned limbs of the Ghost Peak and Albert Canyon anticlines can account for these displacements.

North of the Trans-Canada Highway the two branches of the Standfast Creek fault shown in Price et al. (1981) are also limited in displacement by stratigraphic constraints. The upper Standfast Creek fault is both a brittle strike-slip and a normal (hanging-wall-to-the east) fault within the Lardeau Group. The lower Standfast Creek fault is partly an intrusive contact between Lardeau Group in the hanging wall and hornblende quartz monzonite and Devonian granodiorite gneiss in the footwall and partly a strike-slip fault between Lardeau and the gneiss.

Brittle faults

Parrish et al. (1988) speculated that the extensional part of the Standfast Creek fault diverges from the compressional part south of the highway. They hypothesized that the predominantly ductile normal fault forms the boundary between Devonian granodiorite gneiss and metasediment. This boundary was observed to be a brittle normal fault on the ridge west of North Albert Peak and an intrusive contact on the north side of this ridge. An undeformed dyke from the Albert stock crosscuts the intrusive contact. The brittle fault is probably related to the Twin creeks fault system, a series of high angle east- and west-dipping normal faults mapped by Sears (1979) and Thompson (1972) that have a maximum of a few hundred metres of displacement. A low-angle east-dipping brittle fault with limited displacement occurs beneath Ghost Peak at the Badshot-Index contact and cuts down into underlying Index to the south. A series of low angle east-dipping brittle faults in the Albert Peak area postdate the Albert stock. These faults must have a minimal amount of motion because the rock types are identical across the fault. Other brittle faults of note are the strike-slip faults within Devonian gneiss along the Trans-Canada Highway, south of Mount LaForme, and west and north of North Albert Peak. A brittle strike-slip fault also occurs between similar rock types at the upper Standfast Creek fault mapped by Price et al. (1981) on the ridge north of West Woolsey Creek.

SUMMARY

Recent fieldwork has resulted in these findings: i) the Clachnacudainn terrane is composed mostly of Hamill, Badshot, and Lardeau stratigraphy; ii) large-scale isoclines, with an overall west-vergence, occur throughout the terrane and into the overlying Illecillewaet slice; iii) there is no break in metamorphic grade across the upper boundary of the terrane; iv) intrusives in the Clachnacudainn igneous complex are responsible for the sillimanite grade contact metamorphism in the surrounding metasediments; v) minor brittle faulting and phase three folding are the only deformational events that postdate emplacement of most intrusives in the Clachnacudainn igneous complex; vi) motion along the Standfast Creek fault south of the Trans-Canada Highway is minimal, and north of the highway the fault is nonexistent. These findings indicate that the Clachnacudainn terrane has stratigraphic, structural, and metamorphic continuity with the overlying Selkirk allochthon. The distinguishing feature of the terrane is the strong igneous component, the Clachnacudainn igneous complex. The Clachnacudainn terrane is therefore an integral part of the Selkirk allochthon, and as such is part of the Kootenay terrane.

ACKNOWLEDGMENTS

This study is supported by NSERC Operating Grant A2693 and GSC Research Agreement 174 to R.L. Brown. We thank J.O. Wheeler for reviewing the paper.

REFERENCES

- Brown, R.L. and Lane, L.S.**
1988: Tectonic interpretation of west-verging folds in the Selkirk allochthon of the southern Canadian Cordillera; *Canadian Journal of Earth Sciences*, v. 25, p. 292-300.
- Brown, R.L. and Murphy, D.C.**
1982: Kinematic interpretation of mylonitic rocks in part of the Columbia River fault zone, Shuswap Terrane, British Columbia; *Canadian Journal of Earth Sciences*, v. 19, p. 456-465.
- Carr, S.D.**
1990: Late Cretaceous-early Tertiary tectonic evolution of the southern Omineca Belt, Canadian Cordillera; Ph.D. thesis, Carleton University, Ottawa, Ontario.
- Crowley, J.L., Coleman, M.E., and Brown, R.L.**
1991: Preliminary results of fieldwork: Standfast Creek fault zone, southern British Columbia; in *Current Research, Part A*; Geological Survey of Canada, Paper 91-1A, p. 293-301.
- Gilman, R.A.**
1972: Geology of the Clachnacudainn Salient near Albert Canyon, British Columbia; *Canadian Journal of Earth Sciences*, v. 9, p. 1447-1454.
- Journey, J.M.**
1986: Stratigraphy, internal strain, and thermo-tectonic evolution of northern Frenchman Cap dome: an exhumed basement duplex structure, Omineca hinterland, southeastern Canadian Cordillera; Ph.D. thesis, Queen's University, Kingston, Ontario.
- Journey, J.M. and Brown, R.L.**
1986: Major tectonic boundaries of the Omineca Belt in southern British Columbia: a progress report; in *Current Research, Part A*; Geological Survey of Canada, Paper 86-1A, p. 81-88.
- Parrish, R.R., Carr, S.D., and Parkinson, D.L.**
1988: Eocene extensional tectonics and geochronology of the southern Omineca Belt, British Columbia and Washington; *Tectonics*, v. 7, p. 181-212.
- Price, R.A.**
1986: The southeastern Canadian Cordillera: thrust faulting, tectonic wedging and delamination of the lithosphere; *Journal of Structural Geology*, v. 8, p. 239-254.
- Price, R.A., Monger, J.W.H., and Muller, J.E.**
1981: Cordilleran cross-section - Calgary to Victoria; in *Field Guides to Geology and Mineral Deposits, Calgary '81*, Geological Association of Canada/Mineralogical Association of Canada/Canadian Geophysical Union. p. 216-334.
- Read, P.B. and Brown, R.L.**
1981: Columbia River Fault zone: southeastern margin of the Shuswap and Monashee complexes, southern British Columbia; *Canadian Journal of Earth Sciences*, v. 18, p. 1127-1145.
- Read, P.B. and Thompson, R.I.**
1980: Bulletin 60-Geology of the Akolkolex River area-an addendum; in *Geological Fieldwork, British Columbia Ministry of Energy, Mines, and Petroleum Resources, Paper 80-1*, p. 183-187.
- Sears, J.W.**
1979: Tectonic contrasts between the infrastructure and superstructure of the Columbian orogen, Albert Peak area, western Selkirk Mountains, British Columbia; Ph.D. thesis, Queen's University, Kingston, Ontario, 154 p.
- Thompson, R.I.**
1972: Geology of the Akolkolex River area near Revelstoke, British Columbia; Ph.D. thesis, Queen's University, Kingston, Ontario, 125 p.
- Wheeler, J.O.**
1965: Big Bend map-area, British Columbia; Geological Survey of Canada, Paper 64-32.
- Zwanzig, H.V.**
1973: Structural transition between the foreland zone and the core zone of the Columbian Orogen, Selkirk Mountains, British Columbia; Ph.D. thesis, Queen's University, Kingston, Ontario, 158 p.

The southern tail of the Nelson Batholith, southeast British Columbia: structure and emplacement

James J. Vogl¹ and Philip S. Simony¹
Cordilleran Division, Vancouver

Vogl, J.J. and Simony, P.S., 1992: *The southern tail of the Nelson Batholith, southeast British Columbia: structure and emplacement*; in *Current Research, Part A*; Geological Survey of Canada, Paper 92-1A, p. 71-76.

Abstract

The Nelson Batholith belongs to a suite of Middle Jurassic plutons that intrudes the Kootenay Arc in southeast British Columbia. The batholith has a concordant southern 'tail'. The 'tail' consists of three subvertical, subparallel, compositionally distinct sheets; a western quartz diorite, a central leuco-quartz monzonite and an eastern quartz monzonite. Contact mineral assemblages show that the tail was emplaced at similar depths as the main part of the batholith. Subhorizontal igneous lineations suggest that the sheets were emplaced subhorizontally, southward from the main body. Long, thin screens between the sheets preserve country rock structure.

Zones of highly strained granitic rocks within the tail are considered the continuations of the Waneta and Midge Creek faults. Motion on these faults had a dextral component and was probably synchronous with granite emplacement.

Résumé

Le Batholite de Nelson fait partie d'une suite de plutons du Jurassique moyen qui recoupe par intrusion l'arc de Kootenay dans le sud-est de la Colombie-Britannique. Le batholite comporte une extrémité méridionale concordante. Cette extrémité est composée de trois nappes quasi verticales, quasi parallèles et de composition distincte; une diorite quartzique occidentale, une monzonite quartzique leucocrate centrale et une monzonite quartzique orientale. Les associations minérales de contact montrent que la mise en place de l'extrémité a eu lieu à des profondeurs semblables, formant la partie principale du batholite. Les linéations ignées sub-horizontales indiquent que les nappes se sont mises en place sub-horizontalement, vers le sud par rapport au massif principal. Des écrans longs et minces entre les nappes protègent la structure encaissante.

Les zones de roches granitiques très déformées au sein de l'extrémité sont considérées comme des prolongements des failles Waneta et Midge Creek. Le déplacement de ces failles compte une composante dextre, probablement synchrone à la mise en place du granite.

¹ Department of Geology and Geophysics, University of Calgary, Calgary, Alberta T2N 1N4

INTRODUCTION

In the southern Kootenay Arc in southeast British Columbia Early Jurassic island arc and Upper Paleozoic marginal basin assemblages have been thrust on to elements of the North American Miogeocline and on to their distal equivalents (Klepacki and Wheeler, 1985). Radiometric ages suggest that the thrusting and associated deformation was initiated in Early to Middle Jurassic time (Archibald et al., 1983; Andrew and Hoy, 1991).

A Middle Jurassic suite and a mid-Cretaceous suite of granitic plutons have intruded the Kootenay Arc. The Nelson Batholith belongs to the Middle Jurassic suite and consists of a northern mass of about 1500 km² and a 25 km long southward narrowing 'tail' protruding from the southeast margin. The map pattern of the Nelson Batholith appears to be that of an oblique section through a classical 'tadpole' pluton. Detailed mapping of the 'tail' and its margins was therefore undertaken between latitudes 49°15' and 49°30' (Fig. 1) to test this hypothesis.

The Nelson Batholith was originally mapped by McAllister (1951) and Little (1960) and additional work has since been done by Little (1964, 1982), Brown and Logan (1988) and Andrew and Hoy (1991). All workers recognized that the main mass of the Nelson Batholith is composed of several phases which may represent distinct pulses of intrusion. The southern cordilleran LITHOPROBE line that crosses the main northern mass of the batholith suggests a floor at shallow depth (Cook et al., 1988). A model of emplacement of the northern mass has been proposed by Ghent et al. (in press) on the basis of a geobarometric study and some new field observations.

Geochronology

Several isotopic systems indicate that the various phases of the composite Nelson Batholith were emplaced between 160 and 172 Ma. A list of published dates and references is found in Brown and Logan (1988).

A Rb-Sr whole-rock date on the tail gives an age of 150 ± 9 Ma (Duncan and Parrish, 1979) and two K-Ar biotite dates give ages of 123.9 ± 2.6 Ma and 107.1 ± 2.2 Ma (Archibald et al., 1983). The latter probably indicate that the body did not cool below ~300°C until Cretaceous time.

COUNTRY ROCKS

Because the focus of this study is on the granitic rocks, the supracrustal rocks of the region are grouped into four packages based on similarities in age and tectonic setting as suggested by LeClair (1988) and J.M. Einarsen (pers. comm., 1991).

Slaty argillite, siltstone, semi-pelite and thin-bedded quartzite of the Early Jurassic Ymir Group are found as screens within the tail and in adjacent country rocks west of the tail. West of the tail, the Ymir Group is conformably overlain by Early Jurassic island arc volcanics of the Elise Formation of the Rossland Group. These rocks comprise

assemblage 1 of Figure 2 and are part of the Quesnel Terrane, which is the easternmost of several accreted terranes that make up the Canadian Cordillera (Monger et al., 1982).

Screens within the eastern half of the tail consist of thin-bedded quartzite, limestone, minor black phyllite and possible limestone conglomerate. These rocks are tentatively correlated with the Mississippian Milford Group and the Triassic Slovan Group, which are part of assemblage 2 (Fig. 2). The Permian Kaslo Group, which lies between the Slovan and Milford groups to the north (Le Clair, 1988) and represents the marginal basin assemblage, has not been identified in the map area.

Black phyllite, micaceous quartzite, garnet-mica schist and minor limestone are found east of the tail and are tentatively correlated with the Lower Paleozoic Lardeau Group (assemblage 3 of Fig. 2). These rocks may be in fault contact with the granitic rocks of the tail. External contacts of the tail are discussed below.

Assemblage 4 of Figure 2 is composed dominantly of quartzite and limestone of the North American Miogeocline. These rocks will not be discussed further.

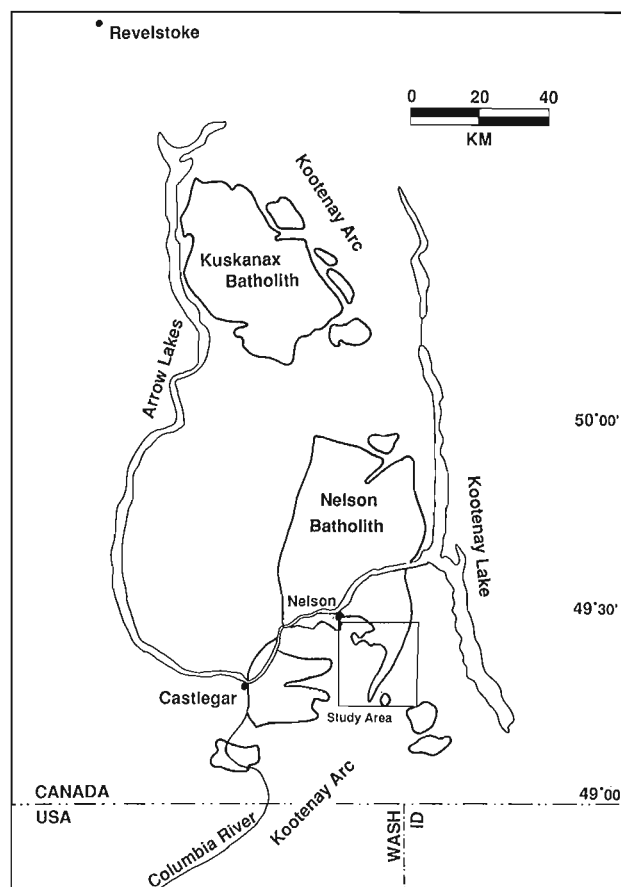


Figure 1. Location map of the Nelson Batholith and other Middle Jurassic plutons intruding the Kootenay Arc. The narrow body protruding from the southeast corner is the 'tail'.

Internal contacts

Long, narrow screens of country rock can be found throughout the tail and large, irregular shaped pendants are numerous near Kutetl Creek. The width of the screens ranges from metres to hundreds of metres and only a few can be shown on Figure 2. Bedding orientations within inclusions are similar to bedding orientations in country rocks outside of the tail suggesting that the screens remained in place throughout intrusion.

Contacts between the three main phases and between the pulses of the western phase are separated by screens of metasedimentary rock. The screens contain plentiful granitoid, pegmatite and aplite lenses and sills parallel to the layering. Screens are also found within phases. Contacts between the granite and screens are strained in most places. However, in the northwest part of the tail where the strain is low, millimetre to centimetre wide mylonite zones are found at the contacts. Lineations in the mylonites plunge gently. The thin mylonite is interpreted as the result of the magma shearing past the screens. The low-angle lineation is thought to represent subhorizontal flow of magma into the tail region.

External contacts

The west contact of the tail is characterized by intrusive contacts. This is indicated by layer-parallel injection of the granite along bedding and a decrease in strain within the granite toward the contact.

The east contact of the tail is poorly exposed. Along the Seeman-Kutetl Creek divide, intrusive relationships similar to those observed at the west contact are present. In contrast, along the western slope of the Ymir valley highly strained quartz monzonite forms the east margin of the tail. Intrusive relationships cannot be demonstrated here and tectonic relations are postulated.

South of Oscar Creek, near its southern limit the tail is divided into two sections by a metasedimentary septum (Fig. 2). The west contact of this septum is sharp and trends slightly east of north. Bedding in the septum strikes northwest up to the contact. The east contact of the metasedimentary strip is gradational and is characterized by extensive dyke injection and stoping so that isolated metasedimentary blocks are surrounded by pegmatite. This indicates a change in intrusive style from concordance in the north to discordance near the southern terminus of the tail.

West of the septum lies the western phase; to the east pegmatite occupies the position occupied by the central phase elsewhere. Due to the poor exposure south of Oscar Creek, the relationship between the pegmatite and the central phase is unknown. Farther east, the eastern phase occupies the same position as in the north although it is thinner, highly altered and fractured.

Apex Creek Plutons

Granitic rock near Apex Creek does not appear to be directly related to the tail. The map pattern (Fig. 2) suggests two granite bodies almost completely separated by a screen. The two bodies may reflect two intrusive pulses and are referred to as the Apex Creek Plutons. The two plutons are homogeneous, fine- to medium-grained biotite-hornblende granite and are distinguished by subtle grain size and compositional differences. The Apex Creek Plutons are in intrusive contact with the Ymir Group and are separated from the tail by screens.

The Apex Creek Plutons are essentially unstrained by comparison to the rocks of the tail. Only mildly strained quartz is observed in some outcrops and thin sections.

Contact aureoles

'Screens in the tail have been thermally metamorphosed within the sillimanite zone and sillimanite, andalusite and staurolite zones are recognized on the west side of the tail. Sillimanite and andalusite zones are found around the Apex Creek Plutons.' A minimum pressure above bathozone 1 is indicated by the widespread occurrence of the assemblage muscovite + quartz + sillimanite (Carmichael, 1978) within the tail while an upper pressure limit is given by the presence of andalusite along the intrusive west contact of the tail. Suitable mineral assemblages to constrain emplacement pressures have not been found. Andalusite occurrence near the tail as well as in the northern margin of the batholith (Cairnes, 1934) indicates that the Nelson Batholith was emplaced at similar pressure along its entire length.

DEFORMATION AND STRAIN

Deformation within screens and pendants

In the large pendant south of Kutetl Creek (Fig. 2), thin-bedded quartzite of the Ymir Group is in contact with deformed white to grey limestone and folded black phyllite injected lit-par-lit by granite. The contact is intruded by pegmatite which incorporates carbonate clasts. Shearing of the carbonate produced a pegmatite/carbonate mélange. A band of highly folded interbedded limestone and quartzite can be traced southward to the ridge south of the headwaters of Seeman Creek. This zone may mark the trace of the Waneta Fault.

Deformation in metasedimentary screens near the east margin of the tail may reflect movement of the Midge Creek Fault. This deformation has produced mylonitic sedimentary rocks on the Oscar/Ymir Creek divide which have been folded and fractured. Along the west slope of Ymir valley a band of grey limestone contains clasts and lenses of granite. It contains clasts and lenses of mylonitic quartz monzonite interpreted as the strained eastern phase. The origin of smaller, more rounded, leucogranite clasts is in doubt and they may represent pebbles in a conglomerate.

Deformation in the granitic rocks

Fabric orientations

Foliations are parallel to bedding in screens within the tail and in adjacent Ymir Group rocks west of the tail. Foliations and bedding dip steeply and strike northwest to north-northeast. The north-northeast-striking foliations/bedding are common in the east half of the tail where deformation is generally strongest. This suggests that the north-northeast-striking foliation and bedding may represent originally northwest-striking foliation rotated into parallelism with a north-northeast-striking shear plane that dips steeply. Kinematic indicators such as 'c-s' fabrics and rotated feldspars in the granite shear zones throughout the tail give a consistent dextral shear sense and lineations are subhorizontal or plunge shallowly southward.

Strain intensity and distribution

Three strain features are important to the deformational history of the tail and the timing and kinematics of the faults.

- (1) The highest strain zones are found throughout the central phase and near the east margin of the eastern phase. Mylonite is common here but the western phase and the remainder of the eastern phase is mildly strained to protomylonitic. The high strain zone within the eastern phase appears to pass out of the tail; it is not observed north of the Ymir/Seeman Creek divide.
- (2) Strain gradients are absent at outcrop scale. Strain within the western phase decreases imperceptibly toward the west contact while the central phase consists of dominantly mylonitic rocks. Inhomogeneities occur in the eastern phase on the scale of tens of metres. Overall, the deformation has produced strikingly homogeneous shear zones.
- (3) A zone of brittlely deformed rock is found along the southeast margin of the tail. This area is poorly exposed, but highly fractured granite can be traced along the eastern margin of the tail southward from Ymir Creek. The fracturing is weak in the northern part of the fault zone where it mildly overprints mylonitic granitic rocks. Brittle deformation is much stronger in the south where the granitic protoliths do not appear to be previously mylonitized. This brittle deformation also affects mylonitic sedimentary rocks on the Oscar/Ymir Creek divide.

Discussion of strain

The homogeneous fabrics observed are typical of high temperature shear zones. Discrete anastomosing mylonite is commonly found in granites deformed under greenschist facies conditions (metamorphic grade of the country rocks in the region of the tail). This suggests that deformation within the tail took place during or shortly after emplacement with the heat from emplacement providing a thermal softening and giving rise to wide homogeneous shear zones. Ductile

deformation of feldspars in the central mylonite and annealed fabrics also suggest a high temperature relative to the low-grade country rocks.

Because the Waneta Fault is truncated around two pendants by the central and eastern phases of the Nelson Batholith the Waneta Fault is inferred to be older than Middle Jurassic. However, a general coincidence of mylonite of the central phase with the trace of the Waneta Fault may indicate that movement on the fault occurred synchronously with emplacement.

The high strain zone near the eastern margin of the tail separates two metasedimentary packages. It coincides with the southward continuation of the Midge Creek Fault with which it is tentatively correlated. Intrusion of the tail into assemblage 3 (Lardeau Group) east of the tail cannot be demonstrated and this probable tectonic contact indicates that movement on the Midge Creek Fault may be Middle Jurassic and younger.

The inverse relationship between the amount of brittle and ductile deformation suggests that longer-lived heat in the north led to ductile deformation there while at the same time the southeast tip of the tail received little heat at its margin producing brittle deformation there at the same time. Alternatively, younger brittle normal faulting may have produced this zone.

Widespread low-angle lineations, the presence of 'C-S' fabrics and dextral kinematic indicators suggest a dextral oblique component to the convergence of the Quesnel Terrane and North American boundary in the area of the tail in the Middle Jurassic. The amount of transcurrent displacement cannot be estimated since no markers exist across the shear zones.

CONCLUSIONS

Similar mineral assemblages in the contact aureole of the tail and the main body of the Nelson Batholith suggest that they were emplaced at similar structural levels. The tail probably does not represent a significantly deeper part of the batholith exposed as an oblique crustal section. Igneous lineations indicate a southward, subhorizontal flow of magma into the tail.

In plan, internal phase contacts bend south-southwestward where they enter the Waneta Fault zone and follow this orientation southward. This suggests that magma flow was controlled by faults active during intrusion and that emplacement of the tail occurred synkinematically with respect to motion on the Waneta and Midge Creek faults. Pre-Nelson movement on the Waneta Fault is shown by granitoid phases cutting obliquely across the fault. No intrusive relationships are found across the Midge Creek Fault. The high temperature nature of the shear zones indicates that motion did not continue during intrusion cooling and thus constrains the age of most of the motion to dominantly Middle Jurassic time.

The significance of the subhorizontal, dextral shearing is unclear. The shear may be a late-stage dextral movement on oversteepened thrust faults or represent a transpressive zone.

REFERENCES

- Andrew, K.P.E. and Hoy, T.**
1991: Geology of the Rossland Group in the Erie Lake area, with emphasis on stratigraphy and structure of the Hall Formation, southeastern British Columbia; in *Geologic Fieldwork 1990*, British Columbia Ministry of Energy, Mines and Petroleum Resources, Paper 1991-1, p. 9-19.
- Archibald, D.A., Glover, J.K., Price, R.A., Farrar, E., and Carmichael, D.M.**
1983: Geochronology and tectonic implications of magmatism and metamorphism, southern Kootenay Arc and neighbouring region as, southeast British Columbia. Part I: Jurassic to mid-Cretaceous; *Canadian Journal of Earth Sciences*, v. 20, p. 1891-1913.
- Brown, D.A. and Logan, J.M.**
1988: Geology and mineral evaluation of Kokanee Glacier Provincial Park, southeastern British Columbia; in *Geologic Fieldwork 1987*, British Columbia Ministry of Energy, Mines and Petroleum Resources, Paper 1988-1, p. 31-48.
- Cairnes, C.E.**
1934: Slocan Mining Camp, British Columbia; *Geological Survey of Canada, Memoir 173*, 137 p.
- Carmichael, D.M.**
1978: Metamorphic bathozones and bathograds: a measure of the depth of post-metamorphic uplift and erosion on the regional scale; *American Journal of Science*, v. 278, p. 769-797.
- Cook, F.A., Green, A.G., Simony, P.S., Price, R.A., Parrish, R.R., Milkereit, B., Gordy, P.L., Brown, R.L., Cofflin, K.C., and Patenaude, C.**
1988: Lithoprobe seismic reflection structure of the southeastern Canadian Cordillera: initial results; *Tectonics*, v. 7, p. 157-180.
- Duncan, I.J. and Parrish, R.**
1979: Geochronology and Sr isotope geochemistry of the Nelson Batholith: a post-tectonic intrusive complex in southeast British Columbia (abstract); *Geological Society of America, Abstracts with Programs*, v. 11, p. 76.
- Ghent, E.D., Nicholls, J., Simony, P.S., Sevigny, J., and Stout, M.Z.**
in press: Hornblende geobarometry of the Nelson Batholith, British Columbia: tectonic implications; *Canadian Journal of Earth Sciences*.
- Klepacki, D.W. and Wheeler, J.O.**
1985: Stratigraphic and structural relations of the Milford, Kaslo and Slocan groups, Goat Range, Lardeau and Nelson map areas, British Columbia; in *Current Research, Part A*; *Geological Survey of Canada, Paper 85-1A*, p. 277-286.
- LeClair, A.D.**
1988: Polyphase structural and metamorphic histories of the Midge Creek area, southeast British Columbia: implications for tectonic processes in the central Kootenay Arc; Ph.D. thesis, Queen's University, Kingston, Ontario, 263 p.
- Little, H.W.**
1960: Nelson map area, west half, British Columbia; *Geological Survey of Canada, Memoir 308*, 205 p.
1964: Ymir map area, British Columbia, *Geological Survey of Canada, Map 1144A*.
1982a: Bonnington map area, British Columbia; *Geological Survey of Canada, Map 1571A*.
- McAllister, A.L.**
1951: Ymir map area, British Columbia; *Geological Survey of Canada, Paper 51-4*, 58 p.
- Monger, J.W.H., Price, R.A., and Tempelman-Kluit, D.J.**
1982: Tectonic accretion and the origin of the two major metamorphic and plutonic belts in the Canadian Cordillera; *Geology*, v. 10, p. 70-75.

Bowser Basin facies and map units in southwest Toodoggone map area, British Columbia

**C.A. Evenchick
Cordilleran Division, Vancouver**

Evenchick, C.A., 1992: Bowser Basin facies and map units in southwest Toodoggone map area, British Columbia; in Current Research, Part A; Geological Survey of Canada, Paper 92-1A, p. 77-84.

Abstract

Three sedimentary facies in the Bowser Lake Group in southwestern Toodoggone map area (NTS 94D) are mappable. They are 1) recessive, dark weathering fine grained sandstone and siltstone; 2) dominantly medium grained sandstone; 3) a sequence composed of more than 40% rusty weathering conglomerate. The conglomerate facies generally overlies the medium grained and fine grained facies, but depositional repetition of these facies is evident in one region. Folded Bowser Lake Group is overlain by Tango Creek Formation of the Sustut Group. Tight to open, and upright to overturned folds in the Bowser Lake Group verge northeast.

Résumé

Trois faciès sédimentaires dans le groupe de Bowser Lake dans le sud-ouest de la zone cartographique de Toodoggone peuvent être cartographiées. Ce sont 1) un grès et un siltstone à grain fin récessifs d'altération foncée; 2) un grès à grain moyen abondant; 3) une séquence composée de plus de 40 % de conglomérat rouillé par altération. Le faciès du conglomérat repose en général sur le faciès à grain moyen et à grain fin, mais la répétition sédimentaire de ces faciès est évidente dans une région. Le groupe de Bowser Lake plissé est surmonté de la formation de Tango Creek du groupe de Sustut. Les plis de fermés à ouverts et de verticaux à déversés dans le groupe de Bowser Lake présentent une vergence au nord-est.

INTRODUCTION

Southwest Toodoggone (94D) map area (Fig. 1) was the focus of fieldwork in the northern Bowser and Sustut basins in 1991. This work is part of a regional mapping project designed to elucidate the sedimentary, structural, and thermal history of the northern Bowser Basin. Previous work in Spatsizi and Telegraph Creek map areas is summarized in Evenchick (1986, 1987, 1988, 1989, 1991a); Evenchick and Green (1990); Ricketts (1990); Ricketts and Evenchick (1991); Green (1991), Greig (1991) and Poulton et al. (1991). The structural style of the region is summarized in Evenchick (1991b). The sedimentary and tectonic evolution of the Sustut Group is described by Eisbacher (1974a). An interpretation of facies of the Bowser Lake Group in southwest Toodoggone area is presented by Eisbacher (1974b). This report contains brief descriptions of the stratigraphy and structure of the Bowser Lake and Sustut groups in the four areas outlined in Figure 2. The Bowser Lake Group includes Middle Jurassic to mid-Cretaceous marine and nonmarine strata (Gabrielse and Tipper, 1984; Evenchick, 1987, 1988, 1989; Cookenboo and Bustin, 1989; Evenchick and Green, 1990; MacLeod and Hills, 1990; Ricketts, 1990; Ricketts and Evenchick, 1991). The Sustut Group is composed of mid-Cretaceous to latest Cretaceous nonmarine strata (Eisbacher, 1974a; Sweet and Evenchick, 1990). Both groups, and underlying strata of Stikinia were deformed by northeast-verging folds and thrust faults of the Skeena Fold Belt in Late Jurassic(?) to latest Cretaceous or Early Tertiary time (Evenchick, 1991b).

DUTI LAKES AREA

Bowser Lake Group

The southern Duti Lakes area is underlain by siltstone and very fine grained sandstone. The strata are dark and recessive weathering, with the exception of rare conglomerate

horizons. They are dominantly laminated black siltstone interbedded with less common fine- to medium-grained sandstone, and are weakly to intensely bioturbated. Rusty weathering claystone beds 2 to 4 cm thick, black massive siltstone, and medium bedded, medium grained sandstone are also present locally. Rare grey weathering conglomerate is 2 to 4 m thick, massive to crudely layered and clast supported. More than 80% of the clasts are radiolarian chert.

The black siltstone/fine grained sandstone facies described above is overlain by about 50 m of medium grained brown, green and grey weathering sandstone and siltstone which contain marine macrofossils. These strata are overlain by an interval with more than 50% rusty weathering conglomerate, in which the proportion of conglomerate increases upward. The conglomeratic facies is more than 500 m thick, and is composed of cycles coarsening up from black, carbonaceous siltstone or shale 5 to 20 m thick, through platy, and planar crossbedded medium grained sandstone intervals 5 to 20 m thick, to 5 to 25 m of chert-pebble conglomerate. In places the base of conglomerate intervals cuts into underlying sandstone beds. Conglomerate is bright rusty weathering, commonly clast supported, massive to vaguely bedded, and in places has large-scale crossbeds. Log impressions are present locally.

Sustut Group

Although the contact between the Tango Creek Formation and folded Bowser Lake Group is covered, it is assumed to be unconformable (as shown by Eisbacher (1974a)). A conglomerate marker is present on 3 ridges about 200 m above the assumed unconformity. The Tango Creek Formation consists of 2500 m or more of interbedded sandstone, siltstone and mudstone with three conglomerate marker beds. Quartz arenite and grit are common near the base. This region is the type locality of the Tango Creek Formation, and the reader is referred to Eisbacher (1974a) for

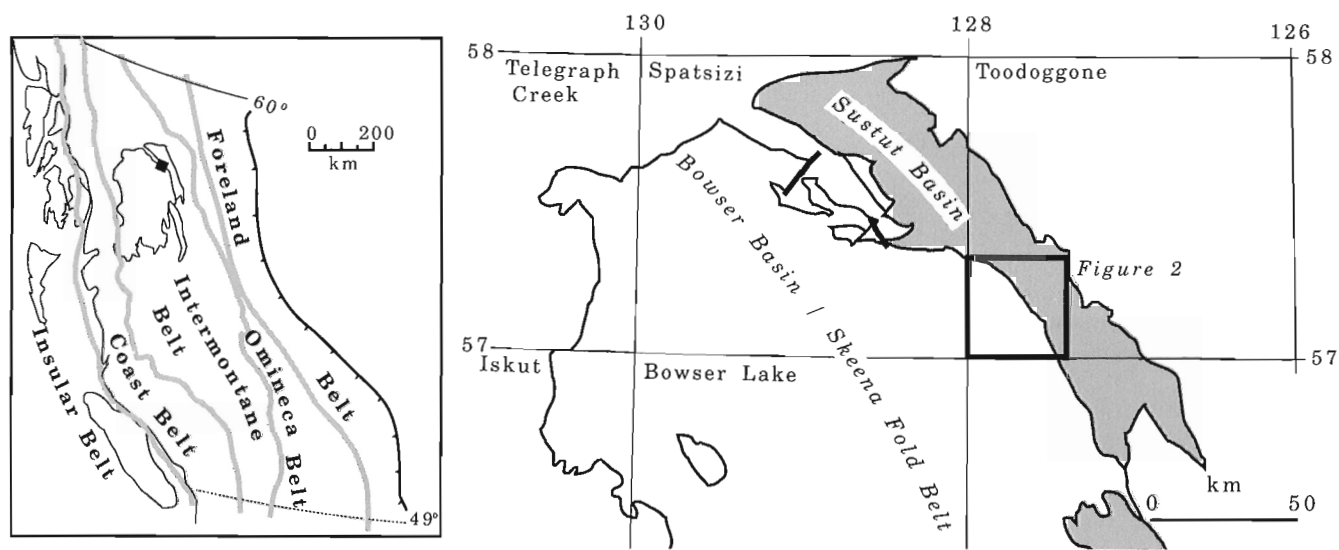


Figure 1. Location of the Bowser and Sustut basins with respect to morphogeological belts in the Canadian Cordillera (left), and location of the study area in Toodoggone map area with respect to the Bowser and Sustut basins (morphogeological belts after Gabrielse and Yorath, 1989).

descriptions of the Sustut Group. Siltstone and sandstone of the Tango Creek Formation are overlain conformably and abruptly by chert and quartz pebble conglomerate which marks the base of the Brothers Peak Formation. More than 40% of the basal 600 m of the Brothers Peak Formation is conglomerate.

Structure

Structures in the siltstone/fine grained sandstone facies of the Bowser Lake Group are poorly displayed and may include unrecognized faults and folds. The siltstone and fine grained sandstone are intensely cleaved, particularly in the south.

The conglomeratic facies is broadly warped (see Fig. 3, section B'C) with the exception of close to tight northeast-verging folds near the base of the unit in two places. These folds may reflect the competency contrast between widespread competent conglomerate sheets and underlying, relatively incompetent, fine grained and thinly layered units. No mesoscopic folds were observed. Macroscopic folds are uncommon; they trend northwest and have little or no plunge (Fig. 4). The Tango Creek Formation is folded into large scale (up to 2 km wavelength) southwest-verging, en echelon folds which plunge gently northwest (Fig. 3, section B'C; Fig. 4). The Brothers Peak Formation dips steeply but flattens gradually to the northeast of section B'C (Fig. 3).

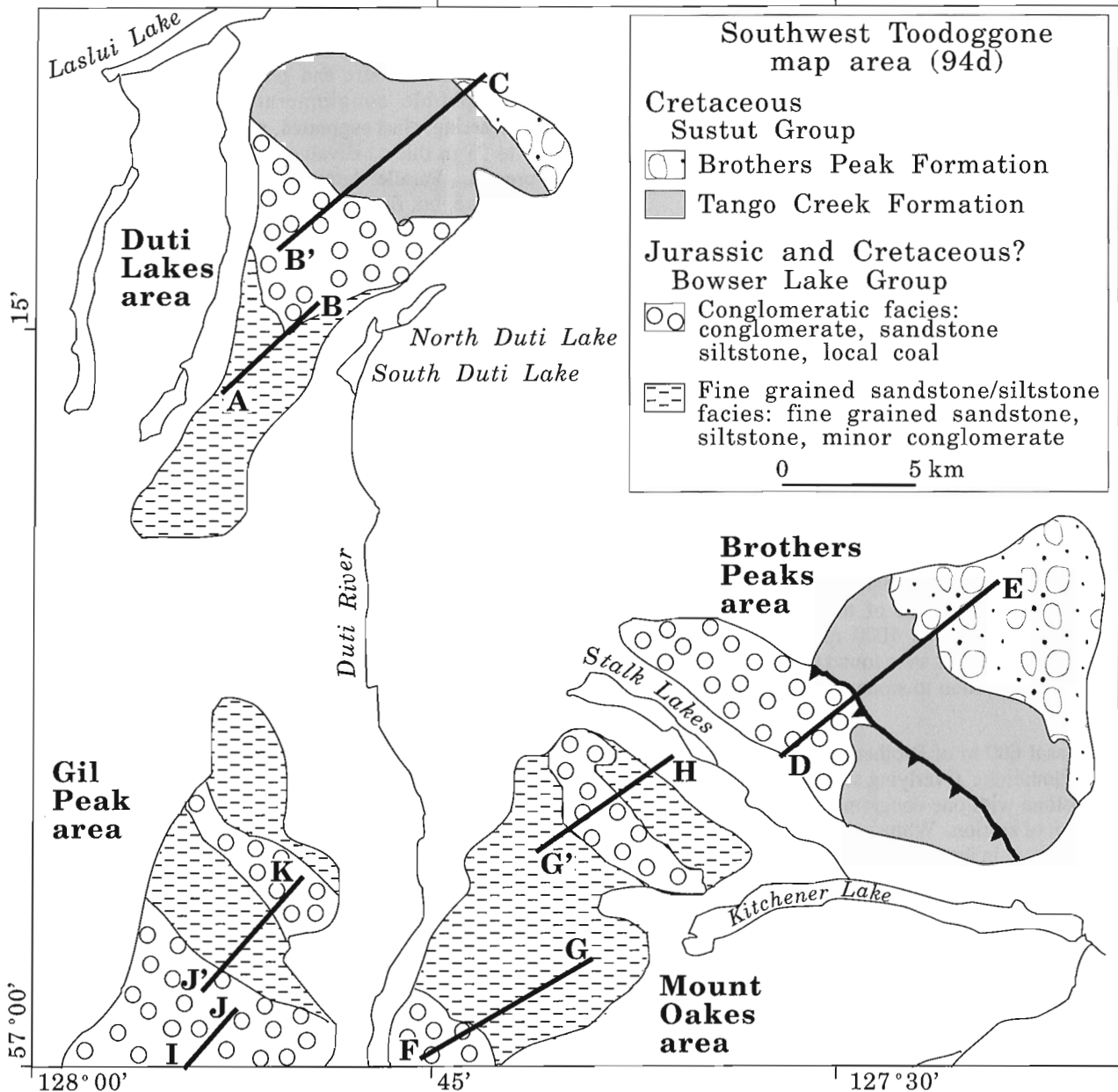


Figure 2. Generalized geological map of southwest Toodoggone map area. Straight lines represent cross-sections shown in Figure 3. Location of Figure 2 is outlined in Figure 1.

BROTHERS PEAKS AREA

Bowser Lake Group

Bowser Lake Group in Brothers Peaks area is generally similar to that of Duti Lakes area and consists of a 400+ m thick section with more than 60% rusty weathering conglomerate. At least 14 conglomerate intervals, each 5 to 20 m thick, are present. They comprise 15 to 30 m thick cycles coarsening up from carbonaceous mudstone and shale (with local coal) at the base, to medium grained platy sandstone and crossbedded sandstone, to chert pebble and cobble conglomerate. Conglomerate is commonly clast supported, and contains large crossbeds and plant impressions. The conglomerate intervals change in thickness along trend, but generally form sheets that can be traced for more than 5 km. Pelecypods and silicified tree fragments are present at several intervals.

Sustut Group

Tango Creek Formation has different structural style on two sides of a thrust fault (Fig. 2,3 section DE). In the northeast its uppermost beds are conformable with the overlying Brothers Peak Formation. Between this stratigraphic contact and its fault contact with the Bowser Lake Group farther south it is intensely folded. The base of the formation is not exposed.

To the southeast, the Tango Creek Formation unconformably overlies folded Bowser Lake Group which is in the hanging wall of the thrust fault. It defines a south-southeast plunging syncline (Fig. 3, section DE; Fig. 4) in which at least 1300 m of continuous section is exposed. The Tango Creek Formation is similar to that at Duti Lakes, with prominent quartz arenite near the base interbedded with siltstone and mudstone. Detrital muscovite is most abundant in an interval about 600 m above the base of the formation. Quartz-pebble conglomerate markers occur 300 m and 500 m above the base of the formation. Chert clasts are minor throughout the lower part of the formation, but become abundant abruptly about 1000 m above the base of the formation. No markers were found to relate the stratigraphic position of this section to strata in the footwall of the thrust fault.

The basal 600 m of Brothers Peak Formation is at least 40% conglomerate. Overlying strata are sandstone, siltstone and mudstone with one conglomerate (10-15 m thick) in at least 800 m of section. White weathering tuff and tuffaceous sandstone occur in intervals to 1+ m thick in the lower 700 m of the formation.

Structure

Folds in the Bowser Lake Group are tight northeast-verging and upright to overturned, or upright, open, and gently doubly plunging (Fig. 3, section DE). A southwest dipping thrust fault with Bowser Lake Group in the hanging wall and Tango Creek Formation in the footwall has northeast-verging folds in the hanging wall. In the footwall of the fault the Tango

Creek Formation is complexly folded and faulted. In the hanging wall it occurs as an open to close syncline which plunges 16° south-southeast (Fig. 4). The Brothers Peak Formation defines a broad open syncline with its core near the northeast limit of mapping. Resistant conglomerate intervals dip consistently 40° northeast, forming the regionally continuous Kitchener Monocline (Eisbacher, 1971).

MOUNT OAKES AREA

In the Mount Oakes area (Fig. 2) a thick section of folded, recessive, dark weathering fine grained clastic rocks is bounded to the northeast and southwest by conglomerate. The fine grained facies is more than 90% laminated black siltstone and fine grained sandstone. Locally these strata are laminated to thinly bedded with fine- to medium-grained sandstone. Beds of medium grained sandstone to 10 cm thick are present but rare and generally underlie and/or overlie chert-pebble conglomerate. Conglomerate is grey weathering, clast supported, and occurs as lenses and sheets 3 to 25 m thick. Bivalves, belemnites and ammonites are present. Parallel lamination is the prevalent sedimentary structure, but fining up beds, cross laminae, and rare flame structures are seen. Fine grained sandstone and siltstone are commonly bioturbated.

Near its southern limit the fine grained facies includes 100 m of thin to thick bedded, grey weathering medium grained chert arenite in 10 m intervals, interbedded with 8 m thick intervals of finer grained sandstone. These strata are overlain by at least 400 m of dark, recessive weathering fine grained bioturbated clastic rocks, which in the upper half increase upward in proportion of chert arenite, to the base of an overlying conglomeratic facies.

The southern conglomerate facies with more than 60% conglomerate is 300+ m thick. Conglomerate occurs in intervals 2 to 20 m thick, separated by 0.5 to 10 m of fine- and medium-grained sandstone. Conglomerate at the base weathers grey but is rusty farther upsection. Conglomerate is mainly clast supported, massive to vaguely bedded; pelecypods are present in the lower half of the unit. Coarsening up cycles similar to those in the Duti Lakes and Brothers Peaks areas are poorly defined. The conglomerate facies is overlain by about 100 m of medium grained chert arenite in thick massive beds, with 20 m of fine grained sandstone in its upper part.

The northern conglomeratic facies also overlies the fine grained facies (section G'H, Fig. 2,3). The lowest conglomerate beds are underlain to the south by about 100 m of dominantly medium grained sandstone, and then by the fine grained facies. To the north the same conglomerate marker is underlain by more than 500 m of medium- and fine-grained sandstone and minor conglomerate (Fig. 3, section G'H). Southward thinning of the interval between the fine grained facies and the conglomerate marker is perhaps a result of southward progradation of the conglomerate facies over the fine grained facies.

The two conglomerate facies belts in the Mount Oakes area are similar, and each overlies the fine grained facies. Their relative stratigraphic position is uncertain in the absence of biostratigraphic control. Their position with respect to a given horizon in the fine grained facies is unknown because of the lack of markers in the fine grained facies.

Structure

Strata in the fine grained facies generally dip gently to steeply southwest, and have strong cleavage. Faults are present, but their displacement is unknown. In section G'H (Fig. 3) siltstone and fine grained sandstone occur in large scale folds overturned to the northeast. Conglomerate and sandstone in the conglomeratic facies delineate upright close to tight folds in the south and large-scale northeast-verging folds, some overturned, in the north (Fig. 3; section G'H; Fig. 4).

GIL PEAK AREA

The Gil Peak area (Fig. 2) is underlain by generally the same facies as the other regions. In the south, a conglomeratic facies at least 600 m thick is composed of coarsening up cycles with 0.5 m thick coal seams in the highest strata. The conglomerate facies is underlain by about 100 m of largely medium grained sandstone which contains marine fossils in the lower part. It is underlain by a fine grained dark weathering sequence with less than 10% conglomerate. As in Mount Oakes and Duti Lakes areas, conglomerate weathers grey and occurs as lenses in this facies. To the north (northeast side of section J'K, Fig. 3), the fine grained facies is underlain by sandstone, and then by more than 300 m of the conglomerate facies. This facies is more than 60% rusty weathering conglomerate, and is itself underlain by sandstone and then a fine grained sandstone facies. No biostratigraphic control is available, but because the fine grained facies is both overlain and underlain by conglomerate facies, stratigraphic

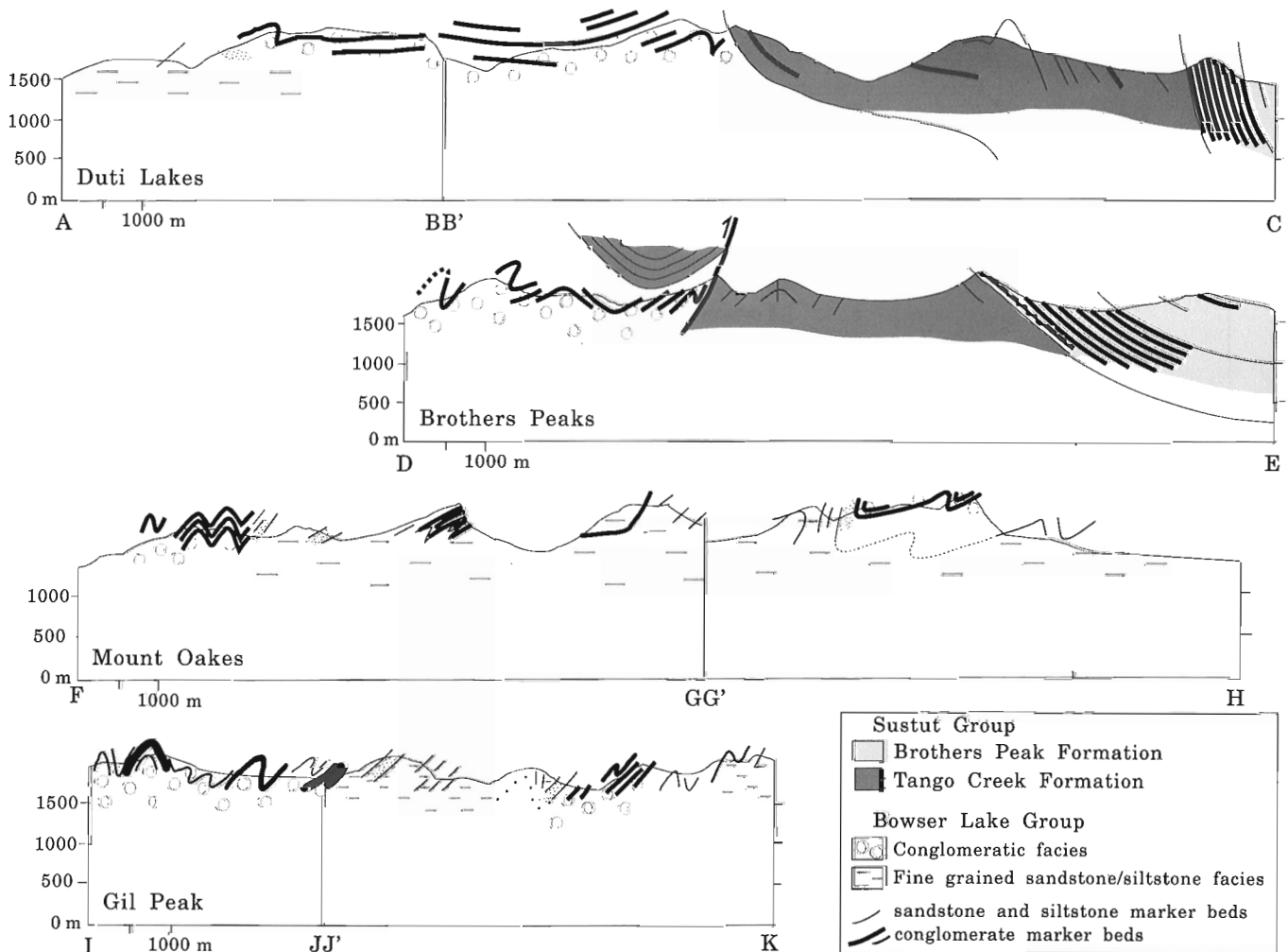


Figure 3. Cross-sections of southwest Toodoggone map area. Locations of sections are shown in Figure 2. The syncline of Tango Creek Formation above section DE is projected from southeast of the section.

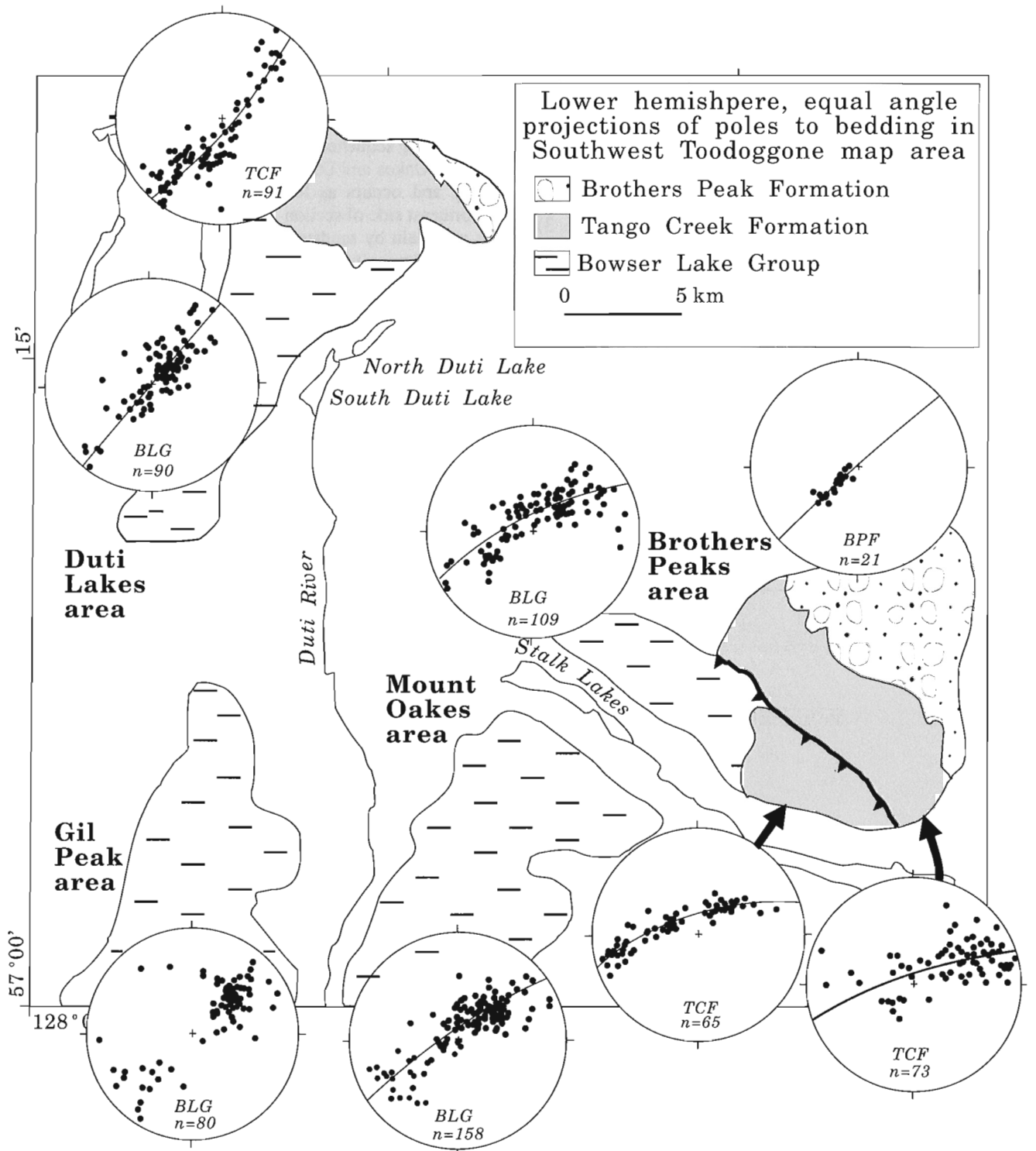


Figure 4. Equal angle, lower hemisphere projections of poles to bedding in the Bowser Lake Group (BLG), Tango Creek Formation (TCF), and Brothers Peak Formation (BPF).

repetition of the conglomeratic facies is required. If no faults modify the intervening strata, they are separated stratigraphically by 1300 m or more of fine grained strata.

Structure

The fine grained facies dips generally southwest, has local faults of unknown magnitude, and rare large-scale overturned folds. The conglomerate facies is characterized by tight northeast-verging folds up to 500 m in amplitude (Fig. 3, section IK).

SUMMARY AND DISCUSSION

Bowser Lake Group strata in southwest Toodoggone area constitute three mappable facies. Dark, recessive weathering laminated siltstone and fine grained sandstone which occurs in Duti Lakes, Mount Oakes, and Gil Peak areas is interpreted to have been deposited on a fine grained clastic marine shelf, and/or slope. Lenses of conglomerate may represent channels which transected the shelf/slope. The siltstone/fine grained sandstone facies is generally overlain by a relatively thin interval of medium grained sandstone gradational between the fine grained facies below and the conglomerate facies above.

The conglomerate facies is generally more than 40% conglomerate, and in the Duti Lakes, Brother Peaks, north Mount Oakes and Gil Peaks areas is strongly rusty weathering. Coarsening up cycles are well defined locally and coal is present, notably in the Brother Peaks and south Gil Peak areas. Marine fossils are known in Duti Lakes, Brother Peaks, and south Mount Oakes areas. The coarsening up cycles, abundance of plant debris and logs, local coal and local marine fossils are interpreted to reflect a coastal, deltaic environment. In Gil Peak area the conglomerate facies is stratigraphically repeated.

The fine grained facies generally resembles the Ashman Formation of Spatsizi map area (Fig. 1; Evenchick 1987, 1988, 1989). Differences are that the fine grained facies in Toodoggone area generally lacks orange/rusty claystone beds and is commonly coarser grained than the Ashman Formation. Bioturbation is moderately common in the fine grained facies but uncommon in the Ashman Formation.

Strata lithologically similar to the rusty weathering conglomerate facies are present in Spatsizi map area (Evenchick, 1987, 1988; Evenchick and Green, 1990). Most are near the present basin margin. A conglomerate unit in south Spatsizi area called the Devils Claw Formation is mid-Cretaceous in age (Cookenboo and Bustin, 1989; MacLeod and Hills, 1990). It differs from the conglomerate facies in Toodoggone map area in weathering grey, not rusty; it lacks marine fossils, and overlies deltaic facies (Cookenboo and Bustin, 1989; MacLeod and Hills, 1990).

The areas mapped fall within facies belts A1, A2, and A3 of the Duti River-Slamgeesh facies defined by Eisbacher (1974b). The three facies belts represent from northeast to southwest, deltaic, prodelta, and sub-sea fan environments. The boundaries of the facies belts from Eisbacher's (1974b)

Figure 3, correspond generally as follows. The conglomeratic, deltaic facies of the Duti Lakes and Brothers Peaks areas of this study correspond roughly to facies belt A1, the deltaic facies. The areas of fine grained facies of this study are equivalent to Eisbacher's A2, the prodelta facies. In addition, the conglomerate facies in Mount Oakes and north Gil Peak areas are in this area. These are deltaic facies which do not fit Eisbacher's (1974b) description of facies A2, which should have little or no conglomerate. Conglomerate facies in south Gil Peak area correspond to Eisbacher's facies A3, the sub-sea fan. The presence of large volumes of conglomerate in coarsening up cycles and of well defined coal seams indicate that the conglomerate facies is deltaic and should be shown as facies A1. In this interpretation the distribution of facies defined by Eisbacher (1974b) is from northeast to southwest: A1, A2, A1.

The differences noted above from Eisbacher's interpretation result from the more detailed mapping in the present study. The concept of a simple distribution of more distal facies away from the margin of the basin margin (Eisbacher, 1974b) is not directly applicable. The primary distribution of facies is complicated enormously by major northeastward shortening in Cretaceous to Early Tertiary(?) time to form the Skeena Fold Belt (Evenchick, 1991b). The structures probably repeat the same facies laterally, and inhibit reconstructions of the primary basin architecture. Today's distribution of facies reflects original distribution, deformation by the Skeena Fold Belt, and erosion.

REFERENCES

- Cookenboo, H. and Bustin, R.M.
1989: Jura-Cretaceous (Oxfordian to Cenomanian) stratigraphy of the north-central Bowser Basin, northern British Columbia; *Canadian Journal of Earth Sciences*, v. 26, p. 1001-1012.
- Eisbacher, G.H.
1971: A subdivision of the Upper Cretaceous - Lower Tertiary Sustut Group, Toodoggone map-area, British Columbia; *Geological Survey of Canada, Paper 70-68*, 16 p.
1974a: Sedimentary and tectonic evolution of the Sustut and Sifton basins, north-central British Columbia; *Geological Survey of Canada, Paper 73-31*.
1974b: Deltaic sedimentation in the northeastern Bowser Basin, British Columbia; *Geological Survey of Canada, Paper 73-33*, 13 p.
- Evenchick, C.A.
1986: Structural style of the northeast margin of the Bowser Basin, Spatsizi map area, north-central British Columbia; in *Current Research, Part B*; *Geological Survey of Canada, Paper 87-1B*, p. 733-739.
1987: Stratigraphy and structure of the northeast margin of the Bowser Basin, Spatsizi map area, north-central British Columbia; in *Current Research, Part A*; *Geological Survey of Canada, Paper 87-1A*, p. 719-726.
1988: Structural style and stratigraphy in northeast Bowser and Sustut basins, north-central British Columbia; in *Current Research, Part E*; *Geological Survey of Canada, Paper 88-1E*, p. 91-95.
1989: Stratigraphy and structure in east Spatsizi map area, north-central British Columbia; in *Current Research, Part E*; *Geological Survey of Canada, Paper 89-1E*, p. 133-138.
1991a: Jurassic stratigraphy of east Telegraph Creek and west Spatsizi map areas, British Columbia; in *Current Research, Part A*; *Geological Survey of Canada, Paper 91-1A*, p. 155-162.
1991b: Geometry, evolution, and tectonic framework of the Skeena Fold Belt, north-central British Columbia; *Tectonics*, v. 10, p. 527-546.

- Evenchick, C.A. and Green, G.M.**
1990: Structural style and stratigraphy of southwest Spatsizi map area, British Columbia; in *Current Research, Part F*; Geological Survey of Canada, Paper 90-1F, p. 135-144.
- Gabrielse, H. and Tipper, H.W.**
1984: Bedrock geology of Spatsizi map area (104H); Geological Survey of Canada, Open File 1005.
- Gabrielse, H. and Yorath, C.J.**
1989: DNAG#4. The Cordilleran Orogen in Canada; Geoscience Canada, v. 16, p. 67-83.
- Green, G.M.**
1991: Detailed sedimentology of the Bowser Lake Group, northern Bowser Basin, British Columbia; in *Current Research, Part A*; Geological Survey of Canada, Paper 91-1A, p. 187-195.
- Greig, C.J.**
1991: Stratigraphic and structural relations along the west-central margin of the Bowser Basin, Oweegee and Kinskuch areas, northwestern British Columbia; in *Current Research, Part A*; Geological Survey of Canada, Paper 91-1A, p. 197-205.
- MacLeod, S.E. and Hills, L.V.**
1990: Conformable Late Jurassic (Oxfordian) to Early Cretaceous strata, northern Bowser Basin, British Columbia: a sedimentological and paleontological model; *Canadian Journal of Earth Sciences*, v. 27, p. 988-998.
- Poulton, T.P., Callomon, J.H., and Hall, R.L.**
1991: Bathonian through Oxfordian (Middle and Upper Jurassic) marine microfossil assemblages and correlations, Bowser Lake Group, west-central Spatsizi map area, northwestern British Columbia; in *Current Research, Part A*; Geological Survey of Canada, Paper 91-1A, p. 59-63.
- Ricketts, B.D.**
1990: A preliminary account of sedimentation in the lower Bowser Lake Group, northern British Columbia; in *Current Research, Part F*; Geological Survey of Canada, Paper 90-1F, p. 145-150.
- Ricketts, B.D. and Evenchick, C.A.**
1991: Analysis of the Middle to Upper Jurassic Bowser Basin, northern British Columbia; in *Current Research, Part A*; Geological Survey of Canada, Paper 91-1A, p. 65-73.
- Sweet, A.R. and Evenchick, C.A.**
1990: Ages and depositional environments of the Sustut Group, north-central British Columbia (abstract); in *Geological Association of Canada, Mineralogical Association of Canada, Abstracts with Program*, A127.

Geological Survey of Canada Project 880027

A preliminary investigation of potential field data from north-central British Columbia

C. Lowe, D. Seemann, and C.A. Evenchick¹
Pacific Geoscience Centre, Sidney

Lowe, C., Seeman, D., and Evenchick, C.A., 1992: A preliminary investigation of potential field data from north-central British Columbia; in *Current Research, Part A; Geological Survey of Canada, Paper 92-1A*, p. 85-93.

Abstract

Analysis of potential field data from north-central British Columbia reveals regional variations in basement lithologies which outline the structure of Mesozoic basins and constrains their tectonic development. A colour-shaded aeromagnetic image delineates the extent of the Bowser and Sustut basins, identifies northwest trending structures in volcanic rocks of the underlying Stikinia, and highlights Tertiary plutons and Neogene volcanic centres within the adjacent Coast Belt. High-amplitude magnetic anomalies occur where Pliocene volcanics pierce and overlap sedimentary assemblages in the Bowser Basin. The existence of both normal and reverse magnetizations attests to a prolonged and episodic volcanism. Mesozoic plutons within Bowser Basin produce a distinctive magnetic anomaly. A similar anomaly centred at 56°13.4'N, 129°34.0'W is also thought to mark a pluton. Regional and high resolution gravity data are presented as a contour map and profile. Correlations between gravity and aeromagnetic data are discussed in a geological context.

Résumé

L'analyse de données relatives au champ potentiel, provenant du centre nord de la Colombie-Britannique, révèle des variations régionales de la lithologie du socle, qui soulignent les contours des bassins d'âge mésozoïque et ont imposé des limites à leur évolution tectonique. Une image aéromagnétique ombrée en couleurs délimite l'étendue des bassins de Bowser et de Sustut, permet de reconnaître des structures de direction générale nord-ouest dans les roches volcaniques du terrane sous-jacent de la Stikinia, et met en relief les plutons d'âge tertiaire et les centres volcaniques d'âge néogène situés à l'intérieur du Domaine côtier adjacent. Des anomalies magnétiques de grande amplitude se manifestent là où des roches volcaniques d'âge pliocène percent des assemblages volcaniques ou les recouvrent partiellement dans le bassin de Bowser. L'existence de magnétisations normales et de magnétisations inverses témoigne d'un volcanisme prolongé et épisodique. Les plutons mésozoïques du bassin de Bowser engendrent une anomalie magnétique distinctive. Une anomalie similaire centrée sur 56°13,4'N 129°34,0'W pourrait également marquer l'emplacement d'un pluton. On présente sous forme de carte en courbes de niveau et de profil, les données gravimétriques régionales et de haute résolution. On examine les corrélations entre les données gravimétriques et les données aéromagnétiques dans un contexte géologique.

¹ Cordilleran Division, Vancouver

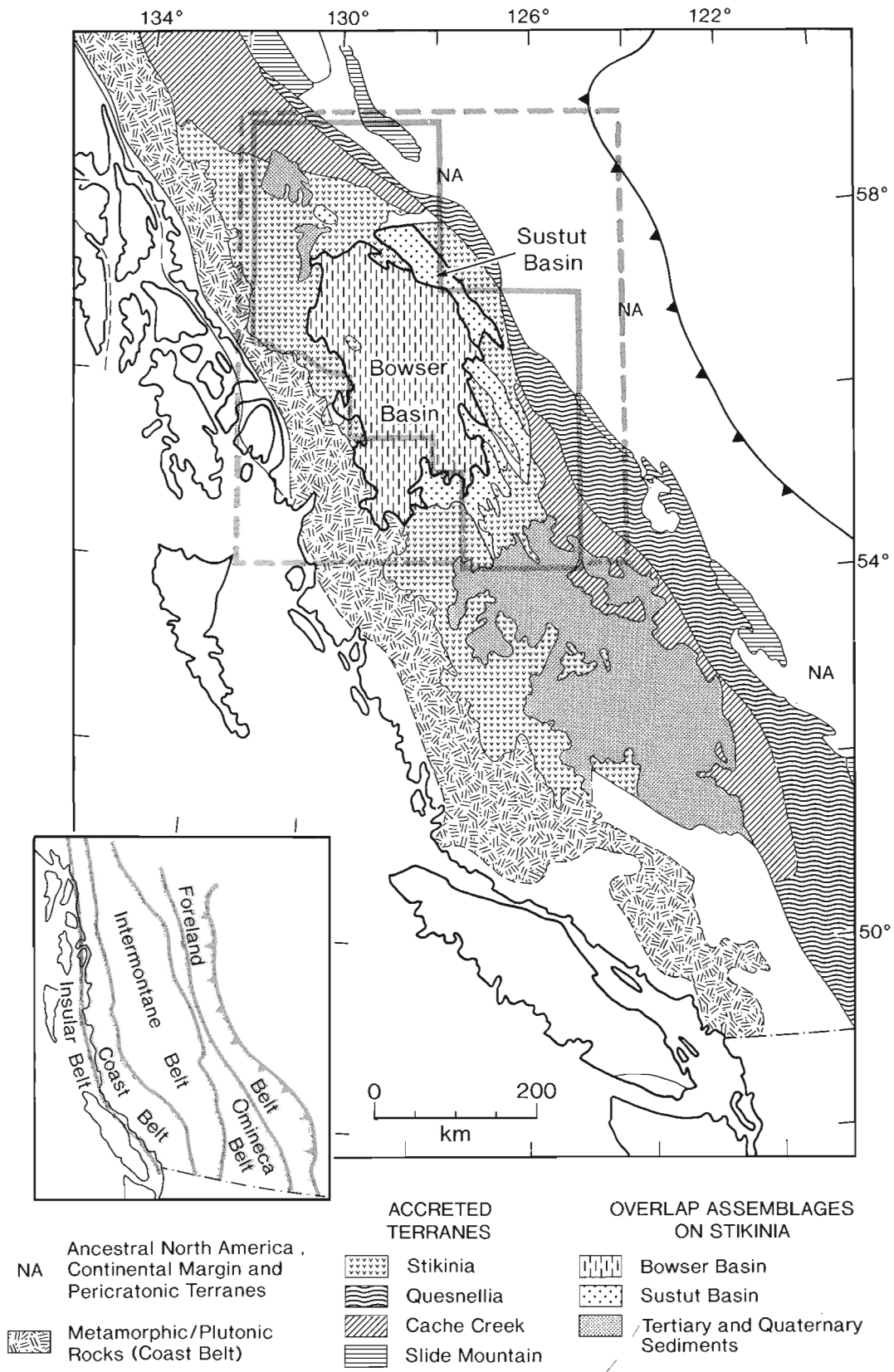


Figure 1. Generalized tectonic map of the northern Canadian Cordillera, modified after Evenchick (1991a). Only terranes in the Intermontane Belt and overlap assemblages in Stikinia are indicated. The locations of Figure 2 and Figure 4 are outlined in continuous and dashed lines, respectively. Inset shows the morphogeologic belts of the Canadian Cordillera.

INTRODUCTION

A potential field study was recently initiated in north-central British Columbia, in an area underlain by Stikinia and overlapping sedimentary assemblages in the Bowser and Sustut basins, (Fig. 1). As part of this study, the regional gravity coverage (station interval 10 km) was extended across the western margin of the Bowser Basin, and high-resolution (station interval 2.5 km) data were acquired along a 170 km northeasterly-trending profile. These data were reduced as Bouguer anomalies, to be incorporated into the National Geophysical Database, Ottawa. A Global Positioning System (GPS) was used to locate gravity stations, and yielded 3-D positions to an accuracy of a few tens of centimetres.

Evenchick (1991a, b) has proposed that a minimum of 44% shortening was accommodated across the northern part of the Bowser Basin, between Latest(?) Jurassic and Early Tertiary times, during the development of a northeasterly directed thrust and fold belt (Skeena Fold Belt). Deformation there is thought to be "thin-skinned", with a basal décollement lying within the upper units of Stikinia. Further to the south, in the Oweege Dome inlier, deformed basement (Stikinia) rocks are also exposed (Greig, 1991).

The objectives of the current study are to analyze variations in thickness of sedimentary rocks within the Bowser and Sustut basins, to examine the relationship of these basins to the underlying accreted terranes, and to determine involvement of basement rocks in the Mesozoic and Tertiary deformation. In this paper, new and pre-existing gravity data and high resolution aeromagnetic data are qualitatively analyzed and correlated with known geology. Future work will focus on quantitative analysis and inverse modelling of these data to develop a 3-D structural model of the area and to provide a framework for testing tectonic hypotheses.

GEOLOGICAL SETTING

On the edges of the study area (Fig. 1) metamorphic and plutonic rocks predominate in the Coast and Omineca belts. In the Coast Belt plutonic rocks range in age from Late-Cretaceous to Tertiary, whereas in the Omineca Belt they are predominantly Early Jurassic and Mid-Cretaceous (Wheeler and McFeely, 1987; Gabrielse, 1991). The centre of the study area is underlain by Stikinia. This is the largest of the accreted terranes and extends across most of the width of the Intermontane Belt. It is overlain by Middle Jurassic to Cretaceous sedimentary assemblages in the Bowser and Sustut basins. Paleozoic and Mesozoic rocks in the accreted Cache Creek and Quesnellia terranes form minor outcrops within the study region. Comprehensive accounts of the geology are given in a number of recent publications (Eisbacher, 1981; Gabrielse, 1985, 1991; Evenchick, 1991a, b; Greig, 1991; Anderson and Thorkelson, 1990).

Stikinia is comprised of a Mississippian to Upper Triassic sequence of platformal carbonates and arc related rocks, which are overlain by felsic to mafic volcanics and associated epiclastics of the Lower to Middle Jurassic Hazleton Group (Greig, 1991; Gabrielse, 1991). A Mid-Jurassic

compressional event emplaced the Cache Creek terrane upon Stikinia. Both terranes were amalgamated with Quesnellia forming the "Intermontane Superterrane", which was subsequently accreted to the North American continental margin (Gabrielse, 1991). The uplift of the Cache Creek Terrane and Stikinia provided clastics to the Bowser Basin (Eisbacher, 1981). The Bowser Lake Group is dominated by a marine to nonmarine succession of siltstone, shale, fine sandstone, and conglomerate, (Eisbacher, 1981). The Sustut Group of Mid to Upper Cretaceous clastics, rests unconformably upon the Bowser Lake Group or upon Stikinia (Evenchick, 1991a). This sedimentary assemblage is divided into an older Tango Creek Formation, and a younger Brothers Peak Formation. The source for the lower Tango Creek Formation was the Omineca Belt whereas clastics in the Upper Tango Creek and Brothers Peak Formations had a westerly source in the Bowser Basin (Eisbacher, 1974).

Compression of the Bowser and Sustut basins from Late Jurassic(?) to Late Cretaceous or Early Tertiary times formed the Skeena Fold Belt (Evenchick, 1991a, b). This thrust and fold belt is presently exposed as a rugged mountainous terrain. Deformation involved both the cover of the Bowser and Sustut basins and underlying units of Hazleton Group rocks in Stikinia (Evenchick, 1991a, b).

The youngest formation is Late Pliocene basalt, erupted through the Bowser Lake Group to form columnar jointed flows and volcanic necks (Evenchick and Green, 1990).

AEROMAGNETIC DATA

High-resolution, aeromagnetic data from the National Geophysical Database were used to generate the image shown in Figure 2 and the profiles shown in Figure 3. The coverage is a composite of several surveys. No data are yet available for the southernmost Bowser Basin or for much of the central part of the Sustut Basin and Omineca Belt. Compilation procedures (including removal of the 1985 International Geomagnetic Reference Field, and interpolation onto a 812.8 m grid) are similar to those described by Dods et al. (1985).

The residual aeromagnetic data were displayed as a shaded-relief color image to enhance small, low-amplitude features. In this paper, the image is photographically reproduced in black and white (Fig. 2). A simple visual inspection indicates four magnetic zones with distinctive characteristics. These zones (labelled I, II, III, and IV, Fig. 2) are effectively outlined by the geologically mapped boundaries of the Bowser and Sustut basins and by the neighbouring terranes. The close correspondence of the magnetic zones to the mapped geology indicates the aeromagnetic data's sensitivity to variations in lithology, uplift, and thermal history. Each zone has a relatively homogeneous internal magnetic fabric, characterized by anomalies of similar amplitude and wavelength, which are easily distinguished from those of neighbouring zones. The black and white image (Fig. 2) portrays the distinctive magnetic fabric, while the profiles (Fig. 3) indicate the

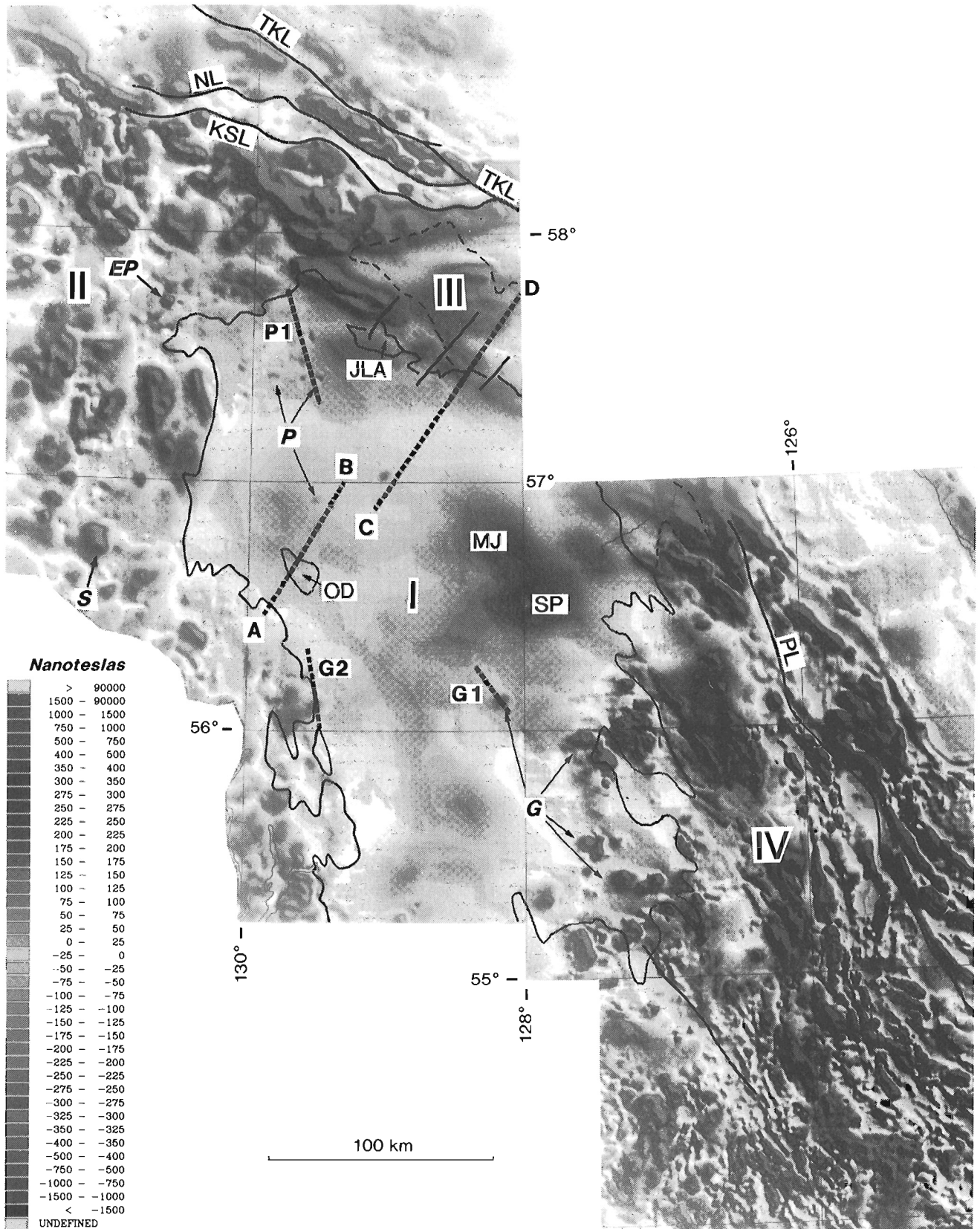


Figure 2. Black and white photographic reproduction of a shaded-relief colour image of aeromagnetic residuals. The mapped boundaries of the Bowser (continuous) and Sustut (dashed) basins are indicated. Magnetic zones referred to in the text are labelled I, II, and IV. **Basement inliers:** Oweegee Dome (OD), Joan Lake Anticline (JLA); **Magnetic lineaments:** Thibert-Kutchok lineament (TKL); Nahlin lineament (NL); King Salmon lineament (KSL); Pinchi lineament (PL); **Transects:** G1, G2, P1, and AB-CD are shown in Figure 3. Plutonic bodies and volcanic rocks are indicated by G and P, respectively.

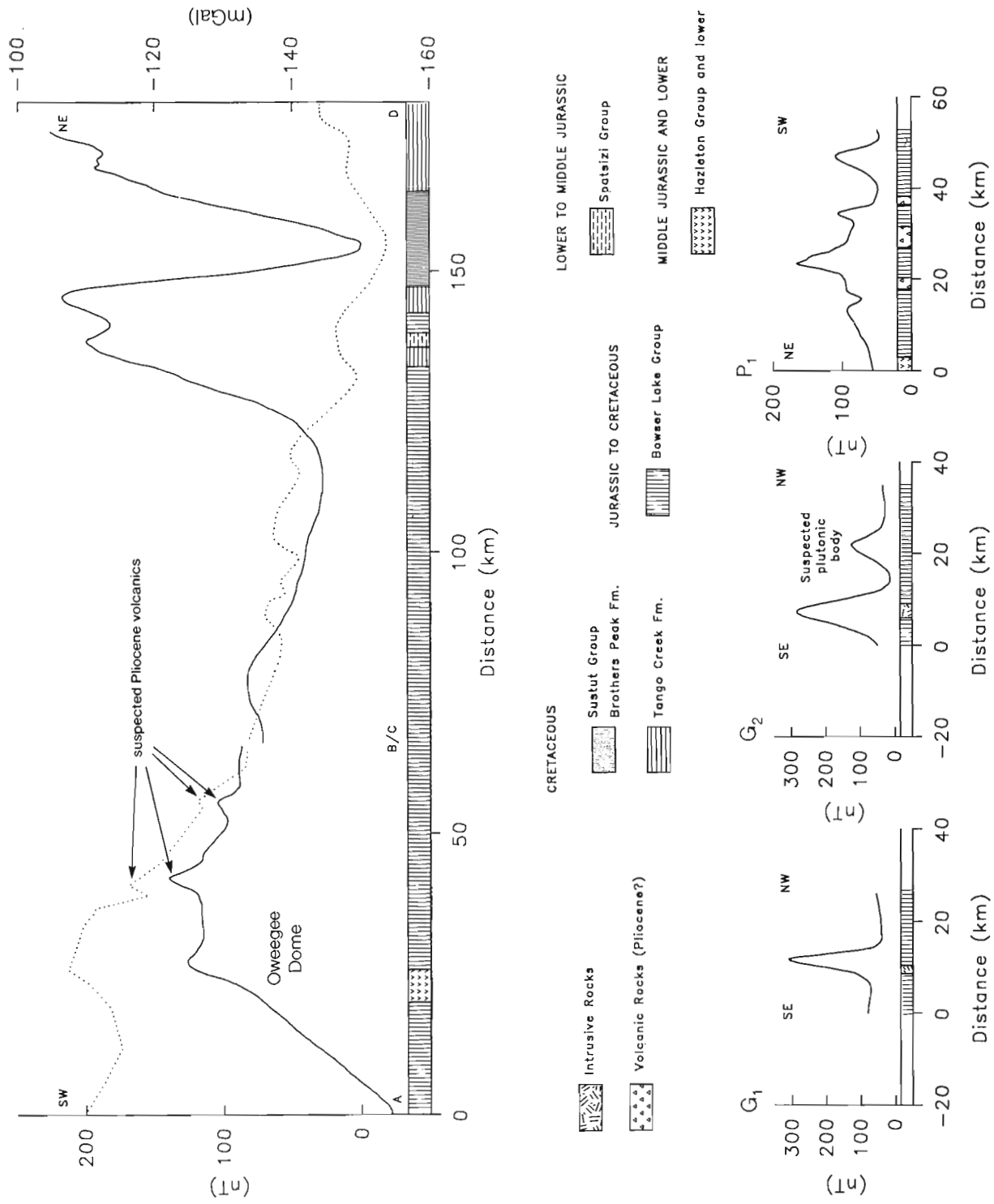


Figure 3. Profiles from the study region; magnetic (solid lines) and gravity (dotted lines). The location of transects are indicated in Figures 2 and 4. Gravity data are displayed as Bouguer anomalies (in mGal) while aeromagnetic data are displayed as residual anomalies (in nT). The geological legend refers to map formations shown as a strip along the base of each profile.

magnitude of intensity variations which are sensitive to the magnetite content and magnetic susceptibility of underlying rocks. A brief description of the four zones is given below:

Zone I

Zone I in the central part of Figure 2 is approximately coincident with the geologically mapped Bowser Basin. The magnetic features in this zone have amplitudes which are usually less than 350 nT and gradients which are less than 3 nT/km. This response indicates both the weak magnetic character of the Bowser sediments and the considerable depth to basement (Stikinia).

The smooth character of the zone is punctuated by two types of short-wavelength anomalies, designated "P" and "G". The "P" anomalies (Fig. 2 and 3) typically have intensities of 30 to 80 nT, wavelengths <10 km, and gradients >9 nT/km. Many correspond with mapped outcrops of Pliocene basalt (Evenchick and Green, 1990; Gabrielse and Tipper, 1984). In some cases, the magnetic anomalies are more extensive than mapped volcanic outcrops, suggesting hypabyssal intrusions beneath surface flows. In profile the anomalies have very simple geometries, consisting of a single intense peak or trough. Peaks predominate, and indicate extrusions during periods of normal magnetization, while troughs of decreased intensity indicate a reversed field at the time of emplacement. In a few cases, single outcrops of volcanics have more complex magnetic responses, suggesting multiple flows, or shallow intrusions magnetized at different times. These more complex features and the existence of both normal and reverse magnetizations suggests the volcanism spanned one or more field reversals.

The "G" anomalies (Fig. 2 and Fig. 3 (G1 and G2)) are normally magnetized, with wavelengths in excess of 10 km, peak magnetic intensities of 100 to 350 nT, and gradients of 8-30 nT/km. Many are associated with outcrops of Mesozoic plutons (for example, G1 in Fig. 3; Geological Survey of Canada, 1957). Compared to mapped plutons the areal extent of many "G" anomalies indicates the plutons are larger at depth. A number of "G" type anomalies do not correspond to mapped plutons. Two such anomalies, "MJ" and "SP", are indicated in Figure 2, while a third is shown in profile in Figure 3 (G2). The latter anomaly has a maximum intensity of 126 nT and a wavelength of 24 km. A simple graphical technique (Vacquier et al., 1951) yields an approximate depth of 1.8 km to the upper surface of the causative body. Mount Jackson (MJ) and Stephen Peak (SP) are the largest isolated magnetic features within the Bowser Basin. The wavelength of both anomalies is approximately 120 km and they have peak magnetic intensities of about 350 nT. The northern part of the Mount Jackson anomaly occurs over the eastern part of the Groundhog Coalfields and the latter (SP) over sediments in the Bowser Lake Group further to the southeast. Both anomalies are elongated in a northwest-southeast direction, parallel to the structural and magnetic grain. Although the nature of these magnetic anomalies is uncertain, we speculate that high-grade anthracite and meta-anthracite

coal seams within the "Carrier" unit of the Groundhog Formation may owe their high rank to a shallow pluton of pre- or Early Tertiary age.

Zone II

Zone II, to the north and west of the Bowser Basin, encompasses part of the Coast Belt in the south, and portions of Stikinia, the Cache Creek Terrane, and Quesnellia in the north (Fig. 1, 2). It is characterized by moderate to elevated magnetic responses (50 to 400 nT). Sub-oval and elongate anomalies are abundant in the Coast Belt as well as further north in the accreted terranes. These anomalies with wavelengths that vary from less than 10 km to more than 60 km have peak magnetic intensities in the range 100 to 500 nT and gradients in excess of 10 nT/km. They are commonly associated with granites, granodiorites, and quartz monzonites which episodically intruded the Coast Belt and western Intermontane Belt between the Mid Jurassic and Tertiary (Wheeler and McFeely, 1987). One such anomaly (labelled "S" in Fig. 2) corresponds to a quartz-monzonite pluton in the Mount Dick region of the Iskut map area (Geological Survey of Canada, 1957). Late Tertiary and Quaternary volcanics within the zone produce elevated magnetic responses particularly at the margins of basaltic plateaux and eruptive centres like Mount Edziza (EP on Fig. 2).

Northwest-trending lineaments marking breaks in the magnetic fabric, extend for more than 100 kilometres. Three such lineaments, in the northern part of Zone II, coincide with traces of the King Salmon (KSL), Nahlin (NL), and Thibert-Kutcho (TKL) fault systems. The Cache Creek Terrane, bounded on the south by the King Salmon Fault and on the north by the Thibert-Kutcho fault system, displays a more subdued magnetic response than either neighbouring terrane. This reflects lithological differences between the terranes; both Quesnellia (to the north) and Stikinia (to the south) contain higher proportions of mafic volcanics than the chert-rich lithologies that dominate the Cache Creek Terrane (Gabrielse, 1991).

Zone III

Zone III, the smallest, lies northeast of zone I, coincident with the map extent of the Sustut Basin (Fig. 1). Within the zone the magnetic response is relatively smooth, with gradients less than 20 nT/km. Maximum intensities, in the range 50-400 nT, are higher than observed in zone I. This observation suggests either elevated magnetic susceptibilities for Sustut sediments as compared to those of the Bowser, or alternatively, a northeasterly shallowing of magnetic basement. As mentioned earlier, sediments of the Bowser Lake Group were derived from chert-rich Cache Creek lithologies, whereas sediments in the Sustut Group were derived in part from metamorphic and plutonic rocks in the Omineca Belt and in part from eroded Bowser Basin sediments (Eisbacher, 1981). Detailed geological studies indicate that while the Sustut Group was deposited directly on volcanics (Stikinia) in the northeast part of the Sustut

Basin, the lowermost units of the Sustut Group are underlain by sediments of the Bowser Lake Group in the southwest (Eisbacher, 1974, 1981). Measurements of magnetic susceptibility and further processing of the magnetic data, including upward continuation and spectral analyses, are planned to evaluate the two alternatives.

The boundary between zones I and III is marked by an elongate band of northwest-trending magnetic anomalies which may be traced into zone II, and with lesser clarity, into zone IV (Fig. 2). Further to the northwest and to the southeast these anomalies are associated with outcrops of Triassic and Jurassic volcanics and epiclastics of Stikinia (Gabrielse and Tipper, 1984; Evenchick, 1991a). In the northwest, the linear band of anomalies is coincident with a mapped anticlinorium in Hazleton Group rocks. The continuity of the magnetic anomalies to the southeast (Fig. 2) suggests this structural high extends beneath the relatively nonmagnetic sediments of the Bowser and Sustut Basins, consistent with the structural interpretations of Evenchick (1991a).

Zone IV

The most complex region is zone IV, to the south and east of the Bowser Basin. The magnetic response is characterized by a strong northwesterly banding parallel to regional strike (Fig. 2). This area contains highly magnetic volcanic sequences of Stikinia, Quesnellia, and the Cache Creek Terrane (Fig. 1). Numerous lineaments correlate with northwest-trending faults. The Pinchi lineament, ("PL" in Fig. 2), extending for more than 250 km, coincides with the mapped trace of Pinchi Fault, separating Cache Creek (to the southwest) from Quesnellia (to the northeast). As in zone II the Cache Creek Terrane has a more subdued magnetic response than Quesnellia.

GRAVITY DATA

A Gravity anomaly map (Fig. 4) was generated from approximately 3000 single gravity readings (average spacing 10 km). The data are available from the National Geophysical Data Centre in Ottawa (note: approximately 70 of these measurements were acquired during the 1991 field season and will comprise the latest additions to the National Geophysical Database). All measurements are referenced to the International Gravity Standardization Net 1971 (Morelli, 1974). Bouguer anomalies were calculated using a standard density of 2.67 g cm^{-3} . Terrain corrections were applied using a 1 km digital elevation file to a distance of 30 km from each reading.

The Bouguer anomaly data (Fig. 4) clearly highlight the northwest trending structural grain, and depict several isolated anomalies. In general, the anomaly pattern is "busier" for basement terranes than for sedimentary overlap assemblages. The regional gravity data are less sensitive to differences between terranes than the aeromagnetic data described above. Bowser, Sustut, and younger sedimentary assemblages, which overlap Stikinia, are characterized by smooth, open contours. Contours within the Bowser Basin

suggest variations in sediment thickness. Generally, higher values are observed over the southern and southwestern parts of the basin.

The eastern boundary of the Sustut Basin is marked by a gravity gradient of 1.3 mGal/km . While Bouguer values to the east of the basin are higher than in the basin, they are low compared to Stikinia exposed west of the Bowser Basin. This suggests lateral variations in density contrasts within Stikinia. Further suggestions of lateral density variations, within and possibly beneath Stikinia, are indicated by the contrasting gravity signatures observed over the Joan Lake Anticline (JLA) and Oweegee Dome (OD) inliers in the Bowser Basin. Both inliers, (Fig. 4) expose volcanic and volcanoclastics of the Hazleton Group, and in addition the Oweegee Dome contains Permian limestones and Triassic volcanics (Greig, 1991). Bouguer values over the Oweegee Dome are comparable to those observed over Stikinia west and north of the Bowser Basin (Fig. 3). In contrast, a large Bouguer low (minimum -156 mGal) overlies the Joan Lake inlier (Fig. 4). This sub-oval anomaly is the largest observed over regions underlain by Stikinia. Density measurements on welded tuffs and porphyritic lavas from the Joan Lake area yield average values of $2.65 \pm 0.09 \text{ g cm}^{-3}$, while densities of $2.60 \pm 0.13 \text{ g cm}^{-3}$ are typical of the surrounding sedimentary rocks. Unless substantial material of lower density remains unsampled, these data suggest that volcanics and volcanoclastics in the Joan Lake region are not responsible for the observed Bouguer low. Alternative hypotheses include underthrusting of Bowser Lake Group sediments beneath the inlier, or low density rocks in the Stikine stratigraphy beneath the exposed Hazleton Group.

The largest isolated gravity low in the study area (minimum -168 mGals) corresponds to granodiorite and quartz-diorite of the Early to Middle Jurassic Hogem Batholith. Sub-oval and elongate Bouguer lows are also associated with the Germansen and Cassiar batholiths (Fig. 4). The latter, one of the largest in the Canadian Cordillera, lies north and east of the Sustut Basin, its elongate outcrop extending northwestwards beyond the study area. These Bouguer lows indicate that the granitic batholiths have lower densities than the surrounding lithologies. Steep, linear, gravity gradients ($0.5\text{-}1.7 \text{ mGal/km}$) are associated with several mapped faults (for example, the Northern Rocky Mountain Trench, the Kechika fault, the Kutcho Fault, and the Pelly Fault, see Fig. 4). Bouguer data indicate significant density and thickness contrasts across these faults. The steepest gradients (1.7 mGal/km), which trend northwestwards across the survey region, are associated with the trace of the Northern Rocky Mountain Trench. This is a major physiographic low across which abrupt changes in stratigraphy have been mapped.

TRANSECT AB-CD

In addition to the regional gravity data acquired in 1991, 67 new measurements (average station interval 2.5 km) were acquired along a 168 km, northeast-trending transect, (AB-CD, Fig. 3, 4). The northern part of this transect is coincident with a structural cross-section presented in

Evenchick (1991a, p. 979). Although regional terrain corrections have been applied to these data, the rugged terrain demands more detailed corrections before an accurate geological evaluation is attempted. This work is currently

underway. More than 1000 density measurements on rocks from the region will be used to constrain the gravity model. While emphasizing their preliminary nature we present some

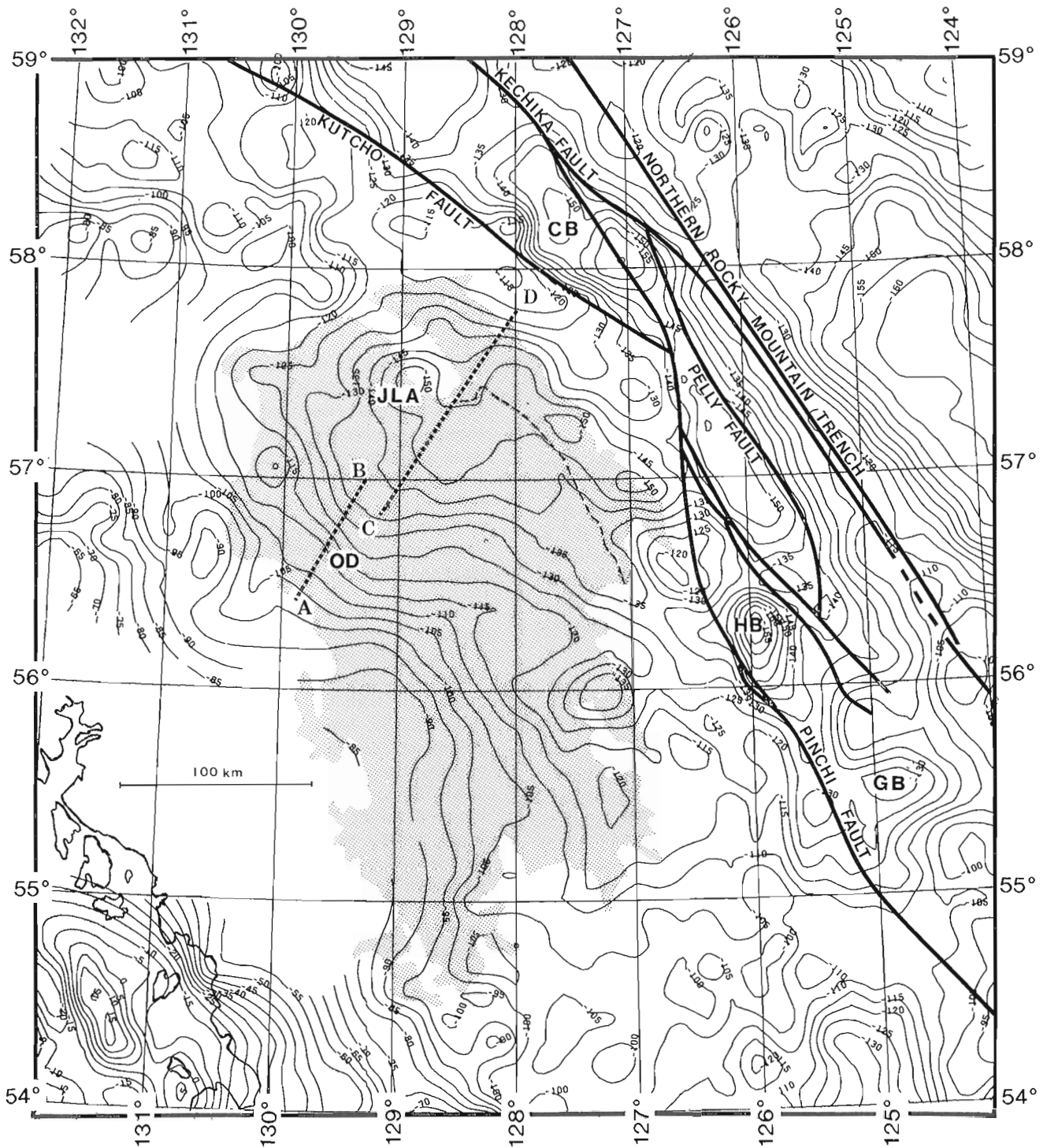


Figure 4. Contoured gravity anomaly data (Bouguer on land, Free-air offshore) for the area outlined in Figure 1. The shaded areas depict the mapped extent of the Bowser and Sustut Basins. **Basement inliers:** Oweege Dome (OD); Joan Lake Anticline (JLA); **Batholiths:** Hogem Batholith (HB); Cassiar Batholith (CB); Germansen Batholith (GB); The mapped traces of several major faults are indicated.

comments on these data and on a coincident magnetic profile (Fig. 3). The magnetic profile was interpolated from the gridded data described above.

The largest Bouguer high having a maximum amplitude of -108 mGal is found at kilometre 25 on the profile (Fig. 3). A corresponding magnetic high (peak intensity 130 nT) is also observed. Both highs are associated with outcrops of Permian limestones, Upper Triassic and Lower to Middle Jurassic volcanics and volcanoclastics (Stuhini and Hazleton groups) in the Oweege Dome (Greig, 1991). The southern boundary of the Oweege Dome is the locus of high gradients in both the gravity and the magnetic data, while to the north gentler gradients are observed.

North of the Oweege Dome two pairs of coincident gravity and magnetic highs are observed (kilometre 42 and 56, Fig. 3). The intensities and wavelengths of the magnetic anomalies are similar to those observed over mapped outcrops of Pliocene basalt farther north (see profile P1, Fig. 3). Density measurements on specimens of Pliocene basalt yield an average value of $2.70 \pm 0.08 \text{ g cm}^{-3}$ which is significantly higher than that of sediments in the Bowser Lake Group ($2.60 \pm 0.13 \text{ g cm}^{-3}$). No Pliocene basalts are mapped in this area and consequently it is thought the potential field observations may reflect unexposed dykes or feeder pipes at shallow depths.

Outcrops of the Brothers Peak Formation (Sustut Group) in the Sustut Basin generate a pronounced magnetic low at kilometre 156 (Fig. 3). A corresponding, though less significant, gravity anomaly is associated with the magnetic low. Magnetic highs, with peak intensities of more than 200 nT, occur both to the north and south of anomaly low. In the south, steep magnetic gradients (27 nT km^{-1}) separate the high from the low. Gabrielse and Tipper (1984) map a structural culmination in volcanics (Stikinia) northeast along strike from the anomaly high. The continuity of this culmination to the south, beneath a thin sedimentary cover, may be the source of the anomaly high. The structural cross-section of Evenchick (1991a) also indicates a basement culmination in this area. A similar magnetic high, at the northeast end of the profile, overlies exposures of volcanics and epiclastics in Stikinia. Magnetic susceptibility measurements on rock samples from this region will be used to quantitatively model the profile.

SUMMARY

Preliminary examination of potential field data from north-central British Columbia highlights a number of subsurface features hitherto unrecognized. The data provide support for a structural culmination in basement rocks beneath the sedimentary cover of the Bowser and Sustut basins. Pronounced variations in magnetic character due to differences in lithology or thermal history are noted for the accreted terranes.

ACKNOWLEDGMENTS

Taimi Mulder (University of British Columbia) is thanked for her enthusiastic field assistance. David Laxton (Mapping and Charting Establishment) provided useful instruction on GPS and associated processing techniques. Constructive reviews were given by Tark Hamilton and Chris Yorath (Pacific Geoscience Centre).

REFERENCES

- Anderson, R.G. and Thorkelson, D.J.**
1990: Mesozoic stratigraphy and setting for some mineral deposits in the Iskut map area, northwestern British Columbia; in *Current Research, Part E*; Geological Survey of Canada, Paper 90-1E, p. 131-139.
- Dods, S.D., Teskey, D.J., and Hood, P.J.**
1985: The new 1:1,000,000 - scale magnetic anomaly maps of the Geological Survey of Canada: compilation techniques and interpretation; in *The Utility of Regional Gravity and Magnetic Maps*, (ed.) W.J. Hintze; Society of Exploration Geophysicists, Tulsa, OK, p. 69-87.
- Eisbacher, G.H.**
1981: Late Mesozoic-Paleogene Bowser Basin molasse and Cordilleran tectonics, western Canada; in *Sedimentation and Tectonics in Alluvial Basins*, (ed.) A.D. Miall; Geological Association of Canada, Special Paper 23, p. 125-151.
1974: Sedimentary history and tectonic evolution of the Sustut and Sifton basins, north-central British Columbia; Geological Survey of Canada, Paper 73-31, 57 p.
- Evenchick, C.A.**
1991a: Geometry, evolution and tectonic framework of the Skeena Fold Belt, north-central British Columbia; *Tectonics*, v. 10, no. 3, p. 527-546.
1991b: Structural relationships on the Skeena Fold Belt on the west side of the Bowser Basin; *Canadian Journal of Earth Science*, v. 28, p. 973-983.
- Evenchick, C.A. and Green, G.M.**
1990: Structural style and stratigraphy of southwest Spatsizi map area, British Columbia; in *Current Research, Part F*; Geological Survey of Canada, Paper 90-1F, p. 135-144.
- Gabrielse, H.**
1985: Major dextral transcurrent displacements along the Northern Rocky Mountain Trench and related lineaments in north-central British Columbia; *Geological Society of America, Bulletin*, v. 96, p. 1-14.
1991: Late Paleozoic and Mesozoic terrane interactions in north-central British Columbia; *Canadian Journal of Earth Science*, v. 28, p. 947-957.
- Gabrielse, H. and Tipper, H.W.**
1984: Bedrock geology of the Spatsizi map area (104H); Geological Survey of Canada, Open File 1005.
- Geological Survey of Canada.**
1957: Stikine River area, Cassiar district, British Columbia; Geological Survey of Canada, Map 9-1957.
- Greig, C.J.**
1991: Stratigraphic and structural relations along the west-central margin of the Bowser Basin, Oweege and Kinskuch areas, northwestern British Columbia; in *Current Research, Part A*; Geological Survey of Canada, Paper 91-1A, p. 197-205.
- Morelli, C. (comp.)**
1974: International Gravity Standardisation Net 1971; International Association of Geodesy, Special Publication no. 4, Paris.
- Vacquier, V., Steenland, N.C., Henderson, R.G., and Zeitz, I.**
1951: Interpretation of Aeromagnetic Maps; Geological Society of America, Memoir 47.
- Wheeler, J.O. and McFeely, P. (comp.)**
1987: Tectonic assemblage map of the Canadian Cordillera and adjacent parts of the United States of America; Geological Survey of Canada, Open File 1565.

The Crevasse Crag Volcanic Complex, southwestern British Columbia: structural control on the geochemistry of arc magmas

R.A. Coish¹ and J.M. Journeay
Cordilleran Division, Vancouver

Coish, R.A. and Journeay, J.M., 1992: *The Crevasse Crag Volcanic Complex, southwestern British Columbia: structural control on the geochemistry of arc magmas*; in *Current Research, Part A; Geological Survey of Canada, Paper 92-1A*, p. 95-103.

Abstract

The Crevasse Crag Volcanic Complex (CCVC) is located 100 km east of the Garibaldi Volcanic Belt in southwestern British Columbia. It unconformably overlies Late Cretaceous and younger intrusive rocks of the Coast Plutonic Complex and is composed of volcanic breccias, tuffs and plagioclase-phyric flows. Near its base, the CCVC has an intrusion breccia containing fragments of volcanic rocks, quartz diorite, and exotic metamorphic and sedimentary clasts. Major, trace and rare earth element analyses indicate that flows near the base of CCVC are basaltic andesites, andesites, and dacites. Furthermore, chemical analyses exhibit a continental, calc-alkaline trend. The CCVC is interpreted to be part of the Pemberton Volcanic Belt, a Late Tertiary arc complex situated inboard of the Pleistocene and Recent Garibaldi arc. Lavas from the CCVC are chemically distinct from Garibaldi rocks; the differences may be attributed to a structural control on the ascent of CCVC magmas.

Résumé

Le complexe volcanique de Crevasse Crag est situé à 100 km à l'est de la zone volcanique de Garibaldi dans le sud-ouest de la Colombie-Britannique. Il repose en discordance sur les roches intrusives du Crétacé supérieur et plus récentes du complexe plutonique côtier et est composé des brèches volcaniques, de tufs et de coulées à phénocristaux de plagioclase. Près de sa base, le complexe contient une brèche d'intrusion formée de fragments de roches volcaniques, de diorite quartzique et de clastes métamorphiques et sédimentaires allochtones. Des analyses des éléments majeurs, des éléments en traces et des terres rares indiquent que les coulées près de la base du complexe sont des andésites basaltiques, des andésites et des dacites. De plus, des analyses chimiques révèlent une tendance calco-alkaline continentale. Le complexe est interprété comme faisant partie de la zone volcanique de Pemberton, qui est un complexe d'arc du Tertiaire supérieur situé dans l'arc de Garibaldi du Pléistocène et du Récent. Les laves du complexe de Crevasse Crag diffèrent chimiquement des roches de Garibaldi; les différences peuvent être attribuables à un contrôle structural sur l'ascension des magmas de ce complexe.

¹ Geology Department, Middlebury College, Middlebury, Vermont 05753, U.S.A.

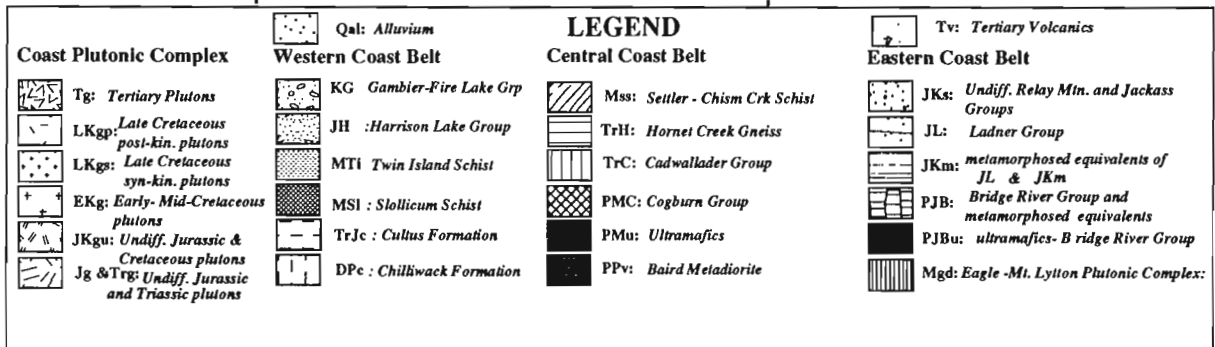
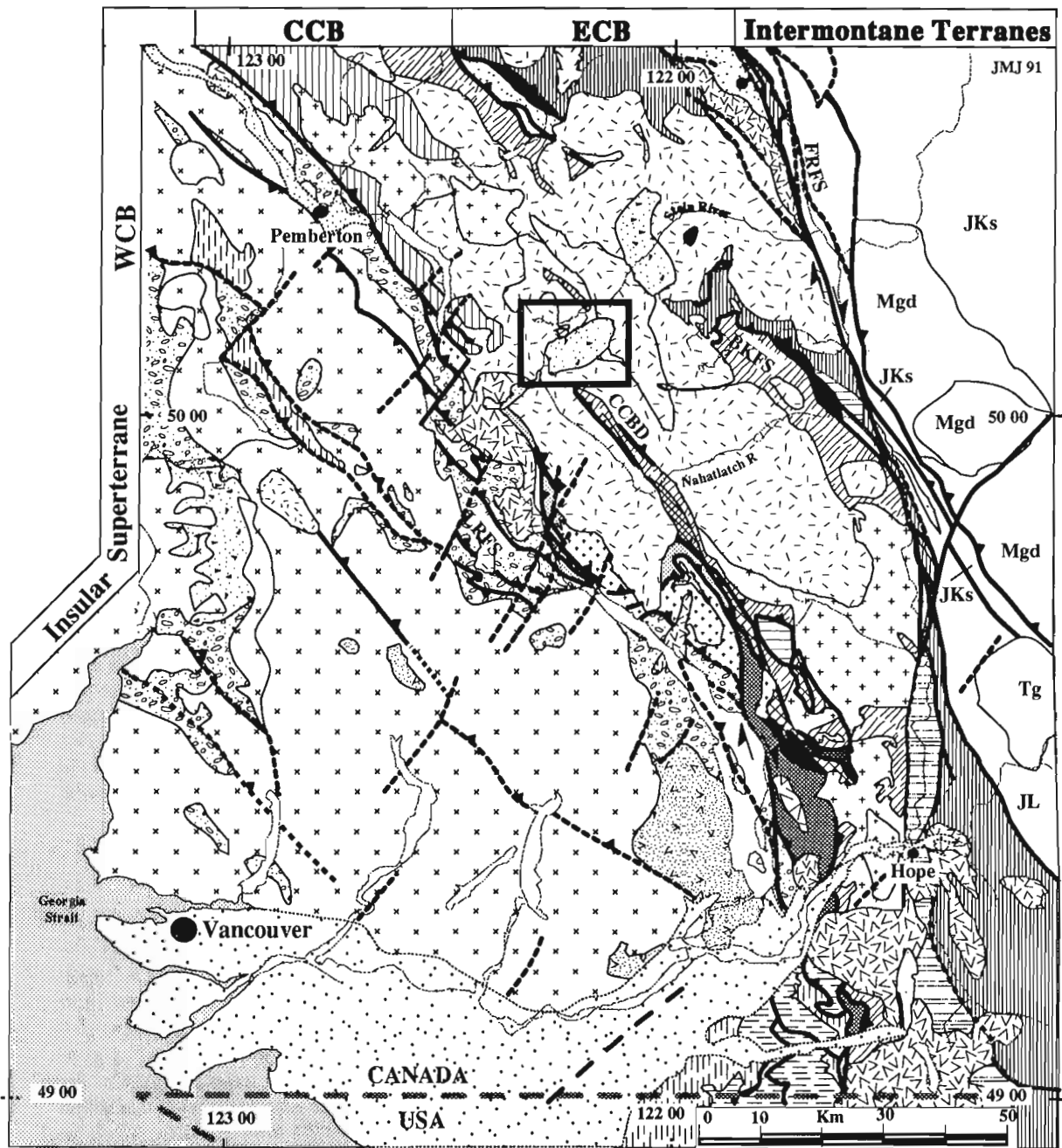


Figure 1. General geological map of southwestern British Columbia (Journeay, 1990) showing location of Crevasse Crag Complex.

INTRODUCTION

This report presents preliminary field, petrographic, and geochemical information on a Tertiary volcanic complex located about 20 km southeast of Lillooet Lake, in the Pemberton map area (Fig. 1). We informally name the unit the Crevasse Crag Volcanic Complex (CCVC) after a prominent topographic feature in the area. This work is based on a reconnaissance visit in 1989 by JMJ, detailed mapping of a small area in 1990 by JMJ and RAC, and petrographic and geochemical work in 1990 and 1991 by RAC.

The CCVC is interpreted as part of the Miocene Pemberton Volcanic Belt (Souther and Yorath, in press). The field relations and geochemistry are consistent with the formation of the complex in a subduction environment. The chemistry of the complex has interesting differences compared to volcanics from the younger Garibaldi belt; we interpret the differences to be related to a structural control on the ascent of CCVC magmas.

REGIONAL SETTING

The CCVC is located in the central Coast Belt, dominated by Mesozoic intrusions and metamorphosed volcanic and sedimentary rocks. The CCVC is one of three Tertiary?-aged volcanic bodies that fall along a northeast trend (Fig. 1). Although the other two bodies, one to the southwest and one to the northeast, have not been sampled or analyzed in detail, reconnaissance field work suggests that the rocks are similar in all three bodies which are thus assumed to be of the same age and origin (Roddick and Hutchison, 1973; Woodsworth, 1977). The southeastern body sits on the Rogers Creek pluton, dated at 16 Ma (Woodsworth, 1977; Friedman, 1990). Until results from K-Ar dating are available, we assume that the CCVC is 16 Ma or younger, based on the correlation of the CCVC with the southeastern volcanic complex that sits on the Rogers Creek pluton.

FIELD RELATIONSHIPS

The CCVC, maximum 12 km long by 8 km wide, has been mapped in detail in one area only. There, the stratigraphy of the lower part of the complex is beautifully exposed in a steep-walled bowl (Fig. 2); all subsequent discussion is based on this region. The stratigraphic sequence includes a plutonic core cut by an intrusion breccia, overlain in turn by coarse volcanic breccia, a mixed flow and tuff unit, a tuff unit, and a plagioclase-phyric flow unit. Northeast-trending dykes and northwest-trending sills cut through the stratigraphy.

The plutonic core is medium- to fine-grained quartz diorite that shows various stages of brecciation. The quartz diorite is composed of plagioclase, quartz, hornblende, biotite with secondary chlorite and calcite. It ranges from intact to completely "replaced" by a heterolithic intrusion breccia. Intermediate stages of the brecciation are seen in areas where en echelon fractures penetrate the quartz diorite and fragment mafic dykes that cut the pluton. The brecciation is interpreted to be due to invading fluids related to the development of the heterolithic breccias, rather than to tectonic movements.

The intrusion breccia, which cuts the quartz diorite and lower parts of the volcanic breccia, contains a spectacular montage of rock fragments. The breccia includes cobble sized fragments of quartz diorite, fine grained mafic, intermediate and felsic volcanic rocks, foliated granite and granodiorite, andalusite-staurolite schist, kyanite-andalusite schist, feldspathic gneiss and quartzite. The fragments range from angular to subrounded, and float in a matrix that comprises quartz and feldspar grains cemented by tuffaceous material. The breccia is thought to be a diatreme that cut like a blow-torch through the pluton and into the lowermost volcanic units. It may represent the lower part of feeder pipes to the overlying volcanic pile.

The volcanic breccia, in contrast to the intrusion breccia, consists of mostly volcanic fragments with minor quartz diorite. The fragments range from 1 m to a few centimetres across, are angular to subrounded, and in places are crudely aligned. The volcanic fragments range from mafic to intermediate lavas, with subordinate intermediate tuffs. The matrix is volcanic ash. The unit contains minor plagioclase-phyric flows which are autobrecciated in places.

Above the volcanic breccia is a unit containing fine grained flows and tuffs. The fine grained flows are dark, nearly aphanitic, with tiny crystals of plagioclase visible in hand specimen. In the thin section, it is seen that plagioclase is the dominant mineral with minor amounts of clinopyroxene and magnetite. Plagioclase grains are aligned presumably due to flow giving a trachytic texture. Minor calcite and chlorite alteration occurs in some samples. The fine grained flows are intercalated with a crystal-lithic tuff, consisting of broken, angular grains of plagioclase, quartz, rock fragments, clinopyroxene and magnetite in a fine grained tuffaceous matrix. Rock fragments are mostly fine- to medium-grained volcanics. In one locality, flattened pumice? fragments are seen.

The crystal-lithic tuff unit consists of fine- to medium-grained tuffs with subordinate amounts of coarse volcanic breccia and plagioclase phyric flows. The tuffs in this unit are similar to those described in underlying unit.

The plagioclase-phyric flow unit comprises andesitic to dacitic flows with prominent plagioclase phenocrysts. Clinopyroxene, magnetite, and rarely amphibole also occur as phenocrysts. The matrix is fine grained plagioclase and pyroxene. Plagioclase is beautifully and complexly zoned; clinopyroxene also shows some zoning. This flow is characteristic of the complex. In higher parts of the stratigraphy, there is very little alteration whereas where these flows are seen near the base calcite alteration can be pervasive. In places, the flows are autobrecciated.

Dykes and sills cut through the stratigraphy. Northeast trending dykes are about 3 to 5 m wide, are andesitic to dacitic, with plagioclase and clinopyroxene phenocrysts, and in places carbonate alteration. They are similar to the plagioclase phyric flows. Northwest-trending sills/dykes again are andesitic and are dominated by plagioclase phenocrysts but also have large percentages of amphibole and pyroxene phenocrysts, which differentiate them from flows in the region.

WHOLE ROCK GEOCHEMISTRY

Whole rock chemical analyses for major and trace elements (including rare earths) were performed on 19 samples of flows, 3 dyke/sill samples and 1 sample of plutonic rock by Chemex labs, North Vancouver (Table 1).

Flows are classified as mostly basaltic andesite and andesite with two basalts and dacites (Fig. 3A, B). On an alkalis-SiO₂ diagram, all samples are subalkaline, plotting below the alkaline/subalkaline line (Irvine and Baragar, 1971). On the AFM and K₂O versus SiO₂ diagrams, the flows plot as calc-alkaline series. However, it should be noted that the trend shown in K₂O versus SiO₂ diagram is across the calc-alkaline field with a higher positive slope than many calc-alkaline rocks. This trend is similar to that exhibited by volcanic rocks associated with extensional regions of the Aleutian arc (Kay et al., 1982).

On Harker variation diagrams, FeO, TiO₂, MgO, Al₂O₃, and CaO all decrease with increasing SiO₂ content, also consistent with a calc-alkaline trend (Fig. 4). However, as is discussed later, Harker trends shown by CCVC rocks differ slightly from younger subduction volcanics in the Cordillera. On mantle-normalized diagrams, the CCVC rocks show an enrichment in incompatible elements relative to more compatible elements, and show a general increase in total incompatible element content with increasing SiO₂ (Fig. 5). Furthermore, the patterns exhibit negative anomalies in Ta and Nb relative to K and La (Fig. 5), characteristic of volcanic rocks formed from sources that have been modified by subducting-plate fluids (Brique et al., 1984). On other diagrams designed to distinguish among tectonic environments, the Crevasse Crag rocks invariably fall in

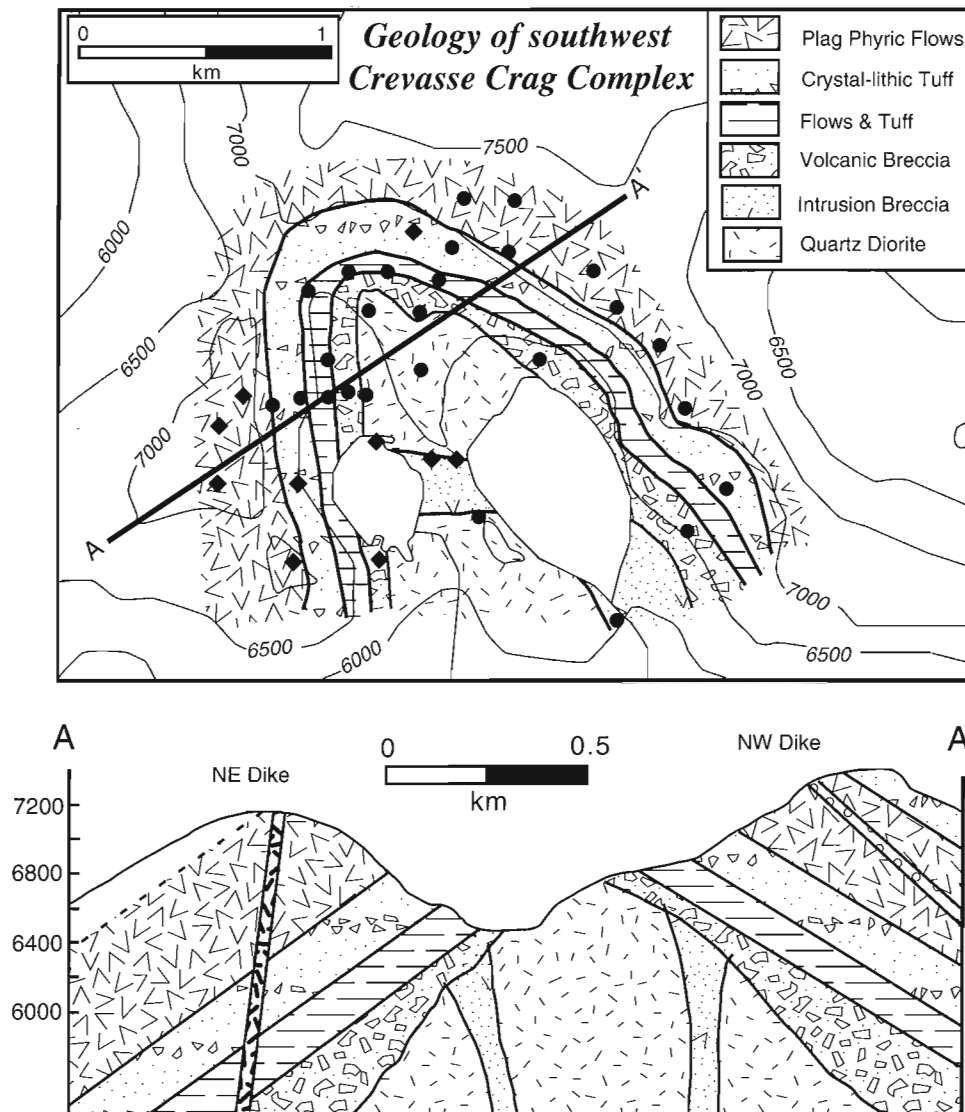


Figure 2. Geological map and cross-section of southwestern part of Crevasse Crag Complex. Station localities are denoted by (♦) for samples with an RC prefix in Table 1, and by (•) for samples with RCJ prefix.

Table 1. Geochemistry of rocks from Crevasse Crag Volcanic Complex (units: PPF (plagioclase-phyric flow), CLT (crystal-lithic tuff), F & T (flows & tuff), (volcanic breccia), QD (quartz diorite); totals recalculated dry; trace elements in ppm).

<i>Unit</i>	PPF	CLT	CLT	F & T	F & T	F & T	F & T	F & T	CLT	F & T
<i>Sample</i>	RC9015	RC9011A	RC9005B	RC9012B	RC9009A	RC9012C	RC9009B	RC9006	RC9004	RC9024
SiO ₂	51.62	52.44	55.29	54.71	54.89	56.53	56.39	59.08	59.32	57.64
TiO ₂	1.04	0.95	0.87	1.32	1.15	1.31	1.14	0.87	0.95	0.89
Al ₂ O ₃	20.05	20.29	19.32	18.54	18.54	18.09	18.24	18.54	18.83	17.89
Fe ₂ O ₃	8.91	8.59	7.97	9.50	9.00	8.96	8.90	6.84	6.94	7.91
MnO	0.19	0.21	0.14	0.15	0.19	0.17	0.16	0.13	0.11	0.15
MgO	5.13	5.10	4.43	3.63	3.30	3.40	3.18	2.44	2.98	3.74
CaO	8.58	8.41	5.40	7.50	7.04	7.10	6.55	7.58	6.64	8.01
Na ₂ O	3.40	3.48	5.21	3.69	4.38	3.50	4.14	3.80	4.24	3.04
K ₂ O	0.84	0.17	1.24	0.59	1.22	0.75	1.39	1.31	1.06	1.03
P ₂ O ₅	0.29	0.29	0.25	0.39	0.41	0.37	0.40	0.28	0.26	0.27
Total	100.04	99.93	100.12	100.01	100.12	100.17	100.51	100.87	101.32	100.57
LOI	4.40	4.53	5.44	3.95	1.75	2.81	2.05	5.93	5.36	1.93
<i>Traces</i>										
Sc	31	26	26	22	24	23	22	24	26	32
V	170	142	166	187	134	184	131	144	183	183
Co	25	26	18	18	14	16	14	12	13	17
Ni	19	36	26	6		8		3	3	5
Rb	5	2	23	5	6	6	0	12	16	11
Sr	453	490	382	483	554	522	510	418	433	6
Y	22	17	24	32	25	27	23	22	21	357
Zr	110	115	116	167	132	185	128	181	111	20
Nb	10	8	10	12	10	12	11	11	10	102
Ba	282	241	307	416	468	432	561	584	602	9
Th	4.3	2.4	3.4	3.1	2.4	3.1	2.7	2.4	2.5	2
Ta	0.7	0.5	0.6	0.8	0.6	0.8	0.7	0.7	0.6	96
Hf	3.1	2.7	3.4	4.7	3.9	5.0	3.5	4.1	4.0	1.7
La	18.6	12.6	19.1	21.5	18.4	21.2	18.5	15.3	18.1	0.6
Ce	48	24	30	48	45	54	45	38	36	3.1
Nd	13	10	28	21	22	18	20	22	23	0.5
Sm	6.3	4.5	4.9	7.3	5.7	7.6	7.1	4.8	5.3	12.5
Eu	2.0	1.7	1.4	2.3	1.5	2.1	2.0	1.3	1.3	27
Tb	2.5	0.6	0.2	2.2	1.1	2.3	1.8	0.8	0.3	16
Yb	2.8	2.1	2.5	3.5	3.4	3.4	3.3	3.2	2.8	4.6
Lu	0.5	0.4	0.4	0.6	0.5	0.5	0.5	0.5	0.4	1.1
<i>Unit</i>										
	F & T	VB	PPF	PPF	PPF	PPF	NW Dike	NE Dike	NE Dike	QD
<i>Sample</i>	RC903A	RC9010	RC9013	RC9017	RC9018	RC1902	RC9014A	RC9007	RC9003B	RC9025
SiO ₂	60.64	63.83	63.54	62.51	63.93	63.68	54.64	61.73	61.83	59.42
TiO ₂	0.83	0.56	0.72	0.66	0.67	0.58	0.84	0.59	0.61	0.69
Al ₂ O ₃	17.02	15.97	17.06	16.08	16.46	15.73	15.58	16.47	16.46	16.38
Fe ₂ O ₃	7.07	5.53	5.46	5.15	5.01	5.24	7.97	5.59	5.54	6.97
MnO	0.14	0.08	0.09	0.10	0.09	0.11	0.13	0.11	0.11	0.11
MgO	3.43	2.64	2.54	2.48	2.29	3.00	7.11	3.98	3.85	4.17
CaO	5.91	5.66	4.98	5.34	5.14	5.41	9.12	6.41	7.02	6.49
Na ₂ O	3.46	3.39	3.53	3.25	4.06	3.72	3.11	3.72	3.29	3.34
K ₂ O	1.13	2.13	2.56	2.06	2.00	2.34	1.07	1.50	1.29	1.78
P ₂ O ₅	0.25	0.21	0.29	0.25	0.13	0.26	0.26	0.25	0.20	0.25
Total	99.88	100.00	100.76	97.88	99.79	100.07	99.83	100.35	100.19	99.61
LOI	4.07	6.88	2.33	0.01	1.69	1.31	2.25	7.07	6.65	2.97
<i>Traces</i>										
Sc	23	17	16	19	18	23	40	20	20	31
V	145	110	101	101	96	103	191	113	115	86
Co	11	16	13	14	11	14	29	15	16	12
Ni	5	9	10	12	8	5	28	31	31	5
Rb	9	25	50	33	25	41	11	23	21	19
Sr	399	361	369	391	374	375	507	484	546	256
Y	22	20	29	20	27	25	15	14	15	24
Zr	104	129	174	175	183	157	107	105	112	510
Nb	9	10	10	10	10	9	8	11	10	9
Ba	636	709	870	820	692	750	358	613	482	278
Th	1.8	7.4	7.8	6.2	6.9	6.7	3.2	5.4	6.1	4.1
Ta	0.6	0.6	0.6	0.6	0.6	0.6	0.5	0.7	0.6	0.6
Hf	3.4	4.0	5.8	6.3	6.3	5.6	3.0	3.7	3.8	3.9
La	13.4	23.3	25.9	24.4	26.1	24.6	15.4	20.7	24.2	16.4
Ce	29	43	66	47	49	45	37	43	34	33
Nd	16	16	17	18	21	20	16	21	20	14
Sm	4.5	5.2	7.3	6.0	6.4	6.5	5.2	3.8	4.3	4.8
Eu	1.5	1.3	1.8	1.3	1.2	1.0	1.6	0.9	1.0	1.0
Tb	0.3	0.5	1.5	1.0	1.0	1.2	0.3	0.5	0.5	0.9
Yb	2.6	2.1	2.9	3.5	3.8	3.4	1.9	1.7	1.9	3.0
Lu	0.4	0.4	0.5	0.4	0.4	0.4	0.4	0.3	0.3	0.4

volcanic arc fields; for example, Rb - Y + Nb, Th/Yb - Ta/Yb (Fig. 6). Moreover, the chemistry is indicative of a continental rather than an oceanic arc (Fig. 6B).

The chemistry of the CCVC rocks is similar to that of the Coquihalla Volcanic Complex, mapped as part of the Miocene Pemberton Volcanic Belt (Berman and Armstrong, 1980; Berman, 1981; Souther, in press). The chemistry of the two complexes overlaps completely on Harker variation diagrams (Fig. 4). (Note that felsic pyroclastic rocks from Coquihalla complex are not included in diagrams because they probably do not represent true liquid compositions). Also, trace element abundances and patterns are identical between the two complexes. Therefore, we consider the CCVC to be part of the Pemberton Volcanic Belt on the basis of its chemical similarity with the Coquihalla Volcanic complex and its age (16 Ma).

In contrast, there are significant differences between the chemistry of the CCVC and that of calc-alkaline rocks in the Quaternary Garibaldi range (Fig. 4). First, on Harker diagrams; Fe, Ti, and V are all higher, and MgO lower, at given SiO₂ values in the CCVC rocks. Secondly, in CCVC rocks Al₂O₃ decreases with increasing SiO₂ but increases in Garibaldi rocks. Thirdly, Sr contents are anomalously high in Garibaldi samples (Table 1). Fourthly, rare earth patterns have steeper slopes in Garibaldi rocks than in CCVC samples; i.e., La/Yb ratios are higher in Garibaldi lavas. These differences can be explained if the CCVC magmas fractionated under drier, lower pressure conditions than Garibaldi magmas. The relative importance of amphibole may be the key. If amphibole fractionation were more important in Garibaldi magmas than in CCVC, then differences in Harker trends can be explained because amphibole fractionation results in lower Fe, Ti, V, and higher La/Yb ratios in derivative magmas. Furthermore, if amphibole fractionation suppressed the crystallization of plagioclase at early stages in Garibaldi magmas, then Sr would increase in derivative magmas, perhaps giving rise to the observed high Sr. There is some independent evidence indicating the importance of amphibole in the origin of Garibaldi magmas. Amphibole is an important phenocryst phase in Garibaldi andesites, and theoretical fractionation models include up to 60% amphibole in calculated fractionated minerals (Green, 1981). In contrast, in CCVC rocks, amphibole is rare and seen only as a minor phenocryst phase in high Si andesites and dacites.

In summary of the geochemistry, Crevasse Crag rocks are calc-alkaline andesites, with minor basalt and dacite. Furthermore, they have the chemical imprint of volcanics formed in a continental subduction zone. Finally, they are chemically similar to the Miocene Pemberton Belt volcanics but show important differences from the Quaternary Garibaldi Belt.

INTERPRETATION AND TECTONIC IMPLICATIONS

Two main Neogene volcanic belts occur in southwestern British Columbia. The Pemberton Volcanic Belt (24-8 Ma) consists of subvolcanic plutons and explosive volcanic rocks,

interpreted here as an arc complex formed above an easterly-dipping oceanic plate (Souther and Yorath, in press). The PVB lies 50 to 100 km northeast of the Garibaldi Volcanic Belt (GVB), which comprises a series of basaltic to andesitic arc volcanoes ranging from ~2.4 Ma to a few thousand years old. The GVB is a northward continuation of the Cascade volcanic arc, formed by subduction of the Juan de Fuca oceanic plate eastwards beneath the North American continent. Volcanism apparently shifted westwards from the PVB to the GCB between 7 Ma and ~3 Ma (Souther and Yorath, in press). Our study indicates that the shift in volcanism was also accompanied by chemical changes in the magma compositions.

We speculate that the chemical differences between the Crevasse Crag and Garibaldi magmas are influenced by tectonic elements. As stated in the previous sections, the increased role of amphibole in early fractionation within the Garibaldi can explain the observed chemical differences. The question then arises: why does amphibole fractionate at an early stage in Garibaldi magmas but not in CCVC magmas. Amphibole stability is controlled principally by P_{H₂O}; thus, controls on fluid pressure are important. If initial fluid contents were different between GVB and CCVC magmas, then clearly P_{H₂O} at successive fractionation stages would be different. However, we have no independent

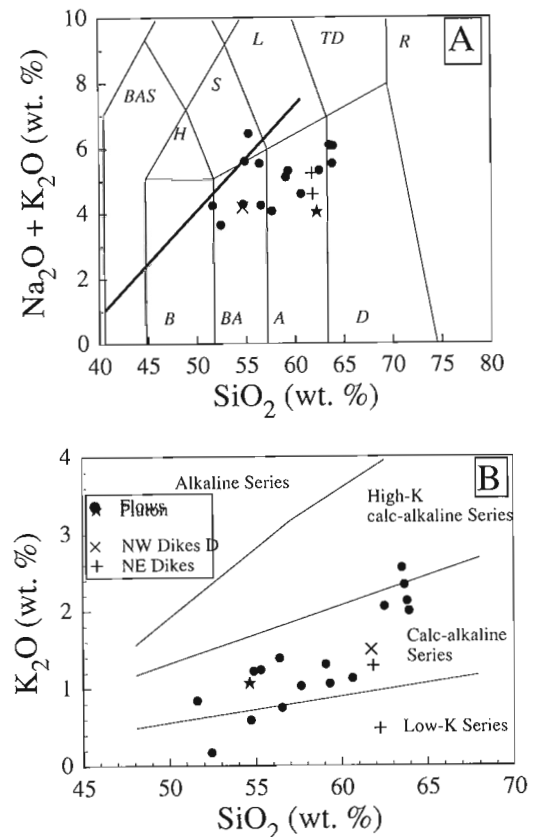
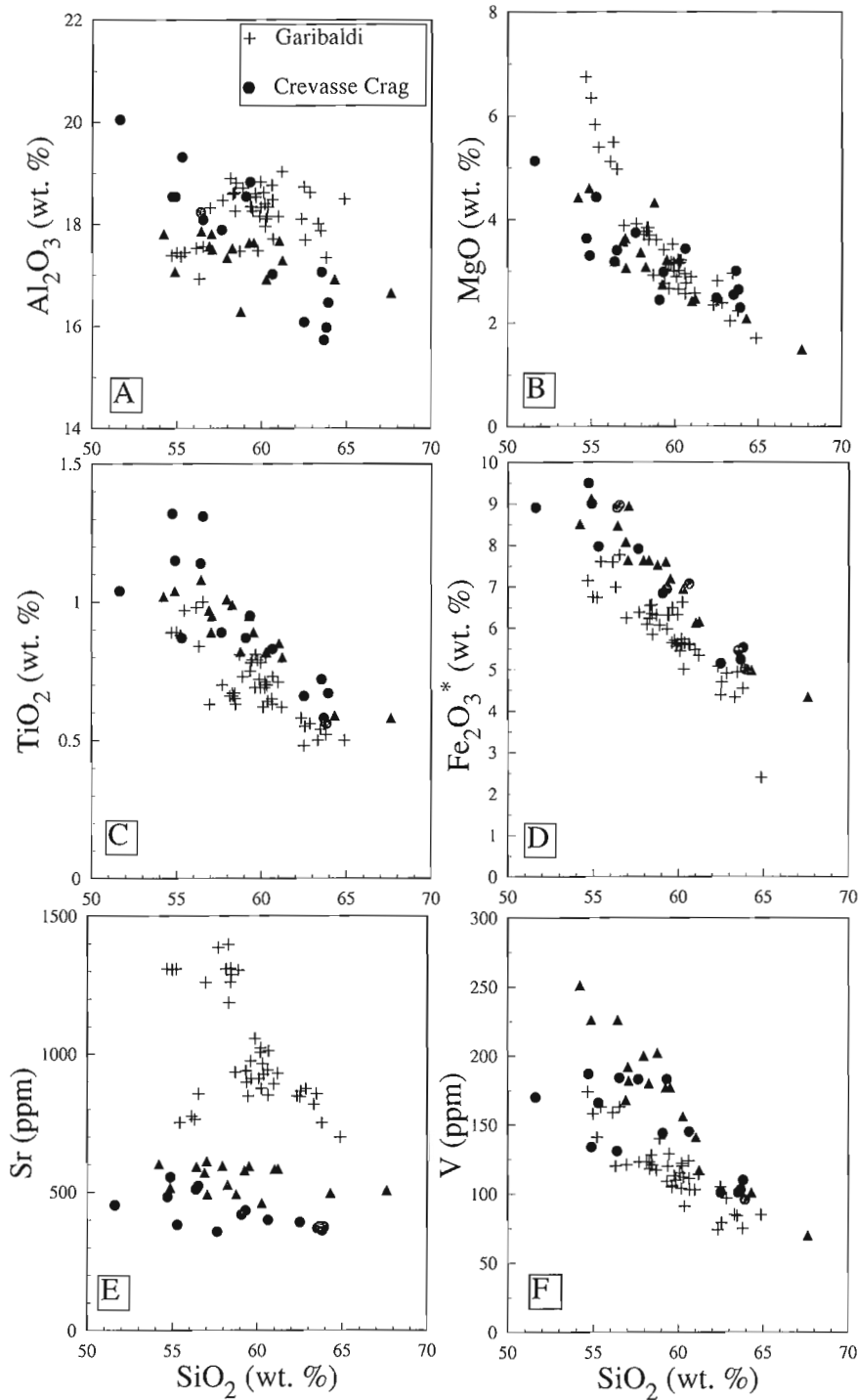


Figure 3. Alkalis versus SiO₂ (A), and K₂O versus SiO₂ (B) classification diagrams for Crevasse Crag Volcanic Complex. Fields in A after LeBas et al. (1986).

information on the nature of the source rocks for the two magma series. Another important control on the fluid pressure may be the plumbing system for the ascent of magmas. In the Crevasse Crag area, northeast-trending faults are associated with intrusion breccias, and thus appear to have

acted as passageways for magma ascent (Journey, 1990). We suggest that magma egress along these faults resulted in the quick release of volatiles, and hence suppressed the build-up of water pressure, which in turn delayed the crystallization of amphibole. We further suggest that



Data Sources: Garibaldi (Green, 1981); Coquihalla (Berman, 1979); Crevasse Crag (this study)

Figure 4. Harker variation diagrams showing data for Crevasse Crag Volcanic Complex, Coquihalla Volcanic Complex, and Garibaldi andesites and dacites.

Garibaldi magmas did not have easy exit to the surface, and therefore, cooled at depth where water pressure could build up to promote early amphibole crystallization.

A rough analog for the above model is seen in magmas produced along the Aleutian arc. Along the arc, segmentation has occurred with faults marking the ends of long arc segments. Near the faulted ends of segments, magmas tend to be intermediate between true calc-alkaline and tholeiitic magmas (Kay et al., 1982; Kay and Kay, 1985). Away from those faults in the middle of arc segments, true calc-alkaline magmas are produced. The intermediate lavas are lower in Ti, Fe, V and higher in Mg at a given SiO₂ content and have flatter REE patterns than the calc-alkaline magmas (Kay et al., 1982); this is exactly how the CCVC magmas differ from Garibaldi magmas (Fig. 4). Kay et al. (1982) relate the chemical differences between the intermediate and calc-alkaline to tectonic controls. The intermediate lavas are produced along faults; thus, they reach the surface quickly, resulting in the suppression of amphibole fractionation.

If, indeed, easy access via faults affects the chemistry of the CCVC lavas in the Miocene, why aren't the Garibaldi magmas affected in a similar fashion? One suggestion is that appropriate fault systems do not exist as feeders for Garibaldi magmas. Between 7 and -4 Ma, volcanism in southwestern

British Columbia jumped westward, perhaps as a result of steepening subduction after formation of the Nootka fault (Riddihough, 1984). Before 7 Ma, the subducting angle was shallow and transfer of stress from the lower to upper plate very effective. Compressive stresses, at right angles to the plate boundary, may have been effectively transferred to the upper plate. Concomitant extensional stresses parallel to the boundary were accommodated by the formation of an oblique-slip, northeast-trending fault system (Journeay, 1990) that provided passageways for magma ascent. Since 4 Ma, if the subducting plate has been descending at a higher angle, perhaps there has been less effective transfer of stress to the upper plate, and hence less chance of the formation of northeast-trending faults.

CONCLUSIONS

The principal results of this study are:

- 1) The Crevasse Crag Volcanic Complex comprises basalt, andesite, and dacite in both fragmental deposits and lava flows. It is probably part of the Miocene Pemberton Volcanic Belt.

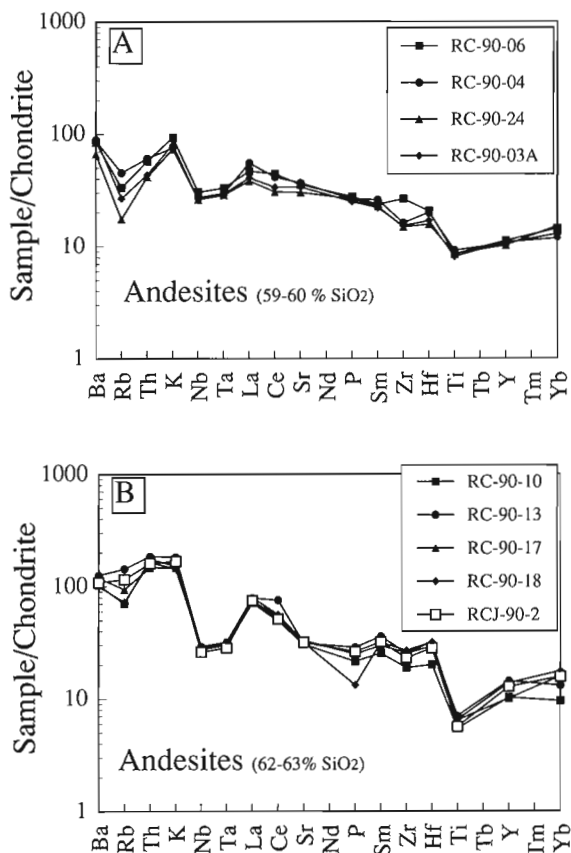


Figure 5. Chondrite-normalized (Thompson et al., 1984) data for selected CCVC lavas. Note the negative anomalies for Nb and Ti; this is typical of subduction-related volcanic rocks.

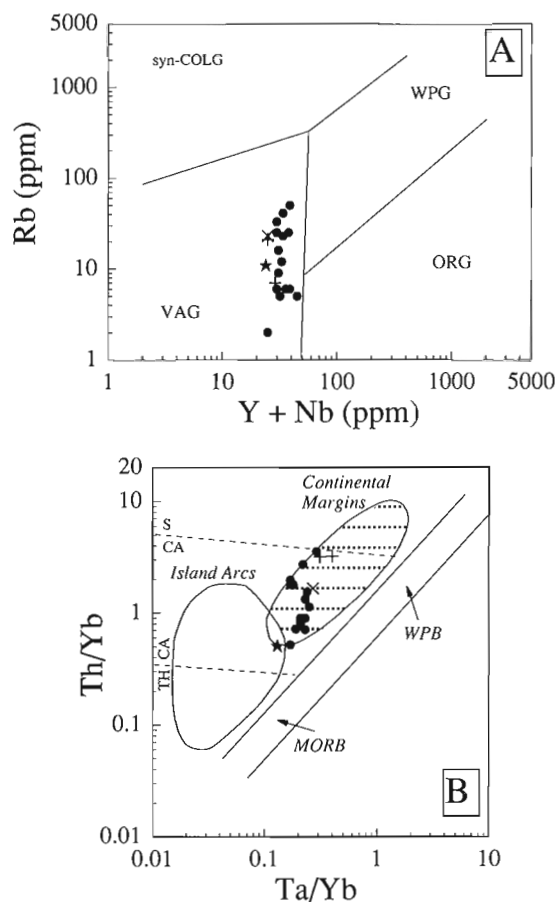


Figure 6. CCVC data plotted in tectonic discriminant diagrams. Symbols for CCVC rocks same as in Figure 3. Abbreviations for tectonic fields: VAG - volcanic arc, WPG - within-plate, ORG - ocean ridge, syn-COLG - syn-collision, MORB - mid-ocean ridge, WPB - within-plate. Note that CCVC rocks plot in volcanic arc fields.

- 2) The lower part of the complex sits on a quartz diorite body, which in places is intruded and thoroughly fractured by an intrusion breccia.
- 3) The intrusion breccia is charged with local clasts of the quartz diorite and exotic fragments of volcanic rocks, schists, gneiss, and sedimentary rocks.
- 4) The chemistry of the lava flows in the CCVC is calc-alkaline in nature, but shows some differences from the calc-alkaline sequence of the younger Garibaldi range.
- 5) The chemical peculiarities of the CCVC relative to Garibaldi rocks can be explained by early suppression of amphibole fractionation in CCVC magmas.
- 6) The CCVC magmas may have ascended to the surface rapidly along northeast-trending, oblique-slip faults. The rapid ascent may be partly responsible for the suppression of amphibole fractionation.

REFERENCES

- Berman, R.G.**
 1979: The Coquihalla Volcanic Complex, southwestern British Columbia; MSc thesis, University of British Columbia, Vancouver.
 1981: Differentiation of calc-alkaline magmas: evidence from the Coquihalla Volcanic Complex, British Columbia; *Journal of Volcanology and Geothermal Research*, v. 9, p. 151-179.
- Berman, R.G. and Armstrong, R.L.**
 1980: Geology of the Coquihalla Volcanic Complex, southwestern British Columbia; *Canadian Journal of Earth Sciences*, v. 17, p. 985-995.
- Brique, L., Bougault, H., and Joron, J.L.**
 1984: Quantification of Nb, Ta, Ti and V anomalies in magmas associated with subduction zones: petrogenetic implications; *Earth and Planetary Science Letters*, v. 68, p. 297-308.
- Friedman, R.M.**
 1990: Mapping in the northeastern part of the Pemberton Dioritic Complex, Pemberton map area, British Columbia; in *Current Research, Part E*; Geological Survey of Canada, Paper 90-1E, p. 213-217.
- Green, N.L.**
 1981: Geology and petrology of Quaternary volcanic rocks, Garibaldi Lake area, southwestern British Columbia; *Geological Society of America Bulletin*, Part II, v. 92, p. 1359-1470.
- Irvine, T.N. and Baragar, W.R.A.**
 1971: A guide to the chemical classification of volcanic rocks; *Canadian Journal of Earth Sciences*, v. 8, p. 523-548.
- Journeay, J.M.**
 1990: A progress report on the structural and tectonic framework of the southern Coast Belt, British Columbia; in *Current Research, Part E*; Geological Survey of Canada, Paper 90-1E, p. 183-195.
- Kay, S.M. and Kay, R.W.**
 1985: Aleutian tholeiitic and calc-alkaline magma series I: The mafic phenocrysts; *Contributions to Mineralogy and Petrology*, v. 90, p. 276-290.
- Kay, S.M., Kay, R.W., and Citron, G.P.**
 1982: Tectonic controls on tholeiitic and calc-alkaline magmatism in the Aleutian arc; *Journal of Geophysical Research*, v. 87, p. 4051-4072.
- LeBas, M.J., LeMaitre, R.W., Streckeisen, A., and Zanettin, B.**
 1986: Chemical classification of volcanic rocks; *Journal of Petrology*, v. 27, p. 746-750.
- Riddihough, R.**
 1984: Recent movements of the Juan de Fuca plate system; *Journal of Geophysical Research*, v. 89, p. 6980-6994.
- Roddick, J.A. and Hutchison, W.W.**
 1973: Pemberton (east half) map-area, British Columbia; Geological Survey of Canada, Paper 73-17, 21 p.
- Souther, J.G.**
 in press: Volcanic Regimes; in *The Cordilleran Orogen, Decade of North American Geology*.
- Souther, J.G. and Yorath, C.J.**
 in press: Neogene assemblages; in *The Cordilleran orogen: Canada, Decade of North American Geology*.
- Thompson, R.N., Morrison, M.A., Hendry, G.L., and Parry, S.J.**
 1984: An assessment of the relative roles of crust and mantle in magma genesis: an elemental approach; *Royal Society of London Philosophical Transactions*, v. 310, p. 549-590.
- Woodsworth, G.J.**
 1977: Pemberton (92J) map area, British Columbia; Geological Survey of Canada, Open File 482.

Geological Survey of Canada Project 890036

Geology of parts of Riske Creek and Alkali Lake areas, British Columbia¹

P.B. Read²
Cordilleran Division, Vancouver

Read, P.B., 1992: *Geology of parts of Riske Creek and Alkali Lake areas, British Columbia*; in *Current Research, Part A; Geological Survey of Canada, Paper 92-1A*, p. 105-112.

Abstract

The map area straddles the dextral strike-slip Fraser Fault. East of the fault, Cache Creek Complex forms a thick siltstone-greywacke sheet faulted(?) onto greenstone-chert blocks in a phyllite matrix preserved in a northerly-trending syncline. West of the fault, correlative rocks include pre-Upper Permian chert and greenstone and thick, Middle to Upper Triassic limestone. Fossiliferous Lower Jurassic sediments pass downward into rhyolite, dacite, and andesite before passing into hypabyssal and plutonic intrusions. Fossiliferous sandstone of Middle to Late Jurassic age and conglomerate unconformably overlie the Triassic rocks. Middle Eocene rhyolite and dacite, and three lithologically indistinguishable olivine basalt flow sequences of Late Miocene, Late Pliocene, and Pleistocene ages partly cover the older rocks on both sides of the fault. West of Fraser Fault, pre-Eocene stratified and intrusive rocks, including Farwell Pluton, form at least four, folded, northeasterly-directed sheets separated by serpentinite or tectonic mélange.

Résumé

La zone cartographique chevauche la faille Fraser à rejet horizontal dextre. À l'est de la faille, le complexe du ruisseau Cache forme une épaisse nappe de siltstone-grauwacke faillée (?) en blocs de roches vertes cherteuses dans une matrice de phyllite conservée dans un synclinal à direction nord. À l'ouest de la faille, les roches équivalentes sont composées notamment de chert et de roches vertes antérieurs au Permien supérieur et un calcaire épais du Trias moyen à supérieur. Les sédiments fossilifères du Jurassique inférieur se transforment vers le bas en rhyolite, dacite et andésite avant de passer à des intrusions hypabyssales et plutoniques. Le grès fossilifère du Jurassique moyen à supérieur et le conglomérat reposent en discordance sur les roches triasiques. La rhyolite et la dacite de l'Éocène moyen ainsi que trois séquences de coulée de basalte à olivine lithologiquement distinctes datant du Miocène supérieur, du Pliocène supérieur et du Pléistocène recouvrent en partie les roches les plus anciennes des deux côtés de la faille. À l'ouest de la faille Fraser, les roches stratifiées et intrusives antérieures à l'Éocène, y compris le Pluton de Fraser, forment au moins quatre nappes plissées à direction nord-est séparées par un mélange de serpentinite ou tectonique.

¹ Contribution to the Frontier Geoscience Program Chilcotin-Nechako Hydrocarbon Province

² Geotex Consultants Limited, #1200 - 100 West Pender St., Vancouver, B.C. V6B 1R8

CENOZOIC	
Quaternary and Tertiary	
Pleistocene	
Pvb	CHILCOTIN GROUP (Pvb to Ms) Grey olivine- and/or plagioclase-phyric subaerial basalt flows
Tertiary	
Pliocene	
Pvb	Grey olivine- and/or plagioclase-phyric subaerial basalt flows
Ps	Unconsolidated fluvialite sandstone and pebble to boulder conglomerate
Miocene	
Mvb	Grey olivine- and/or plagioclase-phyric subaerial basalt flows
Ms	Unconsolidated fluvialite sediments; minor rhyolite ash and diatomaceous earth
Eocene	
Es	Conglomerate, sandstone; minor siltstone and bentonitic shale; rare coal
Ev	Hornblende-plagioclase-phyric dacite and hornblende-biotite-quartz-phyric rhyolite flows and tuff; rare basalt
MESOZOIC	
Jurassic	
Middle to Upper Jurassic	
mJcg	South of Bald Mountain: Red sparsely plagioclase-phyric volcanic conglomerate overlying nonbedded quartz-bearing feldspathic sandstone
mJscg	North of Bald Mountain: Interbedded grey-green volcanic chip conglomerate and nonbedded quartz-bearing feldspathic sandstone
Jqm	Chloritized leucoquartz monzonite, leucoquartz diorite; rare metagabbro. Hypabyssal dacite and felsite intrusions occur marginally
Lower Jurassic	
lJp	Grey noncalcareous siltstone with thin sandstone laminae; minor thin limestone
lJvr	Grey-green and locally maroon porphyritic (plagioclase, quartz) dacite and rhyolite flows and tuffs, felsite- and quartz-feldspar porphyry-bearing tuff; minor green metabasalt flows
Triassic	
Middle to Upper Triassic	
uTs	Grey nonlimy siltstone and minor interbedded thin calcareous sandstone
uTc	Nonbedded light to medium grey micritic limestone
PALEOZOIC	
Permian	
Late Permian	
Pf	FARWELL PLUTON Chloritized and locally foliated metadiorite; minor quartz metadiorite and metagranodiorite
Permian to Jurassic	
Lower Permian to Middle(?) Jurassic	
PJccpw	CACHE CREEK COMPLEX (PJccpw to Pccvb) Western Belt: Grey siltstone, shale; minor grey lithic wacke
PJccv	Western Belt: Meta-andesite and metabasalt breccia and flows
PJcctpc	Western Belt: Tectonic(?) lenses of greenstone, limestone and chert in a grey phyllite matrix
PrMCC	Marble Canyon Formation Grey unbedded micritic limestone
Permian to Triassic	
Prvb	Green and grey-green aphanitic basic metatuff and minor flows
Permian and(?) older	
Lower Permian and(?) older	
Pcctp	Grey, grey-green and minor light green chert, ribbon chert and phyllite
Pcctpl	Light grey unbedded limestone
Pccvb	Grey-green and green greenstone

Figure 1. Legend

INTRODUCTION

The work reported in this paper results from the second year of a three-year geological investigation of the northeast corner of Taseko Lakes map area (92O) at the southern end of the Chilcotin-Nechako Hydrocarbon Province (Hickson, 1990). This year's geological mapping at a scale of 1:50 000 extends from longitude 122°10' to 122°45' and adjoins along its southern edge that previously reported by Hickson et al. (1991). Although many samples were collected for paleontology and radiometric dating, the results from them are unavailable. Because the ages of the units rest on only a few determinations from the localities shown in Figure 1 and listed in Table 1, significant changes may be anticipated.

Earlier regional mapping in the study area (Tipper, 1978) indicated that northeast of the confluence of the Chilcotin and Fraser rivers upper Paleozoic rocks of the Cache Creek Complex, which include limestone of the Marble Canyon Formation, underlie a partly preserved cover of Neogene sediments and basalt flows of the Chilcotin Group. Within the area the northerly-trending Fraser Fault, a major dextral strike-slip structure, forms the western limit of the complex. West of the fault and north of the Chilcotin River, partial erosion of the Chilcotin Group revealed Upper Triassic stratified rocks intruded by Jurassic plutons. Recently determined radiometric ages (Mathews, 1989; Friedman and Armstrong, 1989), and Late Toarcian (late Early Jurassic) (Hickson, 1990) and Middle to Late Triassic (Uyeno, unpubl. data) fossil collections are incorporated into this detailed revision of the regional geology. In this volume, reports on the Taseko Lakes map area (92O) by Broster and Huntley (1992), Friedman and van der Heyden (1992), Hickson (1992), Mahoney et al. (1992), and van der Heyden and Metcalfe (1992) give the results of geological investigations in Taseko Lakes map area south of Riske Creek and Alkali Lake.

STRATIGRAPHY

Late Paleozoic to Middle Jurassic

East of Fraser Fault, the Cache Creek Complex encompasses rocks of mid-Pennsylvanian to Middle(?) Jurassic age (Monger, 1989). West of the fault, pre-Late Permian(?) to Upper Triassic rocks probably correlate with the Cache Creek Complex; the Jurassic rocks are not correlated. On both sides of the fault, the complex consists of a number of fault slices with no stratified unit assuredly common to any of the slices. Because of the present lack of paleontologic ages, most of the rock units are of unknown age, but within some of the slices, the relative order of the units is known from facing criteria. The pre-Late Permian(?) age of some stratified units is based on the U-Pb age of zircons from Farwell Pluton which may intrude these units (see Farwell Pluton, this paper).

Cache Creek Complex east of Fraser Fault

A fairly continuous section along Alkali Creek exposes the entire width of the Western Belt of the Cache Creek Complex and the western edge of the Marble Canyon Formation. Along the north side of Alkali Lake Indian Reservation 1,

Table 1. Fossil and radiometric date localities, Riske Creek (92O/15) and Alkali Lake (92O/16) areas

Number	Easting	Northing	Age (Reference)
1*	EN0526500	EN5755800	Middle to Late Triassic — (Rusmore & Woodsworth, 1991a)
2	EN0524200	EN5754000	Middle to Late Triassic — (Uyeno, unpubl. data)
3	EN0521450	EN5748350	Middle to Late Jurassic — (G.E. Rouse, pers. comm., Aug. 1991)
4	EN0529000	EN5734870	Late Toarcian — (Hickson, 1990)
1**	EN0530000	EN5741800	258 ± 5 Ma — (Friedman and Armstrong, 1989)
2	EN0558850	EN5739150	0.72 ± 0.36 Ma and 0.7 ± 0.3 Ma — (Mathews, 1989)
3	EN0557900	EN5736800	0.9 ± 0.4 Ma — (Mathews, 1989)
4	EN0548250	EN5731100	2.1 ± 0.3 Ma — (Mathews, 1989)
5	EN0543500	EN5719850	1.3 ± 0.1 Ma — (Mathews, 1989)
6	EN0550350	EN5715750	1.4 ± 0.4 Ma — (Mathews, 1989)
7	EN0551500	EN5715050	2.9 ± 0.2 Ma — (Mathews, 1989)

* Fossil Collection localities shown as numbered boxes on Figure 1
** Radiometric date localities shown as numbered circles on Figure 1

unit **PJcpc¹** consists of tectonic(?) lenses of limestone and contorted ribbon chert in a subhorizontally foliated grey phyllite matrix. Green, locally foliated basalt or andesite breccia and flows of unit **PJcvc** cap unit **PJcpc** north and south of the Indian reservation but do not intervene between the unit and the overlying grey nonlimy siltstone and minor light grey lithic wacke of unit **PJcpcw** west of the reservation. To the west, unit **PJcpcw** forms a northwesterly-trending belt up to 8 km wide and 30 km long that is characterized by grey siltstone and lithic wacke, and the absence of chert and ribbon chert. Because rocks dip and face northeastward on the west side of the belt and dip southwestward on the east side, the unit fills the core of a large syncline. Between the western edge of unit **PJcpcw** and Fraser Fault, are lenses (tectonic?) of limestone, and basic metavolcanic rocks in grey ribbon chert and siliceous phyllite. They may be a fold repetition of similar rock types that lie north of the Alkali Lake Indian Reservation 1.

Pre-Late Permian(?) rocks west of Fraser Fault

West of Fraser Fault, Farwell Pluton intrudes a succession of green, unbedded mainly ash to lapilli tuff of andesite and basalt composition that constitutes unit **Pccvb**. Because deformation and metamorphism have overprinted or obliterated the primary volcanic textures, the rocks are now greenstone. The intrusive nature of the plutons and their associated contact metamorphism are clearly exposed along the Fraser River north of its confluence with Chilcotin River and on the north side of Word Creek.

In the lower part of Word Creek, plutonic rocks, lithologically similar to Farwell Pluton, intrude grey and grey-green phyllite, siliceous phyllite, ribbon chert and massive chert of unit **Pcctp**. A lithologically similar sequence

with at least one 30 m thick, locally bedded limestone of unit **Pcctpl** straddles the Fraser River south of Ross Gulch. In both areas, the ribbon chert is commonly radiolaria-bearing.

Upper Triassic rocks west of Fraser Fault

Up to 1000 m of unbedded light grey limestone of unit **uTc** forms the several summits of Bald Mountain and extends 8 km farther north to the head of Thaddeus Creek. Grey nonlimy siltstone and thin interbedded calcareous sandstone of unit **uTs** and a few unbedded limestone layers up to 15 m thick overlie the thick limestone and are probably part of the Upper Triassic succession. The age of unit **uTc** comes from a single conodont locality in the thick limestone exposed on the north shore of the lower of the two lakes at the head of Thaddeus Creek (Table 1). About 5 km northeast of Farwell Canyon, a light grey, unbedded marble knob may be correlated with the dated Triassic limestone on Bald Mountain. Northwest of the knob and separated from it by a zone of tectonic(?) lenses of greenstone, chert, and microdiorite, is a succession of nonlimy grey siltstone and calcareous sandstone which may be of Triassic age.

Jurassic

Fossiliferous Jurassic rocks underlie two areas: (a) within and up to 6 km southwest of the Chilcotin Valley; and (b) from the south side of Bald Mountain northward across Highway 20 to and beyond the northern limit of the mapped area. Near the Chilcotin River, the basal flows are sparsely porphyritic rhyolite and dacite with minor andesite and basalt. These pass up into quartz and feldspar phenocryst-bearing dacite and rhyolite ash and lapilli tuffs. The flows and tuffs are combined in unit **IJvr** which here and there is maroon. The overlying

¹Technical difficulties preclude the use in this text of the specialized symbols found on the map in Figure 1. However, the use of conventional type to approximate these symbols does not seem to introduce any unacceptable problems if the legend of the map is used when referring from text to map.

light green tuffaceous sandstone lacks bedding and has characteristic vitreous clear and grey quartz grains. The fault-terminated top of the Jurassic succession consists of a few thin (5 m) limestone layers of unit **LJc** intercalated in a grey nonlimy fossiliferous siltstone (Table 1) with thin sandstone beds of unit **LJp**. Because the base of the Jurassic stratified rocks lies at the transition into hypabyssal intrusions and the top is a fault, the preserved thickness of Late Toarcian stratified rocks varies from place to place up to a maximum of 500 m.

Near and north of Bald Mountain, conglomerate, unbedded sandstone, and minor nonlimy siltstone and limestone form a sequence unconformably overlying Upper Triassic rocks. On the south slopes of Bald Mountain, a few hundred metre thickness of brick red monomictic conglomerate composed of sparsely plagiophyric dacite clasts constitutes unit **mJcg** and overlies 20 m or less of siltstone and unbedded, quartz-bearing sandstone. The sandstone, characterized by vitreous clear to grey quartz grains, contains *Ptilophyllum arcticum* and yields a Middle to Upper Jurassic age (G.E. Rouse, pers. comm., Aug. 1991) (Table 1). North of Bald Mountain, the proportion of conglomerate and the clast size of the conglomerate diminish and it changes to matrix-supported conglomerate with 1-2 cm chips of felsic to intermediate volcanic rocks in shades of grey, green, and white. Granitic and limestone clasts are less than 5% each of the clasts, but in certain beds limestone clasts exceed 90%. On Bald Mountain, conglomerate overlies a thin sandstone, but north of the mountain the unbedded sandstone and conglomerate are so closely interbedded in subequal amounts over thicknesses of hundreds of metres that the sandstone and conglomerate are combined in the single unit **mJscg**. Unit **mJp** is a grey nonlimy siltstone with rare sandstone beds a few centimetres thick near the top of the fault-truncated sequence. Limestone and limestone breccia beds of unit **mJc** up to 20 m thick are scattered throughout the sediments. Less than a kilometre north of the west end of the lowest lake on Bald Mountain Creek are fine plagiophyric dacite tuffs and flows. Although these rocks form an isolated outcrop area, they have been placed at the base of the Jurassic succession and correlated with the Lower Jurassic volcanic rocks of unit **LJvr** rather than with Upper Triassic rocks. According to Rusmore and Woodsworth (1991a), conodonts from one of the limestone clasts in a conglomerate north of Bald Mountain yielded a Middle to Late Triassic age (Table 1), but unlike them, I do not interpret this as the age of deposition of the conglomerate. Although several kilometres distant from the dated conglomerate clast, the Middle to Upper Jurassic fossil locality is favoured. To check the age of the succession, the dacite tuff has been submitted for zircon U-Pb dating.

East of Farwell Canyon, and southeast of a presumed Triassic limestone is a sequence of bedded tuffaceous sediments and tuffs that pass eastward into green massive tuffs which may be part of the Lower Jurassic volcanic rocks.

Tertiary

West of the Fraser River, poorly exposed volcanic rocks form unit **Ev** of Eocene age and extend westward from west of Riske Creek to the eastern flank of Bald Mountain. South and west of Toosey Indian Reserve 1, rhyolite ash and flows

compose the basal part of the sequence. Farther to the north, these rocks are replaced by aphanitic dacite flows and lapilli breccia with a minimum thickness of 300 m. Although the rocks are undated, they are lithologically similar to the lower part of the Eocene succession exposed 40 km to the south in Gaspard and Churn creeks (Hickson et al., 1991).

Neogene and Quaternary

Chilcotin Group

Erosional remnants of volcanic and locally underlying sedimentary rocks form parts of the valley walls along the Fraser and Chilcotin rivers. Basalt flows are up to 250 m deep in the area and extend outward to underlie thousands of square kilometres of the Interior Plateau. Between Alkali Creek and the Fraser River, a sequence of sandstone and conglomerate of unit **Ps** blankets a 5-km wide zone immediately east of the Fraser River for over 30 km, from Dog to Riske Creek. East of the zone, the sediments are probably less than 30 m thick. A few of the scattered outcrops in the zone show that these sediments were deposited from streams that flowed northward (Hickson et al., 1991) or westward (Mathews and Rouse, 1986). Along the Chilcotin River, Tipper (1978) mapped Pliocene sediments in the valley bottom west of Big Creek, but within the map area sediments are not known to underlie basalt flows along the river.

The olivine basalt flows form three lithologically indistinguishable sequences of differing ages (Table 1). The oldest of these, unit **Mvb**, is Late Miocene (7.9 ± 0.6 to 9.2 ± 0.4 Ma) (Mathews, 1989) and forms parts of the Chilcotin valley walls. It lies directly on a pre-Tertiary basement with up to 150 m of paleo-relief. A Late Pliocene (2.1 ± 0.3 Ma) sequence (Mathews, 1989), unit **Pvb**, up to 10 m thick and containing only a few flows, extends into the south end of the area on the ridge between the Fraser River and Alkali Creek. A Pleistocene sequence (0.9 ± 0.4 to 0.7 ± 0.4 Ma) (Mathews, 1989), unit **Pvb**, containing many flows with a combined thickness of 130 m, extends from the Fraser River southeastward to and beyond Alixton Creek. A probable eruptive centre at 3450' elevation 9.5 km north of the east end of Alkali Lake exposes a basalt breccia containing white marble fragments which lies directly on a marble basement.

INTRUSIONS

Farwell Pluton

The Chilcotin and Fraser rivers, from Farwell Canyon to the mouth of Gaspard Creek, expose Farwell Pluton (**Pf**) and lithologically similar rocks only on the west side of Fraser Fault. The fault forms the eastern edge of the pluton, but a few kilometres north of the confluence of the Chilcotin and Fraser rivers, the northwesterly striking contact of the intrusion deviates from the fault and is intrusive. The pluton is typically a medium grained (2-4 mm) chloritized pyrobole (25-35%) metadiorite. U-Pb dating of zircons from a sample collected from the southwestern abutment of the logging road bridge at Farwell Canyon yielded a Late Permian age (Friedman and Armstrong, 1989) (Table 1). Because the dated locality lies close to or

within a tectonic mélangé and the sampled lithology is more leucocratic and less altered than is typical of Farwell Pluton, application of the date to the entire pluton is uncertain.

Unnamed Jurassic intrusions

On the southwest side of the Chilcotin valley from a few kilometres downstream of the mouth of Big Creek to south of the confluence of the Fraser and Chilcotin rivers, is an intrusive complex (unit **Jqm**). The bulk of the complex is medium grained (1-2 mm) and leucocratic with 5-10% chloritized biotite and/or hornblende quartz monzonite and quartz diorite. Locally the grain size increases to 4 mm and where the intrusions are mafic-rich (35-55%) they form metadiorite or metagabbro permeated by sills and dykes of the common leucocratic rocks. The plutonic rocks pass upwards through hypabyssal dacite and felsite intrusions with scattered quartz and plagioclase phenocrysts into compositionally similar flows of Late Toarcian age. Local zones of intense hydrothermal quartz-sericite-sulphide alteration extend through the hypabyssal intrusions into the supracrustal rocks as on the north bank of the Chilcotin River 4.8 km downstream from the mouth of Big Creek, and 2.0 km west of the mouth of the Chilcotin River.

STRUCTURE

At least two episodes of strong folding and faulting affect Jurassic and older rocks and north-trending faults with large strike-slip displacements control the distribution of Eocene and older rocks. West of Fraser Fault, Jurassic and older rocks are stacked in a series of at least four folded slices with each slice separated by sheared serpentinite surrounding tectonic

blocks of mainly greenstone and rare limestone, chert, or metadiorite (Table 2). The lowest or Wineglass slice forms a northwesterly elongate doubly-plunging window lying along Chilcotin Valley from a few kilometres downstream from Big Creek to the Fraser River (Fig. 1). The slice consists of Lower Jurassic stratified rocks intruded by hypabyssal and plutonic rocks. The base of the slice is unexposed, so the rocks may be autochthonous. The overlying fault contains pods of dolomitized serpentinite and foliated mylonite which parallel the bedding in the underlying Jurassic rocks and dip moderately to steeply northeast along the northeast margin of the window and gently southwest along the southwest side of the window.

The second or Farwell slice is probably very large but poorly exposed beyond the Chilcotin Valley and at present only partly mapped. Near the valley, metadiorite of Farwell Pluton forms the slice, but to the south greenstone of unit **Pccvb** and ribbon chert of unit **Pcctp** probably form the bulk of the slice. North of the valley, stratified rocks of dubious stratigraphic correlation form the upper part of the slice. A zone up to 300 m thick of protoclastic to mylonitic metadiorite and greenstone with small tectonic lenses of marble and grey metachert separates Farwell and Wineglass slices.

The third or Bald Mountain slice is a thrust-bottomed syncline which extends northward 15 km from Bald Mountain to beyond the northern limit of the map area. Serpentinite up to 400 m thick fills the thrust which sets Upper Triassic and Middle to Upper Jurassic rocks of the slice onto Farwell Pluton. At the south end of the slice the northerly dipping foliated serpentinite has a few asymmetric folds which indicate that the Bald Mountain slice moved northeastward relative to Farwell slice. The serpentinites are strongly veined and altered by ferroan dolomite.

Table 2. Compositions of and relationships among thrust slices in the northeast corner of Taseko Lakes map area

Name	Lithology	Name	Lithology
Thaddeus	Aphanitic intermediate to basic volcanics of unknown age	Thaddeus? (near Word Creek)	Aphanitic intermediate to basic volcanics of unknown age
Bald Mtn	Middle to Late Triassic limestone unconformably overlain by Middle Jurassic clastic sediments	Unnamed (Ross Gulch)	Undated limestone and volcanic rocks
Farless	Late Permian metadiorite which intrudes basic volcanics and ribbon chert	Unnamed (Ross Gulch)	Grey and grey-green ribbon chert and limestone
Wineglass	Late Toarcian basic to felsic volcanic rocks and overlying sandstone, shale and limestone	Wineglass (Chilcotin R. upstream from Big Cr.)	Basic and felsic volcanic and overlying sediments
BASE NOT EXPOSED			

The highest of the stacked slices, Thaddeus slice, lies west of a west-dipping serpentinite zone which is up to 500 m wide and includes tectonic blocks of greenstone, chert, and limestone. Aphanitic greenstone of unit **PTvb**, possibly derived from andesite and basalt tuffs and flows, constitutes the slice. Lithologically similar rocks outcrop northeast of Word Creek and may belong to Thaddeus slice.

South of the Chilcotin River, a south-striking serpentinite zone probably is the extension of the south-trending serpentinite-filled Farwell thrust. South of the river, its dip is assumed to be gently to the west. Metadiorite outcrops east of the fault in a few places, but most of Farwell slice is metavolcanic in contrast to its plutonic composition around the Chilcotin River. Parts of other slices such as the two slices exposed southwest of Ross Gulch are not mapped sufficiently to allow their unambiguous placement in the sequence.

The orientations of Wineglass and Farwell thrusts subparallel the bedding of the nearby Jurassic rocks and outline a northwest-trending anticline and northerly-trending syncline, respectively, each about 20 km long. The timing of the thrusting and folding is unknown except that it lies within the limits of Middle to Upper Jurassic from the age of the youngest rock involved in the thrusting to Middle Eocene, the age of the oldest rocks overlying the fault trace northeast of Bald Mountain.

East of Fraser Fault, the same phase of folding may have formed the northerly-trending syncline filled by unit **PJcpcw** of the western belt of the Cache Creek Complex. Basalt flows of the Chilcotin Group covers its southeastward extension. The underlying rocks of unit **PJcpcptc** may represent a folded fault zone composed of tectonic blocks in a highly foliated phyllite matrix.

West of Fraser Fault, pre-Late Permian(?) greenstone of unit **Pccvb** and the highly folded phyllite and chert of unit **Pcctp** are well foliated and veined units. A few occurrences of unfoliated Lower Jurassic rocks with rare clasts of foliated and quartz-veined phyllite, and radiolaria-bearing ribbon chert with the foliation and quartz veins truncated along the margins of the clasts indicate an Early Jurassic or older episode of deformation and metamorphism.

The dextral strike-slip Fraser Fault and its splays are the northward continuation of the Fraser River fault system of Late Eocene to Early Oligocene age. Under a cover of basalt flows of the Chilcotin River, Fraser Fault leaves the margin of Farwell Pluton and continues to strike northerly towards the lower part of Riske Creek. The fault zone has a width of hundreds of metres of crushed rock which are well exposed 5.5 km downstream from the mouth of Riske Creek on the east wall of the Fraser River. Here Fraser Fault has a 40°E dip which corroborates other moderate easterly dips found on subparallel faults close to the trace of Fraser Fault north of Farwell Pluton.

DISCUSSION

The discovery that Middle to Upper Jurassic and older rocks west of Fraser Fault form a series of folded thrust sheets separated by serpentinite-filled faults has important

implications for regional structure on both sides of Fraser Fault. Northeast of Mount Waddington and about 150 km west of the map area, Rusmore and Woodsworth (1991b) have documented northeasterly directed thrust faulting involving Upper Triassic to mid-Cretaceous stratified rocks and plutonic rocks as young as 87 Ma that were folded and faulted in early Late Cretaceous (Fig. 2). They noted that east-vergent thrusting exists for nearly 700 km along the east side of the Coast Plutonic Complex in the form of backthrusts to a slightly older west-verging thrust system on the west side of the complex. The presence of extensive folded thrusts in the present map area indicates that the zone of thrust faulting on the east side of the complex is at least 100 km wider than previously realized at this latitude and that it may extend an additional 40 km into the Ashcroft-Cache Creek area as explained below. The similarity of folding and thrusting in the present area and near Mount Waddington does not necessitate a synchronicity of development. In the present area, the folded thrust faults developed between Middle to Late Jurassic and Early Eocene based on the truncation of Middle to Upper Jurassic sediments on Bald Mountain and the lapping of Middle Eocene volcanics across Farwell fault northeast of Bald Mountain.

Correlation of Triassic and older rocks west of Fraser Fault to the Cache Creek Complex east of the fault implies that the same deformation style should exist to the east. West of Clinton, in the Cache Creek Complex of the Marble Range, Trettin (1980) interpreted a large folded thrust with a minimum strike length of 16.5 km and width of 4.3 km. In the Ashcroft-Cache Creek area, Travers (1978) suggested that the tectonic mélange present in the Cache Creek Complex developed prior to the eastward thrusting during Early Jurassic of the complex, Upper Triassic Nicola Group, and Early to Middle Jurassic Ashcroft Formation. Unpublished mapping by Read in the complex north of Cache Creek outlined a folded serpentinite-bearing tectonic mélange similar to those near the Chilcotin River west of Fraser Fault.

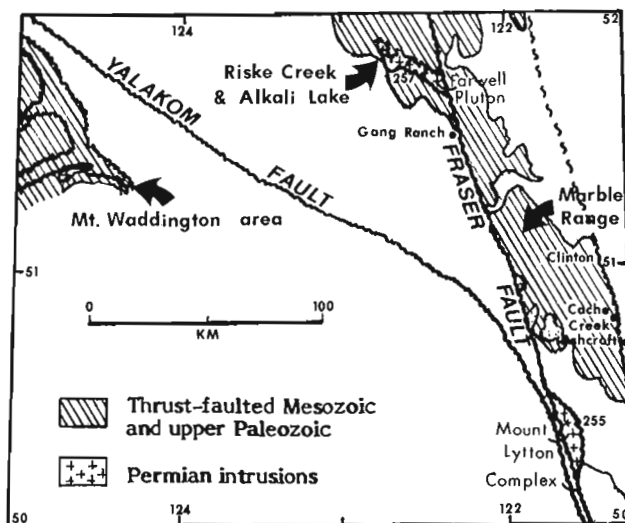


Figure 2. Part of southwestern British Columbia showing the extent of thrust-faulted upper Paleozoic and Mesozoic rocks.

Friedman and Armstrong (1989) suggested that the Permian Farwell Pluton on the west side of Fraser Fault and the Permian northern end of Mount Lytton Complex on the east side yields about 150 km of post-Paleozoic dextral strike-slip displacement on the fault. The discovery that Farwell Pluton is present in one or more thrust slices limits its usefulness in determining fault offset. The displacement measured along Fraser Fault is not a post-Paleozoic displacement, but instead may be a measurement of the strike-slip displacement after the thrust emplacement of the rocks in the interval Middle to Late Jurassic to Early Eocene. Secondly Farwell Pluton is present in a thrust sheet, not a large subvertical body, and therefore the present lateral separation across the fault is sensitive to any dip-slip component of movement. As Mathews and Rouse noted in the Gang Ranch area (1984, p. 1143), the presence of Eocene rocks on the west side of the Fraser Fault and their absence on the east implies at least 1.5 km of downthrow on the west. The thrust setting of Farwell Pluton and the uncertainty concerning the volume of Permian rocks present in the pluton (see this paper) limit the usefulness of the date for fault interpretation. Even if there is no dip-slip component of movement on Fraser Fault, the displacement measured along the fault is post-thrust emplacement and not post-intrusion displacement.

On the west side of Fraser Fault, correlation of the Jurassic and older stratified rocks is hampered by uncertainty of their ages. Rusmore and Woodsworth's (1991a) correlation of most of the rocks with the Cadwallader Terrane and Cadwallader Group specifically depends upon the presence of turquoise green silicified tuff fragments in unit **mJscg** which they assigned a Middle to Late Triassic age. The unit probably has a Middle to Late Jurassic age which is younger than rocks in the Cadwallader Terrane. This unit together with the other Jurassic units are more likely correlative with the Hazelton Group and belong to Stikinia. On the west side of the fault, I have correlated the Triassic and older stratified units with the Cache Creek Complex based on the widespread presence of ribbon chert and greenstone, and the occurrence of massive Middle to Upper Triassic limestone which Beyers (1989) has recently shown to be a common and significant part of the Marble Canyon Formation. On the west side of the fault, Jurassic rocks have been excluded from this correlation because an unconformity separates Jurassic from Upper Triassic and older rocks. This unconformity must cast some doubt on the inclusion of Jurassic rocks in the Cache Creek Complex east of the fault.

ACKNOWLEDGMENTS

The kind assistance and generosity of the Mervyns of Alkali Lake Ranch, and Brian and Jane Durrell of Wineglass Ranch were most appreciated. In these days of so much confrontation and misunderstanding, I appreciate the cooperation of Chief William Chelsea and the band members of the Alkali Lake Band in allowing me access to their lands. Without Dr. C.J. Hickson of the Geological Survey of Canada, this project would not have been funded through the Chilcotin-Nechako Hydrocarbon Province Project, under contract #23254-1-0146/01-XSB. Dr. J.W.H. Monger visited in the field and together with Drs. Tipper and Woodsworth provided a richness of geological expertise. Dr. J.A. Roddick critically reviewed and improved the manuscript. I am grateful to these members of the Survey.

REFERENCES

- Beyers, J.M.**
1989: Upper Permian and Triassic conodont biostratigraphy of the Cache Creek Group, Marble Range, south-central British Columbia; M.Sc. thesis, University of British Columbia, Vancouver, 280 p.
- Broster, B.E. and Huntley, D.H.**
1992: Quaternary stratigraphy in the east-central Taseko Lakes area, British Columbia; in Current Research, Part A; Geological Survey of Canada, Paper 92-1A.
- Friedman, R.M. and Armstrong, R.L.**
1989: U-Pb dating of Permian, Jurassic and Eocene granitic rocks between the Coast Plutonic Complex and Fraser-Pinchi fault system (51°-54°N), B.C. (Abstract); in Abstracts with Programs 1989, Geological Society of America, Cordilleran and Rocky Mountain Section Meetings, v. 21, no. 5, p. 81.
- Friedman, R.M. and van der Heyden, P.**
1992: Late Permian U-Pb dates for the Farwell and Northern Mt. Lytton Plutonic bodies, Intermontane Belt, British Columbia; in Current Research, Part A; Geological Survey of Canada, Paper 92-1A.
- Hickson, C.J.**
1990: A new Frontier Geoscience Project: Chilcotin-Nechako region, central British Columbia; in Current Research, Part F; Geological Survey of Canada, Paper 90-1F, p. 115-120.
1992: An update on the Chilcotin-Nechako Project and mapping in the Taseko Lakes (92O) area, west-central British Columbia; in Current Research, Part A; Geological Survey of Canada, Paper 92-1A.
- Hickson, C.J., Read, P., Mathews, W.H., Hunt, J.A., Johansson, G., and Rouse, G.E.**
1991: Revised geological mapping of northeastern Taseko Lakes map area, British Columbia; in Current Research, Part A; Geological Survey of Canada, Paper 91-1A, p. 207-217.
- Mahoney, J.B., Hickson, C.J., van der Heyden, P., and Hunt, J.A.**
1992: The Late Albian-Early Cenomanian Silverquick conglomerate, Gang Ranch area: evidence for active basin tectonism; in Current Research, Part A; Geological Survey of Canada, Paper 92-1A.
- Mathews, W.H.**
1989: Neogene Chilcotin basalts in south-central British Columbia: geology, ages, and geomorphic history; Canadian Journal of Earth Sciences, v. 26, p. 969-982.
- Mathews, W.H. and Rouse, G.E.**
1984: The Gang Ranch - Big Bar area, south-central British Columbia: stratigraphy, geochronology, and palynology of the Tertiary beds and their relationship to Fraser Fault; Canadian Journal of Earth Sciences, v. 21, p. 1132-1144.
1986: An Early Pleistocene proglacial succession in south-central British Columbia; Canadian Journal of Earth Sciences, v. 23, p. 1796-1803.
- Monger, J.W.H.**
1989: Geology of the Hope and Ashcroft map areas, British Columbia; Geological Survey of Canada, Maps 41-1989 and 42-1989.
- Rusmore, M.E. and Woodsworth, G.J.**
1991a: Distribution and tectonic significance of Upper Triassic terranes in the eastern Coast Mountains and adjacent Intermontane Belt, British Columbia; Canadian Journal of Earth Sciences, v. 28, p. 532-541.
1991b: Coast Plutonic Complex: a mid-Cretaceous contractional orogen; Geology, v. 19, p. 941-944.
- Tipper, H.W.**
1978: Taseko Lakes map-area; Geological Survey of Canada, Open File 534.
- Travers, W.B.**
1978: Overturned Nicola and Ashcroft strata and their relation to the Cache Creek Group, southwestern Intermontane Belt, British Columbia; Canadian Journal of Earth Sciences, v. 15, p. 99-116.
- Trettin, H.P.**
1980: Permian rocks of the Cache Creek Group in the Marble Range, Clinton area, British Columbia; Geological Survey of Canada, Paper 79-17, 16 p.
- van der Heyden, P. and Metcalfe, S.**
1992: Geology of the Piltz Peak plutonic complex, northwestern Churn Creek map area, British Columbia; in Current Research, Part A; Geological Survey of Canada, Paper 92-1A.

Geology of the Piltz Peak plutonic complex, northwestern Churn Creek map area, British Columbia

P. van der Heyden and S. Metcalfe¹
Cordilleran Division, Vancouver

van der Heyden, P. and Metcalfe, S., 1992: Geology of the Piltz Peak plutonic complex, northwestern Churn Creek map area, British Columbia; in Current Research, Part A; Geological Survey of Canada, Paper 92-1A, p. 113-119.

Abstract

The Piltz Peak plutonic complex in the Churn Creek map area (92O17) is composed of weakly to locally strongly strained granitoid and metavolcanic rocks, which may be a southerly extension of the Mt. Alex plutonic complex immediately north of the study area. These rocks are overlain, possibly structurally, by unmetamorphosed volcanic rocks that may correlate with the informal Late Cretaceous Powell Peak formation. Several plutonic phases and deformation episodes can be recognized in the field; relative and absolute ages of most rocks and structures in the area remain unknown. Structures in the Piltz Peak plutonic complex may represent early Tertiary extension, superimposed on Jurassic, Cretaceous, and early Tertiary plutonic and metamorphic rocks. Alternatively, ductile and brittle structures in the Piltz Peak plutonic complex may be the result of Middle to Late Jurassic and/or mid- to Late Cretaceous contraction.

Résumé

Le complexe plutonique de Piltz Peak dans la zone cartographique du ruisseau Churn (92O17) est composé de granitoïdes et de roches métavolcaniques de faiblement à fortement déformés par endroits, qui pourraient être un prolongement méridional du complexe plutonique du mont Alex, situé juste au nord de la zone à l'étude. Ces roches sont surmontées, peut-être structurellement, de roches volcaniques non métamorphosées qui pourraient être corrélées à la formation officielle de Powell Peak du Crétacé supérieur. Plusieurs phases plutoniques et des épisodes de déformation peuvent être établies sur le terrain; les âges relatifs et absolus de la plupart des roches et des structures de la région n'ont pas été déterminés. Les structures dans le complexe plutonique de Piltz Peak pourraient représenter une prolongement du Tertiaire inférieur, superposé aux roches plutoniques et métamorphiques du Jurassique, du Crétacé et du Tertiaire inférieur. Par ailleurs, les structures ductiles et cassantes du complexe plutonique de Piltz Peak pourraient être le résultat d'une contraction du Jurassique moyen à supérieur et (ou) du Crétacé moyen à supérieur.

¹ Department of Geological Sciences, University of British Columbia, 6339 Stores Road, Vancouver, B.C. V6T 2B4

INTRODUCTION

This report outlines preliminary results of 1:50 000 scale mapping in the Piltz Peak area, located in the central Chilcotin District of the Intermontane Belt, British Columbia (Fig. 1). The study is part of an ongoing regional mapping program in Taseko Lakes (92/O) map area (Hickson et al., 1991; Hickson, 1990, 1992), and focuses primarily on the northwest quadrant of Churn Creek (92O/7) map area. The northwest part of the study area is underlain by unfoliated to strongly foliated, locally mylonitic metaplutonic and metavolcanic rocks, here referred to as the Piltz Peak Plutonic Complex (PPPC). The southeast part is underlain by unmetamorphosed volcanic strata that may be correlative with the informal Late Cretaceous Powell Peak formation of Glover et al. (1988).

Previous mapping at a scale of 1:250 000 (Tipper, 1978) suggested that the PPPC consisted of Middle(?) Jurassic gneissic granitoid rocks that extend northward into the Mt. Alex (92O/10) map area. Results of current mapping (this report), and of previous work in the Mt. Alex map area (Hickson et al., 1991; Hickson, 1992), confirm the presence of orthogneiss in both the PPPC and in the Mt. Alex Plutonic

Complex (MAPC). Large tracts of both, however, consist of homogeneous, unfoliated granitoid material. The presence in both complexes of schistose and gneissic metavolcanic screens and pendants, coupled with the local presence of well developed foliations, including mylonites, brittle shear zones, and zones with fracture cleavage, may have contributed to their previous designation as a gneissic unit. Significant strain and metamorphism are restricted to local zones, and the PPPC and MAPC are primarily the product of multiple plutonic magmatic phases. Hence, the affix 'plutonic complex' is preferable to 'gneiss complex' or 'metamorphic complex'.

Deformation and metamorphism have nevertheless clearly played a significant role in the evolution of these plutonic rocks, and the presence of orthogneiss in the PPPC and MAPC may have significant regional tectonic implications. Orthogneiss is uncommon in the Intermontane Belt. The largest and best known exposures are in the Tatla Lake Metamorphic Complex, an Eocene core complex situated about 125 km northwest of the study area (Friedman and Armstrong, 1988). Smaller foliated plutonic bodies, including other candidates for Eocene core complexes, are present elsewhere in the central and southern Intermontane

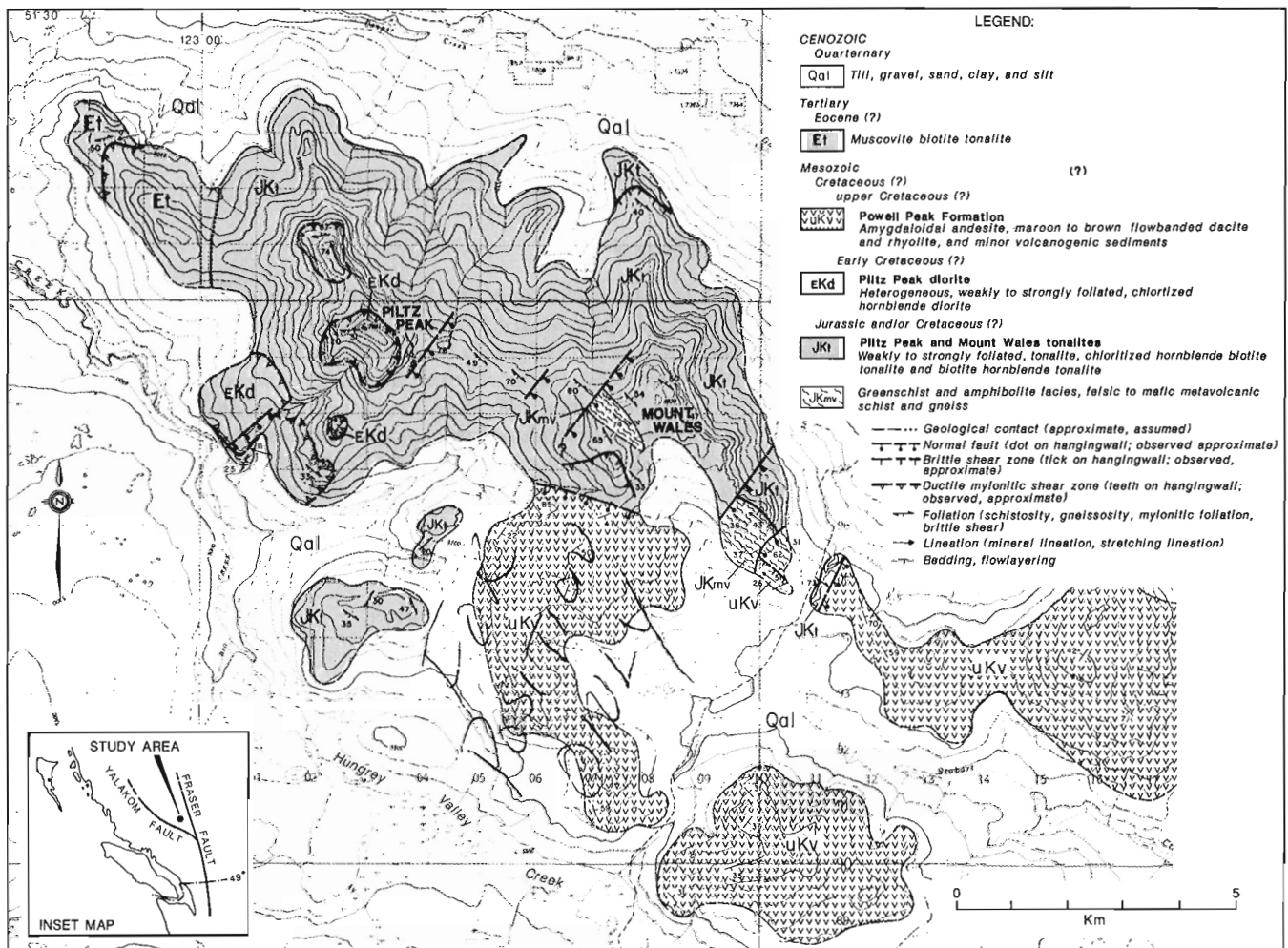


Figure 1. Geology of the study area.

Belt (Friedman and Armstrong, 1989; H.W. Tipper, pers. comm., 1991). Orthogneiss is more widespread along the boundary between the Coast Belt and Intermontane Belt, where both Late Cretaceous (Rusmore and Woodsworth, 1991) and Middle to Late Jurassic (Greig, 1989; van der Heyden, 1989) contractional episodes have been identified. The age of the structures in the study area are not known.

Although broadly similar in terms of lithology and structural style, the MAPC and PPPC almost certainly contain elements of differing age. Previous zircon U-Pb geochronometry of tonalite and diorite from Piltz Peak gave preliminary Late Jurassic (ca. 145 Ma, Friedman and Armstrong, 1989) and Early Cretaceous (ca. 130 Ma, J.W.H. Monger and D. Parkinson, pers. comm., 1987) emplacement ages, respectively. These results suggested that the Piltz Peak area is underlain by a composite plutonic complex, with at least two distinct phases. Recent results of zircon U-Pb geochronometry for the MAPC (Hickson, 1992) indicate that it is at least in part mid-Cretaceous in age (ca. 105 Ma).

A primary goal of this study will be to provide geochronometric constraints on age of emplacement, cooling, and deformation of major units within the PPPC and MAPC, as well as constraints on relations between the two complexes. Results of geochronometry will also hopefully allow the foliated plutonic rocks of the area to be placed in a coherent regional tectonic framework.

RESULTS OF PRESENT MAPPING

The following sections briefly describe the major map units and structures in the study area. Relations between major units remain largely unknown due to poor exposure (total outcrop area is estimated at less than 1%), and geologic contacts between major units were observed at only two locations. Until critical constraints provided by careful geochronometry are available, many of the interpretations offered below must be considered tentative.

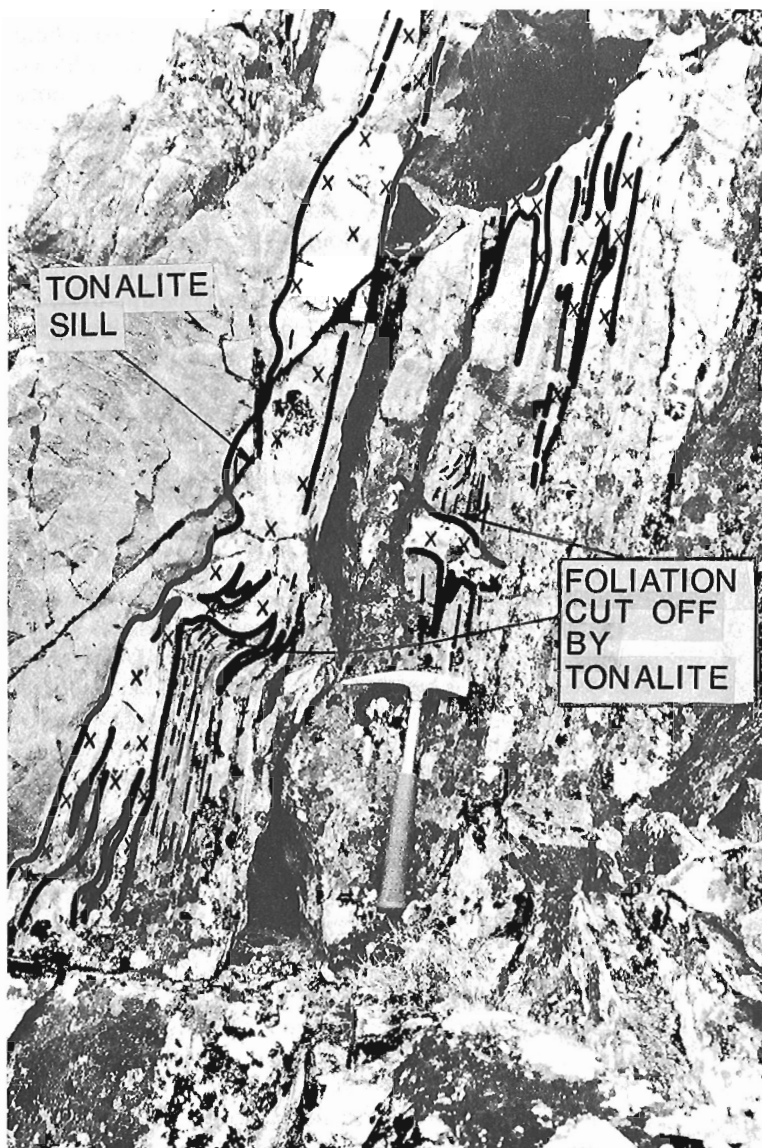


Figure 2. Concordant and crosscutting tonalite dykes in metavolcanic rocks of the Piltz Peak plutonic complex; note folds of the concordant dykes.

Most of the PPPC is underlain by unfoliated to moderately well foliated tonalite and quartz diorite. Foliation in the tonalite is commonly a weakly developed alignment of mafic minerals, which may represent a magmatic foliation. The tonalite is locally gneissic due to the presence of planar aggregates of mafic minerals, which possibly reflect segregation layering, and due to structural interdigitation with metavolcanic gneiss. Local cataclastic, proto-mylonitic and mylonitic fabrics indicate the presence of discrete brittle and ductile shear zones. Several textural and compositional varieties of tonalite can be distinguished; these have here been included in one unit.

Mt. Wales tonalite

Mt. Wales and the surrounding area is underlain by medium grained, mostly unfoliated to weakly foliated tonalite and quartz diorite with varying hornblende and biotite content and local accessory sphene. The mafic minerals are very commonly altered to chlorite and epidote, but locally most hornblende and some biotite remain unaltered, providing fresh material for K-Ar geochronometry. The metavolcanic bodies southeast and southwest of Mt. Wales are extensively invaded by tonalite sills and dykes. Concordant, folded sills with crosscutting apophyses (Fig. 2), and post-kinematic leucotonalite dykes with foliated metavolcanic xenoliths (Fig. 3), indicate that the Mt. Wales tonalite is late- to post-kinematic with respect to development of penetrative foliation in the metavolcanic succession. This is supported by the presence of rare angular to lenticular xenoliths, schlieren, and screens of well foliated metavolcanic material in unfoliated to weakly foliated tonalite of the main pluton.

Southwest of Mt. Wales, near the contact with unmetamorphosed Late Cretaceous(?) volcanic rocks, the Mt. Wales tonalite is locally strongly strained in a 20 m thick porphyroclastic mylonite zone. The mylonite dips gently southwest and is inferred to have formed in a discrete ductile shear zone. Southeast of Mt. Wales, the contact of weakly foliated tonalite with overlying metavolcanic rocks is marked



Figure 3. Post-kinematic tonalite dyke in metavolcanic rocks of the Piltz Peak plutonic complex. Leucocratic layers in the gneissic xenolith are older Mt. Wales tonalite.

by a 15 m thick, steeply southwest dipping cataclasite zone. The cataclasite is characterized by subangular and angular, pea-size tonalite fragments supported in a fine grained, locally weakly foliated, chloritic matrix. It is thought to mark the locus of a major brittle fault. Motion on this fault, and on other brittle shear zones in the tonalite and in the metavolcanic rocks, may significantly postdate the development of penetrative foliations. For instance, a gently southwest dipping brittle shear zone cuts moderately well foliated tonalite about 3.5 km north of Mt. Wales. This zone is characterized by the presence of phacoidal, protoclastic shear fabrics which cut across and postdate a moderately well developed penetrative foliation in the tonalite.

Piltz Peak tonalites

The tonalites exposed near Piltz Peak are generally more leucocratic and coarser grained than those near Mt. Wales. Fabrics, like those in the tonalite near Mt. Wales, range from unfoliated and locally cataclastic, to moderately well foliated, proto-mylonitic and, rarely, mylonitic. Gently dipping proto-mylonitic and mylonitic fabrics, characterized by alignment of quartz ribbon aggregates and local stretching lineations, appear to be common close to the contact with the overlying Piltz Peak diorite (described below). Relations with the Piltz Peak diorite are ambiguous. A foliated tonalite xenolith observed in unfoliated Piltz Peak diorite suggests a younger age for the latter, consistent with previous U-Pb geochronometry of samples from this area (Friedman and Armstrong, 1989; J.W.H. Monger and D. Parkinson, pers. comm., 1987). Rare diorite xenoliths in unfoliated tonalite float, however, as well as unfoliated leucotonalite dykes in the Piltz Peak diorite, suggest an older age for the Piltz diorite. We infer that there were probably two distinct phases of tonalite intrusion near Piltz Peak, separated by emplacement of the Piltz Peak diorite. The relation of either of these tonalite phases to the tonalite of Mt. Wales is unclear; the latter may represent a third, unrelated plutonic body.

Metavolcanic rocks

Foliated metavolcanic rocks occur as isolated xenoliths, schlieren, and small screens throughout the Mt. Wales tonalite. Larger, northwest-striking metavolcanic bodies are exposed less than 1 km southwest and about 3 km southeast of Mt. Wales. Banded, fine to medium grained, greenschist and amphibolite facies metavolcanic schist and gneiss (Fig. 4) are the dominant rock types. Compositional banding in these rocks is a combination of relict primary layering, structural transposition, and tonalite injection parallel to foliation. Composition of individual layers ranges from mafic (metabasalt) to felsic (metarhyolite); locally preserved primary textures indicate a volcaniclastic protolith for some of these rocks.

The metavolcanic rocks southeast of Mt. Wales form a moderately southwest dipping, homoclinal succession, with amphibolite facies granoblastic gneiss close to the contact with the Mt. Wales tonalite grading structurally upward into penetratively foliated greenschist facies metavolcanics.

These, in turn, grade upward into poorly foliated to unfoliated, greenschist facies, mafic to intermediate metavolcanic flows(?). Low grade, locally strongly sheared maroon lapilli tuffs exposed nearby are tentatively correlated with unmetamorphosed Late Cretaceous(?) volcanic rocks (described below). The contact between the metavolcanic rocks and the maroon lapilli tuffs is not exposed.

Penetrative foliation is defined mainly by preferentially oriented chlorite in greenschist facies metavolcanics. Foliation in fine to medium grained, amphibolite facies gneiss is defined by compositional layers ranging from thin laminae to metre scale banding. The development of penetrative foliation in the metavolcanic succession largely predates the emplacement of Mt. Wales tonalite. Semi-brittle and brittle shear planes are mostly subparallel to the foliation in the metavolcanic rocks; local low angle intersections with the foliation produced structures resembling foliation-fish (Hanmer, 1984). These shear planes may have formed during ongoing deformation following emplacement of the Mt. Wales tonalite, or a during a separate, later episode of deformation.

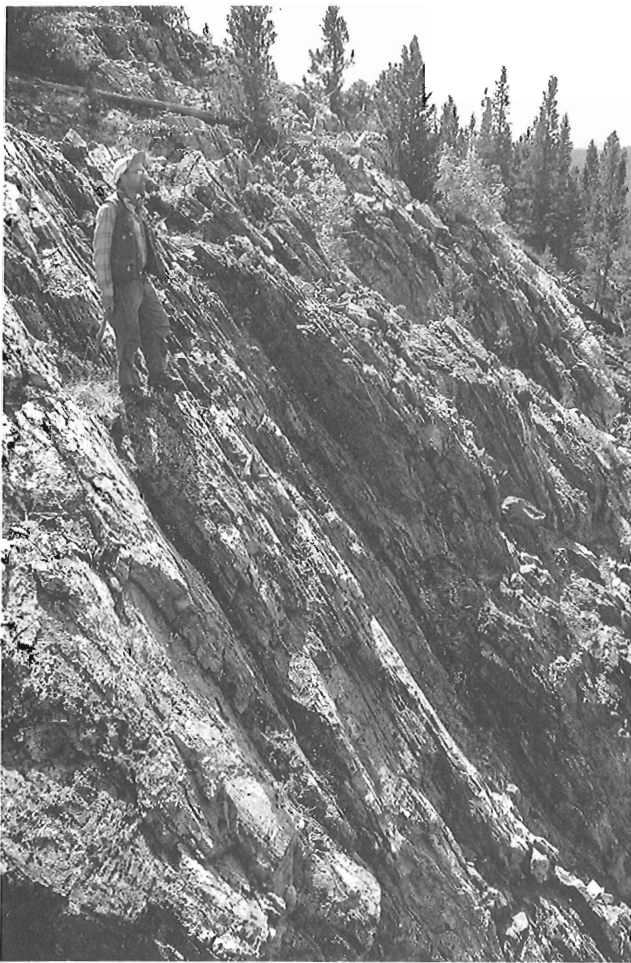


Figure 4. Banded, amphibolite facies metavolcanic rocks southeast of Mt. Wales, Piltz Peak plutonic complex.

Piltz Peak diorite

The Piltz Peak diorite is a mafic, heterogeneous granitoid unit exposed in a gently southwest dipping sheet on Piltz Peak and its southwest flank. Rare xenoliths of foliated tonalite and metavolcanic rocks in unfoliated Piltz Peak diorite suggest a primary intrusive relationship with the underlying Mt. Wales tonalite. The contact between the two map units, however, may be a younger shear zone which structurally detaches the Piltz Peak diorite from the Mt. Wales tonalite. Proto-mylonitic and mylonitic fabrics are common in the Mt. Wales tonalite immediately below the contact, and ductile and semi-brittle shear zones are present in the diorite sheet itself. Shear zones in the Piltz Peak diorite are characterized by strongly foliated and lineated, greenschist facies metaplutonic schist, commonly superimposed by anastomosing, phacoidal brittle shear planes. These shear zones are discrete features, and the Piltz Peak diorite is mostly unfoliated.

The Piltz Peak diorite is texturally and compositionally heterogeneous, commonly at a centimetre scale. It ranges, mostly gradationally, from fine grained to very coarse grained and from hornblende gabbro to leucodiorite. Locally the diorite is porphyritic, with coarse hornblende phenocrysts and aggregates set in a fine grained, microdioritic matrix. Hornblende is commonly severely altered to chlorite and epidote. Abundant dykes of various compositions intrude the Piltz Peak diorite. Included in these is medium to coarse grained tonalite, which, as discussed previously, is inferred to represent the younger of two tonalite phases near Piltz Peak.

Muscovite biotite tonalite northwest of Piltz Peak

The northwest flank of the PPPC consists of medium to coarse grained, mostly unfoliated biotite tonalite, which is readily distinguished from other tonalites in the area by the presence of muscovite and clear quartz grains and by associated muscovite bearing pegmatitic dykes and veins. It also appears to be much less altered than the tonalites near Piltz Peak and Mt. Wales. Local textural gradations include fine grained feldspar porphyry similar to dykes in the Piltz Peak diorite. The muscovite biotite tonalite is identical to a tonalite exposed in the Mt. Alex map area, northwest of the MAPC (Hickson et al., 1991), which has yielded an Eocene U-Pb age (ca. 52 Ma, R.M. Friedman, pers. comm., 1989).

The muscovite biotite tonalite northwest of Piltz Peak is cut by a discrete, approximately 20 m thick, moderately south-southwest dipping mylonite zone. If the tonalite is Eocene, the mylonite zone within it would be Eocene or younger, and other mylonite zones in the PPPC may also be young, Tertiary features.

Dykes and veins in the PPPC

The PPPC is intruded by a variety of dykes and veins. Feldsparphyric andesite and dacite are common, locally comprising up to 50% of the outcrop. Less common varieties include microdiorite and basalt. Felsite is locally abundant,

and includes a 30 m thick rhyolite breccia pipe which cuts across the metavolcanic succession southeast of Mt. Wales. Leucotonalite dykes were observed in all units except in the muscovite biotite tonalite northwest of Piltz Peak.

Lenticular, boudinaged pods and veins of coarse grained quartz are locally present in the foliated metavolcanic and metaplutonic rocks. These were probably emplaced during metamorphism and early deformation of their host rocks, and are readily distinguished from thick, younger extensional quartz veins associated with southeast dipping normal faults. Syntaxial quartz growth and slickensided shear surfaces within the latter veins and their wall rocks, and open-space tension gashes in the wall rocks, indicate emplacement along southeast dipping normal faults during a period of northwest-southeast extension. The veins have been extensively prospected for Au, but are reported to be barren (C. Choate, pers. comm., 1991).

Structures of the PPPC

The PPPC is inhomogeneously foliated. Foliations include schistosity, gneissosity, mylonite fabrics, and brittle phacoidal shears; most of these were described in previous sections. The overall foliation dips moderately southwest (Fig. 5), but locally they dip northeast, probably due to mesoscopic folding about northwest trending axes. Rootless isoclinal folds were seen in some banded schistose and gneissic zones, and foliations are locally crenulated.

Relations between the various structures in different parts of the PPPC are unclear; at least three phases of deformation appear to be represented. An early phase involved the development of schistosity and gneissosity in metavolcanic rocks, and one or more later phases involved the development of schistosity, mylonitic fabrics, brittle shears, and cataclastic zones in the granitoid rocks of the PPPC. Late, southeast dipping normal faults disrupted all older structures and all

map units of the PPPC, with the possible exception of the muscovite biotite tonalite. These late faults may be domino-style rotation structures that formed as a result of northwest-southeast extension.

The mylonitic, phacoidal, and cataclastic shear zones of the PPPC may also be the result of regional northwest-southeast extension. Lineations, including stretching lineations in mylonites, mostly dip gently to the northwest (Fig. 5). The lineations may have rotated, from an original southeast dipping orientation, between late, southeast dipping normal faults. Rare macroscopic kinematic indicators suggest a top to the southeast sense of movement.

Late Cretaceous(?) volcanic rocks

The southeast part of the study area is underlain by unmetamorphosed volcanic and minor sedimentary strata. Tipper (1978) previously assigned these rocks to a regionally extensive Eocene rhyolitic and dacitic unit. The volcanic rocks in the study area, however, are folded on a kilometre scale, in contrast to Eocene volcanics elsewhere in the Taseko Lakes map area, which typically form homoclinal, gently dipping successions. Parts of the unit resemble the informal Late Cretaceous Powell Peak formation of Glover et al. (1988), which is exposed about 30 km south of the study area (C.J. Hickson, pers. comm., 1991). The unmetamorphosed volcanic rocks of the study area are here tentatively correlated with the Powell Peak formation.

Three members were recognized in the field. The lowest member, exposed just north of Hungry Valley, is represented by a few metres of green feldspar porphyry andesite characterized by chlorite and chalcedony amygdules. Elsewhere, lower andesite outcrops are massive or flowbanded. The amygdaloidal andesite is interbedded with and overlain by 1-2 m of fine to medium grained green

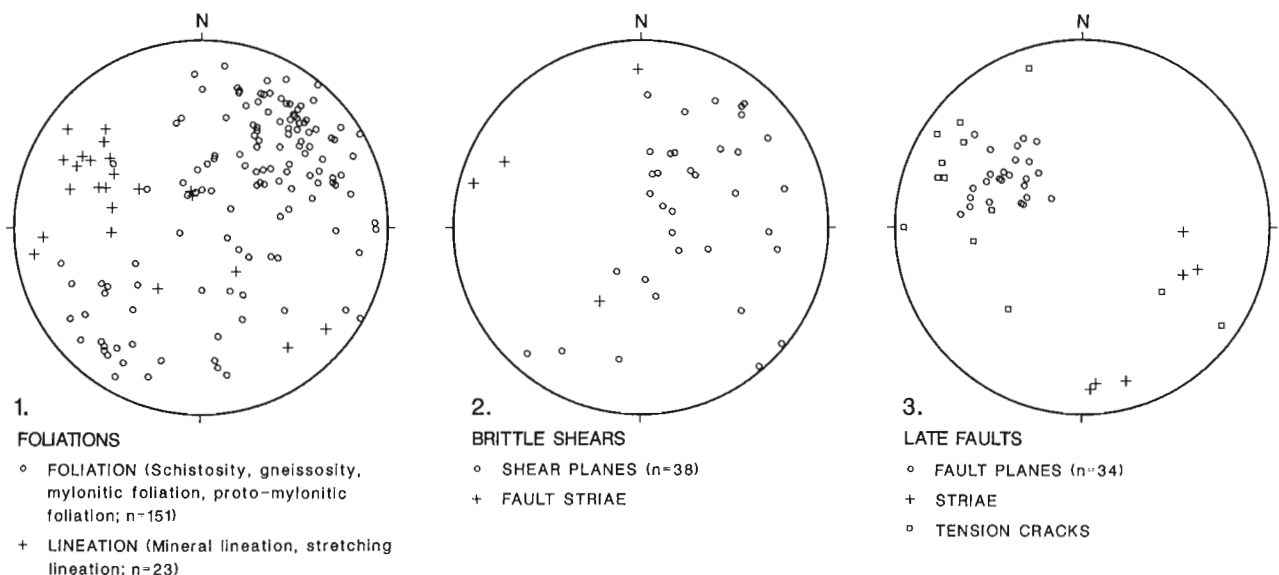


Figure 5. Equal area stereographic projections of structural data, Piltz Peak plutonic complex.

sandstone. These are overlain by the second member, which consists of 10-20 m of dark siltstones, waterlain lapilli tuffs and volcanic sandstone with minor coal and plant fragments, capped by several metres of perlitic rhyolite. This member was probably deposited in a lacustrine environment. The lapilli tuffs contain a minor arkosic component, with quartz and biotite derived from a plutonic source. Overlying the perlite is the third member, consisting of more than 100 m of pink, grey, and brown flowbanded and locally flow-folded rhyolite and dacite.

The contact between the Late Cretaceous(?) volcanic rocks and granitoid rocks of the PPPC is not exposed. Extremely altered, rusty weathering Mt. Wales tonalite immediately adjacent to the inferred contact southwest of Mt. Wales is strongly sheared, brecciated, slickensided, and extensively veined by calcite, limonite, and quartz. The contact here is undoubtedly a major brittle fault. The orientation and sense of movement on this fault remain unknown, and its generalized trajectory can only be inferred from the relative distribution of map units.

The contact between low grade maroon lapilli tuffs and greenschist facies metavolcanic rocks southeast of Mt. Wales is also not exposed. The lapilli tuffs are strongly sheared, and locally brecciated, along gently dipping brittle shear planes similar to brittle shears throughout the PPPC. Fault striae on these shear planes dip gently to the northwest, parallel to lineations in nearby, structurally underlying(?) metavolcanic rocks. The contact here is inferred to be a gently dipping brittle shear zone.

Based on the inferred position of low grade, sheared lapilli tuffs above greenschist facies metavolcanic rocks, we tentatively interpret the primary transition between the PPPC and the Late Cretaceous(?) volcanic unit as a normal fault. Its attitude is inferred to be parallel to brittle shears in the PPPC, but was probably modified by younger folds and disrupted by late, southeast dipping normal faults. We speculate that the fault is extensional in origin.

CONCLUSIONS

The PPPC is composed predominantly of weakly to locally strongly strained metaplutonic and metavolcanic material. Multiple phases of granitoid emplacement and multiple deformation episodes can be distinguished in the field, but relative and absolute ages for many of the units remain obscure. There are hints that the PPPC may, at least in part, represent a Tertiary extensional complex separated from overlying unmetamorphosed Late Cretaceous(?) volcanic rocks by a normal fault. Alternatively, the structures in the PPPC may be the result of older, Middle to Late Jurassic

and/or mid- to Late Cretaceous contraction in the region. An understanding of the tectonic evolution of the study area will depend in large measure on U-Pb and K-Ar geochronometry currently in progress.

ACKNOWLEDGMENTS

This study is a component of an ongoing regional mapping program in the Taseko Lakes (92O) map area, directed by C.J. Hickson. We wish to thank her for support and encouragement of this project.

REFERENCES

- Friedman, R.M. and Armstrong, R.L.**
 1988: The Tatla Lake Metamorphic Complex: an Eocene metamorphic core complex on the southwest edge of the Intermontane Belt, British Columbia; *Tectonics*, v. 7, no. 6, p. 1141-1166.
 1989: U-Pb dating of Permian, Jurassic, and Eocene granitic rocks between the Coast Plutonic Complex and Fraser-Pinchi fault system (51°-54°N), B.C. (Abstract); Geological Society of America, Abstracts with Programs, Spokane, '89, p. 81.
- Glover, J.K., Schiarizza, P., and Garver, J.I.**
 1988: Geology of the Noaxe Creek map area (92/O2); in *Geological Fieldwork 1987*, British Columbia Ministry of Energy, Mines and Petroleum Resources, Paper 1988-1, p. 105-123.
- Greig, C.J.**
 1989: Geology and geochronometry of the Eagle Plutonic Complex, Coquihalla area, southwestern British Columbia (92H/6,7,10,11); M.Sc. thesis, University of British Columbia, Vancouver, 423 p.
- Hanmer, S.K.**
 1984: The potential use of planar and elliptical structures as indicators of strain regime and kinematics of tectonic flow; in *Current Research, Part B*; Geological Survey of Canada, Paper 84-1B, p. 133-142.
- Hickson, C.J.**
 1990: A new Frontier Geoscience Project: Chilcotin-Nechako region, central British Columbia; in *Current Research, Part F*; Geological Survey of Canada, Paper 90-1F, p. 115-120.
 1992: An update on the Chilcotin-Nechako Project and mapping in the Taseko Lakes (92O) area, west-central British Columbia; in *Current Research, Part A*; Geological Survey of Canada, Paper 92-1A.
- Hickson, C.J., Read, P., Mathews, W.H., Hunt, J.A., Johansson, G., and Rouse, G.E.**
 1991: Revised geological mapping of the northeastern Taseko Lakes map area, British Columbia; in *Current Research, Part A*; Geological Survey of Canada, Paper 91-1A, p. 207-217.
- Rusmore, M.E. and Woodsworth, G.J.**
 1991: Coast Plutonic Complex: a mid-Cretaceous contractional orogen; *Geology*, v. 19, p. 941-944.
- Tipper, H.W.**
 1978: Taseko Lakes map-area; Geological Survey of Canada, Open File 534.
- van der Heyden, P.**
 1989: U-Pb and K-Ar geochronometry of the Coast Plutonic Complex, 53°N to 54°N, British Columbia, and implications for the Insular-Intermontane superterrane boundary; Ph.D. thesis, University of British Columbia, Vancouver, 392 p.

Structure of the Vangorda Pb-Zn-Ag deposit, Anvil Range, Yukon Territory

Dennis Brown¹ and Ken McClay¹
Cordilleran Division, Vancouver

Brown, D. and McClay, K., 1992: Structure of the Vangorda Pb-Zn-Ag deposit, Anvil Range, Yukon Territory; in Current Research, Part A; Geological Survey of Canada, Paper 92-1A, p. 121-128.

Abstract

The Vangorda Pb-Zn-Ag deposit is a small polydeformed, polymetamorphosed sedex-type massive sulphide deposit in the Anvil Mining District of the Selwyn Basin, Yukon Territory. The ore body consists of a number of banded, gently southwest-dipping lenses of sulphide lithofacies in the hinge and overturned limb of a southwest verging F_2 fold. Banding in the sulphide lithofacies occurs on a scale of millimetres to centimetres interpreted to be S_1 . The S_1 banding is folded by mesoscopic northwest- to southeast-plunging, tight to nearly isoclinal, class 2 similar style F_2 folds. The deposit is cut by northwest- and northeast-dipping extensional faults with a final stage of strike-slip to oblique-slip movement. F_2 -folded ductile shear zones occur in the sulphide lithofacies.

Preliminary microstructural work indicates that pyrite in the Vangorda deposit deformed by both ductile and brittle mechanisms. Subsequent annealing textures are common.

Résumé

Le gisement à Pb-Zn-Ag de Vangorda est un petit gisement de sulfures massifs de type SEDEX, polydéformé et polymétamorphisé, contenu dans le district minier d'Anvil du bassin de Selwyn (Yukon). Le massif minéralisé est composé d'un certain nombre de lentilles rubanées à lithofaciès sulfuré plongeant faiblement vers le sud-ouest dans la charnière et le flanc déversé d'un pli F_2 à vergence sud-ouest. Le rubanement observé dans le lithofaciès sulfuré est d'échelle millimétrique à centimétrique, interprété comme étant de type S_1 . Le rubanement S_1 est déformé par des plis F_2 mésoscopiques, semblables, de classe 2, à plongement de nord-ouest à sud-est et dont l'aspect varie de serrés à quasi isoclinal. Le gisement est limité par des failles de distension plongeant vers le nord-ouest et le nord-est qui témoignent d'un stade final de décrochement ou de mouvement oblique. Des zones de cisaillement ductile à plis F_2 sont présentes dans le lithofaciès sulfuré.

Des études microstructurales préliminaires indiquent que la pyrite contenue dans le gisement de Vangorda a été déformée à la fois par des mécanismes ductiles et cassants. Les textures dues à des recristallisations par recuit sont courantes.

¹ Department of Geology, Royal Holloway and Bedford New College, University of London, Egham, Surrey, TW20 OEX, United Kingdom

INTRODUCTION

The Vangorda Pb-Zn-Ag deposit is a small (6.9 million tons), sedex-type massive sulphide ore body in the Anvil Mining District of the Selwyn Basin, Yukon Territory (Fig. 1). The deposit is currently being developed as an open pit mine producing approximately 13 500 tonnes of ore per day. The ore body consists of several lenses of fine- to medium-grained pyrite-sphalerite-galena-barite-quartz within the Lower Paleozoic upper Mt. Mye phyllite of the Anvil District. The deposit is polydeformed and polymetamorphosed to mid-greenschist facies. During the 1990 and 1991 field seasons detailed mapping and drill core logging were undertaken to carry out a structural analysis of the Vangorda deposit. The aim of this research is to establish the 3D geometry of the deposit, to define the structural evolution of the orebody and host rocks, and to define the effects of deformation and metamorphism in the sulphides. This paper presents the preliminary results.

REGIONAL GEOLOGY

The Anvil Range lead-zinc-silver district is located within the Omineca Crystalline Belt of the northern Canadian Cordillera, approximately 200 km northeast of Whitehorse, Yukon (Fig. 1). The district lies immediately north of the Cretaceous-Tertiary Tintina fault, a major dextral strike-slip fault in the northern Cordillera (Fig. 2). Rocks in the Anvil District consist of a structurally thickened sequence of upper Proterozoic to lower Paleozoic polydeformed, polymetamorphosed, metasedimentary and metavolcanic

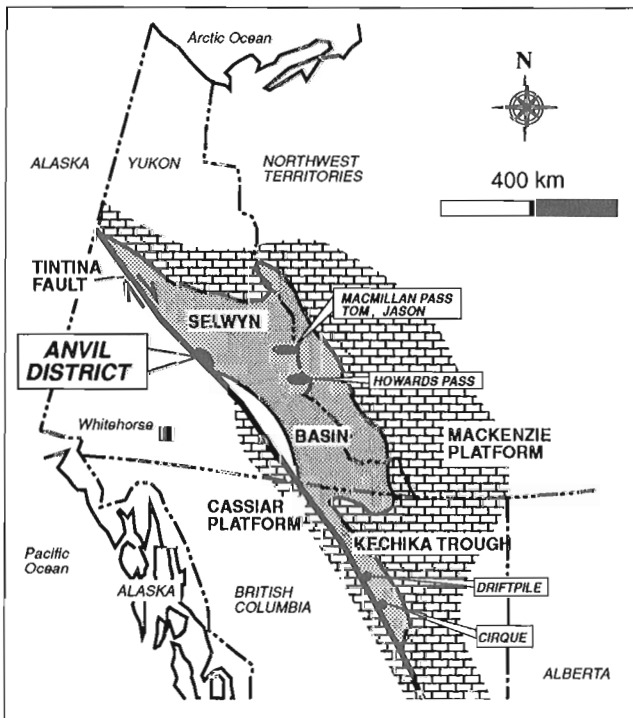


Figure 1. Generalized geological map showing the location of major mineral occurrences in the Selwyn Basin.

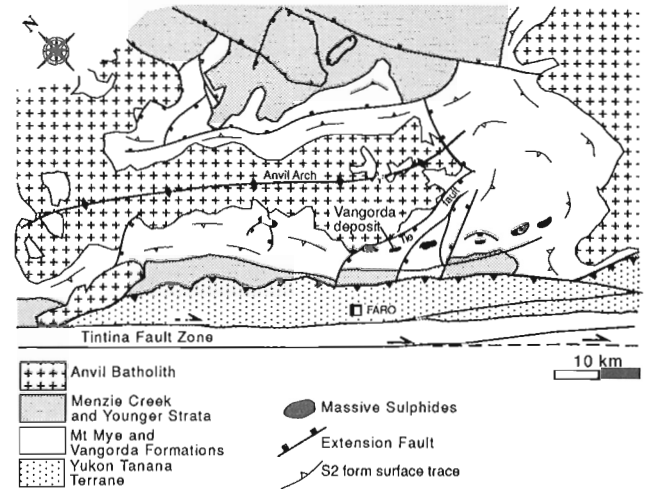


Figure 2. Schematic geological map of the Anvil District. Note the curvilinear distribution of the sulphide deposits. (Redrafted from Jennings and Jilson, 1986).

schist and phyllite (Jennings and Jilson, 1986) interpreted as part of the ancient western North American margin. These rocks are intruded by Cretaceous granite (Pigage and Anderson, 1985) and granodiorite of the Anvil plutonic suite. The dominant structural feature in the district, the Anvil Arch, has a northwest-southeast structural grain outlined by foliation form-surface traces, and is related to uplift during intrusion of the Anvil plutonic suite. Late extensional faults such as the Tie fault (Fig. 2) are interpreted to be related to emplacement and unroofing of the Anvil Batholith (Jennings and Jilson, 1986).

Five ductile deformation events have been recognized in the Anvil district (Jennings and Jilson, 1986). The first two are penetrative and form the dominant structural elements of the district. The first phase, D₁, is interpreted to be related to northeast-directed folding, thrusting, and nappe emplacement during the pre- to mid-Cretaceous docking of outboard terranes onto the ancient North American continent (Tempelman-Kluit, 1979; Mortensen and Jilson, 1985). D₁ resulted in the development of a penetrative regional foliation (S₁), and regional metamorphism reaching greenschist to amphibolite facies (Jennings and Jilson, 1986).

The second deformation event, D₂, is probably related to emplacement of the Anvil plutonic suite. D₂ resulted in southwest-directed folding, development of a penetrative foliation (S₂), greenschist to amphibolite facies contact metamorphism, and extensional faulting. The structural environment of D₂ is essentially that of a metamorphic core complex. The fold overprinting style between F₁ and F₂ is that of a type 3 hook structure (cf. Ramsay, 1967; Jennings and Jilson, 1986). D₃ to D₅ deformation events produced minor folds and steeply dipping crenulation foliations that overprint the D₁ and D₂ structural elements.

The Anvil district is host to five stratiform, massive sulphide deposits with an estimated geological reserve of 120 million tonnes (Jennings and Jilson, 1986) (Fig. 2). The five deposits lie along a northwest-southeast curvilinear trend,

parallel to the regional structural grain of the district (Fig. 2). Ore rocks in the deposits are variably recrystallized metamorphic tectonites (Pigage, 1990) that display deformation textures that can be related to D_1 and D_2 , and locally D_3 to D_5 (cf. Jennings and Jilson, 1986).

LITHOSTRATIGRAPHY

The lithostratigraphy of the Anvil District consists of up to 5 km of polydeformed, late Precambrian to upper Paleozoic metasedimentry and metavolcanic rocks intruded by Cretaceous granites (Jennings and Jilson, 1986) (Fig. 3). Within it are two lithostratigraphic units important to this paper, the lower non-calcareous, carbonaceous Mt. Mye formation and the overlying calcareous, variably carbonaceous Vangorda formation. Near the Vangorda deposit these rocks are chlorite-muscovite phyllite that, in the case of the Vangorda formation, contain calcite and/or dolomite. The Anvil District deposits straddle the boundary between the Mt. Mye and the Vangorda formations, or occur up to 150 m below the stratigraphic contact between the two (Jennings and Jilson, 1986). Ore rocks in the Vangorda

deposit are part of the synsedimentary, stratiform Anvil cycle (Fig. 3) as defined by Jennings et al. (1980) and Jennings and Jilson (1986). These authors envision the Anvil cycle to have formed from hot metalliferous brines discharged along a synsedimentary fault in a terraced fault system.

The Vangorda deposit occurs in the uppermost section of Mt. Mye phyllite directly below the Vangorda formation. The deposit appears to consist of lenses of varying thicknesses and bulk sulphide compositions and are typically accompanied by a footwall biased phyllitic, muscovite-chlorite alteration zone that grades into the ore lithofacies. The salient features of each ore lithofacies in the Vangorda deposit are outlined below.

Ribboned-banded, carbonaceous, pyritic quartzite: these are well banded, sulphide-bearing quartzite, with lesser sphalerite and galena. Bands are on a millimetre- to centimetre-scale and consist of quartz-sulphide and carbonaceous, phyllitic quartzite. Where F_2 folding occurs, S_1 is typically preserved in millimetre- to centimetre-scale lithons. Detailed mapping and drillcore logging shows that this lithofacies may occur alone or be absent from the previously defined Anvil cycle.

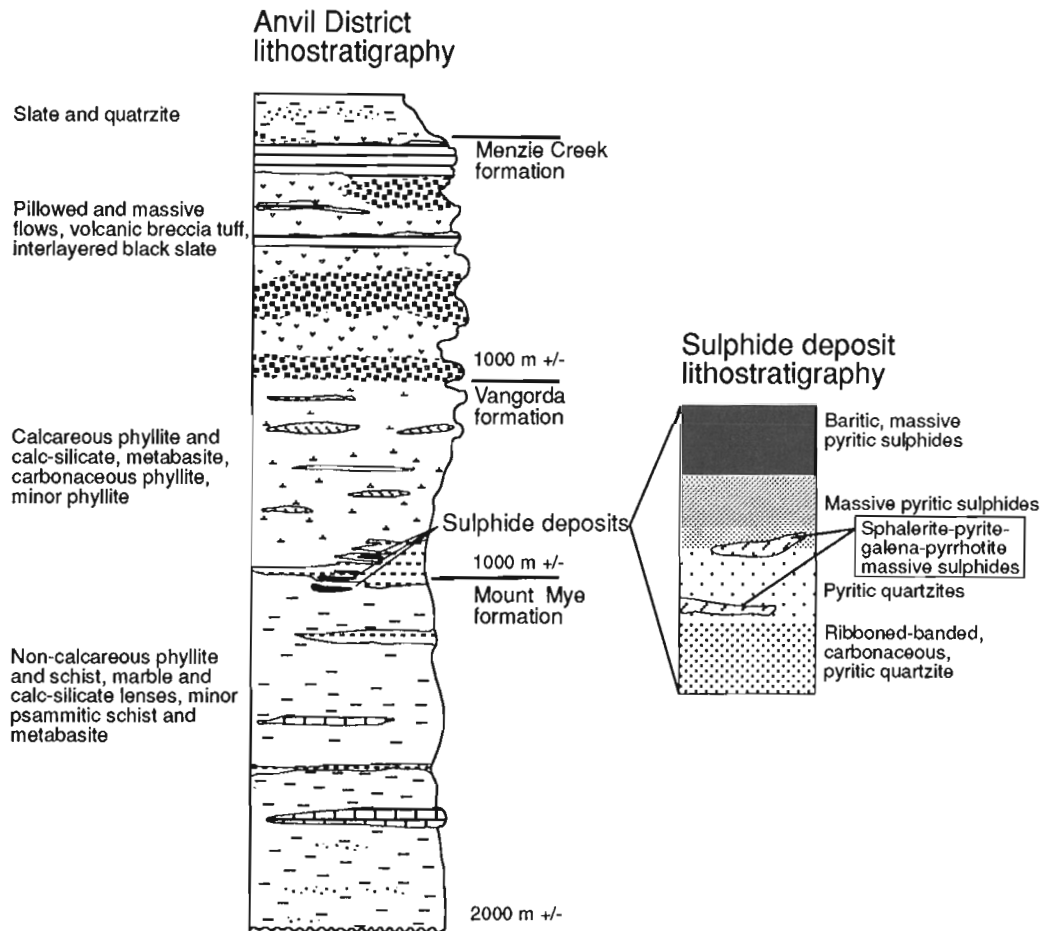


Figure 3. A schematic column of a portion of the Anvil District lithostratigraphy and the sulphide deposit lithostratigraphy. The sulphide deposits occur as lenses in the upper Mt. Mye formation, lower Vangorda formation. (Redrafted from Jennings and Jilson, 1986).

Pyritic quartzite: this consists predominantly of quartz with up to 40% pyrite and minor sphalerite and galena. These rocks are moderately to poorly banded with, locally, a well developed micaceous (muscovite) foliation. Sulphides are typically fine- to medium-grained (0.2-1 mm), with local coarse-grained patches (1-2 mm). Galena, and less commonly sphalerite, may occur in coarse grained aggregates.

Massive pyritic sulphides: these are typically fine- to medium-grained (0.1-1 mm) massive pyrite with less sphalerite, galena, pyrrhotite, and minor magnetite. Quartz, barite, and carbonate are disseminated throughout or occur in aggregates. Total sulphide content ranges from 60% to 100%. Texturally the massive pyritic rocks are homogeneous to banded. Banding is developed on a scale of millimetres to centimetres as alternating thick bands of pyrite and thin bands of sphalerite + magnetite + galena. This lithofacies may be

interbanded with the pyritic quartzites on a scale of centimetres to metres and commonly grades laterally into it. A foliation, defined by chlorite + carbon occurs locally.

Baritic, massive pyritic sulphides: these consist predominantly of barite with fine- to coarse-grained (0.1-2 mm) pyrite, sphalerite, galena, with minor magnetite. Quartz and carbonate are major matrix components. Clasts of pyrite and phyllite are common. Total barite content may be as high as 50%. Millimetre- to centimetre-scale interbanding of pyrite-rich and barite-rich layers is ubiquitous.

As well as the above lithofacies, whose distribution are believed to be relicts of primary depositional ore types, two lithofacies occur in areas of high strain and are interpreted as the result of metamorphic reactions and mobilization during deformation.

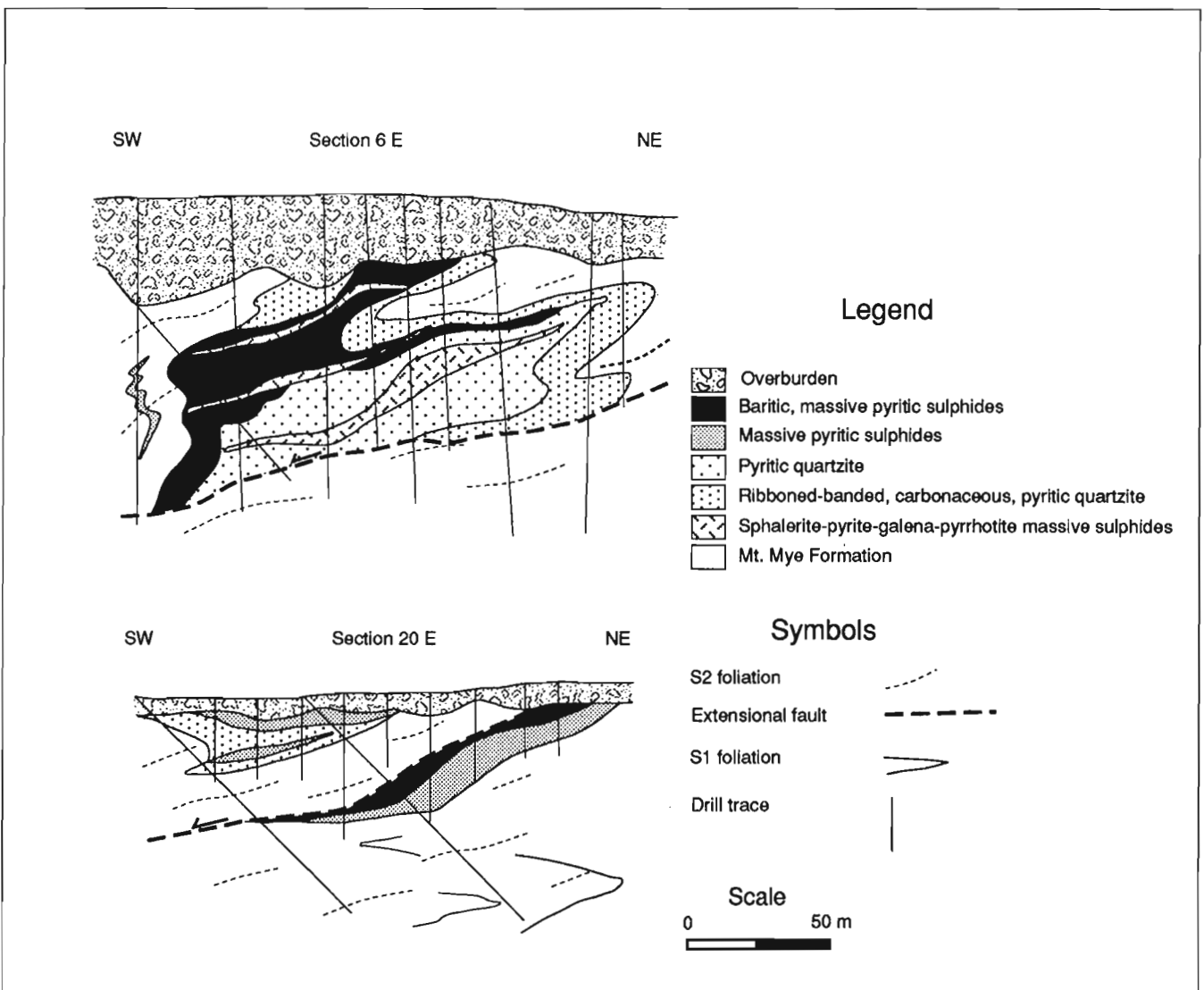


Figure 4. Cross-sections through the Vangorda deposit. Section 6 E contains the complete ore lithostratigraphy. Section 20 E consists of several lenses of sulphide lithofacies that are possibly separated by a fault. Sections were constructed using diamond drillhole data.

Pyrite-sphalerite-galena-pyrrhotite quartzite: this lithofacies is a variant of the pyritic quartzite in which the dominant sulphide is pyrite and sphalerite with lesser galena, and pyrrhotite. Grain sizes range from 0.01 to 2 mm and coarse (2-3 mm) patches of sphalerite or galena are common. Pyrite typically occurs as medium to coarse grained, submillimetre- to millimetre-sized porphyroblasts in an inhomogeneous, discontinuous foliation, or in isolated breccia clasts. These rocks are typically highly strained and commonly contain clasts of other rock types around which a well developed foliation anastomoses. Tailed clasts and rolling structures are common.

Pyrrhotitic massive sulphides: these contain predominantly fine-grained (0.05-1 mm) pyrrhotite with lesser pyrite, sphalerite, galena, and chalcopyrite. Pyrite is commonly porphyroblastic, reaching grain sizes of up to 1 mm. These rocks are typically highly strained and brecciated. Breccia clasts are rounded to angular, and generally have an internal foliation. Clasts may have symmetric or asymmetric tails and rolling structures are common.

THE VANGORDA DEPOSIT

The Vangorda deposit occurs 50 to 120 m beneath the carbonaceous base of the Vangorda formation. It consists of a number of gently northwest-plunging lenses and is elongated northwest-southeast. The deposit is interpreted to lie in the hinge and overturned limb of a macroscopic F₂ fold (Jennings and Jilson, 1986; Pigage, 1990). However, contrary to its structural position the overall lithostratigraphy in this part of the deposit appears to consist of a single, right way up, idealized Anvil cycle (Fig. 4). An extensional fault of unknown offset truncates the orebody to the northwest, and in the southeast the deposit also appears to be truncated by extensional faulting. The deposit is cut approximately in half by a northwest-dipping extensional fault of unknown throw which juxtaposes two fault blocks of contrasting structural and lithostratigraphic styles. Northwest of this fault (Fig. 4, section 6 E) the deposit consists of a thick body of sulphide displaying one complete lithostratigraphic sequence, whereas southeast of the fault (Fig. 4, section 20 E) the orebody consists of thin lenses of individual lithofacies or group of lithofacies.

Regional D₂ metamorphic grade in the area decreases outward from the Anvil Batholith and metamorphism in the Vangorda deposit is thought to be due to contact metamorphism related to intrusion of the batholith (Jennings and Jilson, 1986). Metamorphic grade, recorded by muscovite-chlorite assemblages in wall rock phyllite, is sub- to mid-greenschist facies. The D₁ metamorphic grade regionally reached greenschist to amphibolite facies and in the orebody likely did not exceed greenschist facies.

Rocks in the Vangorda deposit are penetratively deformed by the D₁ and D₂ deformation events, making definition of any primary depositional features on a scale other than microscopic (see below) ambiguous at best. In most lithofacies in the deposit, banding is well developed on a scale of millimetres to centimetres. This banding is

commonly folded by south- to southwest-verging folds presently accepted to be F₂ and is therefore taken to define S₁. Throughout the deposit, S₁ is commonly preserved as lithons in the hinges of F₂ folds in phyllite and the ribbon banded, carbonaceous quartzite. In sulphide-rich lithofacies S₁ is typically transposed into the F₂ axial surface. S₁ is used throughout this paper as the datum for determining the relative ages of the structural elements of the Vangorda deposit.

F₁ folds have not been identified in the Vangorda deposit previously because of penetrative overprinting by F₂ and because exposure was poor before mine development. This study identifies several examples of refolded folds in drill core and in pit wall exposures, indicating that F₁ folding may be important in the present geometry of the deposit. The widespread presence of S₁ in the ore lithofacies, and the evidence for F₁ folding in rocks near the deposit (e.g., Jennings and Jilson, 1986) also point to the relative importance of F₁ folding.

The dominant fold phase in the Vangorda deposit is F₂. F₂ folds are typically east-west- to northwest-southeast-plunging, tight to near isoclinal (interlimb angle is commonly 5-25°) similar folds. F₂ fold morphology changes as a result of relative competency and ductility contrasts between the different lithofacies, but the similar fold style is maintained. Where competency contrast is high, F₂ folds become somewhat disharmonic.

In the surrounding phyllite, a penetrative shallowly southwest-dipping, wavy D₂ axial planar cleavage (S₂) is developed. In some sulphide lithofacies, such as the ribboned-banded, carbonaceous quartzite, a differentiated axial planar S₂ cleavage is well developed. However, S₂ appears to be non-penetrative in the sulphides and is only rarely found in fold hinges. In general, the S₁ banding is transposed into the S₂ orientation, and is easily mistaken for S₂. In high strain zones, such as the overturned limbs of macroscopic folds, S₁ banding in the sulphide lithofacies is discontinuous as a result of shearing and a new, inhomogeneous S₂ foliation is developed.

There is little evidence for the relationship between F₁ and F₂ folds in the Vangorda deposit, but the rare occurrence of refolded folds indicates that the style of overprinting is the same as that recorded regionally, (i.e. type 3 of Ramsay, 1967) (cf. Jennings and Jilson, 1986, Fig. 21).

Locally, steeply south- to southwest-plunging to subvertical, open folds fold the S₂ cleavage and tighten F₂ folds. These folds are here termed F₃. F₃ folds are of minor importance and a local crenulation cleavage is associated with them.

The Vangorda deposit is strongly faulted by brittle extensional faults that, together with F₂ folding, provide the dominant control on the geometry of the orebody. Extensional faults examined truncate the S₂ cleavage and F₂ folds and postdate or are late D₂. Faults in the deposit are typically steeply northwest- to southeast-dipping gouge zones consisting of phyllosilicate and/or sulphide-quartz sand and/or breccia. Locally, these are cemented by a matrix

of quartz and calcite and, in some instances, by pyrite. Breccias contain angular clasts of phyllite and sulphide ranging in size from several millimetres to several centimetres. Clasts are strongly broken and, in many cases, can be fitted back together. Pyrite slickensides on polished fault surfaces are typically subhorizontal or have a shallow pitch angle, indicating a late phase of strike-slip to oblique-slip movement. Faults have an offset of centimetres to several tens of metres. Paucity of marker horizons precludes measurement of exact offset on any fault.

Another type of fault common in the sulphide rocks is characterized by tectonic mixing of angular to rounded clasts of brecciated quartz, phyllite, and sulphide in a ductilely deformed, well foliated, and recrystallized pyrrhothite-rich or sphalerite and galena-rich matrix (Fig. 5a). These faults range in size from several millimetres up to several tens of centimetres wide, generally with sharp boundaries. Clasts are tailed or rotated (5b), and internally folded, with the foliation flowing around them. Pyrite porphyroblasts are common in the matrix and in sulphide clasts. In several instances shear zones are folded by F_2 folds. These shear zones appear to be the extremely high strain end-member of a *durchbewegung* structure (see review by Marshall and Gilligan, 1989) and may represent discrete faults or zones of shearing. Thin breccias and ductile faults are common along boundaries between sulphide lithofacies indicating layer parallel shearing during deformation.

Several low-angle, post- D_2 , northeast-directed thrusts occur within phyllite in the southeast end of the deposit. These cut the S_2 cleavage and have offsets ranging from centimetres up to several tens of metres.

MICROSTRUCTURE

Preliminary studies were carried out on several microstructural aspects of ore rocks from the Vangorda deposit. To date, deformation textures in pyrite have received the bulk of the attention. Selected polished sections were etched with warm, 30% nitric acid (HNO_3) to study growth features (e.g., grain boundaries and overgrowths), mineral phases, and deformation textures (e.g., dislocation structures).

Relict, primary colloform pyrite grains, although rare, occur in the massive pyrite and pyritic quartzite lithofacies within the Vangorda deposit. These are typically 0.05-0.5 mm-sized, equant to xenoblastic grains that occur alone or as cores with overgrowths of secondary, metamorphic pyrite.

Medium- to coarse-grained (0.25-2 mm), secondary, metamorphic pyrite, identifiable by its massive, typically inclusion-poor, equant to idioblastic nature, exhibits both brittle and ductile deformation textures. Zones of intense cataclasis have produced aggregates of angular comminuted grains. Within these zones a foliation, defined by micas and aligned quartz, anastomose around pyrite porphyroblasts. Indentation and axial cracking of large porphyroblasts is common (Fig. 5c).

One sample from the massive pyrite lithofacies shows an excellent example of grain shape preferred orientation of pyrite (Fig. 5d). These elongate grains typically show little or no evidence of brittle deformation, and only minor dislocation microstructure. Grain boundaries are straight to slightly curved, mildly sutured, and lightly indented. No overgrowths are apparent but pressure solution is the likely mechanism responsible for the preferred shape orientation.

Pyrite porphyroblasts commonly have overgrowths, either on relict colloform grains or on secondary metamorphic grains. In some cases numerous phases of grain growth can be recognized in one porphyroblast. These multiple phases of grain growth are evidence of a complex pyrite formation history.

Pyrite also shows annealing textures from metamorphism. In the massive pyritic lithofacies, grains are commonly submillimetre- to millimetre-sized, equant grains with straight to mildly sutured boundaries with 120° triple junctions. In quartz-rich areas and in the pyritic quartzite lithofacies, pyrite commonly forms larger (up to 3 mm locally), equant to idioblastic porphyroblasts.

Etched pyrite grains show dislocation microstructures which are characterized by straight to slightly curved, stepped, or branching dislocation walls and tangles. The dislocation walls and tangles commonly form grid-like arrays denoting the onset of polygonization and subgrain formation and incipient dynamic recrystallization (Fig. 5e).

Subgrain formation is common throughout the samples examined in this study. Subgrains are typically 5-50 μ m, equant grains with straight to slightly curved grain boundaries that meet at 120° triple junctions. Subgrain formation commonly occurs along the boundaries of parent grains (Fig. 5f) resulting in a core-mantle texture.

Pyrite textures such as preferred grain shape orientation, subgrain formation, pressure solution, and dislocation structures indicate pyrite was deformed both by ductile and brittle mechanisms. Many ductile features outlined above have been studied experimentally (cf. Cox et al., 1981) and occur at temperatures of 500 to 650 $^\circ$ C and pressures of \sim 300 MPa.

CONCLUSIONS

This paper illustrates characteristics of the deformational style in the ore rocks of the Vangorda deposit. The dominant fabric element in the deposit is a penetratively developed banding and/or foliation, S_1 , which can be used as a datum for determining the relative age of structural elements.

S_1 is folded by tight to near isoclinal, east-west-plunging F_2 folds with a class 2 similar geometry. In host rocks and some sulphide lithofacies, S_1 is preserved as lithons in the hinge zones of F_2 folds, whereas in fold limbs S_1 has been transposed into the F_2 axial surface. S_2 is typically poorly, or not developed in massive pyritic rocks. The widespread occurrence of S_1 and the relative rarity of S_2 suggests that D_1 played an important role in the deformation and remobilization of the orebody and may be responsible for the

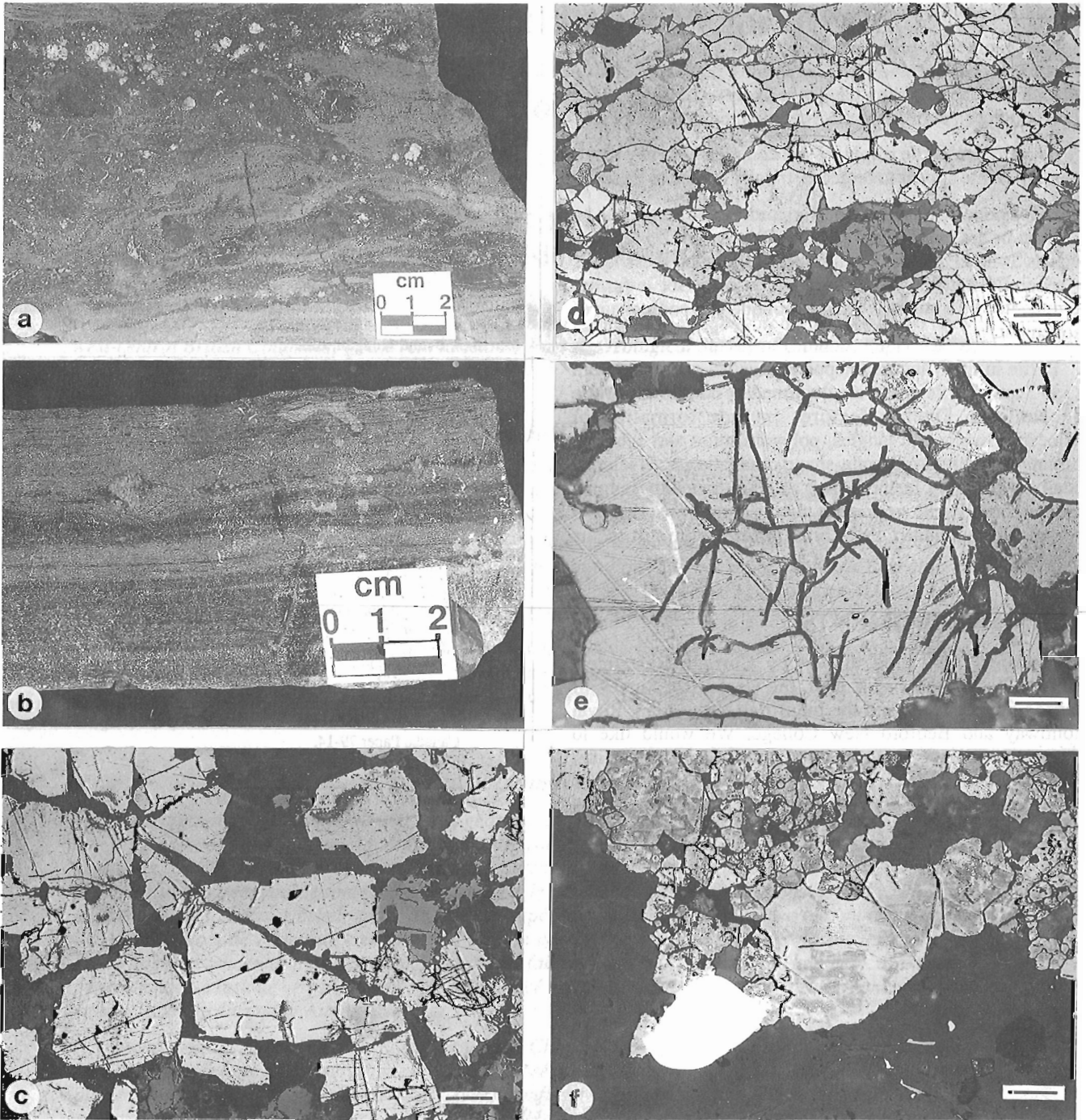


Figure 5(a) Ductile fault zone in massive sulphide. Matrix consists of sphalerite, pyrrhotite, and galena. (b) Sulphide mylonite with tailed, a-type porphyroclasts of quartz. (c) Pyrite porphyroblasts displaying indentation and marked axial cracking. Scale bar is 1.0 mm. (d) Preferred grain-shape orientation in pyrite. Grain boundaries are straight to moderately serrate and meet at 120° triple junctions. Scale bar is 1.0 mm. (e) Dislocation walls and tangles marking the onset of polygonization in pyrite. Scale bar is 0.25 mm. (f) Grain boundary recrystallization and subgrain formation in pyrite. Scale bar is 0.5 mm.

bulk of deformation textures in the sulphides. Strong evidence for this is the occurrence of F₂ folded sulphide shear zones. The D₁ distribution of sulphide lithofacies is tightly folded by F₂ folds.

The geometric relationship between F₁ and F₂ folds remains to be defined. The examples discussed above indicate that the refolding pattern is likely to be a type 3 (or hook structure), similar to that recorded regionally.

Shear zones in the sulphides are complex and may result from D₁. Some appear to be geometrically related to F₂ folds.

Extensional faults in the Vangorda deposit appear to postdate or are late D₂ and clearly offset earlier D₂ features such as S₂ and F₂ folds. The amount of throw on these faults is generally not known. Determination of offset is further complicated by a late strike-slip to oblique-slip component of movement.

Pyrite in the Vangorda deposit ranges in grain size from 0.1 to 3 mm. Pyrite grains are deformed by ductile and brittle mechanisms. Ductile features include formation of dislocation walls and tangles, polygonization and subgrain formation. A preferred grain-shape orientation is developed locally. Annealing features such as grain-boundary bulging are common. Pyrite grains are also indented, cracked, and strongly disaggregated. Primary colloform pyrite still occurs locally.

ACKNOWLEDGMENTS

This project is funded in part by Curragh Resources, D.I.A.N.D., Whitehorse, Yukon, the Geological Survey of Canada (Vancouver), and the Industrial Association, Royal Holloway and Bedford New College. We would like to personally thank Greg Jilson, Lee Pigage, Cam Reed, Mitch Wasel, Steve Morrison, Grant Abbott, and Dirk Tempelman-Kluit. We would also like to thank the people at the Faro mine for their help. Brown is sponsored in part by

the Rothemere Foundation and by the Special Scholarship for Students doing Research in Resource Development administered by Memorial University of Newfoundland. Brenda Fediuk is thanked for her help in getting this paper written.

REFERENCES

- Cox, S.F., Etheridge, M.A., and Hobbs, B.E.**
1981: The experimental ductile deformation of polycrystalline and single crystal pyrite; *Economic Geology*, v. 76, p. 2105 - 2117.
- Jennings, D.S. and Jilson, G.A.**
1986: Geology and sulphide deposits of the Anvil Range, Yukon; in *Mineral Deposits of Northern Cordillera*, (ed.) J.A. Morin; Canadian Institute of Mining and Metallurgy, Special Paper 37, p. 319-361.
- Jennings, D.S., Jilson, G.A., and Pigage, L.C.**
1980: Anvil Range stratigraphy, south-central Yukon Territory (abstract); *Geological Association of Canada, Cordilleran Section, Programme and Abstracts*, p. 16-17.
- Marshall, B. and Gilligan, L.B.**
1989: Durchbewegung structure, piercement cusps, and piercement veins in massive sulphide deposits: formation and interpretation; *Economic Geology*, v. 84, p. 2311-2319.
- Mortensen, J.K. and Jilson, G.A.**
1985: Evolution of the Yukon-Tanana terrane: evidence from southeastern Yukon Territory; *Geology*, v. 13, p. 806-810.
- Pigage, L.C.**
1990: Field guide Anvil Pb-Zn-Ag district, Yukon Territory, Canada; in *Mineral Deposits of the Northern Canadian Cordillera, Yukon-Northeastern British Columbia*, (ed.) J.G. Abbott and R.J.W. Turner; Geological Survey of Canada, Open File 2169, p. 283-308.
- Pigage, L.C. and Anderson, R.G.**
1985: The Anvil Plutonic Suite, Faro, Yukon Territory; *Canadian Journal of Earth Sciences*, v. 22, p. 1204-1216.
- Ramsay, J.G.**
1967: *Folding and Fracturing of Rocks*; New York, McGraw-Hill, 568 p.
- Tempelman-Kluit, D.J.**
1979: Transported cataclasite, ophiolite and granodiorite in Yukon Territory: evidence of arc-continent collision; *Geological Survey of Canada, Paper 79-14*.

An update on the Chilcotin-Nechako project and mapping in the Taseko Lakes area, west-central British Columbia

C.J. Hickson
Cordilleran Division, Vancouver

Hickson, C.J., 1992: *An update on the Chilcotin-Nechako project and mapping in the Taseko Lakes area, west-central British Columbia*; in *Current Research, Part A; Geological Survey of Canada, Paper 92-1A*, p. 129-135.

Abstract

Detailed mapping (1: 50 000) and geochronology in Taseko Lakes (NTS 920) area demonstrated that the mid-Jurassic Mount Alex plutonic complex and overlying volcanic rocks (previously correlated with the Hazelton Group) are mid-Cretaceous (Albian). Correlation of these rocks with the Spences Bridge Group is now more likely. Slightly younger, Late Albian to Cenomanian, volcanic rocks conformably overlie Silverquick conglomerates and may be correlative with Powell Creek volcanics found farther to the southwest. Northwesterly trending, northeasterly verging, reverse (thrust?) faults have displaced and fragmented stratigraphic packages as late as Albian-Cenomanian time.

Miocene to Pleistocene age (Chilcotin Group) lavas overlie much of the region. Discovery of hyaloclastite breccia, along the Fraser River associated with the youngest known lava flows (Dog Creek Formation), confirms regional glaciation about 1 million years ago and incision of the Fraser River valley to a depth of at least 350 m (1800 ft).

Résumé

La cartographie détaillée (1/50 000) et la géochronologie de la région des lacs Taseko (920) montrent que le complexe plutonique de Mount Alex, du Jurassique moyen, et les roches volcaniques sus-jacentes (autrefois corrélées avec le groupe de Hazelton), datent du Crétacé moyen (Albien). Il paraît maintenant plus probable que ces roches sont en corrélation avec le groupe de Spences Bridge. Des roches volcaniques légèrement plus jeunes, s'échelonnant de l'Albien supérieur au Cénomaniens, recouvrent en concordance les conglomérats de Silverquick et sont peut-être en corrélation avec les roches volcaniques de Powell Creek que l'on rencontre plus loin au sud-ouest. Des failles inverses (failles chevauchantes?), de direction générale nord-ouest, de vergence nord-est, ont déplacé et fragmenté des ensembles stratigraphiques à une époque aussi tardive que l'Albien-Cénomaniens.

Des laves d'âge miocène à pléistocène (groupe de Chilcotin) recouvrent une grande partie de la région. La découverte le long du Fraser, d'une brèche composée de hyaloclastite, associée aux coulées de lave les plus récentes connues (formation de Dog Creek), confirme la présence d'une glaciation régionale il y a environ 1 million d'années et le creusement de la vallée du Fraser jusqu'à au moins 350 m de profondeur (1 800 pieds).

INTRODUCTION

The Chilcotin-Nechako project focuses on a region of west-central British Columbia which is part of the Intermontane physiographic subdivision. The region is bounded on the east by the Fraser Fault, the south and west by the Coast Mountains, and extends northward to about 54°. Figure 1 shows the southern half of the region. Field work in this region began under the Chilcotin-Nechako Hydrocarbon Province project in 1989 with a preliminary, two week reconnaissance study (Hickson, 1990). Other, more detailed investigations on thermal maturation of the region (Hunt and Bustin, 1990), Cretaceous and Eocene stratigraphy (Rouse et al., 1990), and geochronology and structure (van der Heyden, 1990) were also started. Funding for the project was through the Federal "Frontier Geoscience Program" which sought to assess the hydrocarbon potential of the Chilcotin-Nechako

Basin (Hickson, 1990) through basic geological and geophysical mapping. Funding levels were insufficient to address all of the problems outlined in the initial project and work focused on the Taseko Lakes (NTS 920) map area (Hickson, 1990). A field program was started in Taseko Lakes (NTS 920) in 1990 (Hickson et al., 1991) while studies of the basin's margin by van der Heyden (1991) and Umhoefer and Tipper (1991) continued. Field work in 1991 is a continuation of the work of Hickson et al. (1991).

Geological and geophysical investigations in the Chilcotin-Nechako region are proposed as a joint Federal-Provincial project under the Mineral Development Agreement between the Province of British Columbia and the Federal Government. Mapping in Taseko Lakes (NTS 920) will continue under present funding initiatives and further mapping in the Anahim Lake (93C), Quesnel (93B) and

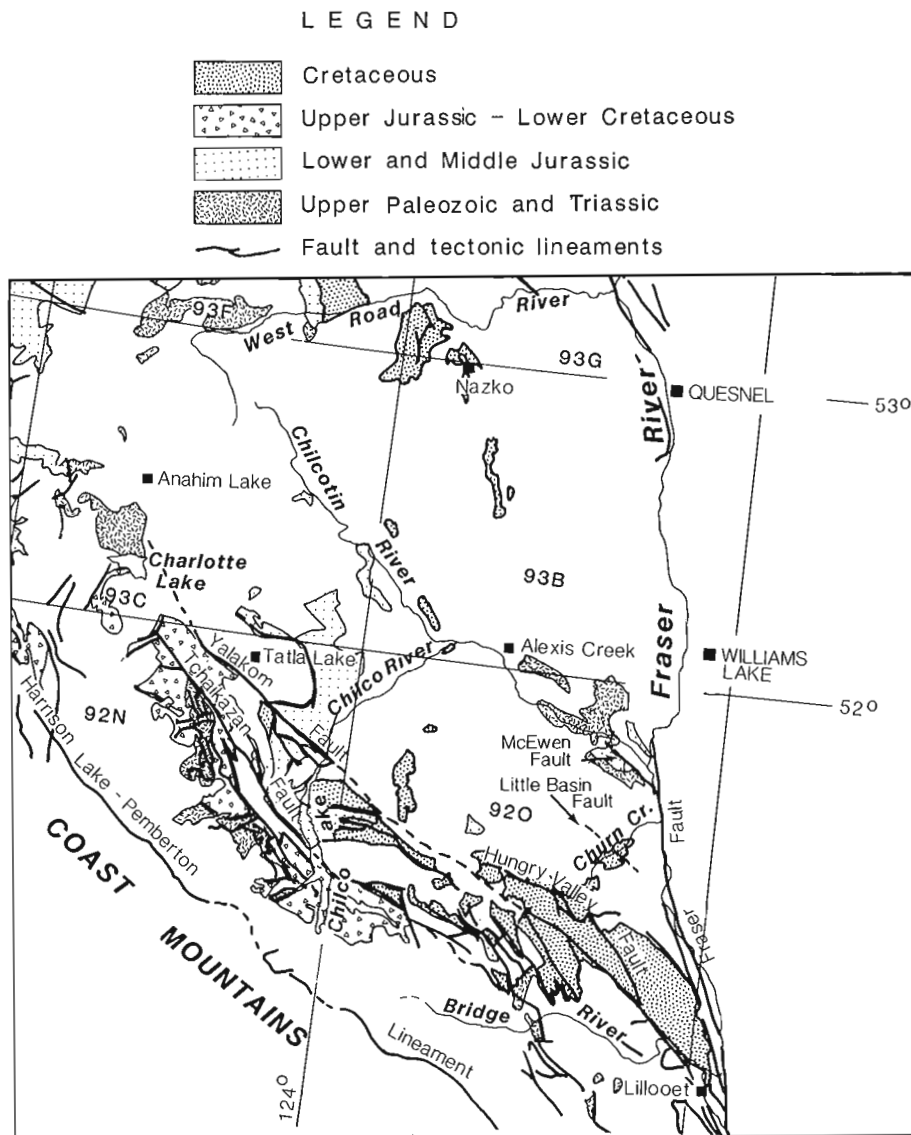


Figure 1. Location map showing the southern portion of the Chilcotin-Nechako Hydrocarbon Province.

Nechako River (93F) map areas will be undertaken by provincial and federal investigators supplemented by geophysical surveys such as aeromagnetic mapping if a mineral development agreement is signed.

STRATIGRAPHY

Paleozoic to early Mesozoic

Paleozoic to early Mesozoic rocks are found within the map area along the east side of the Fraser River (Tipper, 1978), the Chilcotin River (Hickson et al., 1991; Tipper, 1978), and the southern margins of the region (Tipper, 1978; Glover and Schiarizza, 1987; Glover et al., 1987, 1988; Garver et al., 1989; Schiarizza et al., 1989; McLaren, 1990). Continued mapping along the Chilcotin River (parts of NTS 92O/9, 15 and 16), under contract by P. Read of Geotex Consultants Ltd., has shown that the region is more structurally complex than originally reported in Hickson et al. (1991). Read (1992) reports that northeasterly directed thrusting disrupts rocks as old as the Permian (Farwell Pluton) and as young as Early Jurassic (Late Toarcian siltstones).

Jurassic

Jurassic stratigraphy is a separate doctoral thesis study under the Chilcotin-Nechako project conducted by J.B. Mahoney. His study aims to correlate Jurassic sediments from south of the Yalakom Fault northward to the McEwan Fault, details can be found in Mahoney (1992). In 1991 fossiliferous siltstone (**IJp**) of Middle to Upper Jurassic age was discovered north of McEwan Fault (Read, 1992), expanding the known area of Jurassic sediments.

In Hickson et al. (1991) it was suggested that rocks of the Mount Alex plutonic complex (**IKag**, **IKat**, **IKa**), a three phase plutonic complex ranging in composition from quartz diorite to granite, were of possible mid-Jurassic age based on findings by Tipper (1978) and field mapping. The plutonic complex is nonconformably overlain by porphyritic (feldspar) basic to felsic volcanic flows, welded pyroclastics, and breccias. Samples collected during the summer of 1990 for U-Pb dating from the eastern side of the pluton (Fig. 2; sample HHB-90-33-01) and the overlying volcanic rocks (Fig. 2; sample HHB-90-36-09) yielded dates of 105 ± 0.5 Ma and 106 ± 0.5 Ma respectively (R.R. Parrish, written comm., July 21, 1991). These dates clearly establish that much of the plutonic complex, and overlying volcanics are Early Cretaceous (Albian). Tipper (1978) originally correlated the overlying volcanic unit with the Hazelton volcanics, but they are more appropriately correlated with the Spences Bridge Group (Thorkelson and Rouse, 1989).

A plutonic complex to the south (Piltz Peak and Mount Wales, Fig. 2) may be related to the Mount Alex intrusions. This complex is discussed in van der Heyden and Metcalfe (1992).

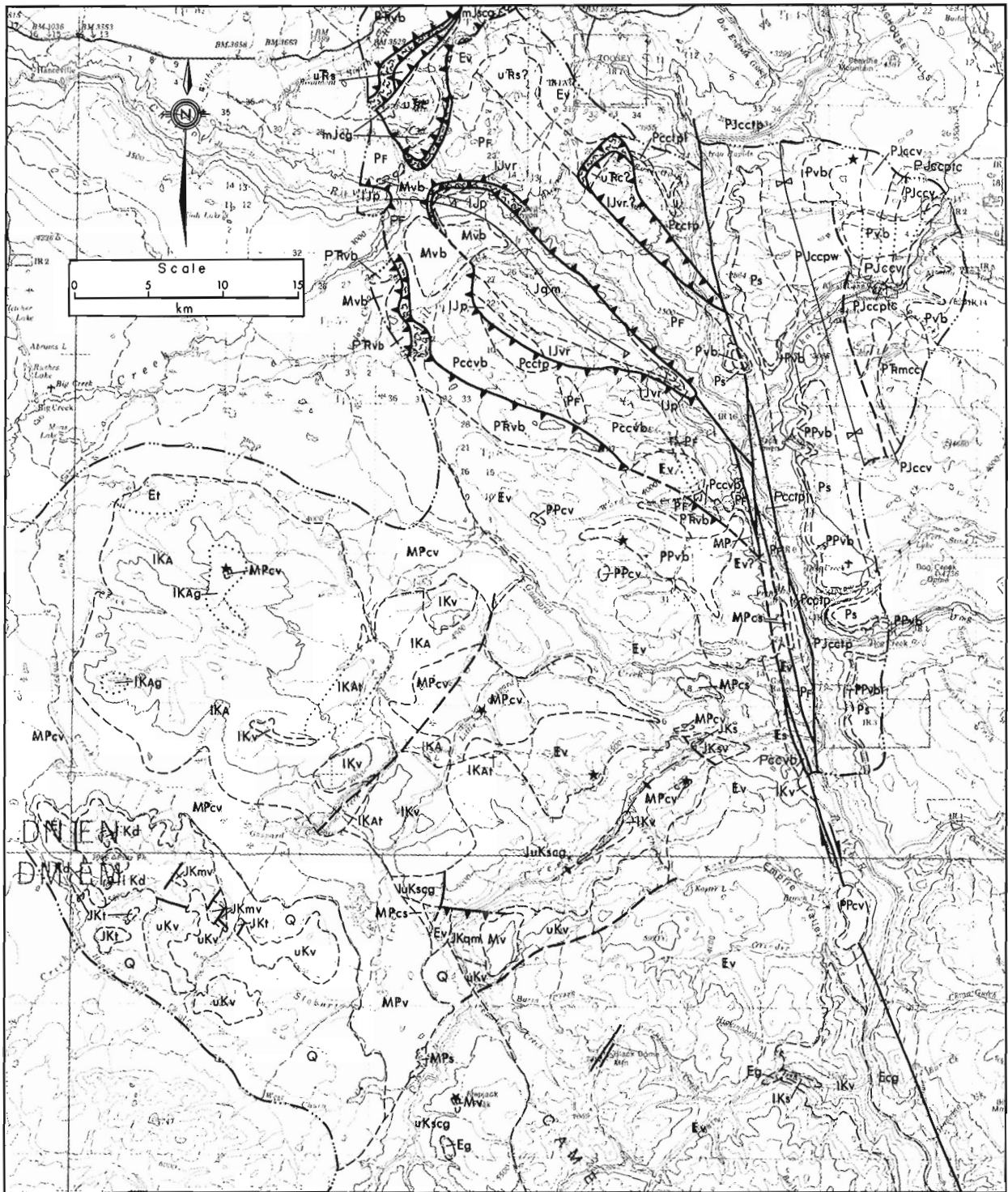
Cretaceous

Further geological complexities were found in the vicinity of Churn Creek. New mapping west of that reported in Hickson et al. (1991) and Rouse et al. (1990) revealed that mid- to Upper Cretaceous sediments are strongly folded and disrupted by reverse faulting (thrusting?). Faulting on the Little Basin Fault places plutonic rocks (**uKp**) over sediments (**uKscg**) (Fig. 2) correlated with the Silverquick conglomerate (Hickson et al., 1991; Mahoney et al., 1992). These sediments were found to be much thicker than previously reported and include clastic material thought to be shed from an over riding fault scarp (Mahoney et al., 1992).

Upper Cretaceous volcanic rocks (**uKv**) previously identified in the area of Churn Creek and southward (Mathews and Rouse, 1984; Green, 1989; Rouse et al., 1990; Hickson et al., 1991) are Cenomanian and present along the south side of Churn Creek where they conformably(?) overlie Silverquick conglomerate (Fig. 2). The volcanic rocks are poorly exposed, but the sequence appears to be made up of intermediate to felsic flows and breccias. The rocks are moderately to strongly porphyritic; feldspar phenocrysts dominate in intermediate end members, but felsic flows have hornblende, biotite, and quartz phenocrysts in addition to feldspar. Heterolithic to monolithic breccias may comprise as much as 50% of the roughly 1000 m thick section. Tilting of the sequence is clearly seen to the south of Churn Creek where the differentially weathering units form a series of south-southwest facing steps dipping from approximately 10° south-southwest to vertical. West of Churn Creek the unit is broadly folded. These volcanic rocks may correlate with the Powell Creek volcanic rocks described from the south western parts of Taseko Lakes (NTS 92O) (Glover and Schiarizza, 1987). Chemically, the volcanic rocks are very similar to the Eocene volcanic rocks (Fig. 3), but this is not a basis for distinguishing them. Further analysis of the data, including trace element and rare earth chemistry, remains to be done.

Tertiary

Mapping of Tertiary volcanic rocks to the south of Churn Creek in the Empire Valley and Churn Creek map areas (NTS 92O/7 and 8) (Fig. 2) suggests Eocene rocks (**Ev**) were extruded on rough paleotopography of Upper Cretaceous volcanic rocks. Eocene volcanic rocks consist of both aerially restricted, high viscosity rhyolite flows and domes, and more laterally extensive mafic to intermediate flows. Blackdome Mine area, the present topographic height of land, most likely is the thickest accumulation of volcanic rocks, possibly the central vent area. Extrusion of felsic lavas from peripheral vents built up thick (up to 100 m), but laterally discontinuous flows. Depressions into which sediments, tephra and coal (**Es**) accumulated were present along the sides of the edifice to the east along the present Fraser River valley (Mathews and Rouse, 1984; Rouse et al., 1990) and the middle reaches of Churn Creek (Fig. 2).



LEGEND	
	Geological contact (approximate) (assumed)
	Geological contact buried beneath Tertiary rocks
	Thrust fault (approximate) (teeth on upper plate) (assumed)
	Strike-slip fault
	Fault buried beneath Neogene rocks
	Melange consisting of blocks in a serpentinite matrix
	Axial trace of folds (northeast overturned anticline) (upright syncline) anticline
	Eruptive centre
	Limit of mapping

Figure 2. Preliminary compilation of mapping completed during 1990 and 1991 field seasons. Geology by C.J. Hickson, P. Read, J. Hunt, P. van der Heyden, B. Mahoney, G. Johansson, S. Metcalfe and K. Green.

Neogene - Quaternary

Chilcotin Group basalt flows (**PPcv** and **MPcv**) cover large areas of the Taseko Lakes (NTS 920) map area (Fig. 2) and range from Miocene to Pleistocene. Along the Fraser River, rocks of the Harper and Dog Creek formations of the Chilcotin Group, form a prominent rim-rock (Mathews and Rouse, 1986). Flows of the Harper Creek Formation (1.3-2.9 Ma), and Dog Creek Formation (1.0 and 1.2 Ma) have sediments between them (Mathews and Rouse, 1986). These sediments are interpreted as representing a proglacial sequence, possibly associated with a previously undocumented regional glaciation (Mathews and Rouse, 1986). Though the time of deposition of these sediments is

clearly bracketed by the lava flows, no direct association with the flows could be ascertained. A succession of hyaloclastite breccia was found north of Canoe Creek along the east bank of the Fraser River (Fig. 2). The breccia contains heterolithic clasts (anvil shaped to subrounded), angular basalt pillow fragments and vesicular basalt clasts set in a yellowish-orange weathering matrix of tuff to lapilli sized basaltic glass (hyaloclastite). The section represents a classic subglacial sequence as described elsewhere by Mathews (1947), Hickson (1987), and others. This deposit clearly indicates volcanism contemporaneous with glaciation, tightening the timing of the major glacial advance postulated by Mathews and Rouse (1986) to explain the deposits to the

LEGEND

CEENOZOIC

Quaternary and Tertiary	
Pliocene and Pleistocene	
CHILCOTIN GROUP (PPcv to MPcs)	
PPcv	Grey olivine and/or plagioclase-phyric basalt flows; locally basal palagonite tuff and pillow breccia
Tertiary	
Miocene to Pleistocene	
MPcv	Grey olivine- and/or plagioclase-phyric subaerial basalt flows; minor interflow breccia
Miocene and(?) Pliocene	
MPcs	Unconsolidated fluvial sediments; minor rhyolite ash and diatomaceous earth
Eocene	
Es	Conglomerate, sandstone; minor siltstone and bentonitic shale; rare coal
Ev	Hornblende-plagioclase-phyric dacite and hornblende-biotite-quartz-phyric rhyolite flows; minor basalt, andesite, pyroclastic flows and ash; rare sediments
Et	Biotite-muscovite tonalite
Eg	felsic intrusive

MESOZOIC

Cretaceous	
upper Lower Cretaceous and Upper Cretaceous	
Powell Creek volcanics (?)	
uKv	Maroon to brown intermediate to felsic flows, tuffs and breccia; minor sediments
Silverquick formation (luKscg to luKs)	
luKscg	Maroon volcanic conglomerate; minor sandstone
luKs	Green to buff chert pebble conglomerate, green to maroon sandstone; minor siltstone
Lower Cretaceous	
lKv	Maroon to green sparsely feldspar-phyric andesite (?) flows, breccia; minor welded rhyolite ash flows
MOUNT ALEX PLUTONIC COMPLEX (lKag to lKa)	
lKag	Hornblende monzogranite and granodiorite
lKat	Chloritized hornblende leucotonalite
lKa	Weakly to strongly foliated, chloritized hornblende quartz monzo-diorite, quartz diorite and diorite
Piltz Peak diorite	
lKd	Heterogeneous, weakly to strongly foliated, chloritized hornblende diorite
lKvo	Amygdaloidal plagioclase-phyric andesite(?) flows; minor pyroclastic rocks
Jurassic and/or Cretaceous	
Lower Jurassic to Lower Cretaceous	
JKsv	Plagioclase-phyric andesite(?) flows; green sandstone and minor siltstone
JKs	Argillaceous, well lithified dark grey siltstone
Piltz Peak and Mount Wales tonalites	
JKt	Weakly to strongly foliated tonalite, chloritized hornblende biotite tonalite and biotite hornblende tonalite

JKmv	Greenschist and amphibolite facies, felsic to mafic metavolcanic schist and gneiss
Jurassic	
Middle to Upper Jurassic	
mJcg	South of Bald Mountain: Red sparsely plagioclase-phyric volcanic conglomerate overlying nonbedded quartz-bearing feldspathic sandstone
mJscg	North of Bald Mountain: Interbedded grey-green volcanic chip conglomerate and nonbedded quartz-bearing feldspathic sandstone
Jqm	Chloritized leucoquartz monzonite, leucoquartz diorite; rare metagabbro. Hypabyssal dacite and felsite intrusions occur marginally
Lower Jurassic	
lJp	Grey noncalcareous siltstone with thin sandstone laminae; minor thin limestone
lJvr	Grey-green and locally maroon porphyritic (plagioclase, quartz) dacite and rhyolite flows and tuffs, felsite- and quartz-feldspar porphyry-bearing tuff; minor green metabasalt flows
Triassic	
Middle to Upper Triassic	
uRs	Grey to nonlimy siltstone and minor interbedded thin calcareous sandstone
uRc	Nonbedded light to medium grey micritic limestone
PALEOZOIC	
Permian	
Late Permian	
FARWELL PLUTON	
Pf	Chloritized and locally foliated metadiorite; minor quartz metadiorite and metagranodiorite
Permian to Jurassic	
Lower Permian to Middle(?) Jurassic	
CACHE CREEK COMPLEX (PJccpw to Pccvb)	
PJccpw	Western Belt: Grey siltstone, shale; minor grey lithic wacke
PJccv	Western Belt: Meta-andesite and metabasalt breccia and flows
PJcctpc	Western Belt: Tectonic(?) lenses of greenstone, limestone and chert in a grey phyllite matrix
Marble Canyon Formation	
PRmcc	Grey unbedded micritic limestone
Permian to Triassic	
PRvb	Green and grey-green aphanitic basic metatuff and minor flows
Permian and(?) older	
Lower Permian and(?) older	
Pcctp	Grey, grey-green and minor light green chert, ribbon chert and phyllite
Pcctpl	Light grey unbedded limestone
Pccvb	Grey-green and green greenstone

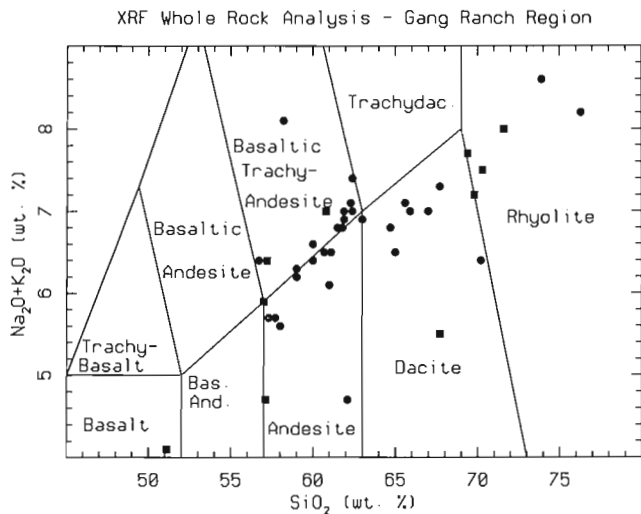


Figure 3. Whole rock XRF analysis of Eocene (circles) and Cretaceous (rectangles) volcanic rocks from the northeast quadrant of Taseko Lakes (92O) map area.

north. The breccia is exposed from an elevation of 884 m (2900 ft) down to an elevation of 550 m (1800 ft) confirming that the Fraser River was already deeply incised one million years ago.

Overlying the Chilcotin and older rocks are thick accumulations of Pleistocene and Holocene sediments, the focus of the doctoral research of D. Huntley. Preliminary findings can be found in Broster and Huntley (1992).

ACKNOWLEDGMENTS

D.W. McDonald provided amiable and able assistance in the field. Logistical and field assistance by S. Metcalfe, J. van der Brink, I. Alarie and D. Halliwell was appreciated. Conversations with R.B. Mahoney, P. van der Heyden, and D. Huntley were most useful. Bev and Larry Ramsted and the staff of Gang Ranch, Bob and Eithia Pepperling of Empire Valley Ranch, and Margo and Chilco Choate of Fosberry Meadows, provided support and access to private land; many thanks. Adroit helicopter piloting by Rob Owens, Wayco Aviation, was appreciated. Horse packing and hospitality by Ron and Daniell Cable was an unforgettable experience. Reviews by R.B. Mahoney and H.W. Tipper were useful and help with manuscript preparation by B. Vanlier and figures by T. Oliveric was most appreciated.

REFERENCES

Broster, B. and Huntley, D.
1992: Quaternary stratigraphy in the east-central Taseko Lakes area, British Columbia; in *Current Research, Part A*; Geological Survey of Canada, Paper 92-1A.

Garver, J.I., Schiarizza, P., and Gava, R.G.
1989: Stratigraphy and structure of the Eldorado Mountain area, Chilcotin Ranges, southwestern British Columbia (92O/2; 92J/15); in *Geological Fieldwork 1988*, British Columbia Ministry of Energy, Mines and Petroleum Resources, Paper 1989-1, p. 131-143.

Glover, J.K. and Schiarizza, P.
1987: Geology and mineral potential of the Warner Pass map sheet (92O/3); in *Geological Fieldwork 1986*, British Columbia Ministry of Energy, Mines and Petroleum Resources, Paper 1987-1, p. 157-169.

Glover, J.K., Schiarizza P., and Garver, J.I.
1988: Geology of the Noaxe Creek map area (92O/02); in *Geological Fieldwork 1987*, British Columbia Ministry of Energy, Mines and Petroleum Resources, Paper 1988-1, p. 105-123.

Glover, J.K., Schiarizza, P., Umhoefer, P.S., and Garver, J.
1987: Geology and mineral potential of the Warner Pass map sheet (92O/3); British Columbia Ministry of Energy, Mines and Petroleum Resources, Open File 1987-3.

Green, K.C.
1989: Geology and industrial minerals in the Gang Ranch area; British Columbia Ministry of Energy, Mines and Petroleum Resources, Open File 1989-27.

Hickson, C.J.
1987: Quaternary volcanism in the Wells Gray-Clearwater area, east-central British Columbia; Ph.D. thesis, Department of Geological Sciences, University of British Columbia, Vancouver, 357 p.
1990: A new Frontier Geoscience Project: Chilcotin-Nechako region, central British Columbia; in *Current Research, Part F*; Geological Survey of Canada, Paper 90-1F, p. 115-120.

Hickson, C.J., Read, P., Mathews, W.H., Hunt, J.A., Johansson, G., and Rouse, G.E.
1991: Revised geological mapping of northeastern Taseko Lakes map area, British Columbia; in *Current Research, Part F*; Geological Survey of Canada, Paper 91-1F, p. 207-217.

Hunt, J.A. and Bustin, R.M.
1990: Stratigraphy, organic maturation, and source rock potential of Cretaceous strata in the Chilcotin-Nechako region (Nazko Basin), British Columbia; in *Current Research, Part F*; Geological Survey of Canada, Paper 90-1F, p. 121-127.

McLaren, G.P.
1990: A mineral resource assessment of the Chilko Lake planning area; British Columbia Ministry of Energy, Mines and Petroleum Resources, Mineral Resources Division, Geological Survey Branch, Bulletin 81, 117 p.

Mahoney, J.B.
1992: Middle Jurassic stratigraphy of the Lillooet area, south-central British Columbia; in *Current Research, Part A*; Geological Survey of Canada, Paper 92-1A.

Mahoney, J.B., Hickson, C.J., van der Heyden, P., and Hunt, J.A.
1992: The Late Albian-Early Cenomanian Silverquick conglomerate, Gang Ranch area: evidence for active basin tectonism; in *Current Research, Part A*; Geological Survey of Canada, Paper 92-1A.

Mathews, W.H.
1947: "Tuyas," flat-topped volcanoes in northern British Columbia; *American Journal of Science*, v. 18, p. 560-570.

Mathews, W.H. and Rouse, G.E.
1984: The Gang Ranch-Big Bar area, south-central British Columbia: stratigraphy, geochronology, and palynology of the Tertiary beds and their relationship to the Fraser Fault; *Canadian Journal of Earth Sciences*, v. 21, p. 1132-1144.
1986: An Early Pleistocene proglacial succession in south-central British Columbia; *Canadian Journal of Earth Sciences*, v. 23, p. 1796-1803.

Read, P.
1992: Geology of parts of Riske Creek and Alkali Lake areas, British Columbia; in *Current Research, Part A*; Geological Survey of Canada, Paper 92-1A.

Rouse, G.E., Mathews, W.H., and Lesack, K.A.
1990: A palynological and geochronological investigation of Mesozoic and Cenozoic rocks in the Chilcotin-Nechako region of central British Columbia; in *Current Research, Part F*; Geological Survey of Canada, Paper 90-1F, p. 129-133.

Schiarizza, P., Gaba, R.G., Garver, J.I., Glover, J.K., Church, B.N., Umhoefer, P.J., Lynch, T., Sajgalik, P.P., Safton, K.E., Archibald, D.A., Calon, T., MacLean M., Hanna, M.J., Riddell, J.M., and James, D.A.R.
1989: Geology of the Tyaughton Creek area; British Columbia Ministry of Energy, Mines and Petroleum Resources, Open File 1989-4.

Thorkelson, D.J. and Rouse, G.E.

1989: Revised stratigraphic nomenclature and age determinations for mid-Cretaceous volcanic rocks in southwestern British Columbia; *Canadian Journal of Earth Science*, v. 26, p. 2016-2031.

Tipper, H.W.

1978: Taseko Lakes (92O) map-area; Geological Survey of Canada, Open File 534.

Umhoefer, P.J. and Tipper, H.W.

1991: Stratigraphic studies of Lower to Middle Jurassic rocks in the Mt. Waddington and Taseko Lakes map areas, British Columbia; in *Current Research, Part A; Geological Survey of Canada, Paper 91-1A*, p. 75-78.

van der Heyden, P.

1990: Eastern margin of the Coast Belt in west-central British Columbia; in *Current Research, Part E; Geological Survey of Canada, Paper 90-1E*, p. 171-182.

1991: Preliminary U-Pb dates and field observations from the eastern Coast Belt near 52°N, British Columbia; in *Current Research, Part A; Geological Survey of Canada, Paper 91-1A*, p. 79-84.

van der Heyden, P. and Metcalfe, S.

1992: Geology of the Piltz Peak plutonic complex, northwestern Churn Creek map area, British Columbia; in *Current Research, Part A; Geological Survey of Canada, Paper 92-1A*.

Geological Survey of Canada Project 890039

Late Permian U-Pb dates for the Farwell and Northern Mt. Lytton plutonic bodies, Intermontane Belt, British Columbia

Richard M. Friedman¹ and Peter van der Heyden
Cordilleran Division, Vancouver

Friedman, R.M. and van der Heyden, P., 1992: Late Permian U-Pb dates for the Farwell and Northern Mt. Lytton plutonic bodies, Intermontane Belt, British Columbia; *in* Current Research, Part A; Geological Survey of Canada, Paper 92-1A, p. 137-144.

Abstract

The Farwell and Northern Mt. Lytton plutons, located in the southern Intermontane Belt of British Columbia, have yielded U-Pb zircon dates of 258 ± 5 Ma and 250 ± 5 Ma, respectively. They lie on opposite sides of, and are both cut by the Fraser Fault system. Restoration of a minimum of 135 km, to a maximum of 160 km of dextral offset along this system brings these bodies into coincidence. These dates document Late Permian magmatic activity in the southern Intermontane Belt of British Columbia.

Résumé

Les datations U/Pb sur le zircon, du pluton de Farwell et du pluton de Mt. Lytton Nord, situés dans la zone sud Intermontagneuse de la Colombie-Britannique, ont indiqué respectivement un âge correspondant à 258 ± 5 Ma et à 250 ± 5 Ma. Ces plutons se trouvent de part et d'autre du champ de failles du Fraser et sont tous deux recoupés par ce champ. On peut faire coïncider ces deux corps ignés, par compensation de 135 km au minimum et de 160 km au maximum du rejet dextre. Ces datations permettent de détailler l'activité magmatique de la zone Intermontagneuse sud de la Colombie-Britannique au Permien supérieur.

¹ Department of Geological Sciences, University of British Columbia, 6339 Stores Road, Vancouver, B.C. V6T 2B4

INTRODUCTION

In this paper we report U-Pb dates for two plutons from the Intermontane Belt of British Columbia, in an area where structural complexities are only now coming to light (Read, 1992). These dates were previously cited by Friedman and Armstrong (1989) and Monger (1989; Northern Mt. Lytton). Some of the possible tectonic implications of these data are also explored.

GEOLOGY

The Farwell and Northern Mt. Lytton plutons are located in the southwestern Intermontane Belt of British Columbia (Fig. 1). They occur on opposite sides of, and are both cut by the Fraser dextral strike-slip fault system. The dated portions of these two intrusions are separated by a distance of 135-160 km. The Farwell Pluton is spatially associated with rocks of the Cache Creek Terrane and the southern extension of Stikinia (Hickson et al., 1991).

EXPLANATION

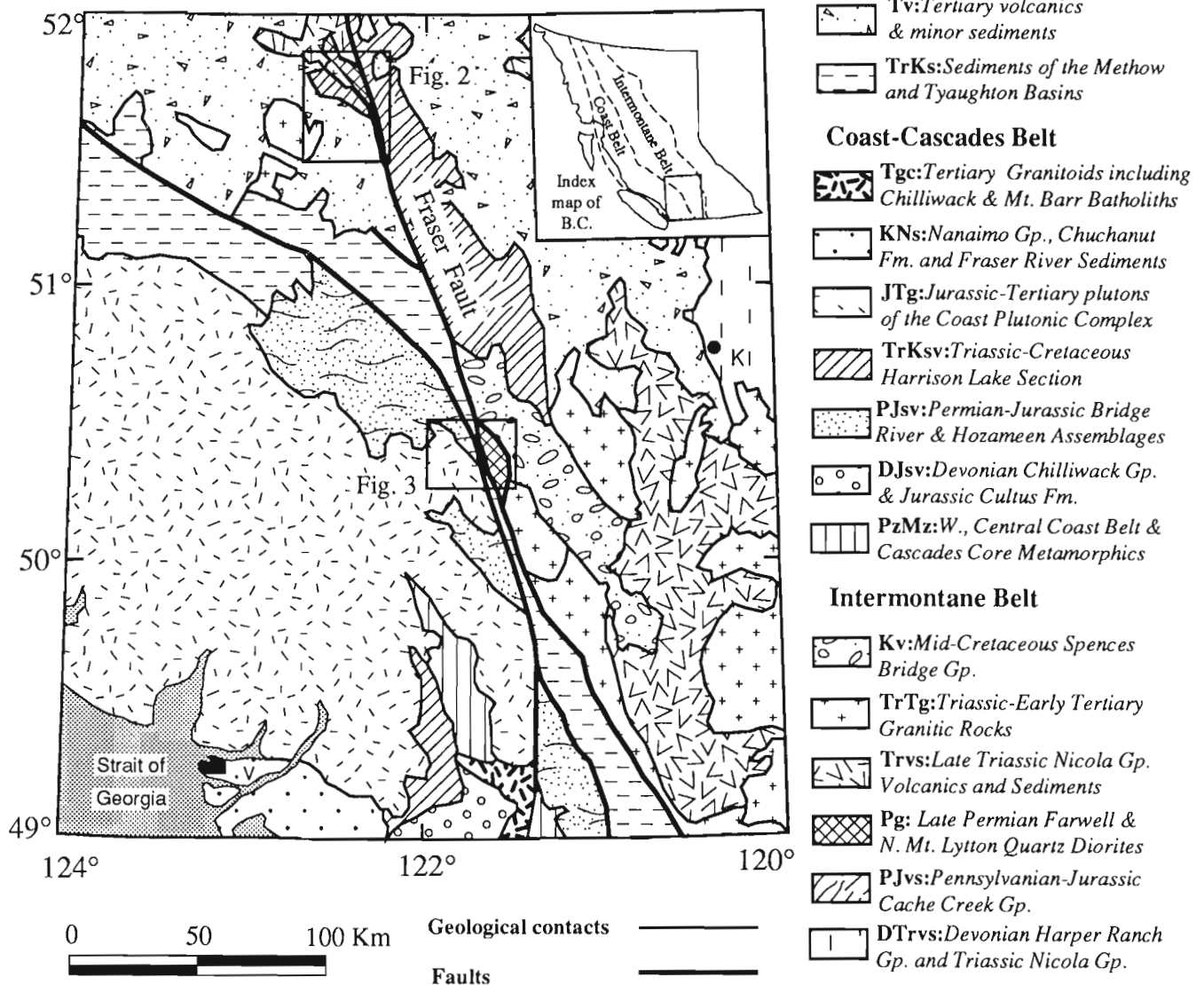


Figure 1. Generalized geological map in the vicinity of the Coast Belt-Intermontane Belt boundary, southwestern British Columbia; K: Kamloops; V: Vancouver.

The Northern Mt. Lytton Pluton is part of a fault-bounded composite body that makes up the northernmost portion of the Mt. Lytton Complex, an assemblage of gneissic and plutonic rocks correlated with Quesnellia (Monger, 1989; Parrish and Monger, in press).

Farwell Pluton

The Farwell Pluton is a massive to locally foliated, quartz diorite to granodiorite body exposed largely in Farwell Canyon of the Chilcotin River. It is cut by the Fraser Fault along its eastern margin (Fig. 2; Tipper, 1978). Recent

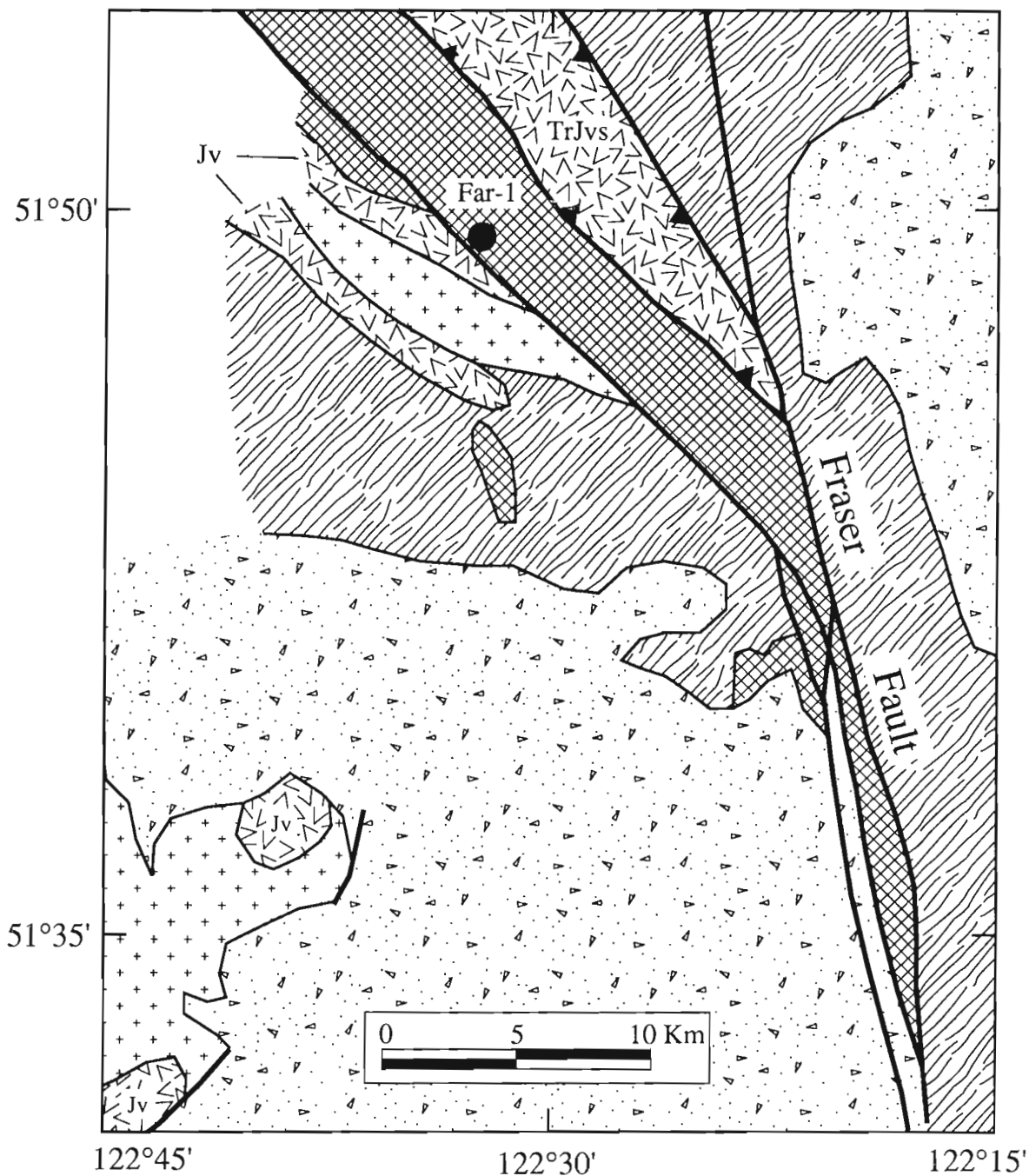


Figure 2. Geological map of the Farwell Pluton area, modified from Tipper (1978), Hickson et al. (1991), and Read (1992). See key on Figure 1 for patterns and symbols. Random v's: TrJvs - probable Upper Triassic and/or Lower Jurassic volcanics; Jv - Jurassic volcanics tentatively correlated with the Hazelton Group.

mapping has revealed that the Farwell Pluton was imbricated along thrust faults (Read, 1992; shown schematically on Fig. 2), and later affected by steep strike-slip (Fraser system) and normal faults (Hickson et al., 1991). This intrusion is spatially associated with rocks of the Cache Creek Group, as well as Upper Triassic and Lower Jurassic volcanic rocks (the latter are probable Hazelton Group equivalents). The dated portion of the pluton appears to be fault bounded (Fig. 2), so that its original relationship to these units remains unclear. However, a panel of the rock in the south, interpreted as part of the Farwell Pluton, and a petrographically similar stock, both intrude and metamorphose rocks of the Cache Creek Group (Fig. 2; Hickson et al., 1991).

The dated sample, (Far-1, Fig. 2) is a nonfoliated, coarse grained biotite-hornblende quartz monzodiorite. It contains saussuritized plagioclase, biotite (largely altered to chlorite),

poikilitic hornblende, quartz with undulose extinction, and K-feldspar. Epidote-rich veins up to about 5 mm in width, and associated 5 mm wide envelopes of brecciated granitic host are common at the sample locality. Dark, rounded, fine grained, centimetre-scale xenoliths also occur at the collection site. These were carefully removed from the sample prior to crushing.

Northern Mt. Lytton Pluton

The Northern Mt. Lytton Pluton is a fault-bounded, locally foliated diorite to granodiorite body, that comprises most of the northern portion of the Mt. Lytton Complex (Monger, 1989). It is associated with quartzofeldspathic and mafic mylonitic gneiss. The Northern Mt. Lytton structural panel is cut to the west by the Fraser system, and by normal faults

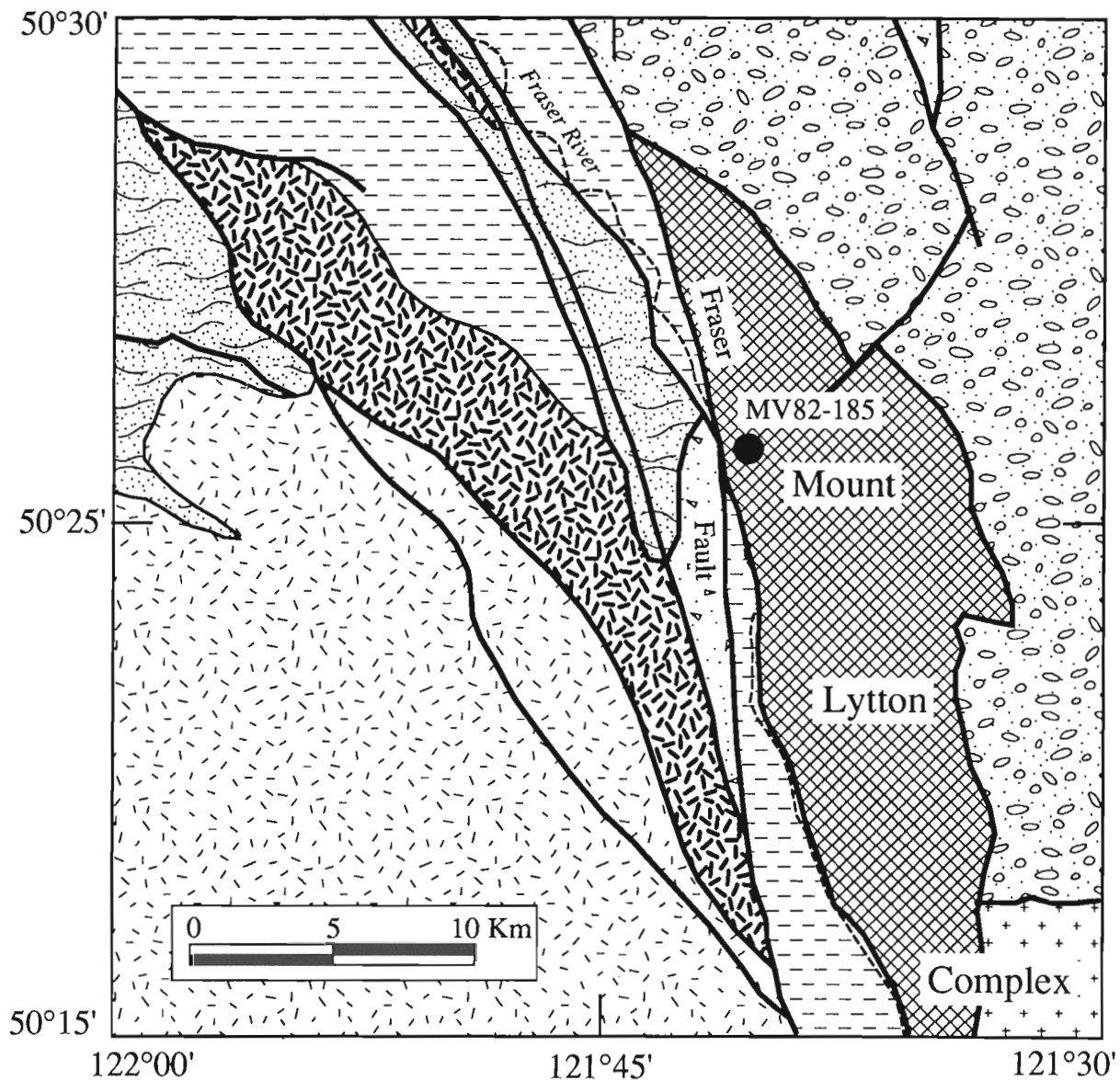


Figure 3. Geological map of the Northern Mt. Lytton Pluton area, modified from Monger (1989). Patterns and symbols as on Figure 1.

along its eastern margin, adjacent to mid-Cretaceous Spences Bridge Group rocks (Fig. 3). The Mt. Lytton Complex has been interpreted by Monger (1989) as roots of the Late Triassic Nicola arc of Quesnellia. A U-Pb zircon date of 225 Ma (by R.R. Parrish, reported in Monger, 1989) was determined for an orthogneiss sample positioned just off the edge of Figure 3, about 5 km east of the Northern Mt. Lytton Block. To the south, the Mt. Lytton Complex merges with the largely Late Jurassic Eagle Plutonic Complex, which was deformed together with adjacent structurally underlying meta-Nicola Group rocks during Late Jurassic and Early Cretaceous time (Greig, 1989).

Sample MV82-185 (Fig. 3) is a massive, altered, coarse grained tonalite, composed of saussuritized plagioclase, quartz with undulose extinction, and minor K-feldspar. Mineral masses made up of mostly chlorite and epidote are all that remain of mafic phase(s), interpreted as originally being hornblende. Xenoliths similar to those described in sample Far-1 of the Farwell Pluton are also common at this collection locality.

U-Pb GEOCHRONOLOGY

U-Pb data for samples from the Farwell and Northern Mt. Lytton plutons are plotted on concordia diagrams (Fig. 4, 5) and listed in Table 1. Three analyses for the latter sample were carried out during a seven year interval, a time in which U-Pb procedures at the University of British Geochronology Laboratory evolved significantly. The various permutations of sample preparation and analytical procedures are briefly outlined in Appendix 1.

Farwell Pluton

Three fractions of zircons from sample Far-1, separated on the basis of size and magnetic properties, were analyzed from the single population of clear to pale amber "football-shaped" (1:w=1:1.2-1:2.2) crystals. The error ellipse associated with the coarse, abraded fraction (Fig. 4, 1a) slightly overlaps the

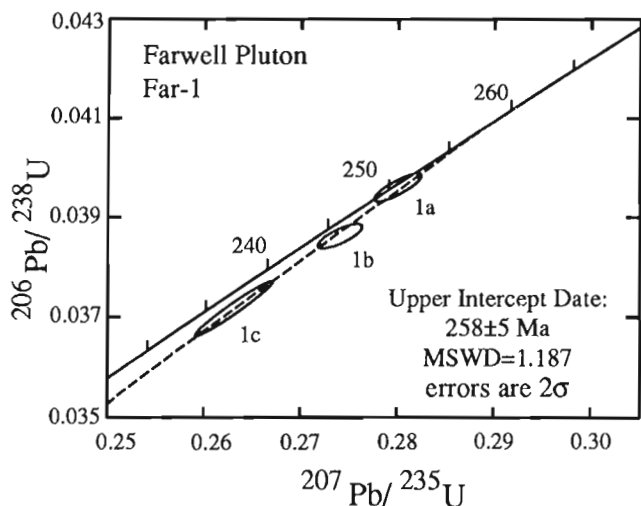


Figure 4. Concordia diagram for sample Far-1 of the Farwell Pluton.

concordia curve at about 250 Ma. The other two (1b and 1c) are situated below concordia in an arrangement suggestive of modern Pb-loss (Fig. 4). A chord fit to the data and 0 Ma gives an upper intercept of 258 ± 5 Ma (2% errors), interpreted as a reasonable age estimate for this rock. A "free-floating" chord gives virtually the same upper intercept with a somewhat larger error envelope. We feel that fitting the discordia line through 0 Ma is justified in this case because it does not change the upper intercept. Furthermore, there is little extrapolation required between the most concordant fraction (1a) and the point of intersection with concordia.

Northern Mt. Lytton Pluton

Three fractions of zircon were analyzed from the single population of transparent, pale pink, doubly terminated crystals (1:w=1:1.5-1:2.5) separated from sample MV82-185. Split 2a (analyzed in 1983) was a massive (about 30 mg), bulk fraction from which impurities were handpicked. The other two, 2b and 2c (done in 1990 and 1985, respectively), both come from a relatively coarse, nonmagnetic split (Table 1), the former being moderately abraded. The distribution of data (Fig. 5) suggest that Pb-loss has taken place, but fraction 2a appears to be largely unaffected as it lies directly on concordia at 250 Ma. A chord fit to the data has upper and lower intercepts of 252 and 137 Ma, respectively, with large errors. The position of this line is strongly controlled by fractions 2c and 2a. We interpret the U-Pb dates for fraction 2a, 250 ± 5 Ma as a reasonable estimate for the age of the Northern Mt. Lytton Pluton because this fraction is concordant and includes the upper intersection point of the regressed discordia line.

CORRELATION OF THE FARWELL AND MT. LYTTON PLUTONS

Interpreted dates for the petrographically similar Farwell (258 ± 5 Ma) and Northern Mt. Lytton (250 ± 5 Ma) plutons exhibit some age overlap, which allows for the suggestion that they were originally part of a single contiguous intrusion.

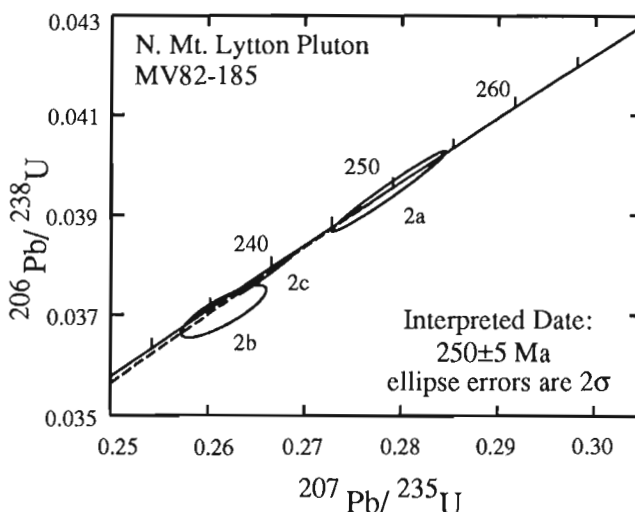


Figure 5. Concordia diagram for sample MV82-185 of the Northern Mt. Lytton Pluton.

Table 1. U-Pb Zircon Analytical Data

Analysis number	Fraction ^a	Wt. mg	U ppm	Pb ^b ppm	Measured 206Pb/204Pb, (Blank Pb, pg) ^c	Pb Isotopic abundance ^d , 206=100 207 208	Isotopic ratios and Dates, (Ma) ^e				
							206Pb/238U	207Pb/235U	207Pb/206Pb		
<i>Farwell Canyon: FAR-1: Lat/Long 51°49.5'N, 122°33.7'W</i>											
1a, -149+74µm, N5°/0.5A		1.6	161	6.6	5039 (100)	0.0038	5.1857	14.2525	0.03959±24 (250.3±1.4)	0.28001±212 (250.7±1.6)	0.05130±20 (254.3±9.2)
2a, -74+44µm, N1°/1A, M0.5°/2A		0.8	262	10.1	2166 (150)	0.0160	5.3818	10.3837	0.03862±20 (244.3±1.2)	0.27410±200 (245.9±1.6)	0.05147±22 (262.0±9.8)
3a, -44µm, N5°/0.5A, M1°/1A		0.8	530	19.4	4999 (100)	0.0096	5.2748	8.8502	0.03717±46 (235.3±2.8)	0.26315±338 (237.2±2.8)	0.05135±14 (256.4±6.6)
<i>Northern Mt. Lytton: Lat/Long 50°75.'N, 121°40.38'W</i>											
2a, Bulk		29.2	440	16.8	11843 (800)	0.0032	5.1718	7.4723	0.03945±68 (249.4±4.3)	0.27873±493 (249.7±4.4)	0.05124±12 (251.8±5.3)
2b, -149+74µm N0.5°/2.0A, Abr		1.8	384	14.2	12820 (50)	0.0047	5.1753	8.5126	0.03782±34 (239.3±2.2)	0.26628±246 (239.7±2.0)	0.05107±4 (243.8±2.0)
2c, -149+74µm, N0.5°/2.0A		1.6	453	16.3	7109 (100)	0.0033	5.1708	7.5560	0.03705±42 (234.5±2.6)	0.26170±340 (236.1±2.8)	0.05123±40 (251.2±17.8)
^a Grain size in micrometres (µm). Magnetic (M) or nonmagnetic (N) when passed across Franz magnetic separator at specified side tilt in degrees, and field strength in Amperes (A); Abr = abraded. ^b Radiogenic and common Pb. ^c Blank estimate derived largely from ongoing total procedural blank analyses. ^d Radiogenic and common Pb, corrected for fractionation and blank Pb (see Appendix 1 for details). ^e Errors are quoted as 2 standard errors of the mean for all isotopic ratios and dates. Common Pb corrections were made assuming the following composition from Stacey and Kramers (1975): 204:206:207:208 = 1:18.318:15.609:38.172 (250 Ma).											

Both bodies are cut by, and lie on opposite sides of the Fraser Fault system, and are separated by a distance of 135-160 km (Fig. 1). Published estimates for dextral offset along the Fraser Fault system include 80-100 km (Monger, 1989), 120 km (Okulitch et al., 1977), 160 km (Anderson, 1977), and 190 km (Misch, 1977). It should be noted that Farwell-Northern Mt. Lytton separation may not be a direct measure of strike-slip motion along the Fraser Fault because the former body occurs in shallowly-dipping, folded thrust slices, and some dip-slip motion has been documented along the Fraser Fault in this vicinity (Mathews and Rouse, 1984).

TECTONIC IMPLICATIONS

We have documented Late Permian (ca. 250-260 Ma) magmatic activity in the southern Intermontane Belt of British Columbia. Major mineralogic characteristics of the Farwell and Mt. Lytton plutons suggest that they are the products of arc magmatism. Although structural complexities and uncertain terrane affinities of the dated bodies preclude speculations on their detailed tectonic significance, some general comments are offered. If, as tentatively suggested by Hickson et al. (1991), Permian granite of the Farwell Pluton intrudes the Cache Creek Terrane, it provides evidence that this assemblage is not purely oceanic in nature, a previously held, reasonable view (Monger, 1989). Furthermore, if a Farwell-Mt. Lytton correlation proves to be valid, it would provide a Late Permian tie between Quesnellia and the Cache Creek Terrane. Further speculation will await continued detailed and regional mapping of the area.

REFERENCES

- Anderson, P.**
1977: Timing of Mesozoic plate tectonics in southwestern British Columbia (abstract); Geological Association of Canada, Program with Abstracts, v. 2, p. 4.
- Friedman, R.M. and Armstrong, R.L.**
1989: U-Pb dating of Permian, Jurassic, and Eocene granitic rocks between the Coast Plutonic Complex and Fraser-Pinchi Fault System (abstract); Geological Society of America, Abstracts with Programs, v. 21, no. 5, p. 81.
- Greig, C.J.**
1989: Geology and geochronometry of the Eagle Plutonic Complex, Coquihalla area, southwestern British Columbia; M.Sc. thesis, University of British Columbia, Vancouver, 423 p.
- Hickson, C.J., Read, P., Mathews, W.H., Hunt, J.A., Johansson, G., and Rouse, G.E.**
1991: Revised geological mapping of the northeastern Taseko Lakes map area, British Columbia: in Current Research, Part A; Geological Survey of Canada, Paper 91-1A, p. 207-217.
- Krogh, T.E.**
1973: A low-contamination method for hydrothermal decomposition of zircon and extraction of U and Pb for isotopic age determination; Geochimica Cosmochimica Acta, v. 37, p. 485-494.
1982: Improved accuracy of U-Pb ages by the creation of more concordant systems using an air abrasion technique; Geochimica Cosmochimica Acta, v. 46, p. 637-649.
- Ludwig, K.R.**
1980: Calculation of uncertainties of U-Pb isotope data; Earth and Planetary Science Letters, v. 46, p. 212-220.
1983: Plotting and regression programs for isotope geochemists, for use with HP-86/87 microcomputers; United States Geological Survey, Open File Report 83-0849, 102 p.
- Mathews, W.H. and Rouse, G.E.**
1984: The Gang Ranch-Big Bar area, south-central British Columbia: stratigraphy, geochronology, and palynology of the Tertiary beds and relationship to the Fraser Fault; Canadian Journal of Earth Sciences, v. 21, p. 1132-1144.

Misch, P.

1977: Dextral displacements at some major strike faults in the Northern Cascades (abstract); Geological Association of Canada Annual Meeting, Abstracts with Programs, v. 2, p. 37.

Monger, J.W.H.

1989: Geology of Hope and Ashcroft map areas, British Columbia; Geological Survey of Canada, Maps 41-1989 and 42-1989.

Okulitch, A.V., Price, R.A., and Richards, T.A.

1977: A guide to the geology of the southern Canadian Cordillera; Geological Association of Canada, Mineralogical Association of Canada, Society of Economic Geologists, Field Trip Guidebook 8, 135 p.

Parrish, R.R.

1987: An improved micro-capsule for zircon dissolution in U-Pb geochronology; *Isotope Geoscience*, v. 66, p. 99-102.

Parrish, R.R. and Krogh, T.E.

1987: Synthesis and purification of ^{205}Pb for U-Pb geochronology; *Isotope Geoscience*, v. 66, p. 111-121.

Parrish, R.R. and Monger, J.W.H.

in press: New U-Pb dates from southwestern British Columbia; in *Radiogenic Age and Isotope studies*, Report 5, Geological Survey of Canada, Paper 91-2.

Parrish, R.R., Roddick, J.C., Loveridge, W.D., and Sullivan, R.W.

1987: Uranium-Lead analytical techniques at the geochronology laboratory; Geological Survey of Canada, Paper 87-2, p. 3-7.

Read, P.B.

1992: Geology of parts of Riske Creek and Alkali Lake areas, British Columbia; in *Current Research, Part A*; Geological Survey of Canada, Paper 92-1A.

Stacey, J.S. and Kramers, J.D.

1975: Approximation of terrestrial lead isotope evolution by a two-stage model; *Earth and Planetary Science Letters*, v. 26, p. 207-221.

Tipper, H.W.

1978: Taseko Lakes (920) map-area; Geological Survey of Canada, Open File 534.

York, D.

1969: Least squares fitting of a straight line with correlated errors; *Earth and Planetary Science Letters*, v. 5, p. 320-324.

APPENDIX 1

Uranium-lead analytical procedures

Sample preparation

Zircons were separated from 30-40 kg samples using standard crushing, Wilfley table and heavy liquid extraction techniques (e.g., Parrish et al., 1987). Zircons were then split into specific fractions based on size, shape, magnetic susceptibility, and physical attributes such as color and clarity of individual crystals. All fractions were air abraded using techniques similar to those of Krogh (1982). Prior to dissolution all zircon fractions were leached in warm 3N HNO₃ for 25 minutes followed by rinsing in high-purity H₂O and acetone.

Uranium-lead methods

Sample dissolution and chemical analyses were carried out with a procedure modified from Krogh (1973) and Parrish (1987). Uranium and lead concentrations for fractions from Far-1 and 2b from MV82-185 (1990 analyses) were determined with a mixed ²⁰⁵Pb/²³⁵U spike (Parrish and Krogh, 1987); a mixed ²⁰⁸Pb/²³⁵U spike was used for 2a and 2c of the latter sample (1984-1985 analyses). All analyses were carried out using a Vacuum-Generators Isomass 54R solid source mass spectrometer in single collector mode. A

Daly multiplier detector was used for all 1990 analyses except for split 2b (Pb, Faraday collector). The Faraday collector was used for all earlier analyses. Faraday runs were corrected for 0.12% (Pb) and 0.06% (U) per amu mass fractionation and Daly runs 0.55% (Pb) and 0.45% (U) per amu relative to National Bureau of Standards SRM981 lead and U500 uranium standards. A nonradiogenic lead correction was made by first subtracting analytical blank lead with the isotopic composition 204:206:207:208 = 1.00:17.7515.50:37.30 (1990 analyses), 1.00:17.75:15.57:37.30 (fraction 2c, 1985), and 1.00:17.75:15.57:37.00 (fraction 2a, 1983). Common lead compositions were estimated using the model of Stacey and Kramers (1975), (see footnotes of Table 1 for common lead isotopic compositions). The magnitude of the common lead correction for each fraction was proportional to the remaining ²⁰⁴Pb after the blank correction.

Precisions for isotopic ratios and calculated dates were determined by numerical error propagation. Error ellipses are plotted as two standard errors of the mean. Uranium-lead concordia plots were generated using a program modified from Ludwig (1983). Intercept dates were calculated using techniques of York (1969) and the algorithm of Ludwig (1980).

Fieldwork in the Oweege and Snowslide ranges and Kinskuch Lake area, northwestern British Columbia

C.J. Greig¹
Cordilleran Division, Vancouver

Greig, C.J., 1992: *Fieldwork in the Oweege and Snowslide ranges and Kinskuch Lake area, northwestern British Columbia*; in *Current Research, Part A*; Geological Survey of Canada, Paper 92-1A, p. 145-155.

Abstract

Skeena fold belt structural culminations along the west-central margin of the Bowser Basin expose Early Jurassic and older Stikine terrane basement. Basement rocks contain a record of Late Triassic to Early Jurassic deformation, uplift and erosion, expressed as a pronounced sub-Hazelton Group angular unconformity. Toarcian epiclastic rocks are the oldest cover rocks in the culminations, and mark the onset of Bowser Basin sedimentation. Toarcian strata and Spatsizi and Bowser Lake group rocks are conformable and record Jura-Cretaceous clastic sedimentation, including Late Jurassic slump folding.

Parasitic folds northeast of the structural culminations change in style away from the more competent basement rock. Fold trends in the cover are conformable around the margins of basement culminations, suggesting a genetic relation. Brittle reverse faults in the basement probably account for only a small portion of the structural shortening in the cover.

Résumé

Les culminations structurales de la zone de plissements de Skeena, sur la marge du centre ouest du bassin de Bowser, laissent affleurer le socle du terrane de Stikine qui date du Jurassique inférieur et de périodes plus anciennes. Les roches du socle témoignent d'épisodes de déformation, de soulèvement et d'érosion survenus du Trias supérieur au Jurassique inférieur, qui se traduisent par une discordance angulaire prononcée au-dessous du groupe de Hazelton. Les roches épicastiques du Toarcien sont les plus anciennes roches de couverture apparaissant dans les culminations, et marquent le commencement de la sédimentation dans le bassin de Bowser. Les strates du Toarcien et les roches des groupes de Spatsizi et de Bowser Lake sont concordantes et témoignent de la sédimentation clastique d'âge jurassique-crétacé, et également du plissement par glissement survenu au Jurassique supérieur.

Le style des plis parasites formés au nord-est des culminations structurales change à mesure que l'on s'éloigne des roches du socle plus compétentes. Dans la couverture, la direction générale des plis est concordante sur les marges des culminations du socle, ce qui semble indiquer une relation génétique. Les failles inverses fragiles qui traversent le socle ont probablement peu d'importance dans la fraction du raccourcissement structural de la couverture.

¹ Department of Geosciences, University of Arizona, Building #77, Tucson, Arizona 85721, U.S.A.

INTRODUCTION

Fieldwork in 1991 in the Oweege and Snowslide ranges and Kinskuch Lake area of northwestern British Columbia comprised the second season of a three season mapping program. The aim of the program is to map structural and stratigraphic relationships along the west-central margin of the Bowser Basin and thereby gain an improved understanding of the tectonic evolution of the region. An in depth discussion of the rationale for the program, and results of 1990 fieldwork, were given in Greig (1991a); results of a reconnaissance lithogeochemical study in the areas mapped in 1990 were presented in Greig (1991b); and speculations on the tectonic setting of the region were presented by Evenchick (1991a,b), Greig et al. (1991), and Ricketts and Evenchick (1991).

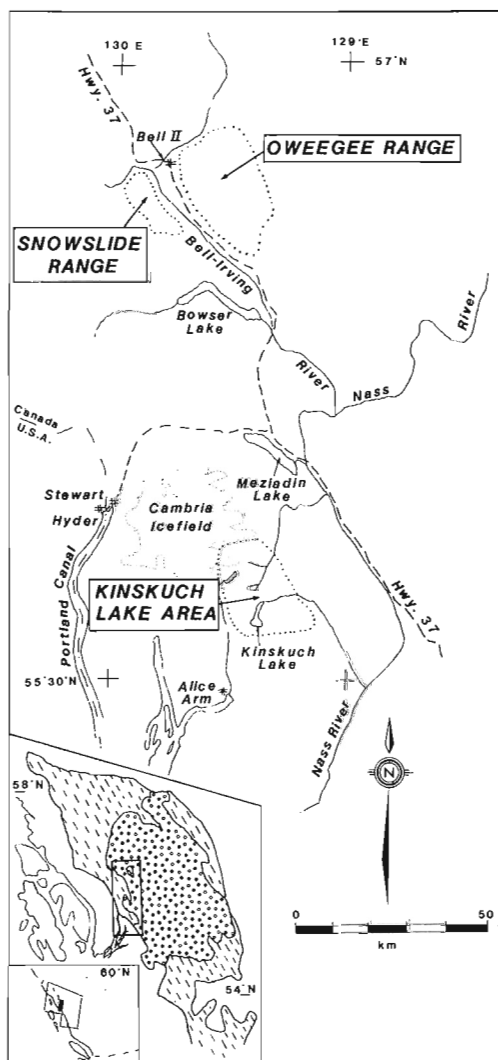


Figure 1. Location map of Oweege and Snowslide ranges and Kinskuch Lake area, northwestern British Columbia. Stippled pattern on insert map represents Bowser Basin strata; hachured pattern represents basement rocks of the Stikine terrane.

The Oweege and Snowslide ranges are located 100 km north-northeast of Stewart, B.C., near Bell II (Fig. 1). The Kinskuch Lake area is located 50 km southeast of Stewart. In both the Oweege and Kinskuch areas, "basement" rocks, which underlie the predominantly sedimentary rocks comprising the Bowser Basin fill or "cover", are exposed in structural culminations of the Skeena fold belt of Evenchick (1991a,b). Mapping in the first season focused mainly on defining the structural style of Skeena fold belt structures in the cover, and southwest vergent folds and faults were recognized in cover rocks on the northeast margins of the dome-like basement culminations (Greig, 1991a). Preliminary work in 1990 failed to identify geometrically compatible structures in the basement, therefore much of the 1991 fieldwork was spent mapping basement rocks. Geological features recognized during fieldwork in the Oweege and Kinskuch regions are described below. The focus is on relations between map units. Lithological description of units is minimized, except where new rock types were recognized or where descriptions are relevant to the discussion of map relations. More extensive lithological descriptions may be found in Greig (1991a).

OWEEGEE AND SNOWSLIDE RANGES

Stratigraphy

In northern Oweege dome, basement rock includes all pre-Bowser Basin Stikine terrane stratigraphy, from the Paleozoic Stikine assemblage through to Toarcian clastic rocks of the uppermost Hazelton Group (Fig. 2, 3). Primary stratigraphic relations were observed between all successive map units except between Permian and Devonian and older(?) rocks of the Stikine assemblage. Faults are common in the basement, but unconformities may play a more significant role in generating map pattern complexity.

Stikine assemblage

Devonian and older(?) volcanic rocks

Rocks in the northern Oweege dome assigned a pre-Permian age by Koch (1973) and Monger (1977), were interpreted by Greig (1991a) to be part of the Lower Jurassic Hazelton Group. A preliminary Devonian U-Pb zircon date was recently obtained by the author from rhyodacite flow-breccia located approximately 3 km north of Oweege Peak, confirming the original age assignment of Koch (1973). Further mapping indicated that tuffaceous Hazelton Group rocks, together with locally abundant boulder and cobble conglomerate (Fig. 4), overlie the Devonian and older(?) rocks along a steeply east-northeast dipping unconformity. Immediately southwest, the Devonian and older(?) rocks structurally overlie Permian limestone and clastic rocks of the Upper Triassic Stuhini Group along a steeply northeast dipping reverse fault. West of Skowill Creek, the Devonian and older(?) rocks form the core of a recumbent fold first recognized by Koch (1973). The fold is interpreted to occur in the hanging wall of a genetically-related(?) reverse fault (Fig. 3).

Devonian and older(?) rocks consist primarily of coarse, feldspar phyric pyroclastic rocks and lesser flows of intermediate(?) to felsic composition; associated epiclastic rocks are less common. They can be distinguished from lithologically similar Hazelton Group rocks by their more pervasive brittle fracture and chlorite alteration overprint, as well as by stratigraphic position. Devonian and older(?) rocks also appear to be more highly fractured and altered than the Permian or Triassic rocks.

Permian limestone

The contact between Permian limestone and Devonian and older(?) rocks, where not demonstrably faulted, is presumed to be depositional. In most places, the contact between limestone and rocks of the Upper Triassic Stuhini Group is a reverse fault, with Stuhini Group rocks in the footwall (see Fig. 5 in Greig, 1991a).

Stuhini Group

Abundant tuffaceous siliciclastic and rare mafic volcanic rocks, chert, and limestone comprise the Upper Triassic Stuhini Group in the Oweege Range. A metre-scale limestone pod collected near the north margin of the Delta glacier yielded Upper Triassic (Carnian) conodonts (M.J. Orchard, written comm., 1991), confirming the Late Triassic age reported by Monger (1977). Stuhini Group rocks conformably overlie Permian limestone near the northeast margin of Oweege dome. There, Permian limestone is overlain by thinly interbedded chert and limestone and brown and dark green poorly sorted sandstone, pebble conglomerate, and mafic volcanic rocks. Siliciclastic rocks west of Skowill Creek, here assigned to the Stuhini Group, also appear conformable with Permian limestone, but the contact is not exposed.

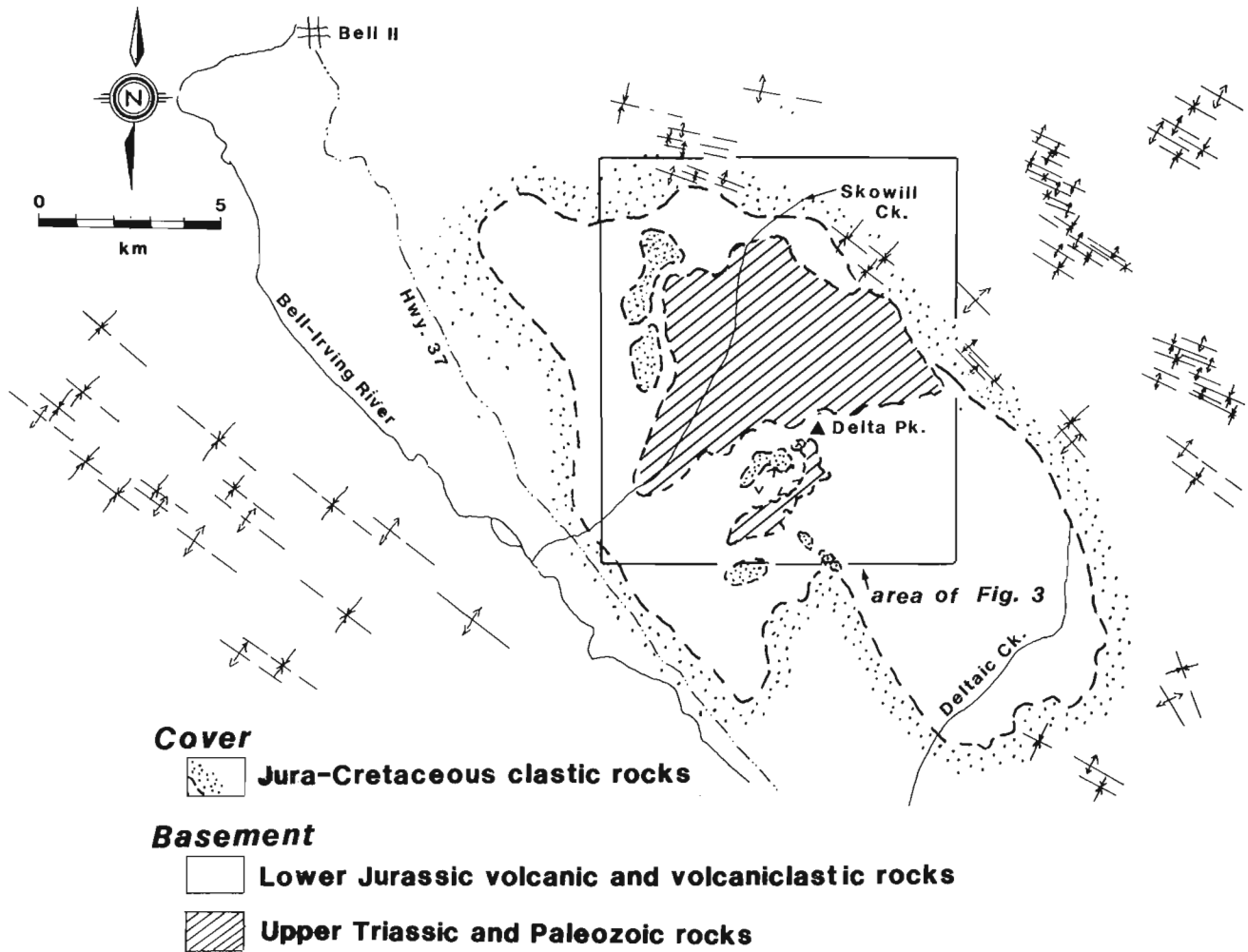


Figure 2. Distribution of basement and cover rocks, Oweege dome.

Hazelton Group

The Hazelton Group is the most extensive map unit in Oweegee dome, and it comprises the southern half of the dome. Rocks of the Hazelton Group sit with pronounced angular unconformity on deformed Upper Triassic, Permian and Devonian and older(?) rocks (Fig. 5), and are interpreted to have been deposited during uplift. Rocks directly overlying the "sub-Hazelton" unconformity include rocks stratigraphically high in the Hazelton Group, and even Toarcian rocks (see below) lie unconformably on pre-Hazelton Group rocks. This suggests that there was significant relief on the unconformity and/or that uplift was concurrent with and followed Hazelton Group deposition.

Significant differences in lithology and thickness occur within the Hazelton Group north and south of their contact with older basement rocks near Delta Peak. To the north, the Hazelton Group is generally considerably thinner (maximum thickness approximately 500 m) than to the south (approximately 1000 m). Polymict conglomerate (Fig. 4), in large part locally derived, is common at the base of the Hazelton Group north of Delta Peak. To the south, conglomerate is absent and monomict coarse pyroclastic

rocks or massive tuffaceous sandstone unconformably overlie Upper Triassic Stuhini Group rocks. In the northern part of the dome there is also a greater abundance of maroon (nonmarine and stratigraphically high?) relative to green (marine and stratigraphically low?) tuffaceous and volcanoclastic rocks. Abundant evidence for soft-sediment deformation within Hazelton Group rocks along the contact with the Stuhini Group near Delta Peak, supports the view that uplift occurred during Hazelton Group deposition. This contact can reasonably be interpreted as a syndepositional fault, as it is overlain to the east by the Middle Jurassic Spatsizi Group. The age of Hazelton Group rocks along this structure is constrained by Middle Sinemurian to Early Pliensbachian bivalves (T.P. Poulton, written comm., 1991) collected near the toe of Delta glacier.

In the Hazelton Group in the southern dome, discordances in the thick tuffaceous volcanic and sedimentary section are common. Volcanic rocks are typically feldspar-rich and in general, individual volcanic units thin toward the top of the section. Dacite and rhyolite appear to be restricted to the upper parts of the section; mafic pyroclastic rocks and rare flows occur throughout the section. The angular discordances, as well as smaller scale evidence for

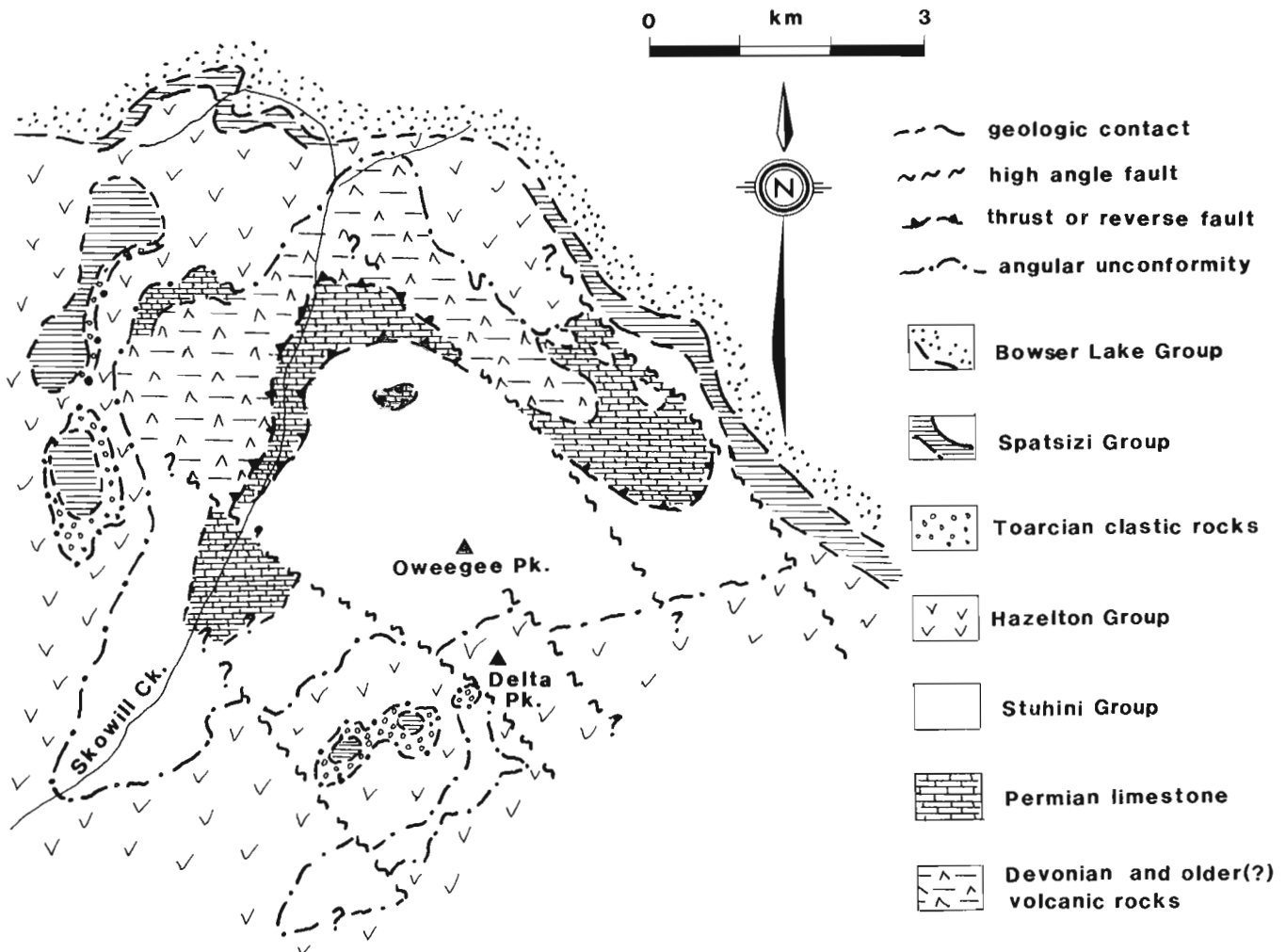


Figure 3. Generalized geology, northern Oweegee Range.

downcutting along the bases of individual tuffaceous units, suggests deposition as ash flows and, where rocks contain a muddy matrix, as debris flows.

Toarcian sandstone and conglomerate

Fossiliferous, dark brown, limy, coarse grained sandstone and local conglomerate is exposed in several places west of Skowill Creek and west-southwest of Delta Peak. A diverse assemblage of marine fossils common to this unit includes belemnites and the coarse-ribbed bivalve *Weyla*, indicating a Toarcian age (T.P. Poulton, written comm., 1991). An angular discordance is present at the base of this unit, but it is typically less than 15°. With one important exception, the Toarcian sandstone rests unconformably on the upper parts of the Hazelton Group. The exception is limy sandstone immediately west-southwest of Delta Peak, which overlies siliceous sandstone and siltstone of the Stuhini Group. While this relationship may be taken to suggest considerable post-Hazelton Group uplift, nearby beds to the west overlie rocks of the uppermost Hazelton Group with very little stratigraphic discordance, and with little evidence of significant relief on the sub-Toarcian unconformity. In addition, the pre-Toarcian rocks of the upper Hazelton Group at this place overlie Stuhini Group rocks unconformably, and nearby, the sub-Toarcian and sub-Hazelton unconformities merge. This is interpreted to represent progressive onlap of Hazelton Group rocks on the basal unconformity, followed by renewed uplift prior to Toarcian time.

Spatsizi and Bowser Lake groups

The Spatsizi and Bowser Lake groups, and perhaps also the Toarcian sandstone, constitute the sedimentary cover to Early Jurassic and older basement of Oweege dome. The clastic succession represents the initiation of widespread sedimentation and its predominance over volcanism in this area.

The Spatsizi Group is a thin but continuous and distinctive unit of thin-bedded siliceous siltstone and dust tuff(?) near the base of the cover succession on all sides of Oweege dome. The Spatsizi Group-Toarcian sandstone contact is everywhere covered, but their spatial association, the occurrence of limy sandstone in both, and a lack of evidence within the Spatsizi Group for an erosive lower contact suggest that they are conformable and probably gradational.

A gradational contact between the Spatsizi and Bowser Lake groups is well exposed on the eastern margin of Oweege dome. The proportion of sandstone and the thickness of individual siltstone and sandstone beds increase upsection through the contact zone, while the abundance of pale green-grey, clay-rich dust tuff(?) layers and the silica content of siltstones decrease.

Fossils collected in 1990 and identified by T.P. Poulton of the Geological Survey of Canada suggest an Oxfordian to Tithonian(?) age for the "turbidite" and "siltstone" facies and a possible Cretaceous age for the "shallow marine" facies of Greig (1991a).



Figure 4. Poorly sorted boulder conglomerate with angular Permian limestone clasts, base of Hazelton Group, 3 km north of Oweege Peak.



Figure 5. Angular unconformity between Hazelton (upper half of photo) and Stuhini groups, south-southwest of Delta Peak.

Bowser Lake Group rocks west of Oweegee dome in the central and southern Snowslide Range consist almost exclusively of alternating medium to thin bedded turbidite sandstone and siltstone. Based on the presence of Oxfordian ammonites in the central part of the Snowslide Range (Grove, 1986), and on the southerly structural plunge in the range, the lower part of the turbidite succession is in part Oxfordian or older. Stratigraphically above the fossil localities are several remarkable horizons of soft-sediment slump folds which are bound above and below by undeformed planar-bedded turbidite sandstone and siltstone (Fig. 6). The slump fold horizons have themselves been folded and can be traced from the southern to the central Snowslide Range, a distance of approximately 8 km. No obvious correlation exists between the slump-folded horizons west of Oweegee dome and Bowser Lake Group rocks east of the dome, although isolated slump folds and several discordances of uncertain origin were noted in the "siltstone" facies of Greig (1991a).

Structure

A full discussion of the structural geology of the Oweegee and Snowslide ranges awaits the compilation and interpretation of structural data, but a number of generalizations can be made. Several lines of evidence suggest that Oweegee dome is a structural culmination which acquired its present form during the development of the Skeena fold belt of Evenchick (1991a,b). Broad arching across the dome of the Bowser Lake and Spatsizi groups, of the less well-preserved Toarcian clastic rocks, and, in the northern dome, of the sub-Hazelton unconformity, suggests that formation of the dome was structural in nature and postdated deposition of the Jura-Cretaceous Bowser Lake Group. Within the Bowser Lake Group folds west of the dome verge to the northeast, whereas those along the north and northeast margins of the dome verge to the south-southwest and southwest, respectively. Bowser Lake Group rocks nearest the dome, in particular along the northern

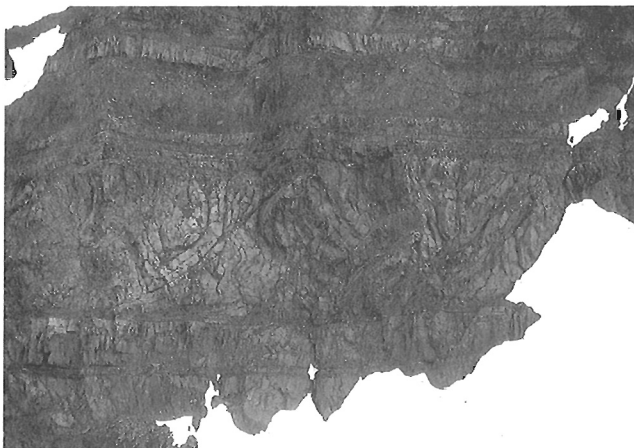


Figure 6. Disharmonic slump folds (central layer) in Bowser Lake Group turbidites, southern Snowslide Range; cliff is approximately 75 m high.

and eastern margins, are more tightly folded (Fig. 7), more disrupted by faults, and possess a more pronounced cleavage than those to the northeast or southwest, away from the dome.

Evidence for folding in the Hazelton Group is rare and common primary stratigraphic discordances complicate their recognition. However, relatively well-layered tuffaceous rocks in upper parts of the section, particularly in the southeast part of the dome, appear to have been folded along north-northwest trending fold axes.

North-northwest trending high angle faults within Oweegee dome may be a partial expression of Skeena fold belt shortening in the basement. Highly fractured and altered rocks and, locally, well-developed topographic lineaments, mark the faults. Most are west-side-up reverse faults, and may be correlative with high angle west-side-up reverse faults in the Bowser Lake Group near the eastern margin of Oweegee dome. In the Bowser Lake Group, the faults disrupt tight southwest vergent folds and have typical displacements of less than 10 m. The faults may reflect northeast directed shortening associated in the Skeena fold belt.



Figure 7. Tight south-southwest vergent folds and related faults in Bowser Lake Group rocks, north margin of Oweegee dome; hillside with folds approximately 200 m high.

Within the older basement rocks of Oweege dome there is good evidence for a major contractional event which predates the development of the Skeena fold belt. North dipping reverse faults juxtapose Devonian and older(?) rocks with Permian limestone and Stuhini Group siliciclastic rocks.

The faults do not involve the Hazelton Group, which sits with pronounced angular unconformity on the older rocks. These relations indicate that faulting occurred between Carnian and Middle Sinemurian to Early Pliensbachian time.

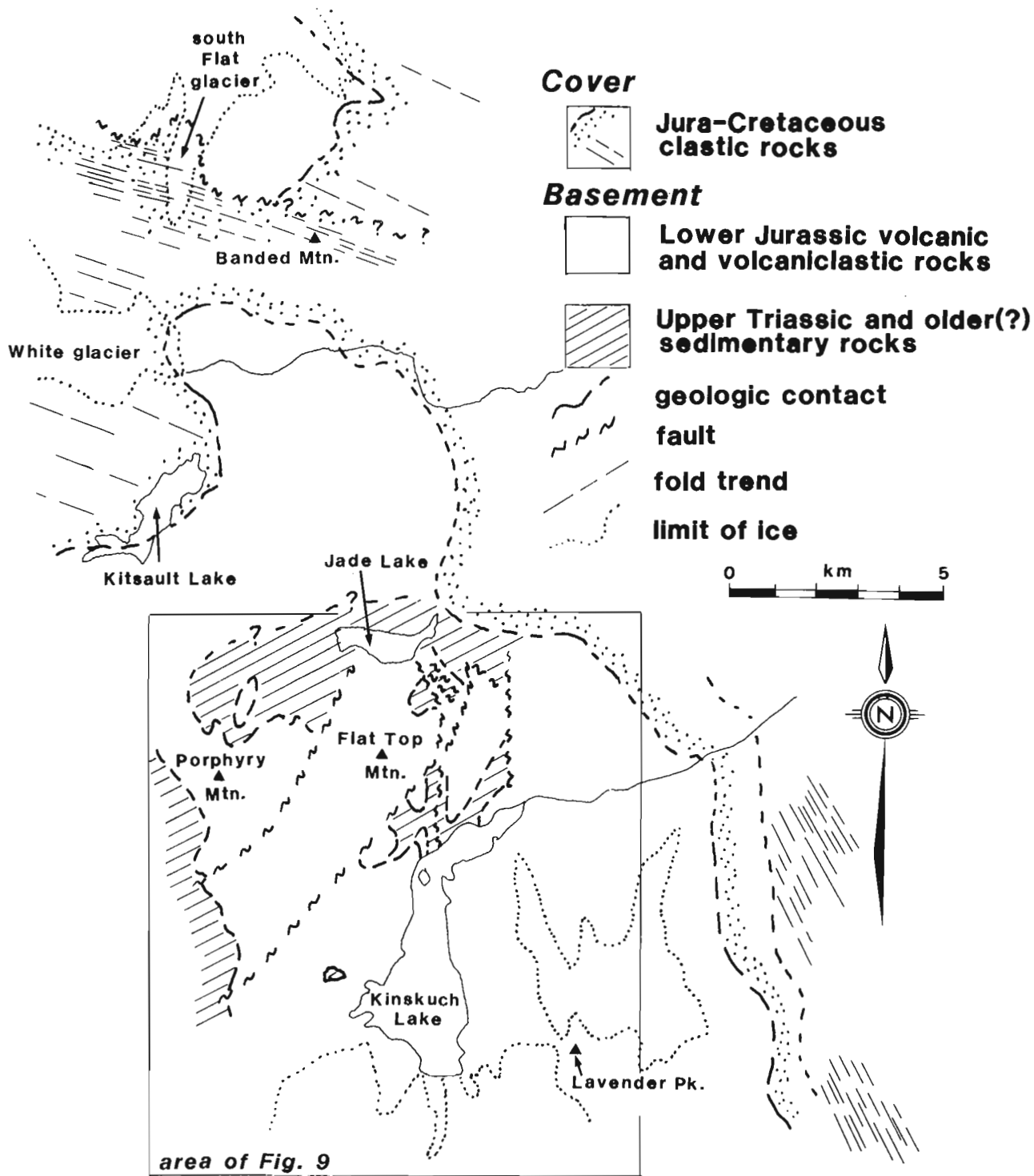
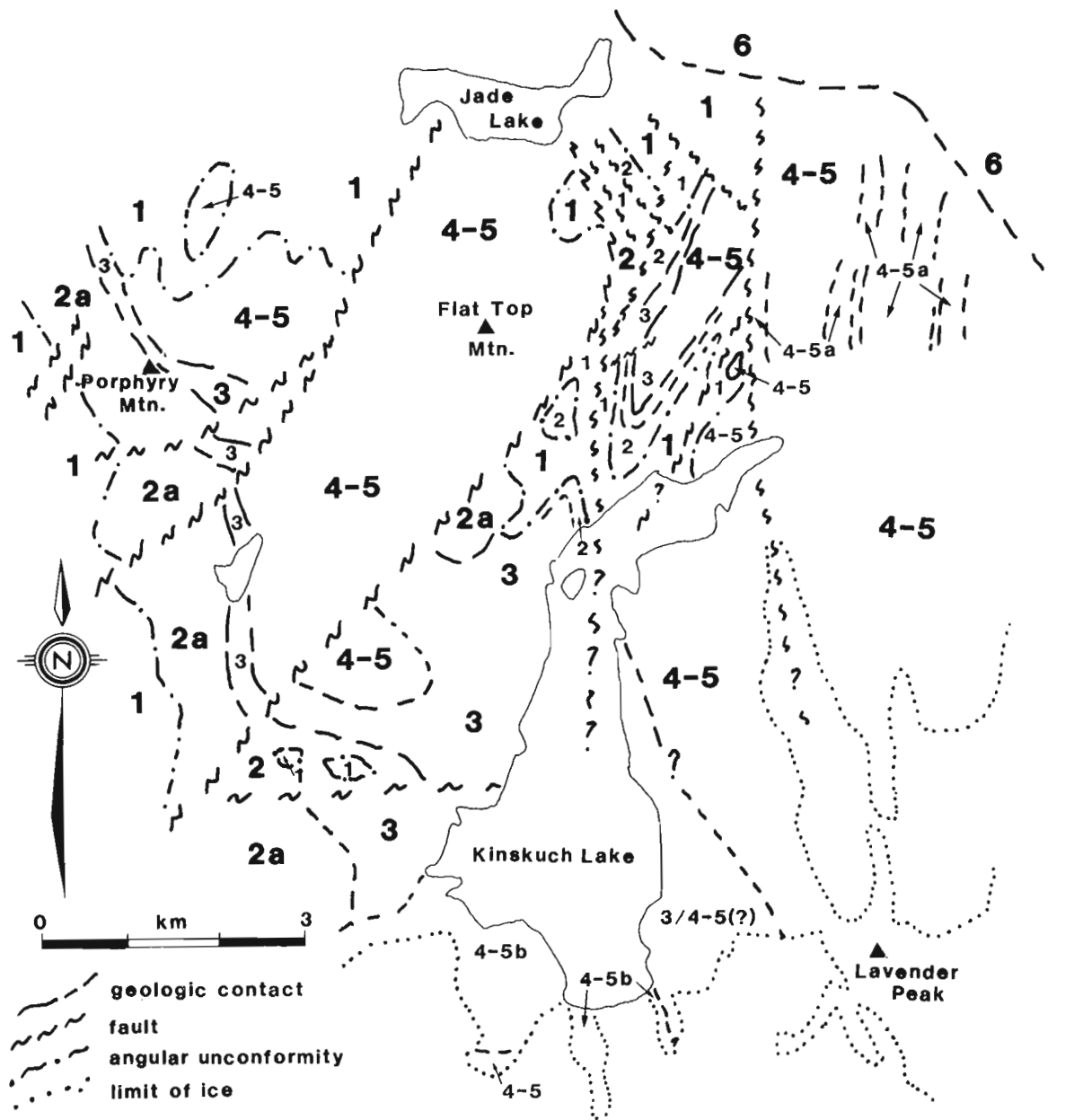


Figure 8. Distribution of basement and cover rocks, Kinskuch Lake area.



Salmon River Formation

6 clastic rocks

Hazelton Group

4-5 intermediate to felsic volcanic rocks;
megacrystic feldspar porphyry flows (4-5a)
high-level intrusive rocks (4-5b)

3 limy clastic rocks

2 mafic volcanic(2a) and volcanoclastic rocks, limestone

Stuhini Group

1 fine-grained black clastic rocks,
radiolarian chert

Figure 9. Generalized geology in the vicinity of Kinskuch Lake.

KINSKUCH LAKE AREA

Stratigraphy

Preliminary work in 1990 near Kinskuch Lake suggested that map units along the west side of the study area were repeated by faults and folds near the north end of the lake, and that these structures may have accommodated some of the southwest-directed shortening observed in overlying Bowser Lake Group rocks to the east (Greig, 1991a). Current mapping (Fig. 8, 9) confirmed these suggestions and revealed several other significant features: 1) Late Triassic or older bedded radiolarian cherts within the lowermost map unit (unit 1); 2) an unconformity between deformed unit 1 rocks and overlying rocks of the Hazelton Group (units 2-5); and 3) important facies changes within the Hazelton Group. Microfossil work on samples collected in 1990 revealed that the assignment of at least part of unit 1 to the Upper Triassic Stuhini Group was correct (see below). However, units 2 and 3, which were also assigned a Late Triassic age, are now interpreted to be the lowermost parts of the Lower and Middle Jurassic Hazelton Group. Units 4 and 5 are probable facies equivalents, and in their lower- and uppermost parts may be age-equivalent with parts of units 3 and 6, respectively.

Stuhini Group

Unit 1: Late Triassic and older(?) fine grained clastic rocks

Along the west margin of the study area, unit 1 is characterized by folded and faulted, thin bedded siltstone and fine grained sandstone (Greig, 1991a). Near the west side of Kinskuch Lake and between Kinskuch and Jade lakes, the unit contains a greater proportion of siliceous rocks, including abundant and distinctive thin-bedded pale green, pale grey, and black radiolarian chert (Fig. 10). Near the top of this unit, two discontinuous centimetre-scale limy lenses, one from the



Figure 10. Pale-coloured, folded Late Triassic or older bedded radiolarian chert (unit 1) overlain by dark coloured, massive mafic tuff-breccia or lahar (unit 2); 2.5 km west of Kinskuch Lake.

western outcrop area and one from near the northwest end of Kinskuch Lake, yielded Upper Triassic conodonts (Late Norian and Middle to Late Norian; M.J. Orchard, written comm., 1991). In neither area is the base of the unit exposed. Unit 1 is characterized by the presence of metre-scale minor folds and brittle-ductile shear-fractures. Phyllitic sub-centimetre interbeds are common between radiolarian chert layers. Deformation responsible for these features predated the deposition of younger map units, because undeformed rocks of the lowermost Hazelton Group rocks commonly overlie unit 1 rocks with pronounced angular unconformity (Fig. 10), and locally contain angular metre-scale clasts of tightly folded and/or phyllitic bedded chert and siliceous argillite of unit 1. In addition, Hazelton Group rocks in the Kinskuch area only very rarely possess evidence for ductile strain, which typifies rocks of unit 1.

Hazelton Group

Unit 2: Mafic volcanic and volcanoclastic rocks and limestone

Although composed of varied lithologies, the stratigraphic position of rocks of this unit at the base of the Hazelton Group helps distinguish them from rocks of overlying map units. In addition, pyroxene and angular chert grains and fragments are commonly present in rocks of unit 2, but less common in rocks of younger units. In the belt of unit 2 rocks trending south-southeast from Porphyry Mountain, and in the small area of outcrop west of north-central Kinskuch Lake (unit 2a, Fig. 9), this unit is easily distinguished by the presence of massive pyroxene-bearing pyroclastic rocks. Near the southwest and northwest ends of Kinskuch Lake, however, unit 2 is typically much thinner, and consists mainly of sedimentary rocks. Massive medium grained sandstone containing angular fragments and grains of chert predominates, but medium to thin bedded sandstone and siltstone are common. Locally, poorly-bedded bioclastic and tuffaceous limestone and limestone breccia (up to 10 m thick) occur at the base of the unit. Chert-bearing clastic rocks are massive and very resistant, and chert fragments are typically white-weathering. This weathering presents a misleading appearance suggestive of felsic tuffaceous rocks, and it belies the common presence of augite grains. Coarser grained varieties, of probable debris flow origin, particularly abundant near the southwest end of Kinskuch Lake, are outwardly similar to coarse grained andesite and dacitic-andesite pyroclastic rocks of units 4 and 5.

Unit 3: Limy clastic rocks

Along the west side of Kinskuch Lake, this unit comprises thin bedded dark grey siltstone and feldspathic turbidite sandstone. Within its respective lower and upper parts it includes lahar which is likely a facies equivalent of coarse pyroclastic deposits common to units 2 and 4.

Units 4 and 5: Intermediate and felsic pyroclastic rocks and associated flows, clastic rocks and high level intrusive rocks

Mapping northeast of Kinskuch Lake and northwest of Banded Mountain suggests that units 4 and 5 of Greig (1991a), and possibly the lowermost part of unit 6, may be age-equivalent lithofacies. For example, the extremely massive coarse lapilli tuff and tuff-breccia of unit 4 which underlies Flat Top Mountain and the ridge to the east, grades laterally to the north and northeast into massive debris flows and siliceous tuffaceous sandstone and siltstone. Debris flows consist of angular volcanic fragments up to tens of centimetres in diameter contained in a matrix of dark grey to black siliceous tuffaceous sandy siltstone or mudstone. East and northeast of Jade Lake, the debris flows grade upward into and are interbedded with siliceous siltstone and sandstone of unit 6.

Massive coarse grained tuffaceous rocks such as those near Flat Top Mountain are also interbedded with green and locally maroon massive crystal lithic ash tuff and with megacrystic potassium feldspar porphyritic flows. The ash tuff is locally the most common lithology in the Hazelton Group (e.g., south of the juncture of the north and south Flat glaciers) and may occur at any stratigraphic level within units 4 and 5. Its lack of layering and the general absence of sedimentary structures suggest that the tuff was deposited as voluminous ash flows. Megacrystic potassium feldspar porphyritic flows (unit 4/5a) contain scattered centimetre-scale potassium feldspar phenocrysts and abundant medium grained plagioclase feldspar phenocrysts. The flows are of probable dacitic composition, may exceed 5 m in thickness, are locally foliated, and are interbedded with pyroclastic rocks typical of units 4 and 5.

Near the southwest end of Kinskuch Lake, units 4 and 5 consist largely of massive fine grained hornblende feldspar porphyritic, high level(?) intrusive rocks (map unit 4/5b). Near its west margin, this unit probably includes both extrusive and intrusive rocks, but internal textures and contact relations with tuffaceous rocks of unit 3 are non-diagnostic. To the east, the unit is texturally more variable (though everywhere fine grained), but an intense alteration overprint obscures contacts between textural varieties. Complicating this problem is their lithological similarity to common hornblende feldspar porphyritic granodiorite(?) dykes which intrude all map units near the southwest margin of the lake (Gale, 1957).

Salmon River Formation

Unit 6: Siliceous clastic and volcanoclastic rocks

At the base of unit 6, rusty weathering laminated and thin bedded (5-15 cm) siliceous siltstone paraconformably overlies coarse, silt matrix-rich debris flows or pyroclastic rocks of the uppermost Hazelton Group. Farther upsection in the Salmon River Formation, siltstone is interbedded with massive dark green, medium grained, locally pebbly, sandstone (AE turbidites) which are locally up to 5 m thick. Sandstone beds commonly contain rusty weathering

carbonate concretions that are nucleated on siltstone rip-up clasts. Along the margins of the south Flat glacier, the Salmon River Formation is intruded by distinctive white weathering sills and dykes of pyritic aphanitic rhyolite up to 5 m thick (Fig. 11).

Bowser Lake Group

Unit 7: Pale grey weathering clastic rocks

Pale grey weathering clastic rocks on the east margin of the study area overlie the Salmon River Formation along a gradational contact. The Bowser Lake Group is distinguished from the Salmon River Formation by its thinner bedded sandstones, its paler weathering colours, and its less siliceous composition.

Structure

As in the Oweegee area, the eastern margin of the Kinskuch basement culmination is the locus for southwest vergent folds in the cover rocks (Greig, 1991a), and structural trends and vergence conform, in part, to the orientation of the margins of the culmination. In the Kinskuch area, several major reverse faults involve basement rocks; these may in part accommodate some of the shortening observed in cover rocks of the Bowser Lake Group and Salmon River Formation.

The contact between Hazelton Group volcanic rocks and clastic rocks of the Salmon River Formation west of Banded Mountain is a north dipping reverse fault; its location to the east is somewhat uncertain. To the northeast, the units are conformable and folded into broad, open folds. To the south and southeast of the fault, south vergent tight to open folds in the Salmon River Formation have angular hinges and long, commonly gently north dipping limbs; short, typically steeply south dipping limbs are locally overturned. Farther south, near the terminus of the White glacier and in the area north and west of Kitsault Lake, folds in the Salmon River Formation are more open and the Hazelton Group is conformable with the Salmon River Formation. The style,



Figure 11. Rhyolite dyke and sill intruding south vergent folds in Salmon River Formation, west margin, south Flat glacier; exposure is approximately 120 m high.

vergence, and distribution of these folds implies that they are genetically related to the fault near Banded Mountain. The eastward projection of the fault in the Salmon River Formation has therefore been drawn between the domain of open folds to the north and that of tight folds to the south and southeast.

Near the northwest side of Kinskuch Lake, a system of north trending, steeply dipping faults and associated folds involve lithologically distinct radiolarian chert of unit 1 and limestone and massive mafic tuff-breccia of unit 2. The structures in this area are therefore relatively easily defined compared to structures elsewhere in the map area, which commonly juxtapose similar lithologies. The faults are near-vertical and mainly east-side-up, as suggested by the westward overturned basal contact of the Hazelton Group northwest of Kinskuch Lake, and by rare pervasive east dipping foliation in Hazelton Group rocks in the fault zone. Displacement on this system of faults may have occurred in response to southwest directed shortening of overlying Bowser Lake Group rocks, which is evident farther east.

SUMMARY AND CONCLUSIONS

In the Oweege and Snowslide ranges and the Kinskuch Lake area, structural culminations within the Skeena fold belt along the west-central margin of the Bowser Basin expose Early Jurassic and older Stikine terrane basement. These basement culminations contain a record of Late Triassic to Early Jurassic deformation, uplift and erosion. Deformation of this age has been described from elsewhere in the Stikine terrane (Terrace, Monger, 1977; Telegraph Creek, Brown and Greig, 1990), but its regional extent was not recognized. Uplift and erosion, which followed the deformation, is expressed as a pronounced angular unconformity at the base of the Hazelton Group; onlap of the stratigraphically highest Hazelton Group rocks onto the unconformity suggests that the erosion surface had substantial relief or that uplift was active during Hazelton Group deposition. Such a depositional environment is in accord with abrupt thickness and facies changes recognized in the Hazelton Group.

Toarcian time marks the onset of dominantly clastic sedimentation and essentially, the cessation of proximal volcanism. In the Oweege and Snowslide ranges, Toarcian sandstone and Spatsizi and Bowser Lake groups are conformable and the only apparent stratigraphic discordances are Oxfordian or younger slump folds in the Snowslide Range. Similarly, Toarcian time in the Kinskuch area is marked by cessation of Hazelton Group volcanism and the inception of dominantly clastic sedimentation, which is there represented by the conformable Salmon River Formation and Bowser Lake Group.

On the northeast margins of the Oweege and Kinskuch basement culminations, structures in Toarcian(?) and younger cover rocks verge to the southwest and are parasitic folds to larger scale structures in the northeast-vergent Skeena fold belt. Conformity of structural trends within the cover rocks around the margins of basement culminations

suggests a genetic relation. The considerable shortening recorded in the cover may be partially accommodated by brittle and brittle-ductile reverse faults in the basement.

ACKNOWLEDGMENTS

David Stiles and Julie Kadar provided excellent assistance in the field. Carol Evenchick, George Gehrels and Bob Anderson offered continued good-humoured advice and encouragement, and Mike Gunning willingly undertook biostratigraphic studies of Stikine assemblage rocks in Oweege dome. Peter van der Heyden, Carol Evenchick, and Bev Vanlier edited the manuscript. Cooperation and geological discussions with Dave Tupper and his Keewatin Engineering crew, with Ian Paterson of Cominco, and with geologists in the employ of Lac Minerals was rewarding and greatly appreciated. The interest of the late Andreas Vogt of Lac Minerals will be greatly missed.

REFERENCES

- Brown, D.A. and Greig, C.J.**
1990: Geology of the Stikine River-Yehiniko Lake area, northwestern British Columbia (104G/11W and 12E); in *Geological Fieldwork 1989*, British Columbia Ministry of Energy, Mines and Petroleum Resources, Paper 1990-1, p. 141-151.
- Evenchick, C.A.**
1991a: Geometry, evolution, and tectonic framework of the Skeena Fold Belt, north-central British Columbia; *Tectonics*, v. 10, no. 3, p. 527-546.
1991b: Structural relationships of the Skeena Fold Belt west of the Bowser Basin, northwest British Columbia; *Canadian Journal of Earth Sciences*, v. 28, p. 973-983.
- Gale, R.E.**
1957: The geology of Kinskuch Lake area; M.Sc. thesis, University of British Columbia, Vancouver, 63 p.
- Greig, C.J.**
1991a: Stratigraphic and structural relations along the west-central margin of the Bowser Basin, Oweege and Kinskuch areas, northwestern British Columbia; in *Current Research, Part A: Geological Survey of Canada, Paper 91-1A*, p. 197-205.
1991b: Reconnaissance lithochemistry, Oweege and Kinskuch areas, northwestern British Columbia (104A/11, 12; 103P/11); in *Exploration in British Columbia 1990*; British Columbia Ministry of Energy, Mines and Petroleum Resources, p. 169-174.
- Greig, C.J., Gehrels, G.E., Anderson, R.G., and Evenchick, C.A.**
1991: Possible transtensional origin for the Bowser Basin, British Columbia (abstract); *Geological Society of America, Abstracts with Programs*, v. 23, p. 30-31.
- Grove, E.W.**
1986: Geology and mineral deposits of the Unuk River-Salmon-Anyox area, British Columbia; *British Columbia Ministry of Energy, Mines and Petroleum Resources, Bulletin 63*, 152 p.
- Koch, N.G.**
1973: The central Cordilleran Region; in *Future Petroleum Provinces of Canada*; Canadian Society of Petroleum Geologists, Memoir 1, p. 37-71.
- Monger, J.W.H.**
1977: Upper Paleozoic rocks of northwestern British Columbia; in *Report of Activities, Part A: Geological Survey of Canada, Paper 77-1A*, p. 255-262.
- Ricketts, B.D. and Evenchick, C.A.**
1991: Analysis of the Middle to Upper Jurassic Bowser Basin, northern British Columbia; in *Current Research, Part A: Geological Survey of Canada, Paper 91-1A*, p. 65-73.

Preliminary results on the stratigraphy and structure of the Lardeau Group in the Illecillewaet synclinorium, western Selkirk Mountains, British Columbia

Maurice Colpron¹ and Raymond A. Price¹
Cordilleran Division, Vancouver

Colpron, M. and Price, R.A., 1992: Preliminary results on the stratigraphy and structure of the Lardeau Group in the Illecillewaet synclinorium, western Selkirk Mountains, British Columbia; *in* Current Research, Part A; Geological Survey of Canada, Paper 92-1A, p. 157-162.

Abstract

Detailed mapping of Lardeau Group rocks in the Illecillewaet synclinorium, south of latitude 51°15', has demonstrated that all mappable units are stratigraphically conformable with underlying strata of the Badshot Formation and Hamill Group. These relationships are incompatible with the hypothesis of the mid-Paleozoic "accretion" of Kootenay terrane. The Illecillewaet synclinorium results from the superposition of two generations of isoclinal folds and a later phase of cross-folds. The occurrence of an inverted panel of the Badshot Formation confirms the suggestion that the area was subjected to early, large scale recumbent folding. Two generations of faults are documented in the area: 1) early, east-verging thrust faults that are now overturned, and 2) later southwest-verging thrust faults.

Résumé

La cartographie détaillée des roches du Groupe de Lardeau dans le synclinorium d'Illecillewaet, au sud de la latitude 51°15', démontre que toutes les unités cartographiques sont en continuité stratigraphique avec les strates susjacentes de la Formation de Badshot et du Groupe de Hamill. Ces relations ne sont pas conformes à l'hypothèse de "l'accrétion" du terrane de Kootenay au Paléozoïque moyen. Le synclinorium d'Illecillewaet résulte de la superposition de deux générations de plis isoclinaux et d'une phase tardive de plis transverses. La présence d'un panneau inversé de la Formation de Badshot confirme l'hypothèse selon laquelle la région aurait été soumise à une phase précoce de plis couchés de grande échelle. Deux générations de failles sont documentées dans la région: 1) failles de chevauchement précoces de vergence est, qui sont maintenant renversées, et 2) failles de chevauchement tardives de vergence sud-ouest.

¹ Department of Geological Sciences, Queen's University, Kingston, Ontario K7L 3N6

INTRODUCTION

The Illecillewaet synclinorium is a west-facing fold in the southwest flank of the Selkirk Fan structure (Wheeler, 1963). It forms a segment of the zone of structural divergence that follows the Omineca crystalline belt and straddles the suture zone between North America and Intermontane "superterrane", from northeastern Washington to southern Yukon (Fig. 1; Price, 1981). The core of the synclinorium is occupied by strata that are assigned to the Lardeau Group (Wheeler, 1963; Zwanzig, 1973). Although the Lardeau Group has traditionally been considered to be conformable with underlying strata of the Badshot Formation (Fyles and Eastwood, 1962; Zwanzig, 1973; Read, 1975; Klepacki and Wheeler, 1985), it has been proposed, on the basis of stratigraphic disparity with homotaxial strata to the east, that the Lardeau Group may represent an allochthonous terrane (*Kootenay terrane* of Wheeler *in* Monger and Berg, 1984) structurally juxtaposed over the North American rocks of the Cordilleran miogeocline. More recently, Gehrels and Smith (1987) and Smith and Gehrels (1990) have proposed, on the basis of regional correlations along the Kootenay Arc, and detailed mapping in the Ninemile Creek-Wilmon Creek-Hunters Creek area of northeastern Washington (Smith, 1991) and the Trout Lake area of southeastern British Columbia (Smith and Gehrels, 1990), that the Lardeau Group is an inverted stratigraphic sequence that was juxtaposed over North American miogeoclinal strata during the mid-Paleozoic Antler orogeny. According to their model, talc-bearing schists such as those reported by Zwanzig (1973) and Sears (1979) may represent the remnants of the "suture" between *Kootenay terrane* and the North American Cordilleran miogeocline.

This paper presents some preliminary results of detailed mapping (1:20 000) of the northern part of the Illecillewaet synclinorium during the summer of 1991. These results have important implications for the interpretation of the relationships between the Lardeau Group and rocks of the Cordilleran miogeocline, and their regional tectonic significance. The study area is located northeast of Revelstoke and north of the Trans-Canada highway (NTS sheets 82N/5 and 82N/4), and is approximately defined to the west and east by the limits of Revelstoke and Glacier National Parks (respectively), and to the north by latitude 51°17'N (Fig. 2).

STRATIGRAPHY

Badshot Formation (Walker and Bancroft, 1929)

The Badshot Formation consists of white dolomitic marble and medium to dark grey muscovite schist. It is gradational into the underlying Mohican Formation of the Hamill Group (Fyles and Eastwood, 1962; Zwanzig, 1973). The marble is light grey to buff weathering and contains darker argillaceous intercalations less than 1 cm-thick that define the bedding. The schist is light grey weathering and non graphitic. It locally contains thin (1-5 cm) beds of light coloured limestone.

Lade Peak Formation (Fyles and Eastwood, 1962; Zwanzig, 1973)

This unit consists of medium to dark grey dolomitic and graphitic limestone interbedded with black calcareous argillite. The bedding within the limestone is generally outlined by thin parallel laminations of argillaceous material. Locally, silty horizons define low-angle crossbeds. Elsewhere, the limestone-argillite sequence contains graded bedding and has imbricate clasts of light coloured limestone at the base of darker limestone beds. As a whole, the Lade Peak Formation appears to represent an interval of basin subsidence. The thickness of the limestone beds decreases from 30 cm at the base to about 5 mm near the top, and the proportion of argillite increases upward. The graphitic limestone grades into the overlying black phyllite unit at the base of the Lardeau Group. Near the base of the sequence, the black dolomitic limestone is interbedded with more competent, 25-30 cm-thick beds of light grey laminated limestone resembling the Badshot Formation. The contact between the Lade Peak Formation and the underlying Badshot Formation appears to be gradational.

Lardeau Group

The remainder of the sedimentary units recognized in the Illecillewaet synclinorium are assigned to the Lardeau Group (Walker and Bancroft, 1929; Fyles and Eastwood, 1962; Wheeler, 1963). Three informal map units were recognized during this phase of field work: a black phyllite unit at the base, a phyllitic grit unit, and a quartzite/phyllite unit at the top.

Black phyllite unit

The lower part of the Lardeau Group corresponds to a thick sequence of dark grey to black, graphitic and calcareous phyllite, schist and argillite. Wheeler (1963) and Zwanzig (1973) have tentatively correlated this unit with the Index Formation in the Ferguson area (Fyles and Eastwood, 1962). This unit is gradational into the overlying phyllitic grit unit. The bedding is generally defined by thin, white siltstone laminae (\approx 1 mm-thick) or 1-10 cm-thick black limestone beds. The black phyllite, however, commonly lacks primary sedimentary structures. Locally, the unit contains siliceous argillite or black siltstone in beds 10-50 cm-thick. Although, intervals of siliceous argillite and siltstone may be as thick as few tens of metres, they do not seem to form a mappable stratigraphic unit within the black phyllite, as suggested by Zwanzig (1973). Massive, light to dark grey quartzite beds, generally less than 1 m-thick, occur locally. East of Corbin Peak, a tan weathering, medium grey calcareous phyllite occupies the core of an anticline within the black phyllite sequence. This phyllite is characterized by an abundance of \approx 1 m-thick beds of dolomitic sandstone.

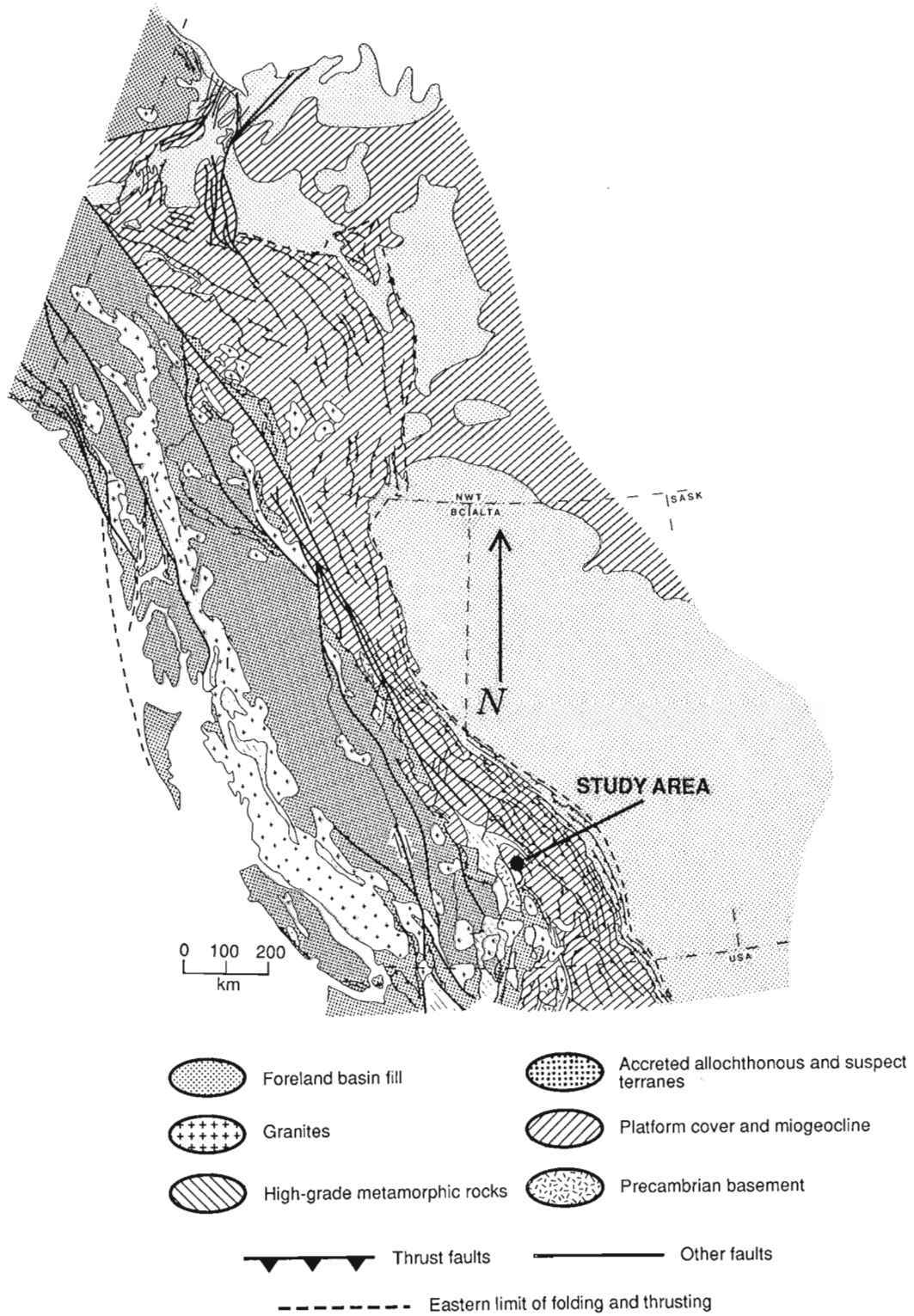


Figure 1. Tectonic sketch map of the Canadian Cordillera showing the location of the study area (modified after Douglas, 1968, and Price, 1986).

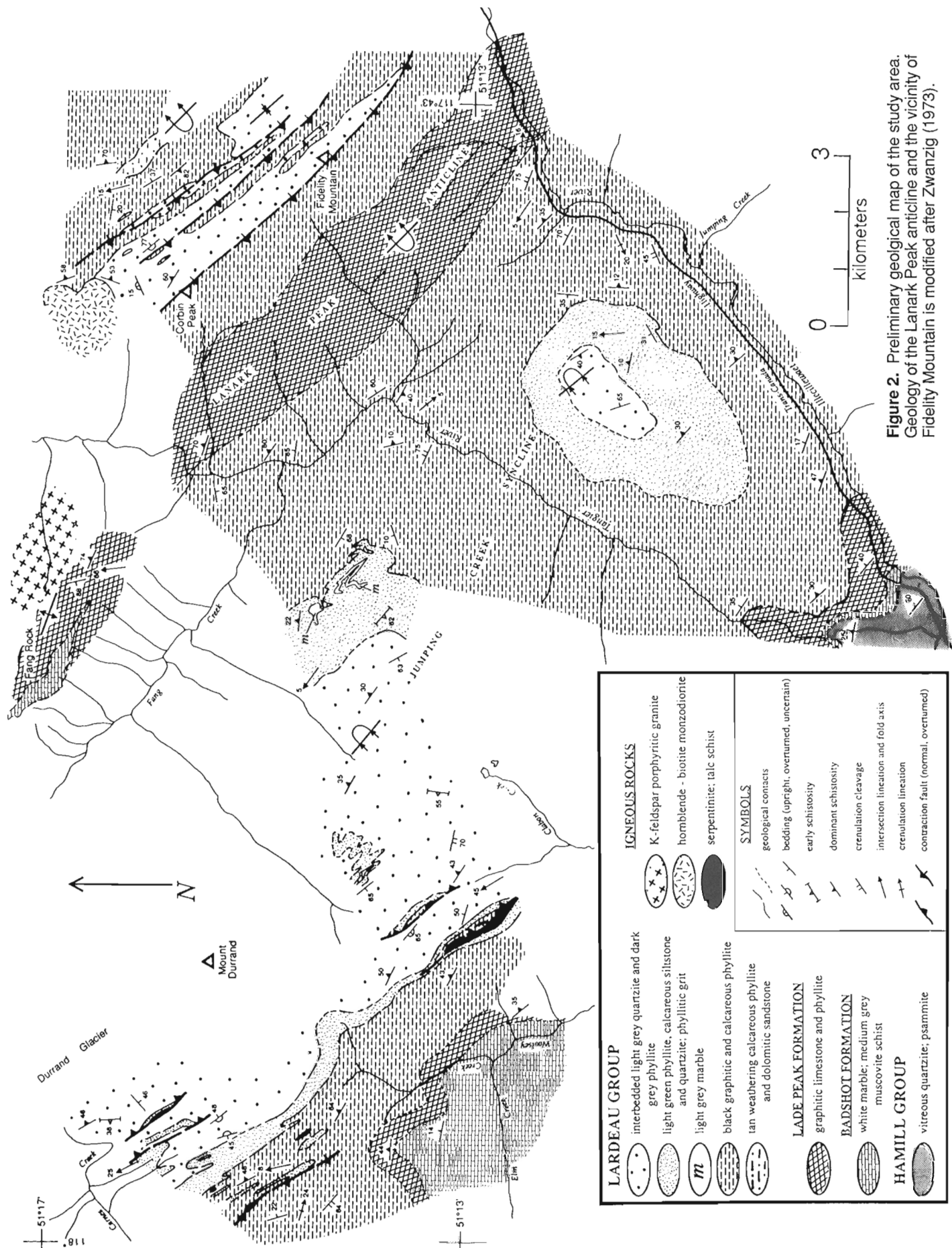


Figure 2. Preliminary geological map of the study area. Geology of the Lanark Peak anticline and the vicinity of Fidelity Mountain is modified after Zwanzig (1973).

Phyllitic grit unit

The phyllitic grit unit is characterized by light green to light grey phyllitic grit and calcareous siltstone. The siltstone layers are generally less than 1 cm-thick and buff weathering. The phyllitic grit generally contains isolated blue (or smoky) quartz granules (≥ 2 mm). Rip-up clasts of graphitic phyllite occur locally. Medium- to coarse-grained quartzose, chloritic and feldspathic grit layers (10 cm to few metres thick) also occur locally. Buff weathering dolostone and/or light grey to white marble occur near the base of the phyllitic grit unit. This carbonate unit is generally discontinuous, but a relatively continuous marble horizon can be mapped along the east flank of the Jumping Creek syncline northwest of Tangier river (*m* in Fig. 2). The transition between the phyllitic grit and the overlying quartzite/phyllite unit is marked by an increase in the amount of quartz in the rock and the appearance of thin interbeds of black lustrous phyllite. In the vicinity of Corbin Peak, the phyllitic grit unit is absent and the black phyllite unit grades upward into the quartzite/phyllite unit.

Quartzite/phyllite unit

The quartzite/phyllite unit consists of interbedded light to medium grey massive quartzite and dark grey to black lustrous (generally non-graphitic) phyllite. The quartzite is generally medium-grained, although it is locally coarse and *gritty*. The beds vary from few centimetres to more than 1 m-thick. The phyllite interbeds are generally thin (~1-5 cm), although they locally are up to 1 m-thick. This unit is remarkable for its abundance of well preserved primary sedimentary structures, particularly graded bedding and load structures. Convoluted and slump beds are also observed. The primary structures are best preserved west of Durrand glacier and east of Corbin Peak. They show that the quartzite/phyllite unit generally faces upward and that it stratigraphically overlies the phyllitic grit and black phyllite units. The stratigraphically highest section mapped in the Corbin Peak area is a unit of black graphitic phyllite that is more than 10 m-thick.

Serpentinite and talc schist

A few serpentinite and talc schist outcrops were mapped in the area. They occur mainly west of Durrand glacier. The serpentinite is generally associated with chlorite schist and greenstone, and, locally, with carbonate alteration and fuschite. Serpentinite occurs within all three stratigraphic units of the Lardeau Group, and, accordingly, the occurrence of serpentinite and talc schist cannot be used to locate a major fault beneath (or within) *Kootenay terrane* (Gehrels and Smith, 1987).

Intrusive rocks

Two types of plutonic rocks are recognized in the area: a K-feldspar porphyritic granite (east of Fang Rock) and a hornblende-biotite monzodiorite (north of Corbin Peak). Both rock types are medium- to coarse-grained and contain

mafic inclusions locally. K-feldspar megacrysts in the Fang granite are generally larger than 2 cm. A few diabase dykes also occur south of Mount Durrand. The dykes are 1-10 m-wide and generally strike north-northwest. All intrusive rocks mapped appear to postdate the dominant phase of deformation.

DISCUSSION OF STRATIGRAPHIC RELATIONS

Observations made during the summer 1991 indicate that the Lardeau Group is positionally linked to the underlying Lade Peak and Badshot formations, and that the bulk of the stratigraphic sequence exposed south of latitude $51^{\circ}15'$ is upright. These observations, therefore, are strong arguments against the hypothesis that the entire Lardeau Group represents an allochthonous terrane, and that it was tectonically inverted and juxtaposed over the North American miogeocline during a mid-Paleozoic orogenic event (Gehrels and Smith, 1987; Smith and Gehrels, 1990).

Read (1975) and Sears (1979) concluded that Lardeau strata in the Illecillewaet synclinorium are lateral equivalents of the Index Formation of the Kootenay Arc. They also suggested that Lardeau strata in the Illecillewaet synclinorium are stratigraphically continuous with the overlying Jowett and Broadview formations in the Akolkolex River and Incomappleux River areas (Read and Wheeler, 1976; Sears, 1979). If these interpretations are correct, then our conclusions regarding the Lardeau Group in the Illecillewaet synclinorium can be extended southward to the classic stratigraphy of the Lardeau Group in the Kootenay Arc (Fyles and Eastwood, 1962; Fyles, 1964; Read and Wheeler, 1976).

STRUCTURE

Three distinct tectonic foliations are recognized regionally within the study area. The oldest foliation is a schistosity that is axial planar to isoclinal folds of bedding. It is best preserved in phyllitic grits and quartzites of the Lardeau Group. Folding of the oldest folds by younger folds has produced type 3 interference patterns (Ramsay, 1962). The sense of vergence of the earliest folds is uncertain.

The second foliation is a pervasive northwest-striking schistosity that is developed in all rock types and is the dominant foliation in the area. It is axial planar to tight to isoclinal southwest-verging and, generally, northwest-plunging folds. Folds of this generation dominate the map pattern.

The third foliation is a west-northwest-striking spaced, crenulation cleavage associated with open folds. The third generation folds result mainly in the local doming and arching of previous structures (type 1 interference pattern). The most conspicuous expression of the third phase of folding is illustrated by the marble marker unit along the west flank of the Jumping Creek syncline, northwest of Tangier river (Fig. 2).

The occurrence of downward-facing marbles of the Badshot Formation in the core of a syncline on the southwestern slope of Fang Rock (Fig. 2; Wheeler, 1963) confirms the suggestion that the area was subjected to an early phase of recumbent folding (Thompson, 1972; Zwanzig, 1973; Sears, 1979; Brown and Lane, 1988). However, the relationships between structures in the vicinity of Fang Rock, and to the north near Mount Moloch (Brown and Lane, 1988), and those mapped to the south by Zwanzig (1973; Fig. 2) have yet to be established.

At least two generations of faults have been documented in the area. The earliest faults are marked by conspicuous, sharp, outcrop-scale truncations of bedding, and associated folding. They are characteristically east-dipping and the sense of shear outlined by truncations and associated folding indicates that they are east-verging contraction faults, which are now overturned and have a normal sense of displacement. These early faults are overprinted by the second generation foliation. The early faults correspond with the overturned east-verging thrust faults that were identified by Zwanzig (1973) in the vicinity of Fidelity Mountain.

A second generation fault, recognized along the southwest flank of the Jumping Creek syncline, south of Mount Durrand, is marked by a zone of stratigraphic disruption that dips northeast, parallel to the dominant schistosity. It is characterized by the juxtaposition of lenses of quartzite, phyllitic grit, black phyllite and serpentine that are up to tens of metres thick.

SUMMARY

Rocks of the Lardeau Group in the Illecillewaet synclinorium are gradational into the underlying miogeoclinal sequence of the Badshot and Lade Peak formations. These relationships are incompatible with the hypothesis that the Lardeau Group is tectonically inverted (Smith and Gehrels, 1990) and that it is allochthonous with respect to the underlying Hamill Group and Badshot Formation (Gehrels and Smith, 1987; Wheeler *in* Monger and Berg, 1984).

The structural evolution of the Illecillewaet synclinorium involved an early phase of recumbent folding (east- or west-verging ?), early east-verging thrust faulting, strong southwest-verging tight to isoclinal folding (and thrusting), and a late phase of doming and arching by cross-folds. The area was intruded by two plutons after the development of the southwest-verging structures.

ACKNOWLEDGMENTS

Financial support for this study was provided by EMR Research Agreement #080-4-91 to R.A. Price, NSERC Collaborative Research Grant #117228 to R.A. Price, NSERC Research Operating Grant #0092417 to R.A. Price, and a FCAR postgraduate scholarship to M. Colpron. Jason Smolensky and Rob Wheelan provided assistance in the field. Thanks to John Carter for his help in resolving logistical problems. The visit of D.M. Carmichael (and the helicopter ride) is greatly appreciated.

REFERENCES

- Brown, R.L. and Lane, L.S.**
1988: Tectonic interpretation of west-verging folds in the Selkirk Allochthon of the southern Canadian Cordillera; Canadian Journal of Earth Sciences, v. 25, p. 292-300.
- Douglas, R.J.W. (Compiler)**
1968: Geological map of Canada; Geological Survey of Canada, Map 1374A.
- Fyles, J.T.**
1964: Geology of the Duncan Lake area, Lardeau district, British Columbia; British Columbia Department of Mines and Petroleum Resources, Bulletin 49, 78 p.
- Fyles, J.T. and Eastwood, G.E.P.**
1962: Geology of the Ferguson area, Lardeau District, British Columbia; British Columbia Department of Mines and Petroleum Resources, Bulletin 45, 92 p.
- Gehrels, G.E. and Smith, M.T.**
1987: "Antler" allochthon in the Kootenay arc?; Geology, v. 15, p. 769-770.
- Klepachi, D.W. and Wheeler, J.O.**
1985: Stratigraphic and structural relations of the Milford, Kaslo and Slocan groups, Goat Range, Lardeau and Nelson map areas, British Columbia, *in* Current Research, Part A; Geological Survey of Canada, Paper 85-1A, p. 277-286.
- Monger, J.W.H. and Berg, H.C.**
1984: Lithotectonic terrane map of western Canada and southeastern Alaska; *in* Siberling, N.J. and Jones, D.L. (eds.); Lithotectonic Terrane Maps of the North American Cordillera, Part B; United States Geological Survey, Open-File Report 84-523, p. B1-B31.
- Price, R.A.**
1981: The Cordilleran foreland thrust and fold belt in the southern Canadian Rocky Mountains; *in* McClay, K.R. and Price, N.J. (eds.); Thrust and Nappe Tectonics: The Geological Society of London, Special Publication No. 9, p. 427-448.
1986: The southeastern Canadian Cordillera: thrust faulting, tectonic wedging, and delamination of the lithosphere; Journal of Structural Geology, v. 8, p. 239-254.
- Ramsay, J.G.**
1962: Interference patterns produced by the superposition of folds of similar types; Journal of Geology, v. 70, p. 466-481.
- Read, P.B.**
1975: Lardeau Group, Lardeau map-area, west half (82K west half), British Columbia; *in* Report of Activities, Part A; Geological Survey of Canada, Paper 75-1, p. 29-30.
- Read, P.B. and Wheeler, J.O.**
1976: Geology of Lardeau W/2 (82K W/2); Geological Survey of Canada, Open File 432.
- Sears, J.W.**
1979: Tectonic contrasts between the infrastructure and suprastructure of the Columbian orogen, Albert Peak area, western Selkirk Mountains, British Columbia; Ph.D. thesis, Queen's University, Kingston, Ontario, 154 p.
- Smith, M.T.**
1991: Geologic strip map of the Ninemile Creek-Wilmont Creek-Hunters Creek area, Ferry and Stevens County, Washington; Washington Department of Natural Resources, Open File Report 91-4, 9 p.
- Smith, M.T. and Gehrels, G.E.**
1990: Geology of the Lardeau Group east of Trout Lake, southeastern British Columbia (Silvercup Ridge, Mount Wagner and Mount Aldridge areas); British Columbia Ministry of Energy, Mines and Petroleum Resources, Open File 1990-24.
- Thompson, R.I.**
1972: Geology of the Akolkolex River area near Revelstoke, British Columbia; Ph.D. thesis, Queen's University, Kingston, Ontario, 125 p.
- Walker, J.F. and Bancroft, M.F.**
1929: Lardeau map-area, British Columbia, general geology; *in* Geological Survey of Canada, Memoir 161, p. 1-16.
- Wheeler, J.O.**
1963: Rogers Pass map-area, British Columbia and Alberta (82N W/2); Geological Survey of Canada, Paper 62-32, 32 p.
- Zwanzig, H.V.**
1973: Structural transition between the foreland zone and the core zone of the Columbian orogen, Selkirk Mountains, British Columbia; Ph.D. thesis, Queen's University, Kingston, Ontario, 158 p.

New developments in the geology of Mayo map area, Yukon Territory¹

C.F. Roots and D.C. Murphy
Cordilleran Division, Vancouver

Roots, C.F. and Murphy, D.C., 1992: New developments in the geology of Mayo map area, Yukon Territory; in Current Research, Part A; Geological Survey of Canada, Paper 92-1A, p. 163-171.

Abstract

Revision geological mapping has clarified the stratigraphy and structure of Mayo map area. The "Keno Hill quartzite" and underlying carbonaceous phyllite and felsic metavolcanic rocks exhibit two episodes of high-strain deformation and late open folding; the earliest high-strain deformation characterizes the Tombstone thrust sheet in the area. Keno Hill mineralization postdates high-strain deformation and may coincide with later, possibly middle Cretaceous, high-angle faulting. In the Robert Service thrust sheet of southern Mayo map area, Cambrian maroon argillite and siltstone, Road River chert, and Earn Group clastic sediments are folded in open, upright folds and cut by Early Cretaceous granite. Delineation of the extent of prospective middle Paleozoic stratigraphy in the Tombstone and Robert Service thrust sheets will aid in exploration for stratiform Cu-Zn and Zn-Pb mineralization.

Résumé

La cartographie géologique, aux fins de révision, a permis de mieux expliquer la stratigraphie et la structure de la région cartographiée de Mayo. Le «quartzite de Keno Hill», et aussi la phyllite carbonée et les roches métavolcaniques felsiques sous-jacentes, témoignent de deux épisodes de déformation intense et de plissements tardifs de type ouvert; l'intense déformation initiale caractérise dans la région la nappe de charriage de Tombstone. La minéralisation de Keno Hill est postérieure à la déformation intense et pourrait coïncider avec la formation de failles ultérieures de fort pendage, datant peut-être du Crétacé moyen. Dans la nappe de charriage de Robert Service, qui se situe dans la région cartographiée du sud de Mayo, l'argile indurée et le siltstone marron, le chert de Road River et les sédiments clastiques du groupe d'Earn, tous d'âge cambrien, ont été déformés par des plis droits ouverts, et ont été recoupés par un granite du Crétacé inférieur. La délimitation des strates qui pourraient dater du Paléozoïque moyen, dans les nappes de charriage de Tombstone et de Robert Service, facilitera la prospection des minéralisations stratiformes en Cu-Zn et Zn-Pb.

¹ Canada-Yukon Co-operation Agreement on Mineral Resources 1991-96

INTRODUCTION

The Canada-Yukon Economic Development Agreement, signed in the spring of 1991, includes provisions for revitalizing geological mapping programs in prospective areas of the Yukon. Under this agreement, the revision geological mapping of the Mayo map area (105M) begun last summer (Roots, 1991) was accelerated with the addition of a second scientist (D.C. Murphy). The release of an up-to-date compilation of the geology of Mayo map area is planned for early 1992. This report contains stratigraphic and structural highlights from 1991 fieldwork.

GEOLOGICAL FRAMEWORK

Mayo map area comprises portions of two regional thrust sheets (Fig. 1). The more northerly Tombstone thrust sheet includes a mid-Paleozoic to Upper Triassic succession characterized by a pronounced foliation and lineation (Abbott, 1990). The southern two-thirds of the map area is underlain by uppermost Proterozoic to Mississippian off-shelf strata of the Robert Service thrust sheet. These rocks are folded and faulted in the south and gradually assume the intense fabrics of the Tombstone thrust sheet to the north (Gordey, 1990). Post-kinematic Early Cretaceous(?) granitic rocks intrude both thrust sheets.

STRATIGRAPHY OF THE KENO HILL REGION

Pre-Mississippian stratigraphy conformably beneath the "Keno Hill quartzite"

Three map units are traditionally recognized in the Keno Hill region, the "lower schist", "Keno Hill quartzite", and "upper schist" (Green, 1971 and references therein). Early workers considered this trio to be a gently folded conformable stratigraphic succession, Precambrian in age (Green and McTaggart, 1960, and references therein). Later work showed that the "lower schist" is in part composed of Paleozoic and Mesozoic rocks as young as Jurassic (Tempelman-Kluit, 1970; Green, 1971; Poulton and Tempelman-Kluit, 1982), whereas part of the "upper schist" is probably correlative with the uppermost Proterozoic-lower Cambrian "Grit Unit" (Poole, 1965; Green, 1971) now referred to as the Hyland Group (Gordey, in press). On the basis of the Jurassic age of underlying rocks and similarity to the Lower Cretaceous Keenan quartzite in Alaska, Tempelman-Kluit (1970) proposed that the "Keno Hill quartzite" was Lower Cretaceous. More recently, Mortensen and Thompson (1990) reported Mississippian conodonts (determination by M.J. Orchard, GSC) from this unit in the Ogilvie Mountains. Unless the "Keno Hill quartzite" is overturned in the Keno Hill district, the Mississippian age implies faults above and below (Robert Service and Tombstone thrusts, respectively).

Two additional considerations imply further complexity. Mortensen and Thompson (1990) reported a Middle Triassic U-Pb zircon and baddeleyite date from a metadiorite and

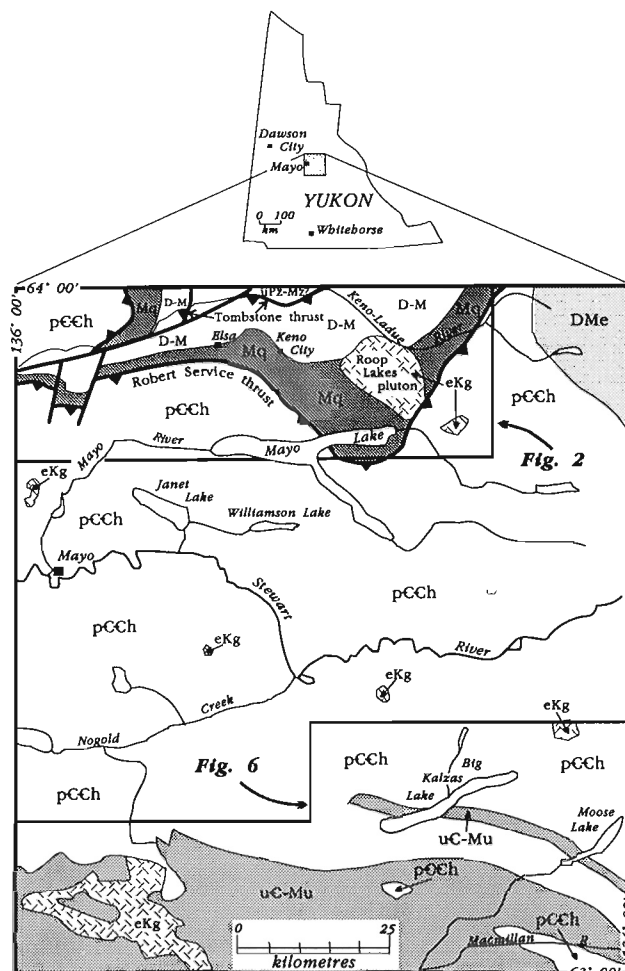


Figure 1. Generalized geological map of Mayo map area (105M) (compiled from Bostock, 1947; Roots, 1991 and references therein as well as new mapping). pCCh, Hyland Group; uC-Mu, undifferentiated Lower to Middle Paleozoic formations (see text); DMe, Earn Group; D-M, undifferentiated Devonian-Mississippian strata conformably below "Keno Hill quartzite" in northern part of map area; Mq, "Keno Hill quartzite" (both Mq and D-M are intruded by voluminous metadiorite and metagabbro bodies of inferred Middle Triassic age); eKg, Early Cretaceous granite, quartz monzonite, quartz syenite. Locations of Figures 2 and 6 are indicated.

metagabbro sill in the "Keno Hill quartzite" in the southern Ogilvie Mountains. Similar sills can be traced eastward along strike for over 200 km into the Keno Hill region, where they also intrude the "lower schist". Although not dated at Keno Hill, the sills there are also considered to be Middle Triassic. Mortensen and Thompson (1990) suggested that this implies (1) that the rocks immediately beneath the "Keno Hill quartzite" at Keno Hill are not Jurassic but pre-Middle Triassic or (2) that the sills are structurally intercalated with younger "lower schist", or (3) that sills of more than one age are present at Keno Hill. Secondly, in the Mt. Westman map area northeast of Keno Hill, Abbott (1990) and Turner and Abbott (1990) mapped foliated and lineated carbonaceous phyllite, siliceous carbonaceous phyllite and siltstone, and porphyritic and non-porphyritic phyllitic felsic metavolcanic

rocks conformably beneath the "Keno Hill quartzite". They correlated these rocks with the Devonian-Mississippian Earn Group. A preliminary Early Mississippian U-Pb zircon age from the felsic metavolcanic host of the MARG VMS deposit supports this interpretation (determination by J. Mortensen, reported in Abbott, 1990; Turner and Abbott, 1990). To reflect this, Abbott (1990) mapped the Tombstone thrust between the unnamed foliated and lineated correlatives of the Earn Group and underlying similar but weakly deformed carbonaceous clastic rocks intruded by metadiorite and metagabbro sills. In the Patterson Range the Tombstone thrust is identified by the sharp strain gradient between these units, rather than at the base of the "Keno Hill quartzite".

During 1991, the distinctive strata beneath the "Keno Hill quartzite" were mapped westwards from the northern edge of the Mayo map area (Fig. 2), extending Abbott's (1990) map. The felsic metavolcanics occur across the region, becoming less porphyritic farther west.

The "upper schist"

In his regional compilation, Green (1971) subdivided the "upper schist" above the "Keno Hill quartzite" into three stratigraphic units (1, 2, and pCy), considered to be Precambrian and to lie conformably below the "Grit Unit". Green's (1971) unit 1 north of Mayo Lake (ruled area, Fig. 2) near its contact with the "Keno Hill quartzite" (Robert Service thrust, Fig. 2) contains highly deformed rocks similar to the "Keno Hill quartzite" intercalated with grey-green, waxy-lustrous phyllonitic quartz-pebble conglomerate, psammite, and phyllitic marble reminiscent of the Hyland Group. Instead of a conformable sequence, unit 1 is interpreted as a structurally imbricated (isoclinally folded or faulted) succession of rocks from immediately above and below the Robert Service thrust.

Structure and structural evolution of the region around Keno Hill

The interpretation of the structure and evolution of the Keno Hill region has evolved with each stratigraphic interpretation. Early workers considered the strata to be disposed in a gently folded conformable sequence. Green and McTaggart (1960) and McTaggart (1960) suspected that the structure was more complicated and proposed an early phase of southwest-trending, low-angle, tight to isoclinal folding and shearing and a later phase of open upright folding. Subsequent fossil discoveries and U-Pb geochronology imply the existence of two regionally important thrust faults, the Robert Service thrust between the "Keno Hill quartzite" and the overlying Hyland Group, and the Tombstone thrust within "lower schist" Earn Group.

Observations made during the 1991 field season necessitate further revision of the structure and evolution of the Keno Hill region. At least four pre-ore deformation phases have been identified: at least two early high strain deformation phases characterized by prominent foliation and/or lineation and tight to isoclinal folding, and two later, possibly coeval, regional-scale open fold phases. Mineralized Keno Hill vein-faults are not affected by the deformation. The vein-faults are generally parallel to and increase in number towards a northeast-trending fault in the valley of the South McQuesten River, implying a possible genetic connection.

Early high-strain structures

All the rocks examined from the Patterson Range westward to Mt. Haldane (Fig. 2) exhibit structural fabrics associated with the earliest phase of deformation; the second phase of high-strain deformation is concentrated between Keno Hill and Mayo Lake. The earliest recognizable phase of

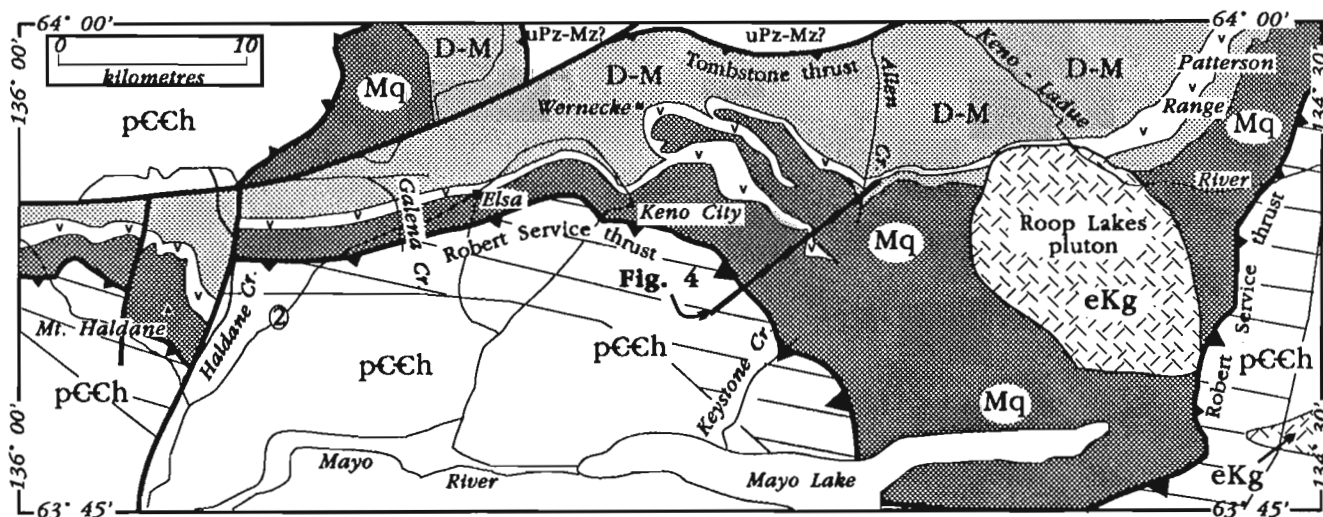


Figure 2. Simplified geological map of the Keno Hill region. Unit designation symbols as in Figure 1. "v" pattern indicates felsic metavolcanic unit below the "Keno Hill quartzite"; metavolcanic strata also occur within the "Keno Hill quartzite" but the contact relations are poorly understood. Ruled area is approximate area underlain by Green's (1971) Unit 1 (see text for discussion).

deformation produced a suite of mesoscopic (handspecimen- to outcrop-scale) planar and linear fabric elements including: (1) compositional layering (mapped as bedding by all workers) and a subparallel foliation defined by the parallel alignment of platy minerals (micas and graphite) in phyllite and phyllitic parting on quartzite surfaces (S_p , the subscript "p" refers to "prominent"); (2) open to isoclinal folds of both compositional layering and foliation but with an axial planar foliation indistinguishable from S_p and parallel to it [including gleitbrett folds of Green and McTaggart (1960), McTaggart (1960), and Green (1971)]; (3) a second, more widely spaced foliation (S_p') that is generally inclined to S_p (with consistent sense of inclination) and deflects it, but is also asymptotic with it, creating sigmoidal foliation domains and boudins of compositional layering; and (4) a pronounced northwest- to west-trending quartz rodding and mineral streaking lineation contained within all of the forementioned planar elements (L_p).

The earliest fabrics are folded by northwest-trending, northeast-vergent tight to isoclinal D_{p+1} folds and locally disrupted by D_{p+1} shear zones (D_{p+1}). This phase of deformation is responsible for the laterally discontinuous outcrop pattern of the "Keno Hill quartzite" on Keno Hill. Boyle (1957) inferred that the lateral discontinuity of the quartzite reflects stratigraphic facies changes. Later, McTaggart (1960) and Green and McTaggart (1960) suggested that the lateral termination was due to isoclinal folding around south- to southwest-plunging hinges. The 1991 mapping shows that the base of the quartzite is folded around the hinge of a southeast-trending and -plunging northeast-overturned isoclinal antiform. The structurally inverted limb of the antiform is characterized by southeast-trending and -plunging, southwest-vergent folds ranging in scale from outcrop to 1:50 000 scale (Fig. 3). The inverted limb heads back toward Keno Hill where it is folded back to the southeast by the closure mapped by McTaggart (1960) east of Wernecke. The base of the quartzite then passes through a second antiform-synform pair before it re-emerges into a long, structurally upright limb that heads northeastward into the Patterson Range (Fig. 2, 4).

D_{p+1} shear zones or isoclinal folds are responsible for the imbrication of the Robert Service thrust above the "Keno Hill quartzite". D_{p+1} fabrics within these shear zones are indistinguishable from D_p fabrics except that they deform L_p and verge to the northeast rather than to the northwest or west.

Kinematic interpretation

The geometry of the fabric elements produced during the earliest phase of deformation implies top-to-the-northwest or -west shearing. S_p' is interpreted as an extensional crenulation or shear band cleavage; its sense of inclination and sense of shear imply a top-to-the-northwest or -west transport direction, parallel to L_p . Fold tightness varies from open to isoclinal and fold hinges range in orientation from perpendicular to L_p to parallel to L_p . Folds with hinges most inclined to L_p are generally more open and uniformly northwest- or west-vergent. Quartz veins in quartzite are either folded or extended into boudins depending on their orientations; the geometry of their deformation also is compatible with top-to-the-northwest or -west shear.

Although morphologically identical to D_p fabrics, D_{p+1} fabrics suggest top-to-the-northeast shearing.

Relationship of high-strain fabrics to thrust faulting

The distribution of D_p fabrics implies a genetic relationship with the Tombstone thrust. These fabric elements are exhibited by all of the rocks in the Keno Hill region, extending structurally downward from well into the Hyland Group in the hanging wall of the Robert Service thrust sheet, through the "Keno Hill quartzite" and into structurally deeper

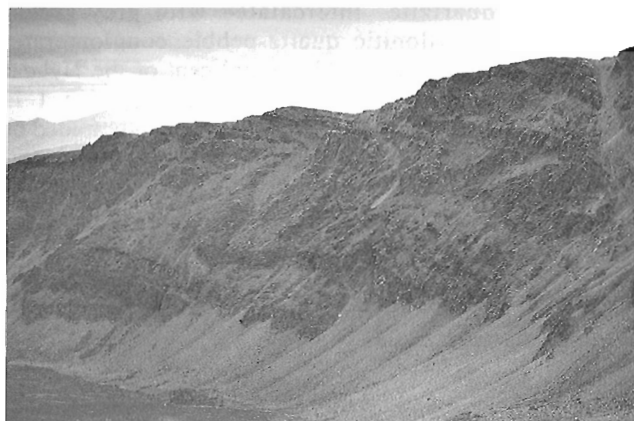


Figure 3. Oblique view of second-order northeast-trending, southwest-vergent fold pair on overturned limb of antiform northeast of Mt. Hinton. View is to the south.

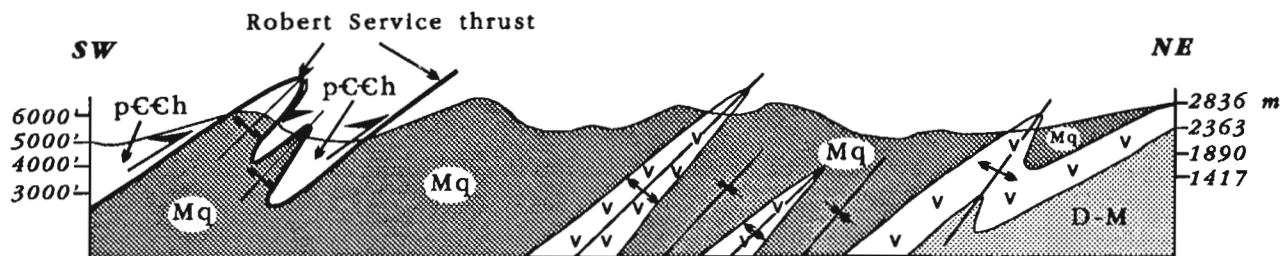


Figure 4. Simplified northeast-trending cross-section illustrating the geometry of D_{p+1} folds of the "Keno Hill quartzite". Location shown in Figure 2.

rocks to the northeast. In the deeper structural levels exposed in the Mt. Westman map area northeast of Keno Hill, Abbott (1990) mapped weakly deformed carbonaceous clastic rocks intruded by Middle Triassic(?) sills. According to Abbott (1990 and pers. comm., 1991), the intervening strain discontinuity coincides with the Tombstone thrust.

The distribution of Tombstone thrust fabrics suggests forelandward propagation of thrust faulting. Because rocks of the structurally higher Robert Service thrust sheet are deformed by these fabrics, the Robert Service sheet must have been emplaced before the onset of displacement on the structurally deeper, more forelandward Tombstone thrust.

The latest high-strain fabrics (D_{p+1}) suggest that the direction of displacement of the Tombstone thrust sheet changed from northwest- or west-directed to northeast-directed late in its movement history.

The location of the Tombstone thrust in the Keno Hill region is not well defined. As the rocks in the Keno Hill area possess the pronounced foliation and lineation of the hanging wall of Tombstone thrust, the thrust either lies outside the Mayo map area, or is in the valley of the Keno-Ladue River between Keno Hill and the southern slopes of the Davidson Range (Fig. 2).

Late open folding

Structures of the two early phases of deformation are folded by two, possibly coeval, phases of open folding, one north-northeast-trending and the other northwest-trending. These two phases of folding are defined by continuous changes in orientation of lithotectonic units and fabric

elements across the northern part of the Mayo map area (Fig. 5). S_p strikes essentially east-west from Haldane Creek to Keno City, northwest-southeast from Keno City to Mayo Lake, and northeast-southwest from Mayo Lake to the Patterson Range. Within S_p , L_p trends and plunges east-southeasterly from Galena Creek eastward to Keno City, trends northwesterly and plunges to both the northwest and southeast from Keno City southeast to Mayo Lake, and trends and plunges southeasterly from Mayo Lake northeastward into the Patterson Range.

High-angle faulting and mineralization in the Keno Hill district

Two phases of faulting cut the rocks of the Keno Hill region. Most early workers mapped a northeast-trending fault in the valley of the South McQuesten River to account for discontinuity of the "Keno Hill quartzite" across the valley (Fig. 2). The mineralized veins around Keno and Galena hills mostly parallel this trend and become more common towards the valley. To account for the discontinuity in the trend of the "Keno Hill quartzite" between the Mt. Haldane and Galena Creek regions, early workers also mapped a north-northeast-trending fault in the valley of Haldane Creek (Fig. 2). The fault hosting mineralization in the Mt. Haldane camp parallels this trend. The parallelism of mineralized veins to mappable faults and the increase in their density near the faults implies a genetic relationship.

A structural model for the Keno Hill district by Lynch (1989) related Keno Hill vein faults to syn-thrusting wrench-style brittle-ductile shear zones. He proposed that the Keno Hill vein faults formed in a northeast-trending sinistral

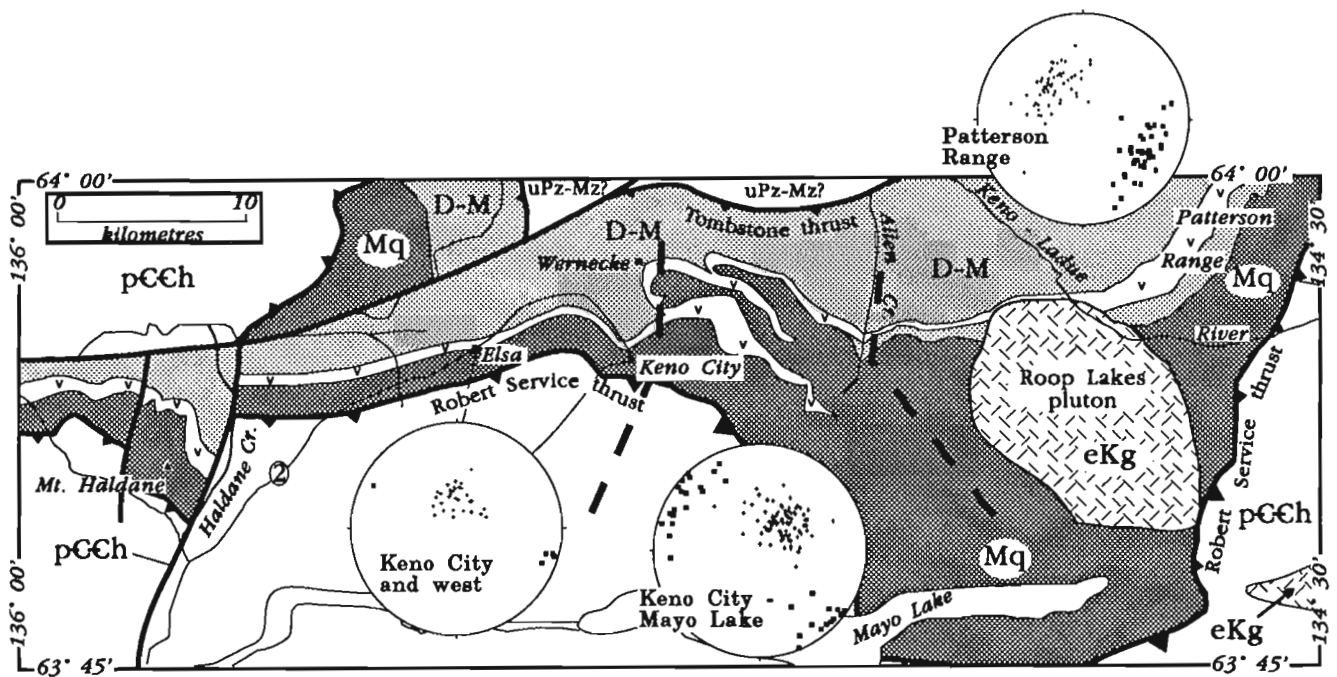


Figure 5. Equal-area stereoplots illustrating the change in orientation of the prominent early foliation, S_p (crosses) and the prominent early lineation, L_p (squares) in the region around Keno Hill. Heavy dashed lines are dip-domain boundaries (approximately the axial surface traces of late open folds).

brittle shear zone having a conjugate relationship to a dextral shear zone inferred to occur in the region east of Keno Hill. The dextral shear zone is inferred on the basis of a change in orientation of early fold hinges. Although the suggestion that the vein faults form a sinistral brittle shear zone is likely correct, there are no data to support the occurrence of a dextral shear zone east of Keno Hill; the changes in orientation of early linear fabrics is due to late warping of the planar elements (S_p) that contain them (Fig. 5).

STRATIGRAPHY OF THE ROBERT SERVICE THRUST SHEET

This structural unit is named after Robert Service Mountain, about 75 km northeast of Dawson, where the Cambrian and older Hyland Group overlap Triassic limestone and shale on a moderately south-dipping zone of thrust faults. In this area, the hanging wall Hyland Group is successively overlain by lower Paleozoic Kechika and Road River stratigraphy with as much as 50 km of overlap.

In the Mayo area all rocks south of the "Keno Hill quartzite" are considered part of this thrust sheet (Fig. 1). The sole fault is not well defined: the "Keno Hill quartzite" is overlain by a variety of units (Green, 1971) and these may represent a zone of complex imbrications as discussed above.

The Robert Service thrust sheet may be divided into two or three structural panels, each with a distinctive stratigraphy and structural style. The two northerly panels contain only Hyland Group – mostly quartzose schist, chlorite-muscovite schist, minor limestone and muscovite or graphite phyllite (Roots, 1991). The area south of Nogold Creek and Big Kalzas Lake is less deformed than the northern panels and includes lower to middle Paleozoic strata.

MAP UNITS IN SOUTHERN MAYO MAP AREA

The Paleozoic succession of folded siltstone, chert, sandstone, and conglomerate extends from adjacent map areas: Glenlyon to the south (105L, Campbell, 1967) and Tay River to the southeast (105K, Gordey, 1987); however broad

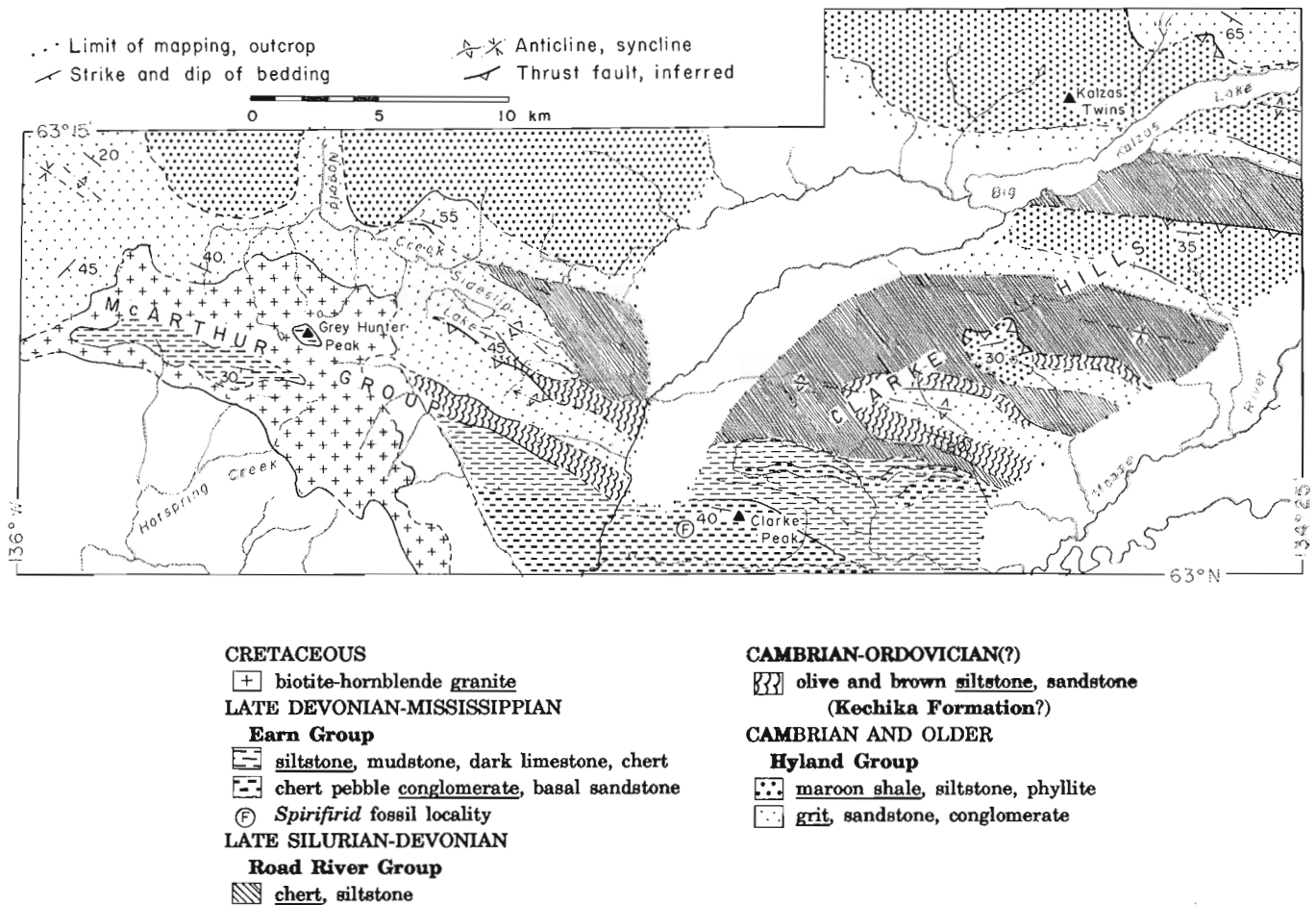


Figure 6. Geology of southern Mayo map area based on 1991 fieldwork.

valleys and vertical faulting in Mayo map area preclude continuous tracing of strata. A single fossil of Mississippian age (i.e., Earn Group) was located in southern Mayo map area (Fig. 6). Other units were identified where distinctive lithology could be matched using published descriptions from adjoining areas, and by personal communication with co-workers.

Hyland Group

Coarse blue-quartz-granule sandstone, conglomerate, and phyllite occur in a broad belt from northwest of Dawson to the Nahanni map area where the unit is defined by Gordey (in press). The Hyland Group is the off-shelf correlative of the Windermere Supergroup and underlies the main part of the lower Paleozoic Selwyn Basin.

In southern Mayo map area the Hyland Group has two parts: a lower unit of medium and thick beds of quartz grit and sandstone (locally bearing 5-10% blue quartz granules) and about a third siltstone, and an upper unit of maroon argillite and siltstone. The maroon argillite is strongly cleaved and bedding is difficult to identify except where white sandstone is interbedded (Fig. 7). In the southern Ogilvie Mountains north of Dawson, Hyland Group maroon argillite contains the trace fossil *Oldhamia* of Middle Cambrian age.

Cambrian-Ordovician unit

Olive and brown siltstone with black laminae, as well as brown and green sandstone overlie the maroon argillite. Bedding surfaces of this unit are coated with trace fossil imprints (*Planelites sp.*). Near the top are thin beds of black bioturbated chert with a knobby appearance.

Cambrian-Ordovician Kechika and Rabbitkettle formations (Gordey, 1987) occur on Dromedary Mountain, 30 km southeast of Clarke Peak. Thick-bedded or massive light brown quartz siltstone is overlain by about 200 m of distinctively banded green and mauve siltstone and carbonate. In Mayo map area only massive, nondescript siltstone is present.



Figure 7. Maroon argillite with planar crossbedded quartz sandstone interbeds of the upper Hyland Group. From 3 km south of the east end of Big Kalzas Lake.

Road River Group

This widely distributed unit characterizes the Selwyn Basin in central Yukon (Cecile, 1982, p. 19-23). In southern Mayo map area its base is drawn below the first occurrence of continuous chert beds. The chert is typically black, but ranges from light grey and green to light blue. Black mudstone forms intercalations (Fig. 8). Grey weathering argillaceous siltstone and black siltstone are common near the top.

Road River Group undergoes facies changes according to the depositional site within Selwyn Basin, and formation names have been given to various facies. The lithology in Clarke Hills area resembles the Duo Lake Formation mapped to the southeast along strike by Gordey (1987). Characteristic orange-weathering, green siltstone marker and graptolite-bearing beds noted by Gordey (1987) have not been found in Mayo map area.

Earn Group

These marine turbiditic chert-rich clastic sedimentary rocks are widely distributed across central Yukon and north-central British Columbia. They were deposited in late Devonian to mid-Mississippian time and were probably derived from underlying Road River rocks to the west (Gordey et al., 1982). In Mayo area as much as 1 km of clastic and carbonate strata are probable with lenses of chert-pebble conglomerate up to several hundred metres-thick and several kilometres-long (?Crystal Peak Formation; Gordey, 1987).

The base of the Earn Group is a brown-weathering fine-grained sandstone and siltstone unit with rare chert pebbles. It is overlain by 500 and 1000 m of fissile black mudstone containing thin lenses of chert-pebble conglomerate, horizons of barite matrix chert breccia, and dark grey, fetid limestone.

The upper part consists of black sandstone and grit containing chert fragments, overlain by chert-pebble conglomerate and beige sandstone. Conglomerate beds are 2-6 m thick and contain subrounded pebbles of black, brown,



Figure 8. Thin-bedded chert with shaly intercalations. These beds, considered to be Road River group, typically have trace fossil imprints on under-surfaces. Locality is 5 km south of the east end of Big Kalzas Lake.

and green chert 0.5-2.0 cm in diameter, closely packed with white calcareous or limonitic matrix. The stratigraphically highest beds, southeast of Clarke Peak, are a black fissile siltstone with a light-grey weathered surface. A *Spiriferid* brachiopod fossil from this unit is similar to Middle Mississippian brachiopods about 23 km to the southeast (S.P. Gordey, pers. comm., 1991).

McArthur Group pluton

The McArthur Group is a series of prominent mountain ridges in southwestern Mayo map area (Fig. 9). These are underlain by post-tectonic granite and resistant rocks of the adjacent contact metamorphic aureole. Most of the pluton consists of medium-grained biotite-hornblende white granite, locally with potassium feldspar phenocrysts to 1 cm long. Alaskitic dykes are common in the pendants and along the margin. The low-angle contact is visible in steep-walled cirques and four pendants of sedimentary rock underlie the highest peaks. It appears that erosion has only exposed the cupola of the intrusion.

STRUCTURAL NOTES

A series of southeast trending cylindrical folds expose the Paleozoic strata across southern Mayo map area. North-verging thrust faults are inferred along base of Hyland Group strata. One of these is exposed on the north side of the 1 km² klippe in Clarke Hills and dips 15° south.

The McArthur Group pluton is elongate, and may have intruded a weakened zone parallel to the Tintina fault, 10 km to the southwest.

IMPLICATIONS FOR MINERALIZATION

(1) Definition of the extent of the Tombstone thrust sheet

The extension of the Tombstone thrust is important to prospectors because: (1) the Earn Group, which hosts many of the stratiform base metal deposits in the Yukon, is now



Figure 9. Grey Hunter Peak, McArthur Group is a pendant of probable Earn Group, on a ridge of jointed granite intruding folded Road River and younger strata.

known to be part of its hanging wall and (2) the hanging wall also contains felsic metavolcanics locally exhibiting VMS mineralization (MARG; Turner and Abbott, 1990).

(2) Recognition of Earn Group strata in southern Mayo map area

In nearby Glenlyon sheet, Earn group strata host stratiform Pb-Zn mineralization (Dromedary Mountain). These deposits occur along the margin of Selwyn Basin (Mac Pass, Howards Pass).

(3) Placer gold in Hyland Group strata

Placer operations occur around Mayo Lake, on Davidson Creek, and near Francis Lake southeast of Mayo. This region is underlain solely by rocks of the Hyland Group. The gold may be derived from mantling Pleistocene glacial deposits, but original sources in the Keno Hill-Galena Hill area are unlikely because these high hills were not glaciated (Hughes, 1982). Instead the McConnell ice sheets moved westward through the valleys. Several of the creeks contain mostly angular fragments of Hyland Group and it could be that this unit, where pulverized (or structures within it) are the source of the gold.

ENVIRONMENTAL CONSIDERATIONS

Mayo map area contains discontinuous permafrost and consequently drainage is poor in wide valleys of glacial till. Nearby hills are typically felsenmeer-covered and dry. The rapid drainage from pyritic rocks, including old workings, is commonly diverted directly to valley bottoms where surface water becomes contaminated. At first this was not a serious hazard because minor carbonate in the host rock buffered potentially acidic water, and sulphate-producing bacteria were less common. Unless remedial steps are taken, the exothermic oxidation reaction will continue (BC AMD Task Force, 1990). Comparison modelling of water chemistry collected in the 1950s with current data would show the extent of acidification and heavy metal loadings.

ACKNOWLEDGMENTS

Fieldwork was funded through the Canada-Yukon Economic Development Agreement and facilitated by Steve Morison of Geology and Exploration Services, Department of Northern Affairs, Whitehorse. David Lucas of Mayo, Stephan Meinke and Fred Roots were able field assistants. We thank Archer Cathro and Associates (1981) Ltd., particularly Lasha Reid, and also Pat and J.D. Randolph of Nogold Farm for their hospitality and help with logistics. The promptness and precision of Trans-North helicopter pilots Dave Reid, Dave Holden and Jamie Bowles is appreciated. The first author is grateful to Betty Lucas, Sharon MeHaffy, Bob Leckie, and Neil Davies for introductions to the community and to Steve Gordey for stratigraphic advice.

REFERENCES

Abbott, J.G.

1990: Geological map of Mt. Westman map area (106D/1); Indian and Northern Affairs Canada, Open File 1990-1.

BC AMD Task Force

1990: Draft acid rock drainage technical guide, v. I and II; British Columbia Acid Mine Drainage Task Force Report, published by Environment Protection, Environment Canada and the Government of British Columbia.

Bostock, H.S.

1947: Mayo, Yukon Territory; Geological Survey of Canada, Map 890A.

Boyle, R.W.

1957: The geology and geochemistry of the silver-lead-zinc deposits of Galena Hill, Yukon Territory; Geological Survey of Canada, Paper 57-1.

Campbell, R.B.

1967: Geology of Glenlyon map area, Yukon Territory; Geological Survey of Canada, Memoir 352.

Cecile, M.P.

1982: The lower Paleozoic Misty Creek Embayment, Selwyn Basin, Yukon and Northwest Territories; Geological Survey of Canada, Bulletin 335.

Gordey, S.P.

1987: Geology of Sheldon Lake and Tay River map areas, Yukon Territory; Geological Survey of Canada, Map 19-1987.

1990: Geology of Tiny Island Lake map area (105M/16), Yukon; Indian and Northern Affairs Canada, Exploration and Geological Services Division, Open File 1990-2.

in press: Evolution of the northern Cordilleran miogeocline, Nahanni map area (105I) Yukon Territory and District of Mackenzie; Geological Survey of Canada, Memoir 428.

Gordey, S.P., Abbott, J.G., Tempelman-Kluit, D.J., and Gabrielse, H.

1982: "Antler" clastics in the Canadian Cordillera; *Geology*, v. 15, p. 103-107.

Green, L.H.

1971: Geology of Mayo Lake, Scougale Creek, and McQuesten Lake map areas, Yukon Territory; Geological Survey of Canada, Memoir 357.

Green, L.H. and McTaggart, K.C.

1960: Structural studies in the Mayo district, Yukon Territory; *Proceedings of the Geological Association of Canada*, v. 12, p. 119-134.

Hughes, O.L.

1982: Surficial geology and geomorphology, Janet Lake (scale 1:100 000); Geological Survey of Canada, Map 4-1982.

Lynch, J.V.G.

1989: Hydrothermal zoning in the Keno Hill Ag-Pb-Zn vein system: a study in structural geology, mineralogy, fluid inclusions, and stable isotope geochemistry; Ph.D thesis, University of Alberta, Edmonton.

McTaggart, K.C.

1960: The geology of Keno and Galena hills, Yukon Territory (105M); Geological Survey of Canada, Bulletin 58.

Mortensen, J.K. and Thompson, R.I.

1990: A U-Pb zircon-baddeleyite age for a differentiated mafic sill in the Ogilvie Mountains, west-central Yukon Territory; in *Radiogenic Age and Isotopic Studies: Report 3*, Geological Survey of Canada, Paper 89-2, p. 23-28.

Poole, W.H.

1965: Mount Haldane (105M/13) and Dublin Gulch (106D/4) map areas; in *Report of Activities, Field, 1964*; Geological Survey of Canada, Paper 65-1, p. 32-34.

Poulton, T.P. and Tempelman-Kluit, D.J.

1982: Recent discoveries of Jurassic fossils in the Lower Schist Division of central Yukon; in *Current Research, Part C*; Geological Survey of Canada, Paper 82-1C, p. 91-94.

Roots, C.F.

1991: A new bedrock mapping project near Mayo, Yukon; in *Current Research, Part A*; Geological Survey of Canada, Paper 91-1A, p. 255-260.

Tempelman-Kluit, D.J.

1970: The stratigraphy and structure of the "Keno Hill quartzite" in Tombstone River-Upper Klondike River map areas, Yukon Territory; Geological Survey of Canada, Bulletin 180.

Turner, R.J.W. and Abbott, J.G.

1990: Regional setting, structure, and zonation of the Marg volcanogenic massive sulphide deposit, Yukon; in *Current Research, Part E*; Geological Survey of Canada, Paper 90-1E, p. 31-41.

Geological Survey of Canada Project 900035

Progress report on the project in comparative metallogenesis and tectonics of the U.S.S.R. Far East, Alaska and the Canadian Cordillera

Kenneth M. Dawson
Mineral Resources Division, Vancouver

Dawson, K.M., 1992: Progress report on the project in comparative metallogenesis and tectonics of the U.S.S.R. Far East, Alaska and the Canadian Cordillera; in Current Research, Part A; Geological Survey of Canada, Paper 92-1A, p. 173-177.

Abstract

Representatives of the Geological Survey of Canada, United States Geological Survey and Alaska Division of Geological and Geophysical Surveys spent four weeks in July-August of 1991 in productive working visits to three Institutes of the Far East Branch of the U.S.S.R. Academy of Sciences, as part of a joint tectonic-metallogenic map project encompassing the northern circum-Pacific regions of the three countries. Productive discussions in Magadan and Vladivostok emphasized the tectonic environments of terranes, comparisons of specific terranes and mineral deposit models, and relationships between metallogeny and terrane tectonics. Preparation of manuscript maps, terrane sections and descriptions and mineral deposit tables is well advanced. Four field excursions were taken in the Magadan and Primor'ye regions. A workshop planned for the summer of 1992 in Anchorage will allow finalization of publications.

Résumé

Des représentants de la Commission géologique du Canada, de la United States Geological Survey et de l'Alaska Division of Geological and Geophysical Surveys ont passé quatre semaines, en juillet-août 1991, à effectuer des visites productives dans trois instituts de la Direction de l'Académie des Sciences de l'U.R.S.S. pour l'Extrême-Orient, dans le cadre d'un projet conjoint de cartographie tectonique-métallogénique englobant les régions circumpacifiques septentrionales des trois pays. Les discussions productives tenues à Magadan et à Vladivostok ont surtout porté sur les milieux tectoniques des terranes, sur les comparaisons entre des terranes spécifiques et les modèles de gisements minéraux, et sur les relations entre la métallogénie et la tectonique des terranes. La préparation des cartes manuscrites, les coupes et les descriptions des terranes et les tableaux relatifs aux gisements minéraux en sont à une étape avancée. On a effectué quatre excursions sur le terrain dans les régions de Magadan et de Primor'ye. Un atelier est prévu pour l'été 1992 à Anchorage, pour la mise au point finale des publications.

INTRODUCTION

Joint geological research agreements, signed in 1988 by representatives of governments of U.S.A. and U.S.S.R., initiated scientific exchanges on comparative studies of ophiolites and metallogenic provinces in the U.S.S.R. Far East and Alaska. Visits by an Alaskan tectonic-metallogenic group to institutes and mines in the U.S.S.R. Far East in 1989 (Bundtzen et al., 1990) was followed by two visits to Alaska by Soviet scientists in 1990, and to the McKelvey Forum in Nevada in 1991 (Grybeck et al., 1991). Representatives of the Geological Survey of Canada, invited to join the 1:5 million map project in 1990, include K.M. Dawson of the Mineral Resources Division (metallogenic maps) and J.W.H. Monger and S.P. Gordey of the Cordilleran Division (tectonic maps).

Working visits to offices of the Academy of Sciences and the Ministry of Geology in Magadan, Vladivostok and Khabarovsk, between July 22 and August 20, 1991, were made by members of the metallogenesis team: Warren J. Nokleberg, U.S.A. Project Chief, U.S.G.S. Branch of Alaskan Geology, Menlo Park; Donald J. Grybeck, U.S.G.S. Branch of Alaskan Geology, Anchorage; Thomas K. Bundtzen, A.D.G.G.S. Fairbanks; and the writer. The team travelled to Magadan from Anchorage on one of Alaska Airlines' new summer excursion flights, but returned from Khabarovsk two days early because of uncertainties surrounding the attempted coup.

OBJECTIVES

Regional metallogenic studies over the past two decades in western North America have incorporated plate tectonic theories in assessing the origin, distribution and potential of mineral resources. A fertile field for the application of terrane-based metallogenic analysis is the Far Eastern region of the U.S.S.R. where proximity to Alaska, contiguity of the two continental shelves and similarities in geology have encouraged geologists from both continents to speculate on the continuity of tectonic and metallogenic trends. Comparisons have been restricted in the past by the classified status of detailed geological and mineral deposit data in the Far East, and the predominance, until recently, of classical tectonic theories over modern plate tectonic terrane analysis in the Soviet Union.

The emergence of an expanding group of 'mobilists' in Moscow and the Far East Branch of the U.S.S.R. Academy of Sciences, and the initiatives of these geologists and managers in establishing working relationships with their North American counterparts, has led to the establishment of this joint tectonic-metallogenic map project. In addition to addressing traditional questions of geologic continuity between northeastern U.S.S.R. and Alaska, the project will establish international tectonostratigraphic and metallogenic legends, assign tectonic environments to terranes, and attempt to correlate terranes, igneous arcs, mineral deposit models and metallogenic belts between the two continents. Substantial interest has already been expressed by the exploration community in planned project publications.

LOCATIONS VISITED

Magadan meetings

The team's first visit was to Magadan, population about 170 000, the administrative centre of the large (ca. 1 million km²) Magadan Oblast or province (Fig. 1).

Twelve days of working sessions at the offices of the North-East Interdisciplinary Science Research Institute of the U.S.S.R. Academy of Sciences were interspersed with two days of field excursions. Hosts and co-authors from the Academy were Anatoly Siderov, Director; Roman Eremin; Stanislav Byalobzhesky; Vladimir Shpikerman; and Tatyana Velikoda, interpreter. Project participants from the R.S.F.S.R. Ministry of Geology were Ilya Rozenblyum, Chief Geologist; Gleb Sosunov and Mary Gorodinsky. The Magadan group presented an excellent manuscript plate tectonic-magmatic map of northeastern U.S.S.R., location maps of 250 lode and 70 placer deposits and a detailed table of deposit descriptions in English and Russian. The release of this volume and standard of data will contribute greatly to the quality of the planned publications. Presentation of Alaskan and Canadian data followed, comparisons were made and legends established. Routine discussions were enlivened by enthusiastic comparisons of terranes, metallogenic belts and post-amalgamation igneous arcs.

Skolnoye Au mine

A helicopter trip to the Skolnoye (schoolboy) Au mine 200 km northwest of Magadan allowed aerial views of several placer and lode Au mines of the Kolyma River district, some of which were 'gulags' operated as prison mines by the infamous Far Eastern Construction Company during the Stalin era. Gold mines of the Magadan region, dominantly placer, currently produce about 77 760 kg or 25% of total U.S.S.R. gold production (Bundtzen et al., 1990). The underground mine produces a modest 200 tonnes/day from a single vein system 10 m wide, 400 m long and 600 m deep. High grade ore, averaging 30 g/t Au, is transported by truck 80 km to a concentrator. Fracture-controlled veins are hosted by hornfelsed and folded Permo-Triassic clastic and volcanoclastic sediments, a Lower Jurassic granodiorite stock and related dykes. Quartz-sericite enveloped quartz veins contain, in addition to free Au, an assemblage of pyrite-arsenopyrite-boulangerite-jamesonite ± molybdenite, wolframite. Exploration is under way and expansion is planned. The excursion was led by district geologist M. Zinnatulín.

Magadan batholith

A second field excursion was two half-day road trips to beach cliff exposures of the Magadan Massif, a granitoid batholith which, like the Skolnoye stock, is within the inner zone of the Okhotsk-Chukotka volcanic-plutonic belt, a late Paleozoic-late Mesozoic post-accretionary igneous arc. The dominantly mid- to Late Cretaceous, granodiorite-tonalite,

magnetite-series plutons are zoned compositionally inward from a Benioff zone related to the Japan arc. The excursions were led by petrologists M.L. Gilman and N.V. Andreyeva.

Vladivostok meetings

On August 5, the North American team arrived in Vladivostok, a cosmopolitan city of 1 million inhabitants and an important seaport and naval base (Fig. 1). Our hosts and co-authors at the Far East Geological Institute of the U.S.S.R. Academy of Sciences were Ivan Nekrasov, Director, Alexander Khanchuk, Deputy Director; Vladimir Ratkin; Ivan Panchenko; and Lydiya Kovbas, interpreter. The Vladivostok group presented a plate tectonic-magmatic map of southeastern U.S.S.R. including Prior'ye, Khabarovsk and eastern Amur (Fig. 1), lode and placer deposits location maps, and detailed descriptions of 80 significant mineral deposits. Their first draft, when completed in the spring of 1992 and combined with similar high quality data from the Magadan group, will constitute the U.S.S.R. portion of a planned map series at 1:5 million scale of the entire circum-North Pacific region. The first week of Vladivostok working sessions, involving detailed reviews of tectonic and metallogenic data from southeastern U.S.S.R., Alaska and the Canadian Cordillera, continued during a weekend visit to an oceanographic research station at Popov Island.

The second week of sessions, a workshop for the preparation of a draft of the tectonostratigraphic terrane map of the North Pacific, included participation by co-authors from other centres including: Leonid Parfenov (Academy of

Sciences, Yakutsk), Boris Natalin (Academy of Sciences, Khabarovsk) and Lev Natapov (Ministry of Geology, Moscow). Stimulating discussions revealed several interesting correlations in terranes, igneous arcs and metallogenic belts between the two continents.

Voznesenka fluorite mine

When the map team made a two-day excursion to the Voznesenka (Ascension) fluorite mine 200 km northeast of Vladivostok, it was the first visit by North Americans to one of the world's largest fluorite deposits. The Voznesenka open pit, with mining reserves of 500 000 tonnes of 40-42% CaF₂, sends 5000 tonnes of ore per day to the concentrator, providing 72% of fluorite production in the U.S.S.R. A second large deposit and several prospects are not yet developed.

The fluorite deposits are hosted by lower Paleozoic shelf sediments derived from the Siberian craton, now part of the Bureya-Khanka superterrane which was amalgamated in Permian time. Pre-amalgamation, Silurian to Early Devonian Li,F-rich granite intruded a folded Cambrian limestone-shale sequence and generated fluorite greisen replacements along granite-limestone contacts. The micas muscovite, zinnwaldite and lepidolite are recovered and stockpiled. Adjacent deposits include stratiform (sedex?) Zn, Pb occurrences, formerly producing Sn,F polymetallic veins in granite and a large Nb,R.E.E. vein system in granite, under development.

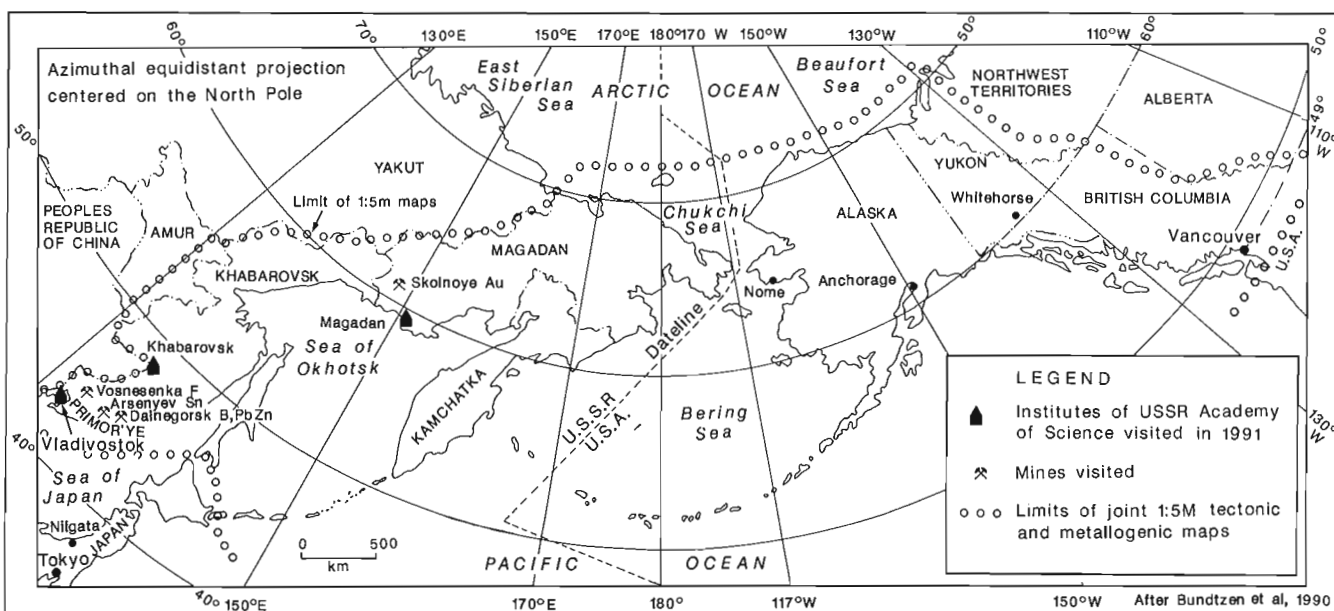


Figure 1. Limits of mapping under the comparative metallogenesis and tectonics of the U.S.S.R. Far East, Alaska and the Canadian Cordillera. A joint project of the Far East Branch of the Academy of Sciences of the U.S.S.R., Magadan, Vladivostok, Khabarovsk, Yakutsk, and Petropavlovsk; the U.S.S.R. Ministry of Geology, Moscow; the R.S.F.S.R. Ministry of Geology, Magadan; the United States Geological Survey, Branch of Alaskan Geology; the Alaska Division of Geological and Geophysical Surveys; and the Geological Survey of Canada, Mineral Resources and Cordilleran Divisions.

Dalnegorsk B, AgPbZn and Kavalerovo Sn districts

During the terrane workshop sessions, a five-day excursion was taken to mines of the Primor'ye region, 300-400 km northeast of Vladivostok (Fig. 1). The writer was accompanied by regional geologist Gennady Vasilenko and his daughter Anya, interpreter. First visited was the large Bor boron skarn at Dalnegorsk, hosted by an Upper Triassic limestone knocker enclosed by Lower Cretaceous turbiditic clastics of the Coastal terrane, a disrupted accretionary melange. The skarn orebody, 400 m by 3000 m by 700 m deep and consisting essentially of concentrically zoned intergrowths of datolite, wollastonite, andradite and hedenbergite, formed in a thermal aureole overlying alkalic granitoid stocks and dykes of Late Cretaceous age and elevated boron content. The integrated open pit mine-metallurgical complex produces about 180 000 tonnes per year of at least 10 boron products, constituting about 80% of U.S.S.R. production and providing exports to Japan and Europe.

The adjacent Nikolayvsky mine, whose production is being increased from 1.5 to 2 million tons of Ag-rich Pb-Zn ore per year, is one of eight economic base metal skarn deposits in the Dalnegorsk district. Lead-zinc ore averages 30-50 g/t Ag but Ag-sulphosalt ores attain grades of 10 kg/t Ag. Like the Bor deposit, the Ag,Pb,Zn skarns are hosted by Triassic limestone knockers, some of which attain 7 km in maximum dimension. The deposit is zoned vertically with Ag decreasing and Cu,Bi increasing with depth. Although

associated with datolite and other borosilicates, the Ag,Pb,Zn skarns are interpreted to be about 10 Ma younger than the B skarns, and related to Upper Cretaceous-Paleocene subvolcanic intrusions of the East Sikhote-Alin volcanic belt (V.V. Ratkin and A.I. Khanchuk, written comm., 1991).

Last visited was Arsenyev Sn mine, the largest of six producing polymetallic Sn vein deposits in the Kavalerovo district. A central concentrator recovers about 900 000 tonnes per year of cassiterite and stannite concentrates from Sn oxide and Sn,Pb,Zn,Cu sulphide ores of the district, accounting for about 20% of Sn produced in the U.S.S.R. Sn veins occur within the late Albian Luzhinsky fold belt, hosted by siltstone and sandstone of a post-accretionary lower Cretaceous clastic sequence, the upper part of a Triassic to lower Cretaceous oceanic terrane. Northwest faults are the dominant control for several stages of Sn veins and intramineral andesite and rhyolite dykes. A large granitoid pluton is inferred to underlie the Arsenyev deposit (Khanchuk et al., 1989).

The last day of the Vladivostok terrane workshop was disrupted by announcements of the coup in Moscow, and the North American team departed by overnight train to Khabarovsk (Fig. 2) with some apprehension. A visit to the Institute of Tectonics and Geophysics the following day was curtailed by the opportunity to make an early departure for Anchorage. Concerns for the future of the map project and our co-workers were allayed by subsequent events.



Figure 2. North American mapping team members bid farewell to some Soviet co-authors and friends at the train station in Vladivostok. News of the coup in Moscow had been received a few hours earlier.

PLANNED PUBLICATIONS

1. A tectonostratigraphic terrane map of the Canadian Cordillera with principal lode and placer deposits, accompanying legend, terrane stratigraphic columns and descriptions and deposit table, at scale 1:5 million, will be published as a G.S.C. open file in the spring of 1992.
2. A tectonostratigraphic terrane map of the circum-North Pacific (U.S.S.R. Far East, Alaska, Canadian Cordillera) region, accompanying metallogenic belt map, lode and placer deposits maps, legend and deposit table, at scale 1:5 million, will be in first draft in the summer of 1992, released as a U.S.G.S. open file in late 1992 or early 1993, and as final coloured maps published simultaneously by the U.S.G.S. and U.S.S.R. in 1993-94.
3. A series of terrane tectonic and metallogenic maps of U.S.S.R. Northeast and mainland Alaska only, at scale 1:4 million, will be published jointly by the Alaska and Magadan-based map project participants. A first draft will be ready in the spring of 1992 followed by a U.S.G.S. open file and U.S.G.S. and U.S.S.R. coloured maps in 1993-94.

CONCLUSION

Significant progress on the joint U.S.S.R. Far East-Alaska-Canadian Cordillera comparative metallogeny and terrane tectonics map project was achieved during a visit to U.S.S.R. Far East by North American map team members in July-August 1991. The team was pleased to receive excellent manuscript maps and detailed mineral deposit data from

Soviet co-authors from several offices of the Academy of Sciences and the Ministry of Geology. Discussions revealed that many potentially correlative terranes, igneous arcs and metallogenic belts exist. Planned working visits to Anchorage and Vancouver by two groups of Soviet co-authors in the summer of 1992 will permit preparation of a first draft of 1:5 million maps. The unprecedented release of previously classified mineral deposit data, in conjunction with application of plate tectonic concepts, will permit, for the first time, a metallogenic comparison of the circum-North Pacific region.

REFERENCES

- Bundtzen, T.K., Swainbank, R.C., Deagen, J.R., and Moore, J.L.**
1990: Alaska's Mineral Industry, 1989; Alaska Division of Geological and Geophysical Surveys, Special Report 44, p. 68-71.
- Grybeck, D.J., Nokleberg, W.J., and Bundtzen, T.K.**
1991: Comparative metallogeny of the Soviet Far East and Alaska; in U.S.G.S. Research on mineral Resources-1991, Seventh Annual V.E. McKelvey Forum on Mineral and Energy Resources, United States Geological Survey, Circular 1062, p. 36.
- Khanchuk, A.I., Golozubov, V.V., Nevolin, P.L., Ratkin, V.V., and Kokorin, A.M.**
1989: Geology and tin occurrences of Kavalerovo Region in Primor'ye; Field trip guidebook, Tectonics, Energy and Mineral Resources of North-West Pacific Symposium, Far Eastern Branch of the Academy of Science of the U.S.S.R., Khabarovsk.
- Ratkin, V.V. and Khanchuk, A.I.**
1991: Lode mineral deposits of the southern U.S.S.R. Far East; written communication.

Geological Survey of Canada Project 740098

Major lithologies of the Ajax West pit, an alkalic copper-gold porphyry deposit, Kamloops, British Columbia¹

Katherina V. Ross², Kenneth M. Dawson,
Colin I. Godwin², and Lorne Bond³
Mineral Resources Division, Vancouver

Ross, K.V., Dawson, K.M., Godwin, C.I., and Bond, L., 1992: *Major lithologies of the Ajax West pit, an alkalic copper-gold porphyry deposit, Kamloops, British Columbia*; in *Current Research, Part A; Geological Survey of Canada, Paper 92-1A*, p. 179-183.

Abstract

Ajax West pit (50°37'N, 120°24'W), in the Afton mine district, lies 13 km west of Kamloops and 420 km northeast of Vancouver, B.C. The pit, on the southwestern side of the alkalic Iron Mask batholith, was developed on copper-gold mineralization at the intersection of three major rock units: two dioritic units of the Iron Mask pluton and a picritic unit of uncertain origin. Porphyry style mineralization is mainly pyrite and chalcopyrite with minor amounts of bornite and chalcocite. Alteration includes intense albitization and less intense K-feldspar, epidote and chlorite ± anhydrite and diopside.

Field work consisted of pit mapping at 1:750 scale and detailed core logging of representative sections. Eleven major lithologies are recognized and arranged in a preliminary chronological order, from oldest to youngest: (1) picrite, (2) monzodiorite, (3) Sugarloaf diorite, (4) pyroxene gabbro, (5) hybrid diorite, (6) pegmatitic hybrid diorite, (7) dioritic dykes, (8) plagioclase porphyry dykes, (9) Cherry Creek monzonite dykes, (10) magnetite-rich diorite dykes, and (11) quartz-eye latite dykes.

Future work will refine descriptions of the lithologies and explain alteration and structural relationships.

Résumé

Le puits de mine Ajax West (50°37'N, 120°24'W), situé dans le district minier d'Afton, se situe à 13 km à l'ouest de Kamloops et à 420 km au nord-est de Vancouver en Colombie-Britannique. Le puits, situé du côté sud-est du batholite alcalin d'Iron Mask, a été établi sur une minéralisation cuprifère-aurifère à l'intersection de trois grandes unités lithologiques: deux unités dioritiques du pluton d'Iron Mask et une unité picritique d'origine incertaine. La minéralisation de style porphyrique se compose principalement de pyrite et de chalcopyrite accompagnées de petites quantités de bornite et de chalcocite. L'altération inclut une intense albitisation et un degré moindre de formation de feldspath potassique, d'épidote et de chlorite ± anhydrite et diopside.

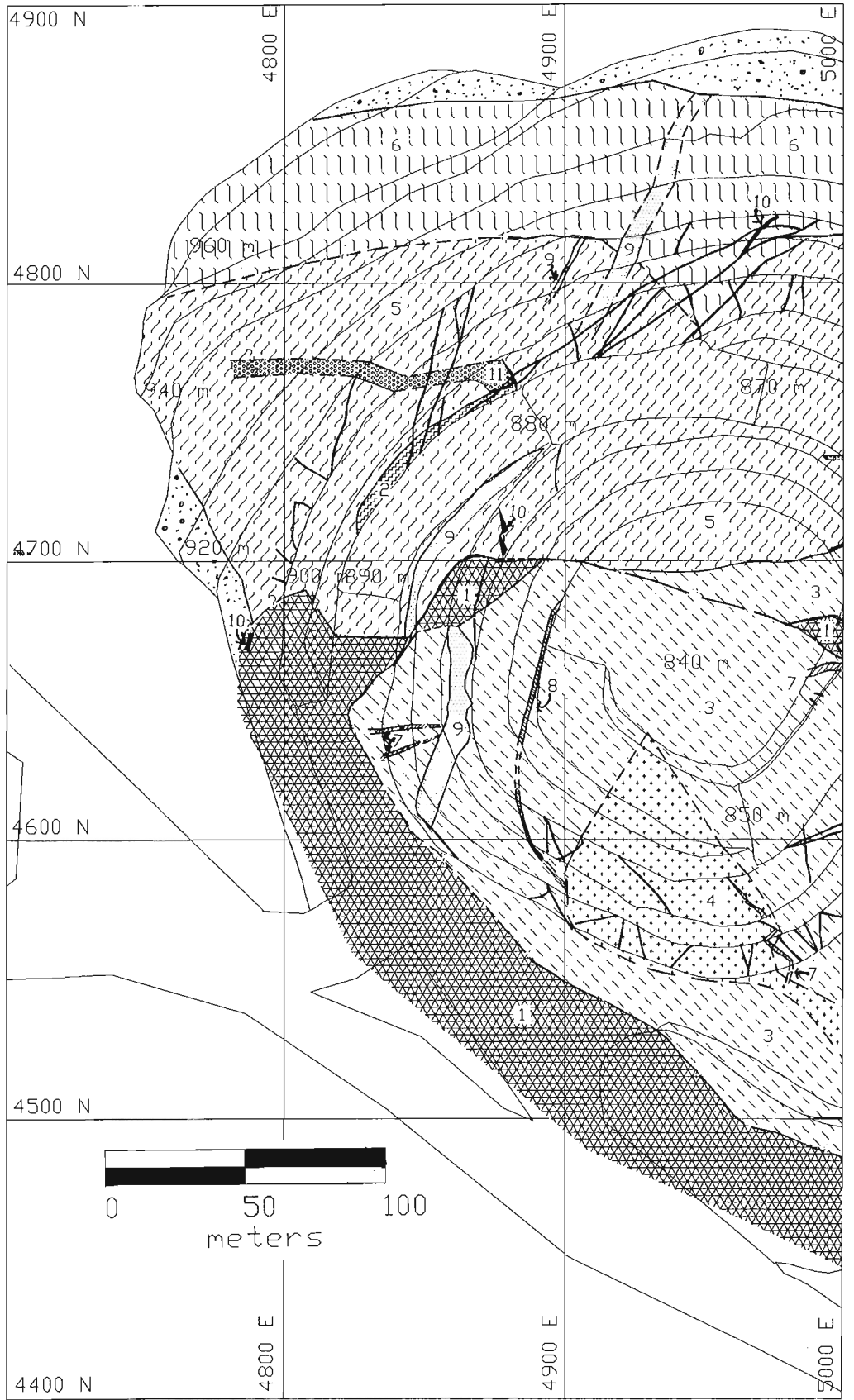
Les travaux sur le terrain comprenaient la cartographie du puits à l'échelle de 1/750 et la diagraphie détaillée de carottes de sondage prélevées dans des coupes représentatives. On a identifié onze grandes lithologies que l'on a disposées selon un ordre chronologique, de la plus ancienne à la plus récente: (1) picrite, (2) monzodiorite, (3) diorite de Sugarloaf, (4) gabbro à pyroxène, (5) diorite hybride, (6) diorite pegmatitique hybride, (7) dykes dioritiques, (8) dykes porphyriques à plagioclase, (9) dykes monzonitiques de Cherry Creek, (10) dykes dioritiques riches en magnétite et (11) dykes de latite à quartz ocellé.

La recherche future permettra d'affiner les descriptions des lithologies et d'expliquer l'altération et les relations structurales.

¹ Mineral Deposits Research Unit, Contribution No. 10.

² Mineral Deposits Research Unit, Department of Geological Sciences, University of British Columbia, 2449 Stores Road, Vancouver, B.C. V6T 2B4

³ Afton Operating Corp., P.O. Box 937, Kamloops, B.C. V2C 5N4



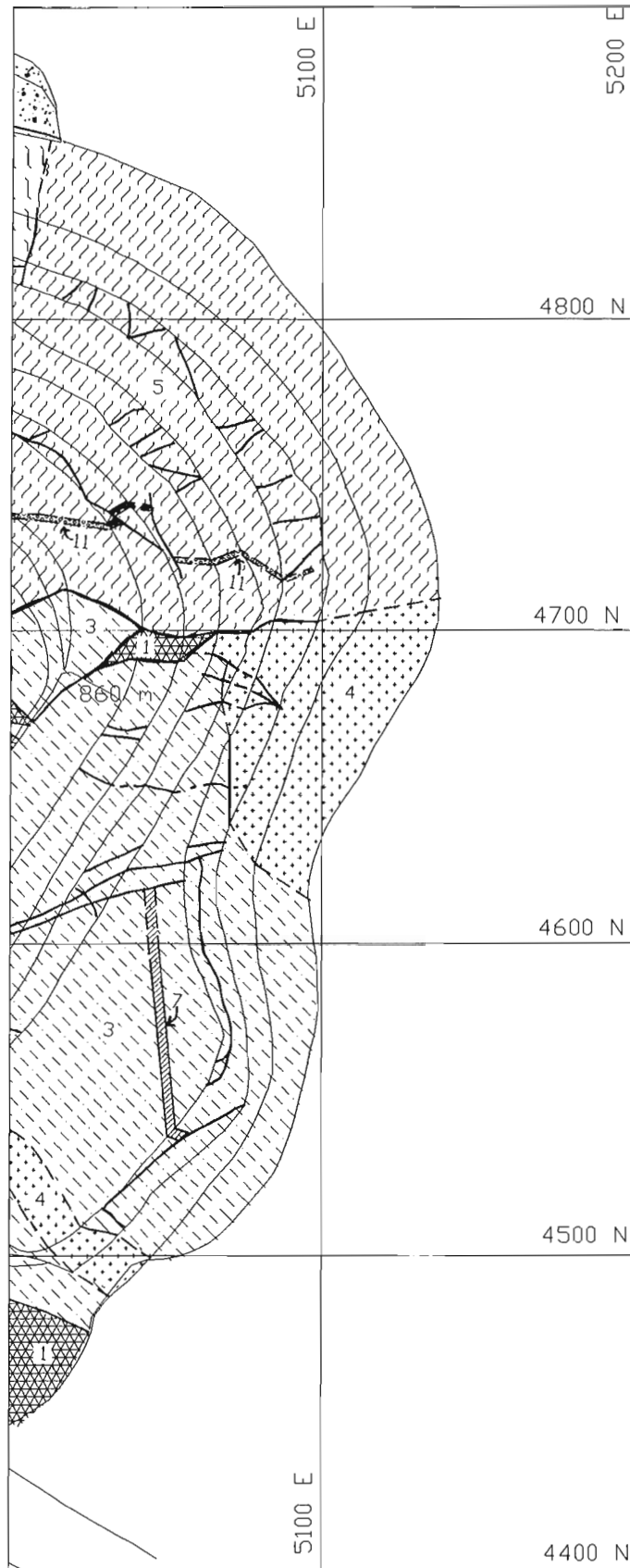
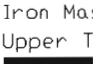
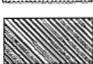


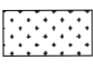

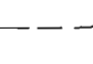




Figure 1. Geology of the Ajax West pit.

LEGEND

-  Overburden
- Tertiary ?
- 11  Quartz-eye Latite Dyke
- Iron Mask Batholith and Related Intrusions
Upper Triassic and Lower Jurassic
- 10  Magnetite-Rich Dyke
- 9  Cherry Creek Monzonite Dyke
- 8  Plagioclase Porphyritic Dyke
- 7  Diorite Dyke
- 6  Pegmatitic Hybrid Diorite
- 5  Hybrid Diorite
- 4  Pyroxene Gabbro
- 3  Sugarloaf Diorite
- 2  Monzodiorite
- 1  Picrite
-  Trace of Faults
-  Geological Contacts, Inferred
-  Open Pit Bench Contours

INTRODUCTION

Estimated open pit reserves in the combined Ajax West and Ajax East zones are 20.7 million tonnes averaging 0.45% copper and 0.01 ounces of gold per tonne (Teck Corporation, 1990 Annual Report). As of 1991, stage 1 of the Ajax West pit has been completed. A stage 2 pit is planned that will significantly enlarge and deepen the existing pit. The pit is situated on the southwestern side of the alkalic Iron Mask batholith at the intersection of three major rock units: two dioritic phases of the Iron Mask pluton and a picritic unit of uncertain origin. Porphyry-style mineralization consists of pyrite and chalcopyrite with minor amounts of bornite and chalcocite (Bond, 1987).

The objective of fieldwork this year was to determine the temporal and structural relationships of the rock units within the Ajax West Pit, as well as to examine the alteration and mineralization related to these units. Mapping was conducted at 1:750 scale. In addition, core from approximately forty drill holes was examined in detail. In this progress report, only the lithologies are described.

GEOLOGY

Pit mapping has delineated eleven significantly different rock units (Fig. 1). Preliminary order, from oldest to youngest, is: picrite, monzodiorite, Sugarloaf diorite, pyroxene gabbro, hybrid diorite, pegmatitic hybrid diorite, dioritic dyke, plagioclase porphyry dyke, Cherry Creek monzonite dyke, magnetite-rich diorite dyke and quartz-eye latite dyke. This provisional sequence of intrusions, which differs from those of previous field and petrographic workers (Carr, 1956; Kwong, 1987; Northcote, 1977 and Preto, 1968) and is based upon observed contact relations alone, will be confirmed by planned zircon U-Pb dating.

(Unit 1) Picrite: basaltic in composition, is characterized by abundant clinopyroxene and serpentinized olivine phenocrysts, and as much as 25% secondary magnetite (Kwong, 1987). It occurs on the southwest side of the pit and as faulted slices within a major east-west fault that divides the pit in half (Fig. 1). Intensely sheared contacts with other units render its relative age unclear.

(Unit 2) Monzodiorite: a fine- to medium-grained porphyritic unit with weakly aligned pyroxene and plagioclase phenocrysts. It has limited exposure in the wall of the pit and may be a screen of older rock caught up in the hybrid diorite (Fig. 1). The contact between this unit and the surrounding hybrid diorite appears to be gradational and irregular. The unit is weakly mineralized.

(Unit 3) Sugarloaf diorite: a fine- to medium-grained porphyry with elongate hornblende and plagioclase phenocrysts enclosed in a medium grey matrix. This unit has been recognized and mapped on a regional scale (Preto, 1968). The unit occurs mainly to the south of the major east-west fault in (Fig. 1). Intense albite alteration has changed much of this unit to a white structureless mass. High grade copper-gold mineralization is closely associated with intense albitization.

(Unit 4) Pyroxene gabbro: medium- to coarse-grained pyroxene and amphibole pyritic unit with a dark grey matrix. It is in sharp contact with the Sugarloaf diorite (Fig. 1), but the two units appear to be interleaved. Copper mineralization is weak.

(Unit 5) Hybrid diorite: a fine grained mafic unit often characterized by the presence of crosscutting veins and alteration envelopes of albite, epidote, potassium feldspar, and calcite. The unit occurs mainly north of the major east-west fault (Fig. 1). Potassic alteration is much more prevalent in this unit than in the Sugarloaf diorite, although the copper content tends to be lower.

(Unit 6) Pegmatitic hybrid diorite: is spatially related to the hybrid diorite and may be a late differentiate and/or zones of recrystallization. It consists of fine- to very coarse-grained plagioclase and hornblende, with or without magnetite. Hornblende crystals up to 3 cm long occur. Contacts with the hybrid diorite are apparently migmatitic and probably gradational. Fine- and coarse-grained phases of the unit crosscut one another. This unit is exposed on the uppermost benches above the north side of the pit (Fig. 1). It is not well mineralized with copper.

(Unit 7) Dioritic dykes: fine- to medium-grained, typically epidotized and mineralized. Several of these dykes cut the Sugarloaf diorite (Fig. 1). The largest dyke is three metres in width.

(Unit 8) Plagioclase porphyritic dyke: white feldspar phenocrysts in a fine grained, greyish purple matrix. A single dyke of this composition was traced up the southern wall of the pit (Fig. 1).

(Unit 9) Cherry Creek monzonite dyke: a fine grained porphyry with hornblende and plagioclase phenocrysts in a potassium feldspar matrix with approximately 2-3% disseminated magnetite. This unit has been recognized and mapped on a regional scale (Preto, 1968). It occurs as a seven metre-wide unmineralized dyke which cuts both the hybrid diorite and Sugarloaf diorite (Fig. 1).

(Unit 10) Magnetite-rich diorite dykes: vary in color from green to grey to purple and are moderately to strongly magnetic. Several small dykes, generally less than one metre in width, and apparently unrelated to mineralization, cut the Sugarloaf and hybrid diorite units (Fig. 1).

(Unit 11) Quartz-eye latite dykes: are hornblende, potassium feldspar, and quartz pyritic. These dykes cut the hybrid diorite unit (Fig. 1). The largest dyke is approximately five metres wide. These dykes postdate alteration, mineralization and many of the faults. Similar dykes are reported in the Afton Pit (Kwong, 1987).

CONCLUSIONS

Detailed mapping of the Ajax West pit has delineated eleven major rock units. The relative ages of these units are provisionally defined by contact relationships. Future petrographic work, accompanied by whole rock analyses and isotope dating of the units will help to establish compositions

and age relationships. Studies will also be conducted on correlations among alteration, mineralization, and structure within the pit.

ACKNOWLEDGMENTS

Afton Operating Corporation, in particular Louis Tsang and Greg Reid, helped in geological and mapping problems in the pit and provided access to company files, drill core and the mine property. Research has been supported by the Geological Survey of Canada and the Mineral Deposit Research Unit (MDRU Contribution No. 10) at the Department of Geological Sciences, the University of British Columbia, through the Collaborative Industry-SCBC-NSERC research project, "Copper-Gold Porphyry Deposits of British Columbia." Financial support from a COSEP Grant to Ross is gratefully acknowledged.

REFERENCES

- Bond, L.**
1987: Geology and Mineralization at the Ajax Mine, unpublished company report.
- Carr, J.M.**
1956: Deposits associated with the eastern part of the Iron Mask Batholith near Kamloops, B.C.; British Columbia Department of Mines, Annual Report, p. 47-69.
- Kwong, Y.T.J.**
1987: Evolution of the Iron Mask Batholith and its associated copper mineralization; British Columbia Ministry of Energy, Mines and Petroleum Resources, Bulletin 77, p. 1-55.
- Northcote, R.E.**
1977: Geology of the southeast half of Iron Mask Batholith; in Geological Fieldwork, 1976, British Columbia Department of Mines and Petroleum Resources, p. 41-46.
- Preto, V.A.**
1968: Geology of the eastern part of the Iron Mask Batholith; in Annual Report 1967, British Columbia Ministry of Mines and Petroleum Resources, p. 137-147.
- Teck Corporation**
1990: Annual Report, p. 1-52.

Geological Survey of Canada Project 740098

A self-arresting moraine dam failure, St. Elias Mountains, British Columbia

John J. Clague and S.G. Evans
Terrain Sciences Division, Vancouver

Clague, J.J. and Evans, S.G., 1992: A self-arresting moraine dam failure, St. Elias Mountains, British Columbia; *in* Current Research, Part A; Geological Survey of Canada, Paper 92-1A, p. 185-188.

Abstract

In June 1990, several thousand cubic metres of water poured out of a moraine-dammed lake in the St. Elias Mountains, northwestern British Columbia. The escaping waters incised the moraine dam, producing a debris flood or debris flow that travelled 4 km on an average slope of 13° to Tats Creek. There, it blocked the stream and diverted it from its former course. The event was triggered by an anomalous flow of water across the crest of the moraine; the cause of this overflow is uncertain. The outburst is one of several from lakes dammed by Neoglacial moraines in the Canadian Cordillera, but differs from previously reported events in that the breaching of the moraine was arrested before the dam completely failed. The event indicates that some moraine-dammed lakes can produce more than one destructive outburst.

Résumé

En juin 1990, plusieurs milliers de mètres cubes d'eau se sont déversés d'un lac de barrage morainique dans le chaînon St. Elias, dans le nord-ouest de la Colombie-Britannique. En s'échappant, les eaux ont entaillé le barrage morainique, et généré une inondation ou coulée de débris qui s'est déplacée sur 4 km suivant une pente de 13° jusqu'au ruisseau Tats. À cet endroit, les débris ont bloqué le cours d'eau et l'ont fait dévier de son cours précédent. Cet épisode a été déclenché par un écoulement anormal d'eau à travers la crête morainique; la cause de ce débordement est incertaine. Cette crue est l'une de plusieurs ayant pour origine des lacs obstrués par des moraines néoglaciales dans la Cordillère canadienne, mais diffère des épisodes antérieurement rapportés en ce que l'entaillage de la moraine s'est arrêté avant la rupture complète du barrage. Cet épisode indique que certains lacs de barrage morainique peuvent être à l'origine de plus d'une crue destructrice.

INTRODUCTION

Many lakes in the glacier-clad mountains of western Canada are dammed by steep-sided Neoglacial moraines comprising bouldery diamicton and gravel with a sand-silt matrix. Such dams tend to be unstable and susceptible to failure through piping, anomalous overflow and incision, and melting of residual ice cores (Blown and Church, 1985; Clague et al., 1985; Evans, 1987). Failure of a moraine dam results in the release of impounded lake water, causing a destructive flood or debris flow that may travel a few kilometres to many tens of kilometres downvalley (Costa and Schuster, 1988).

At present, there is little public awareness of this potentially destructive phenomenon in western Canada, in large part because moraine dam failures have occurred in remote mountain valleys without property damage or loss of life. There is, however, increasing pressure to develop resources in mountain valleys, and this requires a full appreciation of the possibility and likely impacts of outburst floods from moraine-dammed lakes. This report documents the most recent known event of this type, which occurred in the St. Elias Mountains, northwestern British Columbia, in June 1990. Although smaller than other documented outbursts from moraine-dammed lakes, this event is informative in that the failure self-arrested before the dam was completely breached. Further, it is instructive of how the breaching process progresses.

EVENT DOCUMENTATION

The source of the outburst is a small moraine-dammed lake at 1500 m elevation in the drainage basin of Tats Creek (a tributary of Tatshenshini River, 17 km southeast of the proposed Windy Craggy mine (Fig. 1, 2). It is the easternmost of three, similar moraine-dammed lakes that lie in a composite cirque at the head of an unnamed tributary of Tats Creek. The lake has an area of approximately 1 ha and is bordered on three sides by a single, sharp-crested moraine that formed during late Neoglacial time (the Little Ice Age). Along its east side, the lake is in contact with the steep snout of a cirque glacier. The outlet of the lake is located opposite the glacier snout in a low eroded swale in the moraine (Fig. 2, 3c). When examined in July 1991, the outlet channel showed evidence of 0.4 m of recent downcutting. This suggests that the level of the lake dropped 0.4 m during the outburst and that about 4000 m³ of water escaped.

The effects of the outflow are evident on the outer slope of the moraine. A steep-walled trench up to 10 m deep and 25 m wide extends 500 m along the former course of the outlet stream from near the crest of the moraine at 1510 m elevation to its toe at about 1350 m (Fig. 3a, 3b, 4). The walls of the trench, which were actively mass wasting during our visit in July 1991, expose diamicton and poorly sorted, bouldery gravel with crude stratification dipping parallel to the outer slope of the moraine. From measurements of the trench made in the field, and taking into account the pre-outburst geometry

of the moraine, as seen on aerial photographs, we estimate that 5000-15,000 m³ of sediment were eroded by the escaping waters.

The slurry of sediment and water moved downvalley either as a debris flood or debris flow, locally eroding additional sediment from the valley floor. The first 2.3 km of the flow path below the moraine has an average gradient of 11° (Fig. 3). The final 1.3 km to Tats Creek (410 m elevation) slopes 20° on average (maximum gradient = 40°). Considerable sediment may have been incorporated into the flow as it moved down this final steep reach. The flow entered Tats Creek and came to a halt. A fan-shaped mass of debris about 100 m wide and 100 m long (Fig. 5) accumulated on the valley floor and temporarily stemmed the flow of the

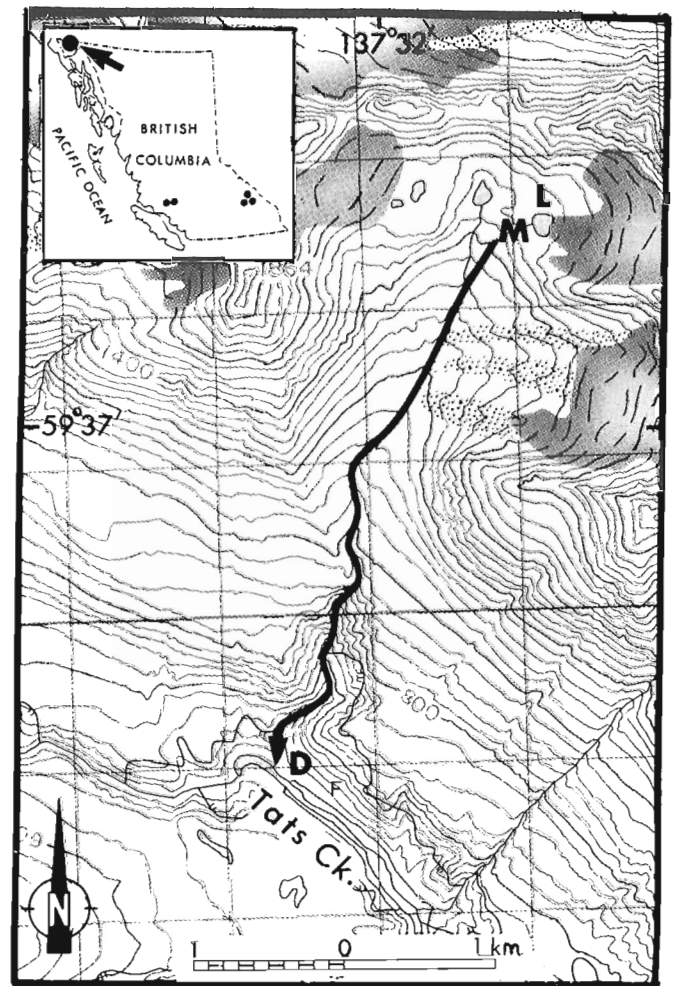


Figure 1. Map showing the location of the outburst event reported in this paper. L = lake; M = crest of moraine dam; D = debris fan at Tats Creek. The path of the debris flow/flood is indicated by the arrowed line. The two lakes west of L are also dammed by moraines. Inset shows locations of other documented moraine dam failures (for details, see Evans, 1987).

creek. Soon, however, the stream overflowed the debris dam and established a new course through forest along the south side of the valley (Fig. 5).

DISCUSSION

The outburst occurred on the afternoon of June 28, 1990 (B. Downing, personal communication, 1991). Although there were no witnesses at the source, the cause can be inferred from the fact that the floor of the outlet channel adjacent to the lake was lowered about 0.4 m during the event. This erosion could have been accomplished only by unusually high overflow. There apparently were no exceptional rainstorms during the period when the outburst occurred, thus the most likely cause of the anomalous overflow is either (1) a sudden influx of water resulting from the drainage of a water body within or beneath the glacier east of the lake, or (2) a wave train generated by an avalanche or calving of ice from the glacier snout. The former explanation is hypothetical because no evidence has been found for the presence of englacial or subglacial water bodies within or beneath the glacier. A few blocks of ice were present in the lake at the time of our visit, but it is not clear if these could produce waves large enough to overtop and incise the outlet.

Whatever the trigger, the overflowing water eroded the outlet of the lake and deeply incised the steep outer flank of the moraine. Incision probably propagated from the steepest part of the moraine back towards the lake. Normally, such a process would continue until the moraine had been completely breached or the lake was empty. In this case,



Figure 2. Source of the 1990 outburst (L). Note trench (arrow) eroded into outer flank of moraine (see Fig. 4). Bedrock is exposed near the upper end of the trench.

however, the process was arrested before the breach became fully formed. One of the reasons for this is that bedrock became exposed along one section of the channel as the breach deepened, severely limiting headward erosion (Fig. 3). Another reason is that downcutting of the outlet adjacent to the lake ceased when a bouldery lag developed in the channel, armouring it from further erosion.

Another interesting aspect of this event is that an apparently small volume of water (estimated to be 4000 m³) initiated a significant debris flow or debris flood that travelled over 4 km from its source. A large amount of sediment was mobilized by this water on the steep outer slope of the moraine dam. It is not known if a viscous flow or a flood traversed the relatively low-gradient section of the valley below the moraine. A considerable amount of debris may have been entrained along the steep, dominantly rocky channel 2.3-3.6 km below the moraine, and there is little doubt that a true debris flow passed down this channel and entered Tats Creek.

In conclusion, the event described in this report is an example of a previously poorly documented type of moraine dam failure, one in which breaching is arrested before drainage is complete. The recognition of such partial breach failures is significant because it raises the possibility that multiple outbursts can occur from a single moraine-dammed lake. Indeed, the conspicuous erosional saddle in the moraine described in this report (Fig. 3c) may record one or more pre-1990 outbursts.

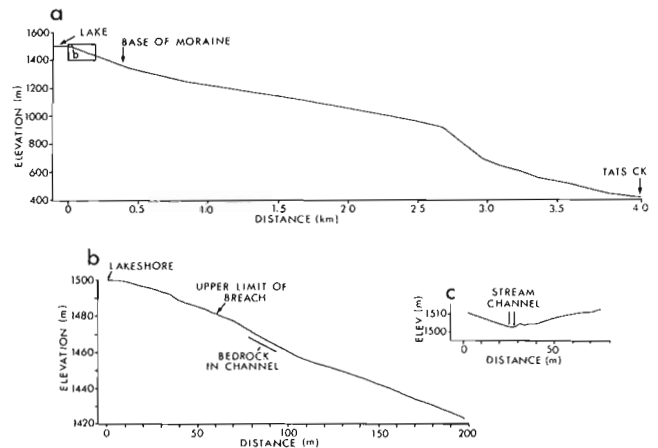


Figure 3. Topographic profiles. (a) Path of debris flow/flood from the source to Tats Creek. (b) Detail of upper part of (a). (c) Crest of the moraine across the outlet of the lake. (a) is plotted from a 1:50 000 topographic map; (b) and (c) were surveyed in the field.



Figure 4. Trench on the outer flank of the moraine; view to the southwest. Person in foreground for scale.

Figure 5. Debris fan deposited during the 1990 outburst. The fan, originating from the stream valley on the right, briefly stemmed the flow of Tats Creek and diverted it through forest (lower left).



REFERENCES

Blown, I. and Church, M.

1985: Catastrophic lake drainage within the Homathko River basin, British Columbia; *Canadian Geotechnical Journal*, v. 22, p. 551-563.

Clague, J.J., Evans, S.G., and Blown, I.G.

1985: A debris flow triggered by the breaching of a moraine-dammed lake, Klattasine Creek, British Columbia; *Canadian Journal of Earth Sciences*, v. 22, p. 1492-1502.

Costa, J.E. and Schuster, R.L.

1988: The formation and failure of natural dams; *Geological Society of America, Bulletin*, v. 100, p. 1054-1068.

Evans, S.G.

1987: The breaching of moraine-dammed lakes in the southern Canadian Cordillera; *Proceedings, International Symposium on Engineering Geological Environment in Mountainous Areas, Beijing*, v. 2, p. 141-150.

Geological Survey of Canada Projects 870017, 830016

Quaternary stratigraphy and history of central British Columbia

Alain Plouffe
Terrain Sciences Division

Plouffe, A., 1992: *Quaternary stratigraphy and history of central British Columbia*; in *Current Research, Part A*; Geological Survey of Canada, Paper 92-1A, p. 189-193.

Abstract

This paper documents some of the Quaternary stratigraphy along Klawli and Nation rivers in central British Columbia. The oldest sediments exposed are glaciotectionised glaciolacustrine deposits which are overlain by a pre-Fraser till. Orientation of structures suggests that ice flowed to the west to southwest during this pre-Fraser Glaciation. On the other hand, ice flow varying from east to northeast prevailed during the Fraser Glaciation as indicated by the surficial morphology. Retreat of Fraser ice was marked by the impounding of local glacial lakes in Nation and Klawli river valleys. Work under progress includes study of till geochemistry and petrography as an aid in interpreting direction of glacial transport.

Résumé

Cet article porte sur la stratigraphie du Quaternaire dans les vallées des rivières Nation et Klawli, dans la partie centrale de la Colombie Britannique. Des dépôts glaciolacustres glaciotectionisés constituent l'unité stratigraphique de base sur laquelle repose un till associé à une glaciation antérieure à la Glaciation de Fraser. L'orientation des structures dans ces sédiments glaciolacustres semble indiquer un écoulement glaciaire ayant une provenance variant de l'est au nord-est pendant cette glaciation antérieure. Par contre, la morphologie en surface indique que la glace s'écoulait vers l'est et le nord-est durant la Glaciation de Fraser. La présence de dépôts glaciolacustres dans les vallées des rivières Nation et Klawli témoigne de l'existence de lacs glaciaires pendant la dernière déglaciation. Les présents travaux en cours comportent des études sur la géochimie et la pétrographie des tills dans le but de renseigner sur la direction du transport glaciaire.

INTRODUCTION

A regional mapping project was undertaken by the Geological Survey of Canada in central British Columbia (Plouffe, 1991) in order to map the surficial materials of two 1 : 250 000 scale map areas (Fort Fraser and Manson River, NTS 93 K and N, respectively) and to establish details of the glacial history. As part of this project, a series of stratigraphic sections exposed along Klawli and Nation rivers were studied in detail during the 1991 field season. This report summarizes the stratigraphy of the area based upon investigations of natural exposures and discusses preliminary interpretation of the two last glacial events : Fraser and pre-Fraser glaciations.

The area of interest is located about 85 km north of Fort St. James, and 25 km northwest of Mount Milligan, a site where Placer Dome Inc. is presently conducting feasibility studies for the possible opening of an open pit copper-gold mine (Fig. 1 and 2).

SETTING

During the last glaciation, the Fraser Glaciation, ice flowed over the central interior of British Columbia from accumulation zones located in the Coast, Cariboo, and Skeena mountains (Tipper, 1971a; Plouffe, 1991). During the onset of the Fraser Glaciation, in the study area, ice flow direction varied from east-southeast to northeast under the influence of topography and coalescence of piedmont glaciers (Fig. 2). According to Tipper (1971a), ice never attained the ice dome stage at the climax of Fraser Glaciation

in central British Columbia, that is, a radial flow from a central accumulation zone. However, this same author suggested that the ice dome stage was reached during a penultimate glaciation as is indicated by the westerly transported erratics in the Coast Mountains and the occurrence of drumlins and glacial grooves above morphological features attributed to the limit of the Fraser

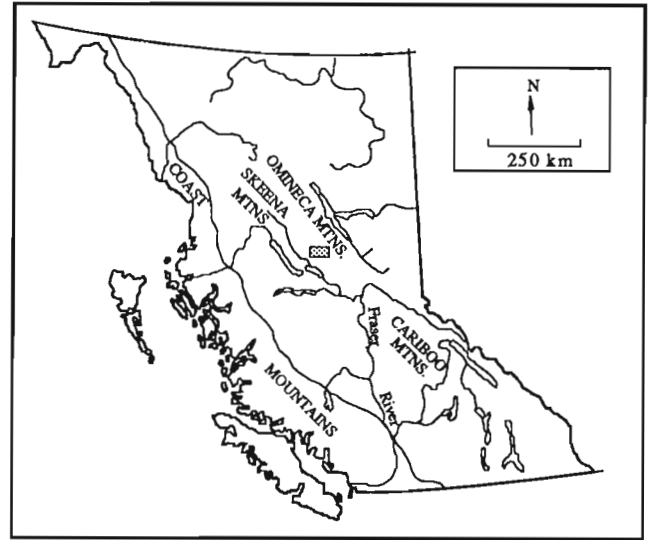


Figure 1. Location of study area (shaded) with surrounding mountain ranges.

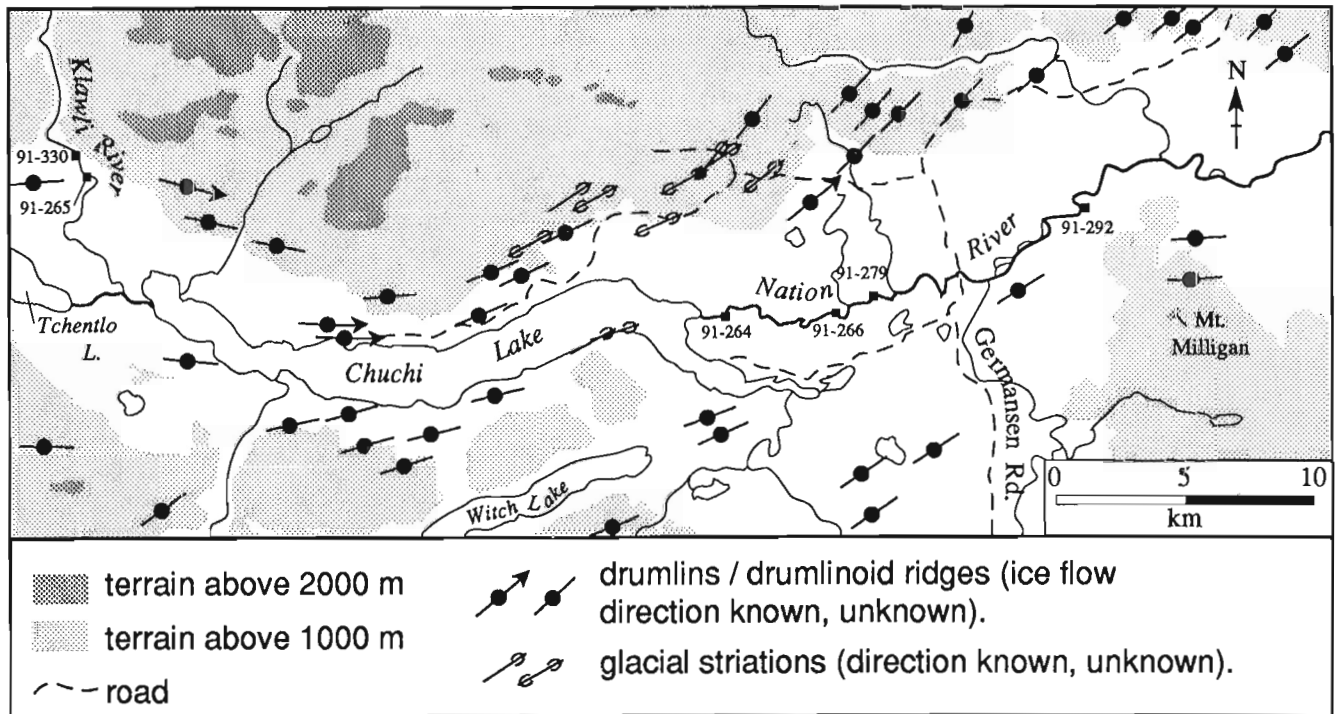


Figure 2. Study area with location of sections and pattern of ice flow direction as deduced from drumlins, glacial grooves, crag and tails, and striations.

ice. At the end of the Fraser Glaciation, glacial lakes impounded behind retreating ice invaded the Stuart, Endako, and Nechako river valleys to the south of the study area (Tipper, 1971b; Plouffe, 1991).

STRATIGRAPHY

Figure 3 summarizes Quaternary stratigraphy in the study area. The following description will deal with stratigraphic sections from west to east.

Klawli River sections

Section 91-330. Unit 1, a massive dark grey clay bed of unknown thickness, was exposed by digging a shallow trench in the scree below unit 2. It is thought to have been deposited

in a glacial lake impounded behind stagnating ice which was wasting towards the Tchentlo Lake valley as indicated by a series of lateral meltwater channels on higher hill slopes.

Unit 2 consists of a bouldery diamicton with clasts averaging 50 to 60 cm and a few reaching 90 cm in diameter. Its matrix is sandy and poorly compacted. The coarse nature of this unit suggests that it was deposited in an ice proximal glaciofluvial environment.

A crossbedded fine sand layer with clay and diamicton interbeds overlies unit 2. Paleocurrent direction in this unit is towards the southeast. This unit was likely deposited in a delta or as distal outwash. However, the presence of cross-stratified sand with clay interbeds could correspond to a proglacial subaqueous environment as described by Rust and Romanelli (1975).

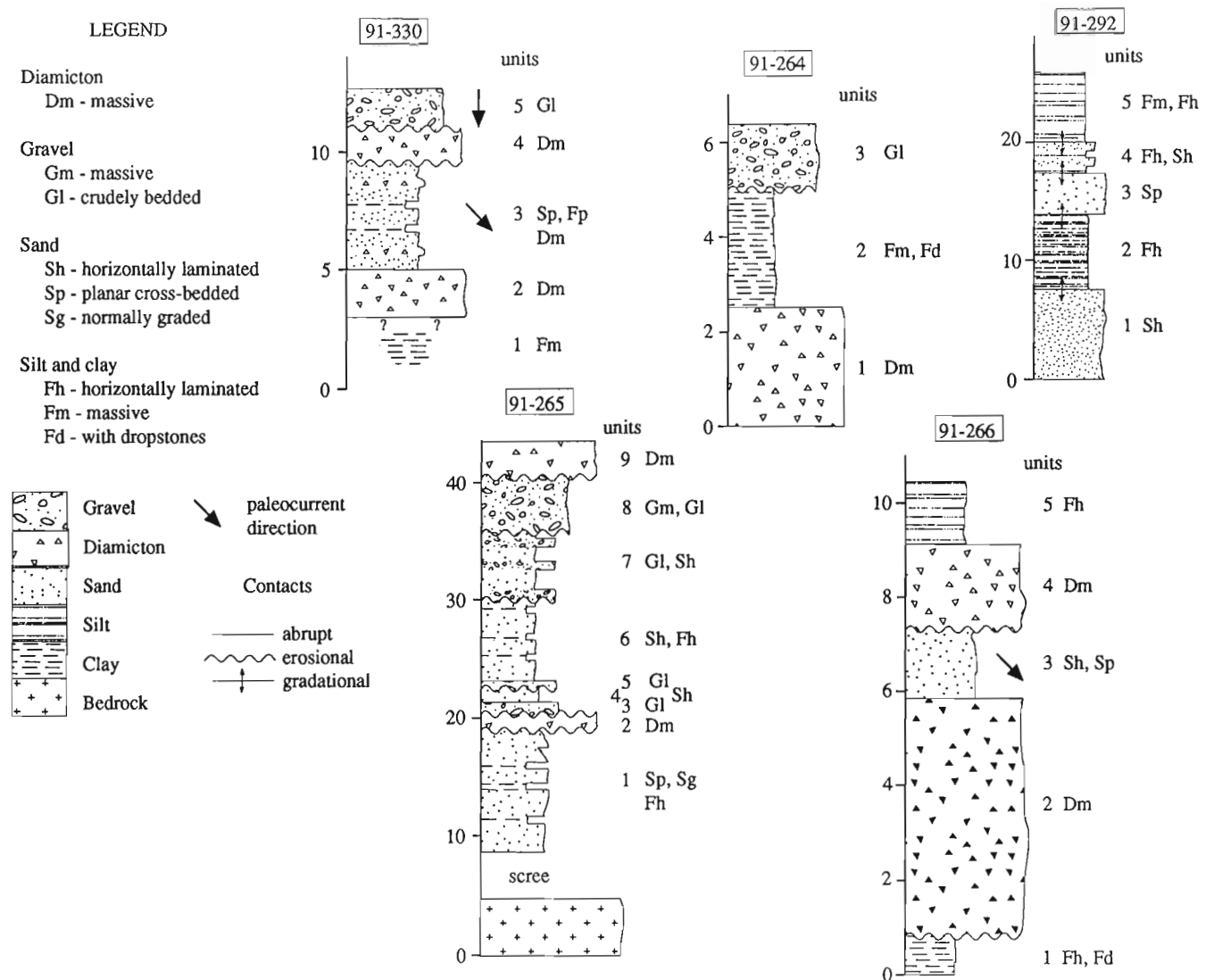


Figure 3. Lithostratigraphic cross-section from Klawli River valley to Nation River valley. Section locations are indicated in Figure 2.

Unit 4, a massive poorly compacted grey-brown diamicton is interpreted as a debris flow deposited during paraglacial sedimentation.

Finally, a bouldery gravel, unit 5, caps the section and is part of the Klawli River alluvial terrace deposited during an aggradation period. Clasts imbrication indicates a current towards the south, that is, the same as present day current direction.

Section 91-265. Quaternary sediments rest upon scree-covered quartz syenite bedrock.

Units 1 to 8 consist of alternating sandy and gravelly layers of varying thicknesses. Most of the sandy units are planar stratified and include several clay interbeds. Coarsening upward cycles are present in the sandy layers (unit 1) and the gravelly units become coarser toward the top of the section. This sequence of sediments is thought to represent distal glaciofluvial deposition in front of the advancing ice. The clay interbeds indicate subaqueous sedimentation.

Unit 9 is a thick, well compacted diamicton (till) deposited during Fraser Glaciation.

Nation River Sections

91-264. Three units are exposed at this section. The lowest unit is a well compacted diamicton (till), with several striated clasts. It is overlain by 2.5 m of massive clay with dropstones deposited in a glacial lake impounded in Nation River valley during the retreat of the ice from the area. The crudely bedded sand and gravel of unit 3 are interpreted to be fluvial sediments deposited during a period of aggradation.

Bison bones fragments (D. Pokotylo, personal communication, 1991) were recovered from this section in 1967, possibly in unit 2. Work is presently under way to identify the bison species, date the bones by radiocarbon method, and relocate their stratigraphic position.



Figure 4. Glaciotectionised glaciolacustrine sediments at station 91-279.

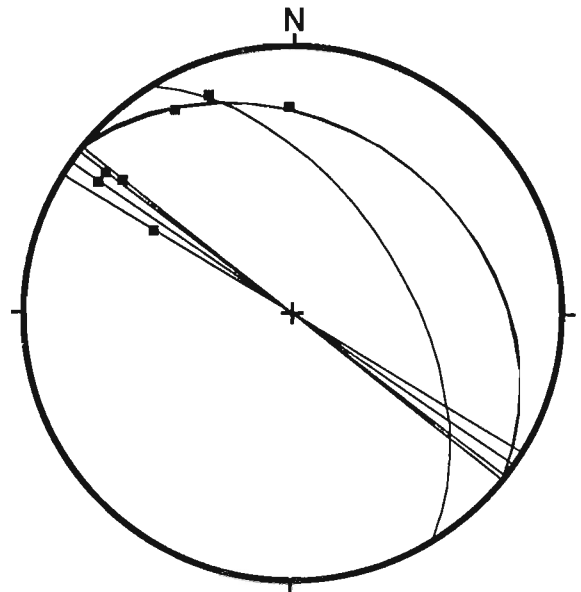


Figure 5. Trend and plunge of fold axes and traces of axial planes in glaciolacustrine sediments at section 91-279 (Fig. 2), plotted on lower hemisphere.

91-266. Two diamictons (tills), units 2 and 4, from pre-Fraser and Fraser glaciations respectively, are exposed at section 91-266 (Fig. 2). Partly contorted and well laminated glaciolacustrine clay, with sporadic dropstones, underlies unit 2 and a well sorted sand unit of deltaic or distal outwash origin, unit 3, conformably (?) overlies this lower till. Cross-stratifications indicate a paleocurrent direction towards the southeast. Finally, the upper till is overlain by well stratified glaciolacustrine silt and clay.

91-279. A single unit of contorted, laminated glaciolacustrine clay is exposed at this section (Fig. 4). It is correlated with the lowest unit of glaciolacustrine sediments of section 91-266 because of the similar textural and structural appearance.

Axes of seven major folds in the glaciolacustrine sediments gently plunge to the north-northwest (Fig. 5). Also, some of the folds are overturned with an axial plane dipping toward the northeast. Those deformations, developed during the pre-Fraser Glaciation, and could indicate ice flow varying from west to southwest. However, more detailed petrographic studies of both tills at section 91-266 are under progress. These will test this hypothesis.

91-292. A series of sections along Nation River, between Germansen Road and station 91-292 (Fig. 2), expose glaciolacustrine and outwash (or deltaic ?) sediments. Only the most complete section, 91-292, will be described in this report. Five units, all separated by gradational contacts, are exposed at this site. Unit 1 is composed of well sorted, planar stratified fine sand with scarce carbonate concretions (Fig. 3). A large channel scour occurs in this unit. Unit 1 is overlain

by planar stratified silt (Unit 2) which reaches a thickness of 8 m in places. Unit 3 consists of well sorted fine sand with convolute bedding and climbing ripples which indicate a paleocurrent direction toward the north to northeast. A planar stratified fine sand and silt with abundant clay interbeds constitute unit 4. Approximately 6 m of glaciolacustrine rhythmites (varves ?) are exposed at the top of the section (unit 5). They are subdivided into 10 couplets of silt and clay. Each individual couplet consists of an approximately 1 m thick silt bed overlain by a thin (2-5 cm) clay layer.

The stratigraphic position of units 1 to 4 under glaciolacustrine sediments (unit 5) suggests that those units were deposited subaqueously. Consequently, they are tentatively interpreted as subaqueous outwash or proglacial deltaic sediments. Variation in grain size amongst the units might indicate a fluctuation in the retreating ice front position and/or a variation in the position of the sediment feeding channel.

QUATERNARY HISTORY

Based upon the stratigraphy exposed along Nation and Klawli rivers, there is evidence of two glaciations in the study area: the pre-Fraser and Fraser glaciations.

At the onset of pre-Fraser Glaciation, a glacial lake was impounded in Nation River valley as indicated from the stratigraphy exposed at section 91-266. Glaciotectionic structures in the glaciolacustrine sediments, beneath pre-Fraser till, suggest an ice flow direction towards west to southwest during the pre-Fraser Glaciation. Ice flow to the west likely occurred during a continental ice sheet stage, that is, during a period of radial flow from an ice dome located to the east of the area. This suggests that the penultimate (pre-Fraser) glaciation was more extensive than the Fraser Glaciation, which agrees with the conclusions of Tipper (1971a). The drainage of Nation River might also have been blocked during the retreat of pre-Fraser ice if unit 3 of section 91-266 is of deltaic origin.

Coarsening upwards glaciofluvial stratified sand and gravel underneath Fraser till, in Klawli River valley, are interpreted to be advance outwash deposited in front of Fraser ice. Ice flow during the Fraser Glaciation ranged from east to northeast as revealed by ice flow indicators (Fig. 2).

The Fraser deglaciation was marked by the formation of local glacial lakes in Klawli and Nation river valleys. In the latter, glaciolacustrine sediments occur to an elevation of about 850 m, which gives a minimum level for the glacial lake. The occurrence of glaciolacustrine sediments in this

valley is limited to an area between Chuchi Lake and station 91-292, which suggests that the glacial lake was of local extent. Finally, if it is assumed that unit 5 of section 91-292 is a more or less complete varve sequence, the glacial lake was of short duration (approximately 10 years).

Ice retreat was followed by fluvial sedimentation conditioned by the abundance of glacial sediments (paraglacial sedimentation). This was followed by stream incision and the cutting of terraces.

CONCLUSION

Most of the unconsolidated sediments exposed along Klawli and Nation river valleys are the result of the Fraser Glaciation. However, fragmentary evidences of a pre-Fraser Glaciation suggest that ice flowed towards the west to southwest during that penultimate glaciation. Till geochemistry and petrography (work under progress) will test this hypothesis.

During the subsequent Fraser Glaciation, ice flowed to the east and northeast from zones of accumulation located in the Coast and Skeena mountains. Retreat of the ice was marked by the formation of local glacial lakes in Klawli and Nation river valleys.

ACKNOWLEDGMENTS

The author would like to thank L.E. Jackson, Jr. and R.J. Fulton for several comments which improved the original manuscript and S. Pohl for valuable field assistance.

REFERENCES

- Plouffe, A.**
1991: Preliminary study of the Quaternary geology of the northern interior of British Columbia; in *Current Research, Part A, Geological Survey of Canada, Paper 91-1A*, p. 7-13.
- Rust, B.R. and Romanelli, R.,**
1975: Late Quaternary subaqueous outwash deposits near Ottawa, Canada; in: *Glaciofluvial and Glaciolacustrine Sedimentation*, (ed.) A.B. Jopling, and B.B. McDonald; Society of Economic Paleontologists and Mineralogists, Special Publication No. 23, p.177-192.
- Tipper, H.W.**
1971a: Multiple glaciation in central British Columbia; *Canadian Journal of Earth Sciences*, v. 8, p. 743-752.
1971b: Glacial geomorphology and Pleistocene history of central British Columbia; *Geological Survey of Canada, Bulletin 196*, 89 p.

Holocene sediments from Saanich Inlet, British Columbia and their neotectonic implications

Andrée Blais¹
Terrain Sciences Division

Blais, A., 1992: *Holocene sediments from Saanich Inlet, British Columbia and their neotectonic implications*; in *Current Research, Part A; Geological Survey of Canada, Paper 92-1A*, p. 195-198.

Abstract

Sediments in piston cores collected from Saanich Inlet, British Columbia consist of varved units intercalated with massive beds. The massive beds are inferred to have been deposited by grain flows or debris flows which may have been generated by earthquakes. Cesium-137 was detected in samples from the tops of some cores; this will help to establish a varve chronology and times of deposition of the massive layers.

Résumé

Les sédiments prélevés avec un carottier à piston dans l'inlet Saanich en Colombie-Britannique se composent d'unités à varves interstratifiées dans des couches massives. Ces dernières ont sans doute été mises en place par des écoulements de particules ou de débris qui ont peut-être été produits par des séismes. On a décelé la présence de césium 137 dans des échantillons provenant du sommet de quelques carottes de sondage; il sera ainsi plus facile d'établir une chronologie des varves et de déterminer les époques de sédimentation des couches massives.

¹ Ottawa – Carleton Geoscience Centre, Carleton University, Ottawa, Ontario

INTRODUCTION

In February 1991 five piston cores were collected from Saanich Inlet, British Columbia as a follow-up to a study initiated by Bobrowsky and Clague (1990). One of the objectives of this study (the author's PhD project) is to ascertain whether massive layers intercalated with varved units in the Holocene sediment sequence are due to failures caused by earthquakes.

STUDY AREA

Saanich Inlet, located at the southern end of Vancouver Island (Fig. 1) is 26 km long, up to 8 km wide, and has average and maximum depths of 120 m and 236 m, respectively. Goldstream River, the only significant stream flowing into the inlet, discharges a small percentage of the 9×10^4 tonnes of sediment that accumulates there each year (Gross et al., 1963; Bobrowsky and Clague, 1990). The main source of terrigenous sediment is Cowichan River which flows into Satellite Channel northwest of the head of the inlet (Fig. 1).

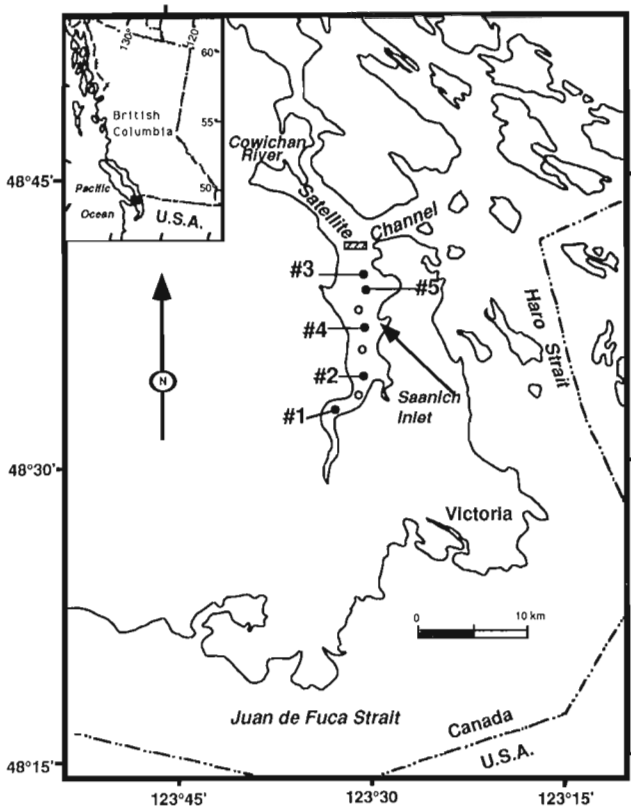


Figure 1. Locality map showing Saanich Inlet and the core sites. The open circles locate the cores of Bobrowsky and Clague (1990); the solid circles locate the cores collected in February 1991. The box across the mouth of Saanich Inlet represents the bedrock sill.

Holocene sediments in Saanich Inlet consist primarily of silt and clay deposited during fall and spring freshets and diatoms deposited during spring and summer blooms. The sediments are rhythmically laminated; individual couplets have been shown to be annual deposits, and thus may be called varves (Gross et al., 1963; Sancetta and Calvert 1988; Bobrowsky and Clague, 1990). The bedrock sill at the north end restricts normal water circulation which creates anoxic conditions in the lower part of the water column. The depth to which anoxic conditions prevail varies throughout the year, from 70 m below sea level in October to 150 m in December (Gross et al., 1963). Because anoxic conditions exist continuously at the sediment-water interface, there is absence of epifauna and infauna; thus the potential for preservation of stratification is high (Bobrowsky and Clague, 1990).

METHODS

The core sites are within the area from which three piston cores were previously collected by Bobrowsky and Clague (1990) (Fig. 1). Five continuous cores were collected from Saanich Inlet using a large (10 cm diameter) piston corer (Fig. 1). The core localities are: Core #1, 48°33.209'N, 123°32.074'W (1191 cm); Core #2, 48°34.936'N, 123°30.229'W (1155 cm); Core #3, 48°39.629'N, 123°30.186'W (1161 cm); Core #4, 48°37.207'N, 123°30.110'W (1030 cm); Core #5, 48°40.742'N, 123°30.220'W (945 cm).

The cores were cut into approximately 1.5 m lengths in the field and stored in a cold room at the Pacific Geoscience Centre (PGC). At PGC, the cores were split longitudinally, sealed in plastic wrap, and stored in plastic D-tubes. One half was archived and the other half was used for logging and sampling. The split cores were photographed and described in detail (colour, contact relationships between units, structure, thickness of units, and fossil content).

One hundred and sixty samples were collected for grain size analysis to detect possible textural differences between the varved and massive units (see also Bobrowsky and Clague, 1990). Grain size analyses will be carried out at PGC during the winter of 1991-1992 using a Micromeritics Sedigraph.

Samples from the top of each core were analyzed at PGC using a gamma ray spectrometer to determine ^{137}Cs concentrations. This radioactive element is a product of atmospheric fallout from nuclear bomb tests in the 1950s and the 1960s. ^{137}Cs first appeared in the atmosphere in 1954 and peaked in 1963; thus its presence can be used to date young sediments (Ritchie et al., 1975; Ashley and Moritz, 1979). Its concentrations in Saanich Inlet sediments should provide absolute dates near the tops of the cores.

Shells and wood fragments were extracted from the cores and sent to IsoTrace Laboratory at the University of Toronto for accelerator mass spectrometry ^{14}C dating.

Mud samples for microfossil identification were also collected.

RESULTS

Results from grain size analysis, microfossil identification, and ^{14}C dating are not yet available. However, traces of ^{137}Cs have been detected in most of the cores (T. Hamilton, personal communication, 1991).

The varved units consist of light-coloured laminae ranging from olive (5Y4/3) to olive brown (2.5Y4/4, Munsell colour determination) and dark-coloured laminae ranging from dark olive grey (5Y3/2) to very dark greyish brown (2.5Y3/2). The massive layers are generally dark olive grey (5Y3/2).

A total of 27 massive layers were found in the cores and these range in thickness from 3 cm to 110 cm. The depths in the core for each massive layer are presented in Table 1; analysis of core #5 is still in progress, thus no data are given for this core.

A 110 cm thick massive bed in core #1 (depth 877-987 cm) is unusual in that it has a 2 cm thick basal pebbly gravel (Fig. 2). The lower contact is sharp and erosional; the upper contact is also sharp, but conformable. Like the

massive layers observed by Bobrowsky and Clague (1990), it is capped by an anomalously thick, light-coloured, olive (5Y4/3) diatom-rich layer (Fig. 3). Although it has a coarse base, this bed was emplaced in the same manner as the other massive layers – by sediment gravity flow.

Table 1. Depths of massive layers in Saanich Inlet cores (cm).

Core 1	Core 2	Core 3	Core 4
63-78	277-282	350-356	306-310
223-247	356-374		448-452
302-308	482-486		547-552
397-401	610-639		810-814
428-439	676-683		
462-468	777-782		
521-528	868-871		
607-612	899-905		
638-651	1058-1063		
831-841	1098-1170		
877-987			
1073-1082			

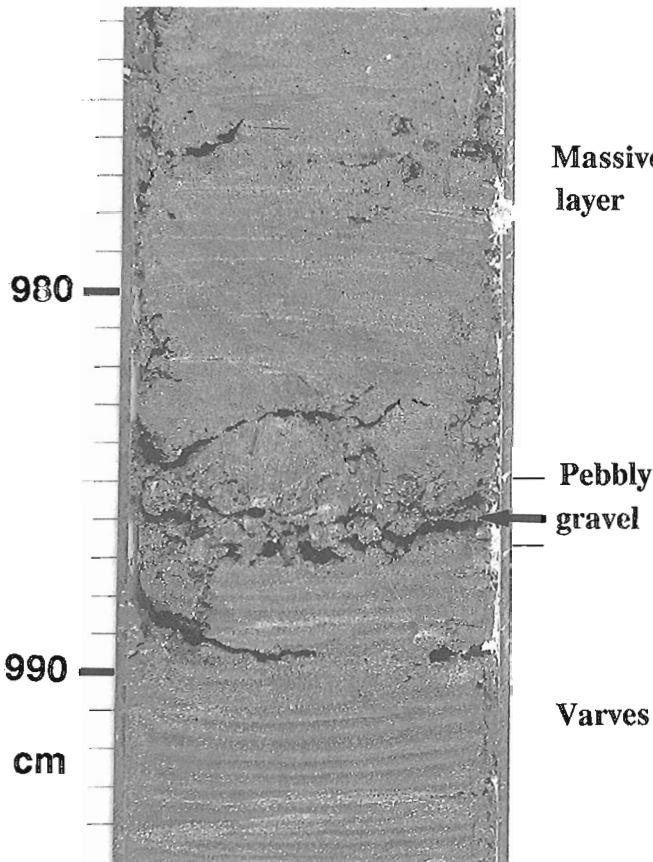


Figure 2. The lower part of a thick massive layer. (877-987 cm, Core 1); pebbly gravel (arrow) unconformably overlies varved sediments.

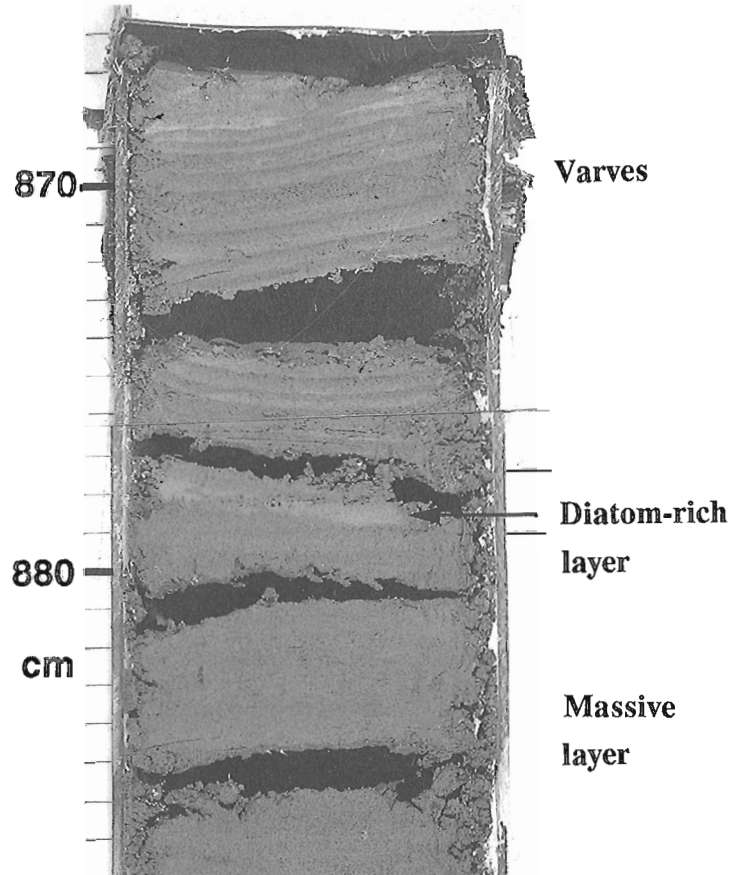


Figure 3. The top of the same thick massive layer shown in Figure 2. Note the diatom-rich layer (arrow) conformably overlain by varves.

DISCUSSION

Bobrowsky and Clague (1990) demonstrated that the massive layers are coarser than bounding varved units and, therefore, concluded that the former are products of resedimentation. They suggested that, due to a lack of grading and the presence of deformed varves beneath a few of the massive beds, these beds were produced by grain flows or debris flows. Because the massive beds observed by the author have the same visual characteristics, they are also assumed to be resedimented deposits emplaced by sediment gravity flows.

Bobrowsky and Clague (1990) argued that, given the common occurrence of seismically triggered sediment gravity flows in lacustrine and marine environments in areas of high seismicity, "the sediments from Saanich Inlet may record earthquakes" (p. 256). The preliminary observations on the second set of cores collected in Saanich Inlet support this interpretation.

Other techniques will be applied to the sediments in an effort to correlate the massive beds from core to core: time series analyses of the varves; micropaleontological study; X-ray diffraction analysis of clay minerals, and paleomagnetic analysis.

ACKNOWLEDGMENTS

The project is being funded by the Geological Survey of Canada under J.J. Clague's supervision (project 870017). Dr. Peter Bobrowsky and Dr. John Clague collected the cores.

The author acknowledges Dr. John J. Clague and Dr. J. Alan Donaldson for critically reviewing the manuscript. Dr. Tark Hamilton and Wanda Bentkowsky provided help with the ^{137}Cs determination. Wayne Stevens and David Corrigan are thanked for their assistance.

REFERENCES

- Ashley, G.M. and Moritz, L.E.**
1979: Determination of lacustrine sedimentation rates by radioactive fallout (^{137}Cs), Pitt lake, British Columbia; Canadian Journal of Earth Sciences, v. 16, p. 965-970.
- Bobrowsky, P.T. and Clague, J.J.**
1990: Holocene sediments from Saanich Inlet, British Columbia, and their neotectonic implications; in Current Research, Part E, Geological Survey of Canada, Paper 90-1E, p. 251-256.
- Gross, M.G., Gucluer, S.M., Creager, J.S., and Dawson, W.A.**
1963: Varved marine sediments in a stagnant fjord; Science, v. 141, p. 918-919.
- Ritchie, J.C., Hawks, P.H., and McHenry, J.R.**
1975: Deposition rates in valleys determined using fallout Cesium-137; Geological Society of America, Bulletin, v. 86, p. 1128-1130.
- Sancetta, C. and Calvert, S.E.**
1988: The annual cycle of sedimentation in Saanich Inlet, British Columbia; implications for the interpretation of diatom fossil assemblages; Deep-Sea Research, v. 35, 1A, p. 71-90.

Geological Survey of Canada 870017

Metamorphic rocks in the Tagish Lake area, northern Coast Mountains, British Columbia: a possible link between Stikinia and parts of Yukon-Tanana Terrane

Lisel D. Currie¹
Continental Geoscience Division

Currie, L.D., 1992: *Metamorphic rocks in the Tagish Lake area, northern Coast Mountains, British Columbia: a possible link between Stikinia and parts of Yukon-Tanana Terrane*; in *Current Research, Part A; Geological Survey of Canada, Paper 92-1A*, p. 199-208.

Abstract

Lithological character and new U-Pb geochronology of metamorphic rocks, previously included in the continental Nisling Terrane, indicate stronger affinities to rocks in arc-like Stikinia and parts of Yukon-Tanana Terrane. Three units with equivalents in Stikinia and Yukon-Tanana Terrane are the Middle Jurassic Tagish Lake suite, which includes the Hale Mountain granodiorite (185 ± 1 Ma; U-Pb zircon and sphene) and the Mt. Caplice gneiss, the mid-Permian Wann River gneiss (270 ± 5 Ma; U-Pb zircon), and the Paleozoic (?) Boundary Ranges metamorphic suite with the Mississippian orthogneiss that intrude it. Preliminary isotopic data for these rocks indicate that they derive from a primitive source, which supports these correlations. This implies that Stikinia and parts of Yukon-Tanana Terrane may be correlative, and that the Stikinia-Nisling Terrane boundary exists in the Tagish Lake area.

Résumé

Le caractère lithologique et les nouvelles datations U-Pb de roches métamorphiques, antérieurement incluses dans le terrane continental de Nisling, indiquent des affinités plus étroites avec les roches contenues dans la Stikinia en forme d'arc et des parties du terrane de Yukon-Tanana. Trois unités comportant des équivalents dans la Stikinia et le terrane de Yukon-Tanana constituent la série de Tagish Lake du Jurassique moyen, incluant la granodiorite de Mount Hale (185 ± 1 Ma; U-Pb sur zircon et sphène) et le gneiss de Mt. Caplice, le gneiss de Wann River du Permien moyen (270 ± 5 Ma; U-Pb sur zircon) et la série métamorphique de Boundary Ranges du Paléozoïque (?) avec l'orthogneiss du Mississippien qui la recoupe. Des données isotopiques préliminaires de ces roches indiquent qu'elles proviennent d'une source primitive, appuyant ces corrélations. La Stikinia et certaines parties du terrane de Yukon-Tanana pourraient donc être équivalentes, et la limite entre la Stikinia et le terrane de Nisling devrait se trouver dans la région du lac Tagish.

¹ Ottawa-Carleton Geoscience Centre, Department of Earth Sciences, Carleton University, Ottawa, Ontario K1S 5B6

INTRODUCTION

Metamorphic rocks exposed in the Tagish Lake area of the northern Coast Mountains (Fig. 1) were originally not divided and their age was unknown (Christie, 1957; Werner, 1977, 1978; Bultman, 1979). Subsequently, they were included in the Nisling Terrane, which is interpreted to be a displaced continental margin assemblage (Wheeler et al., 1988; Fig. 1). However, recent mapping, new U-Pb zircon dates for rocks from this area (this study), and preliminary initial $^{87}\text{Sr}/^{86}\text{Sr}$ isotopic ratios show that some of these rocks more closely resemble rocks found in arc-like Stikinia (Stikine Terrane; Coney et al., 1980; Monger et al., 1982; Wheeler et al., 1988) and parts of Yukon-Tanana Terrane (Mortensen, in press).

Metamorphic rocks in the Tagish Lake area are subdivided into the Boundary Ranges metamorphic suite (Mihalynuk and Rouse, 1988a,b), the mid-Permian Wann River gneiss (Mihalynuk et al., 1990; Currie, 1990, 1991), the Middle Jurassic Tagish Lake suite, and the Florence Range metamorphic suite (Mihalynuk et al., 1990; Currie, 1990, 1991; Fig. 2). Of these, only the Florence Range metamorphic suite includes lithologies, such as quartzites,

indicative of a continental margin setting (ie. Nisling Terrane). The characterization and correlation of the other three units is the focus of this paper.

GEOLOGICAL SETTING

Metamorphic rocks are exposed primarily west of the Llewellyn Fault, which separates them from unmetamorphosed Triassic Stuhini Group volcanic rocks of Stikinia and rocks of the Boundary Ranges metamorphic suite (Fig. 2). To the immediate west of the map area geological mapping is hindered by ice cover, but farther west, in southeastern Alaska, metamorphic rocks are correlated with Yukon-Tanana Terrane rocks (Samson et al., 1991).

ANALYTICAL METHODS

Results from geological mapping, U-Pb zircon geochronometry, and Rb/Sr isotope analyses are used to characterize the rocks from the Tagish Lake area described here. Metamorphic rocks exposed in NTS map areas 104M/1,8,9,10 were mapped at 1:50 000 scale during the

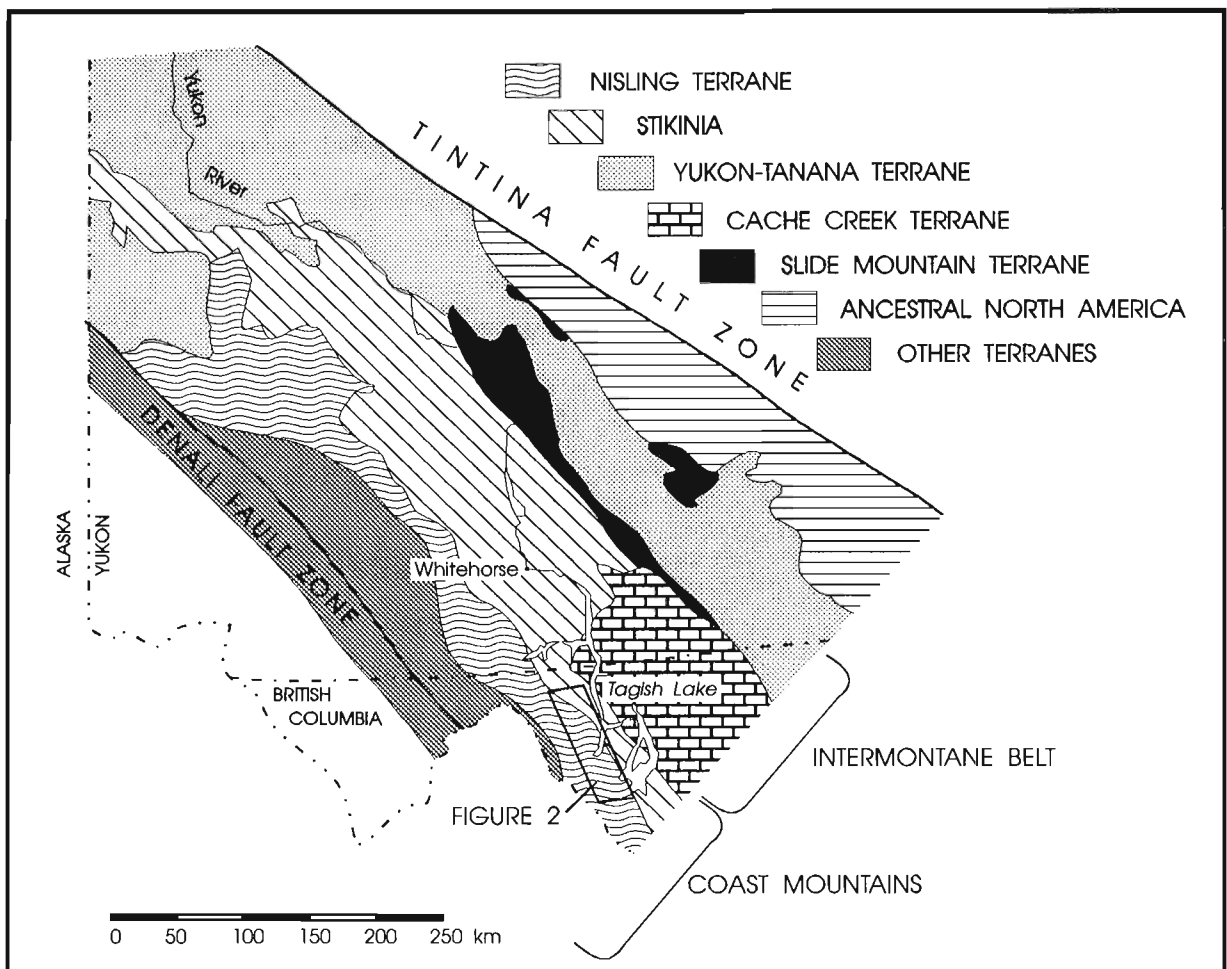


Figure 1. Map showing the location of the Tagish Lake area and the location of exposed Stikine, Yukon-Tanana and Nisling Terrane rocks (modified from Wheeler et al., 1988 and Mortensen, in press).

1989 to 1991 field seasons (Fig. 2; see Mihalynuk and Rouse, 1988a,b; Mihalynuk et al., 1989a,b, 1990; Currie, 1990, 1991).

U-Pb analyses of zircon fractions (Table 1) were performed at the Geological Survey of Canada in Ottawa using analytical procedures summarized by Parrish et al. (1987). Blanks for U are 1 picogram or less, and blanks for Pb range from 7-14 picograms. The clearest crystals were analyzed and all zircon fractions were abraded, but sphene fractions remained unabraded.

Rb/Sr isotopic data (Table 2) was collected at the University of British Columbia between 1970 and 1985 (unpublished data, R.L. Armstrong, pers. comm., 1991).

CHARACTERIZATION OF LITHOLOGICAL UNITS

Boundary Ranges metamorphic suite

The Boundary Ranges metamorphic suite comprises chlorite-actinolite schist and chlorite schist, with minor pyroxene-chlorite schist, biotite schist (\pm garnet, kyanite, staurolite), discontinuous marble layers, chlorite-hornblende schist, graphite schist, and thin fine grained felsic layers (Mihalynuk and Rouse, 1988a,b; Currie, 1990, 1991). At least three phases of deformation are known (Mihalynuk et al., 1989a,b).

A Late Mississippian U-Pb zircon age (preliminary data, not presented in this paper) for a foliated felsic dyke that truncates layers in the Boundary Ranges metamorphic suite (Fig. 2, 3) indicates a Late Mississippian or older age for this suite.

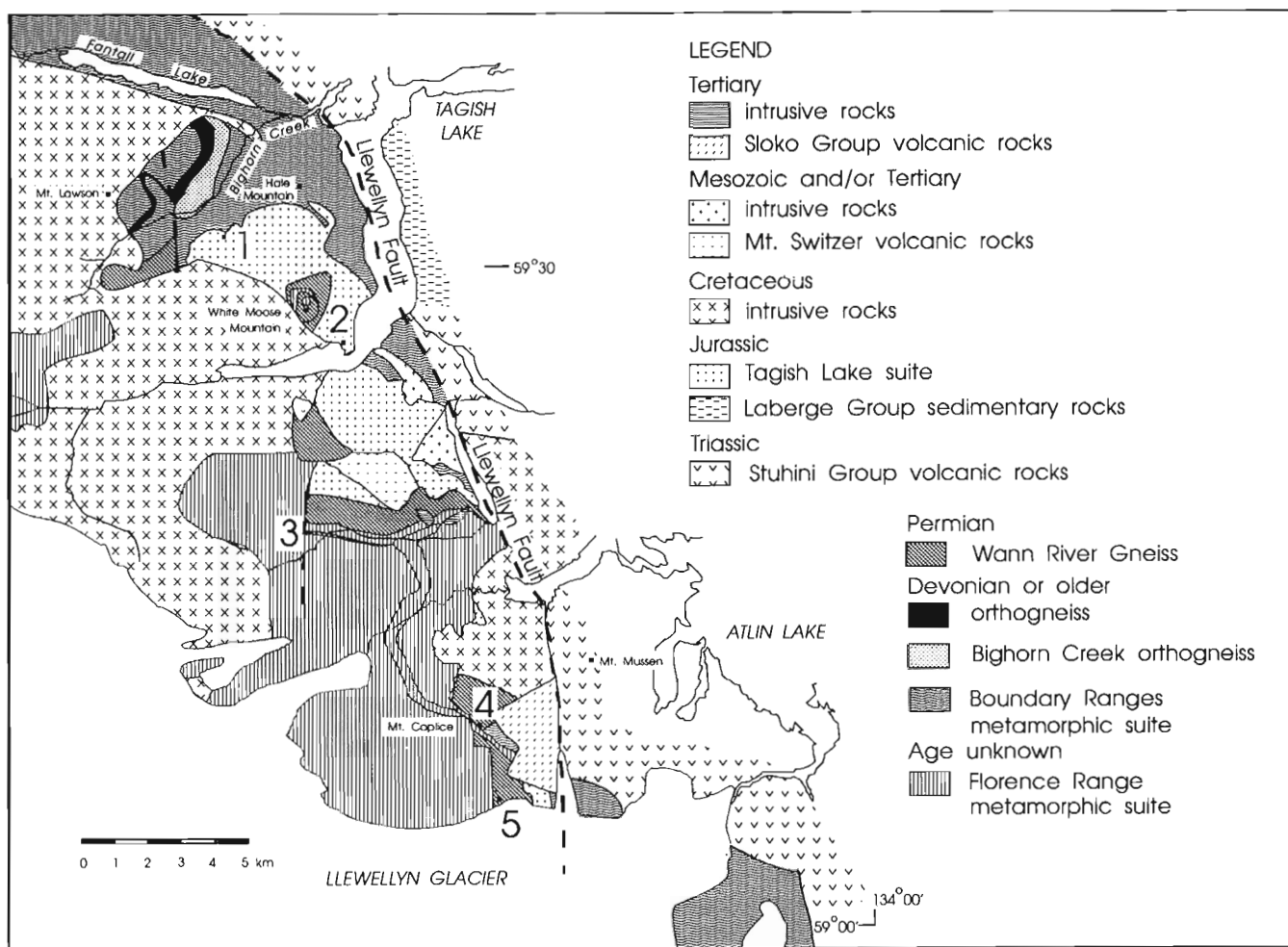


Figure 2. Geological sketch map of the Tagish Lake area. Numbers indicate sample locations for: 1, Hale Mountain granodiorite (LC-88-35-1); 2, Hale Mountain granodiorite (T75-323-6); 3, Wann River gneiss (LC-89-91B); 4, Mt. Caplice granodiorite (LW76-a76c); 5, Wann River gneiss (LW76-a68A).

Included in the Boundary Ranges metamorphic suite is the Early Mississippian (preliminary data, not presented in this paper) granitic Bighorn Creek orthogneiss. The contact between the Bighorn Creek orthogneiss and the adjacent Boundary Ranges metamorphic suite rocks is not observed, and may be intrusive or faulted.

$^{87}\text{Sr}/^{86}\text{Sr}$ and epsilon Nd signatures of Boundary Ranges suite rocks indicate that they were derived from a primitive source (Jackson et al., 1991).

Wann River gneiss

The Wann River gneiss is an intermediate hornblende-plagioclase gneiss with minor epidote. It is characterized by millimetre to centimetre scale compositional layering (cf. Fig. 3 in Currie, 1990), which is folded by one phase of deformation.

An initial $^{87}\text{Sr}/^{86}\text{Sr}$ ratio for a sample of hornblende-plagioclase gneiss correlated with the Wann River gneiss, has a relatively unevolved signature (Table 2, unpublished data, R.L. Armstrong, pers. comm., 1991).

U-Pb Geochronology

Five zircon fractions from the Wann River gneiss were analyzed. They comprise clear, elongate (length:width = 2-3:1), crystals with rounded edges, synneusis twins, minor inclusions, and without visible cores. The zircon analyses plot below concordia reflecting inheritance and possible Pb-loss (Table 1; Fig. 4). For all fractions, the U-Pb ages are slightly younger than the ^{207}Pb - ^{206}Pb ages. This suggests some Pb-loss occurred. Regression of the data yields a lower intercept of 262.7 ± 0.8 Ma (MSWD=0.84), which can only be viewed as an approximate age of crystallization because of potential Pb-loss. The youngest fraction has a ^{206}Pb - ^{207}Pb age of 270 ± 5 Ma (Table 1) which is interpreted as the age of crystallization.

Tagish Lake suite

The Tagish Lake suite is made up of Middle Jurassic hornblende granodiorite plutons exposed in the Tagish Lake area. It includes the Hale Mountain granodiorite and the Mt. Caplice granodiorite.

Table 1. U-Pb data for zircon and sphene fractions

Fraction size ¹	Wt. mg	U ppm	Pb ² ppm	$^{206}\text{Pb}^3$ / ^{204}Pb	Pbc ⁴ pg	^{208}Pb %	$^{206}\text{Pb}^5$ / ^{238}U	$^{207}\text{Pb}^5$ / ^{235}U	Corr. Coeff.	$^{207}\text{Pb}^6$ / ^{206}Pb	$^{207}\text{Pb}^7$ / ^{206}Pb	$^{207}/^{206}$ Age ⁶ age (Ma)	$^{207}/^{206}$ Age ⁷ age (Ma)
LC-88-35-1, Hale Mountain Granodiorite, variably deformed hornblende granodiorite from Hale Mountain, UTM 6596500N, 531925E.													
<u>zircon</u> ⁸													
A (+149)	0.169	405	12	4267	30	11.2	0.02919 ±0.08%	0.2008 ±0.10%	0.8572	0.04989 ±0.05%	0.04985	190.0 ±2.5	188.0
B (+149)	0.182	291	9	4299	23	12.6	0.02904 ±0.09%	0.1996 ±0.11%	0.8954	0.04984 ±0.05%	0.04979	187.4 ±2.4	185.1
C (+149)	0.260	398	12	4010	48	11.6	0.02919 ±0.15%	0.2001 ±0.16%	0.8911	0.04972 ±0.07%	0.04968	181.8 ±3.4	180.2
D (+149)	0.211	390	12	5311	28	11.6	0.02900 ±0.09%	0.1994 ±0.11%	0.9158	0.04987 ±0.04%	0.04983	188.9 ±2.1	187.0
E (+149)	0.182	431	13	8711	16	11.6	0.02897 ±0.11%	0.1991 ±0.12%	0.9303	0.04986 ±0.05%	0.04982	188.4 ±2.1	186.4
F (+149)	0.110	382	11	5756	13	11.6	0.02909 ±0.09%	0.2000 ±0.12%	0.8591	0.04987 ±0.06%	0.04981	188.8 ±2.9	186.1
<u>sphene</u> ⁸													
S1 (+149)	0.256	222	9	161	736	34.4	0.02900 ±0.20%	0.2019 ±0.10%	0.7652	0.05048 ±0.88%		217.3 +40.1/ -41.1	
S2 (+149)	0.310	172	7	146	773	38.9	0.02901 ±0.21%	0.2026 ±0.11%	0.7664	0.05066 ±0.94%		225.5 +43.1/ -44.3	
LC-89-91b, Wann River Gneiss, compositionally layered hornblende-plagioclase gneiss from south of the upper Wann River, 6573525N 536750E.													
<u>zircon</u>													
A (+74)	0.065	218	10	1970	19	16.9	0.04177 ±0.09%	0.2976 ±0.16%	0.6993	0.05166 ±0.11%		270.4 +5.2/ -5.3	
B (+74)	0.052	185	9	3726	7	17.8	0.04602 ±0.09%	0.3465 ±0.13%	0.7730	0.05461 ±0.08%		396.4 ±3.7	
C (+74)	0.033	272	13	1974	12	18.1	0.04190 ±0.12%	0.2990 ±0.17%	0.6773	0.05176 ±0.13%		274.9 +5.8/ -5.9	
D (+74)	0.022	236	11	1187	11	17.4	0.04207 ±0.10%	0.3000 ±0.25%	0.6019	0.05172 ±0.20%		273.0 +9.3/ -9.4	
E (+74)	0.025	202	9	471	30	18.4	0.04220 ±0.12%	0.3017 ±0.44%	0.6068	0.05185 ±0.38%		279.0 +17.2/ -17.4	
Notes: ¹ sizes (i.e. +105) refer to length aspect of crystals in microns; ² radiogenic Pb; ³ measured ratio, corrected for spike and fractionation; ⁴ total common Pb in analysis corrected for spike and fractionation; ⁵ corrected for blank Pb and U, common Pb, errors quoted are one sigma in percent; ⁶ corrected for blank and common Pb, errors are two sigma in Ma; decay constants are those of Steiger and Jager (1977); for analytical details see Parrish et al. (1987); ⁷ corrected for initial Th exclusion, assuming whole rock Th/U=3/1 (see Scharer, 1984); ⁸ common Pb correction made using initial common Pb isotopic compositions from feldspars from Katet Mountain quartz monzonite from the Iskut River area, west-central B.C., $^{206}\text{Pb}/^{207}\text{Pb} = 19.015 \pm 0.1$, $^{207}\text{Pb}/^{204}\text{Pb} = 15.662 \pm 0.1$, $^{208}\text{Pb}/^{204}\text{Pb} = 38.714 \pm 0.2$ (M.L. Bevier, pers. comm., 1991).													

Table 2. Initial $^{87}\text{Sr}/^{86}\text{Sr}$ Ratios

Sample	Lithologic Unit	Easting	Northing	ppm Sr	ppm Rb	$\frac{^{87}\text{Rb}}{^{87}\text{Sr}}$	$\frac{^{87}\text{Sr}}{^{86}\text{Sr}}$	Age(Ma)	$\frac{^{87}\text{Sr}(i)}{^{86}\text{Sr}}$ ¹
LW76-a68A ²	Wann River Gneiss	547918	6552207	414	5.9	0.041	0.7064	262 ±5	0.7062
LW76-a76c ²	Mt. Caplice Granodiorite	545723	6560161	1081	95.9	0.257	0.7056	179	0.7049
T75-323-6 ²	Hale Mtn Granodiorite	538892	6588298	997	36.3	0.104	0.7055	185 ±1	0.7052

¹decay constants are those of Steiger and Jager (1977); ²unpublished data collected at Univeristy of British Columbia, 1970-1985, R.L. Armstrong, pers comm., 1991).

Hale Mountain granodiorite

The Hale Mountain granodiorite is a medium- to coarse-grained hornblende granodiorite characterized by plagioclase phenocrysts and minor sphene and epidote. Near its margins it has a penetrative foliation that is concordant with the bounding shear zones, and a penetrative fabric localized along layers within the pluton. Between the foliated layers the Hale Mountain granodiorite is massive.

The initial $^{87}\text{Sr}/^{86}\text{Sr}$ ratio for a sample of Hale Mountain granodiorite is relatively low and does not reflect the presence of an evolved source (Table 2, unpublished data, R.L. Armstrong, pers. comm., 1991).

U-Pb Geochronology

Six zircon and two sphene fractions from the Hale Mountain granodiorite were analyzed (Table 1). The zircon crystals are clear, euhedral, and elongate (length:width = 2-3:1), with minor inclusions, and no visible cores. The common Pb correction was made using initial isotopic Pb compositions from feldspars from the Katete Mountain Quartz Monzodiorite in the Iskut River area, which may have formed in a similar environment (Stikinia), and which is close in age to the Hale Mountain granodiorite (about 192 Ma; M.L. Bevier, pers. comm., 1991; Table 1). These Pb isotope ratios are close to those determined using the Stacey and Kramers (1975) Pb isotope growth curve for 192 Ma, and therefore do not significantly affect the age determined for the Hale Mountain granodiorite.

Except one, all of the zircon fractions cluster and plot below concordia (Fig. 5). The $^{207}\text{Pb}/^{206}\text{Pb}$ ratio for the fraction above concordia has standard errors about the mean two or more times the errors for other fractions. The reversely discordant deviation is therefore most likely due to



Figure 3. Foliated felsic dyke cutting across layers in the Boundary Ranges metamorphic suite. Note the left side of the leucocratic orthogneiss dyke crosscutting fabrics in the chlorite schist country rocks.

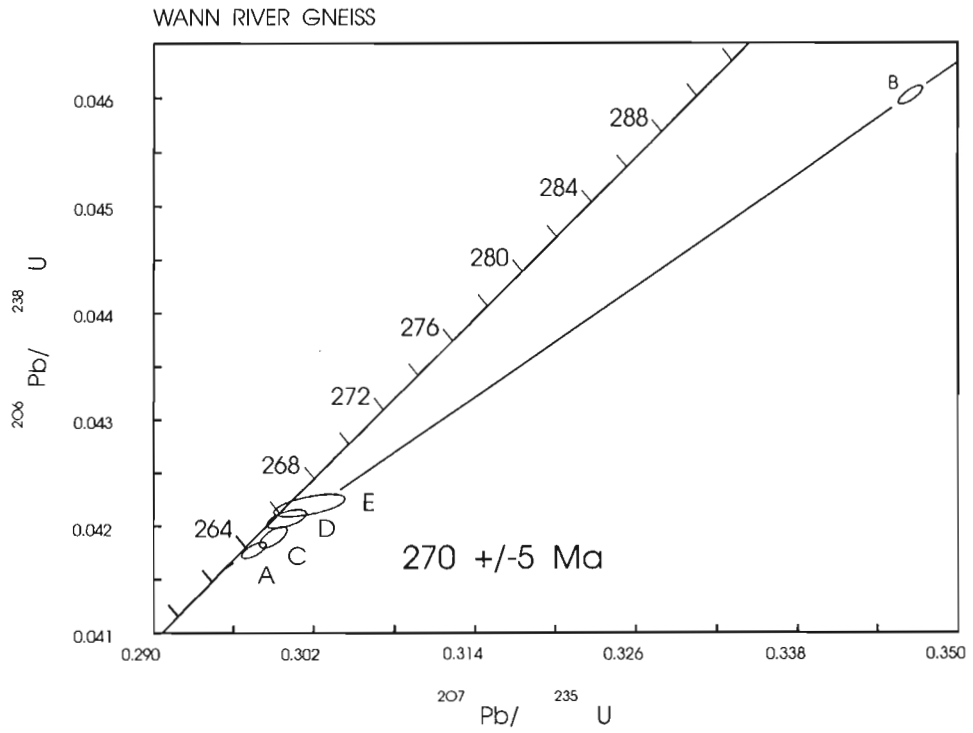


Figure 4. U-Pb concordia diagram for the Wann River gneiss.

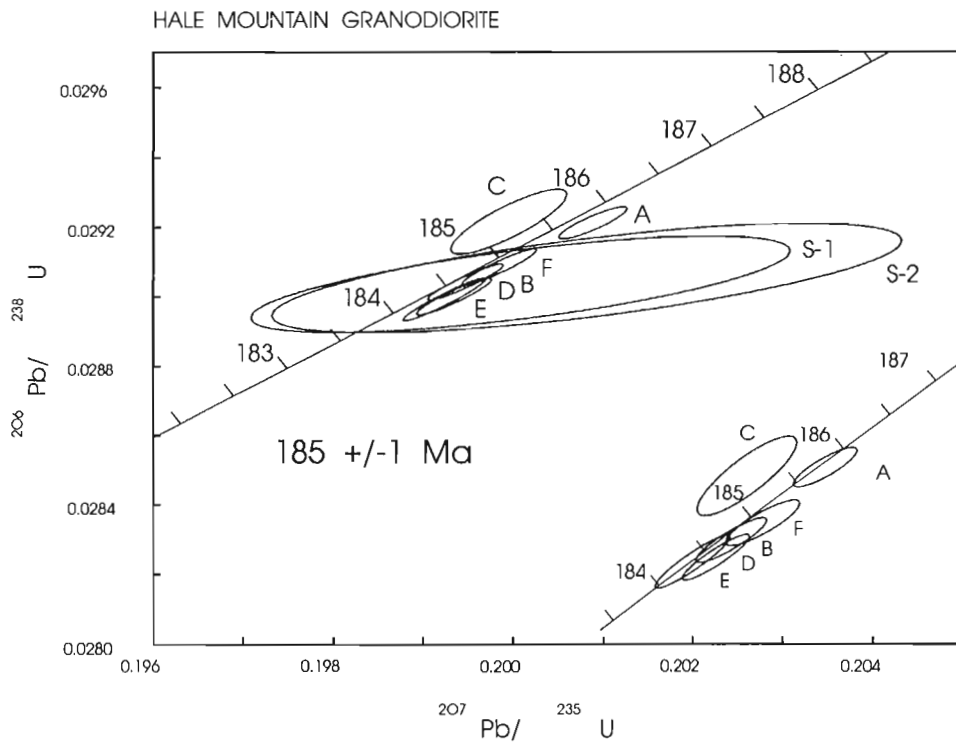


Figure 5. U-Pb concordia diagram for the Hale Mountain granodiorite.

additional, but unspecified analytical error associated with this specific analysis of Pb isotopes. The slight normal discordance of the remaining zircon fractions can be accounted for by the exclusion of ^{230}Th from zircon during crystallization (Mattinson, 1973). Since ^{230}Th is an intermediate daughter product of the ^{238}U - ^{206}Pb decay chain (half life = 7.52×10^4 Ma), "the exclusion of ^{230}Th from zircon during crystallization will result in a deficiency of ^{206}Pb equivalent to the amount of ^{230}Th excluded" (Mattinson, 1973). After correction for excluded ^{230}Th (Table 1), the zircon analyses plot on concordia between 184 and 186 Ma (Fig. 5) and therefore an age of 185 ± 1 Ma (Middle Jurassic) is the considered age of the Hale Mountain granodiorite.

The sphene fractions are concordant and have U-Pb ages within the error associated with U-Pb zircon age for this sample (Table 1; Fig. 5). The errors for sphene fractions are larger than those for zircon fractions because sphene incorporates more common Pb in its structure than zircon during crystallization.

Mt. Caplice granodiorite

The Mt. Caplice granodiorite is a moderately foliated, medium-grained hornblende granodiorite with minor sphene. U-Pb zircon ages (preliminary data, not presented in this paper) indicate that its age is Middle Jurassic.

An initial $^{87}\text{Sr}/^{86}\text{Sr}$ ratio for a sample of the Mt. Caplice granodiorite shows that it derives from a relatively unevolved source (Table 2; unpublished data, R.L. Armstrong, pers. comm., 1991).

INTERPRETATIONS AND CORRELATIONS

Rocks like those of the Boundary Ranges metamorphic suite, Wann River gneiss and Tagish Lake suite, exist in the Yukon-Tanana Terrane and Stikinia (Table 3). In all three areas Devonian to Mississippian, Permian and Jurassic igneous (plutonic and/or volcanic) rocks are represented, and rocks of Permian and Jurassic age preserve unevolved isotopic signatures (Tables 2, 3). Correlations between metamorphic rocks of the Tagish Lake area and metamorphic rocks of the Scotia-Quaal Belt (Coast Ranges of west-central British Columbia) have been made by Gareau (1991).

Correlations between Stikinia and parts of Yukon-Tanana Terrane have previously been discounted because of differences in metamorphic grade and state of strain. In Yukon-Tanana Terrane, Permian and older rocks are foliated, but in central and southern British Columbia, Stikinia rocks are commonly unmetamorphosed and mildly deformed. Consequently, metamorphic rocks in Yukon have been traditionally included in Yukon-Tanana Terrane, whereas in central British Columbia metamorphic rocks are correlated with equivalents of the same age in Stikinia. For example, Middle Jurassic rocks of the Central Gneiss Complex are correlated with coeval less deformed, lower grade rocks of the Gamsby Group, which belong to Stikinia (van der

Heyden, 1982). The Tagish Lake area lies south of exposed Yukon-Tanana Terrane rocks and north of Stikinia exposures in west-central British Columbia, and links these areas.

Boundary Ranges metamorphic suite

Rocks belonging to the Boundary Ranges metamorphic suite are interpreted to be volcanic and sedimentary rocks of probable Paleozoic age (Late Mississippian or older). They are assumed to have formed in an arc setting, and were intruded by felsic plutons and dykes (now orthogneisses) in Mississippian time. A possible correlative within Stikinia is the Paleozoic Stikine Assemblage, which includes sedimentary, volcanic and igneous rocks of Devonian to Mississippian age (Monger, 1977; Anderson, 1989; Brown et al., 1991). In Yukon Devonian to Mississippian orthogneisses (e.g. Pelly Gneiss) are preserved and intrude carbonaceous and non-carbonaceous metasedimentary rocks and metavolcanic rocks comprising the "middle unit" of Yukon-Tanana Terrane of Mortensen (in press). These orthogneisses may be correlative with orthogneisses in the Tagish Lake area and the metasedimentary and metavolcanic rocks may be correlative with those of Boundary Ranges metamorphic suite.

Initial $^{87}\text{Sr}/^{86}\text{Sr}$ ratios for the Boundary Ranges metamorphic suite are low (Jackson et al., 1991), whereas initial $^{87}\text{Sr}/^{86}\text{Sr}$ ratios for Devonian to Mississippian orthogneisses in Yukon are generally high (Mortensen, in press).

Possible pre-Permian unconformity

Equivalence of terranes can be postulated on the basis of corresponding periods of deposition, intrusive activity, non-deposition or erosion. A pre-Permian unconformity has been documented for Stikinia in the Telegraph Creek map area (Souther, 1971, 1972; Read et al., 1989; Brown et al., 1991), where deformed pre-Permian rocks are overlain by less deformed Permian limestone. An equivalent pre-Permian unconformity within the Tagish Lake area metamorphic rocks, between the Late Mississippian or older Boundary Ranges metamorphic suite and the Permian Wann River gneiss, is possible. However, the Boundary Ranges metamorphic suite and the Wann River gneiss are everywhere separated by the Hale Mountain granodiorite and the contact between them is not preserved (Fig. 2). No pre-Permian unconformity is documented in the Yukon-Tanana Terrane, but the absence of rocks between 341 and 263 Ma (Mortensen, in press) allows for postulation that one exists within Yukon-Tanana Terrane.

Wann River gneiss

The Wann River gneiss is interpreted as a metamorphosed volcanic unit, based on the banding in the gneiss which locally preserves primary structures. The gneiss may correlate with volcanic rocks of proposed Permian age (no geochronological data) in Stikinia (Monger, 1977; Anderson, 1989; Brown et al., 1991), and Permian suites of rocks from

Table 3. Comparison of age, composition, and isotopic characteristics of Jurassic, Permian and Paleozoic rocks from Yukon-Tanana Terrane, Tagish Lake area, west-central British Columbia, and Stikinia

	Yukon-Tanana Terrane, Yukon ¹	Metamorphic Rocks NW B.C. ²	Stikinia B.C.
EARLY TO MIDDLE JURASSIC			
Lithologic unit	Includes: Klotassin suite, Aishihik Batholith	Tagish Lake Suite	Includes: Texas Creek plutonic suite, Three Sisters plutonic suite ³
Composition	hornblendite, Hbl/Bt granodiorite, Qtz monzonite, syenite	Ep-Hb granodiorite	(Bt) Hb granodiorite, Qtz monzodiorite, K-spar- phyric andesite dykes, Bt syenite
U-Pb age range(Ma)	185-212	179 to 185	189-195 ³
Sr initial ratios	0.704	0.705	0.703-.705 ⁴
Associated volcanic rocks	none known	none known	Hazelton volcanic rocks
MID-PERMIAN			
Lithologic unit	Includes: Sulphur Creek orthogneiss, Klondike schist metavolcanic rocks and sills.	Wann River Gneiss	Asitka Group ⁵
Composition	Bt-Qtz monzonite, Qtz-Felds porphyry	intermediate Hb-Plag gneiss	
U-Pb age range (Ma)	256-263	270 ±5	
Sr initial ratios	0.706-0.711	0.7062	0.703-.705 ⁴
DEVONIAN/MISSISSIPPIAN			
Lithologic unit(s)	Simpson Range plutonic suite, Selwyn Gneiss, Mt. Burnham orthogneiss, Fiftymile Batholith, Moose Creek orthogneiss	Bighorn Creek orthogneiss, Felsic dykes intruding Boundary Ranges metamorphic suite rocks	Bimodal arc volcanic rocks
Composition	gabbro to granite	granite	
U-Pb age range (Ma)	343-365	320 to 350	
Sr initial ratios	0.709-0.728	no data	no data
Associated volcanic rocks	mafic to felsic metavolcanics (Sr _i =0.709)	not known	no data
References used here may be compilations of earlier data. For original references the reader is referred to these compilations. ¹ Mortensen (1991; in press), ² This paper, ³ Anderson (1989); Anderson and Bevier (1990), ⁴ Samson et al. (1989), ⁵ Monger (1977). Bt - biotite, Ep - epidote, Felds - feldspar, Hb - hornblende, K-spar - alkali feldspar, Ms - muscovite, Plag - plagioclase, Qtz - quartz.			

the "upper unit" of Yukon-Tanana Terrane of Mortensen (in press), including the Simpson Range suite (Mortensen, in press) and Selwyn Gneiss (Tempelman-Kluit and Wanless, 1975; Table 3).

Tagish Lake suite

Hornblende granodiorite in the Middle Jurassic Tagish Lake suite have plutonic equivalents in the Yukon-Tanana Terrane (e.g. Klotassin suite; Tempelman-Kluit and Wanless, 1975; Mortensen, in press) and in Stikinia (e.g. Gamsby Group; van der Heyden, 1982). Low initial $^{87}\text{Sr}/^{86}\text{Sr}$ ratios are characteristic of Jurassic rocks from all three areas (Table 3). Volcanic equivalents of these plutonic rocks are preserved only in Stikinia (Hazelton volcanic rocks).

Florence Range metamorphic suite

As mentioned above, the Florence Range metamorphic suite is considered to belong to Nisling Terrane. Consequently, if other metamorphic rocks in the Tagish Lake area are correctly included in Stikinia, then the Nisling-Stikinia terrane boundary exists in the Tagish Lake area.

Mortensen (in press) has correlated the "lower unit" of Yukon-Tanana Terrane with Nisling Terrane, which implies that the Florence Range metamorphic suite is correlative with the "lower unit" of Yukon-Tanana Terrane. If correlation of the Tagish Lake area metamorphic rocks with Stikinia and Yukon-Tanana Terrane rocks are correct, then the Nisling-Stikinia terrane boundary should continue northward from the Tagish Lake area into Yukon.

CONCLUSION

New U-Pb zircon ages for the Hale Mountain granodiorite (185 ± 1 Ma) and the Wann River gneiss (170 ± 5 Ma), and preliminary data that constrain the age of the Boundary Ranges metamorphic suite to Late Mississippian or older, together with lithological characteristics and initial $^{87}\text{Sr}/^{86}\text{Sr}$ ratios, support correlation of the Boundary Ranges metamorphic suite, Wann River gneiss and Tagish Lake suite with Stikinia and parts of Yukon-Tanana Terrane. If the correlations are correct, then not all metamorphic rocks in the Tagish Lake area belong to the Nisling Terrane, and Stikinia rocks are exposed farther west and Yukon-Tanana rocks are exposed farther south than previously thought. This implies that Stikinia rocks correlate with the "middle and upper units" of Yukon-Tanana Terrane of Mortensen (in press), that the Nisling-Stikinia boundary is exposed in the Tagish Lake area, and that the boundary should continue northward into Yukon-Tanana Terrane.

ACKNOWLEDGMENTS

Fieldwork was funded by Geological Survey of Canada Project 850001 and a Natural Sciences and Engineering Research Council Operating Grant awarded to R.R. Parrish, and by a Northern Scientist Training Program Grant from the Department of Indian and Northern Affairs and a Geological

Society of America Grant awarded to L.D. Currie. Geochronology was performed at the Geological Survey of Canada in Ottawa.

Unpublished initial Sr ratios were generously provided by Dick Armstrong.

Ideas presented in this paper were aided by discussions with Randy Parrish, Jim Mortensen, Dick Brown, Jay Jackson, Susie Gareau and Mitch Mihalynuk. Dirk Tempelman-Kluit is thanked for critically reading and improving the manuscript. However, any errors or omissions are the responsibility of the author.

REFERENCES

- Anderson, R.G.**
1989: A stratigraphic, plutonic, and structural framework for the Iskut River map area, northwestern British Columbia; in Current Research, Part E, Geological Survey of Canada, Paper 89-1E, p. 145-154.
- Anderson, R.G. and Bevier, M.L.**
1990: A note on Mesozoic and Tertiary K-Ar geochronometry of plutonic suites, Iskut River map area, northwestern British Columbia; in Current Research, Part E, Geological Survey of Canada, Paper 90-1E, p. 141-147.
- Brown, D.A., Logan, J.M., Gunning, M.H., Orchard, M.J., and Bamber, W.E.**
1991: Stratigraphic evolution of the Paleozoic Stikine assemblage in Stikine and Iskut rivers area, northwestern British Columbia; Canadian Journal of Earth Sciences, v. 28, p. 958-972.
- Bultman, T.R.**
1979: Geology and tectonic history of the Whitehorse Trough west of Atlin, British Columbia; Ph.D. thesis, Yale University, New Haven, Connecticut, 284 p.
- Christie, R.L.**
1957: Bennett, Cassiar District, British Columbia; Geological Survey of Canada, Map 19-1957.
- Coney, P.J., Jones, D.L., and Monger, J.W.H.**
1980: Cordilleran suspect terranes; Nature, v. 288, p. 329.
- Currie, L.D.**
1990: Metamorphic rocks in the Florence Range, Coast Mountains, northwestern British Columbia; in Current Research, Part E, Geological Survey of Canada, Paper 90-1E, p. 113-119.
- 1991: Geology of the Tagish Lake area, northern Coast Mountains, northwestern British Columbia; in Current Research, Part A, Geological Survey of Canada, Paper 91-1A, p. 147-153.
- Gareau, S.A.**
1991: Geology of the Scotia-Quaal metamorphic belt, Coast Plutonic Complex, British Columbia; Ph.D. thesis, Carleton University, Ottawa, Ontario, 391 p.
- Jackson, J.L., Patchett, P.J., and Gehrels, G.E.**
1991: Preliminary Nd and Sr isotopic analyses from the Nisling assemblage, northern Stikine and northern Cache Creek terranes, northern British Columbia and adjacent Yukon (104M,N); in Geological Fieldwork 1991, British Columbia Ministry of Energy, Mines and Petroleum Resources, Paper 1991-1, p. 153-159.
- Mattinson, J.M.**
1973: Anomalous isotopic composition of lead in young zircons; Carnegie Institute of Washington Yearbook, v. 72, p. 613-616.
- Mihalynuk, M.G. and Rouse, J.N.**
1988a: Geology of the Tutshi Lake area, British Columbia; British Columbia Ministry of Energy, Mines and Petroleum Resources, Geological Survey Branch, Open File Map 1988-5 (104M/15).
- 1988b: Preliminary geology of the Tutshi Lake area, northwestern British Columbia (104M/15); in Geological Fieldwork 1987, British Columbia Ministry of Energy, Mines and Petroleum Resources, Paper 1988-1, p. 217-231.

- Mihalynuk, M.G., Currie, L.D., Mountjoy, K.M., and Wallace, C.**
1989a: Geology of the Fantail Lake (west) and Warm Creek (east) map area; British Columbia Ministry of Energy, Mines and Petroleum Resources, Geological Survey Branch, Open File Map 1989-13 (104M/9W and 10E).
- Mihalynuk, M.G., Currie, L.D., and Arksey, R.L.**
1989b: Geology of the Tagish Lake area (Fantail Lake and Warm Creek) (104M/9W and 10E); in Geological Fieldwork 1988, British Columbia Ministry of Energy, Mines and Petroleum Resources, Paper 1989-1, p. 293-310.
- Mihalynuk, M.G., Mountjoy, K.J., Currie, L.D., Lofthouse, D.L., and Winder, N.**
1990: Geology of the Tagish Lake area (Fantail Lake and Warm Creek) (104M/9W and 10E); British Columbia Ministry of Energy, Mines and Petroleum Resources, Geological Survey Branch, Open File Map 1990-4.
- Monger, J.W.H.**
1977: Upper Paleozoic rocks of the western Canadian Cordillera and their bearing on Cordilleran evolution; Canadian Journal of Earth Sciences, v. 14, p. 1832-1859.
- Monger, J.W.H., Price, R.A., and Tempelman-Kluit, D.**
1982: Tectonic accretion and the two metamorphic and plutonic welts in the Canadian Cordillera; Geology, v. 10, p. 70-75.
- Mortensen, J.K.**
1991: U-Pb zircon ages, Nd isotopic compositions and tectonic significance of Middle and Late Paleozoic magmatism in the Yukon-Tanana Terrane, western Yukon Territory, Canada (Abstract); Geological Society of America, Program with Abstracts, v. 23, p. A434.
in press: Pre-Mid-Mesozoic tectonic evolution of the Yukon-Tanana Terrane, Yukon and Alaska; Tectonics.
- Parrish, R.R., Roddick, J.C., Loveridge, W.D., and Sullivan, R.W.**
1987: Uranium-lead analytical techniques at the geochronology laboratory, Geological Survey of Canada; in Radiogenic Age and Isotopic Studies: Report 1, Geological Survey of Canada, Paper 87-2, p. 3-7.
- Read, P.B., Brown, R.L., Psutka, J.F., Moore, J.M., Journeay, M., Lane L.S., and Orchard, M.J.**
1989: Geology, More and Forrest Kerr creeks (parts of 104B/10, 15, 16, and 104G/1, 2), northwestern British Columbia; Geological Survey of Canada, Open File 2094.
- Samson, S.D., McClelland, W.C., Patchett, P.J., Gehrels, G.E., and Anderson, R.G.**
1989: Evidence from neodymium isotopes for mantle contributions to Phanerozoic crustal genesis in the Canadian Cordillera; Nature, v. 337, p. 705-709.
- Samson, S.D., Patchett, P.J., McClelland, W.C., and Gehrels, G.E.**
1991: Nd isotopic characterization of metamorphic rocks in the Coast Mountains of Alaskan and Canadian Cordillera: ancient crust bounded by juvenile terranes; Tectonics, v. 10, p. 770-780.
- Scharer, U.**
1984: The effect of initial ^{230}Th equilibrium on young U-Pb ages: the Makalu case, Himalaya; Earth and Planetary Science Letters, v. 67, p. 191-204.
- Souther, J.G.**
1971: Geology and mineral deposits of Tulsequah map area; Geological Survey of Canada, Memoir 362, 51 p.
1972: Telegraph Creek map-area, British Columbia; Geological Survey of Canada, Paper 71-44, 38 p.
- Stacey, J.S. and Kramers, J.D.**
1975: Approximation of terrestrial lead isotope evolution by a two-stage model; Earth and Planetary Science Letters, v. 26, p. 207-221.
- Steiger, R.H. and Jager, E.**
1977: Subcommittee on geochronology: convention on the use of decay constants in geo- and cosmochronology; Earth and Planetary Science Letters, v. 36, p. 359-362.
- Tempelman-Kluit, D.J. and Wanless, R.K.**
1975: Potassium-argon age determinations of metamorphic and plutonic rocks in the Yukon Crystalline Terrane; Canadian Journal of Earth Sciences, v. 12, p. 1895-1909.
- van der Heyden, P.**
1982: Tectonic and stratigraphic relations between the Coast Plutonic Complex and the Intermontane Belt, west-central Whitesail Lake map area; M.Sc. thesis, University of British Columbia, Vancouver, 172 p.
- Werner, L.J.**
1977: Metamorphic terrane, northern Coast Mountains west of Atlin Lake, British Columbia; in Report of Activities, Part A, Geological Survey of Canada, Paper 77-1A, p. 267-269.
1978: Metamorphic terrane, north Coast Mountains west of Atlin Lake, British Columbia; in Current Research, Part A, Geological Survey of Canada, Paper 78-1A, p. 69-70.
- Wheeler, J.O., Brookfield, A.J., Gabrielse, H., Monger, J.W.H., Tipper, H.W., and Woodsworth, G.J.**
1988: Terrane map of the Canadian Cordillera; Geological Survey of Canada, Open File 1987.

U-Pb geochronology of plutonic clasts from conglomerates in the Ladner and Jackass Mountain groups and the Peninsula Formation, southwestern British Columbia

Jennifer A. O'Brien¹, George E. Gehrels¹, and J.W.H. Monger
Cordilleran Division, Vancouver

O'Brien, J.A., Gehrels, G.E., and Monger, J.W.H., 1992: U-Pb geochronology of plutonic clasts from conglomerates in the Ladner and Jackass Mountain groups and the Peninsula Formation, southwestern British Columbia; in *Current Research, Part A; Geological Survey of Canada, Paper 92-1A*, p. 209-214.

Abstract

Two plutonic clasts from the Methow terrane yield U-Pb ages of: 1) 235 ± 10 Ma with Pb loss at 75 ± 20 Ma from the Early Jurassic Boston Bar Formation of the Ladner Group; and 2) 156 ± 1 Ma from the lower Albian conglomerate unit of the Jackass Mountain Group. A granitic clast from the base of the Berriasian Peninsula Formation of the Harrison terrane yields a U-Pb age of 164.5 ± 1.5 Ma. Granitic and gneissic rocks with ages roughly the same as those of the Ladner and Jackass Mountain clasts occur in, respectively, Mount Lytton and Eagle plutonic complexes of southwesternmost Quesnel terrane. This suggests that the Methow terrane may have been linked to Quesnel terrane by Early Jurassic time. The Peninsula clast is coeval with granitic rocks that stratigraphically underlie the Peninsula Formation in the southwestern Coast Mountains.

Résumé

Deux roches clastiques plutoniques du terrane de Methow donnent des âges U-Pb de : 1) 235 ± 10 Ma avec perte de plomb à 75 ± 20 Ma pour la formation de Boston Bar du Jurassique inférieur du groupe de Ladner; et de 2) 156 ± 1 Ma pour l'unité conglomératique de l'Albien inférieur du groupe de Jackass Mountain. Une roche clastique granitique de la base de la formation de Peninsula du Berriasien du terrane de Harrison donne un âge U-Pb de $164,5 \pm 1,5$ Ma. Des roches granitiques et gneissiques d'âge relativement équivalent à celles des roches clastiques de Ladner et de Jackass Mountain reposent, respectivement, dans les complexes plutoniques de Mount Lytton et d'Eagle de l'extrême sud-ouest du terrane de Quesnel. Le terrane de Methow pourrait donc avoir eu un lien avec le terrane de Quesnel avant le Jurassique inférieur. Les roches clastiques de Peninsula sont contemporaines des roches granitiques qui reposent stratigraphiquement au-dessous de la formation de Peninsula dans la sud-ouest de la chaîne Côtière.

¹ Department of Geosciences, University of Arizona, Tucson, Arizona, 85721, U.S.A.

INTRODUCTION

The juncture of the Coast and Cascade mountains, southwestern British Columbia, contains several discrete terranes (Fig. 1; Monger, 1989; Tabor et al., 1989). Each has a distinctive stratigraphy and/or lithological association, each is at least partly coeval with neighbouring terranes, and each is bounded by major faults. The paleogeographic relationships between terranes prior to their juxtaposition in mid-Cretaceous time are uncertain.

The U-Pb ages from plutonic clasts given herein are from conglomerates in: 1) the Lower Jurassic section of the Boston Bar Formation of the Ladner Group, Methow terrane; 2) the lower Albian unit of the Jackass Mountain Group, Methow terrane; and 3) the base of the Berriasian Peninsula Formation, Harrison Lake terrane (Fig. 2). The dating was done to determine possible provenances of the plutonic clasts in an attempt to establish terrane linkages.

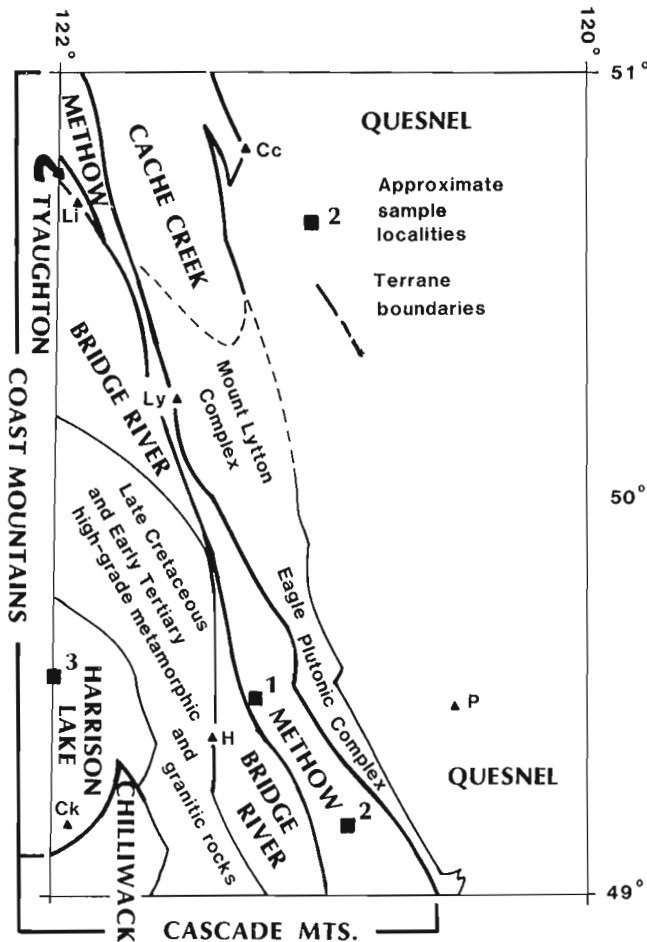


Figure 1. Simplified terrane map showing the location of clasts sampled for U-Pb analysis. Towns for geographic reference include: Cc = Cache Creek, Ck = Chilliwack, H = Hope, Li = Lillooet, Ly = Lytton, and P = Princeton.

The samples were collected by O'Brien and Gehrels in 1986 for a study related to thesis work (O'Brien, 1987) supported during regional mapping of Hope (92H) area (Monger, 1989). The isotopic analyses were made in the Department of Geosciences, University of Arizona.

METHOW TERRANE

The Methow terrane includes volcanic and sedimentary strata that range in age from probable Triassic through early Late Cretaceous. Lowermost is the basaltic Spider Peak Formation and associated greenstone of the Coquihalla serpentine belt (Anderson, 1976; Ray, 1986, 1990). This is overlain by approximately 2000 m of Sinemurian(?) to Aalenian(?) argillite and siltstone with subordinate greywacke and conglomerate of the Boston Bar Formation, of the Ladner Group. These grade upsection and in part

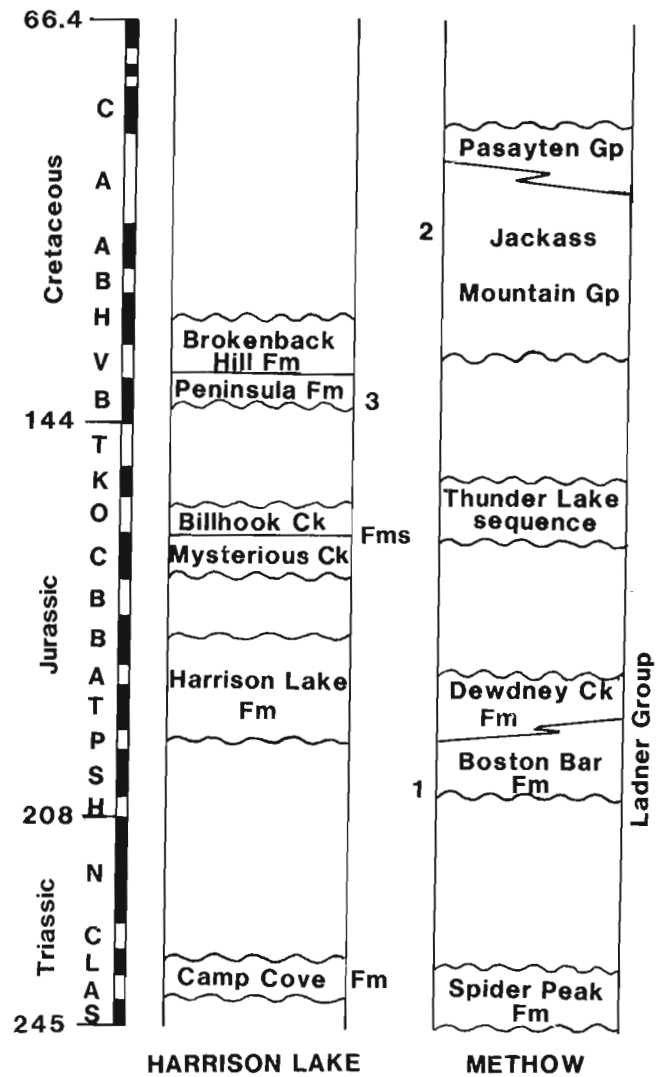


Figure 2. Simplified stratigraphic sections of the Methow and Harrison Lake terranes. The stratigraphic positions of the three samples are indicated by number. The time scale includes a schematic representation of the stages, indicated by initials.

laterally into volcanogenic clastics and flows of the Aalenian to Bajocian Dewdney Creek Formation, of the Ladner Group. Disconformably above are volcanic sandstone and argillite of the Oxfordian to Tithonian Thunder Lake sequence (O'Brien, 1986, 1987). On the west side of the terrane this sequence is disconformably overlain by about 4500 m of Hauterivian through Albian argillite, sandstone, and conglomerate of the Jackass Mountain Group. Sandstone and conglomerate of the Pasayten Group are in part coeval with and partly overlie the Jackass Mountain Group (Coates, 1974).

Boston Bar Formation

The basal Boston Bar Formation is characterized by conglomerate and associated coarse sandstone, siltstone, and argillite. This distinctive section is nearly 200 m thick in the vicinity of Carolin Mine, but tapers rapidly to the north and south. Individual conglomeratic horizons rarely exceed 30 m in thickness (Ray, 1986, 1990). Sub- to well-rounded clasts up to 50 cm in diameter are supported in a matrix of sheared mudstone or immature sandstone. Locally derived greenstone and gabbro are the most common detrital components, but a variety of granitic and felsic to intermediate volcanic rock types and limestone are present. The conglomerate horizon sampled is exposed north of Carolin Mine workings at an elevation of 3700 ft. (Fig. 1; Table 1). The age of this conglomerate is poorly constrained. The maximum age is dictated by the underlying Early(?) Triassic Spider Peak Formation (Ray, 1986) and the minimum age is loosely constrained by the occurrence of the bivalve *Weyla* (Sinemurian through Toarcian) within overlying argillaceous strata (O'Brien, 1987).

The clast sampled for analysis was a well-rounded boulder of medium grained, biotite quartz diorite, about 40 cm in diameter. Biotite has been altered to chlorite; plagioclase feldspar contains abundant secondary calcite and sericite. Brittle shear planes and thin quartz veins are common in the rock. The shear planes and quartz veins must have formed early in the history of this quartz diorite because they do not extend into the sedimentary matrix. Of interest for the mineralization in the region is the occurrence of $\leq 100\mu\text{m}$ -size gold particles in the heavy mineral separate from this clast. This occurrence raises the possibility that some of the gold mineralization in the Carolin Mine area is derived from these clasts.

Five zircon fractions from this sample are all discordant and lie along a line with concordia intercepts of 235 ± 10 Ma and 75 ± 20 Ma (95% confidence level; MSWD = 0.8) (Fig. 3a; Table 1). The occurrence of the five fractions near the upper intercept, combined with the probable Early Jurassic depositional age of the conglomerate, indicates that the upper intercept records crystallization and the lower intercept records isotopic disturbance, presumably by Pb loss.

Jackass Mountain Group

The lower Albian conglomerate sampled for U-Pb analysis was collected along Highway 3 in Manning Park (map unit 4 of Coates, 1974). The age is constrained by the occurrence

of Barremian fossils collected from argillites directly below the conglomerate and lower Albian pelecypods collected within the unit along strike from the sample locality (Coates, 1974). This poorly sorted conglomerate contains sub- to well-rounded clasts up to about 50 cm in diameter. Clasts are predominantly foliated plutonic rock (80%) with lesser amounts of intermediate volcanic rock (10%), undeformed plutonic clasts (5-10%), and minor chert (1%).

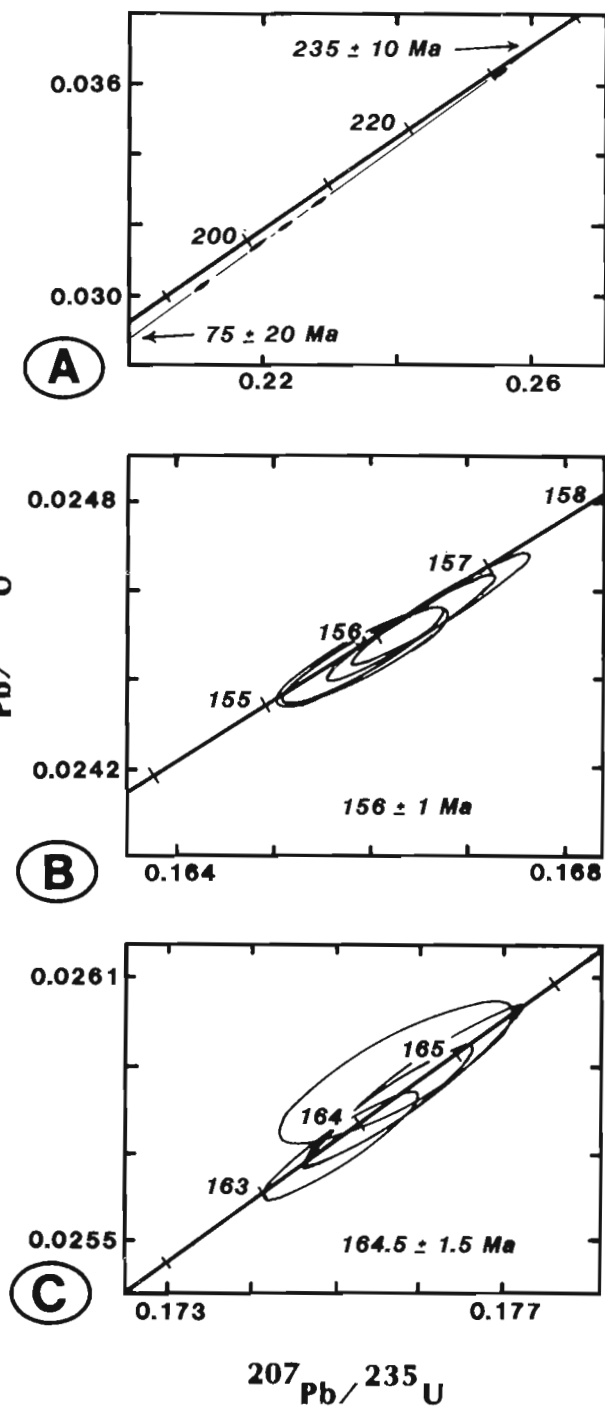


Figure 3. Concordia diagrams of: A) Ladner Group sample; B) Jackass Mountain Group sample; and C) Peninsula Formation sample.

A foliated plutonic clast, 35 cm in diameter, was collected from the conglomerate. The sample analyzed is a plagioclase porphyritic, medium grained, biotite tonalite. Four zircon fractions from this sample are concordant and yield a crystallization age of 156 ± 1 Ma (95% confidence level) (Fig. 3b; Table 1).

HARRISON LAKE TERRANE

The Harrison Lake terrane comprises a remarkably well preserved stratigraphic section of Middle Triassic to middle Albian age (Crickmay, 1930; Arthur, 1986; Monger, 1989, 1991). The lowest unit, the Middle Triassic Camp Cove Formation, consists of cherty argillite and mafic volcanic rocks.

Table 1. U-Pb isotopic data and apparent ages

Wt (mg)	Size (μm)	Concentration (ppm)		Isotopic Composition				Apparent ages	
		U	Pb	^{206}Pb ----- ^{204}Pb	^{206}Pb ----- ^{207}Pb	^{206}Pb ----- ^{208}Pb	$^{206}\text{Pb}^*$ ----- ^{238}U	$^{207}\text{Pb}^*$ ----- ^{235}U	$^{207}\text{Pb}^*$ ----- $^{206}\text{Pb}^*$
<i>Sample 1: Quartz diorite from base of Ladner Group (NTS 92H/11; UTM 10U 602390m E 5485500m N)</i>									
2.21	30-45	340.2	10.55	25000 (1500)	19.554 (9)	7	192.1 (0.9)	194.4 (1.0)	223 (7)
2.12	45-63	347.6	11.18	22000 (1300)	19.502 (9)	6	199.2 (0.9)	201.3 (1.1)	226 (9)
1.57	80-100	254.4	8.30	6300 (150)	18.872 (6)	6	202.7 (0.8)	204.7 (0.9)	228 (7)
1.80	100-125	229.4	7.67	14800 (700)	19.334 (9)	8	206.9 (0.8)	208.9 (0.9)	231 (9)
0.27a	125-175	222.2	7.89	3050 (30)	17.969 (10)	10	230.3 (0.9)	230.9 (1.0)	237 (9)
<i>Sample 2: Foliated biotite granodiorite from Jackass Mountain Group (NTS 92H/2; UTM 10U (624550m E 5484650m N)</i>									
1.06	30-45	286.4	7.23	12500 (150)	19.860 (18)	6	156.1 (0.6)	156.3 (0.7)	159 (9)
1.45	45-63	330.0	8.35	11600 (180)	19.821 (19)	6	156.4 (0.7)	156.6 (0.7)	159 (9)
0.56	100-125	226.6	5.58	4160 (60)	18.982 (15)	8	155.7 (0.6)	155.9 (0.7)	158 (9)
0.42a	125-175	125.7	3.10	2310 (20)	18.010 (16)	7	155.7 (0.6)	155.9 (0.7)	158 (10)
<i>Sample 3: Hornblende-biotite granodiorite from basal Peninsula Formation (NTS 92G/9; UTM 10U (572400m E 5485380m N)</i>									
1.93	30-45	302.4	7.88	11500 (600)	19.780 (11)	8	164.3 (0.7)	164.3 (0.8)	165 (9)
1.63	45-63	559.6	14.25	752 (6)	14.568 (10)	7	164.8 (0.8)	164.4 (1.1)	159 (12)
2.12	63-80	499.6	13.16	4160 (50)	18.940 (9)	8	164.6 (1.0)	164.6 (1.1)	164 (8)
0.87	80-100	436.7	11.46	5000 (120)	19.148 (8)	8	163.7 (0.8)	163.8 (0.7)	165 (7)
*Radiogenic Pb									
a = abraded to approximately 1/2 of original size in air abrasion device									
Information about analytical techniques is provided in Gehrels et al. (1991). All zircon fractions are non-magnetic at 1.8 amps, 5° side slope, and 15° forward slope. Constants used: $^{238}\text{U}=1.55125 \times 10^{-10}$, $^{235}\text{U}=9.8485 \times 10^{-10}$, $^{238}\text{U}/^{235}\text{U}=137.88$. All uncertainties (in parentheses) are reported at the 95% level. Isotopic compositions listed above have been adjusted only for Pb and U added with ^{205}Pb - ^{233}U - ^{235}U spike. In calculating concentrations and apparent ages the isotopic ratios are adjusted as follows:									
(1) Mass-dependent correction factors of: 0.14 (\pm 0.06) %/AMU for Pb, and 0.08 (\pm 0.04) %/AMU for UO_2 .									
(2) Pb ratios have been corrected for 0.010 (\pm 0.005) ng blank with: $^{206}\text{Pb}/^{204}\text{Pb} = 18.6$ (\pm 0.30), $^{207}\text{Pb}/^{204}\text{Pb} = 15.5$ (\pm 0.3), and $^{208}\text{Pb}/^{204}\text{Pb} = 38.0$ (\pm 0.8).									
(3) Uranium aliquot has been corrected for 0.001 (\pm 0.0005) ng blank.									
(4) Common Pb remaining after correcting for blank Pb is interpreted to be initial Pb and is assigned a composition of: $^{206}\text{Pb}/^{204}\text{Pb} = 18.5$ to 18.3 (\pm 2.0), $^{207}\text{Pb}/^{204}\text{Pb} = 15.60$ to 15.59 (\pm 0.30), and $^{208}\text{Pb}/^{204}\text{Pb} = 38.5$ to 38.0 (\pm 2.0). These values are interpreted from Stacey and Kramers (1975).									

The base of this unit is not exposed. Unconformably above are approximately 3000 m of Lower and Middle(?) Jurassic (Toarcian-Bathonian(?)) intermediate to felsic flows, tuffs, volcanogenic sediments, and minor argillite and conglomerate of the Harrison Lake Formation. Disconformably above are Middle and Late Jurassic (Callovian to lower Oxfordian) sedimentary Mysterious Creek and volcanic Billhook Creek formations, with a thickness of about 1000 m. Above are the Early Cretaceous (lower Berriasian to middle Albian) sedimentary Peninsula and volcanic Brokenback Hill formations (Arthur, 1986; Arthur et al., in press).

The nature of the contact at the base of the Peninsula Formation is uncertain. In places it appears to be disconformable, but elsewhere, Middle Jurassic argillites below the last break are more strongly cleaved than those above. This is the basis for the "Agassiz Orogeny" of Crickmay (1930). On the west side of the southern Coast Mountains there is evidence for contractional deformation between Early and Late Jurassic time (185 Ma and 155 Ma) and probable normal faulting during Late Jurassic and Early Cretaceous time (Monger, 1991). Coarse conglomerates widespread at the base of the Cretaceous section in the southern Coast Mountains may be the sedimentary expression of this faulting (Monger, 1991).

Peninsula conglomerate

The conglomerate sampled is located at the base of the Berriasian Peninsula Formation. The outcrop containing the largest clasts (up to 40 cm in diameter) was found on a logging road 9 km west of Harrison Lake, approximately 1.6 km north-northwest of the confluence of Eagle Creek and the Chehalis River. This poorly sorted conglomerate is composed predominantly of fine- to coarse-grained granodiorite (90%) with minor diorite and pyroxenite. These sub- to well-rounded clasts are supported in an arkosic matrix with abundant detrital mica.

A well-rounded clast 35 cm in diameter was sampled for analysis. It is an unfoliated, medium grained, hornblende-biotite granodiorite. Four zircon fractions from this sample are concordant and yield a crystallization age of 164.5 ± 1.5 Ma (95% confidence level) (Fig. 3c; Table 1).

DISCUSSION

The 235 ± 10 Ma upper intercept age for the clast from the Ladner Group can most closely be correlated in this region with U-Pb ages from the Mount Lytton complex (Fig. 1) of 225 ± 5 Ma (Parrish and Monger, in press) and 257 Ma (R.M. Friedman, pers. comm., 1991). The Mount Lytton complex lies immediately east of the northern part of the Methow terrane. It consists of layered quartzofeldspathic granitoid rock interleaved with layers of amphibolite, diorite, altered quartz diorite, and minor marble. The complex includes a crosscutting, relatively fresh biotite-hornblende granodiorite

which yielded a U-Pb age of 212 ± 1 Ma (Parrish and Monger, in press). Similar ages are recorded for the Guichon Creek batholith (Mortimer et al., 1990), which is separated from the Mount Lytton complex by the stratigraphically overlying mid-Cretaceous Spences Bridge Group.

As the Guichon Creek batholith is an integral part of the Quesnel terrane, it is reasonable to suggest that the Mount Lytton complex is exposed basement of at least part of the Quesnel terrane. Derivation of the clast from the Mount Lytton complex accordingly suggests that the Methow and Quesnel terranes were contiguous in Early Jurassic time.

The concordant 156 ± 1 Ma U-Pb age from the Jackass Mountain conglomerate is correlative with dates reported by Greig (1989) from older parts of the Eagle plutonic complex. This complex is located directly east of the Methow terrane, along strike to the south of the Mount Lytton complex. Unlike the Mount Lytton, the Eagle is a Late Jurassic and mid-Cretaceous plutonic complex composed largely of foliated to gneissic tonalite with minor amphibolite. It intrudes metamorphosed volcanic rocks of the Nicola Group (Greig, 1989), which are a major component of Quesnel terrane. Late Jurassic deformation evident along both the eastern and western margins of the Eagle plutonic complex (Greig, 1989) is not recognized within the Methow terrane. The Mount Lytton and Eagle plutonic complexes likely comprise the westernmost part of the Quesnel terrane, uplifted in the mid-Cretaceous (Greig, 1989; Monger, 1989).

The U-Pb age from the Jackass Mountain clast was expected. Lithological comparisons and current direction measurements have long suggested that the Eagle plutonic complex is the source for abundant foliated plutonic clasts present in the Jackass Mountain conglomerate (Coates, 1974; Tennyson and Cole, 1978). Kleinspehn and Woodsworth, (in Stevens et al., 1982) obtained K-Ar dates of 160 ± 11 , 133 ± 16 , and 134 ± 16 Ma from clasts in Jackass Mountain conglomerates of the Camelsfoot Range, west of the Fraser River.

The Peninsula Formation conglomerate appears to have a local source. The western part of the southern Coast Mountains contains abundant granitic rocks with ages of 173-147 Ma (Friedman and Armstrong, 1990; Monger, 1991; Parrish and Monger, in press). Within the general area of the conglomerate, pre-Cretaceous granitic rocks emplaced into the underlying stratified rocks gave a U-Pb age of 162 ± 2 Ma (Friedman and Armstrong, 1990), a K-Ar (biotite) date of 159.6 ± 2.8 Ma, and a preliminary U-Pb age of 160 Ma (Monger, 1989).

ACKNOWLEDGMENTS

A.J. Arthur, C.J. Greig, and G.E. Ray were all involved in the site selection for conglomerate clasts and numerous discussions in the field. C.J. Greig offered constructive criticism on the manuscript.

REFERENCES

- Anderson, P.**
1976: Oceanic crust and arc-trench gap tectonics in southwestern British Columbia; *Geology*, v. 4, p. 443-446.
- Arthur, A.J.**
1986: Stratigraphy along the west side of Harrison Lake, southwestern British Columbia; in *Current Research, Part B*; Geological Survey of Canada, Paper 86-1B, p. 715-720.
- Arthur, A.J., Smith, P.L., Monger, J.W.H., and Tipper, H.W.**
in press: Mesozoic stratigraphy and Jurassic paleontology west of Harrison Lake, southwestern British Columbia; Geological Survey of Canada, Bulletin.
- Coates, J.A.**
1974: Geology of the Manning Park area, British Columbia; Geological Survey of Canada, Bulletin 238, 177 p.
- Crickmay, C.H.**
1930: The structural connection between the Coast Range of British Columbia and the Cascade Range of Washington; *Geological Magazine*, v. 67, p. 482-491.
- Friedman, R.M. and Armstrong, R.L.**
1990: U-Pb dating, southern Coast Belt, British Columbia; in *Project Lithoprobe: southern Canadian Cordillera Transect workshop volume*, University of Calgary, Alberta, p. 146-155.
- Gehrels, G.E., McClelland, W.C., Samson, S.D., and Patchett, P.J.**
1991: U-Pb geochronology of detrital zircons from a continental margin assemblage in the northern Coast Mountains, southeastern Alaska; *Canadian Journal of Earth Sciences*, v. 28, p. 1285-1300.
- Greig, C.J.**
1989: Geology and geochronometry of the Eagle Plutonic Complex, Coquihalla area, southwestern British Columbia; M.Sc. thesis, University of British Columbia, Vancouver, 423 p.
- Monger, J.W.H.**
1989: Geology of Hope and Ashcroft map-areas, British Columbia; Geological Survey of Canada, Maps 41-1989 and 42-1989, scale 1:250 000.
1991: Georgia Basin Project: structural evolution of parts of southern Insular and southwestern Coast belts, British Columbia; in *Current Research, Part A*; Geological Survey of Canada, Paper 91-1A, p. 219-228.
- Mortimer, N., van der Heyden, P., Armstrong, R.L., and Harakal, J.**
1990: U-Pb and K-Ar dates related to the timing of magmatism and deformation in the Cache Creek terrane and Quesnellia, southern British Columbia; *Canadian Journal of Earth Sciences*, v. 27, p. 117-123.
- O'Brien, J.A.**
1986: Jurassic stratigraphy of the Methow Trough, southwestern British Columbia; in *Current Research, Part B*; Geological Survey of Canada, Paper 86-1B, p. 749-756.
1987: Jurassic biostratigraphy and evolution of the Methow Trough, southwestern British Columbia; M.Sc. thesis, University of Arizona, Tucson, 150 p.
- Parrish, R.R. and Monger, J.W.H.**
in press: New U-Pb dates from southwestern British Columbia; in *Radiogenic Age and Isotopic Studies: Report 5*, Geological Survey of Canada, Paper 91-2.
- Ray, G.E.**
1986: The Hozameen fault system and related Coquihalla serpentine belt of southwestern British Columbia; *Canadian Journal of Earth Sciences*, v. 23, p. 1022-1041.
1990: The geology and mineralization of the Coquihalla gold belt and Hozameen fault system, southwestern British Columbia; British Columbia Ministry of Energy, Mines and Petroleum Resources, Geological Survey Branch, Bulletin 79, 97 p.
- Stacey, J.S. and Kramers, J.D.**
1975: Approximation of terrestrial lead isotope evolution by a two-stage model; *Earth and Planetary Science Letters*, v. 26, p. 207-221.
- Stevens, R.D., Delabio, R.N., and Lachance, G.R.**
1982: Age determinations and geological studies, K-Ar isotopic ages, Report 15; Geological Survey of Canada, Paper 81-2, p. 10.
- Tabor, R.W., Haugerud, R.A., Miller, R.B., Brown, E.H., and Babcock, R.S.**
1989: Accreted terranes of the North Cascade Range, Washington; 28th International Geological Congress, Washington, DC, Guide Book to Field Trip 307.
- Tennyson, M.E. and Cole, M.R.**
1978: Tectonic significance of upper Mesozoic Methow-Pasayten sequence, northeastern Cascade Range, Washington and British Columbia; in *Mesozoic Paleogeography of the Western United States*, (ed.) D.G. Howell and K.A. MacDougall; Pacific Section, Society of Economic Paleontologists and Mineralogists, p. 499-508.

Tectonic assemblages of the Eastern Coast Belt, southwest British Columbia

J.M. Journeay and B.R. Northcote¹
Cordilleran Division, Vancouver

Journeay, J.M. and Northcote, B.R., 1992: Tectonic assemblages of the Eastern Coast Belt, southwest British Columbia; in Current Research, Part A; Geological Survey of Canada, Paper 92-1A, p. 215-224.

Abstract

The Eastern Coast Belt (ECB) straddles the boundary between the Intermontane and Insular superterranes of the southern Canadian Cordillera. It consists primarily of Late Paleozoic to Late Mesozoic fault-bounded crustal fragments and overlap assemblages. These rocks are intruded by Late Cretaceous and Early Tertiary magmatic arc sequences of the Coast Plutonic Complex. Our mapping in the Cayoosh and Bendor ranges demonstrates that the Bridge River Terrane and overlying basin successions of the Cayoosh Assemblage are linked stratigraphically. We recognize an important quartz-rich clastic facies in the Cayoosh Assemblage and Brew Group that may record the impingement and/or emergence of volcanic arc and crystalline basement terranes in the Late Jurassic and Early Cretaceous. These data provide important clues about the history of terrane accretion and crustal imbrication in the Eastern Coast Belt.

Résumé

Le Domaine côtier oriental chevauche la limite entre les superterranes intramontagneux et insulaire de la Cordillère canadienne méridionale. Il est principalement composé de fragments de croûte et d'assemblages de chevauchement limités par des failles du Paléozoïque supérieur au Mésozoïque supérieur. Ces roches sont recoupées par intrusion de séquences d'arc magmatiques du Crétacé supérieur et du Tertiaire inférieur du complexe plutonique côtier. La cartographie des chaîons Cayoosh et Bendor, dans la chaîne Côtière, fait ressortir ces contacts. Le terrane de la rivière Bridge et les successions de bassin sus-jacentes de l'assemblage de Cayoosh sont liés stratigraphiquement (bassin de Methow); la présence d'un important faciès clastique quartzique pourrait indiquer un empiètement par des terranes d'arc volcanique et de socle cristallin, ou leur émergence, durant le Jurassique supérieur et le Crétacé inférieur. Ces données donnent des indices importants sur l'histoire de l'accrétion des terranes et de l'imbrication de la croûte dans le Domaine côtier oriental.

¹Department of Geological Sciences, University of British Columbia, 6339 Stores Road, Vancouver, B.C. V6T 2B4

INTRODUCTION

The Eastern Coast Belt (ECB) segment of the Pemberton (1:250 000) map area encompasses more than 450 km² of rugged terrain in the Cayoosh, Bendor, and Chilcotin ranges of the southern Coast Mountains (Fig. 1). It is situated along the boundary between the Intermontane and Insular

superterrane and is made up primarily of fault-bounded crustal fragments and overlap assemblages which record a rich and complex history of terrane accretion and crustal imbrication (Wheeler et al., 1989).

Fieldwork during the 1991 season focused on the structural and stratigraphic framework of the ECB (Fig. 2) and involved 1:50 000 scale mapping of the Cayoosh and

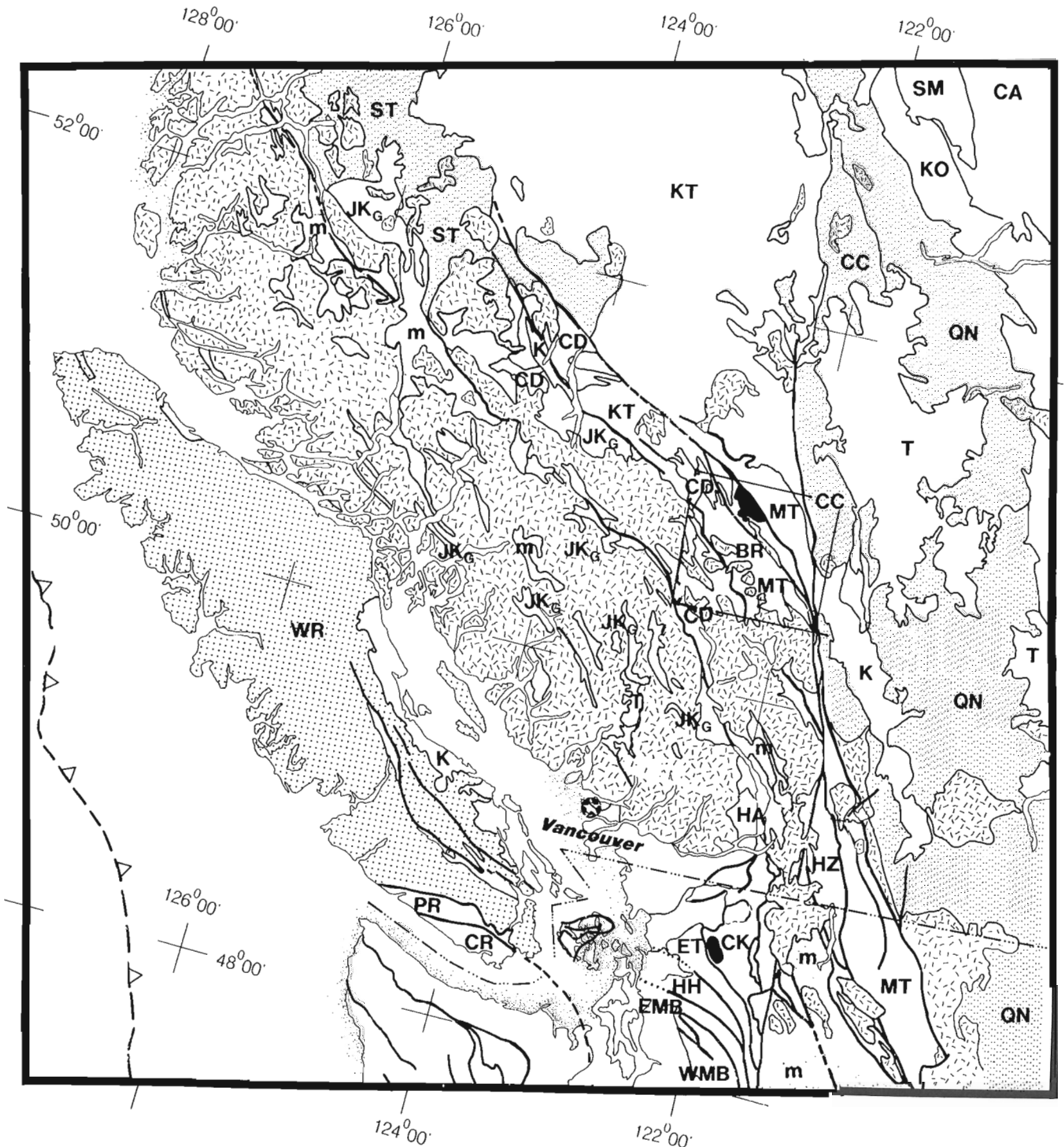


Figure 1. Tectonic framework of the southwest Canadian Cordillera.

Bendor ranges, south of Carpenter Lake. 1:25 000 scale mapping and structural investigations of fault systems in the western Cayoosh Range were carried out in collaboration with Carlo Sanders, Jan-Henk Van Konijnenburg, and Monique Jaasma from the Free University of Amsterdam (see Journeay et al., 1992). Our work is a follow-up to 1:250 000 scale mapping of the region by Roddick and Hutchison (1973) and complements recent 1:50 000 scale mapping of the adjacent Chilcotin Range by Schiarizza et al. (1989, 1990), Garver et al. (1989), Monger (1989), and Coleman (1990). Our mapping provides new 1:50 000 scale geological coverage of the Duffey Lake (92J/8), Shalalth (92J/9), and Bralorne (92J/15) map areas, and establishes a framework for more detailed studies of the geology, tectonic history, mineral potential, and environmental hazards of the Eastern Coast Belt region.

This paper presents our findings on the stratigraphic framework and distribution of tectonic assemblages in the ECB domain, with particular emphasis on the region south of Carpenter Lake. The structural setting and deformation history of this region are discussed separately (see Journeay et al., 1992).

REGIONAL GEOLOGY

The Coast Belt of southern British Columbia comprises an array of fault-bounded island arc and oceanic terranes that were accreted along the continental margin in Middle Jurassic to Early Cretaceous time. This early history of terrane accretion is obscured by the intrusion of Middle Jurassic and younger plutonic suites of the Coast Plutonic Complex, and by mid- to Late Cretaceous deformation and regional metamorphism along the inboard margin of the Insular superterrane.

The structural framework of the ECB is defined by a network of northwest-trending contractional and strike-slip fault systems that record a complex history of post-middle Cretaceous shortening and transpression. These include southwest-verging thrust faults and high-angle reverse faults of the Bralorne-McGillivray Pass-Twin Lakes Fault system and the Shulaps imbricate zone (Journeay et al., 1992; Calon et al., 1990); left-lateral oblique slip contractional faults of the Tyaughton Creek fault system (Schiarizza et al., 1990); northeast-vergent thrust faults of the Castle Pass system (Garver, 1991); dextral strike-slip and related extensional faults of the Downton Creek, Yalakom, Marshall Creek, and Mission Ridge fault systems (Schiarizza et al., 1990; Coleman, 1990; Journeay et al., 1992). These structures are offset by dextral transcurrent faults of the Fraser Fault System (Monger, 1989), and reappear more than 100 km to the south in the Cascades of northern Washington.

TECTONIC ASSEMBLAGES

The Eastern Coast Belt domain (ECB) lies structurally above the high-grade metamorphic-plutonic core of the Central Coast Belt (CCB). It comprises a wide variety of fault-bounded tectonic assemblages ranging in age from Late Paleozoic to Early Tertiary (Woodsworth, 1977; Rusmore,

1985; Schiarizza et al., 1989, 1990). These include Late Paleozoic mafic and ultramafic rocks of the Bralorne-East Liza and Shulaps complexes, Triassic arc sequences of the Cadwallader Group and Bridge River Complex, Mesozoic sedimentary sequences of the Tyaughton and Methow basins, and imbricated metamorphic rocks of the Chism Creek Schist. These rocks are overlapped by Cretaceous synorogenic clastic facies of the Taylor Creek Group and are intruded by Late Cretaceous and Early Tertiary igneous rocks of the Coast Plutonic Complex.

Bralorne-East Liza Complex

Recent studies in the Bralorne mining district (Leitch, 1989) and in the western Shulaps Range (Schiarizza et al., 1989, 1990) have identified a suite of metavolcanic greenstones, gabbros, and ultramafic rocks of Late Paleozoic age. In the Bralorne district, these include metavolcanic flows and flow breccias along the Cadwallader River, (previously mapped as Pioneer Formation; Cairnes, 1937; Church, 1987), the Sumner Gabbro, and sheared serpentinite of the President ultramafic complex (Cairnes, 1937). These rocks are intruded by hornblende-quartz diorite and plagiogranite (soda granite) of the Bralorne suite, which yield zircons of Early Permian age (270 Ma; Leitch, 1989). Correlative rocks in the western Shulaps Range include imbricated greenstone and gabbro of the East Liza Complex (Calon et al., 1990). These rocks, known collectively as the Bralorne-East Liza Complex (P. Schiarizza, pers. comm., 1991) are exposed in fault slivers across a 65 km wide zone bounded to the west by the Bralorne Fault Zone and to the east by the Yalakom Fault.

Our mapping extends the Bralorne-East Liza Complex southward into the Bendor and Cayoosh ranges. Rocks that we consider part of this Complex are exposed northeast of Mount Truax, along the ridge system between Mount Piebiter and Star Mountain, and along the full extent of the McGillivray Pass, Twin Lakes, and Kwoiek Creek fault zones. Slivers of these mafic and ultramafic rocks occur along major fault strands throughout the ECB. Although tectonically significant, most of these fault slivers are less than 50 m in width.

The widespread occurrence of these mafic and ultramafic rocks throughout the ECB suggests to us that the Bralorne-East Liza Complex may be part of an ophiolite that separated Bridge River and Cadwallader terranes prior to their imbrication along the continental margin. This ophiolite complex most likely served as a zone of detachment during later episodes of crustal shortening.

Cadwallader Group

The Cadwallader Group, as defined by Rusmore (1985), comprises a sequence of metavolcanic greenstone (Pioneer Formation) and conformably overlying turbidite and siltstone (Hurley Formation). Metavolcanic greenstones of the Pioneer Formation are characterized by green to purplish-weathering basaltic flows and flow breccias with major and trace element geochemical signatures that are transitional between modern island arc tholeiites and mid-ocean ridge basalts. The Hurley

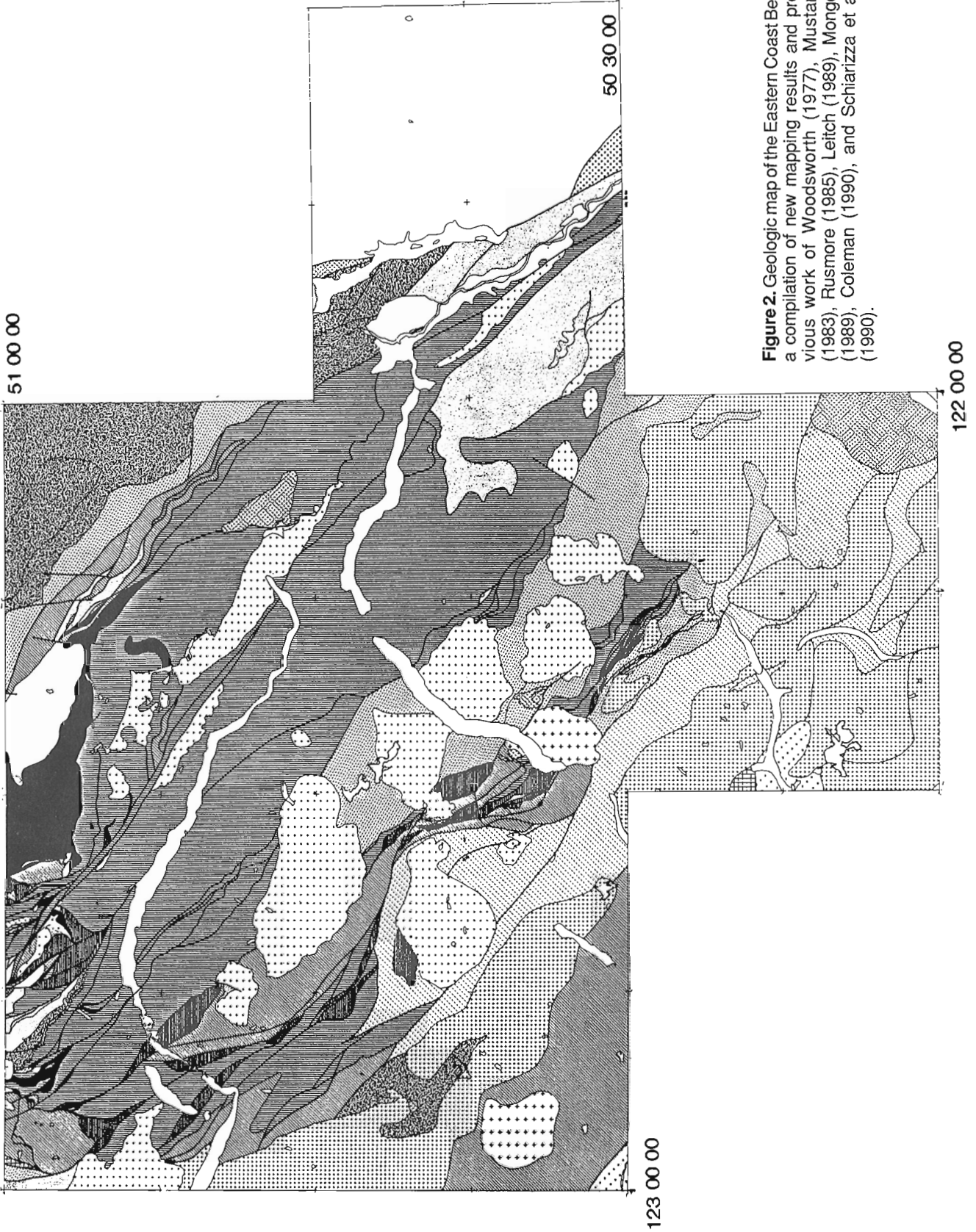


Figure 2. Geologic map of the Eastern Coast Belt; a compilation of new mapping results and previous work of Woodsworth (1977), Mustard (1983), Rusmore (1985), Leitch (1989), Monger (1989), Coleman (1990), and Schiarizza et al. (1990).

Formation consists of an upward fining sequence of thin-bedded volcanoclastic wacke, greywacke-siltstone turbidite, and calcareous siltstone (Rusmore, 1985). Intercalated with these fine grained sediments are distinctive pebble and cobble conglomerates containing fragments of limestone, felsic volcanic, and granitoid rocks that are presumably derived from an adjacent arc complex. Fossils

collected from limestones near the top of the Pioneer Formation and from overlying rocks of the Hurley Formation range from late Carnian to middle Norian (Rusmore, 1985).

Tectonic slivers of the Cadwallader Group have been mapped along the trace of the Bralorne-McGillivray Pass Fault Zone (Leitch, 1989), beneath imbricated mafic and ultramafic rocks of the Bralorne-East Liza and Shulaps complexes, and with younger rocks of the Relay Mountain Group along the northeastern slopes of the Yalakom and Bridge rivers (Schiarizza et al., 1989, 1990).

Although widespread in the Chilcotin Ranges, rocks of the Cadwallader Group represent a minor component of the ECB in the region south of Carpenter Lake. Green- and purplish-weathering metavolcanic flows, volcanoclastic turbidites, and pebble conglomerates, characteristic of the transitional facies separating the Pioneer and Hurley formations of the Cadwallader Group, outcrop east of McGillivray Pass in fault slivers that are structurally interleaved with mafic and ultramafic rocks of the Bralorne-East Liza Complex. South of Whitecap Mountain, thin-bedded turbidites, calcareous siltstones, and limestone-pebble conglomerates of the Hurley Formation are capped by thin-bedded quartzites of the Cayoosh Assemblage, and are in fault contact with mafic greenstones of the Bralorne-East Liza Complex.

The disappearance of Cadwallader Group rocks in the ECB south of Anderson Lake suggests to us one of two possibilities. Either the Cadwallader arc tapers out to the south, or it has been structurally overridden and tectonically buried beneath rocks of the Bralorne-East Liza and Bridge River complexes.


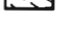
Bridge River Complex

The Bridge River Complex (Schiarizza et al., 1990) is characterized by widespread and monotonous exposures of interbedded and structurally imbricated greenstone and bedded chert with subordinate siltstone, greywacke,



Figure 3. Pillowed basalts of the Bridge River complex (Western Assemblage).

LEGEND

-  Tertiary
Volcanics (undivided)
-  Upper Cretaceous
Powell Creek Volcanics
-  Silverquick Conglomerate
-  Lower Cretaceous
Taylor Creek Group
-  Middle Jurassic - Lower Cretaceous
Relay Mountain Group
Brew Group
-  Lower - Middle Jurassic
Cayoosh Assemblage
-  Upper Triassic
Tyaughton Group
-  Cadwallader Group
Hurley Formation
Pioneer Formation
-  Upper Paleozoic - Jurassic
Bridge River Complex
-  Shulaps Ultramafic Complex
-  Bralorne - East Liza Complex
-  Metamorphic Rocks (age unknown)
Chism Creek Schist
-  Tertiary Intrusions
-  Late Cretaceous
Bendor Intrusions
-  Scuzzy - Mt. Rohr Pluton
Lillooet Range Plutonic Suite
-  "Middle" Cretaceous
Spetch Creek Pluton
-  Diorite (age unknown)
-  Fault Melange

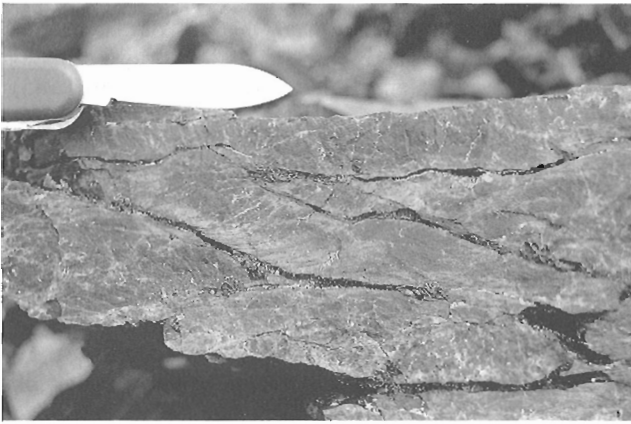


Figure 4. Thin-banded ribbon cherts of the Bridge River Complex (Western Assemblage).

metavolcanic tuff, limestone, and sheared serpentinite (Roddick and Hutchison, 1973; Potter, 1983; Schiarizza et al., 1989, 1990). It includes rocks previously mapped in part as the Fergusson Series or Fergusson Group in the western Chilcotin and Bendor ranges (Cairnes, 1937; Church, 1987), and what others have identified as Bridge River Group (Roddick and Hutchison, 1973), Bridge River Assemblage (Potter, 1983), and Bridge River Schist (Schiarizza et al., 1990; Coleman, 1990). Radiolarian cherts and siliceous siltstones of the Bridge River Complex range from Mississippian to lower Middle Jurassic and, if deposited as one continuous basin sequence, would represent one of the longest-lived and widest oceans known in the geologic record (Cordey, 1988).

In addition to greenstone-chert *mélange* of the eastern Bridge River Complex, we recognize large tracts of greenstone, chert, and related sedimentary rocks in the western Bendor and Cayoosh ranges which, although cut by younger faults, preserve primary stratigraphic relationships. We informally refer to these two different parts of the Bridge River Complex as the eastern and western assemblages. The boundary between these assemblages coincides with the Downton Creek Fault in the central Cayoosh Range, but is obscured by arrays of strike-slip and contractional faults along strike to the northwest in the Chilcotin Range.

The Eastern Assemblage of the Bridge River Complex is well-exposed in the eastern Cayoosh Range and along the shores of Seton and Carpenter lakes. It consists primarily of discontinuous lenses of mafic greenstone, bedded and massive chert, greenstone-chert *mélange* and minor volcanoclastic siltstone and limestone. The Western Assemblage of the Bridge River Complex is well-exposed along ridge systems of the western Cayoosh Range and along the east flank of the Bendor Range. Although we have no constraint on the age or stratigraphic complexity of the Western Assemblage, it is possible to map coherent successions of massive and pillowed greenstone (Fig. 3), calcareous greenschist, chert (Fig. 4), and fine grained volcanoclastic siltstones at a scale of 1:50 000.

The significance of these two distinct assemblages within the Bridge River Complex is uncertain. Middle Triassic blueschists (230 Ma; Archibald et al., 1991) in the central Chilcotin Range (Garver et al., 1989), and greenstone-chert *mélange* throughout much of the Bridge River Complex suggests a long history of deformation in a subduction zone/accretionary complex setting. Coherent greenstone-chert-siltstone successions of the Western Assemblage are basement to overlying deep water marine sequences of the Cayoosh Assemblage, and may represent fragments of a Bridge River ocean that lay west of or within an Early Mesozoic accretionary complex.

Cayoosh Assemblage

We have mapped a thick succession of turbidite, thin-bedded siltstone, sandstone, and shale in the western Cayoosh Range, informally referred to as the Cayoosh Assemblage. Although undated, these rocks overlie and are structurally interleaved with greenstone and chert of the Bridge River Complex, and have strong affinities with Jurassic and Cretaceous sequences of the Methow Basin. The Cayoosh Assemblage is best



Figure 5. Volcanic sandstones, siltstones, and shales of the Cayoosh Assemblage in the headwater region of Melvin Creek (western Cayoosh Range).

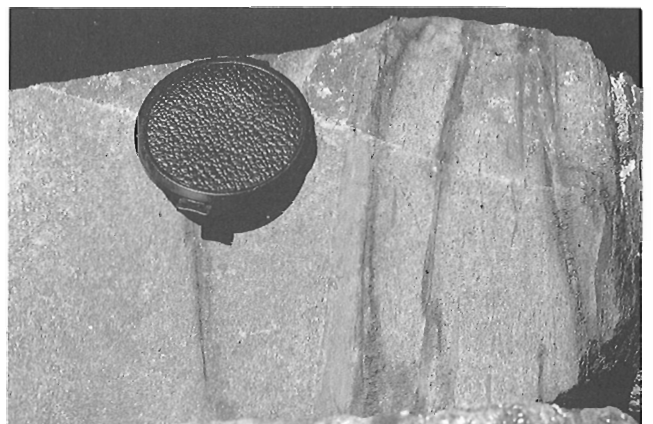


Figure 6. Interlayered volcanoclastic sandstones and siltstones of the Cayoosh Assemblage.

exposed in ridge systems of the west-central Cayoosh Range (Fig. 5), where it forms a northwest-trending belt more than 10 km wide and 50 km long. It extends northwestward into the Bendor Range, where it overlaps and is structurally imbricated with rocks of the Bridge River and Bralorne-East Liza complexes, and southeastward into the Lillooet Ranges where it is intruded by Late Cretaceous granodiorite of the Scuzzy pluton (Fig. 2). Imbricate thrusting, isoclinal folding, and transposition of bedding have structurally thickened the assemblage and obscured primary sedimentary features. However, stratigraphic relationships between major lithofacies are locally well preserved and permit a partial reconstruction of the basin succession.

The basal unit of the Cayoosh Assemblage is well exposed along the ridge north of Melvin Creek and on the overturned limb of a regional isoclinal syncline near the headwaters of Downton Creek. It consists primarily of dark grey phyllitic siltstone and graphitic slate, locally interlayered with lenses of dark grey sandy siltstone and limestone. The contact between the Cayoosh Assemblage and interlayered chert and siltstone of the underlying Bridge River Complex is gradational, and mapped at the top of the highest coherent chert horizon. Chert pods, along with thin metavolcanic flows, occur locally near the base of the Cayoosh Assemblage, but rapidly disappear upsection. Graphitic siltstones and slates grade upward into a sequence of thin-bedded, rhythmically interlayered siltstone-greywacke turbidites, locally containing thin and thick-bedded greenish-weathering volcanoclastic sandstone. Greywacke horizons are fine grained and generally less than 5 cm thick. Collectively, these rocks resemble thin-bedded siltstone successions of the Lower Jurassic Boston Bar Formation in the Anderson River and Coquihalla regions of the Methow Basin (O'Brien, 1986). In its type locality, the Boston Bar Formation unconformably overlies mafic greenstone of the Spider Peak Formation (Bralorne-East Liza Complex?) and greenstone-chert successions of the Hozameen-Bridge River Complex.

Stratigraphically above this lower siltstone-greywacke succession is a sequence of thin- and thick-bedded, immature volcanoclastic sandstone, and dark grey slate and phyllite.

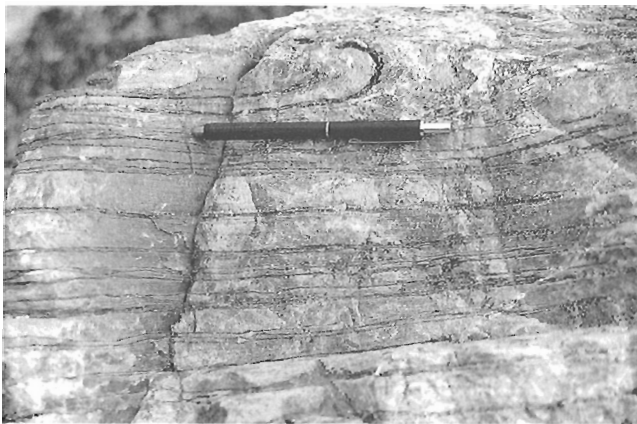


Figure 7. Thin-bedded quartzites of the upper Cayoosh Assemblage.

Sandstone horizons are fine- to medium-grained and locally well graded (Fig. 6). Coarse sandstone beds range from 10 cm to several metres thick. They are locally channelled and contain both shale rip-up clast and pebbly mudstone horizons. Although composed primarily of volcanic detritus, sandstone horizons near the top of this sequence are locally interlayered with arkosic wackes and may contain as much as 10% detrital quartz. The composition and bedding characteristics of this unit resemble volcanic sandstone sequences in the Dewdney Creek Formation of the Ladner Group. In its type locality, the Dewdney Creek Formation is conformable with Lower Jurassic siltstone turbidite of the Boston Bar Formation, and is unconformably overlain by Upper Jurassic greywacke and tuffaceous siltstone of the Thunder Lake Sequence.

The volcanic sandstone facies of the Cayoosh Assemblage is structurally overlain and apparently gradational upward into a fine grained succession of dark grey siltstone and pyritiferous shale. This succession is well exposed along the ridge that separates Melvin and Downton creeks, and extends southeastward into the northern Lillooet Ranges, where siltstones are interdigitated with greenish weathering tuffaceous siltstone, thin- and thick-bedded quartzite (Fig. 7), pillowed metavolcanic flows, and minor limestone. The assemblage of interbedded quartzite and siltstone resembles lower sequences of the Brew Group (Duffell and McTaggart, 1952), which are believed to be Upper Jurassic to Lower Cretaceous.

We interpret the Cayoosh Assemblage to be part of the Methow Basin; a deep water marine succession that overlaps rocks of the Bridge River and Bralorne-East Liza complexes. Volcanoclastic and quartz-rich sandstone facies that occur in the upper parts of this assemblage may record either the impingement and/or emergence of volcanic arc and crystalline basement terranes in Upper Jurassic and Early Cretaceous time. The stratigraphic linkage between this succession and age-equivalent basin sequences of the Tyaughton Trough are uncertain.

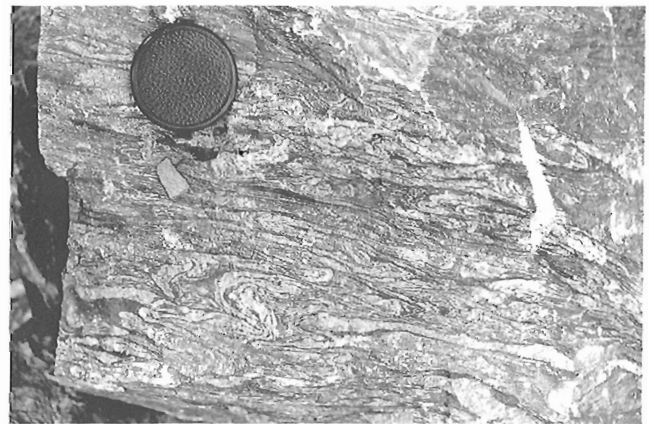


Figure 8. Thin-laminated quartzite facies of the Brew Group. Note transposition of layering.



Figure 9. Boulder conglomerate of the upper Brew Group.

Brew Group

The Brew Group comprises a thick succession of thin bedded, shaly siltstone, greywacke, quartzite, and boulder conglomerate, locally metamorphosed to lower amphibolite grade (Duffell and McTaggart, 1952). Type localities of the Brew Group, well exposed in the vicinity of Mount Brew and along ridge systems that extend southeastward toward the Fraser River, are flanked to the north and west by the low-angle Cayoosh River Fault (Coleman, 1990; Journeay et al., 1992), to the east by the Marshall Creek Fault, and to the south by Tertiary granodiorite of the Coast Plutonic Complex. Although estimated to be more than 2500 m thick (Duffell and McTaggart, 1952), upper and lower contacts of the Brew Group have never been formally defined. Studies in the vicinity of Mount Brew (Mustard, 1983) have identified a regional antiformal syncline with an overturned limb several kilometres long. Continuity of map units, minor structures, and stratigraphic top indicators reveal that the upper and lower siltstone-quartzite successions (each approximately 1000 m thick), as defined by Duffell and McTaggart (1952), occur on opposite limbs of the syncline and are, therefore, correlative (Mustard, 1983). It follows that boulder conglomerates that core the syncline must stratigraphically overlie the siltstone-quartzite succession.

The lower succession of the Brew Group is well exposed on the upright lower limb of the syncline and consists primarily of interlayered thin- and thick-bedded quartzite, dark grey siltstone and siltstone-greywacke turbidite. Thin amphibolite lenses near the base of the succession are interpreted to be metamorphosed volcanic flows. Quartzites include a distinctive thinly-laminated facies (Fig. 8) in which centimetre-scale sandstone beds are separated by thin phyllitic partings, and a thick-bedded facies in which sandstone and siltstone layers are 1-5 m thick. This lower quartzite facies is gradational upward into a thick sequence of thinly-laminated dark grey siltstone, sandy siltstone, and quartzite. Rhythmically interlayered siltstone and sandstone laminae are interpreted as turbidites. Higher in the succession, sandstone layers become thicker, compositionally and texturally less mature, and include lenses of calcarenite, fine grained greywacke, and tuffaceous

siltstone. Near the top of this succession are fossiliferous limy sandstones from which Duffell and McTaggart (1952) collected shell fragments identified by Jeletzky as pelecypods (sp. *Aucella* ex. gr. *crassicollis* Keyserling) of lower Early Cretaceous age. At the top of this succession are clast- and matrix-supported conglomerates containing pebbles, cobbles, and boulders of granite, granodiorite, and subordinate (20-30%) siltstone, black chert, and minor quartzite (Fig. 9).

Quartzite-siltstone successions of the Cayoosh Assemblage resemble the lower clastic facies of the Brew Group and are most likely part of the same sequence. These quartz-rich successions represent a mature clastic facies which, although not previously described, is widespread in the southern Coast Mountains. Our mapping documents quartz-rich sedimentary rocks in both Central and Eastern Coast belts. These rocks occur both as thin, unmappable units and as thick coherent successions. In the Bendor Range, pebble conglomerates and overlying thin- and thick-bedded quartzites sit stratigraphically above greenstone-chert assemblages of the Bridge River Complex and mafic greenstone and ultramafic rocks of the Bralorne-East Liza Complex. Northeast of Mount Noel, pebbles and cobbles of quartzite occur in a coarse matrix-supported conglomerate. These conglomerates are interpreted to be a synorogenic clastic facies of the Taylor Creek Group (Runsmore, 1935).

We consider quartz-rich clastic facies of the Brew Group and upper Cayoosh Assemblage to be part of an Upper Jurassic or Lower Cretaceous overlap assemblage derived from exhumed crystalline terranes of the Intermontane or Omineca belts to the east. Thinly-laminated quartzites, locally containing zones of chaotic intrastratal deformation, suggest deposition as distal turbidites along the continental margin.

Chism Creek Schist

The name Chism Creek Schist was coined by Rusmore (1985) to facilitate mapping of structurally interleaved amphibolite grade metamorphic rocks of the eastern Cadwallader Range. As defined, the Chism Creek Schist is not a stratigraphic unit, but a composite tectonic assemblage comprising imbricated slivers of bedded metachert, amphibolite, mafic and ultramafic rock, pelitic schist, micaceous and phyllitic quartzite, and minor marble (Rusmore, 1985). The areal extent of the Chism Creek Schist was unknown when the unit was formally defined, although reconnaissance mapping of Rusmore (1985) and Woodsworth (1977) had identified slivers of micaceous quartzite and biotite-hornblende schist near Birken and south of Anderson Lake. Our mapping confirms these observations and extends the limits of the Chism Creek Schist to include fault slivers of the Bralorne-McGillivray Pass-Twin Lakes Fault Zone. In the lower plate of this fault zone, rocks of the Chism Creek Schist define a coherent tectonic assemblage that extends more than 50 km southeastward into the Lillooet Ranges, where it is intruded by postkinematic granodiorite and diorite of the Coast Plutonic Complex. Pendants of Chism Creek Schist extend southward to Nahatlatch Creek and are considered to

be part of the Settler Schist Assemblage exposed in the high-grade metamorphic hinterland of the southern Coast Belt thrust system (Journey, 1990).

Protoliths of the Chism Creek Schist are varied (Rusmore, 1985). Thin-bedded metachert and associated amphibolite form tectonic slivers in the Bralorne Fault Zone and are probably derived from upper plate rocks of the Bridge River Complex. Mafic and ultramafic metaplutonic rocks, including meta-peridotite, serpentinite, and talc-carbonate schist occur throughout the Bralorne-McGillivray Pass-Twin Lakes Fault Zone, and are presumably derived from upper plate ophiolites of the Bralorne-East Liza and Shulaps complexes. Calcareous metasedimentary rocks and associated marble horizons near Chism Creek, in the eastern Cadwallader Range, may be derived in part from the Hurley Formation of the Cadwallader Group. Massive and thin-bedded quartzite, pelitic schist, and graphitic phyllite are by far the most abundant and distinctive rocks of the Chism Creek Schist south of Birkenhead Lake. For reasons outlined above, we consider these rocks to be part of the Cayoosh Assemblage.

SUMMARY AND CONCLUSIONS

Late Paleozoic mafic and ultramafic rocks of the Bralorne-East Liza Complex are widespread throughout the ECB, occurring primarily as tectonic slivers along both southwest- and northeast-vergent contractional fault systems. They are interpreted to be part of an ophiolite complex that may have separated Bridge River and Cadwallader terranes prior to their imbrication along the continental margin.

The Cadwallader Group represents a Late Triassic arc complex that is overlapped by basin sequences of the Tyaughton Trough. Paleogeographic relationships between this arc and oceanic rocks of the Bridge River Complex are not clear. Our mapping shows that the Cadwallader Group and overlying Tyaughton Trough, although widespread in the Chilcotin and Cadwallader ranges, are not significant components of the ECB south of Carpenter Lake. We suggest that these rocks either taper to the south, or have been structurally overridden by oceanic rocks of the Bridge River Complex.

We recognize two components of the Bridge River Complex; an eastern assemblage of greenstone-chert-siltstone mélange and a western assemblage in which coherent stratigraphic sequences of greenstone, bedded chert, and siltstone are locally preserved. Both assemblages are basement to marine successions of the overlying Cayoosh Assemblage. Differences in structural style are attributed to deformation in and adjacent to a subduction zone and/or accretionary complex.

The Cayoosh Assemblage sits conformably above interbedded greenstone, chert, and siltstone of the western Bridge River Complex, and is structurally interleaved with greenstone/chert mélange of the eastern Bridge River Complex. These rocks represent a previously unrecognized basin succession in the ECB, and have strong affinities with Jurassic and Cretaceous rocks of the Methow Basin. Basal

and medial sequences of the Cayoosh Assemblage resemble the Early Jurassic Boston Bar Formation and the conformably overlying Dewdney Creek Formation, respectively. The upper quartzite-siltstone succession is correlated with Late Jurassic and lower Early Cretaceous clastic sequences of the Brew Group. Stratigraphic linkages between these rocks and age-equivalent basin successions of the Tyaughton Trough are uncertain.

Quartz-rich clastic rocks of the Brew Group and upper Cayoosh Assemblage unconformably overly older volcanic arc and oceanic terranes of the ECB, and are recognized to be an important component of the Chism Creek Schist and Settler Schist of the CCB. They are interpreted to be part of a widespread overlap assemblage that may record the emergence of crystalline basement terranes to the east and/or the impingement of arc complexes along the continental margin during final stages of accretion in the Late Jurassic and Early Cretaceous.

The Chism Creek Schist is a composite tectonic assemblage of polydeformed metamorphic rocks derived from the Cadwallader Group, Bralorne-East Liza and Bridge River complexes, and the overlying Cayoosh Assemblage. It forms the footwall to imbricated lower grade rocks of the ECB, and is correlated with the Settler Schist along strike to the south in the metamorphic hinterland of the CCB. Deformation and metamorphism of these rocks are attributed to crustal imbrication associated with impingement and eastward underplating of the Insular Superterrane in the Late Cretaceous (Journey, 1990).

ACKNOWLEDGMENTS

Mapping of tectonic assemblages in the western Cayoosh Range was carried out in collaboration with Carlo Sanders, Jan-Henk Van Konijnenburg, and Monique Jaasma from the University of Amsterdam. We are grateful for their contributions to the mapping project and for their good humour throughout the summer. Our understanding of the stratigraphic framework of the ECB has evolved through discussions with Paul Schiarizza and Jim Monger. We thank them for sharing their experience and ideas. Helicopter and logistical support were provided by John and Patricia Goats of Pemberton Helicopters and by Bob Thurston and Bob Holt of Cariboo-Chilcotin Helicopters.

REFERENCES

- Archibald, D.A., Schiarizza, P., and Garver, J.I.
1991: $^{40}\text{Ar}/^{39}\text{Ar}$ evidence for the age of igneous and metamorphic events in the Bridge River and Shulaps complexes, southwestern British Columbia (92O/2; 92J/15,16); in Geological Fieldwork 1990, British Columbia Ministry of Energy, Mines and Petroleum Resources, Paper 1991-1, p. 75-83.
- Cairnes, C.E.
1937: Geology and mineral deposits of the Bridge River mining camp, British Columbia; Geological Survey of Canada, Memoir 213, 140 p.
- Calon, T.J., Malpas, J.G., and Macdonald, R.
1990: The anatomy of the Shulaps Ophiolite; in Geological Fieldwork 1989, British Columbia Ministry of Energy, Mines and Petroleum Resources, Paper 1990-1.

- Church, B.N.**
1987: Geology and mineralization of the Bridge River mining camp (92J/15, 92O/2, 92J/10); in Geological Fieldwork 1986, British Columbia Ministry of Energy, Mines and Petroleum Resources, Paper 1987-1, p. 23-29.
- Coleman, M.E.**
1990: Eocene dextral strike-slip and extensional faulting in the Bridge River Terrane, southwest British Columbia; M.Sc. thesis, Carleton University, Ottawa, Ontario, 87 p.
- Cordey, F.**
1988: Etude des radiolares Permians, Triassiques et Jurassiques des complexes ophiolitiques de Cache Creek, Bridge River et Hozameen (Columbie Britannique, Canada): implications paleographiques et structurales; Ph.D. thesis, Universite Pierre et Marie Curie, Paris, France.
- Duffell, S. and McTaggart, K.C.**
1952: Ashcroft map area, British Columbia; Geological Survey of Canada, Paper 67-10, 55 p.
- Garver, J.I.**
1991: Kinematic analysis and timing of structures in the Bridge River Complex and overlying Cretaceous sedimentary rocks, Cinnabar Creek area, southwestern British Columbia (92J/15); in Geological Fieldwork 1990, British Columbia Ministry of Energy, Mines and Petroleum Resources, Paper 1991-1, p. 65-75.
- Garver, J.I., Schiarizza, P., and Gabba, R.G.**
1989: Stratigraphy and structure of the Eldorado Mountain area, Cariboo-Chilcotin Mountains, southern B.C. (92O/02, 92J/15); in Geological Fieldwork 1988, British Columbia Ministry of Energy, Mines and Petroleum Resources, Paper 1989-1, p. 131-143.
- Journey, J.M.**
1990: Structural and tectonic framework of the southern Coast Belt, British Columbia; in Current Research, Part E; Geological Survey of Canada, Paper 90-1E, p. 183-197.
- Journey, J.M., Sanders, C., Van-Konijnenburg, J.H., and Jaasma, M.**
1992: Fault systems of the Eastern Coast Belt, southwest British Columbia; in Current Research, Part A; Geological Survey of Canada, Paper 92-1A.
- Leitch, C.H.B.**
1989: Geology, wall-rock alteration and characteristics of the ore fluid at the Bralorne mesothermal gold-vein deposit, southwestern British Columbia; Ph.D. thesis, University of British Columbia, Vancouver, 483 p.
- Monger, J.W.H.**
1989: Geology of Hope and Ashcroft map areas, British Columbia; Geological Survey of Canada, Maps 41-1989 and 42-1989.
- Mustard, J.F.**
1983: The geology of the Mount Brew area, Lillooet, British Columbia; M.Sc. thesis, University of British Columbia, Vancouver, British Columbia, 74 p.
- O'Brien, J.**
1986: Jurassic stratigraphy of the Methow Trough, southwestern British Columbia; in Current Research, Part A; Geological Survey of Canada Paper, 86-1A, p. 749-756.
- Potter, C.J.**
1983: Geology of the Bridge River Complex, southern Shulaps Range, British Columbia: a record of Mesozoic convergent tectonics; Ph.D. thesis, University of Washington, Seattle, 192 p.
- Roddick, J.A. and Hutchison, W.W.**
1973: Pemberton (east half) map-area, British Columbia; Geological Survey of Canada, Paper 73-17, 21 p.
- Rusmore, M.E.**
1985: Geology and tectonic significance of the Upper Triassic Cadwallader Group and its surrounding faults, southwestern British Columbia; Ph.D. thesis, University of Washington, Seattle, 170 p.
- Schiarizza, P., Gaba, R.G., Glover, J.K., and Garver, J.I.**
1989: Geology and mineral occurrences of the Tyaughton Creek area (92O/2, 92J/15,16); in Geological Fieldwork 1988, British Columbia Ministry of Energy, Mines and Petroleum Resources, Paper 1989-1, p. 115-130.
- Schiarizza, P., Gaba, R.G., Coleman, M., Garver, J.I., and Glover, J.K.**
1990: Geology and mineral occurrences of the Yalakom River area (92O/1,2, 92J/15,16); in Geological Fieldwork 1989, British Columbia Ministry of Energy, Mines and Petroleum Resources, Paper 1990-1, p. 53-73.
- Wheeler, J.O., Brookfield, A.J., Gabrielse, H., Monger, J.W.H., Tipper, H.W., and Woodsworth, G.J.**
1989: Terrane map of the Canadian Cordillera; Geological Survey of Canada, Open File 1894.
- Woodsworth, G.J.**
1977: Pemberton (92J) map area, British Columbia; Geological Survey of Canada, Open File 482.

Fault systems of the Eastern Coast Belt, southwest British Columbia

J.M. Journeay, C. Sanders¹,
J.-H. Van-Konijnenburg¹, and M. Jaasma¹
Cordilleran Division, Vancouver

Journeay, J.M., Sanders, C., Van-Konijnenburg, J.-H., and Jaasma, M., 1992: Fault systems of the Eastern Coast Belt, southwest British Columbia; in Current Research, Part A; Geological Survey of Canada, Paper 92-1A, p. 225-235.

Abstract

The structural framework of the Eastern Coast Belt is defined by a network of northwest-trending contractional and strike-slip fault systems that record a complex history of post-middle Cretaceous shortening and transpression. Our mapping in the Cayoosh and Bendor ranges of the southern Coast Mountains documents the geometry, kinematics and relative timing of these fault systems and establishes a link with regional fault systems in adjacent parts of the ECB. These data provide the basis for reconstructing the history of deformation along the boundary between the Insular and Intermontane superterranes in Late Cretaceous and Early Tertiary time.

Résumé

Le cadre structural du Domaine côtier oriental est défini par un réseau de failles de contraction et de décrochements à direction nord-ouest relatant un raccourcissement et une transpression complexes, postérieurs au Crétacé moyen. Les travaux de cartographie effectués dans les chaînons Cayoosh et Bendor dans le sud de la chaîne Côtière permettent d'en mieux connaître la géométrie, la cinématique et la chronologie de ces réseaux de failles dans des parties adjacentes du Domaine côtier oriental. Ces données forment la base de la reconstitution de la déformation le long de la limite entre les superterranes insulaire et intramontagneux au Crétacé supérieur et au Tertiaire inférieur.

¹ Geovusie, Instituut voor Aardwetenschappen-VU, De Boelelaan 1085, 1081 HV Amsterdam

essential for reconstructing the history and mechanisms of crustal deformation, and has important implications for those interested in structural controls on mineralization in the upper crust and the geological hazards of living in a mountainous region that is dissected by faults.

This study is part of a regional mapping project aimed at resolving the structural framework and tectonic history of the southern Coast Belt. Fieldwork for the 1991 season focused primarily on the region south of Carpenter Lake, and involved both 1:50 000 and 1:25 000 scale mapping and structural analyses of fault systems in the Bendor, Cayoosh and northern Lillooet ranges of the southern Coast Mountains (Fig. 2). Our work represents the first systematic study of fault systems and related structures in this part of the ECB, and complements 1:50 000 scale mapping of the adjacent Chilcotin Range by Garver et al. (1989), Monger (1989), Schiarizza et al. (1989, 1990), and Coleman (1990).

This report conveys the preliminary results of our study. Open-file geological maps and structural sections of these regions, along with the results of our structural and kinematic analyses will follow. The stratigraphic framework and distribution of tectonic assemblages in this region of the ECB are discussed separately (see Journeay and Northcote, 1992).

FAULT SYSTEMS OF THE ECB

Overview

The structural framework of the ECB is defined by a network of northwest-trending contractional and strike-slip fault systems which record a complex history of post-middle Cretaceous shortening and transpression. These structures obscure an older history of subduction-related deformation that is preserved locally in Triassic blueschists and in post-early Middle Jurassic mélangé of the Bridge River Complex (Garver et al., 1989; Schiarizza et al., 1989, 1990).

The geometry and kinematics of post-mid-Cretaceous fault systems are well established in the Chilcotin Range of the Coast Mountains (Schiarizza et al., 1989, 1990). The most prominent of these structures include northeast-dipping thrust faults and high-angle reverse faults of the Bralorne-McGillivray Pass and Shulaps Range imbricate zones (Rusmore, 1985; Calon et al., 1990); left-lateral oblique-slip and associated contractional faults of the Tyaughton Creek Fault System (Schiarizza et al., 1990); southwest-dipping thrust faults and related folds of the Castle Pass Fault System (Garver, 1991); and dextral strike-slip and related extensional faults of the Yalakom, Mission Ridge and Marshall Creek systems (Coleman, 1990; Schiarizza et al., 1990). These structures are offset by dextral transcurrent faults of the Fraser Fault System (Monger, 1989) and reappear in the eastern Cascades of Washington State, more than 100 km to the south.

Our work focuses on the geometry and kinematics of fault systems in the Bendor, Cayoosh and Lillooet ranges of the southern Coast Mountains. We have traced major fault systems southeastward from Carpenter Lake to their cut-off with the Fraser Fault, and have identified several new

structures of regional significance. These include northeast-dipping imbricate thrusts and related folds of the Twin Lakes Fault Zone, sinistral oblique-slip structures of the Truax Fault Zone, southwest-dipping thrust faults of the Castle Pass Fault System, dextral oblique-slip structures of the Downton Creek Fault Zone, the Cayoosh Creek Fault, and high-angle dextral strike-slip and normal faults of the Marshall Creek Fault Zone.

Bralorne-McGillivray Pass Fault Zone

The Bralorne-McGillivray Pass Fault Zone (Rusmore, 1985; Leitch, 1989) marks the western edge of the Bridge River terrane in the Bendor Range, and is the tectonic boundary between the Central and Eastern Coast Belt domains. It extends southeastward along the Cadwallader River Valley, through McGillivray Pass to D'Arcy, where it has been mapped at 1:10 000 scale by J. Pautler of Teck Resources (J. Pautler, written comm., 1989). Individual faults are 1-5 m wide, and are marked by zones of intense ductile and/or brittle deformation that dip steeply to the northeast. Fault slivers in the Bralorne-Goldbridge region include sheared mafic and ultramafic rocks of the Bralorne-East Liza Complex and penetratively deformed greenstones, cherts and low-grade metasedimentary rocks of the Bridge River Complex and Cadwallader Group.

In the McGillivray Pass region, these rock units are imbricated with phyllites, slates and thin-bedded quartzites of the Cayoosh Assemblage. To the west, these upper plate units are structurally interleaved with lower plate metamorphic rocks of the Chism Creek Schist and with syn-orogenic clastic facies of the Taylor Creek and Kingsvale groups (Rusmore, 1985). Total thickness of the fault zone locally exceeds 8 km along the Hurley River road.

Structural studies of the Bralorne-McGillivray Pass Fault Zone have documented a complex history of deformation that can be linked to distinct episodes of contractional and strike-slip faulting (Rusmore, 1985; Leitch, 1989; Schiarizza et al., 1990). The earliest history of displacement is represented by north- and northwest-striking thrust faults and related folds. These include the Eldorado and Fergusson faults of the Bralorne-Goldbridge district (Rusmore, 1985; Leitch, 1989), and several unnamed faults along strike to the southeast in McGillivray Pass (this study). Asymmetric folds that occur in both upper and lower plates of these faults are inclined along steep northeast-dipping axial surfaces, and are overturned to the southwest. In multi-layered sequences, these folds are tight to isoclinal and are cut by an axial planar cleavage. This early cleavage represents the dominant schistosity throughout upper structural levels of the fault zone. Stretching lineations are, developed only along faults that flank the eastern and western margins of the fault zone, and are steeply inclined. Kinematic indicators observed in several localities along strike of these faults record a top-to-the-southwest displacement history (Schiarizza et al., 1990). The timing of this early thrusting (100-85 Ma) is bracketed by imbrication of the Kingsvale Group and by post-kinematic intrusions of the Coast Plutonic Complex (Rusmore, 1985).

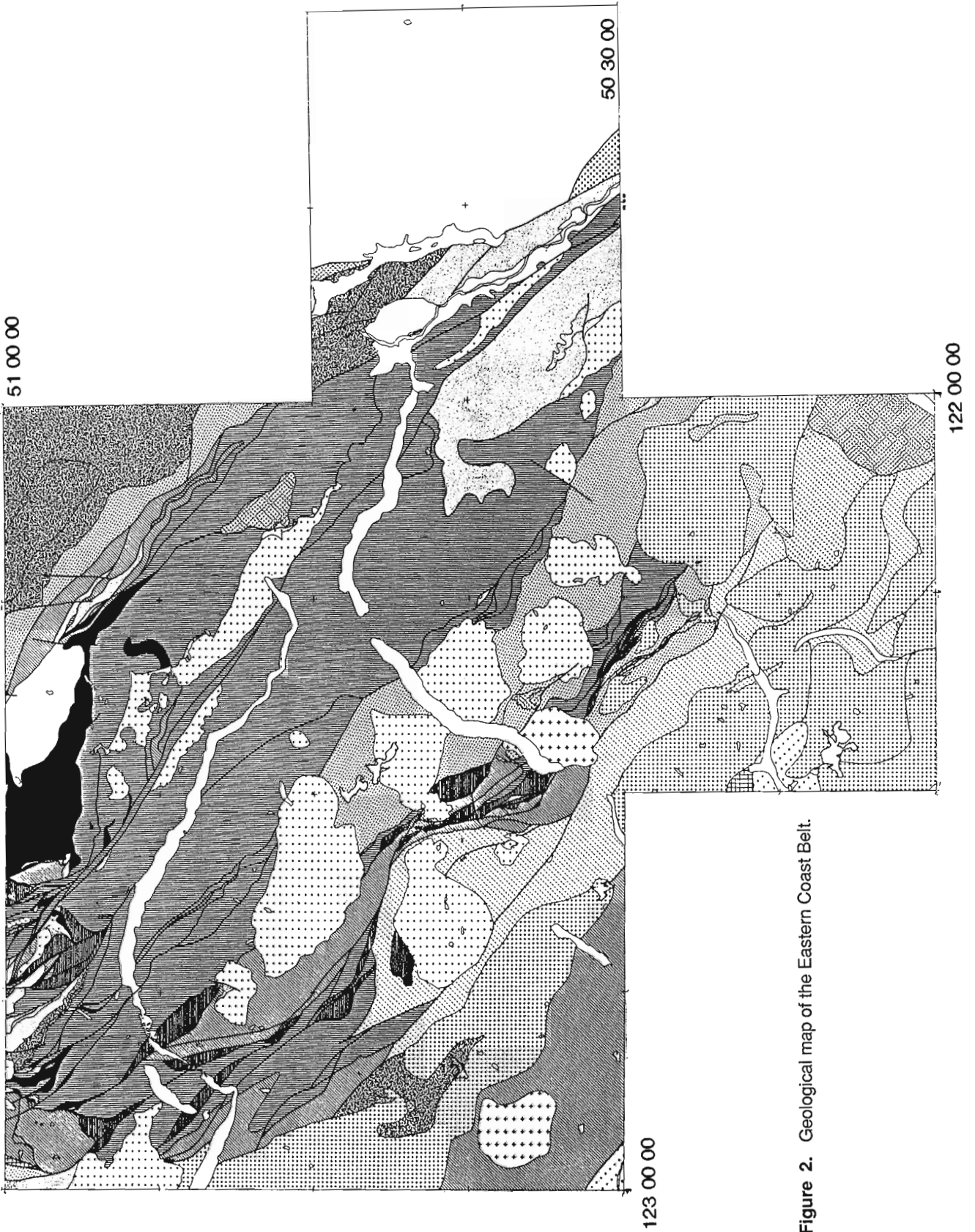


Figure 2. Geological map of the Eastern Coast Belt.

Vein systems and shear fractures that cut the dominant schistosity are the principal structures controlling gold mineralization in the Bralorne-Goldbridge district. These structures are interpreted to be part of a conjugate riedel shear system formed in a left-lateral strike-slip regime (Leitch, 1989). They predate the main stage of gold mineralization,

dated at 91-86 Ma (Leitch, 1989), and are interpreted to be linked to major left-lateral oblique slip along the Tyaughton Creek Fault and related structures (Scharizza et al., 1990).

Twin Lakes Fault Zone

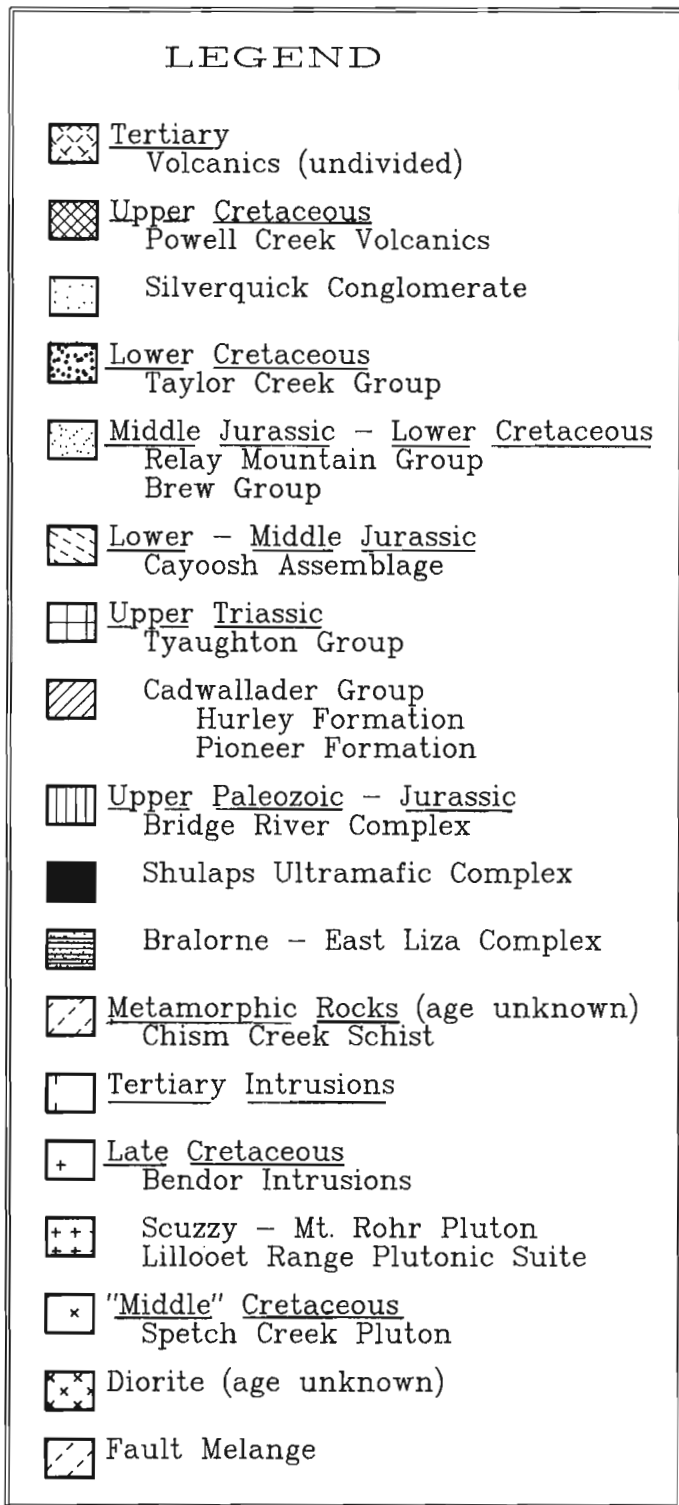
Our studies in the western Cayoosh Range have identified a system of northwest-trending imbricate faults that we refer to collectively as the Twin Lakes Fault Zone. The fault system extends southeastward from D'Arcy, across the Cayoosh Range into the northern Lillooet Ranges, where it is cut by post-kinematic granodiorite of the Scuzzy Pluton (Fig. 3). It represents a link in the system of faults that define the western edge of the Bridge River Terrane in the southern Coast Mountains.

Individual faults, marked by narrow mélangé zones (1-5 m thick), contain exotic slivers of sheared ultramafic rock (serpentinite and talc-chlorite-carbonate schist) and lenticular pods of greenstone, chert and metasedimentary rocks derived from both upper and lower plate domains. The lower plate comprises polydeformed metamorphic rocks of the Chism Creek Schist, which include distinctive micaceous and phyllitic quartzites, phyllitic siltstones, metavolcanic schists and marble derived in part from the Cayoosh Assemblage. Minor structures record a two-stage history of isoclinal folding, faulting and fabric development. Compositional layering is transposed by early generation isoclinal folds that contain a well-developed axial planar schistosity. These structures are overprinted by a crenulation cleavage that is axial planar to asymmetric southwest-verging folds. In multilayered sequences, these late generation folds are tight to isoclinal and steeply inclined to the northeast.

The axial part of the fault system is defined by two distinct zones of imbricate thrusting that separate stratigraphically coherent panels of low-grade sedimentary rocks. The lower fault panel comprises dark grey and black graphitic siltstone, shale, thin-bedded turbidite, greenish-grey tuffaceous siltstone and greywacke. The upper fault panel consists primarily of thin and thick-bedded volcanic sandstone and dark grey siltstone. Graded bedding and asymmetric cleavage relationships indicate that both fault panels are structurally overturned. They are interpreted to have been derived from folded upper plate rocks of the Cayoosh Assemblage.

Arrays of imbricate thrust faults flanking these two panels have the overall geometry of a hinterland-dipping duplex, and define the main locus of displacement for the fault system. Floor and roof thrusts contain a well-developed down-dip stretching lineation and are locally mylonitic. Shear bands and asymmetric flattening foliations documented in several localities along these fault zones record top to-the-southwest displacement (Fig. 4).

We consider the Twin Lakes, McGillivray Pass and Bralorne Fault zones to be part of a regional southwest-verging thrust system formed in response to



large-scale crustal shortening and imbrication along the eastern margin of the Insular Superterrane in Late Cretaceous time. In the Harrison Lake region, these structures are known to have been active between 96 and 91 Ma (Friedman et al., 1992; Journeay and Friedman, in press). Constraints on the timing of deformation in the Bralorne Fault Zone (Leitch, 1989) are consistent with this hypothesis.

Truax Fault

The Truax Fault is defined by a 50 m wide shear zone that cuts mafic and ultramafic rocks of the Bralorne-East Liza Complex. The fault zone dips steeply to the northeast and is well exposed on the ridge north of Mount Truax. It is characterized by an impressive array of mylonites, sheared

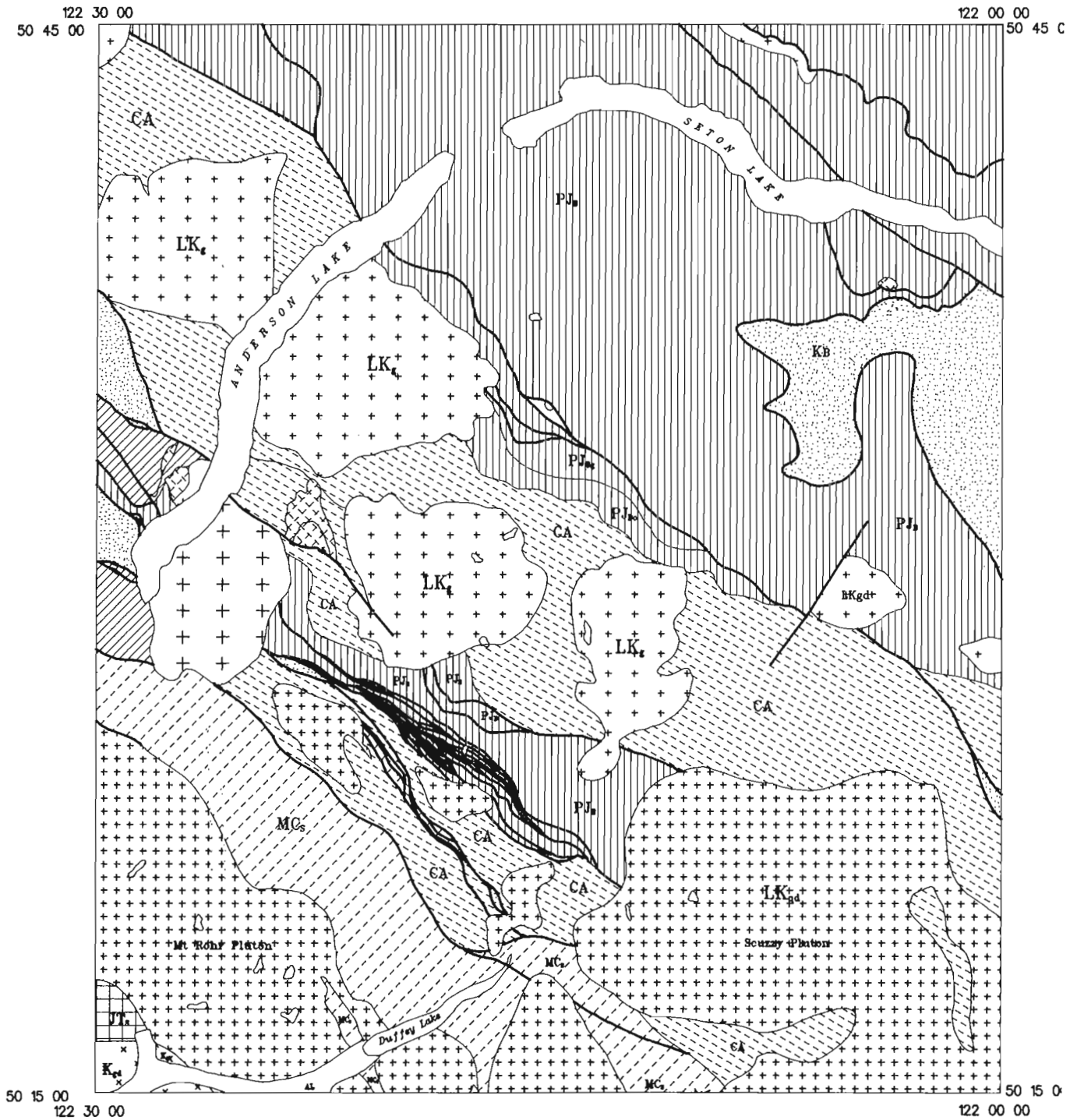


Figure 3. Geology of the Cayoosh Range.

chert breccia and serpentinite mélange. Shear bands and asymmetric flattening foliations occur throughout the fault zone. The orientation of these structures with respect to bounding shear zones indicates an oblique, upper plate to the northwest (sinistral) sense of shear. The fault zone is on strike with sinistral oblique-slip faults in the vicinity of Goldbridge (Schiarizza et al., 1990), and is considered to be part of the Tyaughton Creek Fault System. These structures postdate southwest-verging thrust faults and related folds of the western Chilcotin Range, and apparently predate gold mineralization (91-86 Ma) in the Bralorne mining district (Leitch, 1989).

Castle Pass Fault System

Recent mapping in the Cinnabar Creek region of the southern Chilcotin Range (Schiarizza et al., 1990; Garver, 1991) has identified an array of northeast-verging folds and associated thrust faults that are known collectively as the Castle Pass Fault System. These structures deform Albian and Cenomanian syn-orogenic basin sequences of the Taylor Creek Group, and are believed to have been active between 91 and 86 Ma (Garver et al., 1989). As such, these structures are coeval with shortening and associated gold mineralization in the Bralorne Fault Zone (Leitch, 1989). Our mapping extends the Castle Pass Fault System southeastward into the Bendor Range, and documents several northeast-verging thrust faults that occur along the east flank of the McGillivray Pass Fault Zone, and in isolated regions of the Cayoosh and northern Lillooet ranges. Although not contiguous, we consider these structures to have formed as part of the same fault system.

Northeast-verging thrusts of the Castle Pass system are well exposed in alpine ridges south of Carpenter Lake, between Truax and Tommy creeks. The faults imbricate steep southwest-dipping panels of Bridge River greenstone

and chert, and are marked by discrete brittle and ductile shear zones containing slivers of serpentinite, talc-chlorite-carbonate schist and chert breccia. Along strike to the southeast, these faults are cut by undeformed granodiorite of the Bendor pluton. Shear bands and asymmetric fabrics documented in two localities along the westernmost fault strand of this system record top-to-the-northeast displacement.

In the McGillivray Pass region, northeast-verging faults occur along the ridge system joining the Bendor and Anderson Lake plutons. These faults define a zone of imbricate thrusting that includes fault slivers of sheared serpentinite, talc-chlorite-carbonate schist, greenstone and chert derived from the Bralorne-East Liza and Bridge River complexes. These fault slivers lie structurally above dark grey phyllite, metavolcanic (tuffaceous) siltstone and quartzite of the Cayoosh Assemblage. The roof thrust of this fault system cuts across older southwest-verging faults of the McGillivray Pass Fault Zone, and is marked by ductile shear zones, locally containing mylonites and down-dip stretching lineations. Asymmetric fault zone fabrics documented in two localities along this zone, and in other fault strands of the same system record top-to-the-northeast displacement. The fault zone flanking the east margin of the Bralorne-East Liza Complex north of Mount Truax may be part of this system. The southern extension of this fault system has not yet been mapped.

An isolated but regionally significant northeast-verging fault occurs in the Northern Lillooet Ranges along the headwater regions of Boulder, Molybdenite and Texas creeks. The fault juxtaposes upper and lower plate metasedimentary rocks of the Cayoosh Assemblage and, like other contractional faults of the ECB, is defined by a structural mélange of sheared greenstone, chert and ultramafic rocks derived from the Bralorne-East Liza, Shulaps (?) and Bridge River complexes. Mylonites occur



Figure 4. Asymmetric fault zone fabrics along the roof thrust of the Twin Lakes Fault Zone. Fabrics indicate a top-to-the-southwest displacement history.

along a network of ductile shear zones that contain down-dip stretching lineations. S-C fabrics in quartz-rich mylonites collected from two localities at the head of Molybdenite Creek record a top-to-the-northeast sense of shear.

Downton Creek Fault

The Downton Creek Fault represents an important tectonic boundary in the Eastern Coast Belt. It extends northwestward across the Cayoosh and Bendor ranges and is on strike with a system of faults that occur north of Carpenter Lake (Fig. 2). In the Cayoosh and Bendor ranges, this fault marks the boundary between coherent greenstone-chert-argillite successions of the western Bridge River assemblage and sheared greenstone-chert mélangé of the eastern Bridge River assemblage (Fig. 3). It cuts the overturned limb of a regional southwest-verging syncline and associated thrust faults in the northern headwater region of Downton Creek, and apparently cuts across northeast-verging thrusts and related folds of the Castle Pass System in the Chilcotin, Bendor and northern Lillooet ranges. East of this fault is a system of anticlinoria and synclinoria that deform previously folded rocks of the eastern Bridge River Complex. These are upright, gently inclined folds that plunge to the northeast, nearly orthogonal to the trace of the Downton Creek Fault.

Structures that can be linked to the Downton Creek Fault record a complex history of southwest-vergent thrusting and dextral strike-slip displacement. Where exposed along the north shore of Anderson Lake, the fault juxtaposes an upper plate assemblage of sheared greenstone and chert against structurally thickened and imbricated lower plate siltstones and graphitic shales of the Cayoosh Assemblage. Layer-parallel brittle/ductile shear zones in the lower plate are 1-2 m thick and form a network more than 750 m wide. Stretching lineations are not well-developed. However, long axes of boudinaged siltstone layers and reclined intrafolial fold hinges define a pronounced L-tectonite fabric that is steeply inclined in the dominant schistosity (Fig. 5). Shear bands and asymmetric folds observed along several fault strands of the footwall domain record top-to-the-southwest

thrusting. However, strike-slip fault zones, containing subhorizontal lineations and asymmetric southeast-verging folds of foliation occur along the full extent of the Downton Creek Fault and record a less pronounced, but regionally significant component of right-lateral displacement (Fig. 6). The timing and magnitude of displacement along the Downton Creek Fault are unknown. It apparently cuts northeast-verging thrusts and folds of the Castle Pass System, believed to have formed between 91 and 86 Ma (Garver et al., 1989), and is intruded by post-kinematic granodiorite of the Cayoosh pluton which is part of the 63-57 Ma Bendor intrusions (Roddick, 1987). No other major contractional faults of this age are known southwest of the Marshall Creek Fault. However, southwest-verging thrust faults that occur in and along the flanks of the Shulaps Complex (Calon et al., 1990; Schiarizza et al., 1990) are intruded by late-kinematic hornblende porphyry dykes which yield Ar ⁴⁰/₃₉ cooling dates of 77 ± 11 Ma (Archibald et al., 1990a,b). Although offset by the Marshall Creek Fault, these structures clearly define an important Late Cretaceous system of southwest-verging thrust faults of which the Downton Creek Fault may be a part.

Cayoosh Creek Fault

The Cayoosh Creek Fault (Coleman, 1990) is a shallow northeast-dipping structure that places deformed and metamorphosed schists of the Bridge River Complex structurally above recumbent folded metasedimentary rocks of the Brew Group. The fault has not been mapped in detail, but is well-exposed in the cliffs north of Cayoosh Creek (Fig. 3). The fault is curvilinear and appears to be continuous with a shallow northwest-dipping fault mapped by Roddick and Hutchison (1973). The surface trace of this fault extends southeastward along the flanks of the Cayoosh Creek valley to Downton Creek, and southeastward along the Phair Creek valley. Contrary to previous reports (Mustard, 1983), we found no evidence that this fault cuts the Phair Creek pluton. Although emphasized by differential erosion, the western contact of the pluton is weakly foliated and locally cut by brittle faults with measurable offset.

Figure 5. Early-generation (F1) folds of compositional layering and associated axial planar foliations developed in metavolcanic succession of Bridge River Complex (Western Assemblage), near the headwaters of Downton Creek.



Structures in the lower plate of the Cayoosh Creek Fault are characterized by mesoscopic and map-scale isoclinal folds, well-exposed along the Cayoosh Creek valley and along alpine ridges adjacent to Mount Brew (Mustard, 1983; Coleman, 1990). The largest of these structures is an antiformal syncline exposed south of Mount Brew. The fold duplicates siltstone-quartzite successions of the Brew Group and has an overturned limb length of several kilometres. Minor folds and stretched pebble conglomerates in the hinge region indicate this is an early generation, westerly-verging syncline which plunges gently to the southeast.

Recumbent isoclinal folds in the Cayoosh Creek valley deform an older schistosity and are non-cylindrical along gently dipping axial surfaces. Stretching lineations plunge to the northwest and to the southeast. Asymmetric folds, shear bands and S-C fabrics are well-developed in quartz-rich mylonites. In two localities, these fault zone fabrics record top-to-the-northwest displacement. The Cayoosh Creek Fault has been interpreted by Coleman (1990) as a low-angle thrust fault across which deformed and metamorphosed rocks of the Bridge River Complex were displaced northwestward over younger basin sequences of the Brew Group. Our observations are consistent with this hypothesis, but do not rule out the possibility that the Cayoosh Creek Fault may have rooted to the northwest as a low-angle extensional fault.

Similar structures, including northwest-vergent folds and mylonitic shear zones are documented in the lower plate of the Marshall Creek Fault, along the south shore of Seton Lake (this study). We consider these structures to be part of the Cayoosh Creek Fault. They are cut by weakly deformed granite dykes that resemble the Eocene Mission Ridge pluton (47.5 Ma; Coleman, 1990), and are overprinted to the east by extensional shear zones which record top-to-the-southwest displacement. These top-to-the-southwest shear zones are interpreted by Coleman (1990) to be kinematically linked with right-lateral displacement along the Yalakom Fault.

Marshall Creek Fault

The Marshall Creek Fault extends northwestward from its cut-off with the Fraser Fault System in the Ashcroft map area (Monger, 1989) to its junction with the Relay Mountain and Yalakom faults in the Noaxe Creek Map area (Glover et al., 1988; Schiarizza et al., 1990); a strike distance of more than 135 km. North of Carpenter Lake, the Marshall Creek Fault consists of two separate strands. The northeast strand juxtaposes greenschist and prehnite-pumpellyite facies rocks of the Bridge River Complex and is estimated to have accommodated more than 10 km of right-lateral strike-slip displacement. The southwest strand locally cuts Eocene sedimentary successions and is interpreted to be a steep southwest-dipping normal fault. These two fault strands merge south of Carpenter Lake and continue southeastward as a single composite fault zone. Where it crosses Seton Lake, the Marshall Creek Fault comprises a system of shallow, northeast-dipping shear zones and steep, southwest-dipping brittle faults. Northeast-dipping shear zones record a dextral, top-to-the-southeast displacement, similar to those documented in the lower plate of the Mission Ridge Fault to the east (Coleman, 1990). These structures may be part of a low-angle zone across which displacement was transferred southeastward from the Marshall Creek Fault to the Yalakom Fault.

Down-to-the-southwest normal displacement across the Marshall Creek Fault has apparently down-dropped a segment of the northeast-dipping Mission Ridge Fault near Seton Lake. Restoration of hanging wall and footwall cut-offs suggest a minimum down-dip displacement of 3.5 km (Coleman, 1990). This displacement is believed to have been tied to uplift and unroofing of the Bridge River schists in Eocene time.



Figure 6. Late-generation (F2) folds of foliation in footwall of Downton Creek Fault.

SUMMARY AND CONCLUSIONS

Our work, combined with that of Schiarizza et al. (1989, 1990) allows a partial reconstruction of the deformation history for the ECB. We recognize five important episodes of deformation for the region south of Carpenter Lake. Timing constraints are based on the results of geochronological studies by Leitch (1989), Archibald et al. (1989, 1990a,b), Coleman (1990) and Friedman and Armstrong (1990). These timing constraints bracket, but do not necessarily date specific deformation events.

***96-91 Ma:** Southwest-vergent folding and associated thrusting of terranes throughout the southern Coast Belt. The main locus of displacement in the ECB during this episode of crustal shortening was along the Bralorne-McGillivray Pass-Twin Lakes Fault System. This fault system marks the western margin and may represent the basal detachment for oceanic rocks and overlying basin successions of the Bridge River Terrane. Structures in lower plate rocks of the ECB record a polyphase history of deformation and metamorphism. Structures in upper plate rocks of the ECB record only one major episode of southwest-vergent deformation and associated fabric development. These relationships suggest that the Bralorne-McGillivray Pass-Twin Lakes Fault System is likely out-of-sequence with respect to other contractional fault systems of the Central and Western Coast belts (Journey, 1990). Left-lateral oblique slip faults of the Tyaughton Creek System are interpreted to have formed late in this episode of crustal shortening and may have accommodated an important component of orogen-parallel displacement.

***91-86 Ma:** Northeast-vergent folding and associated thrusting. Major structures of the ECB that are known to have been active during this period of deformation include northwest-striking faults and folds of the Castle Pass System and southwest-dipping thrust faults in the western Bendor Range and in the headwater region of Boulder and Texas creeks in the northern Lillooet Ranges. These structures cut southwest-vergent thrust faults and are interpreted to have been active during gold mineralization in the Bralorne district (91-86 Ma; Leitch, 1989). However, we can not rule out the possibility that northeast-vergent faults may have been active at deeper crustal levels over a longer period of time.

***86-68 Ma:** Oblique, southwest-vergent thrusting and associated dextral strike-slip faulting. The Downton Creek Fault marks the boundary between western and eastern assemblages of the Bridge River Complex, and may be linked to southwest-vergent thrusting in the imbricate zone of the Shulaps Complex. Kinematic linkages between these structures and major dextral strike-slip fault systems of the ECB, such as the Yalakom Fault, are uncertain.

***68-48 Ma:** Detachment and northwestward displacement of the Bridge River Complex along the Cayoosh Creek Fault. Recumbent isoclinal folds in the lower plate of the Cayoosh Creek Fault may reflect either the distributed strain associated with northwestward overthrusting of the Bridge River Complex, or the effects of

older (96-91 Ma) southwest-vergent thrusting. Linkages between these structures and the Yalakom Fault are probable, but can not be proven.

The Mission Ridge Fault and steep southwest-dipping brittle shears along the Marshall Creek Fault represent outward-dipping extensional faults that flank Tertiary-age metamorphic rocks of the Bridge River Complex. These structures cut dextral strike-slip of the Marshall Creek Fault, and record a two-stage history of displacement; down-to-the-northeast displacement along the Mission Ridge Fault, followed by down-to-the-southwest displacement along the Marshall Creek Fault (Coleman, 1990). These structures predate dextral transcurrent displacement along the Fraser River Fault System, dated at 46-36 Ma.

ACKNOWLEDGMENTS

We gratefully acknowledge the mapping and scientific contributions of Bruce Northcote, who traversed with JMJ for most of the summer. CS, JHVK and MJ are responsible for 1:25 000 mapping of the Twin Lakes Fault Zone, and thank Harry Stehl and the University of Amsterdam for supervision and financial support. We thank John and Patricia Goats of Pemberton Helicopters, and Bob Thurston and Bob Holt of Cariboo-Chilcotin Helicopters for air, radio and logistical support throughout the summer.

REFERENCES

- Archibald, D.A., Glover, J.K., and Schiarizza, P.
1989: Preliminary report on Ar⁴⁰/Ar³⁹ geochronology of the Warner Pass, Noaxe Creek and Bridge River map areas (92O/3,2; 92J/16); in Geological Fieldwork 1988, British Columbia Ministry of Energy, Mines and Petroleum Resources, Paper 1989-1, p. 145-151.
- Archibald, D.A., Schiarizza, P., and Garver, J.I.
1990a: ⁴⁰Ar/³⁹Ar dating and the timing of deformation and metamorphism in the Bridge River Terrane, southwestern British Columbia (92O/2; 92J/15); in Geological Fieldwork 1989, British Columbia Ministry of Energy, Mines and Petroleum Resources, Paper 1990-1, p. 45-51.
1990b: ⁴⁰Ar/³⁹Ar evidence for the age of igneous and metamorphic events in the Bridge River and Shulaps Complexes, southwestern British Columbia (92O/2; 92J/15); in Geological Fieldwork 1989, British Columbia Ministry of Energy, Mines and Petroleum Resources, Paper 1990-1, p. 75-85.
- Calon, T.J., Malpas, J.G., and Macdonald, R.
1990: The anatomy of the Shulaps Ophiolite; in Geological Fieldwork 1989, British Columbia Ministry of Energy, Mines and Petroleum Resources, Paper 1990-1.
- Coleman, M.E.
1990: Eocene dextral strike-slip and extensional faulting in the Bridge River Terrane, southwest British Columbia; M.Sc. thesis, Carleton University, Ottawa, Ontario, 87 p.
- Friedman, R.M. and Armstrong, R.L.
1990: U-Pb dating, southern Coast Belt; in Lithoprobe Southern Canadian Cordillera Workshop Report, p. 146-156.
- Friedman, R.M., Tyson, T.M., and Journey, J.M.
1992: U-Pb age of the Mt. Mason Pluton in the Cairn Needle area, southern Coast Belt, British Columbia; in Current Research, Part A; Geological Survey of Canada, Paper 92-1A.
- Garver, J.I.
1991: Kinematic analysis and timing of structures in the Bridge River Complex and overlying Cretaceous rocks, Cinnabar Creek area, southwestern British Columbia (92J/15); in Geological Fieldwork 1990, British Columbia Ministry of Energy, Mines and Petroleum Resources, Paper 1991-1, p. 65-75.

- Garver, J.I., Schiarizza, P., and Gaba, R.G.**
 1989: Stratigraphy and structure of the Eldorado Mountain area, Chilcotin Ranges, southwestern British Columbia (92O/2 and 92J/15); in Geological Fieldwork 1988, British Columbia Ministry of Energy, Mines and Petroleum Resources, Paper 1989-1, p. 131-143.
- Glover, J.K., Schiarizza, P., and Garver, J.I.**
 1988: Geology of the Noaxe Creek map area (92O/2); in Geological Fieldwork 1987, British Columbia Ministry of Energy, Mines and Petroleum Resources, Paper 1988-1, p. 105-123.
- Journey, J.M.**
 1990: Structural and tectonic framework of the southern Coast Belt, British Columbia; in Current Research, Part E; Geological Survey of Canada, Paper 90-1E, p. 183-197.
- Journey, J.M. and Friedman, R.M.**
 in press: The Lillooet River Fault System: evidence of Late Cretaceous shortening in the Coast Belt of SW British Columbia; Tectonics.
- Journey, J.M. and Northcote, B.R.**
 1992: Tectonic assemblages of the Southern Coast Belt, southwest British Columbia; in Current Research, Part A; Geological Survey of Canada, Paper 92-1A.
- Leitch, C.H.B.**
 1989: Geology, wall-rock alteration and characteristics of the ore fluid at the Bralorne mesothermal gold-vein deposit, southwestern British Columbia; Ph.D. thesis, University of British Columbia, Vancouver, 483 p.
- Monger, J.W.H.**
 1989: Geology of Hope and Ashcroft map areas, British Columbia; Geological Survey of Canada, Maps 41-1989 and 42-1989.
- Mustard, J.F.**
 1983: The geology of the Mount Brew area, Lillooet, British Columbia; M.Sc. thesis, University of British Columbia, Vancouver, 74 p.
- Roddick, J.A.**
 1987: Coast Plutonic Complex; in Cordilleran cross-section: Calgary to Vancouver, R.A. Price et al. (eds.), IUGG XIX General Assembly Guidebook for Excursion A1.
- Roddick, J.A. and Hutchison, W.W.**
 1973: Pemberton (east half) map-area, British Columbia; Geological Survey of Canada, Paper 73-17, 21 p.
- Rusmore, M.E.**
 1985: Geology and tectonic significance of the Upper Triassic Cadwallader Group and its surrounding faults, southwestern British Columbia; Ph.D. thesis, University of Washington, Seattle, 170 p.
- Schiarizza, P., Gaba, R.G., Coleman, M., Garver, J.I., and Glover, J.K.**
 1990: Geology and mineral occurrences of the Yalakom River area (92O/1,2,92J/15,16); in Geological Fieldwork 1989, British Columbia Ministry of Energy, Mines and Petroleum Resources, Paper 1990-1, p. 53-73.
- Schiarizza, P., Gaba, R.G., Glover, J.K., and Garver, J.I.**
 1989: Geology and mineral occurrences of the Tyaughton Creek area (92O/2, 92J/15,16); in Geological Fieldwork 1988, British Columbia Ministry of Energy, Mines and Petroleum Resources, Paper 1989-1, p. 115-130.
- Varsak, J.L., et al., (8 authors)**
 in press: Lithoprobe crustal reflection structure of the Southern Canadian Cordillera II: Coast Mountain Transect; Tectonics.

Geological Survey of Canada Project 890036

Quaternary stratigraphy in the east-central Taseko Lakes area, British Columbia

Bruce E. Broster¹ and David H. Huntley¹
Cordilleran Division, Vancouver

Broster, B.E. and Huntley, D.H., 1992: Quaternary stratigraphy in the east-central Taseko Lakes area, British Columbia; in Current Research, Part A; Geological Survey of Canada, Paper 92-1A, p. 237-241.

Abstract

The stratigraphy and nature of glaciogenic sedimentation in the Quaternary sequences of east-central Taseko Lakes area, British Columbia (map sheets 920/7-10) was examined by surficial mapping and detailed examination of exposures along the Fraser River in the vicinity of Gang Ranch.

This report summarizes the results of surficial mapping and gives a brief description of sediments examined along the Fraser River and tributaries during the summer of 1991.

Résumé

La stratigraphie et la nature de la sédimentation glaciogène dans les séquences quaternaires reposant dans le centre-est de la région des lacs Taseko (Colombie-Britannique) (les cartes 920/7-10) ont été étudiées par la cartographie en surface et l'examen détaillé des affleurements longeant le fleuve Fraser dans les environs du ranch Gang.

Le présent rapport donne un résumé des résultats de la cartographie de surface et une brève description des sédiments analysés le long du fleuve Fraser et de ses affluents durant l'été de 1991.

¹ Department of Geology, The University of New Brunswick, P.O. Box 4400, Fredericton, New Brunswick, E3B 5A3

INTRODUCTION AND RESEARCH OBJECTIVES

Fieldwork during the 1991 season focused on map sheets 920/7 to 920/10 (1:50 000 scale; Fig. 1). Within this area, two principal contemporary depositional environments are recognized: upland and plateau areas; and the Fraser River and associated valleys.

The Fraser Plateau comprises the northern two-thirds of the study area. The plateau consists largely of rolling to level upland, with isolated hills rising above the plateau, and dissected by the deeply incised valley of the Fraser River. In the southern portion of the study area, the topography gives way to alpine conditions of the Marble Range and the Camelsfoot Range in the southeast, and the Chilcotin Ranges of the Coast Mountains to the south and southwest.

The Fraser River and its associated drainage incises Paleozoic, Mesozoic and Tertiary metamorphic, sedimentary and igneous sequences underlying the plateau. Extensive vertical and lateral sequences of Quaternary sediments overlie bedrock and are exposed along the Fraser in sections up to 245 m thick. The valley was eroded prior to the Fraser Glaciation and has been infilled by aggrading conditions that may include sediment units older than the Fraser Glaciation (Clague, 1981).

Previous work

Preliminary descriptive accounts of the Quaternary sequences in east-central Taseko Lakes area, British Columbia (map sheet 920; Fig. 1) were made by Tipper (1971) and Heginbottom (1972). These were undertaken as large aerial reconnaissance studies and precluded detailed examination of the thick sedimentary sequences exposed along the Fraser River and its tributaries. More recently, stratigraphic and process studies have been undertaken in adjacent areas. To the north, Mathews and Rouse (1986) have examined the stratigraphy of early Pleistocene glacial deposits in Dog Creek (map sheet 920/9) and deposits relating to advance and retreat of the Fraser Glaciation have been examined around Williams Lake and Soda Creek (Clague, 1986; Broster and Clague, 1987; Eyles et al., 1987). To the south, deglacial terrace development has been examined along the Fraser River at Lillooet by Ryder and Church (1986).

Purpose and methodology

Detailed studies of the stratigraphy, sedimentation processes and glacial dispersion as recorded in Quaternary sequences of Taseko Lakes area are lacking. To this end, research conducted in 1991, had the following objectives. First, to determine the range of lithofacies associated with

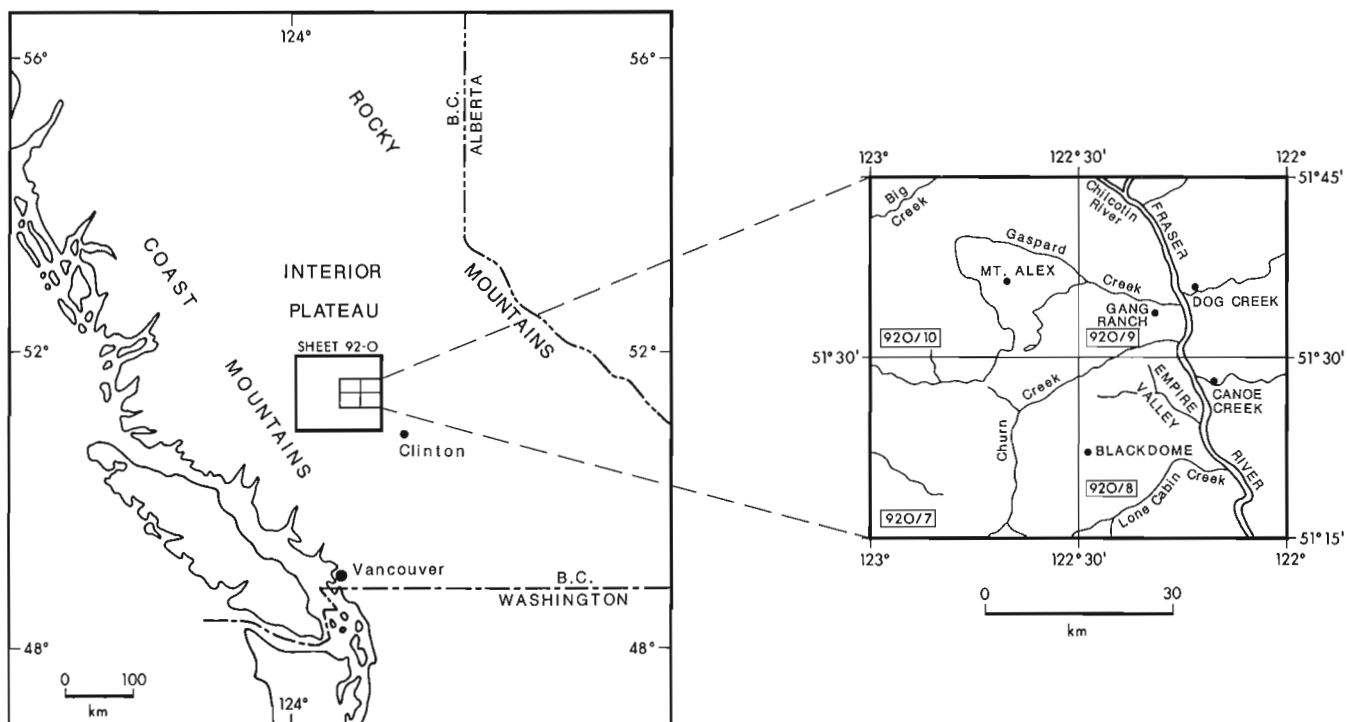


Figure 1. Location of study with detail of map sheets 920/7 to 920/10.

depositional environments operating in the area during the Quaternary. Second, to establish the stratigraphy and depositional history of these deposits. These objectives would build on earlier work (e.g., Tipper, 1971; Heginbottom, 1972) and contribute to present studies in the area by C.J. Hickson of the Geological Survey of Canada.

Field methods combined air photo interpretation with sedimentologic mapping procedures. Landforms were delineated from 1:60 000 (1987) and 1:20 000 (1967) scale air photos and field sketches. Emphasis was placed on the identification of glacial landforms, including till plains, drumlin fields, eskers, melt-water channels and spillways. In conjunction with landform mapping, Quaternary sediments were mapped at a scale of 1:50 000 from ground traverses. In addition, the extent of Fraser River valley fill and landslides have been delineated from mapping completed this year. Four 1:50 000 scale maps (NTS 92O/7, 8, 9, and 10) are in preparation, that will compliment the outlined objectives.

Key exposures were identified and their geometries established by field sketching and photographic documentation. Graphic logs of these sections were produced to determine the range of facies types and stratigraphic relationships. Vertical profile logs were measured with a Thommen altimeter (to an accuracy of ± 5 m). Horizontal profile logs were either measured with a 30 m tape or paced. Sediments were described using non-genetic lithofacies coding similar to Eyles et al. (1983). At each section logged, pebble fabrics, structural

measurements and bedding attitudes were measured and sediment samples were collected for later granulometric and lithological analyses.

Data and samples will be analyzed at the University of New Brunswick. These analyses will support descriptions of lithofacies types and stratigraphy, in addition to providing baseline data on regional geochemical signatures.

PRELIMINARY FINDINGS AND FUTURE RESEARCH OBJECTIVES

Lithostratigraphy

The plateau and valley-fill environments have distinct but complex facies associations, making it difficult to correlate with confidence between these environments. In both environments, stratigraphy is interpreted from incised river sections and exposure in road cuts.

Along the Fraser River valley, crude correlation over large distances is possible because of consistent stratigraphy, unit lithology and thickness. Between 150-245 m of valley fill is exposed in river sections along the Fraser from its confluence with the Chilcotin River to its confluence with Lone Cabin Creek; a distance of approximately 50 km (Fig. 1). Local variation occurs from channel cut and fill within some units. At some sections, large portions of the exposed sediments have experienced reorientation due to landsliding. However, the major units exposed along the

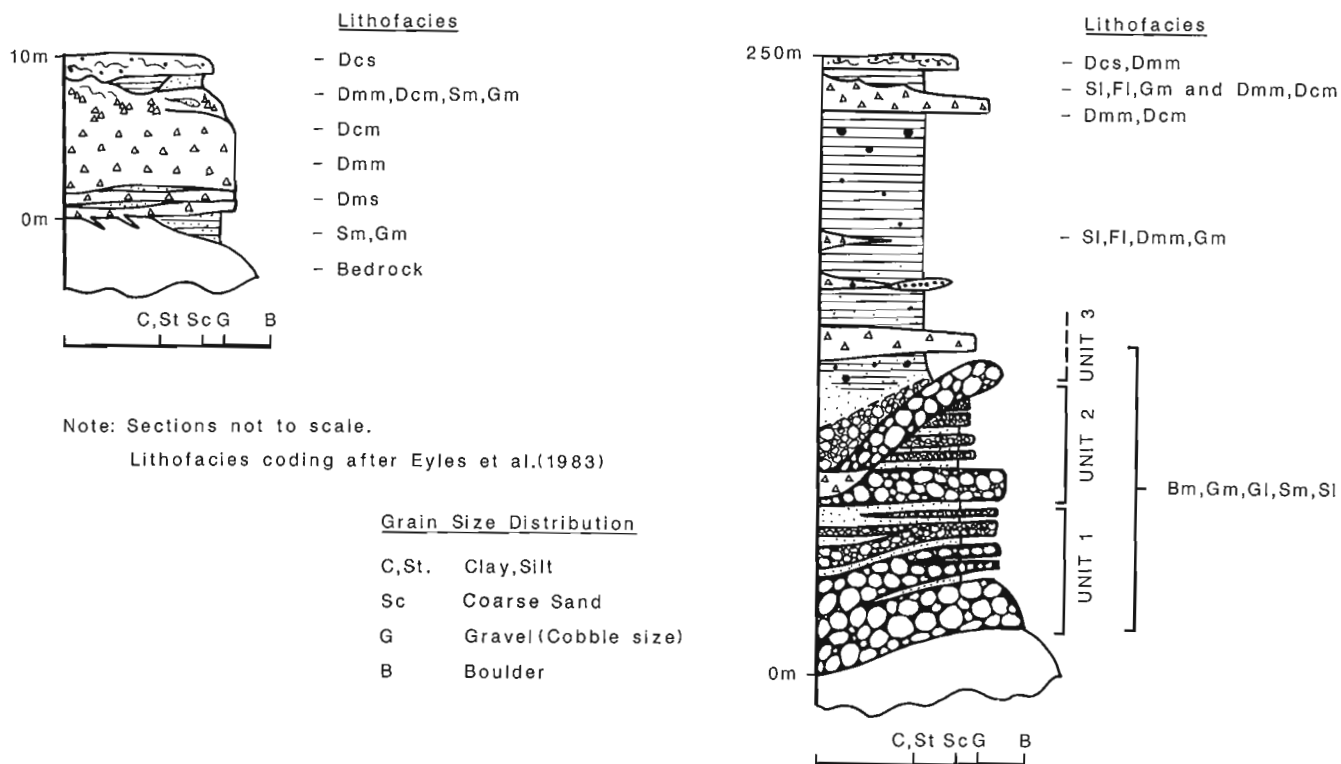


Figure 2. Generalized stratigraphy of principal depositional environments, of Upland and Plateau (left) and Fraser River and associated valleys (right). Lithofacies coding similar to Eyles et al. (1983).

Fraser River are lithologically distinctive and extensive enough to permit reliable correlation between exposures across the river and farther along the valley.

The lithostratigraphic information obtained is summarized below and in Figure 2. Further descriptions of facies types and depositional environments will accompany provisional 1:50 000 editions of landform and facies maps for sheets 92O/7 to 92O/10. Future research in the area will concentrate on regional correlation and establishing debris dispersal patterns within mapped glacial sediments.

Fraser River and its associated valleys

Bedrock:

Quaternary sediments are underlain by late Paleozoic to Tertiary metamorphic, igneous and sedimentary sequences. These sequences are under investigation as part of a regional bedrock mapping program supervised by C.J. Hickson.

Boulder conglomerates (Bm), Gravel (Gm, Gl) and Sands (Sm, Sl):

These sediments are restricted to the Fraser River and comprise the basal 140 m of valley fill. Three upward-fining cut and fill sequences are recognized.

Boulder conglomerates are massive-bedded, clast-supported units up to 20 m thick. Clasts are well-rounded, with a maximum diameter of 2 m. Although boulder conglomerates have a polymictic lithological composition, locally-derived basaltic clasts are proportionally dominant. Gravel conglomerates are also clast-supported and polymictic. These units are interbedded with sands and display massive, laminar and foreset bedding. Foresets indicate a general southward paleoflow.

Laminated sands (Sl), Silt and clay (Fl), Diamict (Dmm) and Gravel (Gm):

These sediments occur between 1600 ft (490 m) and 2100 ft (640 m) along the Fraser River valley. They appear as a monotonous sequence of laminated fine sands, silts and clays. Rounded and faceted boulders (with rare striations) are randomly dispersed throughout these sediments. The mean diameter of these boulders apparently increases towards the top of the sequence. Minor cut and fill gravels and debris flow deposits occur locally. At least one laterally persistent massive, matrix-supported diamict (**Dmm**) is documented within this sequence.

Massive, matrix supported diamict (Dmm), Massive, clast-supported diamict (Dcm):

Within the Fraser River valley a range of diamicts is observed. **Dcm** and **Dmm** overlie bedrock and stratified gravels in Lone Cabin Creek, Grinder Creek and Churn Creek. In addition, **Dmm** is found in an erosional channel at the confluence of Churn Creek and the Fraser River.

In the Gang Ranch area, laminated sands, silts and clays are passively overlain by **Dmm**. This diamict contains striated polymictic clasts and varies between 5 and 15 m in thickness. Drumlinoid and elongated ridge-like features are preserved within the upper surface of this diamict.

Diamicts (Dmm, Dcm), Massive and laminated sands and silts (Sm, Sl, Fl), and Gravels (Gm):

This facies assemblage is restricted to tributary valleys on the east side of the Fraser River (including: Alkali Creek, Harpers Creek, Dog Creek, Canoe Creek and China Gulch). At the confluence of these valleys with the Fraser River, terrace-like features, comprising sands (**Sm**, **Sl**) and silts (**Fl**) are found. Along the valley floors, fluviially re-worked diamict (**Dmm**, **Dcm**) and conical sand deposits (**Sm**) are observed. At the heads of valleys, close to the plateaus, gravels (**Gm**) and coarse sands (**Sm**) occur.

Laminated sands (Sl), Laminated silts (Fl), and Massive gravels (Gm):

These sediments are preserved in the Fraser River valley and typically form crosscutting terraces that partly obscure earlier valley-fill deposits. In general, they appear as repetitive upward fining sequences. These deposits (in addition to earlier sediments) are crosscut by failure planes oriented parallel to the present basinal axis.

Stratified, clast-supported diamict (**Dcs**), and Massive, clast-supported diamict (**Dcm**): Along the east side of the Fraser River and within tributary valleys, **Dcm** and **Dcs** are draped over Quaternary sediments and bedrock. These diamicts are predominantly composed of locally-derived material and thin towards the plateau escarpment at 3000 ft (915 m).

Upland and plateau areas

Bedrock:

Exposure of bedrock is typically confined to elevations above 4500 ft (1370 m) and valley sides. Bedrock is rarely striated, indicating northeast ice-flow (Churn Creek; 92O/7) and westerly ice flow (Dog Creek; 92O/9). In the Chilcotin Ranges, and on peaks above 6500 ft (1980 m), bedrock is obscured by extensive blankets of felsenmeer and patterned ground.

Massive, matrix-supported diamict (Dmm), Stratified, matrix-supported diamict (Dms) and Massive, clast-supported diamict (Dcm):

On slopes between 15° and 5°, **Dmm** and **Dcm** is preserved as a blanket deposit. Thickness varies, but locally may be up to 10 m thick in the Churn Creek map sheet (92O/7).

Diamicts typically contain a mixture of locally and distally-derived lithologies and some clasts are striated. **Dmm** facies are typically vertically and laterally transitional with **Dcm** facies. **Dms** facies, comprising layers of matrix-supported diamict interbedded with sands, are rare.

Massive sands (Sm), Massive gravels (Gm) and Diamicts (Dmm, Dcm):

On slopes below 5°, and within valleys, **Dmm** and **Dcm** is commonly overlain by massive sands and gravels. Sands and gravels are often associated with ridge-like features overlying diamict. Gravels are typically clast-supported and pebbles are well-rounded with occasional preferred alignment parallel to valley orientation. These sediments are commonly buried by significant thicknesses of organic material.

Stratified clast-supported diamict (Dcs):

This facies type is commonly preserved on slopes above 15°, and can overlie all facies types.

SUMMARY

Maps and descriptions by Tipper (1971) and Heginbottom (1972) have been revised for the east-central Taseko Lakes area (map sheets 92O/7 to 92O/10) by the current study. A provisional version of these maps and interpretations are in preparation.

Two principal depositional environments are recognized: upland and plateau areas; and the Fraser River and associated valleys. Both environments have distinct facies assemblages that are laterally and vertically discontinuous, making regional stratigraphic correlation between the two environments difficult.

The units in this portion of the Fraser River have been deposited as valley-fill in an ancestral valley under aggrading conditions. Basal coarse-grained boulder units were deposited in response to episodic fluctuations in base-level and stream energy. Overlying fine-grained sediments were deposited as a result of aggradation and ponding. At present the cause of the ponding is open to speculation, but is likely related to advancing glaciers during the early stages of the Fraser Glaciation. Initially, glacial advance in the Gang Ranch area was probably into a waterfilled basin. At the confluence of Churn Creek and the Fraser River, channel cuts with proglacial dropstones and diamict cut through the fine-grained unit and into the underlying coarse gravel units. Sediment gravity flows and disoriented blocks of sediment are interspersed with waterlain and glaciogenic deposits comprising some of the valley-fill.

Deglaciation was accompanied by ponding of the Fraser and stagnation of glacial masses on the adjacent plateau areas. Glacial sediments are overlain by fluvial, eolian and colluvial sediments. Downcutting and mass-movements represent the major erosional processes since deglaciation.

Although probably initiated because of deglaciation (cf. Broster, 1991), the mass-wasting process has continued to the present and has been responsible for blockage of the Fraser and some tributaries since postglacial time. Major mass-wasting is still ongoing and represents a potential economic and geomorphic hazard because of the possibility of river blockage causing upstream and downstream flooding.

The nature of glacial and postglacial depositional processes are currently under investigation. Topics of concern include: the origin of ridge features in the Gang Ranch area; the dynamics of ice-disintegration at the end of the Fraser Glaciation; and the nature, timing and consequences of late-glacial and postglacial mass-movements along the Fraser River Valley. Future research emphasis will focus on an understanding of glaciogenic dispersal patterns within glacial sediments mapped during the 1991 field season.

ACKNOWLEDGMENTS

Assistance during field work was provided by Irene Alarie. Enlightening discussions were also provided by P. van der Heyden, S. Metcalf, J.J. Clague and W.H. Mathews. Assistance with final manuscript preparation by B. Vanlier was much appreciated. Under A-base funding, additional support for travel and preparation of this report was through EMR Contract No. 23254-1-0145/01-XSB.

REFERENCES

- Broster, B.E.**
1991: Application of glacial geology in the assessment of neotectonics in coastal environments (abstract); Canadian Quaternary Association, Abstracts with Program, p. 18.
- Broster, B.E. and Clague, J.J.**
1987: Advance and retreat deformation at Williams Lake, British Columbia; Canadian Journal of Earth Sciences, v. 24, p. 1421-1430.
- Clague, J.J.**
1981: Late Quaternary geology and geochronology of British Columbia. Part 2: Summary and discussion of radiocarbon-dated Quaternary history; Geological Survey of Canada, Paper 80-35, 41 p.
1986: Quaternary stratigraphy of Williams Lake, British Columbia; Canadian Journal of Earth Sciences, v. 23, p. 885-894.
- Eyles, N., Clark, B.M., and Clague, J.J.**
1987: Coarse-grained sediment gravity flow facies in a large supraglacial lake; Sedimentology, v. 34, p. 193-216.
- Eyles, N., Eyles, C.H., and Miall, A.D.**
1983: Lithofacies types and vertical profile models: an alternative approach to the description and environmental interpretation of glacial diamict and diamictite sequences; Sedimentology, v. 30, p. 393-410.
- Heginbottom, J.A.**
1972: Surficial geology of Taseko Lakes map area British Columbia; Geological Survey of Canada, Paper 72-14, 9 p.
- Mathews, W.H. and Rouse, G.E.**
1986: An early Pleistocene proglacial succession in south-central British Columbia; Canadian Journal of Earth Sciences, v. 23, p. 1769-1803.
- Ryder, J.M. and Church, M.**
1986: The Lillooet terraces of Fraser River: a paleoenvironmental enquiry; Canadian Journal of Earth Sciences, v. 23, p. 869-884.
- Tipper, H.W.**
1971: Glacial geomorphology and Pleistocene history of central British Columbia; Geological Survey of Canada, Bulletin 196, 89 p.

Middle Jurassic stratigraphy of the Lillooet area, south-central British Columbia

J. Brian Mahoney¹
Cordilleran Division, Vancouver

Mahoney, J.B., 1992: Middle Jurassic stratigraphy of the Lillooet area, south-central British Columbia; in Current Research, Part A; Geological Survey of Canada, Paper 92-1A, p. 243-248.

Abstract

An elongate outcrop belt (~75 km long) of Middle Jurassic volcanic sandstone occurs on the northeast side of the Yalakom Fault from south of Lillooet to the headwaters of the Yalakom River. This unnamed unit comprises granule to pebble volcanic conglomerate, arkosic litharenite, laminated siltstone, and carbonaceous shale lithofacies. The stratigraphic base of the unit is not exposed, and the lower contact is everywhere the Yalakom Fault. The upper contact is a disconformity(?) with the overlying Cretaceous Jackass Mountain Group. Ammonite biostratigraphy indicates an Aalenian to Bajocian age. Paleocurrent indicators suggest transport to the northeast during deposition. The Middle Jurassic volcanic sandstone unit records mass sediment gravity flow deposition in a marine basin proximal to a volcanic source during Aalenian to Bajocian time.

Résumé

Un affleurement de grès volcanique du Jurassique moyen (~75 km de longueur) s'allonge sur le compartiment nord-est de la faille Yalakom, du sud de Lillooet jusqu'au cour supérieur de la rivière Yalakom. Cette unité non désignée comprend un conglomérat volcanique caillouteux, une arénite lithique arkosique, un siltstone laminé et un lithofaciès de shale carboné. La base stratigraphique de l'unité n'est pas exposée, et le contact inférieur est partout constitué de la faille Yalakom. Le contact supérieur est une discordance (?) avec le groupe de Jackass Mountain du Crétacé sus-jacent. La biostratigraphie des ammonites indique un âge de l'Aalénien au Bajocien. Les indicateurs de paléocourants révèlent un transport vers le nord-est durant la sédimentation. L'unité de grès volcanique du Jurassique moyen révèle une sédimentation par coulée de gravité dans un bassin marin à proximité d'une source volcanique durant la période allant de l'Aalénien au Bajocien.

¹ University of British Columbia, Department of Geological Sciences, 6339 Stores Road, Vancouver, B.C. V6T 2B4

INTRODUCTION

A Middle Jurassic volcanic sandstone exposed along the Yalakom River, northwest of Lillooet, was examined during the 1991 field season. Detailed mapping and stratigraphic analysis document lateral and vertical facies changes, clarify regional stratigraphic relations, and define the depositional environment. The strata record submarine mass sediment gravity flow deposition adjacent to a volcanic source during Aalenian-Bajocian time.

This investigation is part of a regional study of mid-Jurassic stratigraphy in south-central British Columbia concentrating on stratigraphic analysis and regional correlation. The purpose of the study is to constrain the timing of orogenic events during the middle to late Jurassic. Documentation of the stratigraphy, age range, and depositional environment of the middle Jurassic volcanic sandstone will aid in regional stratigraphic correlation and Jurassic basin reconstruction. The study is part of a doctoral thesis jointly sponsored by Geological Survey of Canada and The University of British Columbia, Department of Geological Sciences. Field work during the 1991 field season concentrated on the area northeast of the Yalakom Fault (Fig. 1), in conjunction with regional 1:50 000 scale mapping of the Taseko Lakes (920) map area.

REGIONAL GEOLOGY

Middle Jurassic volcanic sandstone is exposed on the west side of the Fraser fault in an approximately 75 km long, northwest-trending outcrop belt that extends from the junction of the Fraser and Yalakom faults near Lillooet to the headwaters of the Yalakom River on the northeast side of the Yalakom Fault (Fig. 1). Northeast of the Yalakom Fault the unit is steeply southwest dipping, overturned, and youngs to the northeast. The Yalakom Fault separates the unit from structurally complex imbricate fault slices of the Bridge River complex and the structurally higher Triassic Hurley Formation (Fig. 1).

In the study area, the Yalakom Fault is a high angle, vertical to east dipping structure that parallels bedding in the volcanic sandstone unit. The Yalakom Fault forms the base of the volcanic sandstone unit, and, near this contact, the unit contains west vergent mesoscopic folds with northwest-trending fold axes that parallel the trace of the fault.

The Yalakom Fault is interpreted as a dextral strike-slip fault with offset of 80 to 190 km, based on stratigraphic displacements and kinematic indicators within the fault zone (Tipper, 1978; Monger, 1985; Glover et al., 1988; Schiarizza et al., 1990). The presence of fault-parallel west vergent mesoscopic folds adjacent to the fault, the bedding-parallel attitude of the fault, and the apparent lack of strike-slip shear features in the volcanic sandstone unit near the fault suggest reverse movement along the Yalakom Fault has been significant in the study area.

The volcanic sandstone unit is overlain by lithic sandstone and conglomerate of the mid-Cretaceous (Barremian to Albian) Jackass Mountain Group with no apparent structural discordance. Both the volcanic sandstone and the overlying Jackass Mountain Group strata are deformed into simple, northwest-trending megascopic folds. The lack of structural discordance and similarity in structural style between the formations suggest the contact may be a disconformity.

PREVIOUS INVESTIGATIONS

Duffell and McTaggart (1952) mapped a sequence of argillite, greywacke, volcanic conglomerate and tuffaceous sandstone near Lillooet as the Lower Cretaceous Lillooet Group. Leech (1953) mapped middle Jurassic volcanic sandstone along the Yalakom River, north of the area described by Duffell and McTaggart (1952). Trettin (1961) described the Lillooet Group between the Bridge River and Lillooet, measured stratigraphic sections, and subdivided the unit into 3 divisions. Frebold et al. (1969) briefly described the lithology and paleontology of the unit at the northern end of the outcrop belt.

Woodsworth (1977) mapped the volcanic sandstone unit described by Trettin (1961) as the upper Jurassic-lower Cretaceous Relay Mountain Group. Tipper (1978) correlated the rocks east of the Yalakom River with the lower Jurassic Tyughton Group. Monger (1989) abandoned the name Lillooet Group for the rocks near Lillooet, and correlated the strata with the upper Jurassic-lower Cretaceous Relay Mountain Group. They remapped a small area near the confluence of the Bridge and Fraser rivers as the Lower Jurassic Ladner Group (Fig. 2). Schiarizza et al. (1990) mapped the volcanic sandstone described by Leech (1953) and Woodsworth (1977) along the Yalakom River as an unnamed mid-Jurassic volcanic sandstone (**mJvs**), and suggested a tentative correlation between the rocks along the Yalakom River and those near Lillooet.

The stratigraphic nomenclature in the literature is confusing due to discontinuous exposure, a lack of fossils, and the wide age range of the fossils that have been recovered (Table 1). Geological mapping, stratigraphy, and paleontology completed during this study document the lateral continuity of the unit throughout its outcrop belt, and indicate that the rocks near Lillooet are continuous with those to the northwest along the Yalakom River.

STRATIGRAPHY

Lithofacies

The middle Jurassic volcanic sandstone unit comprises granule to pebble volcanic conglomerate, arkosic litharenite, laminated siltstone and carbonaceous shale lithofacies. Whereas the recessive weathering fine-grained lithofacies are volumetrically more abundant, the resistant arkosic litharenite and conglomerate lithofacies form prominent ribs throughout the outcrop belt and locally dominate the stratigraphy. A 585 m thick partial section was measured along the Yalakom River northeast of its confluence with

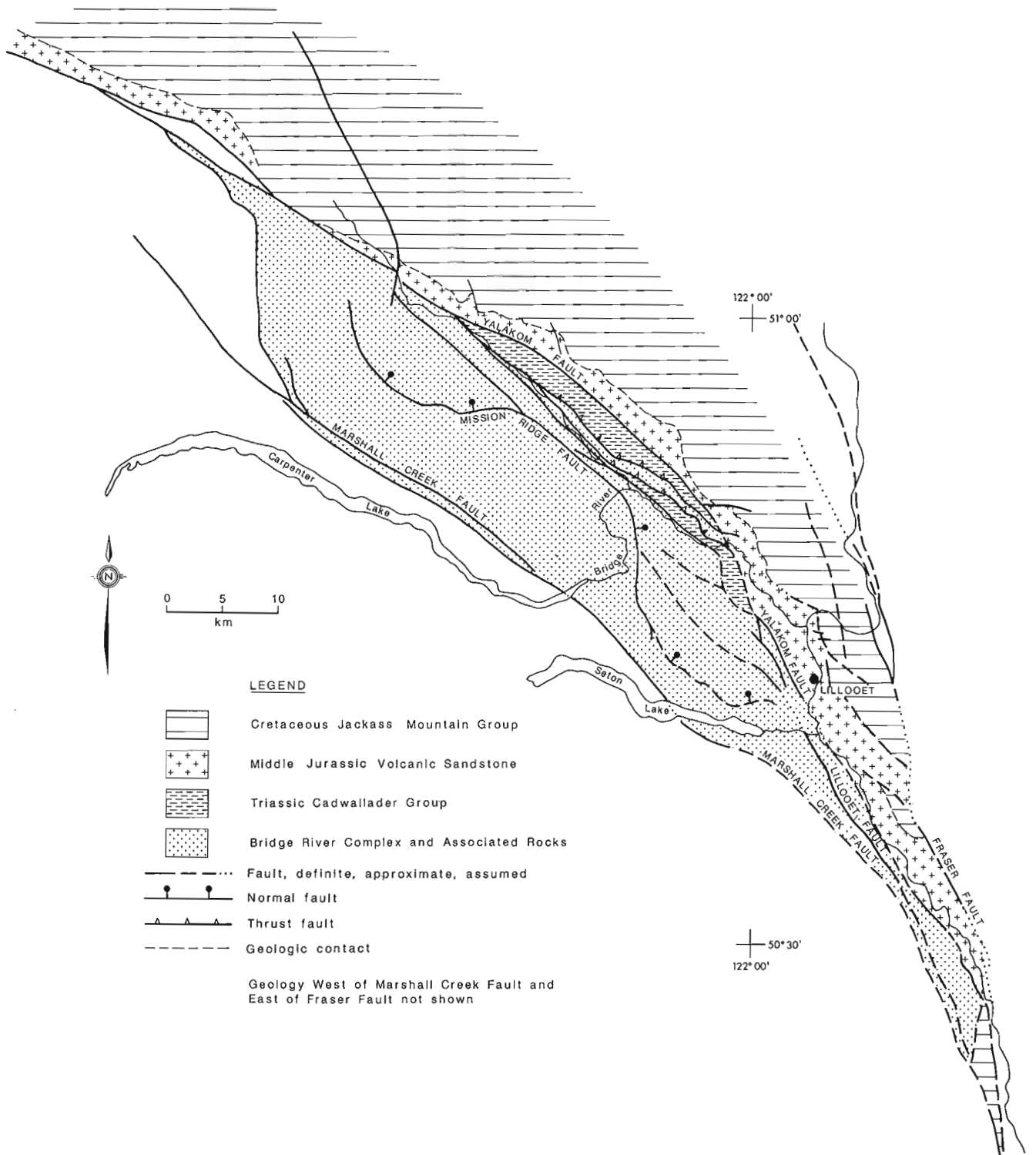


Figure 1. Simplified geologic map of the Lillooet area, showing major faults and the distribution of the middle Jurassic volcanic sandstone unit and associated units. Modified from Woodsworth (1977), Coleman (1989), Monger (1989), Schiarizza, et al. (1990).

Blue Creek (Fig. 2). The maximum thickness of the unit is estimated to be approximately 800 m. The stratigraphic base of the unit is not exposed; the basal contact of the unit is everywhere the Yalakom Fault. An unknown amount of section has been structurally removed. The upper contact of the unit is an unconformity with the overlying Jackass Mountain Group.

The granule to pebble conglomerate lithofacies is medium to thick bedded, and contains angular to subangular clasts of chert, volcanic, and minor sandstone clasts in a medium- to coarse-grained, poorly sorted arkosic litharenite matrix. Angular plagioclase feldspar crystals are locally abundant in the matrix. Abundant platy, angular to subangular mudstone clasts (2-8 cm) commonly occur near the base of beds, and display a preferential alignment parallel to bedding. Bedding appears tabular and laterally continuous, although lenticular beds 25 to 30 m wide and 1 to 2 m deep occur locally. Beds have sharp, scoured basal contacts and are commonly graded. The conglomerate lithofacies displays well-developed fining and thinning upward sequences (1-2 m thick). Thick-bedded, structureless conglomerate grades upward into thin- to medium-bedded, medium- to coarse-grained arkosic litharenite, which is gradationally overlain by thin-bedded, parallel laminated fine- to coarse-grained siltstone. Individual 1 to 2 m thick conglomerate to siltstone sequences aggregate into 5 to 15 m thick fining and thinning upward intervals; each successive conglomerate/siltstone sequence is more fine-grained and thinly bedded than the one below.

The arkosic litharenite lithofacies consists of medium to thick bedded (0.25-1 m), medium to coarse grained, moderately sorted, arkosic volcanic lithic sandstone characterized by an abundance of angular (euhedral) plagioclase grains. Beds are commonly graded, have sharp bases, and become finer grained and parallel laminated near the upper contact. Pebble to granule conglomerate stringers are locally abundant, particularly near the base of beds. Angular mudstone clasts occur locally at the base of beds. Fining and thinning upward sequences are common. Medium- to thick-bedded, medium- to coarse-grained

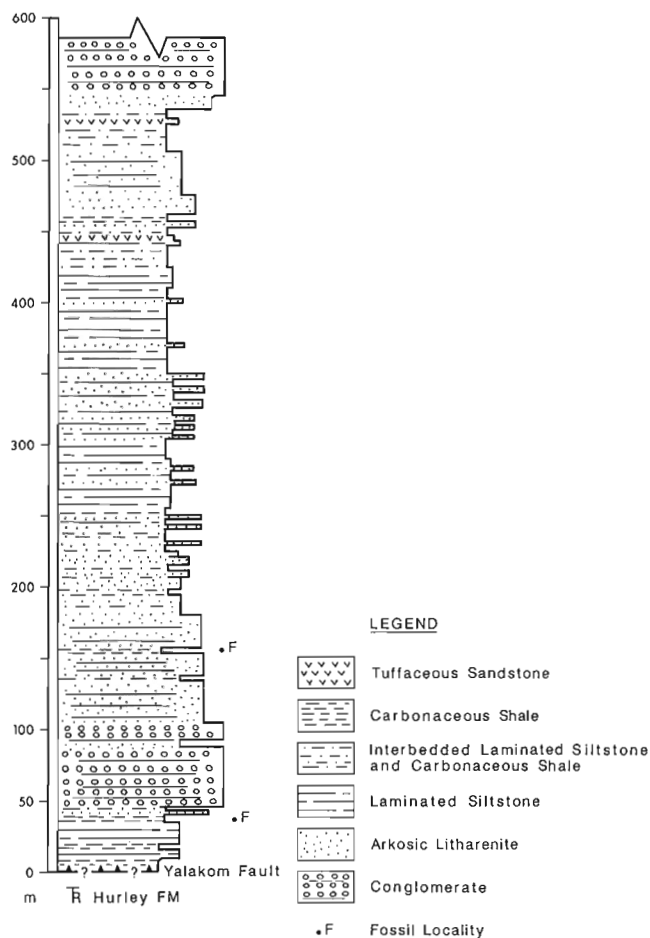


Figure 2. Measured stratigraphic section of the middle Jurassic volcanic sandstone unit. Section measured upstream from the confluence of Blue Creek and the Yalakom River (10U EN, 537800mE, 565370mN)

Table 1. Review of Jurassic stratigraphic nomenclature near Lillooet, B.C.

Formation name	age	location	author
Lillooet Group	Neocomian*	Lillooet	Duffel and McTaggart, 1952
unnamed	Aalenian*	Blue Creek	Leech, 1953
Lillooet Group	Neocomian	Bridge River	Trettin, 1961
unnamed	Bajocian*	Blue Creek	Frebald, et al., 1969
Relay Mountain Group	U. Jurassic to L. Cretaceous	east of Yalakom R.	Woodsworth, 1977
Tyughton Group	Sinemurian to Bajocian	east of Yalakom R.	Tipper, 1978
Relay Mountain Group	Neocomian	Lillooet	Monger, 1989
middle Jurassic volcanic sandstone	Aalenian to Bajocian	east of Yalakom R.	Schiazza et al., 1990
middle Jurassic volcanic sandstone	Aalenian to Bajocian*	east of Yalakom R. to south of Lillooet	this study

* indicates new data presented

sandstone grades upward into thin- to medium-bedded, fine-grained sandstone to coarse siltstone that is capped by dark grey fine- to medium-grained siltstone. The arkosic litharenite lithofacies locally aggregates to 10 to 25 m, but commonly occurs as medium- to thick-bedded interbeds within the conglomerate lithofacies, or as thin beds intercalated within the fine-grained lithofacies.

The laminated siltstone lithofacies is composed of thin-bedded fine- to coarse-grained siltstone and very fine grained sandstone. The lithofacies commonly consists of rhythmic interbeds of thin bedded, parallel to crosslaminated, fine sandstone to coarse siltstone gradationally overlain by thin- bedded, parallel laminated fine siltstone to mudstone. Tuffaceous intervals occur locally. The laminated siltstone lithofacies commonly occurs near the top of coarse-grained intervals, where it may be intercalated with the conglomerate or arkosic litharenite lithofacies, or may form homogeneous sequences up to 50 to 60 m thick. Wood fragments are common on bedding planes.

The carbonaceous shale lithofacies consists of thin bedded, thinly laminated, fissile dark grey shale with locally abundant ammonite and *Buchia* pelecypod impressions. The lithofacies occurs as thin beds intercalated with all other lithofacies, and does not aggregate to greater than 1 m. Faunal impressions are most abundant in the 0.25 to 1 m thick carbonaceous shale intervals. The lithofacies comprises less than 20% of the entire unit.

Minor amounts of thin-bedded, silty micrite and micritic siltstone occur throughout the unit as thin ribs within the laminated siltstone or carbonaceous shale lithofacies. The calcium carbonate content apparently fluctuates throughout the unit, but is highest in the fine-grained lithofacies that are devoid of coarse clastic detritus.

Age

Duffell and McTaggart (1952) assigned an Early Cretaceous age to the Lillooet Group based on pelecypods (??) (*Aucella*) collected south of Lillooet (Table 1). Trettin (1961) supported the Neocomian age determination. Monger (1989) correlated the rocks north of Lillooet with the Upper Jurassic Relay Mountain Group based on lithological similarities and the pre-existing fossil collections of Duffell and McTaggart (1952). However, Monger (1989) mapped a small area at the confluence of the Bridge and Fraser rivers as Ladner Group, based on a probable early Jurassic ammonite.

Leech (1953) and Frebald et al. (1969) collected Aalenian to Bajocian ammonites from the northern end of the outcrop belt. In the same area, two new fossil collections from the measured section (from 46 and 155 m) yielded specimens of *Tmetoceras scissum*, an Aalenian ammonite (P.L. Smith, written comm., 1991). A new fossil collection above the confluence of the Bridge and Fraser rivers, near the southern end of the outcrop belt, yielded the Bajocian ammonite *Stephanoceras* (P.L. Smith, written comm., 1991). This collection is believed to be from the upper one-third of the volcanic sandstone unit, suggesting the entire unit may be Aalenian to Bajocian.

Detailed mapping demonstrates that the Aalenian to Bajocian strata described by Leech (1953), Frebald et al. (1969) and in this report is laterally continuous with the Lillooet Group of Duffell and McTaggart (1952). This correlation suggests the age of the Lillooet Group is Aalenian to Bajocian. The Neocomian age reported by Duffell and McTaggart (1952) is problematic, as the stratigraphic position the Neocomian fauna is unknown. This fauna may indicate a disconformity within the volcanic sandstone unit, or may have been recovered from a lithologically similar but unrelated unit. Detailed mapping and stratigraphic analysis south of Lillooet is needed to resolve this question.

Paleocurrents

The majority of the mid-Jurassic volcanic sandstone unit is structureless or parallel laminated, and paleocurrent indicators are rare. Flute casts measured at the base of arkosic litharenite beds in two stratigraphic levels (at 75 m and 420 m) indicate a northeast (020-040°) paleocurrent during deposition (n=18).

DEPOSITIONAL ENVIRONMENT

The lithofacies in the middle Jurassic volcanic sandstone are interpreted as the product of mass sediment gravity flow in a subwave base marine environment. The conglomerate lithofacies and interbedded arkosic litharenite represent top-cut-out (TAB) coarse-grained turbidites, with minor complete (TABCDE) turbidites. The apparently tabular and laterally continuous conglomerate beds locally contain shallow channel features, and are lenticular on a kilometre scale. Abundant fining and thinning upward stratigraphic intervals suggest deposition by a migrating distributary system. Angular mudstone clasts are interpreted as rip-up clasts due to basal scour by mass sediment gravity flows.

The arkosic litharenite lithofacies consists primarily of top-cut-out turbidites (TAB). Granule to pebble stringers within massive, thick-bedded arkosic litharenite are interpreted as lag deposits within amalgamated TAAA sequences. Beds are tabular and laterally continuous, have sharp bases and graded bedding, and display no evidence of channelling, suggesting deposition by unchanneled turbidity currents.

The laminated siltstone lithofacies comprises base-cut-out partial turbidites (TCDE,DE), as indicated by the sharp basal contacts, graded bedding, parallel and crosslaminations, and the tabular, laterally continuous character of the lithofacies. The carbonaceous shale lithofacies represents hemipelagic deposition during periods of reduced clastic influx. A hemipelagic interpretation is supported by the significant amount of faunal preservation in this lithofacies.

The lithofacies present in the middle Jurassic sandstone unit are contained in fining and thinning upward sequences that represent deposition by both channelized and unchanneled turbidity currents in a migrating distributary system. The conglomerate lithofacies is interpreted to be

deposited in shallow anastomosing channels in the mid-fan region of a submarine fan. The arkosic litharenite and laminated siltstone lithofacies were deposited by unchannelized turbidity currents in the mid- to outer fan region. The carbonaceous shale lithofacies represents hemipelagic deposition between channels in the mid-fan and during periods of low clastic influx on the outer fan.

Proximity to a volcanic source is required by the abundance of volcanic debris in the middle Jurassic volcanic sandstone unit, particularly the amount of unaltered plagioclase. The angularity of the lithic clasts and preservation of coarse plagioclase grains suggest limited transport distance. The locally abundant wood debris suggests proximity to a land mass, and the minor tuffaceous interbeds indicate contemporaneous volcanism. Paleocurrent data suggest the source terrane lay to the southwest of the depositional site. The middle Jurassic volcanic sandstone unit is interpreted to represent submarine fan deposits in a marine basin near a volcanic highland, perhaps in an actively subsiding marginal basin during Aalenian to Bajocian time.

REFERENCES

Coleman, M.

1989: Geology of Mission Ridge, near Lillooet, British Columbia (92I, J); in Geological Fieldwork 1988; British Columbia Ministry of Energy, Mines and Petroleum Resources, Paper 89-1, p. 99-104.

Duffell, S. and McTaggart, K.C.

1952: Ashcroft map area, British Columbia; Geological Survey of Canada, Memoir 262, 122 p.

Frebold, H., Tipper, H.W., and Coates, J.A.

1969: Toarcian and Bajocian rocks and guide ammonites from southwestern British Columbia; Geological Survey of Canada, Paper 67-10, 55 p.

Glover, J.K., Schiarizza, P., and Garver, J.I.

1988: Geology of the Noaxe Creek map area (92O/2); in Geological Fieldwork 1987, British Columbia Ministry of Energy, Mines and Petroleum Resources, Paper 1988-1, p. 105-123.

Leech, G.B.

1953: Geology and mineral deposits of the Shulaps Range, southwestern British Columbia; British Columbia Department of Mines, Bulletin 32, 54 p.

Monger, J.W.H.

1985: Structural evolution of the southwestern Intermontane Belt, Ashcroft and Hope map areas, British Columbia; in Current Research, Part A; Geological Survey of Canada, Paper 85-1A, p. 349-358.

1989: Geology, Ashcroft, British Columbia; Geological Survey of Canada, Map 41-1989, sheet 1, scale 1:250 000.

Schiarizza, R., Gaba, R.G., Coleman, M., Garver, J.I., and Glover, J.K.

1990: Geology and mineral occurrences of the Yalakom River area, in Geological Fieldwork 1989, British Columbia Ministry of Energy, Mines and Petroleum Resources, Paper 1990-1, p. 53-72.

Tipper, H.W.

1978: Taseko Lakes (92O) map area; Geological Survey of Canada, Open File 534.

Trettin, H.P.

1961: Geology of the Fraser river valley between Lillooet and Big Bar Creek; Ph.D. thesis, University of British Columbia, Vancouver, 109 p.

Woodsworth, G.J.

1977: Pemberton (92J) map area; Geological Survey of Canada, Open File 482.

Geological Survey of Canada Project 890039

The Late Albian-Early Cenomanian Silverquick conglomerate, Gang Ranch area: evidence for active basin tectonism

J.B. Mahoney¹, C.J. Hickson, P. van der Heyden, and J.A. Hunt¹
Cordilleran Division, Vancouver

Mahoney, J.B., Hickson, C.J., van der Heyden, P., and Hunt, J.A., 1992: The Late Albian-Early Cenomanian Silverquick conglomerate, Gang Ranch area: evidence for active basin tectonism; in Current Research, Part A; Geological Survey of Canada, Paper 92-1A, p. 249-260.

Abstract

Well exposed sections of chert pebble and volcanic clast conglomerate, correlated with the Albian to Cenomanian Silverquick conglomerate, are present in Churn Creek (1:50 000, map areas 92O17 and 8). The section is 1100 m thick and is made up of a 315 m thick lower, chert pebble conglomerate unit, a middle, 500-600 m thick volcanic-clast conglomerate, and an upper 175 m thick volcanic and plutonic cobble to boulder conglomerate. The sediments represent deposition in a fluvial environment; most likely a braided river. The strata record significant changes in provenance and basin margin tectonism. The transition from the lower chert dominated unit (probably representing eroded Bridge River/Cache Creek terrane) to the volcanic-clast dominated lithofacies, suggest close proximity to a volcanic source. The coarse angular character and lack of fluvial features suggest the upper unit may have been deposited as an alluvial fan adjacent to a proximal highland, possibly associated with reverse faulting along the Little Basin Fault.

Résumé

Au ruisseau Churn (zones cartographiques 92O17 et 8, échelle de 1150 000), on observe des coupes bien exposées d'un conglomérat de cailloux de chert d'origine volcanique corrélé au conglomérat cénomanien de Silverquick. La coupe mesure 1100 m d'épaisseur et est composée d'une unité inférieure de 315 m d'épaisseur de conglomérat de clastes volcaniques et d'un conglomérat supérieur de galets à blocs d'origine volcanique et plutonique de 175 m d'épaisseur. Les sédiments témoignent d'une accumulation dans un milieu fluvial; fort probablement dans un cours d'eau anastomosé. Les couches indiquent des changements importants de provenance et de tectonisme en marge de bassin. La transition d'une unité inférieure principalement cherteuse (représentant probablement le terrane érodé de la rivière Bridge) à un lithofaciès dominé par des clastes volcaniques, pourrait révéler l'étroite proximité d'une source volcanique. La présence de sédiments grossiers anguleux et l'absence de caractéristiques fluviales indiquent que l'unité supérieure a pu se déposer sous forme de cône alluvial près de hautes terres proximales, probablement associées à la formation de failles inverses le long de la faille du bassin Little.

¹ Department of Geological Sciences, The University of British Columbia, 6339 Stores Road, Vancouver, British Columbia V6T 1Z4

INTRODUCTION

Well exposed sections of chert pebble and volcanic clast conglomerate of the Silverquick conglomerate are present along Churn Creek, south of Gang Ranch, British Columbia (Fig. 1). Fluvial sedimentation in a tectonically active basin during Albian to Cenomanian time is indicated by stratigraphic studies and structural analysis of coeval basin-bounding faults. These studies were undertaken in conjunction with regional mapping (1:50 000 scale) of the eastern third of the Taseko Lakes (92O) map sheet (Fig. 2). This work is part of the Chilcotin-Nechako Hydrocarbon Province under the Frontier Geoscience Program (Hickson, 1990; Hickson et al., 1991).

REGIONAL GEOLOGIC SETTING

The eastern third of Taseko Lakes map area is located within the Intermontane Belt, and straddles the dextral strike-slip Fraser Fault (Fig. 1). In this paper, the Churn Creek area refers to the Churn Creek drainage north of Little Basin (Fig. 1). The Fraser Fault is immediately east of the Churn Creek area, and separates Jurassic(?), Cretaceous, and Eocene volcanic and sedimentary rocks on the west from Lower Permian to Middle(?) Jurassic chert, argillite and limestone of the Cache Creek Complex to the east (Fig. 2).

In the Churn Creek area, moderately folded Lower to Upper Cretaceous sedimentary rocks of the Silverquick conglomerate apparently unconformably overlie amygdaloidal andesite lava of probable late Early Cretaceous age. An isolated exposure of Jurassic(?) black argillite on the north side of Churn Creek suggests that older sedimentary units may underlie these Cretaceous units (Fig. 2). The Cretaceous rocks are unconformably overlain by a thick sequence of Eocene volcanic and sedimentary rocks. Basalt flows and intercalated sedimentary rocks of the Plio-Pleistocene Chilcotin Group unconformably overlie all older units (Fig. 2).

SILVERQUICK CONGLOMERATE

Previous work

The Silverquick conglomerate is the informal name assigned to the roughly 1500+ m thick sequence of late Albian-Cenomanian chert-pebble and volcanic clast conglomerate exposed near the Silverquick Mine along Taylor Creek in the Noaxe Creek (92O/2, 1:50 000) map area (Glover et al., 1988a; Garver, 1989; Garver et al., 1989). The unit was originally named the Silverquick formation (Glover et al., 1988a), but the informal designation Silverquick conglomerate has become entrenched in the literature (Garver, 1989; Garver et al., 1989), and that convention is followed in this paper. The Silverquick conglomerate and the gradationally overlying Late Albian to Cenomanian Powell Creek volcanics comprise the informal Battlement Ridge group (Glover et al., 1988a). Glover et al. (1988a) subdivide the Silverquick conglomerate into a lower chert pebble-rich conglomerate member and an overlying cobble to boulder volcanic clast conglomerate member that is interpreted to grade upward into the Powell Creek volcanics.

Hickson et al. (1991) document a transition from chert-rich conglomerate to volcanic clast-rich conglomerate and massive volcanic breccia in Albian to Cenomanian rocks along Churn Creek. Similarities in age, lithology, stratigraphy, and depositional environment support the assignment of the Albian to Cenomanian conglomerate along Churn Creek to the Silverquick conglomerate.

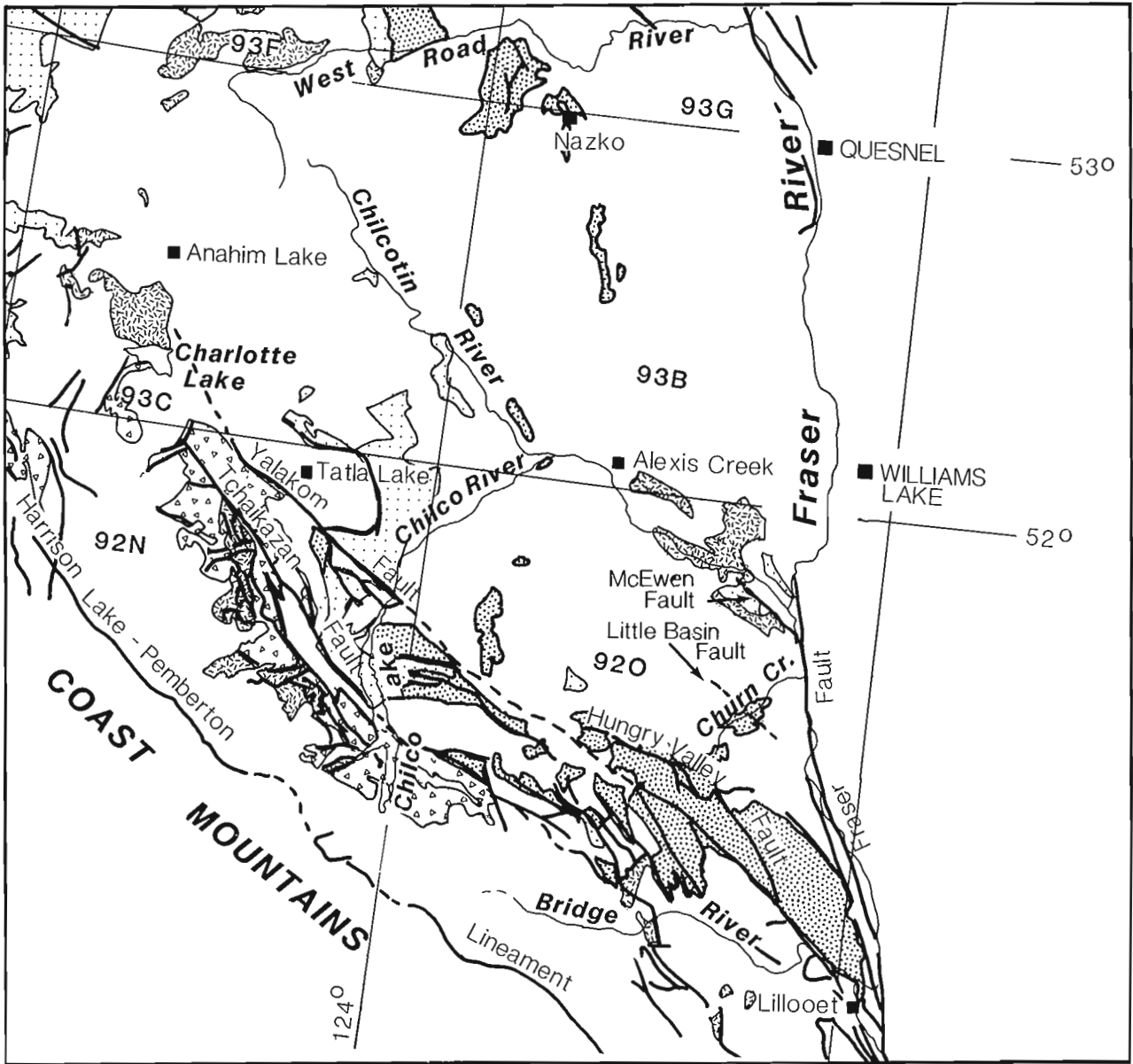
The Silverquick conglomerate is exposed in steep cliffs along the western side of Churn Creek, approximately 25 km southeast of Gang Ranch (Fig. 1, 2). It is extensively exposed in fault panels in the Warner Pass (92O/3) and Noaxe Creek (92O/2) map areas south and west of the study area (Glover et al., 1987, 1988b). The exposures along Churn Creek represent the northernmost extent of the currently recognized Silverquick conglomerate. Coeval conglomerates are sporadically exposed to the north, where they are tentatively assigned to the Skeena Group.

Stratigraphy of Silverquick conglomerate on Churn Creek

Two well-exposed sections of Silverquick conglomerate west of Churn Creek, totalling about 1100 m of strata, were examined during the 1991 field season (Fig. 2, 3). The northern section (section A, Fig. 3) contains the lower 600 m of strata, and consists of green lithic arenite, chert-pebble conglomerate, volcanic cobble to boulder conglomerate, and massive volcanic breccia. This section was measured in 1990, and was re-examined in 1991 (Hickson et al., 1991). The southern section (section B, Fig. 3) comprises the upper 600 m of strata, and primarily consists of cobble to boulder volcanic conglomerate with up to ~20% plutonic clasts, and lesser amounts of massive volcanic breccia, arkosic lithic arenite, and purple siltstone (Fig. 3). The two sections are correlated via a massive volcanic breccia (100+ m) exposed at the top of section A that thins to the south, where it occurs as a 30+ m thick breccia in the lower third of section B (Fig. 3).

The base of the Silverquick conglomerate in Churn Creek occurs in the core of an anticline, where amygdaloidal, extensively fractured brown to green andesitic lava is interpreted to unconformably underlie the basal sandstone and conglomerate of the Silverquick conglomerate (Rouse et al., 1990; Hickson et al., 1991) (Fig. 3). Pervasive alteration in the andesite prevents radiometric dating, but field evidence, including stratigraphic position and the amygdaloidal, zeolite-rich character of the volcanic rock suggests the unit correlates with Lower Cretaceous volcanic rocks to the southeast (Fig. 1).

The Silverquick conglomerate in the Churn Creek area may be subdivided into 3 distinct units based on clast composition and, to a lesser extent, grain size: 1) a lower unit containing coarse sand to pebble chert-rich sediments; 2) a middle unit containing cobble to boulder volcanic clast conglomerate and coarse interbedded arkosic lithic sandstone; and 3) an upper unit containing cobble to boulder volcanic clast conglomerate with a significant proportion of pink quartz monzonite clasts. Each unit of the Silverquick conglomerate in this area is characterized by rapid lateral and vertical facies changes; the following thicknesses and stratigraphic descriptions are approximate.



L E G E N D



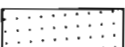


-  Cretaceous
-  Upper Jurassic - Lower Cretaceous
-  Lower and Middle Jurassic
-  Upper Paleozoic and Triassic
-  Fault and tectonic lineaments

Figure 1. Simplified regional geologic map of Chilcotin-Nechako area, showing major structures and the distribution of Mesozoic units.

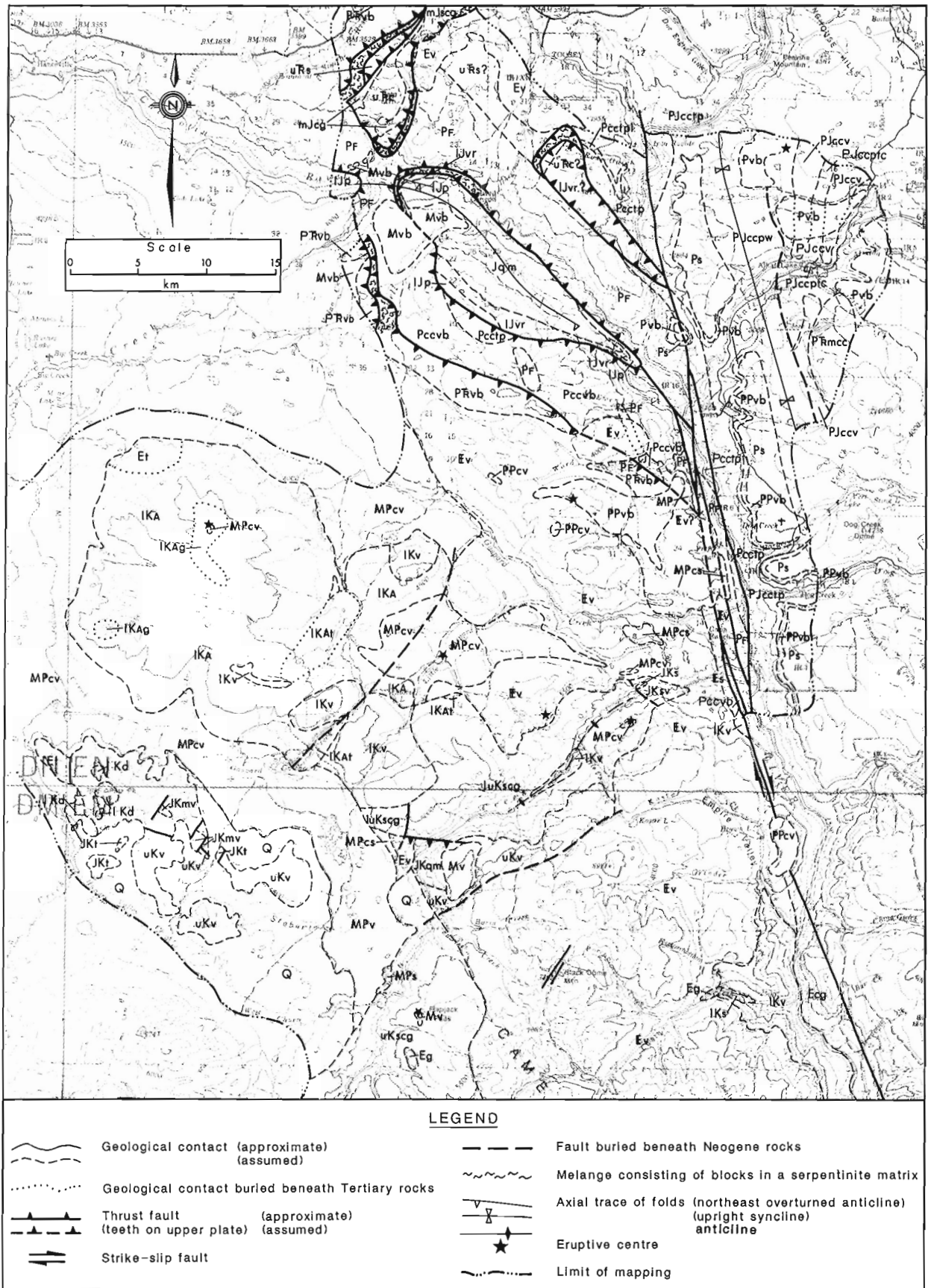


Figure 2. Simplified geologic map of the eastern third of the Taseko Lakes map area, showing location of measured stratigraphic sections. (Modified from Hickson, 1992: Fig. 2).

Lower unit

The lower unit of the Silverquick conglomerate in Churn Creek is approximately 315 m thick, and consists of thin- to thick-bedded sandstone interbedded with medium bedded to massive, matrix- to clast-supported, chert pebble conglomerate. The sandstone is well sorted, very coarse- to fine-grained chert-rich lithic arenite, pebbly in part, with poorly developed parallel laminae, graded bedding, and rare planar or trough crossbeds. The sandstone locally displays 10-15 cm thick fining upward sequences that grade upward from very coarse sand to pebbles at the base into fine- to medium-grained sandstone. The fine grained sandstone is locally micaceous (muscovite) and rich in organic matter. Pebbly channels, from 2-6 m wide and 0.2-0.7 m deep are interspersed within 5-20 m sandstone sequences. Tabular, 0.5-5 m thick chert pebble conglomerate beds composed of varicoloured angular to subrounded, fine to coarse pebble chert clasts with minor volcanic and rare granitic clasts are

interbedded with the sandstone. The conglomerate varies from clast- to matrix-supported, with a matrix of well sorted coarse- to very coarse-grained chert lithic arenite. Conglomerate beds appear tabular and laterally continuous, but locally display well-developed channels. The conglomerate locally contains repetitive 10-15 cm thick fining upward cycles that grade from a pebble rich base into crudely laminated coarse grained sandstone. Crude parallel laminae and rare trough crossbeds occur in the upper portions of channels and fining upward sequences. The lower unit is gradationally overlain by the middle unit across an approximately 40 m thick transition zone.

Middle unit

The middle unit is about 500-600 m thick, and is dominated by clast-supported volcanic conglomerate, with lesser amounts of arkosic lithic sandstone, purple siltstone, and

LEGEND

CENOZOIC		JKmv	Greenschist and amphibolite facies, felsic to mafic metavolcanic schist and gneiss
Quaternary and Tertiary		Jurassic	
Pliocene and Pleistocene		Middle to Upper Jurassic	
CHILCOTIN GROUP (PPcv to MPcs)		mJcg	South of Bald Mountain: Red sparsely plagioclase-phyric volcanic conglomerate overlying nonbedded quartz-bearing feldspathic sandstone
PPcv	Grey olivine and/or plagioclase-phyric basalt flows; locally basal palagonite tuff and pillow breccia	mJscg	North of Bald Mountain: Interbedded grey-green volcanic chip conglomerate and nonbedded quartz-bearing feldspathic sandstone
Tertiary		Jqm	Chloritized leucoquartz monzonite, leucoquartz diorite; rare metagabbro. Hypabyssal dacite and felsite intrusions occur marginally
Miocene to Pleistocene		Lower Jurassic	
MPcv	Grey olivine- and/or plagioclase-phyric subaerial basalt flows; minor interflow breccia	IJp	Grey noncalcareous siltstone with thin sandstone laminae; minor thin limestone
Miocene and(?) Pliocene		IJvr	Grey-green and locally maroon porphyritic (plagioclase, quartz) dacite and rhyolite flows and tuffs, felsite- and quartz-feldspar porphyry-bearing tuff; minor green metabasalt flows
MPcs	Unconsolidated fluvial sediments; minor rhyolite ash and diatomaceous earth	Triassic	
Eocene		Middle to Upper Triassic	
Es	Conglomerate, sandstone; minor siltstone and bentonitic shale; rare coal	uRs	Grey to nonlimy siltstone and minor interbedded thin calcareous sandstone
Ev	Hornblende-plagioclase-phyric dacite and hornblende-biotite-quartz-phyric rhyolite flows; minor basalt, andesite, pyroclastic flows and ash; rare sediments	uRc	Nonbedded light to medium grey micritic limestone
Et	Biotite-muscovite tonalite	PALEOZOIC	
Eg	felsic intrusive	Permian	
MESOZOIC		Late Permian	
Cretaceous		FARWELL PLUTON	
upper Lower Cretaceous and Upper Cretaceous		Chloritized and locally foliated metadiorite; minor quartz metadiorite and metagranodiorite	
uKv	Powell Creek volcanics(?) Maroon to brown intermediate to felsic flows, tuffs and breccia; minor sediments	Permian to Jurassic	
luKscg	Silverquick formation (luKscg to luKs) Maroon volcanic conglomerate; minor sandstone	Lower Permian to Middle(?) Jurassic	
luKs	Green to buff chert pebble conglomerate, green to maroon sandstone; minor siltstone	CACHE CREEK COMPLEX (PJccpw to Pccvb)	
Lower Cretaceous		Western Belt: Grey siltstone, shale; minor grey lithic wacke	
lKv	Maroon to green sparsely feldspar-phyric andesite (?) flows, breccia; minor welded rhyolite ash flows	PJccv	
MOUNT ALEX PLUTONIC COMPLEX (lKAg to lKA)		Western Belt: Meta-andesite and metabasalt breccia and flows	
lKAg	Hornblende monzogranite and granodiorite	PJcctpc	
lKAi	Chloritized hornblende leucotonalite	Western Belt: Tectonic(?) lenses of greenstone, limestone and chert in a grey phyllite matrix	
lKA	Weakly to strongly foliated, chloritized hornblende quartz monzo-diorite, quartz diorite and diorite	Marble Canyon Formation	
Piltz Peak diorite		Grey unbedded micritic limestone	
lKd	Heterogeneous, weakly to strongly foliated, chloritized hornblende diorite	Permian to Triassic	
lKvo	Amygdaloidal plagioclase-phyric andesite(?) flows; minor pyroclastic rocks	P Rvb	
Jurassic and/or Cretaceous		Green and grey-green aphanitic basic metatuff and minor flows	
Lower Jurassic to Lower Cretaceous		Permian and(?) older	
JKsv	Plagioclase-phyric andesite(?) flows; green sandstone and minor siltstone	Lower Permian and(?) older	
JKs	Argillaceous, well lithified dark grey siltstone	Pcctp	
Piltz Peak and Mount Wales tonalites		Grey, grey-green and minor light green chert, ribbon chert and phyllite	
JKt	Weakly to strongly foliated tonalite, chloritized hornblende biotite tonalite and biotite hornblende tonalite	Pcctpl	
		Light grey unbedded limestone	
		Pccvb	
		Grey-green and green greenstone	

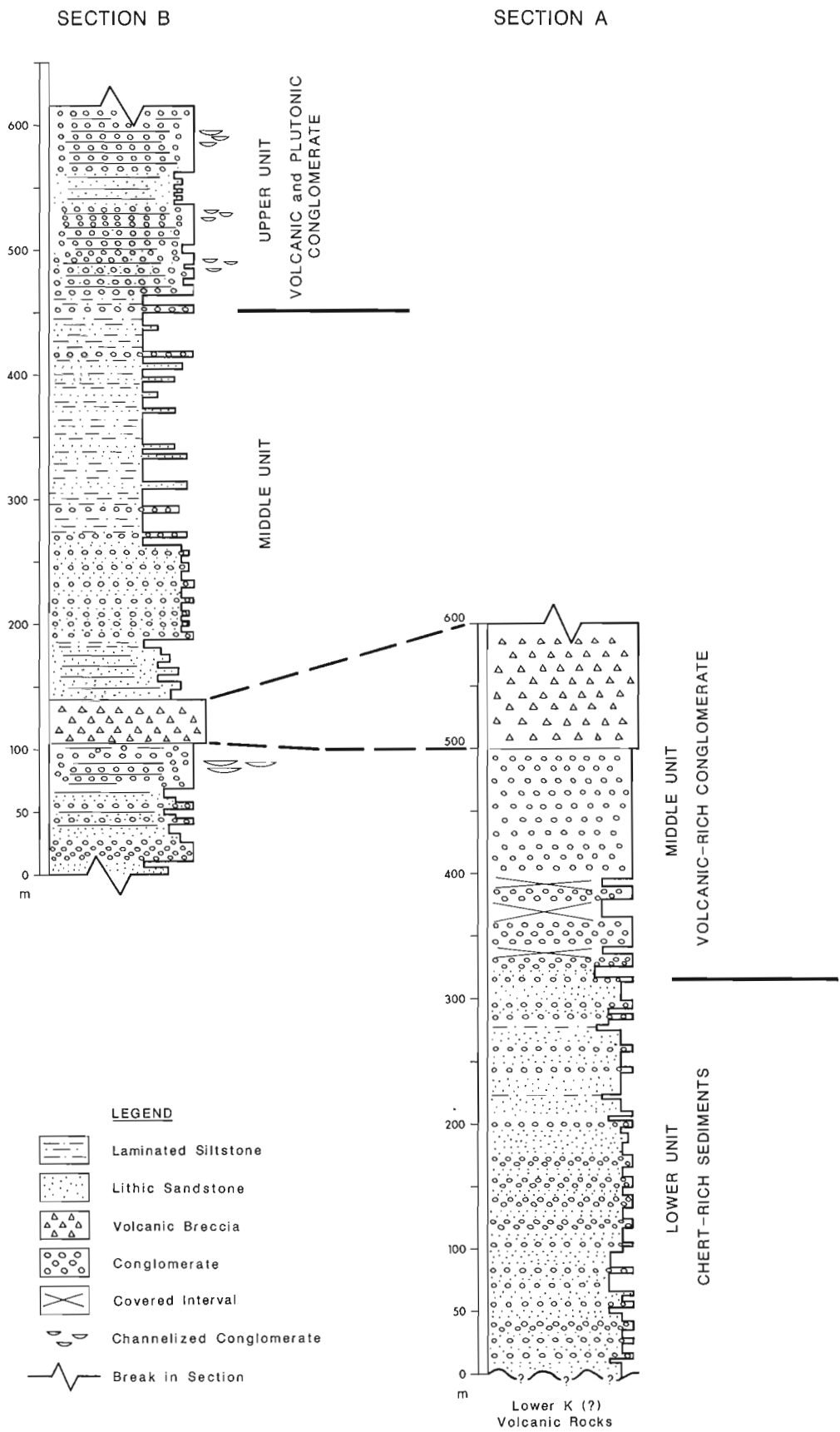


Figure 3. Measured stratigraphic sections of the Silverquick conglomerate on Churn Creek. Section locations shown on Figure 2.

massive volcanic breccia (Fig. 3). Although lateral facies changes are common, the exposures in Churn Creek suggest the middle unit generally fines upward, from massive conglomerate at the base, to interbedded purple siltstone with sandstone/conglomerate channels at the top.

The conglomerate ranges from thick bedded to massive, and is a crudely stratified, poorly sorted, volcanic cobble to boulder conglomerate containing rounded to subangular andesite, dacite, flow-banded dacite and rhyolite, and rare granitoid clasts together with subrounded to rounded pebble-sized chert clasts. The percentage of chert pebbles in any conglomerate bed appears to be inversely proportional to the size of the volcanic clasts within the bed, but nowhere exceeds about 20%. Granitoid clasts are rare, but increase in abundance upsection, and indicate a gradational contact between the middle and upper units. The volcanic clasts locally display a preferred long axis alignment subparallel to bedding. Conglomerate beds vary from tabular and laterally continuous to lenticular with well-developed channels that grade laterally into medium- to thick-bedded, coarse grained lithic sandstone. Nested channel sets are locally evident. Fining and thinning upward sequences 15-20 m thick are common, and consist of thickly bedded to massive conglomerate that grade upward into crudely laminated coarse lithic sandstone with pebble stringers, which in turn grade upward into thin- to medium-bedded, medium grained sandstone and minor siltstone. Lenticular matrix supported volcanic clast conglomerate occurs locally, and consists of subangular to subrounded volcanic clasts in a dark grey, poorly sorted coarse siltstone to sandstone matrix. The volcanic clast conglomerate decreases in grain size, increases in chert pebble content, and contains a higher number of sandstone interbeds to the south.

Massive volcanic breccia forms an important marker bed in the strata along Churn Creek. Section A contains a 100+ m thick breccia composed of angular to subangular boulders of purple to green dacite in a dark grey, fine grained matrix. The breccia is interpreted as a lahar, based on its massive, unsorted character, the homogeneity of the volcanic clasts, and the absence of sedimentary structures (Rouse et al., 1990). This unit thins rapidly to the south, and occurs as a 30+ m thick massive volcanic breccia near the base of section B (Fig. 3).

Medium- to very coarse-grained arkosic lithic arenite is interbedded with volcanic clast conglomerate and locally dominates the stratigraphy of the middle unit. The thin- to medium-bedded lithic arenite is primarily tabular and laterally continuous, and displays erosive basal contacts, weak parallel and crosslaminae, graded bedding, and pebble stringers. Pebble to cobble conglomerate channels are evident in part, and pebble stringers locally define trough crossbeds. The lithic arenite displays both fining and thinning upward and coarsening and thickening upward sequences. Sandstone beds (5-20 m thick) are locally repetitively interbedded with conglomerate beds (0.5-5 m thick).

Sandstone/conglomerate sequences locally grade upward into 1-20 m thick purple siltstone intervals (Fig. 3, section B). The purple siltstone is parallel laminated, fine- to

coarse-grained, and contains matrix-supported fine pebbles in part. The siltstone weathers recessively, and forms reddish-purple slopes between resistant sandstone and conglomerate interbeds. Well developed, lenticular channels (1-10 m wide) of coarse sandstone and conglomerate are interspersed within thick siltstone intervals. Purple siltstone-dominated intervals grade laterally into sandstone and conglomerate intervals over less than 50 m.

Upper unit

The middle unit of the Silverquick conglomerate along Churn Creek is conformably overlain by the upper unit. In section B (Fig. 3), the contact is marked by a rapid transition from purple siltstone and lenticular sandstone into thick bedded to massive volcanic and plutonic clast conglomerate, and appears abrupt. However, the presence of pink quartz monzonite clasts, characteristic of the upper unit below the contact suggests the contact is gradational. The minimum thickness of the upper unit is 175 m. The upper contact of the Silverquick conglomerate in this area is the modern erosion surface. The plutonic and volcanic-rich conglomerate of the upper unit is not documented to the south (Glover et al., 1988a). This upper conglomerate may represent the highest stratigraphic level preserved in the Silverquick conglomerate in the region, or may be the result of a local intrabasinal influx of plutonic debris.

The upper unit of the Silverquick conglomerate is dominated by volcanogenic cobble to boulder volcanogenic conglomerate with a significant percentage (up to ~30%) of angular to subangular pink quartz monzonite clasts. The conglomerate is primarily clast-supported, and contains clasts of subangular to subrounded, pebble- to boulder-sized andesite and dacite, pebble-sized varicoloured chert, and cobble- to boulder-sized angular to subangular pink quartz monzonite clasts. The distinctive pink quartz monzonite clasts increase in size both upsection and laterally to the south. The conglomerate is highly lenticular, and contains abundant, locally overlapping, channels that are 3-5 m thick and 15-20 m wide. Channels aggregate into roughly tabular, laterally continuous beds. Channels have sharp, erosive bases, contain clast-supported boulder conglomerate at the base, and grade upward into matrix supported conglomerate and crudely laminated and crossbedded, coarse grained lithic sandstone with abundant pebble stringers. Parallel laminated, thin- to medium-bedded, fine- to medium-grained lithic sandstone and reddish-brown coarse siltstone locally cap channelized intervals. Parallel laminated, fine grained sandstone and coarse siltstone locally aggregate to 2-10 m thick intervals (Fig. 3). Lenticular, matrix supported conglomerate, with a matrix of coarse lithic sandstone, is common within this unit.

Age

Palynomorphs collected during the 1990 field season from a siltstone within the lower unit of the Silverquick conglomerate yielded a late Albian-early Cenomanian assemblage (Hickson et al., 1991). This age is in agreement with the post-mid-Albian, pre-Santonian age imposed by

stratigraphic constraints to the south (Garver, 1989) (Fig. 4). Several palynomorph samples collected from the upper portion of the middle unit during the 1991 field season have been submitted for analysis.

Depositional environment

Strata of the Silverquick conglomerate exposed along Churn Creek record fluvial deposition in a rapidly subsiding depocenter. Crude parallel and cross-stratification, poor sorting, weak clast imbrication, normal grading, rapid lateral facies changes, pebble lag deposits, and the ubiquitous presence of channels indicate deposition in a braided fluvial system. While the depositional environment of all three units is similar, the lithologic variation among units records important changes in provenance and basin margin tectonism during late Albian to Cenomanian time.

The lower unit of the Silverquick conglomerate is dominated by well-sorted, chert-rich sandstone and pebble conglomerate. Although the lower unit is believed to unconformably overlie Lower Cretaceous volcanic rocks, volcanic detritus is notably absent. Crossbeds from a 2 m thick interval in the upper portion of the lower unit indicate a south-southwest directed paleocurrent, but may not be representative of the entire unit (Hickson et al., 1991). The Cache Creek terrane, exposed to the northeast, represents the probable source terrane for chert in this portion of the section. Garver (1989) suggests the Bridge River terrane, which forms the present day eastern margin of the Silverquick conglomerate to the south, is the primary source of chert detritus in the south. The specific source for the chert in the lower unit remains problematic, and requires additional study.

The transition from chert-dominated lithofacies to volcanic-dominated lithofacies at the boundary between the lower and middle unit marks an important change in source area and basin dynamics. The well-sorted, well bedded sandstone and pebble conglomerate of the lower unit are overlain by thickly bedded to massive cobble to boulder volcanic clast conglomerate and poorly sorted, coarse grained lithic sandstones of the middle unit. The dramatic increase in grain size, decrease in sorting, and the lack of stratification evident in the middle unit suggests rapid deposition proximal to a major volcanic source. The presence of 100+ m thick massive lahar supports proximal active volcanism. We suggest that the contact of the lower and middle units records the onset of volcanism in adjacent areas. Near Mt. Alex, approximately 10 km to the northeast, radiometric dating has identified an Albian (106 Ma) dacite lava and granodiorite pluton (Hickson, 1992). These dates are equivalent to radiometric and palynological ages within the Spences Bridge Group and to palynomorph ages from the Silverquick conglomerate (Thorkelson and Rouse, 1989) (Fig. 4). Although precise age control is lacking, the coeval Spences Bridge Group, exposed to the east and south, is the most likely source for much of the detritus in the middle unit.

The dramatic increase in plutonic debris and grain size at the contact of the middle and upper units suggests an important change in basin margin tectonism. The upper

unit coarsens upward, and contains a significant proportion of boulder-sized angular pink quartz monzonite clasts that increase in size and abundance both upsection and to the south. The upper unit contains abundant channels and lenticular, poorly sorted coarse sandstone, as well as pebbly purple siltstone interpreted to be overbank or interchannel

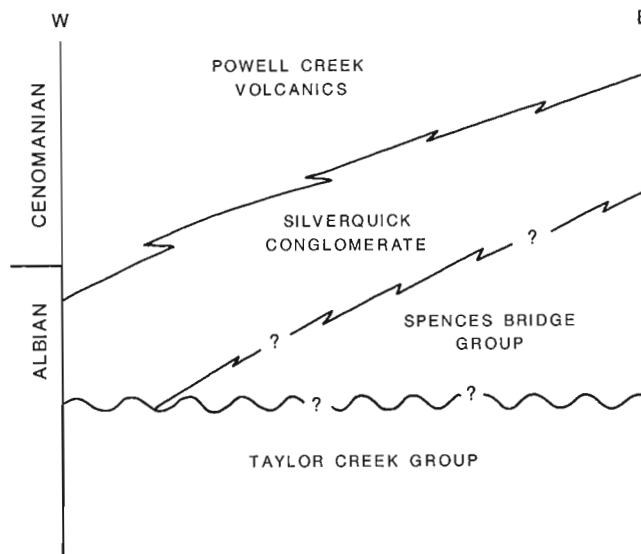


Figure 4. Regional stratigraphic correlation chart of Albian-Cenomanian strata. Data from Garver (1989), Thorkelson and Rouse (1989), and Hickson et al. (1991).

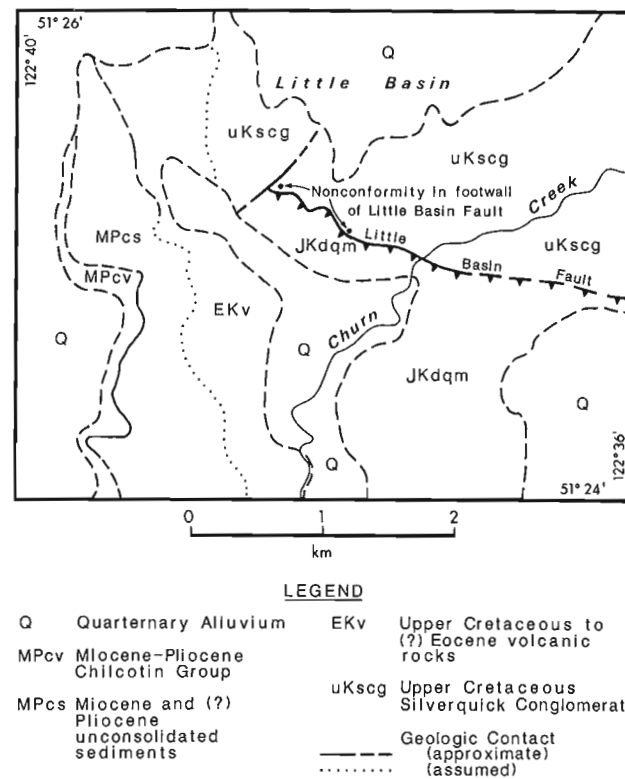


Figure 5. Simplified geologic map (1:250 000) of the Churn Creek area near the Little Basin Fault.

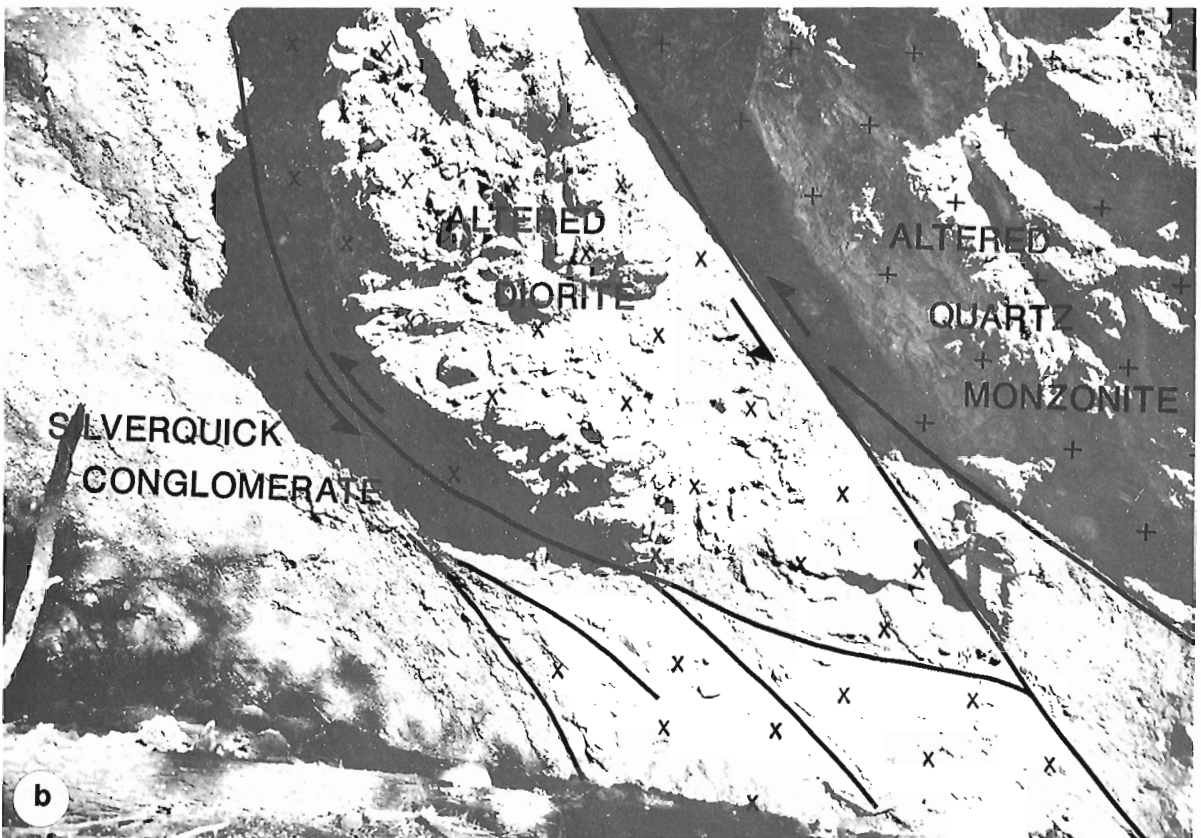
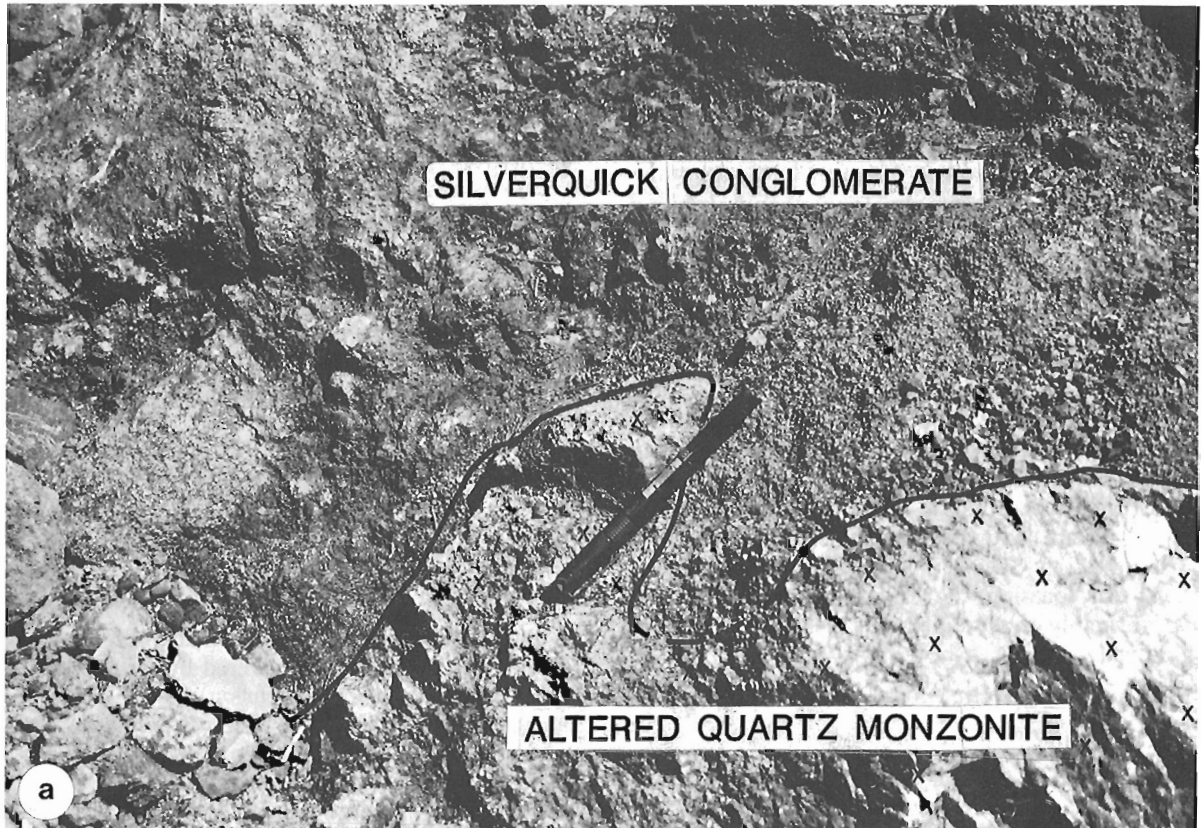


Figure 6. a) Photograph of nonconformity between upper unit of the Silverquick conglomerate and the underlying pink quartz monzonite. Note grussy character of altered quartz monzonite. b) Photograph of Little Basin Fault and associated structures.

deposits in a braided fluvial system. The abundance of coarse grained detritus, angular plutonic boulders that increase in size and abundance both vertically and laterally, and the apparent wedge shaped geometry suggest the upper unit may represent an alluvial fan facies adjacent to a proximal highland. This interpretation is supported by structural analyses to the south of the measured sections (Fig. 2, 4).

LITTLE BASIN FAULT

Previous mapping by Tipper (1978) documented Upper Cretaceous quartz monzonite in contact with Upper Cretaceous sedimentary rocks along Churn Creek. The relationship between these plutonic and sedimentary units was unknown; the contact is now known to be an important southwest dipping reverse fault, referred to as the Little Basin Fault (Fig. 2, 5). Plutonic rocks of unknown age in the hanging wall are juxtaposed against sediments of the Albian-Cenomanian Silverquick conglomerate in the footwall. At this location, the Silverquick conglomerate lies nonconformably on plutonic rocks identical to those in the hanging wall.

Stratigraphic relations

The nonconformable relation between the Silverquick conglomerate and underlying plutonic rocks in the footwall of the Little Basin Fault was observed in two places (Fig. 5). At the eastern location, the Little Basin Fault juxtaposes relatively unaltered quartz monzonite in the hanging wall against extremely altered quartz monzonite in the footwall. The latter grades upward into a zone of red stained quartz monzonite and red, friable material believed to be altered regolith. An irregular but sharp lithologic break marks the depositional contact with the nonconformably overlying conglomerate (Fig. 6a). At the western location, the conglomerate appears to fill small erosional depressions in altered hornblende diorite, but relations here are not definitive due to disruption by a northeast-trending normal fault.

Adjacent to the fault, the Silverquick conglomerate is characterized by extremely coarse, clast supported volcanic and granitic boulder conglomerate. The granitoid component in these sediments was undoubtedly derived from the plutonic rocks adjacent to the Little Basin Fault. A rapid northeasterly decrease in granitoid clast size and abundance away from the fault strongly suggests active faulting during deposition. The Little Basin Fault may have formed a northeast-facing fault scarp from which plutonic and volcanic detritus was shed into the adjacent Silverquick depocenter.

Plutonic rocks

The pluton exposed along Churn Creek is composed of varying proportions of medium grained, biotite hornblende diorite and medium- to locally coarse-grained, pink quartz monzonite. Quartz monzonite stringers locally intrude the diorite, providing a measure of relative age. Absolute ages for the plutonic rocks are presently unknown, but they must

be older than the nonconformably overlying Albian-Cenomanian Silverquick conglomerate. Uranium-lead geochronometry is in progress.

The plutonic rocks are commonly strongly altered, and are extensively fractured and veined by quartz, calcite, and zeolites. Moderately southwest dipping brittle shears, characterized by anastomosing networks of slickensided surfaces, are very common within both rock types. Shear planes also define most contacts between strongly shattered diorite and quartz monzonite. Cataclastic fabrics were observed locally near some shear planes. Relatively non-fractured and unaltered diorite and quartz monzonite is preserved in lozenge-shaped lenses between shear networks.

Little Basin Fault and associated structures

The Little Basin Fault is a discrete, moderately southwest dipping, reverse fault which juxtaposes plutonic rocks in the hanging wall against Silverquick conglomerate in the foot wall (Fig. 6b). About 1.5 km west of Churn Creek, the fault is cut by a younger, northeast-trending normal fault; east of Churn Creek, the fault is covered by Quaternary alluvium (Fig. 5). A northwesterly extension of the fault may be present along Gaspard Creek, about 9 km northwest of Churn Creek, where altered diorite similar to that along Churn Creek is juxtaposed against volcanic rocks of the Lower Cretaceous Spences Bridge Group (Fig. 2). The contact between plutonic and volcanic rocks is not exposed along Gaspard Creek, but southwest dipping brittle shears similar to those along Churn Creek (described below) are common in both units.

The Little Basin Fault cuts up-section through strata of the Silverquick conglomerate, from an observed location within the pluton upward through the nonconformity. Fault attitudes relative to bedding in the conglomerate indicate that the fault cuts up-section at an overall moderate angle of 40-50°. Locally the angle is less, and in several places relations are obscured by folding of the Silverquick conglomerate, which appears to have preceded initial movement on the fault. Crosscutting shear sets indicate at least two periods of movement along the fault. Associated shears within the conglomerate cut through boulders, indicating that the conglomerate was well lithified by the time of the latest fault movement.

Some degree of structural interleaving took place along the Little Basin Fault, however, the transition from pluton to conglomerate across the fault is generally abrupt. Southwest dipping shears associated with and subparallel to the Little Basin Fault are ubiquitous both in the pluton and in the conglomerate. Asymmetry of lenticular domains enclosed by these shear planes suggests reverse motion on the fault. This is confirmed by the orientation of downdip fault striae and grooves, attitudes of associated slickenside steps, and the relative positions of plutonic rocks in the footwall and hanging wall of the Little Basin Fault. Total throw on the fault is unknown as the Silverquick conglomerate is not exposed in the hanging wall.

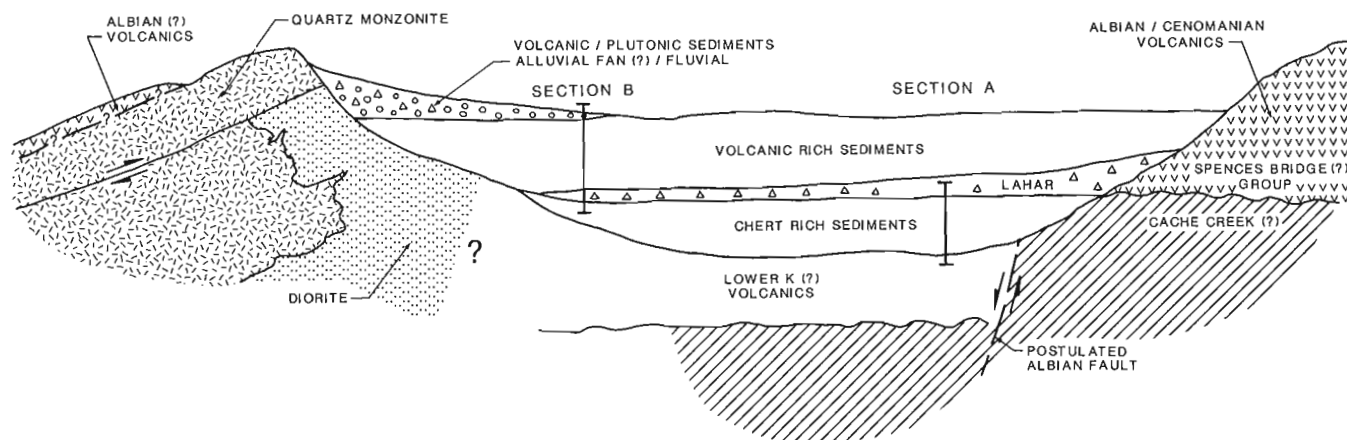


Figure 7. Schematic diagram of Silverquick depositional basin during the Cenomanian.

There is some evidence for structural imbrication of the Silverquick conglomerate northwest of the northeast-trending normal fault shown on Figure 5. Several southwest dipping, bedding parallel faults, associated with apparent repetitions of stratigraphy, were observed in the Silverquick conglomerate in this area. Stratigraphic and structural relations, however, are complicated by folding and north to northeast trending normal faults. The tentative conclusion reached here is that the Little Basin Fault may be one of several reverse faults in a northeast directed imbricate sequence.

CONCLUSIONS

The stratigraphy of the Silverquick conglomerate along Churn Creek provides evidence for important regional tectonic events during late Albian to early Cenomanian time. Chert pebble conglomerate in the lower unit requires a chert-rich source area to the northeast, possibly the Cache Creek terrane, during the late Albian to early Cenomanian. Volcanic clast conglomerate and associated debris flows in the middle unit record the onset of volcanism in adjacent areas, most likely associated with the coeval Spences Bridge Group (Thorkelson and Rouse, 1989). This influx of volcanic material apparently flooded the depocenter, overwhelming northerly derived chert-rich sediment (Fig. 7).

Angular plutonic debris and crudely stratified volcanic clast conglomerates of the upper unit suggest proximity to a plutonic and volcanogenic source terrane by Cenomanian(?) time (Fig. 7). Structural analysis of excellent exposures of a moderately southwest dipping reverse fault documents uplift of plutonic rocks adjacent to the Silverquick depocenter. Uplifted plutonic rocks in the hanging wall supplied abundant coarse grained material to the upper unit of the Silverquick conglomerate in the Churn Creek area, indicating that contractional tectonics controlled sedimentation in the Silverquick depocenter during this time (Fig. 7). Further

work is needed to determine the extent of structural control on Silverquick sedimentation throughout the region. Stratigraphic and structural evidence supports northeast vergent thrust faulting in the Churn Creek area during the Cenomanian(?), which agrees with the regional contractional model proposed by Rusmore and Woodsworth (1991).

REFERENCES

- Garver, J.I.
1989: Basin evolution and source terranes of Albian-Cenomanian rocks in the Tyaughton basin, southern British Columbia: implications for mid-Cretaceous tectonics in the Canadian Cordillera; Ph.D. thesis, University of Washington, Seattle, 227 p.
- Garver, J.I., Schiarizza, P., and Gava, R.G.
1989: Stratigraphy and structure of the Eldorado Mountain area, Chilcotin Ranges, southwestern British Columbia (92O/2; 92J/15); in Geological Fieldwork 1988, British Columbia Ministry of Energy, Mines and Petroleum Resources, Paper 1989-1, p. 131-143.
- Glover, J.K., Schiarizza, P., Umhoefer, P., and Garver, J.I.
1987: Geology of the Warner Pass map area (92O/3); British Columbia Ministry of Energy, Mines and Petroleum Resources, Open-File Map 1987-3A, scale 1:50 000.
- Glover, J.K., Schiarizza, P., and Garver, J.I.
1988a: Geology of the Noaxe Creek map area (92O/2); in Geological Fieldwork 1987, British Columbia Ministry of Energy, Mines and Petroleum Resources, Paper 1988-1, p. 105-123.
- Glover, J.K., Schiarizza, P., Garver, J.I., and Umhoefer, P.
1988b: Geology of the Noaxe Creek map area (92O/2); British Columbia Ministry of Energy, Mines and Petroleum Resources, Open-File Map 1988-3, scale 1:50 000.
- Hickson, C.J.
1990: A new Frontier Geoscience Project: Chilcotin-Nechako region, central British Columbia; in Current Research, Part F; Geological Survey of Canada, Paper 90-1F, p. 115-120.
- 1992: An update on the Chilcotin-Nechako Project and mapping in the Taseko Lakes (92O) area, west-central British Columbia; in Current Research, Part A; Geological Survey of Canada, Paper 92-1A.
- Hickson, C.J., Read, P., Mathews, W.H., Hunt, J.A., Johansson, G., and Rouse, G.E.
1991: Revised geological mapping of northeastern Taseko Lakes map area, British Columbia; in Current Research, Part A; Geological Survey of Canada, Paper 91-A, p. 207-217.

Rouse, G.E., Mathews, W.H., and Lesack, K.A.

1990: A palynological and geochronological investigation of Mesozoic and Cenozoic rocks in the Chilcotin-Nechako region of central British Columbia; in Current Research, Part F; Geological Survey of Canada, Paper 90-1F, p. 129-133.

Rusmore, M.E. and Woodsworth, G.J.

1991: Coast Plutonic Complex: a mid-Cretaceous contractional orogen; *Geology*, v. 19, no. 9, p. 941-944.

Tipper, H.W.

1978: Taseko Lakes (920) map area; Geological Survey of Canada, Open File 534.

Thorkelson, D.J. and Rouse, G.E.

1989: Revised stratigraphic nomenclature and age determinations for mid-Cretaceous volcanic rocks in southwestern British Columbia; *Canadian Journal of Earth Sciences*, v. 26, no. 10, p. 2016-2031.

U-Pb age of the Mt. Mason Pluton in the Cairn Needle area, southern Coast Belt, British Columbia

Richard M. Friedman¹, Thornton M. Tyson², and J.M. Journeay
Cordilleran Division, Vancouver

Friedman, R.M., Tyson, T.M., and Journeay, J.M., 1992: U-Pb age of the Mt. Mason Pluton in the Cairn Needle area, southern Coast Belt, British Columbia; in Current Research, Part A; Geological Survey of Canada, Paper 92-1A, p. 261-266.

Abstract

A U-Pb date of 91.5 ± 2 Ma has been determined for a tonalite from the eastern portion of the Mt. Mason Pluton, in the Cairn Needle area of the southern Coast Belt. This intrusion truncates the Butter Creek Fault, and therefore postdates significant ductile deformation in the area. The date provides a minimum age for shortening along this segment of the Coast Belt-Northwest Cascades Thrust system. The 96 Ma Breakenridge Gneiss was affected by most or all of the deformation within this fault zone, allowing a short time window of about 5 Ma (91-96 Ma) during which this structural zone was active.

Résumé

Une tonalite de la partie orientale du pluton de Mt. Mason, dans la région de Cairn Needle du Domaine côtier méridional a été datée par la méthode U-Pb à $91,5 \pm 2$ Ma. Cette intrusion tronque la faille du ruisseau Butter; elle est donc postérieure à l'importante déformation ductile qui a affecté la région. Cette datation permet d'établir un âge minimal pour le raccourcissement observé le long de ce segment du système de chevauchement du Domaine côtier et de la zone de Northwest Cascades. Le gneiss de Breakenridge de 96 Ma a été affecté par une grande partie sinon par toute la déformation de cette zone faillée, ouvrant une fenêtre d'environ 5 Ma (91-96 Ma) pendant laquelle cette structure était active.

¹ Department of Geological Sciences, University of British Columbia, 6339 Stores Road, Vancouver, B.C. V6T 1Z4

² Department of Geological Sciences, AJ-20, University of Washington, Seattle, Washington, U.S.A. 98165

INTRODUCTION

For several decades the core of the Coast Belt, to the east and north of Harrison Lake, southwestern British Columbia (Fig. 1), has been recognized as an area with a complex history of shortening, amphibolite grade metamorphism, and intrusion of Coast Plutonic Complex granitoid rocks (Roddick, 1965). Detailed mapping studies have begun to unravel the structural and metamorphic history of this area (Journey and Csontos, 1989; Journey, 1990; Tyson, 1990). They serve to underline the close temporal and spatial relationship of mid- to Late Cretaceous plutonism with deformation and metamorphism (Journey and Friedman, in press). These plutonic rocks provide an important opportunity to precisely determine the time of deformation in the southern Coast Belt. In this study we report a U-Pb date

for the eastern portion of the Mt. Mason Pluton, which was intruded at the end of ductile deformation in the southern Coast Belt. This date provides a minimum age for shortening in the Cairn Needle area.

GEOLOGY

The Cairn Needle area is located in the southern Coast Belt of southwestern British Columbia, within the Coast Belt-Northwest Cascades Thrust zone, a major west-vergent contractional system (Fig. 1; Journey 1990). The following sections briefly describe the geology of the Cairn Needle area, (Fig. 2), focusing on the nature and relative timing of intrusion of the Mt. Mason Pluton. These findings are taken from a detailed study of the area by Tyson (1990, 1991).

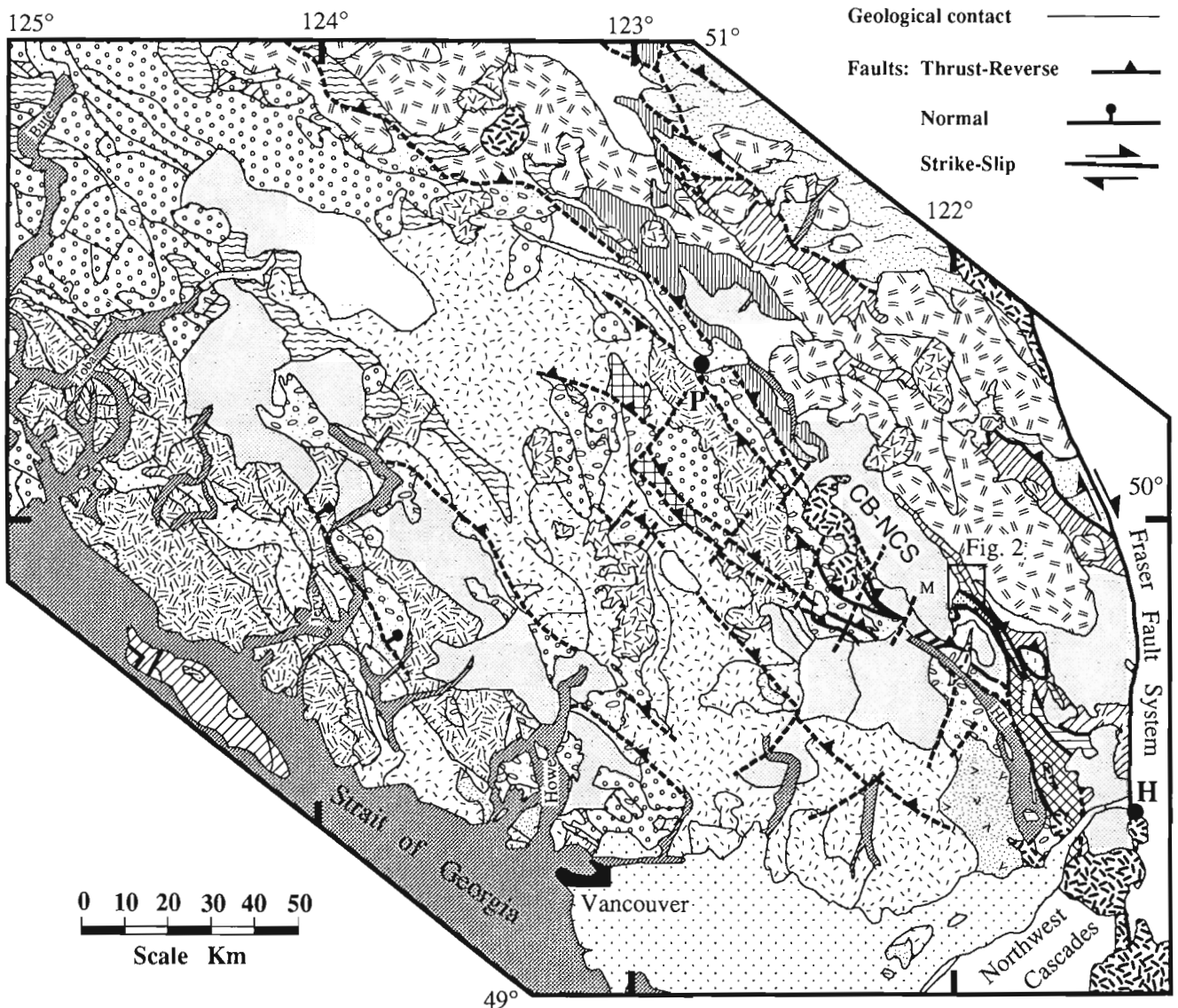


Figure 1. Geological map of the southern Coast Belt, southwestern British Columbia. An outline surrounds the Cairn Needle area depicted in Figure 2. M: Mt. Mason Pluton; CB-NCS: Coast Belt-Northwest Cascades System; HL: Harrison Lake; P: Pemberton; H: Hope. Sources for this compilation map are: Roddick and Hutchison (1973), Woodsworth (1977), Roddick and Woodsworth (1977, 1979), Monger (1989), and Journey (1990).

Plutonic rocks

Four plutonic units are exposed in the Cairn Needle area (Fig. 2), the oldest of which is the 96 Ma Breakenridge Gneiss (U-Pb date by R.R. Parrish, cited in Monger, 1990), a leucocratic orthogneiss body that has participated in all phases of regional deformation. An undated and unnamed foliated granodioritic sill is correlated with the mid-Cretaceous syntectonic Spuzzum Pluton (ca. 95 Ma,

U-Pb, Walker and Brown, 1990), located southeast of the study area (Fig. 1). The next youngest unit is the Mt. Mason Pluton, dated in this study and discussed below. The youngest is the 84 Ma Scuzzy Pluton (U-Pb date by R.R. Parrish, cited in Monger, 1990), a nonfoliated biotite granodiorite body that postdates ductile deformation in the southern Coast Belt.

Stratigraphic units

Two stratigraphic units are exposed in the Cairn Needle area. The Twin Islands Group (Roddick, 1965) consists of lower metavolcanic and structurally overlying metasedimentary members, the former dominated by garnet amphibolites, and the latter by quartz-plagioclase-biotite-amphibole-garnet schists. These rocks have been correlated with the Stollicum Schist to the south (Fig. 1; Monger, 1989; Journeay, 1990). The structurally overlying Hunger Creek group is largely composed of quartz-plagioclase-biotite-amphibole-garnet schists, with minor marble, calc-silicate, pebble conglomerate, quartzite, and amphibolite. Both portions of this unit (Fig. 2) may correlate with the Settler and Chism Creek schists, however the western area could be correlative with the Cogburn Creek Group (Fig. 1; Gabites, 1985; Monger, 1989; Journeay, 1990).

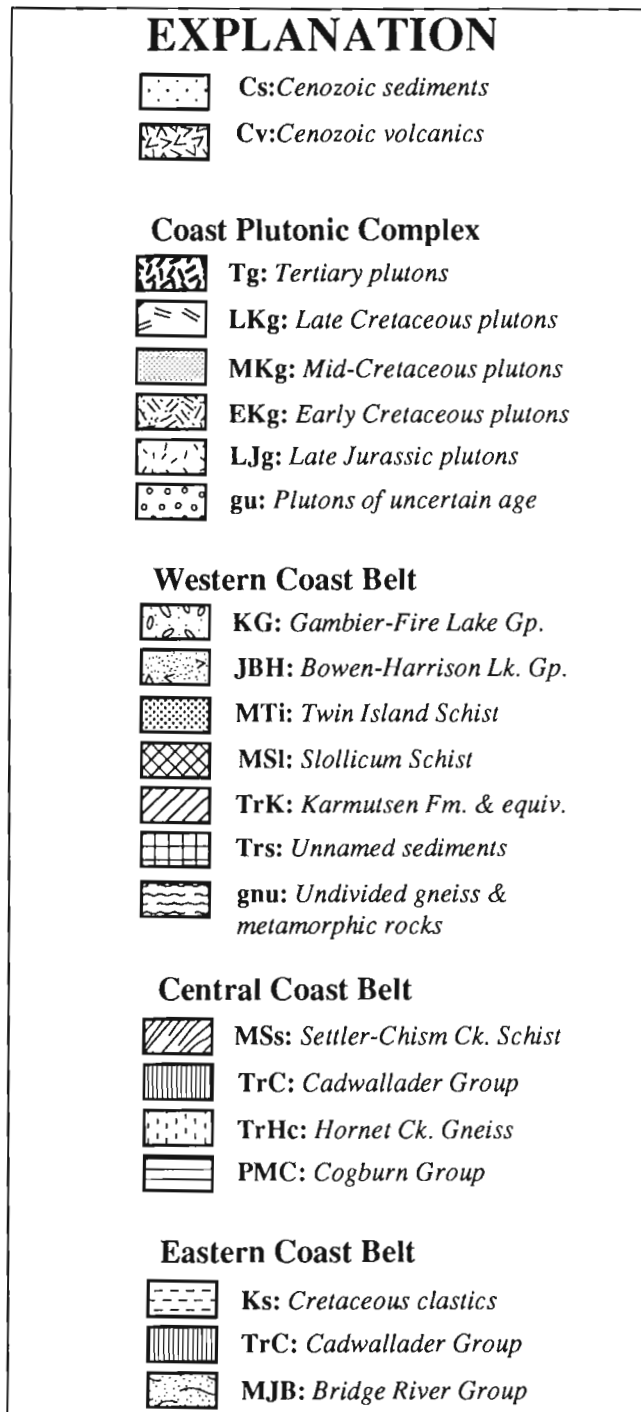
Deformational history

The Hunger Creek and Twin Islands groups and the Breakenridge Gneiss all record two distinct deformation events. The first resulted in isoclinal folding and transposition of compositional layering, development of stretching and down-dip mineral lineations, and imbrication of the Breakenridge Gneiss and Twin Islands Group along a layer-parallel fault zone. The second event is characterized by formation of tight northwest-trending folds at all scales and motion along the steep Butter Creek Fault (Fig. 2). The sense and magnitude of displacement along the Butter Creek Fault are unknown within the study area, but it is thought to have accommodated west-vergent reverse movement along strike to the southeast (Monger, 1989). The second phase of deformation in the Cairn Needle area is correlated with regionally recognized folds and high-angle reverse faults which accommodated northwest directed telescoping of previously imbricated terranes (Journeay and Csontos, 1989). Both style and relative timing of deformational events recognized in the study area are consistent with the two-stage contractional model of Journeay and Csontos (1989), and Journeay (1990).

Metamorphism

Mineral assemblages in metasedimentary rocks of the Hunger Creek and Twin Islands groups indicate that middle amphibolite facies conditions were attained throughout the Cairn Needle area. Key index minerals are garnet, biotite, hornblende, and fibrolite. Garnet-biotite geothermometry indicates peak conditions of 680 MPa 50°C. Garnet-Al₂SiO₅-quartz-plagioclase (GASP) and garnet-hornblende geobarometry both give pressures of 590-780 MPa.

Figure 1 Legend



A pressure of 700 ± 100 MPa is assigned for both groups. Fabric development and growth of synkinematic garnet and amphibole clearly indicate that middle amphibolite conditions were attained during the first deformational event. The presence of syn- to post-kinematic garnet and fibrolite indicates that metamorphic recrystallization outlasted the first, and possibly the second deformational events.

Mt. Mason Pluton

The Mt. Mason Pluton is a hornblende-biotite tonalite body that cuts the Butter Creek Fault (Fig. 2), therefore postdating much of the second phase of deformation. It has a weakly foliated core, and a 30 m zone along its eastern contact with well developed margin-parallel fabric. This foliation extends about 30 m into the country rock, overprinting regional schistosity. The weak foliation in the core is interpreted as being magmatic in origin based on its discontinuous nature at outcrop scale and the presence of plagioclase with normal oscillatory zoning, and undeformed quartz and plagioclase. Intense fabric development within the pluton-country rock contact zone suggests that it is related to emplacement of this body. Deformed dykes and shear zones with little apparent offset that cut the pluton suggest that it was intruded during the waning stages of ductile deformation.

U-Pb GEOCHRONOLOGY

A sample of weakly foliated hornblende biotite tonalite was collected from the southeastern portion of the Mt. Mason Pluton. Three fractions of zircons, separated on the basis of size and magnetic properties, were analyzed from the single population of clear to light amber elongate (1:w = 1:2.5-1:5.0), euhedral prismatic crystals. The analyzed fractions are

plotted as error ellipses (at a precision of two standard errors of the mean) on the concordia diagram in Figure 3. Fractions a and c intersect concordia and exhibit mutual overlap, whereas the position of the ellipse representing split b suggests possible minor Pb-loss. We interpret the U-Pb dates of fraction a, which are the most concordant of the three,

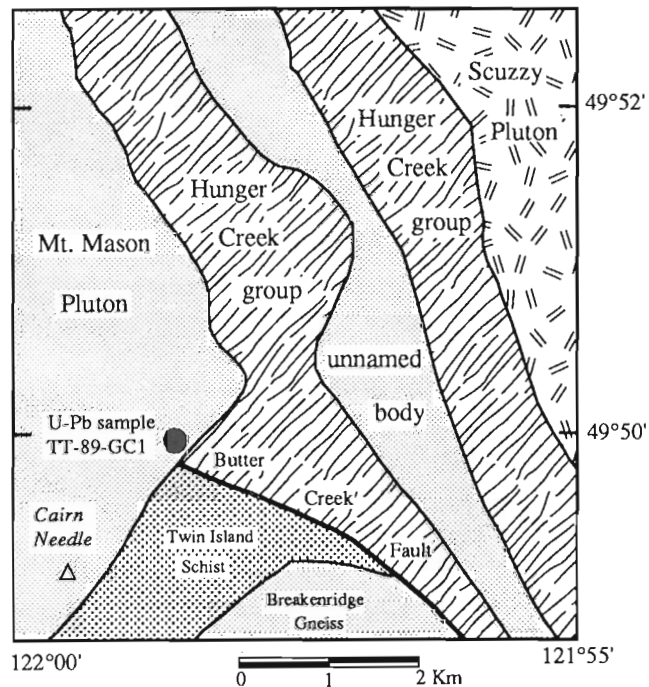


Figure 2. Geological map of the Cairn Needle area showing the location of U-Pb dated sample. See explanation on Figure 1 for patterns and symbols.

Table 1. U-Pb Zircon Analytical Data

Analysis number,	Fraction ^a	Wt. mg	U ppm	p _{Pb} ^b ppm	Measured ²⁰⁶ Pb/ ²⁰⁴ Pb, (Blank Pb, pg) ^c	Pb Isotopic abundance ^d , 206=100			Isotopic ratios and Dates, (Ma) ^e		
						204	207	208	²⁰⁶ Pb/ ²³⁸ U	²⁰⁷ Pb/ ²³⁵ U	²⁰⁷ Pb/ ²⁰⁶ Pb
<i>Mount Mason Pluton: TT-89-GC1, Lat/Long: 49°50'00" N, 121°58'39" W, elevation: 6020 feet</i>											
a,	+149µm, N0.5°/2.1A, Abr	2.3	159	2.3	3250 (50)	0.0152	5.0100	9.6761	0.01429±6 (91.5±0.4)	0.09428±48 (91.5±0.4)	0.04785±12 (92.1+6.0/-6.2)
b,	-149+134µm, N0.5°/2.1A, Abr	3.6	397	5.5	5942 (50)	0.0127	4.9781	8.7408	0.01416±10 (90.7±0.6)	0.09355±68 (90.8±0.6)	0.04791±6 (94.8±3.2)
c,	-134+74µm, Abr N1°/1.5A, M0.5°/2.1A	4.3	216	3.1	3712 (50)	0.0207	5.0999	9.1444	0.01431±6 (91.6±0.4)	0.09462±46 (91.8±0.4)	0.04795±6 (96.9±3.4)

^a Grain size in micrometres (µm). Magnetic (M) or nonmagnetic (N) when passed across Franz magnetic separator at specified side tilt in degrees, and field strength in Amperes (A); Abr = abraded.

^b Radiogenic and common Pb.

^c Blank estimate derived largely from ongoing total procedural blank analyses.

^d Radiogenic and common Pb, corrected for 0.43% per amu relative to NBS standards (see Appendix 1 for details) and blank Pb with the composition 204:206:207:208 = 1.00:17.75:15.50:37.30.

^e Errors are quoted as 2 standard errors of the mean for all isotopic ratios and dates. Common Pb corrections were made assuming the following composition from Stacey and Kramers (1975): 204:206:207:208 = 1:18.559:15.622:38.457 (95 Ma).

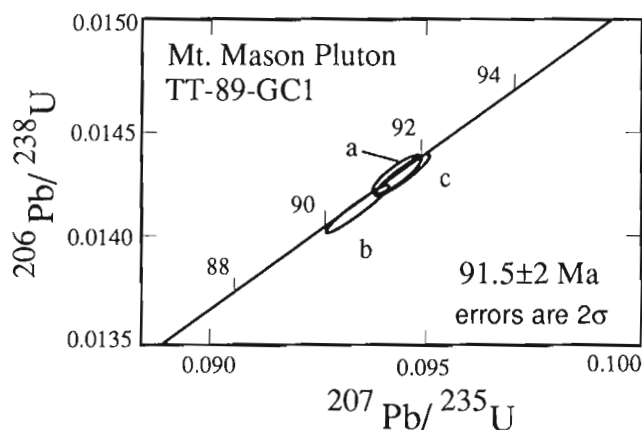


Figure 3. Concordia diagram showing error ellipses for the three analyzed zircon fractions from sample TT-89-GC1 of the Mt. Mason Pluton. See Table 1 for analytical data and Appendix 1 for sample preparation and U-Pb procedures.

as a reasonable age for this rock; 91.5 ± 2.0 Ma. A sample from the western portion of the Mt. Mason pluton gave a U-Pb zircon date of $92 \pm 8/-3$ Ma (Journey and Friedman, in press).

CONCLUSIONS

The eastern portion of the Mt. Mason Pluton in the Cairn Needle area has been dated as 91.5 ± 2 Ma, employing the U-Pb technique on zircon. This date is interpreted as the time of crystallization for this part of the intrusion. The Mt. Mason Pluton cuts the Butter Creek Fault and its emplacement postdates significant ductile deformation in the area. It provides a minimum age for shortening along this segment of the Lillooet River Fault system. The 96 Ma Breakenridge Gneiss has seen most or all of the deformation in this fault zone, allowing a short time window of about 5 Ma (91-96 Ma) during which this structural zone was active. This conclusion is in agreement with results of a regional study along Coast-Belt-Northwest Cascades System fault strands (Lillooet River Thrust System) to the west of the Mt. Mason Pluton (Journey and Friedman, in press).

ACKNOWLEDGMENTS

U-Pb dating was carried out at the Geochronology Laboratory of the University of British Columbia, and was funded by Lithoprobe and NSERC. RMF acknowledges the late Dr. R.L. Armstrong, J.W.H. Monger, and J.M. Journey for their support during the southern Coast Belt studies.

REFERENCES

Gabites, J.E.

1985: Geology and geochronometry of the Cogburn Creek-Settler Creek area, northeast of Harrison Lake, B.C.; M.Sc. thesis, University of British Columbia, Vancouver, 153 p.

Journey, J.M.

1990: A progress report on the structural and tectonic framework of the southern Coast, British Columbia; in Current Research, Part E; Geological Survey of Canada, Paper 90-1E, p. 183-195.

Journey, J.M. and Csontos, L.

1989: Preliminary report on the structural setting along the southeast flank of the Coast Belt, British Columbia; in Current Research, Part E; Geological Survey of Canada, Paper 89-1E, p. 177-187.

Journey, J.M. and Friedman, R.M.

in press: The Lillooet River Fault System: evidence of Late Cretaceous shortening in the Coast Belt of southwestern British Columbia; Tectonics.

Krogh, T.E.

1973: A low-contamination method for hydrothermal decomposition of zircon, an extraction of U and Pb for isotopic date determination; Geochimica Cosmochimica Acta, v. 37, p. 485-494.

1982: Improved accuracy of U-Pb ages by the creation of more concordant systems using an air abrasion technique; Geochimica Cosmochimica Acta, v. 46, p. 637-649.

Ludwig, K.R.

1980: Calculation of uncertainties of U-Pb isotope data; Earth and Planetary Science Letters, v. 46, p. 212-220.

1983: Plotting and regression programs for isotope geochemists, for use with HP-86/87 microcomputers; United States Geological Survey, Open File Report 83-0849, 102 p.

Monger, J.W.H.

1989: Geology of Hope and Ashcroft map areas, British Columbia; Geological Survey of Canada, Maps 41-1989 and 42-1989.

1990: Georgia Basin: regional setting and adjacent Coast Mountains geology, British Columbia; in Current Research, Part F; Geological Survey of Canada, Paper 90-1F, p. 95-107.

Parrish, R.R.

1987: An improved micro-capsule for zircon dissolution in U-Pb geochronology; Isotope Geoscience, v. 66, p. 99-102.

Parrish, R.R. and Krogh, T.E.

1987: Synthesis and purification of ^{205}Pb for U-Pb geochronology; Isotope Geoscience, v. 66, p. 111-121.

Parrish, R.R., Roddick, J.C., Loveridge, W.D., and Sullivan, R.W.

1987: Uranium-lead analytical techniques at the geochronology laboratory; Geological Survey of Canada, Paper 87-2, p. 3-7.

Roddick, J.A.

1965: Vancouver North, Coquitlam and Pitt Lake map area, British Columbia; Geological Survey of Canada, Memoir 335, 276 p.

Roddick, J.A. and Hutchison, W.W.

1973: Pemberton (east half) map-area, British Columbia; Geological Survey of Canada, Paper 73-17, 21 p.

Roddick, J.A. and Woodsworth, G.J.

1977: Bute Inlet; Geological Survey of Canada, Open File 480.

1979: Geology of Vancouver, west half, and mainland part of Alberni; Geological Survey of Canada, Open File 611.

Stacey, J.S. and Kramers, J.D.

1975: Approximation of terrestrial lead isotope evolution by a two-stage model; Earth and Planetary Science Letters, v. 26, p. 207-221.

Tyson, T.M.

1990: Geology of the Cairn Needle area east of Harrison Lake, southwestern British Columbia; in Current Research, Part E; Geological Survey of Canada, Paper 90-1E, p. 205-213.

1991: Structures, plutonism, and metamorphism of the Cairn Needle area, southern Coast Mountains, B.C.: implications for mid-Cretaceous orogenesis; M.Sc. thesis, University of Washington, Seattle, 62 p.

Walker, N.W. and Brown, E.H.

1990: Zircon U-Pb geochronometry of mid-Cretaceous plutonic rocks in the western crystalline core, North Cascades, Washington: implications for timing and nature of orogenesis (abstract); Geological Association of Canada, Mineralogical Association of Canada, Programs with Abstracts, v. 15, p. A137.

Woodsworth, G.J.

1977: Pemberton (92J) map area, British Columbia; Geological Survey of Canada, Open File 482.

York, D.

1969: Least squares fitting of a straight line with correlated errors; Earth and Planetary Sciences Letters, v. 5, p. 320-324.

APPENDIX 1

Uranium-lead analytical procedures

Sample preparation

Zircons were separated from 30-40 kg samples using standard crushing, Wilfley table and heavy liquid extraction techniques (e.g., Parrish et al., 1987). Zircons were then split into specific fractions based on size, shape, magnetic susceptibility, and physical attributes such as color and clarity of individual crystals. All fractions were air abraded using techniques similar to those of Krogh (1982). Prior to dissolution all zircon fractions were leached in warm 3N HNO₃ for 25 minutes followed by rinsing in high-purity H₂O and acetone.

Uranium-lead methods

Sample dissolution and chemical analyses were carried out with a procedure modified from Krogh (1973) and Parrish (1987). Uranium and lead concentrations were determined with a mixed ²⁰⁵Pb/²³⁵U spike (Parrish and Krogh, 1987), and were carried out using a Vacuum-Generators Isomass 54R solid source mass spectrometer in single collector mode

(Daly multiplier detector). Uranium and lead were corrected 0.44% and 0.43% per amu, respectively, relative to National Bureau of Standards SRM981 lead and U500 uranium standards. A nonradiogenic lead correction was made by first subtracting analytical blank lead with the isotopic composition 204:206:207:208 = 1.00:17.75:15.50:37.30 (Table 1). Common lead compositions were estimated using the model of Stacey and Kramers (1975), (see footnotes of Table 1 for common lead isotopic compositions). The magnitude of the common lead correction for each fraction was proportional to the remaining ²⁰⁴Pb after the blank correction.

Errors assigned to isotopic ratios and calculated dates were determined by numerical error propagation. Error ellipses are plotted as two standard errors of the mean. Uranium-lead concordia plots were generated using a program modified from Ludwig (1983). Intercept dates were calculated using techniques of York (1969) and the algorithm of Ludwig (1980).

Report on fieldwork in the southern Big Salmon metamorphic complex, Teslin map area, Yukon Territory

S.A. Gareau
Cordilleran Division, Vancouver

Gareau, S.A., 1992: Report on fieldwork in the southern Big Salmon metamorphic complex, Teslin map area, Yukon Territory; in *Current Research, Part A; Geological Survey of Canada, Paper 92-1A*, p. 267-277.

Abstract

A new project in the southern Big Salmon Range aims at defining and describing lithological units, documenting their age, protolith and metamorphic history, and understanding the context of fabric development in the Early Cretaceous Lone Tree pluton. The southern Big Salmon complex is composed of biotite quartzite to semi-schist, hornblende gneiss, biotite \pm hornblende metaplutonic rock and mylonite interspersed with plutonic rock such as the Lone Tree biotite granodiorite and undeformed biotite granodiorite to granite of probable mid-Cretaceous age. Deformational style away from the Lone Tree pluton is characterized by folding and strong planar fabric, and contrasts with intense mylonitization in an approximately 1 km aureole to the Lone Tree pluton. Regional greenschist-lower amphibolite metamorphic conditions are suggested by mineral assemblages.

Résumé

Un projet entrepris cet été dans le sud de la chaîne Big Salmon a pour but de définir et décrire les unités lithologiques de la région, de documenter l'âge, le protolith et l'histoire métamorphique de ces roches et de comprendre le contexte de développement des fabriques dans le pluton Lone Tree. Le complexe Big Salmon sud est formé de quartzite et semi-schiste à biotite, de gneiss à hornblende, de roche métaplutonique à biotite \pm hornblende et de mylonites, accompagnées de roches plutoniques telles la granodiorite à biotite Lone Tree et la granodiorite-granite à biotite non déformée probablement d'âge crétacé moyen. Le style de déformation des roches métamorphiques situées en-dehors de l'aureole du pluton Lone Tree est caractérisé par des plis et des fabriques planaires fortement exprimées et diffère du style structural des mylonites dans l'aureole du pluton. Des conditions de faciès métamorphique de schiste vert à amphibolite inférieur sont suggérées par les assemblages minéralogiques.

INTRODUCTION

A project was recently initiated in the southern Big Salmon Range, Teslin map area (Fig. 1), Yukon Territory. Five weeks were spent mapping the study area, a part of the Big Salmon metamorphic complex located east of Teslin Lake and south of the Canol Road (Fig. 1) in the Lone Tree Creek map area (105C/7).

Mapping is aimed at defining and describing lithological units as a framework for detailed metamorphic and geochronological study. The main goals are to document the protolith, metamorphic history and terrane affiliation of the

belt. The study will provide additional data towards understanding the complex boundary zone between allochthonous terranes and ancestral North American rocks. Rocks to the northwest and along trend with the southern Big Salmon Complex have been studied extensively (Quiet Lake and Laberge map areas) by Hansen (e.g., 1988, 1989; Hansen et al., 1989, 1991) and are under study in the northern Big Salmon Range (Stevens, 1991, 1992). Previous work in the study area includes regional mapping by Mulligan (1963). Mapping of the Teslin area at 1:250 000 and 1:50 000 scales is in progress (Gordey, 1991, 1992).

REGIONAL SETTING

The study area forms part of a metamorphic-plutonic belt faulted on its western side (unnamed and Teslin faults, Fig. 1) against Mesozoic (?) volcanic and volcanoclastic rocks and unmetamorphosed Cache Creek Group (Gordey, 1991) and bounded on the east by passive continental margin sediments of the Cassiar platform and marginal basin rocks of Slide Mountain terrane (Fig. 1; partly relabelled by Wheeler et al., 1988 as Dorsey terrane based on lack of ultramafic lithologies). Metamorphosed and intensely deformed rocks of unknown age composing the northwesterly-trending belt which extends from northwestern British Columbia, throughout the Yukon Territory and into east-central Alaska have been classified as Yukon-Tanana terrane (Monger and Berg, 1987; Fig. 1; Kootenay terrane of Wheeler et al., 1988). This terrane structurally overlies North American autochthonous rocks to the east and is faulted against accreted oceanic and island-arc terranes of the Intermontane belt to the west (Tempelman-Kluit, 1979; Hansen, 1989 and Mortensen, 1991).

The study area is located along the southern extension of the Teslin suture zone, a ductilely-deformed steeply-dipping portion of the otherwise flat-lying Yukon-Tanana terrane (Tempelman-Kluit, 1979; Hansen, 1988). The Teslin suture zone marks the boundary between rocks deposited along the ancient margin of North America and allochthonous terranes to the west. Deformation and metamorphism in the zone have been interpreted as having occurred between Permian and Early Jurassic time (Hansen et al., 1989).

LITHOLOGICAL DESCRIPTION

In Figure 2 the southern Big Salmon Range is divided into a northern region composed of foliated to mylonitized metamorphic rock, a central region of deformed plutonic rock (Lone Tree pluton) and a narrow southern region of mylonitic rock in faulted contact with unmetamorphosed sandstone, siltstone and shale (Gordey, 1991).

Metamorphic rocks

The first three units described below occur in the northern region and consist of varying proportions of biotite- and hornblende-bearing rocks.

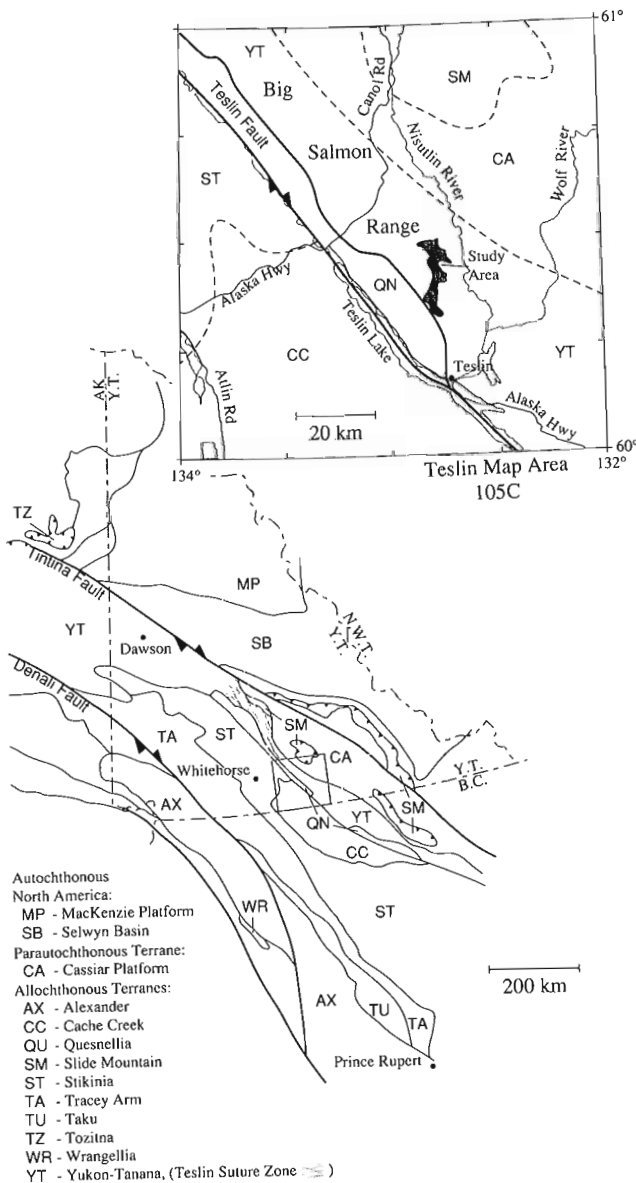


Figure 1. Terrane map of northern British Columbia, Yukon and east-central Alaska (after Tempelman-Kluit, 1979; Jones et al., 1987; Monger and Berg, 1987). The location of the study area is shown in the enlargement of Teslin map area (105C).

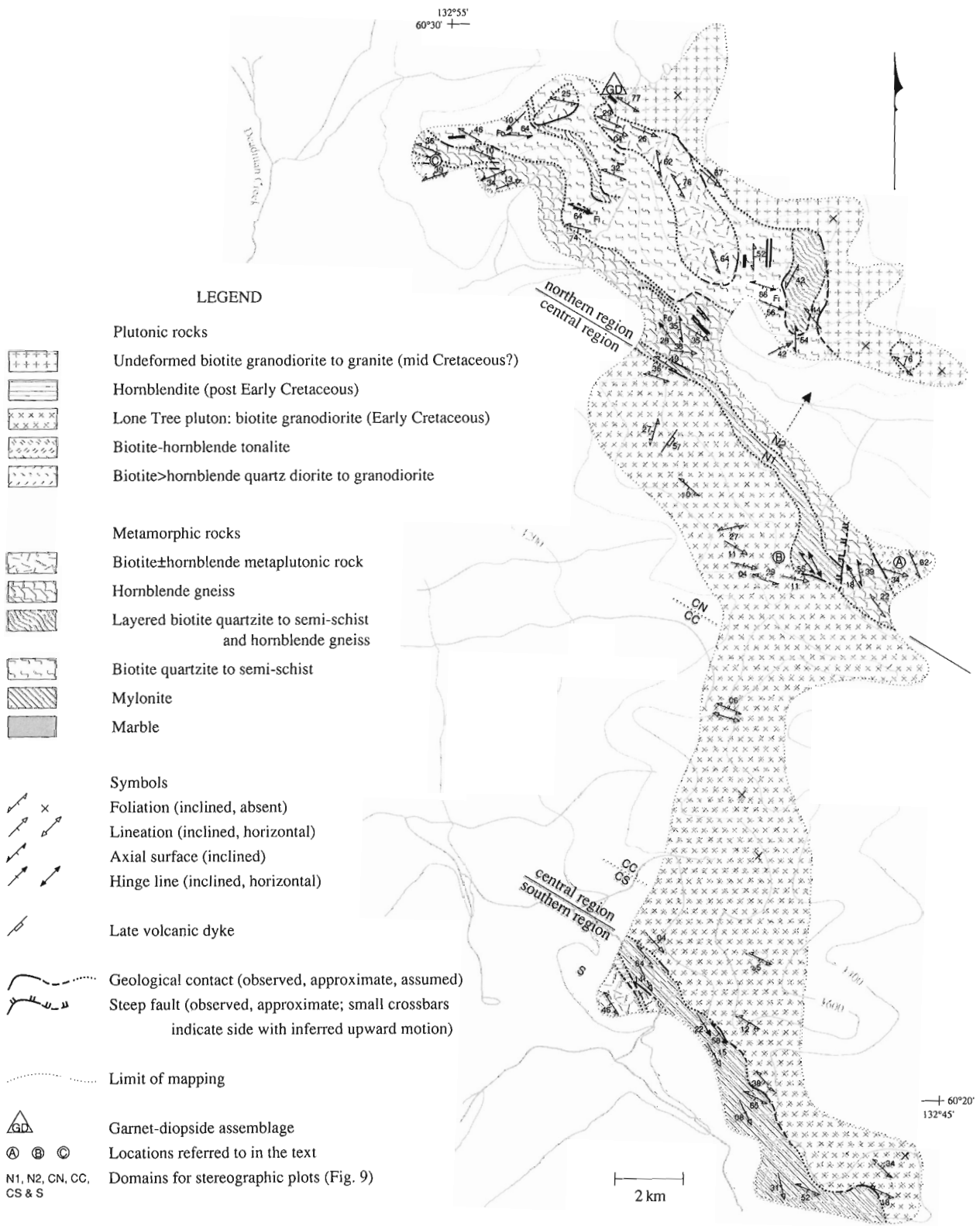


Figure 2. Simplified geological map of the study area.

A) Biotite quartzite to semi-schist

This unit is composed dominantly of biotite quartzite to semi-schist (Fig. 3), but also contains rare (<5% of outcrop) layers of rusty weathering muscovite ± biotite semi-schist to schist and marble. Amphibole + plagioclase ± epidote ± biotite bands and graphitic biotite semi-schist also occur (<1% of outcrop). The relative proportion of semi-schist to quartzite is variable with quartzite locally making up 95% of an outcrop while elsewhere constituting as little as 30%. The distinctive features of this unit are the almost complete absence of hornblende-bearing rocks and the presence of marble bands and muscovite-bearing rocks.

The main rock type is composed of fine grained (≤1 mm) biotite and sugary quartz ± plagioclase. Biotite content varies between 2 and 5%. It is generally disseminated throughout the semi-schist and concentrated along thin (<1 mm) planes approximately 5 mm apart in the quartzite. The quartzite is generally finely laminated.

Concentration and planar alignment of biotite define the foliation in the quartzite. Foliation in the biotite semi-schist is exhibited by planar alignment of biotite and felsic aggregates. Locally, lens-shaped biotite aggregates define a faint lineation.

B) Layered biotite quartzite to semi-schist and hornblende gneiss

In gradational contact with the biotite quartzite to semi-schist, this unit (Fig. 4) is distinguished from the former based on increased hornblende-bearing rock proportion (between 20 and 70%) and absence of marble and muscovite-bearing rocks. The contact zone between the two units spans up to 100 m and is characterized by a gradual increase in hornblende-bearing layers.



Figure 3. Typical appearance of the biotite semi-schist to quartzite unit. Foliation is strong and lineation generally weak to absent.

The biotite quartzite to semi-schist in this unit is similar to that of the previous unit, except that biotite semi-schist dominates over biotite quartzite. The hornblende-bearing rock is generally slightly coarser grained (~1 mm quartz and plagioclase and up to 2 mm long hornblende) than the biotite quartzite to semi-schist. A gneissic appearance results from variations in mafic content. The dominant rock type is a hornblende + plagioclase + quartz ± biotite ± epidote metamorphite. Amphibolite occurs in lesser proportion.

Hornblende is generally oriented in the foliation plane, but rarely aligned to form a lineation. In rocks where hornblende lineation is observed, other hornblende crystals are randomly oriented suggesting that hornblende growth may have continued after deformation or that hornblende crystals were reoriented to varying degrees during deformation postdating metamorphic mineral growth. The sporadic occurrence of hornblende lineation suggests that strain was not distributed homogeneously throughout the region.

C) Hornblende gneiss

Also in the northern region, this unit is composed of dark green weathering greenstone, hornblende-biotite gneiss to amphibolite and minor biotite semi-schist. On one ridge, marble bands occur in the uppermost part of the unit. The basis for distinguishing this package from the two previously described is the near absence of biotite semi-schist. The unit rests beneath biotite quartzite to semi-schist. At the one location where it was observed, the contact is sharp. The contact with mylonites that rest beneath the unit is also sharp.

The greenstone is an aphanitic to very fine grained, locally pyrite-bearing siliceous green rock. It is locally massive, but elsewhere shows foliation-parallel layers defined by variations in grain size. Pyrite occurs in trace amounts in 7 to 10 mm diameter pods.



Figure 4. Layered biotite semi-schist and hornblende gneiss unit. Compositional banding varies from centimetre (as in this picture) to metre scale. Strong foliation parallels compositional layering. Lineation is generally weak to absent.

Strongly foliated, fine to medium grained (average 1 mm diameter felsic minerals and 2 mm length hornblende) biotite-hornblende gneiss varies in mafic content and in

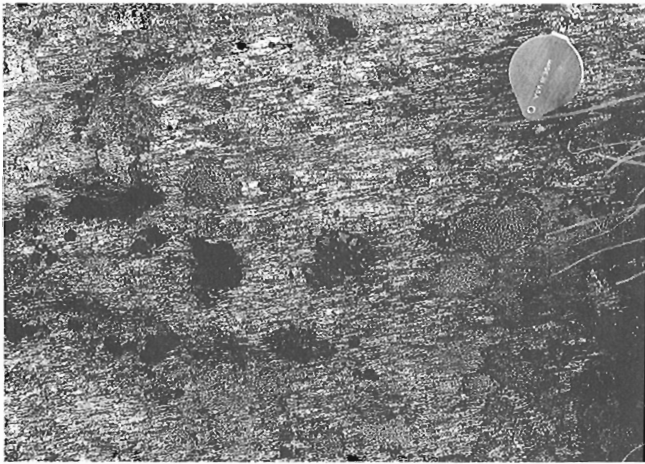


Figure 5. Strong fabric and augen texture in biotite ± hornblende metaplutonic rock.

relative proportion of ferromagnesian minerals. Quartz content reaches approximately 10% and epidote occurs in minor amounts. Locally epidote is more abundant and forms, associated with feldspar, 1 to 2 cm thick layers within the more typical hornblende-rich rock. Layering in this rock type, represented by variations in mafic content and grain size, parallels the local foliation.

Medium grained biotite semi-schist resembles rocks of the same name described earlier, but is generally slightly coarser grained.

Foliation in the greenstone is marked by traces of micas forming rare, thin planes and locally by parting of the rock into 1 to 3 cm thick slabs. Mineral alignment defines the foliation in other rock types. Hornblende lineation occurs locally.

D) Biotite ± hornblende metaplutonic rock

Several peaks in the northern region are underlain by a homogeneous, blocky, grey weathering biotite ± hornblende semi-schist. The unit rests above the biotite quartzite to semi-schist unit with which it is in sharp contact. At one

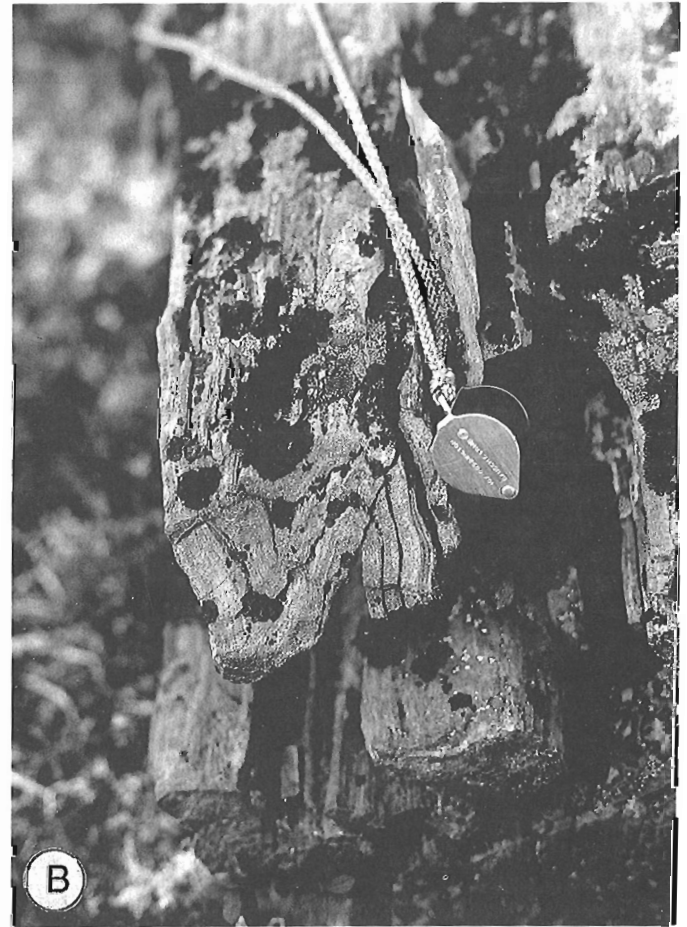
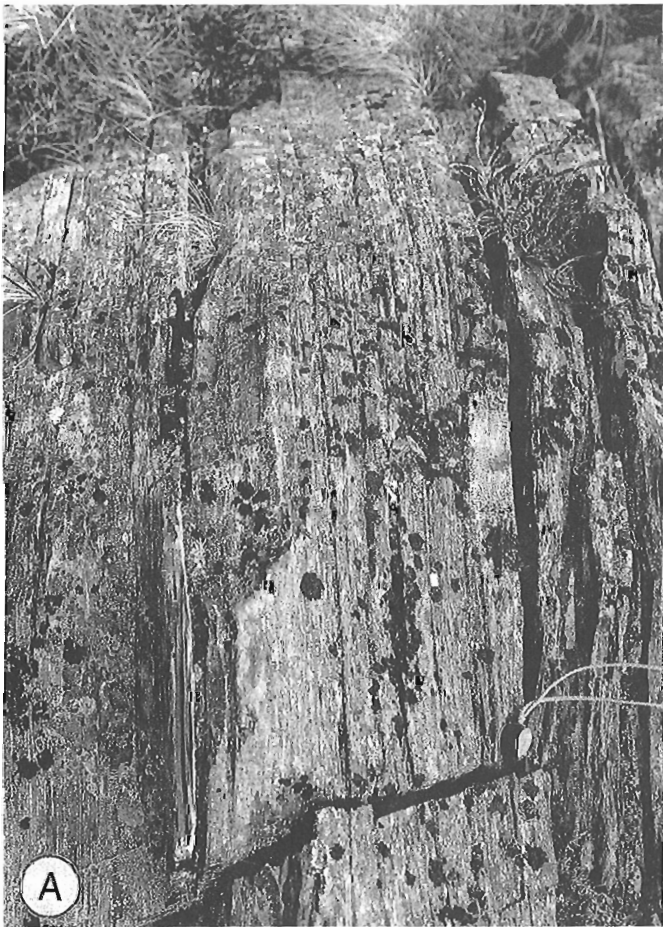


Figure 6. Typical appearance of mylonite unit. The rock is very fine grained and strongly foliated (A) and linedated. Hinge lines of folds (B) parallel the strong lineation.

location, a horizontal contact between the two units appears to be a small fault: it is marked by increasing schistosity within 10 cm of the contact and by occurrence of epidote veins suggestive of fluid movement in the contact zone. Yet, at other locations the contact appears intrusive, with concordant bands of the biotite ± hornblende semi-schist within the biotite quartzite to semi-schist unit as far away as 1 km from the contact. The hornblende content increases slightly towards these contacts.

The medium grained rock predominantly contains biotite (5-10%), hornblende (0-3%) and sugary quartz + plagioclase. Plagioclase locally forms 7 mm long augen (Fig. 5). Chlorite and epidote occur in trace amounts; chlorite as isolated crystals probably after biotite, and epidote in rare pods ($\leq 1\%$). At one location, a fine grained biotite-rich rock occurs as inclusions in the more typical host.

This unit is generally moderately to strongly lineated and moderately to weakly foliated. Where foliation is present, a crenulation is locally observed.

The homogeneous nature of this metamorphic rock over a large part of the study area and the presence of plagioclase augen suggest a plutonic protolith for this unit.

E) Mylonite

Located both in the northern and southern regions, this unit occurs immediately adjacent to the large, deformed Early Cretaceous plutonic body composing the central region of the study area (Lone Tree pluton). The mylonite unit is composed of rusty-brown weathering, flinty and fissile (into 5 mm-2 cm thick plates) siliceous rock locally containing pyrite. This rock is very fine grained and finely laminated (Fig. 6A,B). Minor amphibole-rich and micaceous layers are present ($< 5\%$).

This unit is characterized by extreme lineation and strong foliation. Although generally too fine grained to allow hand-specimen observation of kinematic indicators, the strong planar and linear fabric, the finely laminated nature of the rock, the very fine grain size and the presence of asymmetric plagioclase augen indicate that this rock has been mylonitized. Detailed petrographic analysis is planned in order to substantiate this conclusion and determine sense of movement. Mylonitization appears related to emplacement of the Early Cretaceous Lone Tree pluton. These rocks could be mylonitized equivalents of the biotite quartzite to semi-schist unit.

The mylonites rest sharply beneath hornblende gneiss and above the Lone Tree pluton (Fig. 7A).

Intrusive rocks

A) Biotite-hornblende tonalite

Plutonic rocks richer in hornblende than biotite are relatively rare in the study area. They occur at only three locations (A, B and C, Fig. 2) in the northern region. Dating of

biotite-hornblende tonalite from two of these locations (A and B) is planned in order to investigate a possible correlation between these geographically separated similar rocks. At the easternmost location (A), a biotite-chlorite schist separates the hornblende gneiss unit from the biotite-hornblende tonalite. At location B, the hornblende-bearing tonalite is included within biotite plutonic rock. The contact appears sharp, but the extent of hornblende-bearing plutonic rock and its relationship with the more typical biotite-bearing rock was not defined.

The unit consists of 7 to 15% medium to coarse grained (on average 5 mm long, but reaching 15 mm long) euhedral hornblende, $< 5\%$ euhedral biotite (~ 5 mm diameter), 10 to 25% fine grained (~ 2 mm) sugary quartz, anhedral plagioclase of varying grain size and fine grained accessory titanite. Locally, K-feldspar occurs as 1 cm long phenocrysts (up to 5%). Fine grained epidote occurs locally in trace amounts. In places, variation in hornblende content and in grain size produces a layering at 5 cm scale. At one location, a rusty weathering lens (approximately 2 by 10 m) of pyrite-bearing, hornblende-epidote-rich rock occurs within the tonalite.

This unit is moderately foliated and, at the easternmost location (A), strongly lineated.

B) Biotite granodiorite-Lone Tree pluton

The Lone Tree pluton, named herein after nearby Lone Tree Creek, is a homogeneous intrusive rock that underlies the central region of the study area. A sample from this unit collected in 1990 by S. Gordey (60°25.92'N, 132°50.88'W) gives a zircon U-Pb date of 123.1 ± 1.7 Ma (J.K. Mortensen, pers. comm., 1991). The medium grained rock (2-3 mm) is largely composed of biotite ($\leq 10\%$), titanite (trace), quartz ($\sim 15\%$) and feldspar. Hornblende occurs locally, as well as trace garnet in a small region near the centre of the body. This unit is in sharp contact with surrounding mylonitic rocks (Fig. 7A). Bands of metamorphic rocks ($\leq 5\%$ of outcrop) up to 10 m in width, are included in the outermost 1.5 km of the intrusive body (Fig. 7B).

The intrusive rock is variably foliated and lineated. Strongest fabric is localized near the margins of the pluton and decreases in intensity towards the core of the body where foliation and lineation are absent. The foliation is marked by planar alignment of mafic minerals as well as that of felsic aggregates and feldspar augen (Fig. 7C). Metamorphic bands parallel the plutonic foliation. The alignment of elongate mafic mineral aggregates define the lineation.

The unit is cut by numerous leucocratic hornblende-garnet dykes and biotite pegmatites. Dykes are absent in the core of the body, and form up to 90% of the outcrop, but generally $< 40\%$, close to the pluton's margins. These dykes vary in width between 10 cm and 15 m. They crosscut the body's fabric, but also generally possess a weak foliation parallel to that of the host. A late volcanic dyke approximately 50 cm in width is undeformed and crosscuts the foliated intrusive rock.

C) Hornblendite

A dark green weathering hornblendite band occurs within the southern region. It is composed of euhedral, approximately 5 mm long hornblende accompanied by various proportions of plagioclase. Vague, irregular layering results from

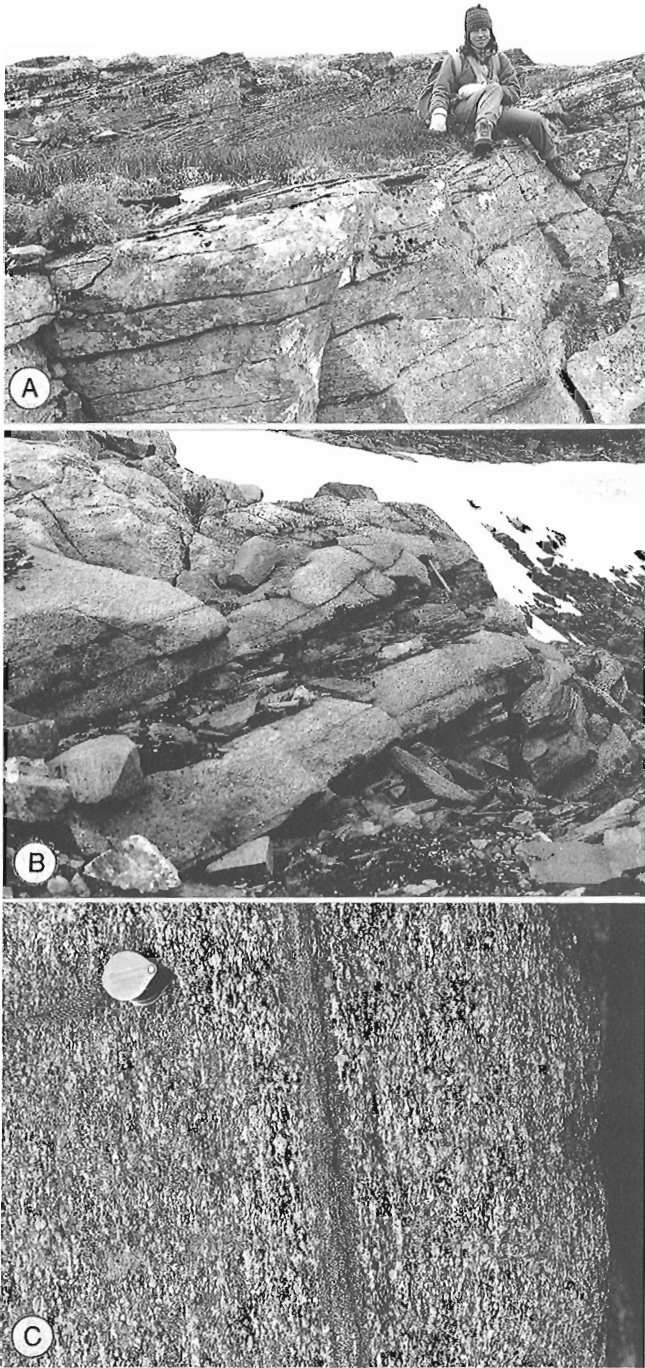


Figure 7. (A) Sharp contact between the Lone Tree pluton (bottom) and mylonite unit (top). (B) Metamorphic inclusions (dark) in the Lone Tree pluton (light grey). (C) Strong fabric in the Lone Tree pluton.

variation in plagioclase content. The absence of foliation and lineation in the sample suggests that emplacement of this unit occurred relatively late in the overall history of the area.

D) Undeformed biotite granodiorite to granite

A late undeformed plutonic rock intrudes metamorphic rocks in the northern region of the study area. The coarse grained (≥ 5 mm), generally porphyritic granodiorite to granite is composed of approximately 5% biotite occurring as ≤ 5 mm plates, approximately 25% anhedral quartz between 4 and 7 mm in diameter, euhedral K-feldspar (~ 5 mm) and plagioclase (~ 3 mm), and fine grained accessory titanite.

The plutonic rock is undeformed except near its very sharp contact with metamorphic rocks, where it is weakly foliated. Apophyses of intrusive rock, up to 1 m in width, occur in the metamorphic rock within 10 m of the contact.

Granitic bodies from this area are generally considered to be coeval with similar, widespread mid-Cretaceous plutons (Mulligan, 1963; Gordey, 1991). The lack of widely developed fabric suggests that this rock is younger than the Early Cretaceous foliated and lineated Lone Tree pluton.

E) Biotite \pm hornblende quartz diorite

A small area of medium grained (1-4 mm) biotite \pm hornblende quartz diorite to granodiorite occurs on the western side of the northern region. Approximately 10% biotite consists of fresh, dark brown flakes of approximately 2 mm diameter. Oriented biotite forms a moderate foliation in the rock. Hornblende occurs as 4 mm long euhedral laths. Quartz and feldspar occur as fine, spherical grains. Quartz content varies between approximately 10 and 20%. Fine grained accessory titanite is also present. Foliation-parallel and crosscutting pegmatitic dykes of 2 to 30 cm width intrude the granitic body and compose up to 50% of the outcrop.

The foliated nature of the rock suggests that it is not related to late biotite-bearing plutonic rock bounding the area to the east. Moreover, the abundance of biotite and the minor proportion of hornblende differentiate this unit from the biotite-hornblende tonalite occurring sporadically throughout the area. Although no mylonites occur in contact with this unit, the dominance of biotite over hornblende, the presence of titanite and the abundance of pegmatitic dykes are suggestive of an association with the Lone Tree pluton.

F) Dykes

Leucocratic dykes cut all units throughout the study area. Fine grained (~ 1 mm) siliceous dykes contain $< 5\%$ biotite or hornblende and trace amounts of garnet. Biotite pegmatites also occur. The dykes are undeformed to slightly foliated. They are locally folded in metre-scale warps (Fig. 8) interpreted to result from late open folding.

STRUCTURE

Foliation

Foliation is marked by preferred orientation of phyllosilicates and prismatic minerals as well as of felsic aggregates and plastically deformed felsic minerals. Compositional layering parallels the foliation.

In the northern region away from the Lone Tree pluton (N1, Fig. 9), poles to foliation define in stereographic projection a great circle girdle pattern suggesting an east-southeast orientation for axes of large-scale folding. Dispersion in the girdle pattern probably arises from noncylindrical nature of folding and late refolding of foliation. Weak foliation in the metaplutonic body may reflect its timing of emplacement with respect to development of the foliation or competency differences between the body and surrounding rock. Foliation in the mylonites strikes consistently to the northwest and dips moderately to the northeast (N2, Fig. 9). The dip of planar fabric decreases gradually towards the Lone Tree pluton.

Foliation in the central region dips shallowly to moderately towards the northeast or the southwest (C, Fig. 9). Northeasterly dips occur predominantly in the northern part of the body close to the plutonic/metamorphic contact. The central part of the pluton is weakly to non-foliated.

In the southern region, dips of foliation are shallow to steep to the southwest and the northeast (S, Fig. 9). Northeast-dipping foliation occurs predominantly in proximity of fold hinges.

Lineation

Although developed throughout the study area, lineation is strongest in metamorphic rock within 1.5 km of the Lone Tree pluton contact (N2 and S domains). It is marked by alignment of mineral aggregates and amphiboles as well as quartz rods.

In the northernmost part of the study area, lineation which is only significantly developed in the biotite \pm hornblende metaplutonic rock generally plunges shallowly to steeply to the east-southeast (N1, Fig. 9). As the Lone Tree pluton is approached (N2), scattering in orientation decreases and lineations dip moderately towards 90 to 123°. Lineation is not well developed in the Lone Tree pluton except close to its margins where linear fabrics are oriented similarly to that in nearby metamorphic rock. Shallowly plunging linear fabrics trend approximately 140 to 150° in the southern region.

Folding

Two fold generations were identified in the study area. Rare rootless, 10 to 30 cm scale amplitude isoclinal folds display both angular and curved hinges. They fold compositional layering and apparently foliation, and their limbs are coplanar with the foliation. Poles to axial surfaces from the southern region are dispersed along a great circle girdle (Fig. 9; AS_i) suggesting reorientation during later deformation. The girdle's π -axis as well as hinge lines of isoclinal folds (Fig. 9;

HL_i) are oriented similarly to the strongly developed local lineation. This is consistent with mylonitization in the proximity of the Lone Tree pluton postdating isoclinal folding in the area.

Late open folding of 0.5 to 1 m amplitude affects both foliation and compositional layering. Folding of late, weakly foliated to undeformed dykes (Fig. 8) present in all units including the Early Cretaceous Lone Tree pluton indicate a relatively young age for this episode of deformation. A few orientations of axial surfaces and hinge lines are shown in Figure 9 (AS_o and HL_o).

Fault

A vertical fault was mapped on the easternmost side of the northern region. The fault is marked in the field by an approximately 20 m wide steep-walled depression along the ridge line in which rocks occur as nearly vertical blocks. Felsic mylonites and overlying hornblende-rich rock occur on the western side of the fault. The sharp contact between the two units strikes approximately 300°, dips moderately to the northeast and is cut by the approximately north-trending fault. Hornblende-rich rocks only are present on the eastern side of the fault suggesting a downward movement of the eastern block.

Mylonitic fabric

Very few macroscopic kinematic indicators were found in the N1 domain. In fact, lineation occurs only sporadically in this region, possibly reflecting localized mylonitization. Rare asymmetric boudins suggest top to the southeast movement, but are too few for statistically significant interpretation. Strong foliation appears to result dominantly from folding. The nature of the fabric in these rocks contrasts sharply with that of rocks in the N2 and S domains where all rocks are uniformly and strongly mylonitized. Kinematic indicators



Figure 8. Open folding of late fine grained leucocratic dyke and host rock.

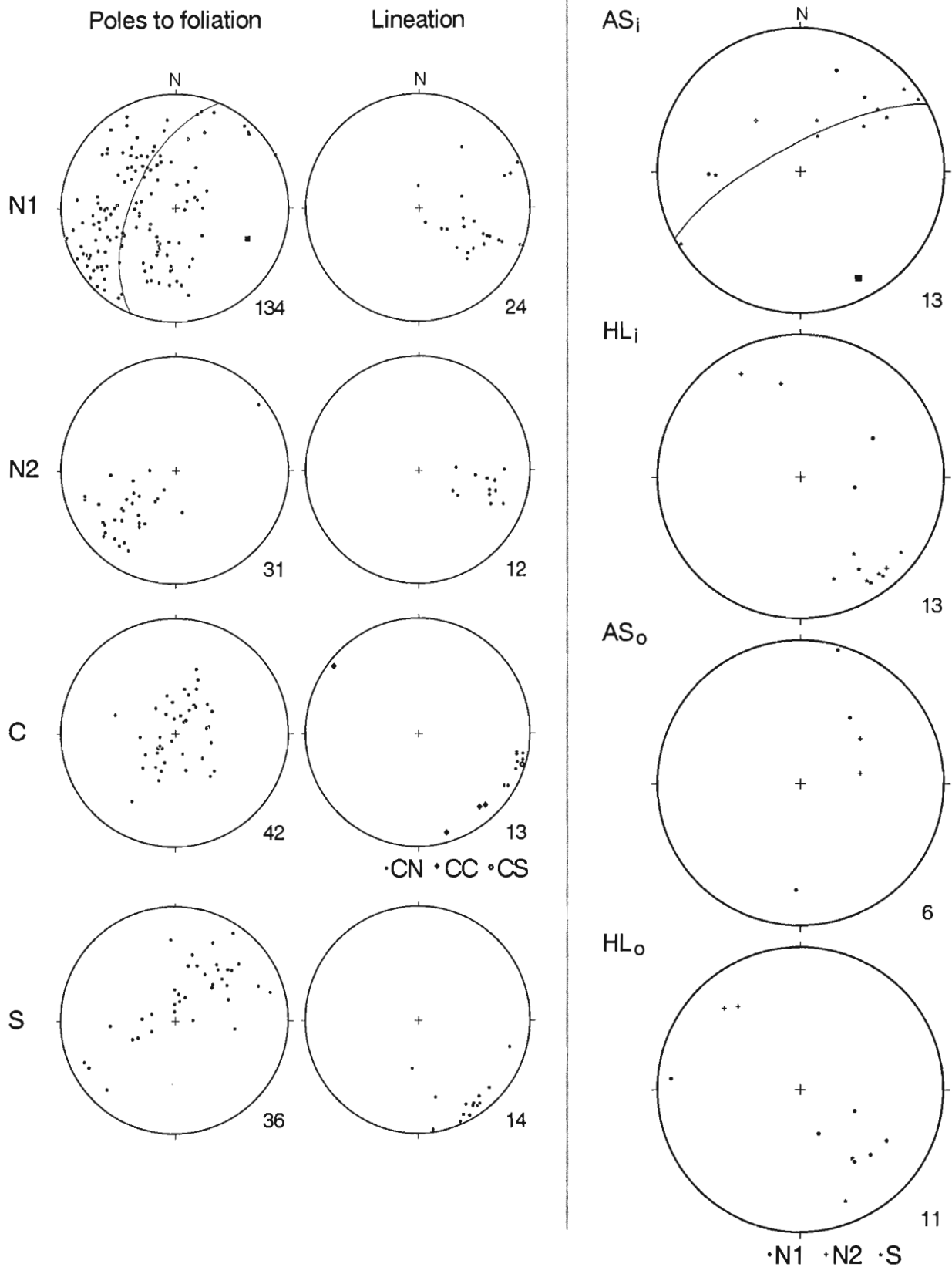


Figure 9. Equal area plots of planar and linear elements in the study area. Poles to foliation and lineations are shown on separate projections for the northern, central and southern regions defined in Figure 2. N1 and N2 represent two distinct domains within the northern region (Fig. 2). CN, CC and CS are domains of the central region and S refers to the only domain composing the southern region. Other abbreviations are: AS_i: axial surfaces of isoclinal folds; HL_i: hinge lines of isoclinal folds; AS_o: axial surfaces of open folds and HL_o: hinge lines of open folds. Numbers in lower right corners are population sample sizes for each stereonet.

include asymmetric folds and augens, and C/S bands. Mylonitic fabric is present locally in the central region, particularly at the pluton's margin.

METAMORPHISM

The dominant rock types of the study area contain only weakly diagnostic mineral assemblages suggesting greenschist and/or lower amphibolite facies metamorphic conditions. Quartzite and quartz semi-schist contain biotite, lesser white mica and minor chlorite. Amphibole, biotite, epidote and chlorite occur in the hornblende gneiss unit. It is not known whether the absence of garnet from these two rock types results from compositional constraints, metamorphic conditions or both factors.

Rare siliceous marble bands contain minerals such as talc, tremolite and phlogopite consistent with inferred greenschist-lower amphibolite metamorphic conditions. The garnet-diopside assemblage, indicative of higher temperature conditions, is stable in a marble inclusion within late undeformed intrusive rock (Fig. 2) and most likely results from contact metamorphism. Detailed petrographic and electron microprobe work will hopefully reveal more information with respect to the metamorphic history of these rocks.

DISCUSSION

Metamorphosed and deformed quartz-rich sedimentary rocks, hornblende-rich rocks of unknown protolith, and granodiorite of the Big Salmon complex fit descriptions of Nisutlin allochthon by Tempelman-Kluit (1979) and Yukon-Tanana terrane by Monger and Berg (1987). U-Pb dating of these units will hopefully provide protolith ages for comparison with these packages at other locations. Petrographic analysis may provide clues to the protolith(s) of the hornblende-rich unit which retains no primary texture observable in the field. In addition, geochronological and petrographic work will be aimed at unravelling the metamorphic history of the complex.

The wide range in orientation of planar fabrics in the Big Salmon Range differentiates the area from the Teslin suture zone documented along trend to the north. The southern Big Salmon area appears transitional between a western zone of steeply dipping fabrics such as the Teslin suture zone and gently dipping rocks to the east. At the latitude of the study area, the Teslin suture zone appears to have been cut by younger faults (Teslin and unnamed) which juxtapose the Big Salmon complex to unmetamorphosed rocks to the west.

An Early Cretaceous age for the foliated and lineated Lone Tree pluton is contrary to regional evidence that development of fabric occurred prior to Early Jurassic time and indicates that at least local deformation occurred between Early Cretaceous Lone Tree pluton emplacement and intrusion of undeformed biotite granodiorite to granite of assumed mid-Cretaceous age. The tectonic regime under which the Lone Tree pluton was emplaced into the Big Salmon complex remains to be defined through petrographic

and geochronological work. The ductile nature of deformation in the pluton, gradational decrease in intensity of fabric from margin to core and the variable deformational state of probably comagmatic felsic dykes in the pluton suggest that deformation in the pluton was synchronous with (or very closely followed) emplacement of the pluton. Moreover, deformation appears closely related to Lone Tree pluton emplacement because a mylonitic aureole surrounds the pluton, development of these mylonites appears to postdate regional deformation and the orientation of planar and linear fabric in the pluton is consistent with that of surrounding mylonites.

ACKNOWLEDGMENTS

This project was suggested by Steve Gordey whom I thank warmly for his support and encouragement. Lively discussions with Rob Stevens while visiting him in the field are acknowledged. Jim Mortensen showed me key lithologies of the Yukon and discussed many controversial issues. Susan Creighton's competent field assistance is acknowledged. Excellent helicopter support was provided by Norm Graham (Discovery Helicopters, Atlin). Thanks to Mitch Mihalynuk and his crew for the use of their cabin. Steve Gordey's helpful comments and suggestions on the manuscript are appreciated.

REFERENCES

- Gordey, S.P.**
1991: Teslin map area, a new geological mapping project in southern Yukon; in *Current Research, Part A*; Geological Survey of Canada, Paper 91-1A, p. 171-178.
1992: Geological fieldwork in Teslin map area, southern Yukon Territory; in *Current Research, Part A*; Geological Survey of Canada, Paper 92-1A.
- Hansen, V.L.**
1988: A model for terrane accretion: Yukon-Tanana and Slide Mountain terranes, northwest North America; *Tectonics*, v. 7, p. 1167-1177.
1989: Structural and kinematic evolution of the Teslin suture zone, Yukon: record of an ancient transpressional margin; *Journal of Structural Geology*, v. 11, p. 717-733.
- Hansen, V.L., Heisler, M.T., and Harrison, T.M.**
1991: Mesozoic thermal evolution of the Yukon-Tanana composite terrane: new evidence from $^{40}\text{Ar}/^{39}\text{Ar}$ data; *Tectonics*, v. 10, p. 51-76.
- Hansen, V.L., Mortensen, J.K., and Armstrong, R.L.**
1989: U-Pb, Rb-Sr and K-Ar isotopic constraints for ductile deformation and related metamorphism in the Teslin suture zone, Yukon-Tanana terrane, south-central Yukon; *Canadian Journal of Earth Sciences*, v. 26, p. 2224-2235.
- Jones, D.L., Silberling, N.J., Coney, P.J., and Plafker, G.**
1987: Lithotectonic terrane map of Alaska (west of the 141st Meridian); United States Geological Survey, Map MF-1874-A, scale 1:2 500 000.
- Monger, J.W.H. and Berg, H.C.**
1987: Lithotectonic terrane map of western Canada and southeastern Alaska; United States Geological Survey, Map MF-1874-B, scale 1:2 500 000.
- Mortensen, J.K.**
1991: Pre-mid-Mesozoic tectonic evolution of the Yukon-Tanana terrane, Yukon and Alaska; *Tectonics*.
- Mulligan, R.**
1963: Geology of the Teslin map area, Yukon Territory (105C); Geological Survey of Canada, Memoir 326.

Stevens, R.A.

- 1991: The Teslin suture zone in northwest Teslin map area, Yukon; in Current Research, Part A; Geological Survey of Canada, Paper 91-1A, p. 271-277.
- 1992: Regional geology, fabrics and structure of the Teslin suture zone in northwest Teslin map area, Yukon; in Current Research, Part A; Geological Survey of Canada, Paper 92-1A.

Tempelman-Kluit, D.J.

- 1979: Transported cataclasite, ophiolite and granodiorite in Yukon: evidence of arc-continent collision; Geological Survey of Canada, Paper 79-14.

**Wheeler, J.O., Brookfield, A.J., Gabrielse, H., Monger, J.W.H.,
Tipper, H.W., and Woodsworth, G.J.**

- 1988: Terrane map of the Canadian Cordillera; Geological Survey of Canada, Open File 1894, scale 1:2 000 000.

Geological Survey of Canada Project 900036

Geological fieldwork in Teslin map area, southern Yukon Territory

S.P. Gordey
Cordilleran Division, Vancouver

Gordey, S.P., 1992: Geological fieldwork in Teslin map area, southern Yukon Territory; in Current Research, Part A; Geological Survey of Canada, Paper 92-1A, p. 279-286.

Abstract

Revision geological mapping of selected areas within Teslin map area (105C) focused on a) Permian and Mesozoic volcanics of Cache Creek and Lewes River groups, b) intensely deformed Triassic-Jurassic chert and greywacke of the Cache Creek Group, c) Mesozoic clastic strata of Quesnel Terrane, and d) strata of the North American margin (hitherto Dorsey Terrane) within the Thirtymile Range.

Résumé

Les cartes géologiques révisées de zones choisies de la région cartographique de Teslin (105C) mettent en évidence a) les roches volcaniques permienne et mésozoïques des groupes de Cache Creek et de Lewes River, b) le chert et le grauwacke triasiques-jurassiques très déformés du groupe de Cache Creek, c) les couches clastiques mésozoïques du terrane de Quesnel, et d) les couches de la marge nord-américaine (jusqu'à maintenant le terrane de Dorsey) au sein de la chaîne Thirtymile.

INTRODUCTION AND REGIONAL SETTING

Fieldwork in 1991 constituted the second season of a five year project to remap the geology of Teslin map area (NTS 105C; 60-61°N; 132-134°W) in southern Yukon (Fig. 1). The aim of this project is to produce a revised 1:250 000 scale map and reports as well as 1:50 000 scale maps of selected areas, to understand the regional stratigraphic, structural and tectonic context of the area's mineral resources and its environmental geological framework. The fieldwork of Mulligan in the early 1950s (Mulligan, 1963) established a geological framework, but little other work has been done until recently (Jackson, 1990; Gordey, 1991; Stevens, 1991; and Cordey et al., 1991).

Although underlain by diverse terranes of the Omineca and Intermontane belts, (see Wheeler et al., 1988) the bedrock geology of Teslin map area can be described in terms of three geological segments. A narrow fault-bounded panel which trends diagonally northwest across the central part of the area (Fig. 1) forms one segment and separates additional segments to the northeast and the southwest. The southwest block is divided approximately along the Alaska Highway. Southeast of the highway, late Paleozoic greenstone, chert, and limestone of the Cache Creek Group is basement(?) to

Triassic and Jurassic chert and clastic rocks (Lewes River assemblage of Wheeler and McFeely, 1987). Northwest of the highway Triassic and Jurassic sediments and volcanics of the undivided Lewes River and Laberge groups (Inklin assemblage of Wheeler and McFeely, 1987) are intruded by several ultramafic plutons.

The northeast block is underlain by sheared Proterozoic and Paleozoic strata deposited along the North America margin overlain by allochthons of Late Paleozoic greenstone, sheared and metamorphosed Paleozoic siliceous sediment and mylonitized granitic rock. Isotopic age data from other regions to the northwest (Hansen et al., 1989) indicate the fabric and metamorphism in allochthonous rocks are post-Permian and pre-Early Jurassic.

The central fault-bounded panel has poorly understood Mesozoic(?) volcanic and volcanoclastic strata. At least 150 km of pre-Late Cretaceous dextral displacement is distributed along its bounding faults as indicated by offset along the Thibert Fault in northwestern British Columbia to which they may join (Gabrielse, 1985, Fig. 9). The northeast bounding fault separates unmetamorphosed and weakly deformed strata on the southwest from mylonitized sedimentary and granitic rocks of high metamorphic rank in the Big Salmon Range on the northeast. Regional folding and faulting of strata across the map area is broadly

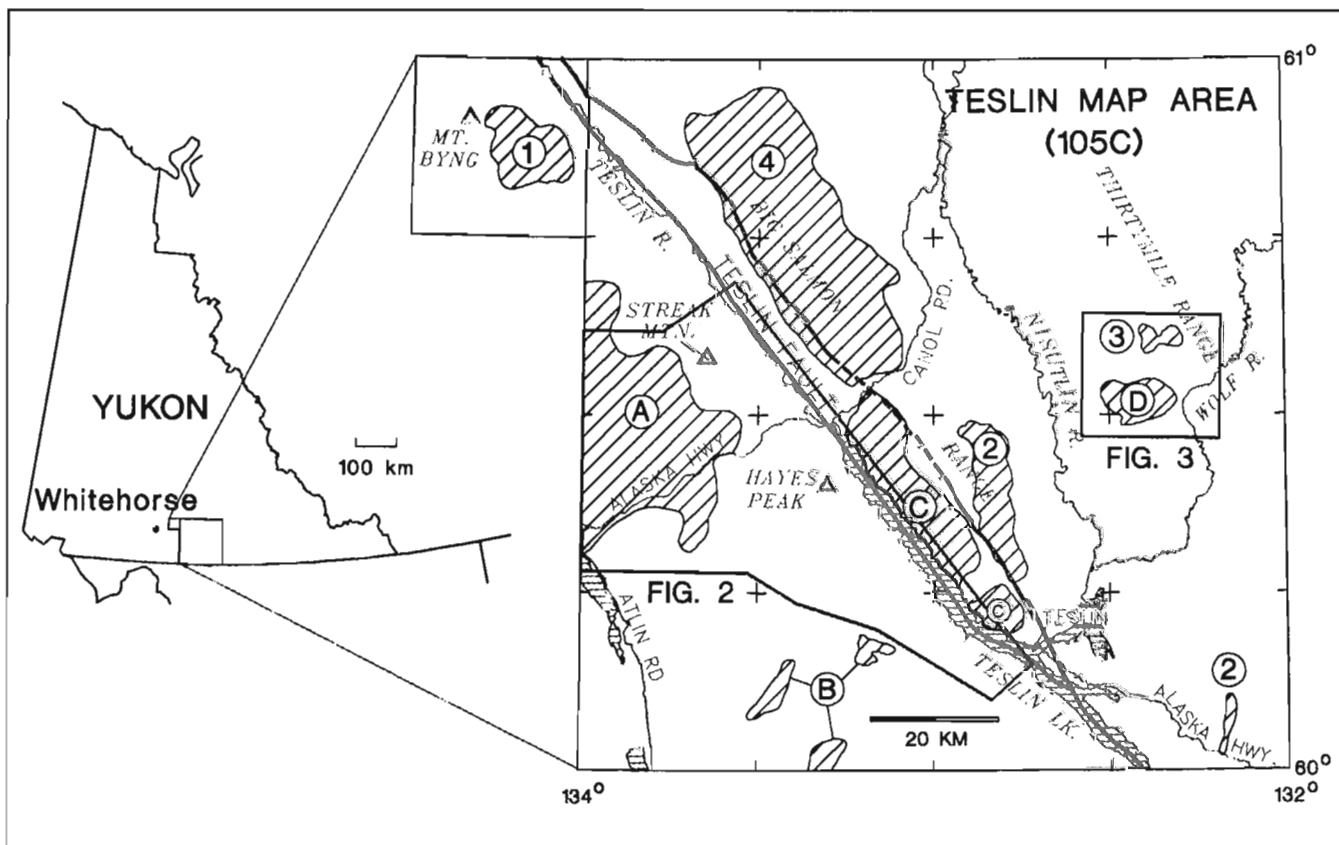


Figure 1. Location of Teslin map area. Hatched areas A-D indicate areas described in this paper. Other hatched areas show location of concurrent fieldwork supported by the Teslin project (1-3) or by EMR Research Agreement (4). See text for details. The dashed lines indicate locations of Figure 2 and Figure 3.

Jura-Cretaceous, as is obduction of allochthons of metamorphosed and mylonitized rock onto North American strata. Unfoliated, post-tectonic mid-Cretaceous granitic plutons occur across the map area.

Four areas were examined (Fig. 1, areas A-D). Other work in the region fully supported through the Teslin project included Master's thesis study of the sedimentology and stratigraphy of Mesozoic strata near Mount Byng, in northeast Whitehorse map area (Fig. 1, area 1), and a postdoctoral study of the metamorphism and structure of the southern Big Salmon Range (Fig. 1, area 2) (Gareau, 1992). Partial logistical support was provided for detailed examination of strata in part of the Thirtymile Range (Fig. 1, area 3) (Harms, 1992). In addition, a structural study of metamorphic rocks of the northern Big Salmon range is currently supported by an EMR Research Agreement (Fig. 1, area 4) (Stevens, 1992). The descriptions that follow are field-based; petrographic and laboratory analysis remains to be done.

VOLCANIC AND INTRUSIVE ROCKS NORTHWEST OF ALASKA HIGHWAY

Strata northwest of the Alaska Highway (Fig. 1, area A; Fig. 2) are mostly massive volcanic rocks (Mulligan, 1963, unit 7). Two volcanic suites are distinguished (see Fig. 2). Northwestern exposures consist of andesite, basalt and minor dacite that typically weather grey to orange-grey. On fresh surface the rocks are light to dark grey, greenish grey, dark olive, or black. The volcanics are characterized by their aphyric, massive character and fine grain size. Calcite amygdules are rare. Well displayed fragmental textures are unusual. Local quartz porphyry is the only porphyritic rock-type and contains 5-10% euhedral and embayed quartz within a dark grey to black aphanitic matrix. Except where fractured, the rocks are extremely well indurated.

At one locality grey-green weathering, massive, aphanitic, medium green volcanics show well developed pillows, and irregular bulbous forms. The pillows range up to 1.5 m across, and in places have an outer spherulite-bearing rind 5-10 cm thick. Grey-white to rust weathering laminated grey chert and siliceous argillite is associated with these volcanics locally.

The second volcanic suite which occurs immediately northwest of the Alaska Highway (Fig. 2) comprises orange-grey and brown-grey weathering, massive, aphyric andesite and/or basalt. Fresh surfaces in fine crystalline varieties range from drab olive, to grey or green. Aphanitic types are typically mottled grey, purplish grey and chrome green, and display a swirly, wispy lamination. Some may be fine fragmental rocks. Coarse, fragmental textures were not seen in any of the volcanics, but could be masked by weathering, alteration and fracturing. Light to dark grey clasts of conchoidally fractured chert are a characteristic component of the volcanics. The proportion of chert varies from 50% in some exposures, to only a few per cent in others. In size, the chert clasts range from fist-sized up to about 40 m across. Rarely they display bedding, although original

bedding may be obscured by close fractures. The chert generally weathers like the surrounding volcanics so that its identity is revealed only upon close inspection. The volcanics also contain rare small to large clasts of medium grey carbonate. One block, at least 30 m across, weathers light blue-grey and contains blobs and irregular patches of dark grey chert. Blocks of chert at least 30 cm across, occur near this particular example. At another locality one of several carbonate blocks (to 20 m across) contains large crinoid columnals. The chert and carbonate blocks were probably incorporated into the volcanic from fault scarps, slumps, or explosive activity during eruption.

Bedding is not seen in the two volcanic units so the effect of faults and folds on stratigraphic thickness is unknown. Based on their aerial extent and relief where exposures occur, the thickness for either succession is estimated at 500 m or more.

The age, stratigraphic relations and affiliation of the two volcanic suites are uncertain. Mutual contacts and those with other rock units are not exposed and where constrained by topography are steep-dipping. The succession on the northwest is continuous with undated volcanic rocks in adjacent Whitehorse map area surmised by Wheeler (1961) to be part of the lower Lewes River Group, and therefore of possible Triassic age. However, the relations of these volcanics with probable Lewes River Group strata in western Teslin map area are not understood (Mulligan, 1963, unit 8; Fig. 2). Volcanics of the same succession underlie the bulk of Streak Mountain.

The volcanics to the southeast are also of uncertain age, but an older limit is given by the youngest age of contained sedimentary fragments (for which microfossil extraction is in progress). The carbonate block mentioned above that carries large crinoid stem fragments was likely derived from upper Mississippian-Pennsylvanian limestone of the Cache Creek Group that is characterized by large crinoid columnals (Monger, 1975, p. 33). The crinoidal limestone clast provides a stratigraphic link to the Cache Creek Group, and based on broad correlation with the volcanic French Range Formation (Monger, 1975) of the group, a Permian age for the succession in Teslin map area is suggested. The French Range Formation occurs on the east side of the Cache Creek belt south of Teslin map area, and locally contains carbonate clasts. Massive basic volcanic rocks forming a fault-bounded panel on the west side of Teslin Lake (Fig. 2) also contain clasts of chert and carbonate (Gordey, 1991) and belong to the same succession as that immediately north of the Alaska Highway.

East-northeast trending fault(s) south of Streak Mountain and near the western margin of the map area partly bound the two volcanic successions (Fig. 2). Further work is required to clarify structural relationships of the two units between Hayes Peak and Streak Mountain (see Fig. 2). However, if the age and affinities of the two volcanic sequences suggested above are correct, the northwest boundary of the Cache Creek Terrane in Teslin map area is a northeast trending fault separating the two assemblages. An implication is that the Cache Creek Group cannot be demonstrated to plunge

northwesterly to become basement to Mesozoic clastic strata of the Lewes River/Laberge groups in northwest Teslin map area.

Two ultramafic bodies, oval in plan, were examined northwest of the Alaska Highway (Fig. 2, unit 11*). They are compositionally alike and consist of peridotite cores flanked

by margins of serpentinite. Peridotite composed of pyroxene 0.5-1.0 cm in diameter in a dark greenish grey to black, fine crystalline matrix comprises the bulk of both bodies. The pyroxene crystals stand out on the orange weathering surface as whitish knots, giving the rock a rough-textured surface. Rarely, variations in concentration of these large pyroxenes

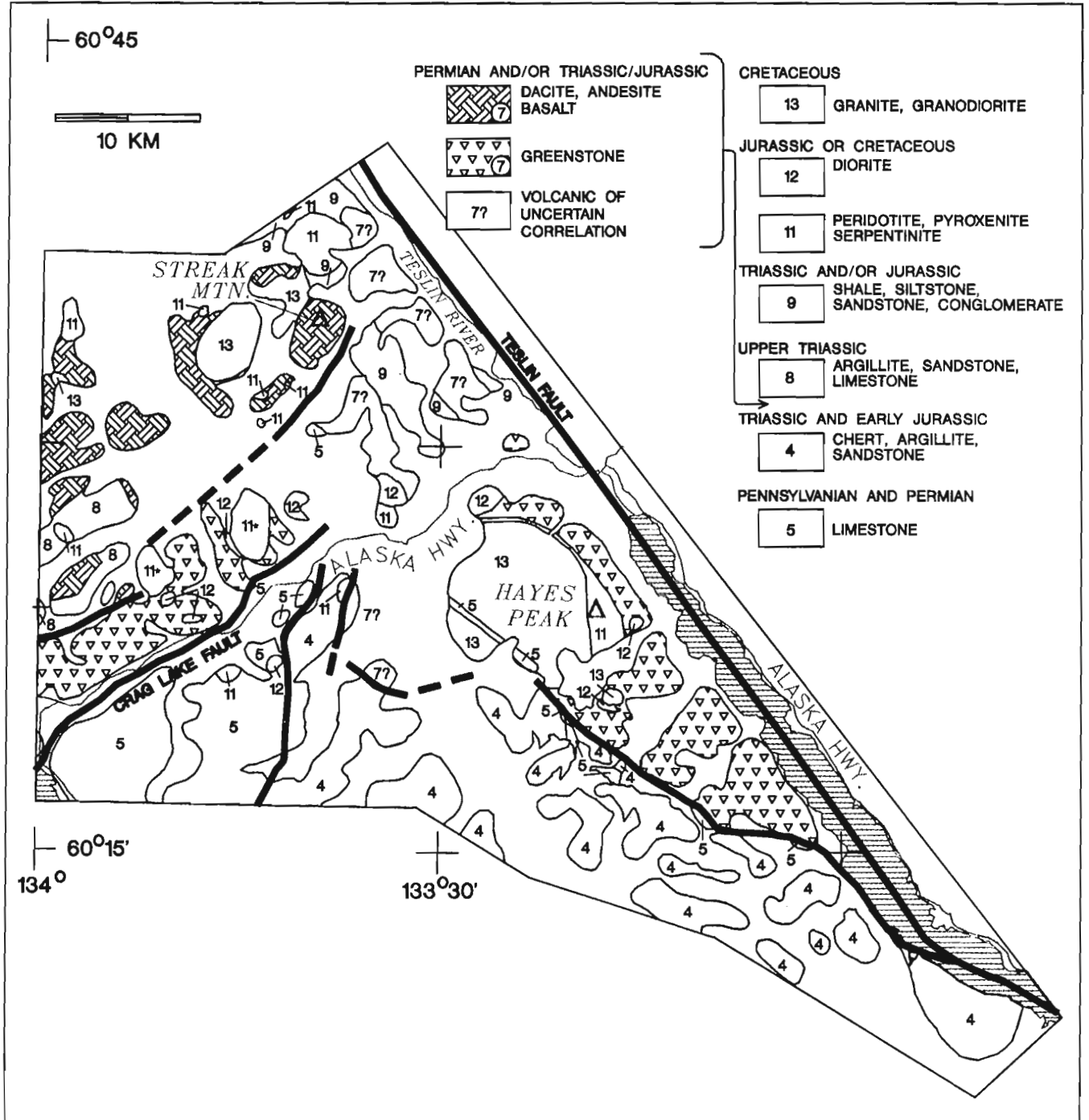


Figure 2. Geological map of part of western Teslin map area. For location see Figure 1. The geology is slightly modified from Mulligan (1963) and for reference retains his map unit designations. Mulligan's unit 7 is subdivided into two volcanic suites. To the northwest are dacite, andesite and basalt of possible Late Triassic(?) age and to the southeast are andesite and basalt of possible Permian(?) age. Ultramafic bodies indicated by asterisk (ie. unit 11*) are referenced in text.

defines a weak foliation and lends the rock a weakly layered aspect. However, well defined mineralogical segregation is not present. Diffuse and irregular patches that lack the large pyroxene crystals occur locally. These have smooth-textured, orange to red weathering surfaces, and approach dunite in composition. The peridotite is locally cut by irregularly oriented 1-3 cm (or more) wide veins of serpentine-magnetite.

Also occurring northwest of the Alaska Highway are small chloritized hornblende(?) diorite intrusions (Fig. 2, unit 12). The diorite typically weathers brown to green and on fresh surface its mafic minerals, amounting from 40-70%, form a speckled dark green to black colour against the white feldspar background. The rocks are massive, and grain size varies from fine to medium grained.

Contacts of the ultramafic and diorite bodies with the country rocks are not exposed. However, the oval shapes and probable steep contacts of the ultramafics argue for an intrusive origin. The diorite is also intrusive and contains inclusions of volcanic country rock. The relative ages of diorite and ultramafic are unclear.

SOUTH TESLIN MAP AREA

Three areas in the south part of Teslin map area underlain by Mesozoic chert and greywacke of the Lewes River assemblage were examined (Mulligan, 1963, unit 4; Wheeler and McFeely, 1987, Fig. 1, area B; Gordey, 1991). The chert is orange, white, grey or black weathering and most commonly black, medium grey, or greyish green on fresh surface. A pale chrome-green variety is rare, but conspicuous. Exposures display excellent, even to lensoidal bedding with bed thickness from 2-8 cm and locally up to 10-15 cm. Black or green argillite forms shaly partings to very thin beds between the chert ribbons. Locally the chert is massive, but this could be partly an artifact of folds and intense fractures obscuring the trace of bedding planes. Radiolaria are abundant and most conspicuous as dark specks on white to light grey weathering surfaces.

The clastic rocks comprise argillite, greywacke and granule to pebble conglomerate. Greywacke forms the bulk of clastic intervals and weathers orange-grey, the orange colour being caused by weathering of disseminated pyrite. On fresh surfaces greywacke is green-grey to dark blue-grey. It is very well indurated. Grain size is typically medium to coarse. Black siliceous argillite interbeds are rare within the greywacke, although some covered intervals could be underlain by this recessive rock type.

In places, the sandstone has scattered clasts of angular, medium to light grey weathering chert that is dark grey to black on fresh surfaces. These most commonly range up to 2-3 cm in diameter; larger chert clasts up to 6 cm across are rare and tend to be rounded. Many chert clasts contain radiolaria. Uncommon, light grey weathering, rounded to angular clasts of black siliceous argillite range up to 8 cm across. The proportion of chert clasts rarely exceeds 10%, and only locally is it large enough to form clast-supported conglomerate. The sandstone is massive and lacks

sedimentary structures. It probably represents sediment gravity flow deposits formed in a submarine fan setting (Gordey, 1991).

The chert and greywacke occur in alternating members 10 to 200 m thick. With rare exception chert beds are not found within the clastic rock and vice versa. Chert members vary from being weakly deformed to intensely crumpled, and in both cases near-vertical dips are commonplace. The greywacke-dominated clastic members lack internal deformation and cleavage. Although greywacke and chert are locally interbedded, the repetition of alternating members of these lithologies over large areas is likely an artifact of intense structural imbrication of a positionally thinner sequence. This structural style persists across strike (ie. west southwesterly) for about 60 km, the width across which these strata are exposed in southwest Teslin map area (ie. unit 4 of Mulligan, 1963). Radiolaria recovered from chert and argillite in this belt are dominantly Late Triassic in age, but range from Middle Triassic (Ladinian) to Early Jurassic (Pliensbachian or early Toarcian) (Cordey et al., 1991).

EAST OF TESLIN LAKE

Strata within the fault-bounded panel east of Teslin Lake (Fig. 1, area C) include clastic and minor volcanic rocks, and minor chert. These are intruded(?) by dunite and highly altered diorite. The exposed thickness may amount to 600(?) m, but the lack of markers combined with possible structural repetition makes this an estimate.

Radiolarian-bearing chert is found low in the succession at several localities where it forms grey to brown weathering well bedded exposures with beds from 10 to 15 cm thick. Black to dark grey argillite forms partings and thin beds. The bulk of the succession is interbedded argillite, siltstone and sandstone. The argillite varies from grey to orange-grey to gunsteel-blue weathering, and on fresh surfaces is dark grey, blue-grey or black. It is commonly highly siliceous, and locally burrowed. The siltstone weathers shades of green to tan and is greenish on fresh surfaces. It typically displays parallel lamination, but is locally graded. The sandstone occurs as massive members from 1 m to at least 50 m thick that weather grey to orange-grey. It is fine to coarse grained and on fresh surfaces is light to medium green. Contacts of sand beds with argillite and siltstone are sharp. Whether some of the thicker sand bodies are multiple beds deposited in rapid succession is unclear. Except for local parallel lamination and centimetre to locally decametre-sized argillite clasts the sandstone is devoid of sedimentary structures. The sandstone contains quartz, much feldspar and as much as 10% fresh, in places euhedral, augite (\pm hornblende?). At one locality sandstone contains suspended rounded clasts up to 15 cm across of augite and augite feldspar porphyry. The augite in the clasts, similar to that in the matrix, is fresh, euhedral and ranged up to a centimetre in diameter.

Non-fragmental volcanic rocks are uncommon within the succession and consist exclusively of augite porphyry. These bodies are no more than 10 m across and typically only 2-3 m. The augite porphyry weathers grey with a surficial orange

weathering rind. On fresh surface it displays euhedral black augite crystals up to a centimetre across and forming about 10% of the rock, set in an aphanitic grey-green matrix. Wherever contact relations are seen, the augite porphyry occurred as dykes, or sills crosscutting bedding at low angles.

Sedimentary features of the sandstones suggest they were deposited as sediment gravity flows. The freshness, abundance and euhedral character of the augite, suggests resedimentation of poorly indurated pyroclastic deposits.

Some sandstones resemble crystal lithic tuff. The augite is unlikely to have remained euhedral and fresh if it had been derived from weathering of an indurated flow-rock.

An ultramafic body about 5.5 km long and 1.3 km across flanks either side of Lone Tree Creek (for location see Mulligan, 1963, unit 11). The ultramafic rocks are dark green dunite which, aside from a centimetre thick orange weathering rind, is remarkably fresh. Serpentinite, and alteration and veining are minimal. Fresh, grey weathering, coarse grained pyroxenite/peridotite is found in one cluster

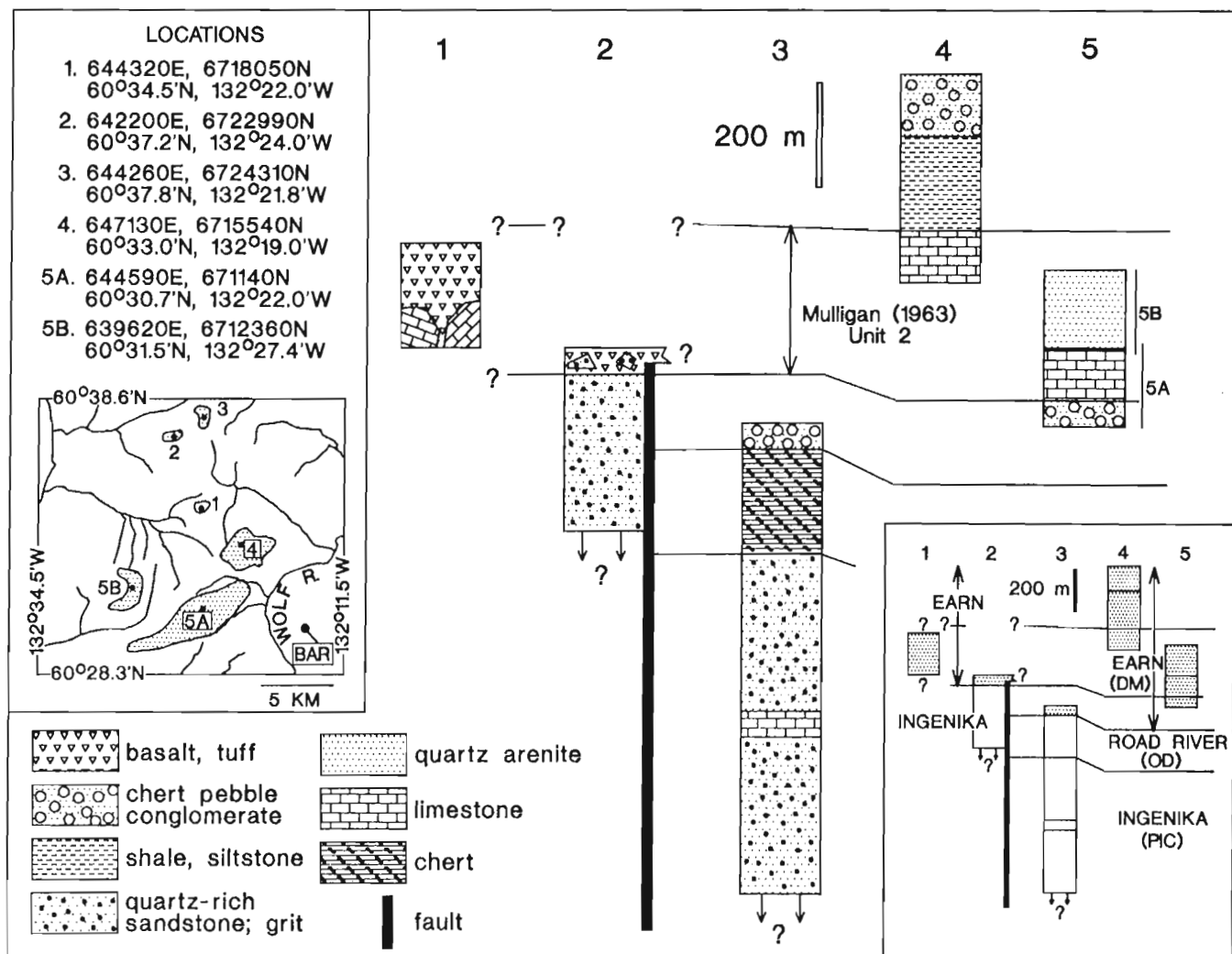


Figure 3. Schematic cross-section showing possible stratigraphic relations for part of the Thirtymile Range, northeast Teslin map area. The fault shown is hypothetical, to account for possible missing stratigraphy beneath the volcanics at location 2 (see text). For location of index map see Figure 1. Co-ordinates are for points shown on the index map, although the sections are derived from map relationships within an entire shaded area. The BAR is a stratabound Pb-Zn-Ag-barite occurrence (INAC, 1990) underlain(?) by Mississippian carbonate of unit 2. The inset stratigraphic section indicates to which strata of the North American margin the Teslin strata are lithologically alike, and the ages inferred from such comparison. Note that some or all of the chert for location 3 could correspond to the Earn (which is chert-bearing) rather than Road River succession as indicated. For reference to North American margin strata see Mansy and Gabrielse (1975) and Murphy (1988) (Ingenika), Gordey and Irwin (1987) (Road River), and Gordey (1988) (Earn). PIC-Proterozoic to Lower Cambrian, OD-Ordovician to Devonian, DM-Upper Devonian and Mississippian.

of exposures at least 100 m across, but its relations to the dunite are uncertain. The ultramafics presumably intrude the surrounding sediments, but contacts are covered. This ultramafic differs from those seen southwest of the Teslin fault. The latter are dominantly peridotite with large resistant pyroxenes in a fine grained matrix (Gordey, 1991).

Flanking either side of Lone Tree Creek at its head (Mulligan, 1963, unit 10b) is highly altered diorite in which original hornblende and/or pyroxene is highly chloritized. Grain size varies widely so that fine and even grained diorite grades into coarse grained pyroxene(?) -feldspar rock within a decametre. At one locality pyroxenite inclusions are pervaded by wispy, and somewhat nebulous injections of fine grained diorite. At other localities, inclusions of felsite and/or baked fine grained sandstone are common. The compositional variations and inclusions weather alike, making it difficult to estimate proportions or to see rock textures. Fine to medium grained diorite with a colour index of about fifty predominates. The diorite may be intrusive or faulted in position.

The sedimentary strata are weakly folded, and for the most part form a homoclinal succession. Bedding most commonly strikes 280-320° and dips 40-60° north. Rarely bedding is near vertical and where tops can be demonstrated, is facing southwest. Cleavage, developed in the fine grained clastics, strikes about 300° and dips 60° (range of 40-90°) to the northeast. Outcrop scale folds are absent. Overall southwest-vergence of folds with long, moderate northeast-dipping limbs and short near vertical southwest-facing limbs is presumed.

Two cherts from low in the stratigraphic section have yielded Upper Triassic (Norian) conodonts (M.J. Orchard, pers. comm., 1991), the first fossils recovered from the succession (ie. from unit 10 of Mulligan, 1963). The nearest similar and partly correlative strata are the Nazcha and Shonektaw formations in Jennings River map area 100 km to the southeast (Gabrielse, 1969). The Shonektaw, a volcanic unit characterized by augite porphyry, massive greenstone and lesser agglomerate and tuff is probably Upper Triassic. The younger Nazcha comprises well bedded volcanic conglomerate, tuff, arkose, siltstone and argillite that ranges into the Early Jurassic (Sinemurian) (H. Gabrielse, pers. comm., 1991).

Because of their age and augite content, the rocks described above (ie. area C, Fig. 1) have been grouped in the Quesnel terrane by Wheeler et al. (1988). These strata (ie. area C) differ from Mesozoic clastic strata along strike in the northwest part of the central panel (Mulligan, 1963, unit 9; see Gordey, 1991) against which they are in uncertain, but probably faulted contact.

THIRTYMILE RANGE

The Thirtymile Range (Fig. 1, area D) is underlain by quartz sandstone, chert, chert pebble conglomerate, andesite and carbonate, that are disrupted by variable and locally intense bedding parallel mylonitization and steep normal faults. Foliation and bedding dip gently. The nature of contacts is

obscured by deformation, but a stratigraphy can be pieced together from different parts of the range. A preliminary working interpretation based on regional correlation and apparent stratigraphic position, but with limited fossil control follows. Figure 3 summarizes previous stratigraphic relations outlined by Gordey (1991), and incorporates new data. Stratigraphic thicknesses are estimated. For fuller lithological descriptions see Gordey (1991).

The only fossiliferous map unit is a limestone containing corals of probably Carboniferous age (Mulligan, 1963, unit 2). Where examined (Fig 1, area D), this carbonate is separated into three members by a central fine to medium grained, massive, quartz arenite. The limestone is overlain by shale, siltstone and finally chert quartz sandstone and chert and quartzite clast conglomerate. Beneath the limestone in order downward are chert-pebble conglomerate, bedded chert, and thick gritty quartz sandstone. The latter is characterized by blue quartz granules, minor interbedded siltstone, and a locally mappable limestone member. At locality 2 (Fig. 3), basaltic volcanics rest directly above the gritty quartzose clastic rocks (see Harms, 1992). The volcanics contain clasts of the underlying quartzite. At locality 1 (Fig. 3), carbonate blocks resembling Carboniferous limestone, rest in a tuffaceous volcanic matrix and are overlain by a basaltic flow, succeeded by volcanic and carbonate matrix conglomerate (Gordey, 1991). The age of these volcanic rocks is uncertain, but must be Carboniferous or younger if the age of the clasts is Carboniferous. A syn-carbonate age is suspected because some beds at locality 1 (Fig. 3) contain volcanic clasts in a largely carbonate matrix. A Mississippian age for basaltic volcanism, combined with the stratigraphic(?) omission beneath them at locality 2 imply block-fault uplift, and erosion before and probably during volcanism. Formation of the BAR, a stratabound barite-Pb-Zn-Ag occurrence (INAC, 1990), southeast of the area studied (Fig. 3), may be linked to this tectonic setting. It rests within a succession of shale, chert, chert sandstone, and minor volcanics (K. Dawson, pers. comm., 1991) that overlies(?) limestone that has yielded conodonts of Mississippian (Late Tournaisian to Early Viséan) age (K. Dawson and M.J. Orchard, pers. comm., 1991).

This area is assigned to the Dorsey Terrane by Wheeler et al. (1988), but the components of the stratigraphic succession have counterparts in North American margin strata (see Fig. 3; Gordey, 1991). A Mississippian age for volcanism and block faulting in the Thirtymile Range is in keeping with Devonian-Mississippian tectonism elsewhere along the North American margin which is characterized by block-faulting, local volcanism, and deposition of chert-rich clastic rocks and local carbonate (Gordey, 1988).

CRETACEOUS MYLONITIC FABRIC IN BIG SALMON RANGE

Gordey (1991) presented a sketch map of part of the southern Big Salmon Range (roughly the main body of area 2, Fig. 1), which includes a large area underlain by foliated and lineated granite. Because of its fabric the granite was thought to be pre-Early Jurassic in age, although it compositionally

resembles unfoliated mid-Cretaceous plutons. A preliminary U-Pb zircon age of 123.1 ± 1.7 Ma (sample location $60^{\circ}25.92'N$, $132^{\circ}50.88'W$) has now been determined for this body (J.K. Mortensen, written comm., 1991), which implies an Early Cretaceous or younger age for its mylonite fabric. The northwest trend of the lineations and their age are consistent with emplacement in a regional stress system dominated by northwest trending dextral faulting, as exemplified by faults bounding the narrow central panel of Figure 1 (see introduction). The Early Cretaceous age also brings into question the age of mylonitic fabrics in other parts of the Big Salmon Range. Are they pre-Early Jurassic as might be assumed through regional correlation (ie. Hansen et al., 1989), or Early Cretaceous or younger, or both?

GUIDE FOR MINERAL EXPLORATION

The present work revealed no new mineral showings. Because of their lack of mineral segregation, the ultramafic bodies described above do not seem promising for economic platinum or chromium deposits. Nor was significant asbestos seen in these bodies.

Occurrences of probable Devonian-Mississippian strata in Thirtymile Range represent a potential for base metal deposits. A hallmark of these strata in other parts of the Cordillera are deposits of stratiform Ag-Pb-Zn-barite such as at Macmillan Pass, Yukon (Bailes et al., 1986) and at the Cirque deposit (Pigage, 1986) in northern British Columbia. Thirtymile Range strata have a good candidate for this type of deposit in the BAR showing (INAC, 1990), mentioned above.

ACKNOWLEDGMENTS

Excellent floatplane support was provided by Aerokon Aviation in Whitehorse. TransNorth Helicopters (Whitehorse) and Discovery Helicopters (Atlin) provided efficient helicopter service. The use of facilities and co-operation of Steve Morison, Chief Geologist, Geological and Exploration Services, Indian and Northern Affairs Canada (Whitehorse) is sincerely appreciated. Rob Stevens, Peter Daubeny, John Paul Rankin, and Stephan Meinke provided superb assistance in the field.

REFERENCES

Bailes, R.J., Smee, B.W., Blackadar, D.W., and Gardner, H.D.
1986: Geology of the Jason lead-zinc-silver deposits, Macmillan Pass, Yukon; in *Mineral Deposits of the Northern Canadian Cordillera*, (ed.) J.A. Morin; Canadian Institute of Mining and Metallurgy, Special Volume 37, p. 87-99.

Cordey, F., Gordey, S.P., and Orchard, M.J.
1991: New biostratigraphic data for the northern Cache Creek Terrane, Teslin map area, southern Yukon; in *Current Research, Part E*; Geological Survey of Canada, Paper 91-1E, p. 67-76.

Gabrielse, H.
1969: Geology of Jennings River map area, British Columbia (104O); Geological Survey of Canada, Paper 68-55, 37 p.
1985: Major dextral transcurrent displacements along the Northern Rocky Mountain Trench and related lineaments in north-central British Columbia; *Geological Society of America Bulletin*, v. 96, p. 1-14.

Gareau, S.
1992: Report on fieldwork in the southern Big Salmon metamorphic complex, Teslin map area, Yukon; in *Current Research, Part A*, Geological Survey of Canada, Paper 92-1A.

Gordey, S.P.
1988: Devonian-Mississippian clastic sedimentation and tectonism in the Canadian Cordilleran miogeocline; in *Devonian of the World*, (ed.) N.J. McMillan, A.F. Embry, and D.J. Glass; Canadian Society of Petroleum Geologists, Memoir 14, vol. II, p. 1-14.
1991: Teslin map area, a new geological mapping project in southern Yukon; in *Current Research, Part A*; Geological Survey of Canada, Paper 91-1A, p. 171-178.

Gordey, S.P. and Irwin, S.E.B.
1987: Geology of Sheldon Lake and Tay River map areas, Yukon Territory, Yukon Territory; Geological Survey of Canada, Map 19-1987.

Hansen, V.L., Armstrong, R.L., and Mortensen, J.K.
1989: Pre-Jurassic ductile deformation and synchronous metamorphism of the Yukon Tanana terrane: geochronologic constraints from the Teslin suture zone, Yukon; *Canadian Journal of Earth Sciences*, v. 26, p. 2224-2235.

Harms, T.
1992: Stratigraphy of the southern Thirtymile Range, Teslin map area, southern Yukon; in *Current Research, Part A*; Geological Survey of Canada, Paper 92-1A.

INAC
1990: Yukon exploration, 1989; Exploration and Geological Services Division, Yukon, Indian and Northern Affairs Canada.

Jackson, J.
1990: Geology and Nd isotope geochemistry of part of the northern Cache Creek terrane, Yukon: implications for tectonic relations between Cache Creek and Stikine (abstract); in *Geological Association of Canada and Mineralogical Association of Canada Joint Annual Meeting, Program with Abstracts*, v. 15, p. A64.

Mansy, J.L. and Gabrielse, H.
1975: Stratigraphy, terminology and correlation of Upper Proterozoic rocks in Omineca and Cassiar mountains, north-central British Columbia; Geological Survey of Canada, Paper 77-17, 17 p.

Monger, J.W.H.
1975: Upper Paleozoic rocks of the Atlin Terrane, northwestern British Columbia and south-central Yukon; Geological Survey of Canada, Paper 74-47, 63 p.

Mulligan, R.
1963: Geology of Teslin map area, Yukon Territory (105C); Geological Survey of Canada, Memoir 326.

Murphy, D.C.
1988: Geology of Gravel Creek (105B/10) and Irvine Lake (105B/11) map areas, southeastern Yukon; Indian and Northern Affairs Canada, Exploration and Geological Services, Yukon, Open File 1988-1, 61 p.

Pigage, L.C.
1986: Geology of the Cirque barite-zinc-lead-silver deposits, northeastern British Columbia; in *Mineral Deposits of the Northern Canadian Cordillera*, (ed.) J.A. Morin; Canadian Institute of Mining and Metallurgy, Special Volume 37, p. 71-86.

Stevens, R.A.
1991: The Teslin suture zone in northwest Teslin map area, Yukon; in *Current Research, Part A*; Geological Survey of Canada, Paper 91-1A, p. 271-277.
1992: Regional geology, fabrics and structure of the Teslin suture zone in northwest Teslin map area, Yukon Territory; in *Current Research, Part A*; Geological Survey of Canada, Paper 92-1A.

Wheeler, J.O.
1961: Whitehorse map area (105D), Yukon Territory; Geological Survey of Canada, Memoir 312, 156 p.

Wheeler, J.O. and McFeely, P.
1987: Tectonic assemblage map of the Canadian Cordillera and adjacent parts of the United States of America; Geological Survey of Canada, Open File 1565.

Wheeler, J.O., Brookfield, A.J., Gabrielse, H., Monger, J.W.H., Tipper, H.W., and Woodsworth, G.J.
1988: Terrane map of the Canadian Cordillera; Geological Survey of Canada, Open File 1894.

Regional geology, fabric, and structure of the Teslin suture zone in northwest Teslin map area, Yukon Territory

R.A. Stevens¹
Cordilleran Division, Vancouver

Stevens, R.A., 1992: Regional geology, fabric, and structure of the Teslin suture zone in northwest Teslin map area, Yukon Territory; *in* Current Research, Part A; Geological Survey of Canada, Paper 92-1A, p. 287-295.

Abstract

The Teslin suture zone in northwest Teslin map area includes three metasedimentary and three metaigneous rock units. Ductile deformation under greenschist to lower amphibolite facies conditions produced protomylonite and mylonite in much of the area. Detailed mapping along two east trending transects about 20 km apart reveals that the suture zone has domains of contrasting structural style with different fabric orientations. In both transects, a western domain of L-S tectonites with well formed mineral lineations passes to the east into a domain dominated by ductile flexural-slip folding with mineral lineations parallel to fold axes, which in turn passes to the east into a domain of poorly formed L-S tectonites with variable fabric orientations. The southern transect intersects a fourth domain farther east that includes L-S tectonites with moderately well formed mineral lineations. The orientation of fabrics are different in the two transects.

Résumé

La zone de suture de Teslin dans le nord-ouest de la région cartographique de Teslin comprend trois unités métasédimentaires et trois unités ignées métamorphisées. La déformation ductile dans des conditions de métamorphisme allant du faciès des schistes verts au sous-faciès inférieur des amphibolites a produit des protomylonites et des mylonites dans une grande partie de cette zone. La cartographie détaillée de la zone longeant deux transects à direction est et espacés d'environ 20 km, révèle que la zone de suture comporte des domaines de style structural contrastant, caractérisés par des orientations de fabrique différentes. Le long des deux transects, un domaine occidental de tectonites L-S, présentant des linéations minérales très nettes, se transforme vers l'est en un domaine où prédomine un plissement par flexure et glissement comportant des linéations minérales parallèles aux axes des plis qui, à son tour, se transforme à l'est en un domaine de tectonites L-S mal formées à orientations de fabrique variables. Le transect sud recoupe un quatrième domaine plus à l'est qui comporte des tectonites L-S à linéations minérales modérément bien formées. Les orientations de fabrique diffèrent le long des deux transects.

¹ Department of Geology, University of Alberta, Edmonton, Alberta T6G 2E3

INTRODUCTION AND REGIONAL SETTING

The Teslin suture zone is part of the Yukon-Tanana composite terrane (Kootenay terrane of Wheeler et al., 1988) of southern Yukon and east-central Alaska. It forms the fundamental boundary between deformed autochthonous North American rocks of the Omineca Belt to the east and accreted terranes of the Intermontane Belt to the west. It has been defined by Hansen (1989) to be "the package of rocks comprising the 15-20 km wide steeply-dipping portion of the Yukon-Tanana terrane in southern Yukon".

Studies of the Teslin suture zone in the Laberge map area recognized three assemblages of ductilely deformed L-S tectonites metamorphosed in the greenschist to albite-epidote amphibolite facies during the early to mid-Mesozoic (Tempelman-Kluit, 1977, 1979, 1984; Erdmer, 1985; Hansen, 1989; Hansen et al., 1989). On the basis of stretching lineation orientation and shear fabric asymmetry Hansen (1989) divided the suture zone into structural domains. Together, the domains record a complex history of deformation that involves extensional shear, thrust shear and strike-slip shear, and are interpreted to result from terrane accretion during oblique plate convergence.

The geology of the Teslin map area is described by Mulligan (1963) and the geology of the northwestern quarter of the map area by Lees (1936). The Teslin map area is being remapped at 1:50 000 and 1:250 000 scales by the Geological Survey of Canada (Gordey, 1991, 1992). Teslin suture zone-related rocks in the southern half of the Teslin map area are the topic of a study in progress (see Gareau, 1992).

This report outlines the regional geology and structural characteristics of the Teslin suture zone in Northwest Teslin map area. An introduction to the regional geology of the area was presented in Stevens (1991). During the summer of 1991, 1:50 000 scale mapping expanded on that completed in 1990. Two detailed structural transects across the suture zone were also completed.

TESLIN SUTURE ZONE MAP UNITS

The geology of the study area is shown in Figure 1. Rock units are grouped into two categories on the basis of fabric development. Rock units in the first category, referred to as Teslin Suture Zone Map Units, display penetrative ductile deformation fabrics and are discussed below. Rocks in the second category, referred to as Other Units, lack a foliation and thus are considered to postdate the development of the Teslin suture zone. Descriptions of these units can be found in Stevens (1991).

Graphitic Phyllite Unit (OD_N?)

This unit consists of sheared, fissile, rusty red to black, fine grained (<1 mm), pyritic graphitic phyllite, calcareous graphitic phyllite, siliceous graphitic phyllite and marble. Tentative interpretations correlate this unit with the Ordovician-Devonian Nasina formation (Stevens, 1991).

Siliceous Schist and Quartzite Unit (PMs)

This unit outcrops in the central part of the map area as an elongate northwest-trending band of quartzite, schist, and phyllite. The predominant rock types are protomylonitic to mylonitic, quartz-muscovite ± chlorite ± epidote ± biotite ± amphibole schist to impure quartzite, muscovite ± chlorite quartzite, and marble. Locally the schists contain feldspar, garnet, pyrite and other opaques. Less common rock types include chlorite-quartz schist, chloritic greenstone and tremolite ± epidote ± garnet calc-silicate. Rocks of this unit are interpreted as part of the Nisutlin Allochthon (Stevens, 1991).

Structural slices of **PM_{tqd}** rocks are interleaved within this unit locally, especially near **PM_{tqd}** bodies. They outcrop as bands 10-300 m wide in contact with **PMs** rocks along fabric-parallel structural contacts.

A 5 m wide band of mafic intrusive rock interpreted as a volcanic fragmental in Stevens (1991), is a xenolithic dyke. It extends for at least 200 m and consists of 30-50% xenoliths in a fine-grained matrix of biotite, amphibole, feldspar and minor pyroxene. The xenoliths are mostly subrounded and show evidence of reaction with the matrix. They are 70-80% massive hornblende and hornblende rich diorite, and foliated diorite, with 20-30% included country rocks (quartzite, marble and schist), and minor possible felsic plutonics. The dyke is massive and cuts the host rock fabric. A massive crosscutting tonalite to quartz-diorite dyke was also found within unit **PMs**; it lacks xenoliths.

Two sub-units rich of **PMs** are recognized. The first is a biotite-amphibole unit, **PM_{sb}** (Fig. 1). The rocks are quartzofeldspathic-biotite ± amphibole schist to biotite bearing meta-arkose. The second, **PM_{sp}**, consists of quartz-muscovite ± graphite ± biotite phyllite, quartzite and possible meta-chert. Locally, the **PM_{sp}** rocks are schistose. The presence of graphite and the phyllitic nature distinguish this sub-unit.

Marble (PM_m)

Marble, unit **PM_m** in Figure 1, is grey to buff, medium grained and sucrosic-textured. It commonly contains 5-40% quartz evenly distributed throughout or in separate bands 3-10 cm wide. Tremolite and epidote are noted locally. Marble is also found within units **OD_N** and **PMs** as 10-30 m wide bands or pods (Stevens, 1991).

Greenstone (PM_{gr})

A greenstone body occurs southeast of the Sawtooth Range (Fig. 1) and includes massive, fine grained, medium to dark green amphibole-chlorite-epidote ± biotite quartzofeldspathic greenstone with 10-50% megacrysts of medium- to coarse-grained hornblende. Other rock types in this unit include fine grained greenstone and amphibolite. Most of the unit is massive, except along its southern margin where strong L-S fabric has developed (Stevens, 1991).

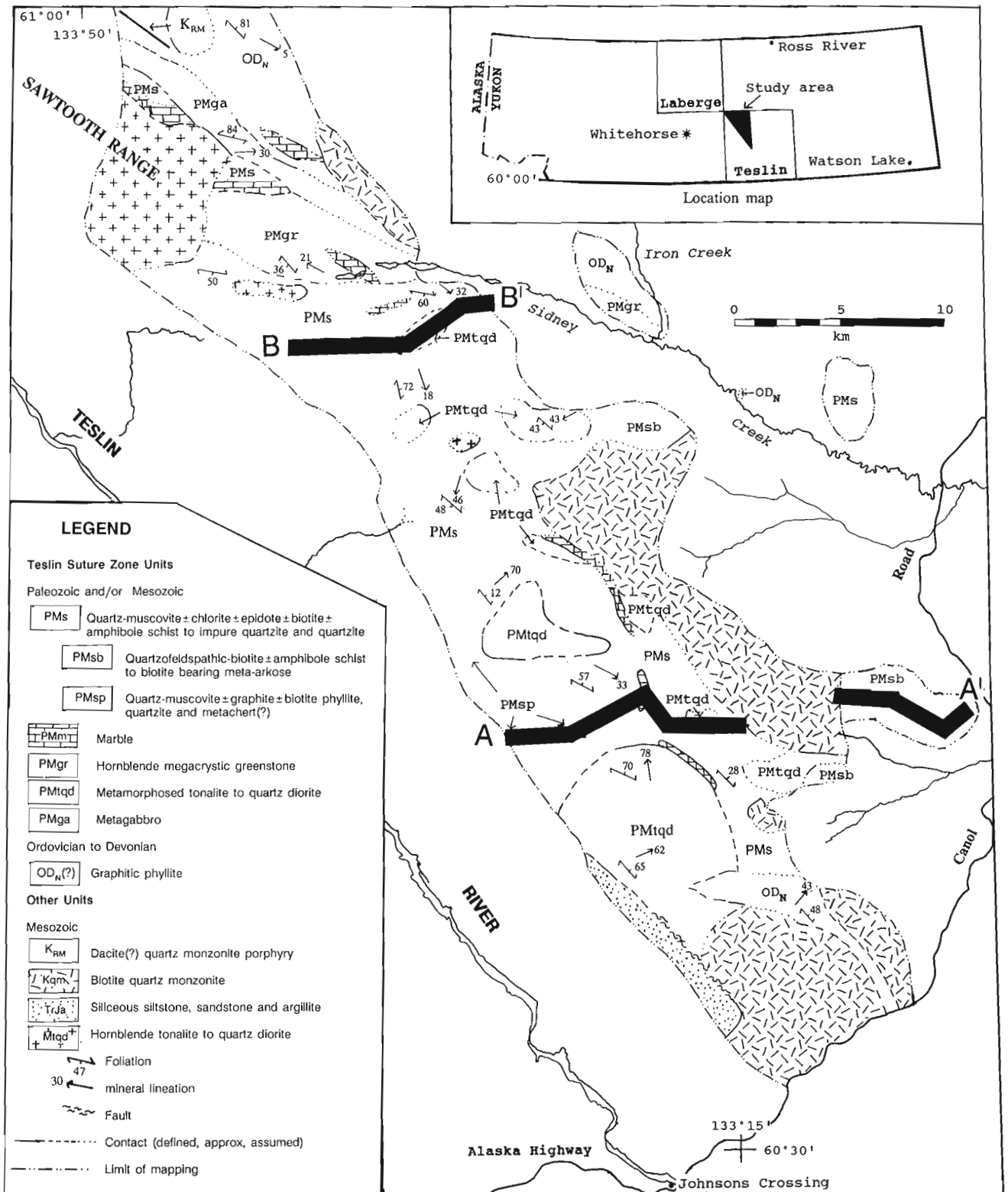


Figure 1. Location map and simplified geological map of the study area modified from Stevens (1991). AA' and BB' are the location of detailed structural transects.

Tonalite to Quartz Diorite (PMtd)

Rocks of this unit outcrop as small bodies in the southern half of the map area. The main rock type is metamorphosed mesocratic tonalite to quartz diorite. Mafic minerals constitute 10-50% and are mainly hornblende, chlorite and biotite. Most of the chlorite and some biotite appear to be alteration products of hornblende. Feldspars are strongly altered to fine grained white mica and epidote. A number of massive mafic dykes cut this unit.

PMtd rocks range from weakly deformed to mylonitic. Areas of weakly deformed rocks are commonly cut by, or grade into, areas of protomylonite and mylonite.

Intrusive contacts with units **PMs** and **OD_N** were observed in a few places, but most contacts are fabric parallel and lack intrusive characteristics. Structural slices of metasedimentary rocks of unit **PMs** are found within some of the bodies, especially near their margins.

Gabbro (PMga)

This unit outcrops as a northwest-trending band east of the Sawtooth Range (Fig. 1). It consists of massive to mylonitic green and white coarse-grained gabbro. Foliated fabric-parallel mafic dykes constitute up to 5% of this unit. The gabbro consists of 50-60% feldspar highly altered to clinozoisite and epidote, 35-60% amphibole, biotite, chlorite, white mica and possible minor pyroxene and <3% quartz. The biotite and chlorite appear to be alteration products of amphibole. This unit was reported as diorite (unit **PMd**) in Stevens (1991). However, the alteration of feldspars to calcic minerals suggests that the anorthite component of the feldspar is greater than 50%, making the rock a gabbro.

METAMORPHISM

The major syn-deformational metamorphic minerals are muscovite, biotite, chlorite, epidote, and, less commonly, amphiboles and garnet. This suggests that metamorphism took place at greenschist to lower amphibolite facies conditions. Garnet is more common in the northern and western parts of the map area than in other parts. Garnet rim-matrix biotite geothermometry on one mylonite sample from unit **PMs** gave a temperature estimate of 380°C ± 50° @ 5 kbar using the calibration of Ferry and Spear (1978). Post-deformational growth of metamorphic minerals occurred locally and may be related to thermal heating accompanying intrusion of quartz-monzonite plutons (unit **Kqm**). However, clear evidence of contact metamorphism is not apparent adjacent to these plutons.

MICROSTRUCTURES AND THE STATE OF DEFORMATION

Rocks from the study area have undergone varying amounts of ductile deformation, producing weak to mylonitic fabrics. In order to characterize the degree of ductile deformation the microstructural characteristics of quartz, and phyllosilicates

and the degree of micro-fabric development are considered. Emphasis is placed on quartz microstructures as they are well documented in the literature (Bell and Etheridge, 1973; Vernon, 1976; Tullis et al., 1982; and Barker, 1990), and quartz is a major constituent of most rocks from the study area.

Under ductile conditions, quartz microstructures are produced mainly by deformation, dynamic recovery and dynamic recrystallization (Bell and Etheridge, 1973). Deformation produces undulose extinction, deformation bands and deformation lamellae developed by intracrystalline slip (Barker, 1990). These dislocation structures impose strain energy on quartz grains that increases with the density of the dislocations. The stored strain energy provides a force for the dynamic recovery (formation of subgrains) and recrystallization (formation of new grains) of the quartz. Figure 2A illustrates some of the quartz microstructures.

Mylonite as used here is a strongly foliated and commonly lineated cohesive rock consisting of 10-50% primary grains or porphyroclasts in a matrix of dimensionally aligned finer grains. The primary grains or porphyroclasts are usually remnant quartz or feldspar grains that are commonly strongly strained, with subgrains and new grains developed at their margins. Mylonite is produced by tectonic grain-size reduction by crystal-plastic processes (ductile deformation).

The following section describes the transition of microstructural characteristics in four stages ranging from weakly deformed to mylonitic. The characteristics are based on observation of more than 175 thin sections from the map area.

Weakly deformed rocks (Fig. 2B) appear massive and undeformed in the field. In thin section quartz grains locally show undulose extinction and deformation bands. Feldspars are unaffected by deformation and phyllosilicates may show minor undulose extinction. Grain size reduction and alignment of minerals is not apparent. Weakly deformed Teslin suture rocks comprise up to 10% of the map area. They occur mostly in units **PMtd** and **PMgr** and rarely in other units.

In moderately deformed rocks (Fig. 2C), quartz grains display undulose extinction, deformation bands, deformation lamellae and subgrains. Some development of new grains and minor grain size reduction is visible. Feldspars, if present, are commonly fractured. Phyllosilicates and occasionally quartz define a weak to moderate foliation, although phyllosilicates are locally variably oriented. Rocks at about the moderately deformed stage underlie 15-20% of the map area and occur predominately in units **PMtd**, **PMgr** and **PMga**.

In strongly deformed and/or protomylonitic rocks (Fig. 2D), many new grains have formed, but 50-90% of the rock consists of strained primary grains or porphyroclasts. The strained primary grains or porphyroclasts are mostly quartz, showing strong undulose extinction, deformation bands, deformation lamellae and subgrains. The margins of many grains include strain-free new grains one-half to one-tenth the size of the original grain. These new grains are

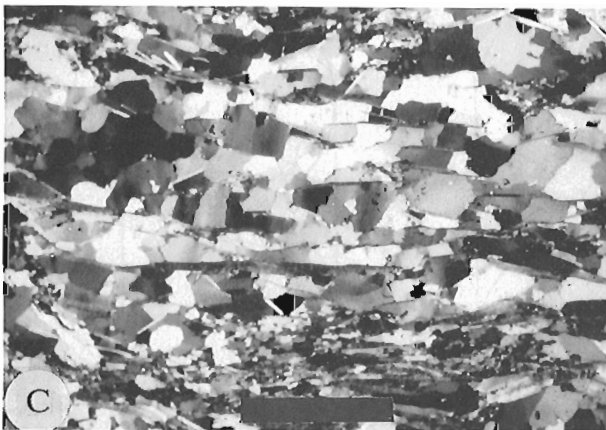
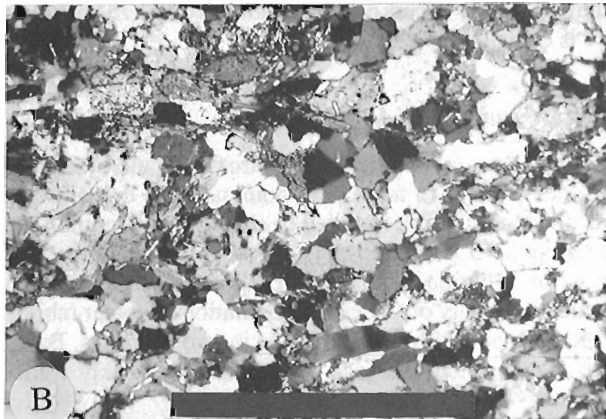
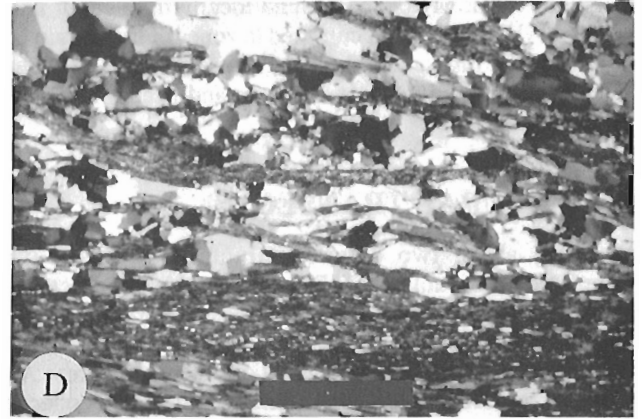
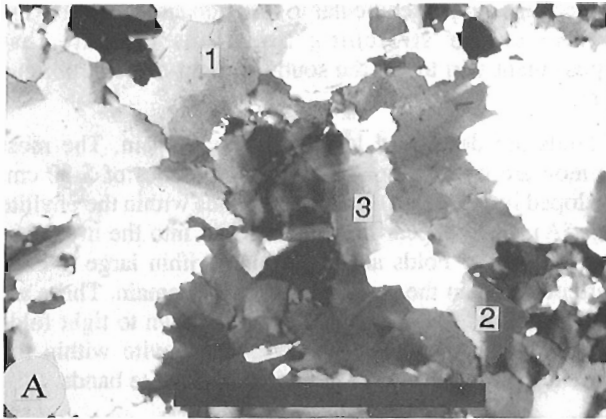


Figure 2. A. Quartz microfabrics illustrated by a muscovite-bearing quartzite, 1-undulose extinction, 2-deformation band, 3-deformation lamellae. B. Weakly deformed rock illustrated by a biotite-bearing arkose. C. Moderately deformed rock illustrated by a muscovite-chlorite quartzite. D. Strongly deformed or protomylonitic rock illustrated by a quartz-muscovite-biotite schist. E. Mylonite rock illustrated by a quartzofeldspathic mylonite derived from hornblende-biotite tonalite. Scale bar on all photos = 1 mm.

commonly elongate in the fabric direction. Areas of small (<0.1 mm) new grains may form bands or zones that alternate or mix with areas, usually augen shaped, of larger (>0.2 mm) strained grains. Phyllosilicates do not show grain size reduction, but are smaller and more elongate than in moderately deformed rocks. They define a moderate to strong foliation that anastomoses around porphyroclasts or augens of strained grains. Kinematic indicators are present in these rocks. Protomylonitic rocks make up 40-60% of the rocks from the map area, mainly in units **PMs** and **ODn**.

The most strongly deformed rocks from the map area are mylonite (Fig. 2E) and rarely ultramylonite. Mylonite consists of 10-50% porphyroclasts or strained primary grains, in a strongly foliated matrix of elongate strain-free grains consisting mostly of quartz and phyllosilicates. The phyllosilicates show dimensional and crystallographic alignment. Grain size reduction is widespread and apparent around the margins of strained primary grains, where smaller new grains formed at the expense of the original larger grains. Kinematic indicators are present in these rocks. Mylonite underlies about 20-30% of the map area particularly in units

PMs and **ODn**. Mylonite is found locally throughout units **PMs** and **OD_N**, and is not confined to zones of high strain but occurs locally throughout these units. In units **PM_{tqd}**, **PM_{ga}** and **PM_{gr}**, mylonite is not common and occurs in narrow zones of high strain.

STRUCTURAL TRANSECTS

Mapping along two detailed structural transects was completed in the summer of 1991. The southern transect (AA' on Fig. 1) is approximately 18 km wide, the northern (BB' on Fig. 1) about 9 km wide. Measurement stations were located 150-250 m apart, resulting in a total of 91 stations across AA' and 45 across BB'. At least one oriented sample was collected at each station.

Four separate structural domains are recognized along AA' and three along BB'. Figures 3 and 4 are strip maps of these transects with contoured stereoplots for each domain.

AA' - Domain 1

L-S tectonites characterize the structure of this domain. Planar fabrics are dominated by mylonitic foliation which clusters near an orientation of 310°/70° (Fig. 3). Mineral and stretching lineations consist of smeared graphite and muscovite, alignment of elongate muscovite, biotite and quartz grains and rodding of quartz. The lineations form a tight cluster plunging 64° towards 2°. C-S fabrics observed in

thin sections cut perpendicular to foliation and parallel to the mineral and/or stretching lineations indicate that displacement was top to the south, or right-reverse, oblique shear.

Folds are developed locally in this domain. The most common are tight to isoclinal with amplitudes of 5-30 cm, developed in small (<10 cm) quartz bands within the phyllite (Fig. 5A). They appear to be transposed into the mylonitic fabric direction. Folds are also found within large (>1 m) quartzite bands in the eastern half of this domain. These are small (amplitudes 1-2 cm) and irregular open to tight folds marked by thin (<1 mm) layers of muscovite within the quartzite. These folds were not noted in phyllite bands.

The western boundary of this domain coincides with the approximate western margin of Teslin suture zone rocks. The eastern boundary occurs over a distance of 0.5-0.75 km where there is a change of structural style.

AA' - Domain 2

Pervasive, flexural slip folds with stretching and/or mineral lineations parallel to folds axes dominate this domain. The folds are open to tight, rounded to chevron, with amplitudes averaging 5-15 cm (Fig. 5B). They fold schistosity and mylonitic foliation. Intense folding across most of this domain commonly obscures the orientation of planar fabrics. An axial planar cleavage was noted in two locations. Bands up to 100 m wide that lack folding or are weakly folded

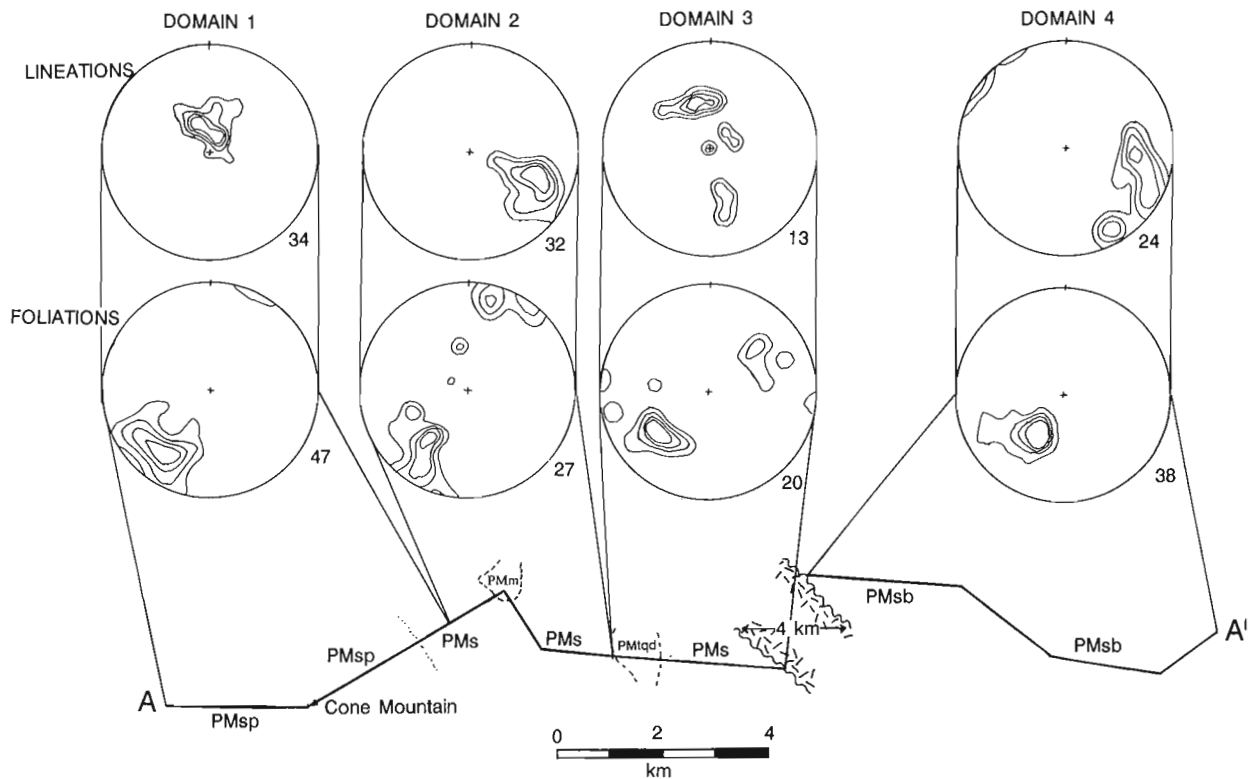


Figure 3. Strip map for transect AA' showing rock types along the transect line. Stereographic projection plots are for the four structural domains recognized in this transect. Contours are densities expressed as multiples of a uniform density. Contours are at densities of 3, 6, 9 and 12.

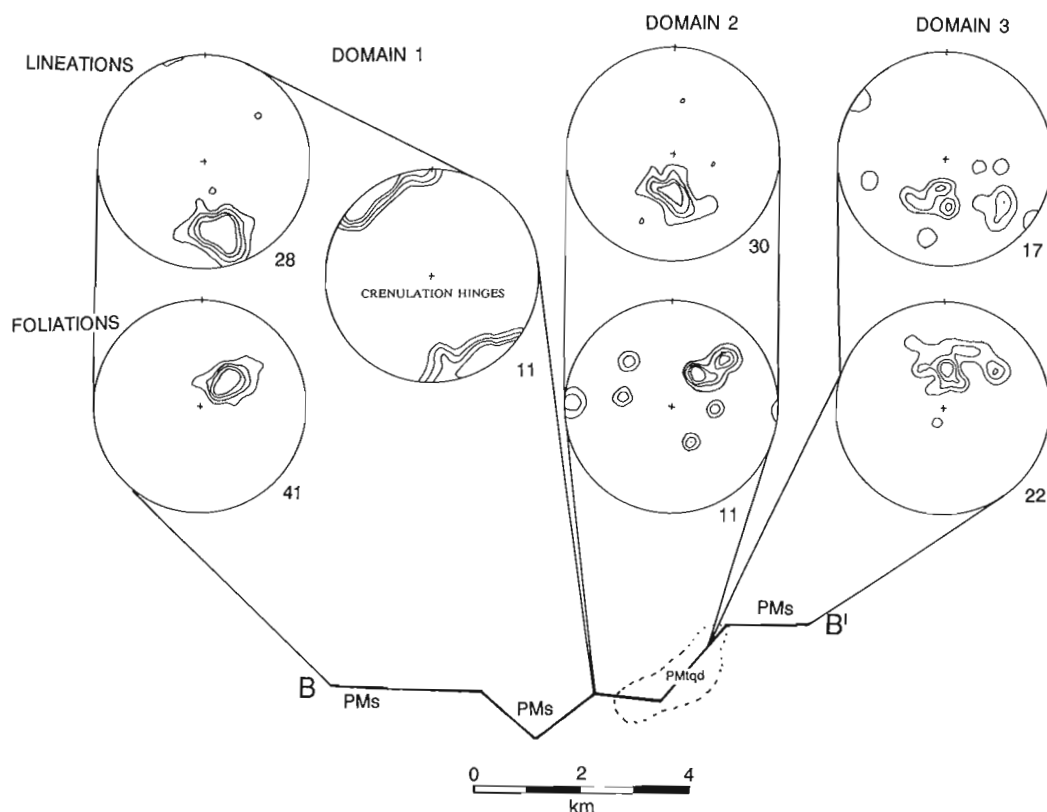


Figure 4. Strip map for transect BB' showing rock types along the transect line. Stereographic projection plots are for the three structural domains recognized in this transect. Contours are densities expressed as multiples of a uniform density. Contours are at densities of 3, 6, 9 and 12.

commonly display mineral lineations defined by quartz, muscovite, chlorite and elongate blade-like grains of chlorite after hornblende. Mineral lineations can also be found within the folded layers. Mineral lineations and fold axes plunge 27° towards 117° on average.

Folds at the outcrop scale or larger are not readily evident in the field. However, poles to schistosity and mylonitic foliation roughly form a great circle perpendicular to the average fold axis, suggesting that the planar fabrics are folded (Fig. 3).

The eastern boundary is <0.5 km wide and is marked by the loss of folds and by the contact to a small body of **PMtd** rocks in domain 3.

AA' - Domain 3

Moderately to strongly deformed and variably oriented L-S tectonites are the most common features of this domain. Figure 3 illustrates the variations in orientation of planar and linear fabrics. Lineations are found in about half of the outcrops. None are strongly developed. Folds are rare and are rootless tight to isoclinal structures transposed into the foliation.

The eastern boundary of this domain is the contact with a massive biotite quartz-monzonite pluton (unit **Kqm**).

AA' - Domain 4

Structures are dominated by L-S tectonites with poorly formed mineral lineations. Foliations cluster around $310^\circ/50^\circ$. Mineral lineations defined by biotite, amphibole and quartz trend southeast and plunge $0-30^\circ$ (Fig. 3). Tight to isoclinal, hand-specimen scale folds are present locally. These appear to be transposed into the fabric.

The western boundary of this domain is at the contact with a massive biotite quartz-monzonite pluton of unit **Kqm**, and the eastern margin is constrained by lack of exposure.

BB' - Domain 1

L-S tectonites dominate this zone. Schistosity and mylonitic foliations cluster near $143^\circ/40^\circ$. Mineral lineations defined by quartz rodding and elongate grains of quartz, muscovite, chlorite, biotite and amphibole plunge 24° towards 170° on average (Fig. 4). A second, less common and generally obscure subhorizontal, crenulation lineation trends northwest or southeast. The relative ages of the two lineations are not clear, but the crenulation lineations are related to minor crenulations that fold the planar fabrics containing the mineral lineations. Small (amplitudes <10 cm), isolated tight to isoclinal folds transposed into the schistosity are present locally.

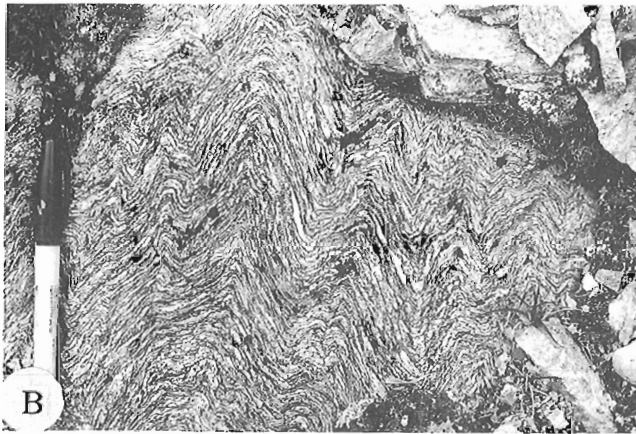
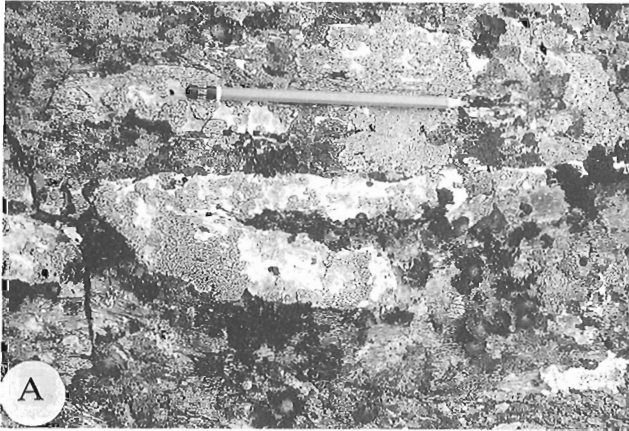


Figure 5. A. Transposed, isoclinal fold of quartzite within a muscovite-biotite-graphite phyllitic mylonite. The pencil is roughly parallel to the mylonitic foliation. This type of fold is present locally in most structural domains. **B.** Ductile flexural-slip folds that have mineral lineations parallel to their fold axes. These folds characterize the structure of domain 2 in AA' and BB'.

The western margin of this domain is constrained by lack of outcrop near the western margin of the suture zone. The eastern boundary is a zone 0.5-1.0 km wide in which folding gradually increases in intensity, mineral lineations are less apparent and fold axes begin to plunge moderately steeply.

BB' – Domain 2

Pervasive, disharmonic, flexural-slip folds with stretching and/or mineral lineations parallel to fold axes dominate this domain. Folds are open to tight and rarely isoclinal, with rounded to chevron hinges. Amplitudes range from <5-30 cm. Mineral lineations defined by quartz rodding, muscovite, biotite, amphibole and elongate chlorite after hornblende can be found in bands of weakly folded rock and less commonly within the folds. Mineral lineations and folds axes plunge 50° towards 180° on average (Fig. 4). Folding has obscured the original orientation of planar fabrics over much of this domain.

The eastern limit of this domain is a zone <0.5 km wide in which folding decreases and becomes a minor component of the structure.

BB' – Domain 3

Inconsistent and commonly weak planar and linear structures are typical of this domain. Foliations strike east to southeast with dips of 40-50° south to southwest (Fig. 4). Mineral lineations are locally developed. The most common trends are south to southeast, with plunges of 30-50°. Small folds, similar to those in domain 2 are present locally.

The eastern limit of the domain is constrained by loss of outcrop in the valley of Sidney Creek.

DISCUSSION

Transects AA' and BB' have similarities and differences. Both have well developed L-S tectonites in the west that pass to the east into a domain dominated by folding, with mineral lineations parallel to fold axes. This in turn grades eastward into a zone of less deformed L-S tectonites with variable mineral lineations. Domain 4 of transect AA' has no equivalent in transect BB'. Deformation decreases eastward in both transects. The difference lies in the orientation of structural fabrics, particularly schistosity and mylonitic foliation which dip north to northeast along AA' but dip south to southwest along BB'. Broad scale late folding may explain the difference in dip direction. However, a simple rotation of structures about the fold axes from the map area do not bring the fabrics from similar domains into common orientation.

Two generations of folds are present. The first, found locally in all domains, are transposed, tight to isoclinal, and commonly rootless. They likely formed as more open folds early in the deformation event, and were subsequently rotated into the X-Y plane of the strain ellipsoid. The later generation are flexural-slip folds that dominate the structure of domain 2 in AA' and BB'. They fold mylonitic foliations and have stretching and/or mineral lineations parallel to their fold axes. Folds with axes parallel to mineral lineations are found within many ductile shear zones (Mattaer et al., 1981; Ghosh and Sengupta, 1987; Malavieille, 1987; and Hansen, 1989; Henderson and Broome, 1990). They are commonly thought to have formed oblique to the shear direction and progressively rotated with increasing strain (Malavieille, 1987). The folds in this study appear to have formed late in the shearing event and do not show evidence of rotation. The origin of this type of folds is poorly understood (Bell and Hammond, 1984; Malavieille, 1987).

ACKNOWLEDGMENTS

Field work was supported by a joint EMR/NSERC research agreement to P. Erdmer and a Northern Scientific Training Program grant from the Department of Indian Affairs and Northern Development, a grant from the Canadian

Circumpolar Institute of the University of Alberta and a Geological Society of America grant awarded to R.A. Stevens. Logistical support provided by the Department of Indian Affairs and Northern Development and the Geological Survey of Canada is greatly appreciated. While in the field I enjoyed visits by S.A. Gareau and D.A. Jones. P. Erdmer is thanked for his help in preparing this manuscript and for reviewing an earlier version of it. D.J. Tempelman-Kluit is thanked for reviewing the manuscript. Andy Turnbull provided excellent assistance in the field.

REFERENCES

- Barker, A.J.**
1990: Introduction to metamorphic textures and microstructures; Blackie and Sons Ltd., London, 169 p.
- Bell, T.H. and Etheridge, M.A.**
1973: Microstructure of mylonites and their descriptive terminology; *Lithos*, v. 6, p. 337-348.
- Bell, T.H. and Hammond, R.L.**
1984: On the internal geometry of mylonites zones; *Journal of Geology*, v. 92, p. 667-686.
- Erdmer, P.**
1985: An examination of the cataclastic fabrics and structures of parts of Nisutlin, Anvil and Simpson allochthons, central Yukon: test of the arc-continent collision model; *Journal of Structural Geology*, v. 7, no. 1, p. 57-72.
- Ferry, J.M. and Spear, F.S.**
1978: Experimental calibration of the partitioning of Fe and Mg between biotite and garnet; *Contributions to Mineralogy and Petrology*, v. 66, p. 113-117.
- Gareau, S.A.**
1992: Report on fieldwork in the southern Big Salmon metamorphic complex, Teslin map area, Yukon; in *Current Research, Part A*; Geological Survey of Canada, Paper 92-1A.
- Ghosh, S.K. and Sengupta, S.**
1987: Progressive development of structures in a ductile shear zone; *Journal of Structural Geology*, v. 9, no. 3, p. 277-287.
- Gordey, S.P.**
1991: Teslin map area, a new geological mapping project in Southern Yukon; in *Current Research, Part A*; Geological Survey of Canada, Paper 91-1A, p. 171-178.
1992: Geological fieldwork in Teslin map area, southern Yukon; in *Current Research, Part A*; Geological Survey of Canada, Paper 92-1A.
- Hansen, V.L.**
1989: Structural and kinematic evolution of the Teslin suture zone, Yukon: record of an ancient transpressional margin; *Journal of Structural Geology*, v. 11, no. 6, p. 717-733.
- Hansen, V.L., Mortensen, J.K., and Armstrong, R.L.**
1989: U-Pb, Rb-Sr, and K-Ar isotopic constraints for ductile deformation and related metamorphism in the Teslin suture zone, Yukon-Tanana terrane, south-central Yukon; *Canadian Journal of Earth Sciences*, v. 26, p. 2224-2235.
- Henderson, J.R. and Broome, J.**
1990: Geometry and kinematics of Wager shear zone interpreted from structural fabrics and magnetic data; *Canadian Journal of Earth Sciences*, v. 27, p. 590-604.
- Lees, E.J.**
1936: Geology of the Teslin-Quiet Lake area Yukon Territory; Geological Survey of Canada, Memoir 203.
- Malavieille, J.**
1987: Kinematics of compressional and extensional ductile shearing deformation in a metamorphic core complex of the northeastern Basin and Range; *Journal of Structural Geology*, v. 9, no. 5/6, p. 541-554.
- Mattauer, M., Faure, M., and Malavieille, J.**
1981: Transverse lineation and large-scale structures related to Alpine obduction in Corsica; *Journal of Structural Geology*, v. 3, no. 4, p. 401-409.
- Mulligan, R.**
1963: Geology of the Teslin map area, Yukon Territory (105C); Geological Survey of Canada, Memoir 326.
- Stevens, R.A.**
1991: The Teslin suture zone in northwest Teslin map area, Yukon; in *Current Research, Part A*; Geological Survey of Canada, Paper 91-1A, p. 271-277.
- Tempelman-Kluit, D.J.**
1977: Quiet Lake (105F) and Finlayson Lake (105G) map areas, Yukon; Geological Survey of Canada, Open File 486.
1979: Transported cataclasite, ophiolite and granodiorite in Yukon: evidence of arc-continent collision; Geological Survey of Canada, Paper 79-14.
1984: Geology, Laberge (105E) and Carmacks (115I), Yukon Territory; Geological Survey of Canada, Open File 1101.
- Tullis, J., Snoke, A.W., and Todd, V.R.**
1982: Significance and petrogenesis of mylonitic rocks: Penrose conference report; *Geology*, v. 10, p. 227-230.
- Vernon, R.H.**
1976: Metamorphic processes: reactions and microstructure development; George Allen and Unwin Ltd., 247 p.
- Wheeler, J.O., Brookfield, A.J., Gabrielse, H., Monger, J.W.H., Tipper, H.W., and Woodsworth, G.J.**
1988: Terrane map of the Canadian Cordillera; Geological Survey of Canada, Open File 1894.

Stratigraphy of the southern Thirtymile Range, Teslin map area, southern Yukon Territory

Tekla A. Harms¹
Cordilleran Division, Vancouver

Harms, T.A., 1992: *Stratigraphy of the southern Thirtymile Range, Teslin map area, southern Yukon Territory*; in *Current Research, Part A; Geological Survey of Canada, Paper 92-1A*, p. 297-302.

Abstract

Detailed mapping in the Thirtymile Range in Teslin map area (105C) documents a stratigraphy that includes carbonate strata, grit, basalt, bedded chert, chert pebble conglomerate, argillite, and siliceous arenite. Different stratigraphic sequences of contrasting lithologies are separated in some places by steeply dipping faults, and elsewhere by low-angle, layer-parallel faults. Direct lithological correlation between these sequences is not possible. Without age data for strata of the study area, it is not clear whether the stratigraphic sequences are telescoped or attenuated facies of equivalent age; sequences of different ages that together comprise a single Precambrian to Paleozoic stratigraphic column; or unrelated assemblages.

Résumé

La cartographie détaillée de la chaîne Thirtymile dans la région cartographique de Teslin (105C) permet de mieux connaître une stratigraphie composée de couches carbonatées, de grès grossier, de basalte, de chert stratifié, de conglomérat de cailloux de chert, d'argilite et d'arénite siliceuse. Différentes séquences stratigraphiques de lithologies contrastantes sont séparées à certains endroits par des failles fortement inclinées, et ailleurs, par des failles faiblement inclinées parallèles aux couches. Il n'est pas possible d'établir de corrélation lithologique directe entre ces séquences. Sans données sur l'âge des couches de la zone à l'étude, on ne peut établir clairement si les séquences stratigraphiques sont des faciès télescopés ou atténués d'âge équivalent; ou si les séquences d'âge différent comporte une seule colonne stratigraphique du Précambrien au Paléozoïque; ou encore si ce sont des assemblages sans liens entre eux.

¹ Department of Geology, Amherst College, Amherst, Massachusetts 01002 USA

INTRODUCTION

Bedded rocks that underlie the Thirtymile Range in Teslin map area (105C) of southern Yukon (Fig. 1) have been included, first, within the domain of the Yukon-Tanana terrane (Monger and Berg, 1987) and, later, within the newly defined Dorsey terrane (Wheeler et al., 1988). This ambiguity has been a consequence of the lack of detailed geological knowledge regarding rocks of the range. Until the regional mapping project presently underway (see Gordey, 1991, 1992), interpretations of the tectonic setting of the Thirtymile Range were based on work by Mulligan (1963) several decades ago.

Recently, Gordey (1991, 1992) has drawn attention to similarities between lithologies in the Thirtymile Range and Precambrian to Paleozoic strata of ancestral North America's continental margin. So that this and any other possible correlations can be tested, 1:25 000 scale mapping and associated geological investigations were initiated in the southern part of the range (Fig. 1) during the 1991 field season. This report outlines the stratigraphy recognized in the study area, and assesses the role of structures that complicate the present distribution of the stratigraphic sequence.

GEOLOGY OF THE SOUTHERN THIRTYMILE RANGE

Stratigraphy

Several contrasting, faulted segments of stratigraphic sequences are recognized within the Thirtymile Range study area (Fig. 2, 3). Lithological differences between the sequences, and the lack of age data for nearly all the units mapped, preclude direct correlation of strata between the various sequences. It is not yet possible to compile a single depositional succession for the study area or to recognize possible facies relationships that may exist amongst the sequences. Stratigraphic sequences that have been mapped in the study area are described below and presented diagrammatically in Figure 3.

Sequence A: A buff weathering, calcareous, grey and silvery grey siltstone (*unit a1*) occurs at the base of this sequence. The siltstone has irregular cleavage which was observed at a high angle to bedding, as expressed by colour banding. The base of this unit is faulted, its structural thickness is approximately 10 m. The siltstone is overlain by a massive grey limestone (*unit a2*), which corresponds to part of unit 2 of Mulligan (1963) and was also described by Gordey (1991). The limestone is recrystallized but preserves

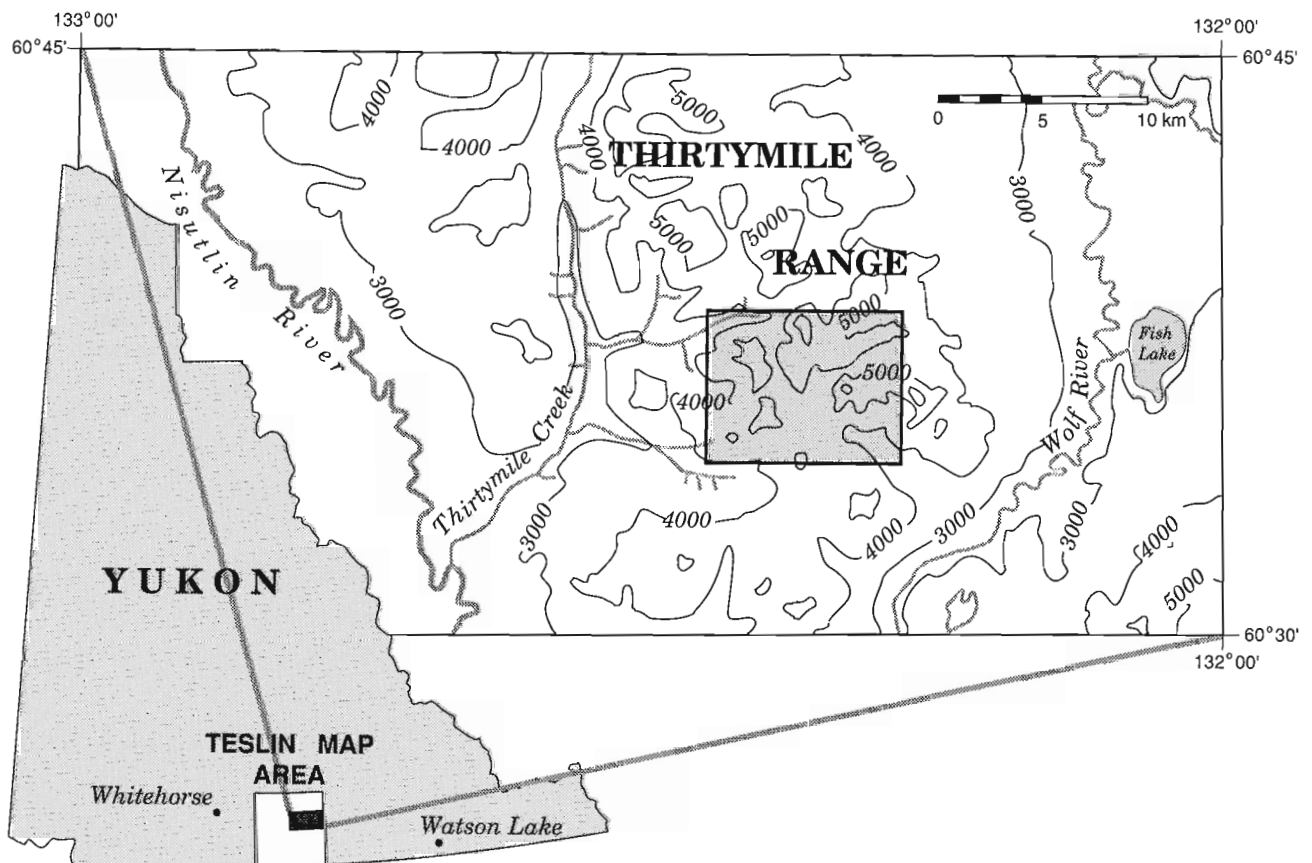


Figure 1. Location of the Thirtymile Range study area in Teslin map area (105C). Area of Figure 2 is shown in light stipple. Contours and drainage taken from 1:250 000 scale topographic base NTS 105C (contour interval 1000 feet).

crinoid columnals, locally abundant and some as large as 1.5 cm in diameter, and rare solitary corals. Blebs and stringers of silicification occur within the limestone and silica-replacement of fossils is present in some domains. Approximately 20 m of this limestone are exposed in the study area. Similar strata nearby have yielded Mississippian fossils (Mulligan, 1963).

Sequence B: This sequence consists of interbedded grey shale or siltstone, silvery green shale or tuffaceous shale, and 1-3 m thick layers of olive-green quartzite (*unit b*). Several small diabasic pods, less than 5 m across, were observed within the outcrop area of sequence B. At the top of sequence B, in fault contact with overlying sequence A, a penetratively sheared quartzite occurs. Foliation in the sheared rock is folded into numerous 1-5 cm wavelength parasitic folds and one northwest-trending outcrop scale fold. The protolith of this rock was quartz-rich but is otherwise indeterminate as no primary sedimentary structures or grains are preserved. The top of sequence B is faulted and the base has not been mapped, consequently its thickness is unknown.

Sequence C: The base of sequence C is a massive marble (*unit c1*) which produces distinctive, although recessive, white outcrops in the study area. It is distinguished from unit

a2 by its greater recrystallization, and a lack of silicification and fossils. The base of this unit was not mapped, but locally as much as 200 m of marble is exposed.

The marble is overlain by 50 m or less of a distinctive clastic rock (*unit c2*) in which elongate, rounded, and flattened carbonate fragments (90%) and less abundant, smaller black siliceous argillite fragments (10%) occur in a very fine grained, crystalline, siliceous matrix. The matrix is predominately white, but includes grey- or light green-coloured irregular, discontinuous seams. This unit interfingers abruptly along strike with marble in unit c1, showing considerable relief (tens of metres) along the contact.

The next overlying unit is a thick (approximately 250 m) sequence of strongly silicified grit (*unit c3*). The grit occurs in massive, 3-5 m thick layers which commonly pinch out along strike over distances of 20-30 m. Thin (approximately 5-10 cm) layers of black argillite or minor chert lie between grit layers in some places, and are more prevalent in the northwesternmost exposures in the study area. Pea green tuffaceous argillite horizons occur sporadically near the top of the grit. Both grading and inverse grading were observed in the westernmost exposures of grit within the study area. In general, the grit has an aphanitic, siliceous, dark to light grey

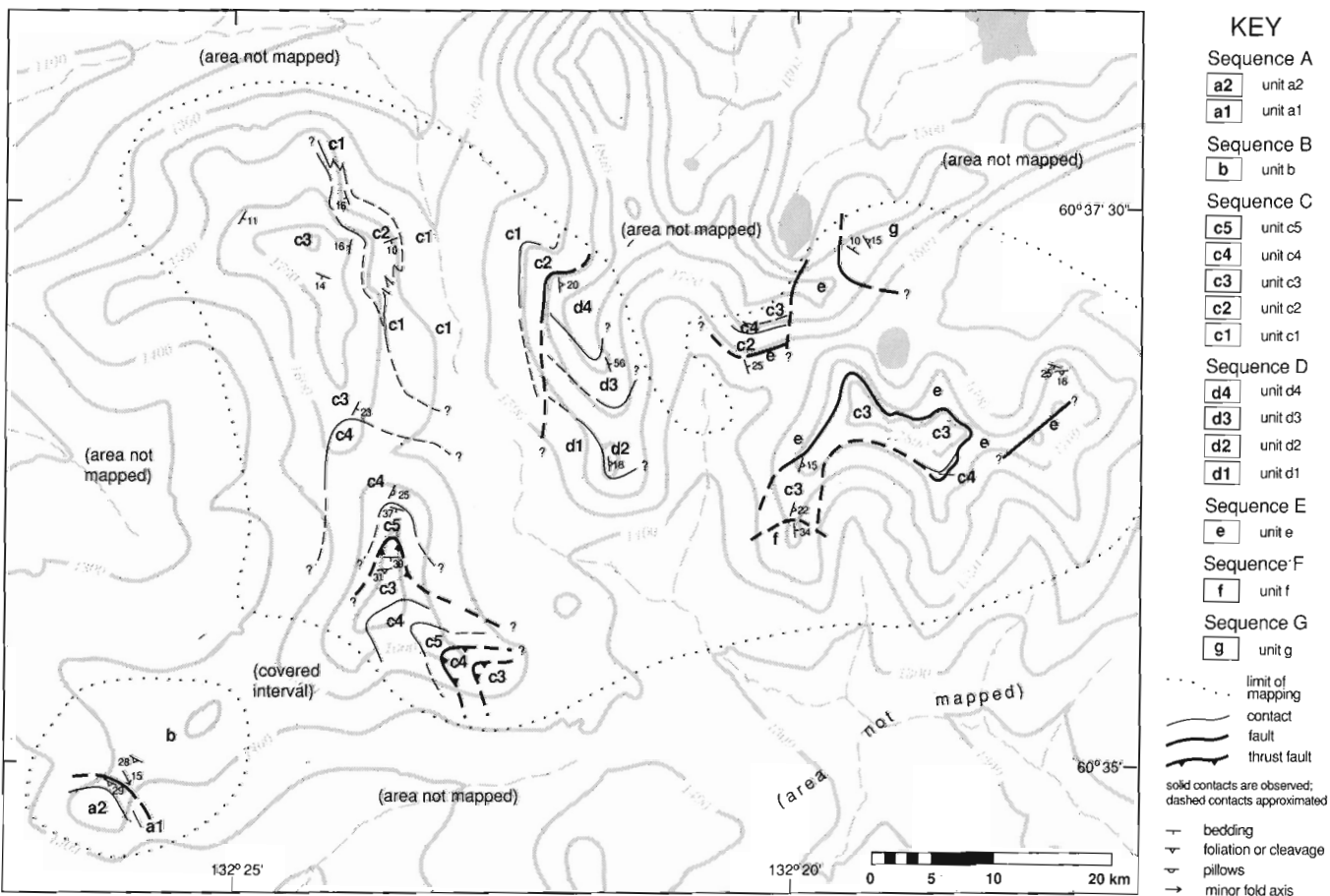


Figure 2. Preliminary geological map of the Thirtymile Range study area. Contours and drainage from 1:50 000 scale metric topographic base NTS 105 C/9 (contour interval 100 m).

matrix with matrix-supported, 1-2 mm, round quartz grains. Some layers have much larger (3-7 mm) quartz and feldspar single-crystal clasts (described in Mulligan, 1963, p. 30).

The grit is overlain by a basaltic flow and pyroclastic unit (*unit c4*) that ranges up to 40-50 m thick. The basaltic extrusive rock is purple-black and dark green. It has irregular scoriaceous to vesicular texture, with well developed, round vesicles, in some places. Pillow shapes were noted in two exposures. The extrusive rock is accompanied by green or purple-grey, fine sand to silt-sized tuff and minor lapilli tuff. Basalt bombs were observed within the tuff at one location. Rare cobbles of grit occur within the volcanoclastic component of this unit, and very large blocks (up to several metres across) of limestone were seen in the basalt in nearly every outcrop. Minor layers of grit, and isolated 1-4 m thick lenses of massive chert occur within the basalt as well. Less than 5 m of distinctive purple slate with green reduction domains occurs discontinuously at the top of the basaltic flows and pyroclastic deposits.

Green bedded chert (*unit c5*) overlies the basaltic unit, and is the top of sequence C as it occurs within the study area. The chert has 3-7 cm thick beds with thinner grey siliceous argillite interlayers. This chert is thoroughly recrystallized, so much so that bedding is obscured in some places.

The distinctive basalt, slate and chert units above the thick grit of sequence C are repeated along 2 or 3 thrust faults at the top of the sequence, in the south-southwestern part of the study area.

Sequence D: This sequence is dominated by chert pebble conglomerate, which occurs at both its base and top, but includes several other, distinct units as well. In the lower, massive chert pebble conglomerate (*unit d1*), there is a continuum in clast size up from a framework of 2-3 mm diameter clasts to larger, 6-10 cm clasts that are matrix supported. All clasts are angular. One large 6 m by 20 m chert olistolith(?) was observed. Clasts in the conglomerate are composed of white chert, grey chert, black siliceous argillite, and chert pebble conglomerate. Throughout the

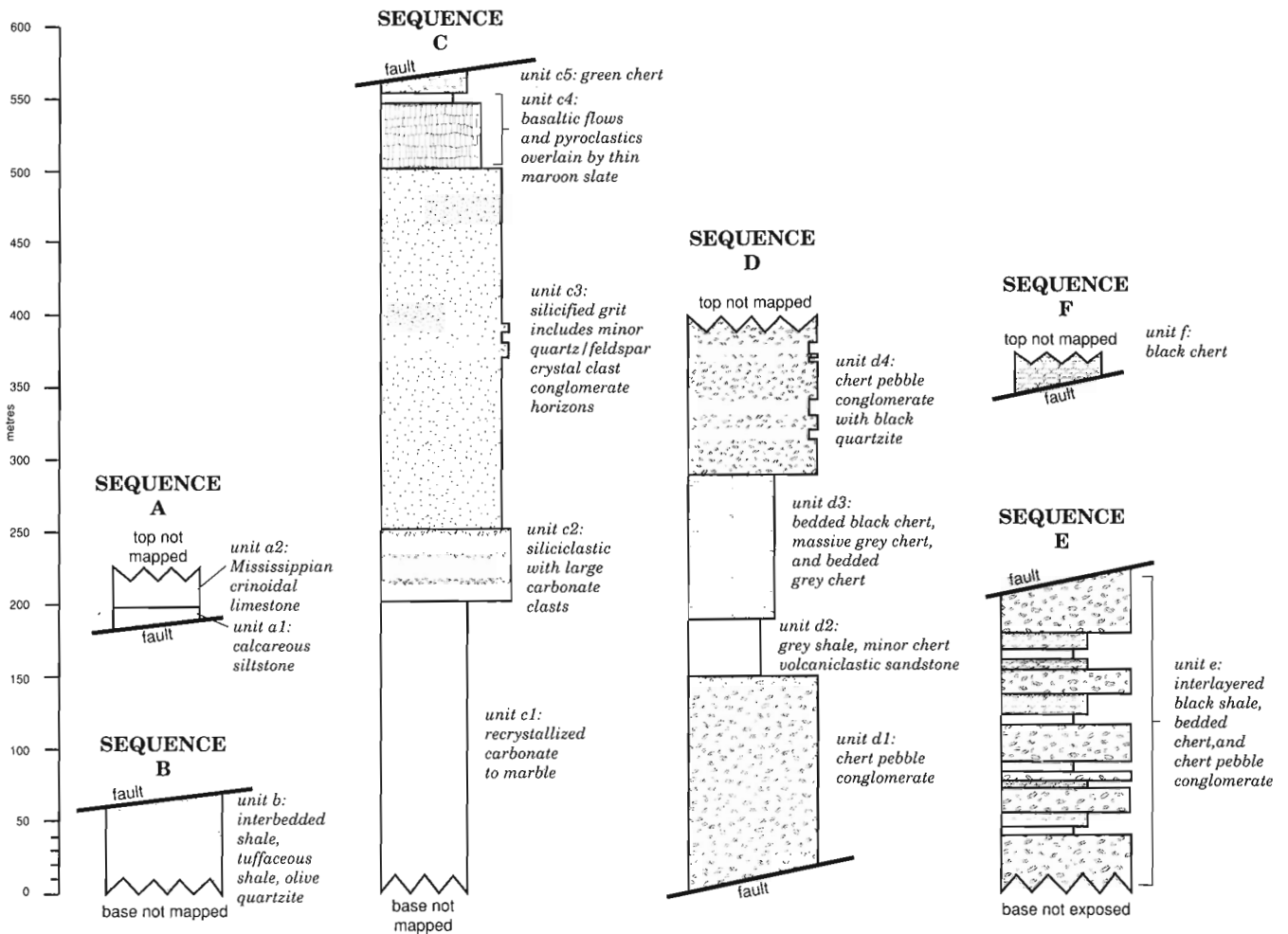


Figure 3. Stratigraphic sequences of the southwestern Thirtymile Range. Thickness of units shown have been estimated based on their outcrop distribution and dip; columns do not represent measured sections. Sequence G (Fig. 2) was observed over only a very limited area and consequently is not included.

approximately 150 m of conglomerate exposed (the base of unit d1 is covered), no reliable bedding indicators were observed.

Approximately 30 m of fissile, dark grey blocky shale to slate with minor grey chert (*unit d2*) overlies the lower chert pebble conglomerate. Minor diabasic dykes crosscut cleavage in this unit. A thin (not more than 10 m), but distinctive horizon of massive, dark green to black volcanoclastic(?) tuff and sandstone occurs above the shale. Fine laminae in this rock are locally contorted by soft-sediment deformation.

Unit d2 is succeeded by thinly bedded (up to 5 cm) black chert with black argillite interlayers. This grades upward into massive, strongly recrystallized, light to dark grey chert, which in turn grades up into bedded grey chert. Altogether, these cherts (*unit d3*) are approximately 100 m thick.

The upper chert pebble conglomerate (*unit d4*) of sequence D overlies chert of unit d3. Conglomerate in unit d4 is indistinguishable from that of unit d1, however, unit d4 also includes interlayered black, fine grained quartzite. The top of unit d4 is truncated by a fault; as exposed, the unit is not less than 100 m thick.

Sequence E: Sequence E consists of interlayered black siliceous argillite and shale with well developed cleavage, bedded black chert in 4 cm beds with 1-2 cm shale interlayers, and chert pebble conglomerate (together constituting *unit e*). Each of these lithologies occurs in individual layers that range from 1 m to approximately 10 m thick. Conglomerate in this sequence is like that in sequence D but is somewhat better sorted. Although angular, clasts predominately range only up to 3-4 cm from a sand-sized matrix. In addition to common light grey chert, chert conglomerate, and black siliceous argillite clasts, fragments of olive-grey chert, chert arenite, and black chert were observed. Locally, pebbles in the conglomerates are strongly flattened and cleavage is developed in the matrix. The base of sequence E is not exposed, and the top of the sequence may be faulted. Not less than 200 m of the sequence is exposed in the study area. Sequence E may correlate with all or part of sequence D, but if so, an abrupt or telescoped facies transition must lie between the two to account for the substantial differences in thickness of individual conglomerate layers and the diverse character of lithologies interlayered with conglomerate. The inclusion of a boulder of grit within unit e in the easternmost part of the study area suggests that sequence E postdates sequence C.

Sequence F: This succession, observed only on the southern margin of the study area, consists of thickly bedded (10-12 cm) white-weathering black chert (*unit f*).

Sequence G: Sequence G comprises interbedded grey chert, massive black siliceous argillite, and grey argillite (*unit g*). Layer-parallel, tabular domains of penetrative deformation occur within this unit, so that in some places the rock is essentially undeformed whereas in others cleavage is developed and in still others chert beds are disrupted or transposed and the rock is strongly and finely foliated. Outcrop-scale, tight to close folds are common.

Structure

The absence of age data in the Thirtymile Range hampers structural as well as stratigraphic analysis, nevertheless, some structural characteristics of the study area have emerged. First, most stratigraphic sequences in the study area are juxtaposed by either steep or shallow dipping faults (Fig. 3). This is most commonly demonstrated by the truncation of units along strike, although in places the faults are accompanied by localized penetrative strain (for example, the fault contact between sequences A and B). Due to lack of age control, it cannot yet be determined if faults between different sequences represent thrust faulting and telescoping or normal faulting and attenuation. Second, several of the stratigraphic sequences appear to be upright. The relative ages of some units can be determined from primary sedimentary indicators of the direction of depositional younging: clasts of underlying units are included in some subsequent deposits (clasts of unit c1 are abundant in unit c2; clasts of unit c3 are found in pyroclastic deposits of unit c4; one boulder of c3(?) grit was observed in unit e), graded bedding occurs rarely (unit c3), and pillow structures were observed in unit c4. Based on this faults within sequence C are thrust faults; they duplicate portions of that sequence and place relatively older units over units higher in the stratigraphic sequence.

Based on the succession of strata found there, in contrast, sequence C underlying ridge tops in the eastern study area (the vicinity of latitude 60°36' to 60°37', longitude 132°19') may be overturned. The facing direction of sequence C at latitude 60°37' between longitude 132°20' and 132°21', and of sequence E that underlies both these areas of sequence C, is uncertain. The nature of the contact between sequences C and E in this location is also not constrained. The absence of much of sequence C's stratigraphy suggests a fault contact, however field evidence for the existence of a fault (truncation of beds or secondary fault structures) does not occur. A depositional contact, albeit overturned, would corroborate evidence from an included grit clast that suggests sequence E is younger than sequence C. It would also require an unconformity with considerable relief along the contact surface. Tectonism during the time span of deposition represented by strata of the study area would be implied.

PRELIMINARY INTERPRETATIONS

Some lithologies mapped within the Thirtymile Range study area, such as bedded radiolarian(?) chert, basalt, chert arenite, and argillite, are known from the adjacent, Late Paleozoic, oceanic Slide Mountain terrane (Harms, 1984, 1986). The sequences in which those rock types occur, however, are distinct from any mapped within the Slide Mountain terrane to date. Furthermore, the Slide Mountain terrane is characterized by the absolute lack of any correlation between adjacent fault-bounded lithotectonic sequences (Harms, 1985, 1986), whereas future field work in the study area may substantiate correlations between sequences D and E based on chert pebble conglomerate, or between sequences C and E based on conglomerate clast provenance.

Other distinctive lithologies in the study area, in particular: grit, Mississippian carbonate, and interbedded chert pebble conglomerate, black argillite and black chert, are similar to those described by Gordey (Gordey et al., 1982; Gordey and Irwin, 1987) for distal North American Precambrian and Paleozoic depocentres in the northern Cordillera (see also Gordey, 1991). Less singular lithologies such as basalt, argillite, and bedded chert have counterparts in North American assemblages but are not, by themselves, diagnostic. It is not yet certain, however, whether lithologies common to both the Thirtymile Range study area and distal North America occur in correlatable stratigraphic sequences (see Gordey, 1992). Clearly, acquisition of fossil and radiometric age dates from units of the Thirtymile Range will improve the strength and reliability of these comparisons.

ACKNOWLEDGMENTS

Acknowledgement is made to the Donors of The Petroleum Research Fund, administered by the American Chemical Society, for partial support of this research. Field work was also supported by a grant from the National Science Foundation and through significant logistical assistance of the Geological Survey of Canada. The contribution of Josh Scala, Amherst College, and of Norm Graham, Capitol Helicopters to the completion of this work is gratefully appreciated.

REFERENCES

- Gordey, S.P.**
 1991: Teslin map area, a new geological mapping project in southern Yukon; in *Current Research, Part A*; Geological Survey of Canada, Paper 91-1A, p. 171-178.
 1992: Geological fieldwork in Teslin map area, southern Yukon Territory; in *Current Research, Part A*; Geological Survey of Canada, Paper 92-1A.
- Gordey, S.P., Abbott, J.G., and Orchard, M.J.**
 1982: Devonian-Mississippian (Earn Group) and younger strata in east-central Yukon; in *Current Research, Part B*; Geological Survey of Canada, Paper 82-1B, p. 93-100.
- Gordey, S.P. and Irwin, S.E.B.**
 1987: Geology of the Sheldon Lake and Tay River map areas, Yukon Territory; Geological Survey of Canada, Map 19-1987.
- Harms, T.A.**
 1984: Structural style of the Sylvester Allochthon, northeastern Cry Lake map area, British Columbia; in *Current Research, Part A*; Geological Survey of Canada, Paper 84-1A, p.109-112.
 1985: Cross-sections through Sylvester Allochthon and underlying Cassiar Platform, northern British Columbia; in *Current Research, Part B*; Geological Survey of Canada, Paper 85-1B, p. 341-346.
 1986: Structural and tectonic analysis of the Sylvester Allochthon, northern British Columbia: implications for paleogeography and accretion; Ph.D. dissertation, University of Arizona, Tucson, 80 p.
- Monger, J.W.H. and Berg, H.C.**
 1987: Lithotectonic terrane map of western Canada and southeastern Alaska; United States Geological Survey, Map MF-1874-B.
- Mulligan, R.**
 1963: Geology of Teslin map area, Yukon Territory (105C); Geological Survey of Canada, Memoir 326.
- Wheeler, J.O., Brookfield, A.J., Gabrielse, H., Monger, J.W.H., Tipper, H.W., and Woodsworth, G.J.**
 1988: Terrane map of the Canadian Cordillera; Geological Survey of Canada, Open File 1894.

Permian and older rocks of the southwestern Iskut River map area, northwestern British Columbia

W.C. McClelland¹
Cordilleran Division, Vancouver

McClelland, W.C., 1992: *Permian and older rocks of the southwestern Iskut River map area, northwestern British Columbia*; in *Current Research, Part A; Geological Survey of Canada, Paper 92-1A*, p. 303-307.

Abstract

The Paleozoic Stikine assemblage in the Iskut River-Craig River region of the Iskut River map area consists of 1) quartzose turbiditic strata, 2) fine-grained tuffaceous clastic rocks of uncertain age, 3) mafic volcanic rocks and argillite of probable Carboniferous age, and 4) Lower Permian limestone and mafic and subordinate felsic volcanic and volcanoclastic rocks. The structurally and inferred stratigraphically lowest unit of quartzose clastic rocks is similar and likely equivalent to continental-derived clastic strata of the Yukon-Tanana terrane in southeastern Alaska, suggesting that parts of the Paleozoic Stikine assemblage may be correlative with Paleozoic rocks of the Yukon-Tanana terrane.

Résumé

L'assemblage de Stikine du Paléozoïque dans la région des rivières Iskut et Craig de la zone cartographique de la rivière Iskut est composé de 1) couches turbiditiques quartzieuses, 2) de roches clastiques tufacées à grain fin d'âge incertain, 3) de roches volcaniques mafiques et d'argilite d'âge probablement carbonifère et 4) de calcaire du Permien inférieur et de roches volcaniques et volcanoclastiques mafiques et felsiques subordonnées. L'unité de roches clastiques quartzieuses la plus basse structurellement et établie par inférence stratigraphique est semblable et probablement équivalente aux couches clastiques d'origine continentale du terrane de Yukon-Tanana dans le sud-est de l'Alaska, indiquant que des parties de l'assemblage de Stikine du Paléozoïque pourraient être corrélées aux roches paléozoïques du terrane de Yukon-Tanana.

¹ Department of Geological Sciences, University of Santa Barbara, Santa Barbara, California 93106

INTRODUCTION

Paleozoic rocks included in the Stikine assemblage (Monger, 1977) are well exposed east of the Coast Belt between the Taku and Iskut rivers (Fig. 1). Recent studies have provided insight into the age and stratigraphy of Lower to Middle Devonian, Carboniferous, and Permian strata of the Stikine assemblage in the Forrest Kerr-Newmont Lake and Scud River regions (e.g., Anderson, 1989; Brown et al., 1991; Gunning, 1992). These studies provide a framework for interpretation and correlation of poorly known, Permian and older rocks outlined by Kerr (1948) and Geological Survey of Canada (1957) south of the Iskut River in the southern Iskut map area (NTS 104B) (Fig. 2).

The nature of the contact between Paleozoic rocks of the Stikine assemblage and metamorphic rocks in the Coast Belt to the west is uncertain. Recent studies in southeastern Alaska suggest that metamorphic rocks west of and within the Coast Belt are correlative with the Yukon-Tanana and/or Nisling terranes (e.g., Gehrels et al., 1990, in press; Gareau, 1991; Rubin and Saleeby, 1991; Samson et al., 1991; McClelland et al., in press) (Fig. 1). Although the juvenile Sm-Nd isotopic signature of the Stikine terrane is distinguished from the evolved signature characteristic of the Yukon-Tanana terrane (Samson et al., 1991). McClelland and Mattinson (1991) suggested that the Stikine assemblage may be partly correlative with mid-Paleozoic rocks in the Yukon-Tanana terrane.

Field work in the Iskut River map area during 1991 focused on pre-Permian rocks of the Stikine terrane to establish and compare the age, character, and geological relationships of the Stikinian basement with the Yukon-Tanana terrane. Permian or older metamorphic rocks exposed south of the Iskut River in the Craig River-Inhini River region (Fig. 2) were examined to provide a stratigraphic and structural framework for geochronological and isotopic studies. The following article summarizes field observations from this region. Results of conodont, macrofossil, geochronological, and isotopic studies underway will be reported elsewhere.

PERMIAN AND OLDER ROCKS IN THE ISKUT RIVER-CRAIG RIVER REGION

Kerr (1948) and Geological Survey of Canada (1957) outlined the regional distribution of metamorphic rocks that underlie limestone of known or suspected Permian age in the Stikine and Iskut rivers region. Schistose to gneissic argillite, metavolcanic rocks, quartzite, and limestone were reported (units 9 and Ga, Gb of Kerr, 1948 and Geological Survey of Canada, 1957, respectively) and examined in this study south of the Iskut River at localities shown in Figure 2. The preliminary descriptions below summarize the lithological sections observed at these localities but will be revised as the results of structural analysis and fossil and geochronological results demand.

Brunt Creek

Brunt Mountain is underlain by a massive section of clinopyroxene porphyritic tuff, flows, volcanoclastic rocks, and argillite of probable Late Triassic age (Kerr, 1948; Geological Survey of Canada, 1957). These volcanic rocks overlie a section of interlayered black argillite, siliceous tuff, fine-grained volcanoclastic rocks, and discontinuous layers of light grey weathering, white marble (Fig. 3a). The marble layers may either be 1) Permian in age based on along strike projection of limestone of probable Permian age exposed at the mouth of Brunt Creek and along the Craig River or 2) Triassic in age based on comparison of this sequence with similar rocks in the Telegraph Creek area (Souther, 1972; D.A. Brown, pers. comm., 1991). In Brunt Creek, the marble-bearing section is underlain by phyllitic argillite and fine-grained volcanoclastic rocks with subordinate brown weathering marble and mafic pillow flows, fragmental rocks, and tuff of uncertain but possible Carboniferous age. In Brunt Creek and north of Brunt Mountain (Fig. 2), hornblende-clinopyroxene gabbro and diorite that are inferred to be Late Triassic in age (Alldrick et al., 1990) and appear compositionally similar to the uppermost volcanic sequence of probable Late Triassic age intrude all of the above units.

Craig River-Simma Creek

The ridge between the Craig River and Simma Creek is underlain by a thick sequence of garnet-biotite-white mica-feldspar-quartz schist derived from fine-grained

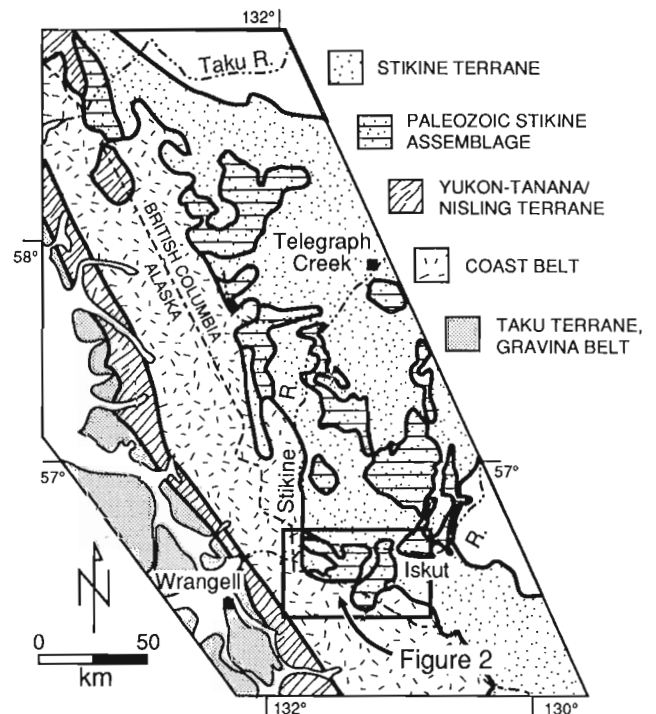


Figure 1. Simplified tectonostratigraphic map showing the location of the study area and distribution of the Paleozoic Stikine assemblage (modified after Wheeler and McFeely, 1987 and Brown et al., 1991).

quartzose turbiditic strata and quartzite (Fig. 3b). Eastern exposures of the clastic sequence are intruded by foliated hornblende-biotite quartz diorite of unknown age. To the west, the quartzose turbidites grade upwards into a thick sequence of light green tuffaceous clastic rocks dominated by centimetre-scale beds of fine-grained sandstone, siltstone, and mudstone. These rocks are in turn overlain by black argillite interlayered with dark brown marble and biotite-amphibole schist derived from mafic tuff and flows. The argillite and volcanic section is capped by light grey weathering, white marble that is apparently laterally continuous with limestone of probable Permian age exposed along the Inhini River (Fig. 2).

Quartz-rich clastic rocks at the base of this section are similar to continent-derived sediments of the Yukon-Tanana terrane in southeastern Alaska (e.g., Gehrels et al., 1990). This correlation and the apparent depositional relationship between the quartzose clastic rocks and Permian rocks of the Stikine terrane suggest that the Paleozoic Stikine assemblage either depositionally overlies or laterally grades into the Yukon-Tanana terrane.

Dick Creek-Inhini River

East of the Inhini River, limestone of probable Permian age is faulted against a thick sequence of pyroxene crystal lithic tuff and volcanoclastic rocks likely correlative with the Upper Triassic Stuhini Group (Fig. 2, 3c). Nonetheless, the contact is likely a faulted depositional contact. Rocks depositionally underlying the limestone in the unnamed creek south of Fizzle Mountain (Fig. 2) include tuffaceous siltstone and sandstone, siliceous siltstone, mafic tuff, and minor brown weathering limestone. North-dipping, massive Permian limestone along the north side of Dick Creek is underlain by probable Carboniferous interlayered green to brown tuffaceous siltstone, mafic flows, lapilli tuff, and breccia. Thin limestone lenses within the volcanic section contain abundant crinoid fragments and rugose corals. Volcanoclastic rocks at the base of the unit grade down into light grey siliceous argillite. The upper portion of the argillite contains a relatively thin (<10 m) coarsely crystalline white marble. Exposures south of Dick Creek are dominated by a thick section of light green, tuffaceous to quartzose turbiditic rocks that are similar to the clastic rocks overlying the sequence of quartzose turbidites and quartzite south of Simma

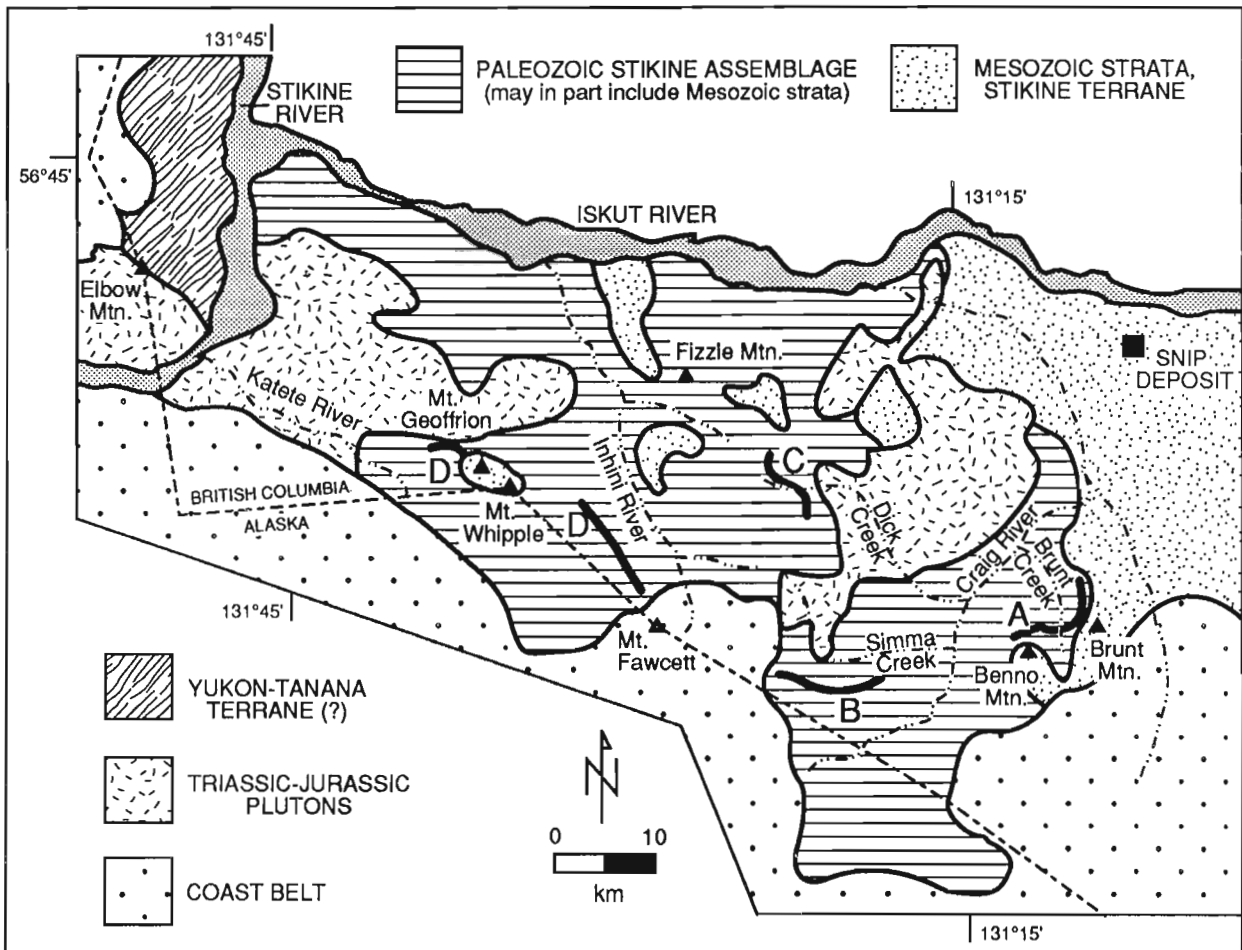


Figure 2. Location of study area showing the distribution of the Stikine assemblage (modified after Kerr, 1948 and Wheeler and McFeely, 1987) and general location of schematic columns A-D shown in Figure 3.

Creek (described above). Centimetre-scale beds of fine-grained sandstone, siltstone, and mudstone that make up the section may be Carboniferous or older because they appear to underlie the volcanic section exposed north of Dick Creek.

Mount Geoffrion-Mount Fawcett

Mount Geoffrion and Mount Whipple (Fig. 2) are underlain by a thick sequence of probable Triassic mafic to intermediate, pyroxene-, amphibole- and plagioclase-bearing tuff, debris flows, volcanoclastic rocks, and subordinate argillite (Fig. 3d) that depositionally overlies massive light grey to white limestone of known Permian age (D.A. Brew, unpub. data). West of Mount Geoffrion, the limestone overlies centimetre-scale beds of fine-grained volcanoclastic rocks, tuff, and argillite. The lower sequence contains at least two, undated, massive, 5 to 20 m-thick limestone layers. Probable Permian limestone along the ridge north of Mount Fawcett

(Fig. 2) is underlain by mafic volcanic rocks, argillite, and fine-grained tuffaceous clastic rocks. This section is similar to that observed below limestone of probable Permian age south of Simma Creek.

SUMMARY

A generalized sequence for the poorly dated Stikine assemblage in the Iskut-Craig rivers region can be inferred from the sections presented in Figure 3. Lower Permian limestone generally overlies probable Carboniferous mafic volcanic rocks and argillite. The Carboniferous sequence overlies a thick fine-grained tuffaceous clastic and subordinate mafic volcanic rock unit of unknown age. The clastic rocks in turn grade down into quartzose turbiditic strata that resemble continental-derived clastic strata of the Yukon-Tanana terrane in southeastern Alaska.

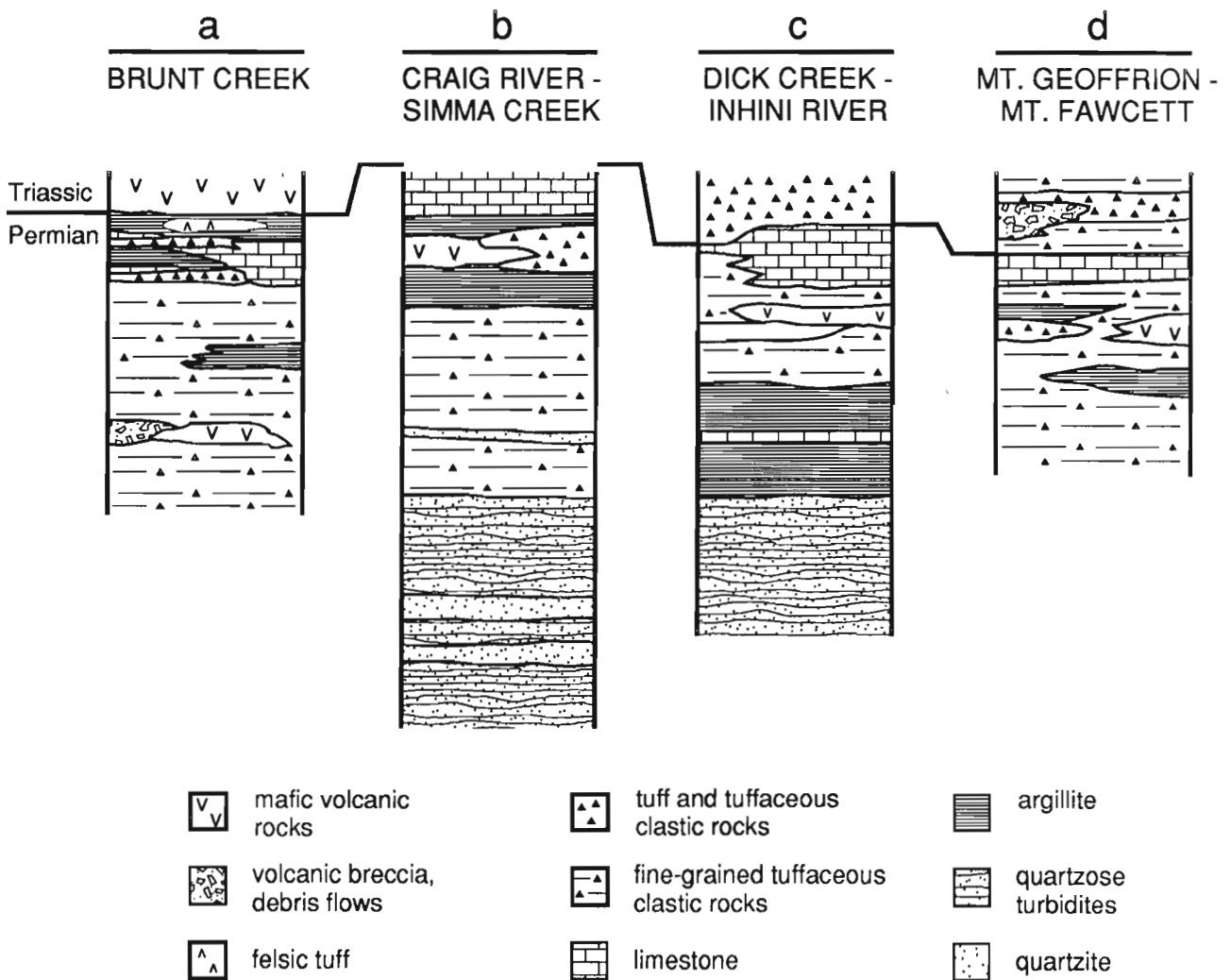


Figure 3. Schematic stratigraphic columns of the Paleozoic Stikine assemblage in the Iskut River-Craig River region. (a) Brunt Creek. (b) Craig River-Simma Creek. (c) Dick Creek-Inhini River. (d) Mount Geoffrion-Mount Fawcett. See Figure 2 for general location.

ACKNOWLEDGMENTS

Field work in the Iskut River map area, funded by the Geological Survey of Canada (Project 840046) and by NSF grant EAR-8917316 (awarded to J.M. Mattinson), was conducted in close collaboration with R.G. Anderson. The field observations outlined above are the result of coordinated mapping efforts of myself, M.H. Gunning and J. Rublee.

REFERENCES

Alldrick, D.J., Britton, J.M., Maclean, M.E., Hancock, K.D., Fletcher, B.A., and Hiebert, S.N.

1990: Geology and mineral deposits of the Snippaker area; British Columbia Ministry of Energy, Mines, and Mineral Resources, Geological Survey Branch, Open-File Map 1990-16.

Anderson, R.G.

1989: A stratigraphic, plutonic, and structural framework for the Iskut River map area, northwestern British Columbia; *in* Current Research, Part E; Geological Survey of Canada, Paper 89-1E, p. 145-154.

Brown, D.A., Logan, J.M., Gunning, M.H., Orchard, M.J., and Bamber, W.E.

1991: Stratigraphic evolution of the Paleozoic Stikine assemblage in the Stikine and Iskut rivers area, northwestern British Columbia; *in* Contributions to the Geology and Geophysics of Northwestern British Columbia and Southeastern Alaska, (ed.) R.G. Anderson; Canadian Journal of Earth Sciences, v. 28, p. 958-972.

Gareau, S.A.

1991: The Scotia-Quaal metamorphic belt: a distinct assemblage with pre-early Late Cretaceous deformational and metamorphic history, Coast Plutonic Complex, British Columbia; *in* Contributions to the Geology and Geophysics of Northwestern British Columbia and Southeastern Alaska, (ed.) R.G. Anderson; Canadian Journal of Earth Sciences, v. 28, p. 870-880.

Gehrels, G.E., McClelland, W.C., Samson, S.D., and Patchett, P.J.

in press: U-Pb geochronology of detrital zircons from the Yukon crystalline terrane in the northern Coast Mountains batholith, southeastern Alaska; Canadian Journal of Earth Sciences.

Gehrels, G.E., McClelland, W.C., Samson, S.D., Patchett, P.J., and Jackson, J.L.

1990: Ancient continental margin assemblage in the northern Coast Mountains, southeast Alaska and northwest Canada; *Geology*, v. 18, p. 208-211.

Geological Survey of Canada

1957: Stikine River area, Cassiar District, British Columbia; Geological Survey of Canada, Map 9-1957.

Gunning, M.H.

1992: Carboniferous limestone, Iskut River region, northwest British Columbia; *in* Current Research, Part A; Geological Survey of Canada, Paper 92-1A.

Kerr, F.A.

1948: Lower Stikine and western Iskut river areas, British Columbia; Geological Survey of Canada, Memoir 246, 94 p.

McClelland, W.C. and Mattinson, J.M.

1991: U-Pb (zircon) constraints on the age of the Yukon-Tanana terrane in the Coast Mountains, central southeast Alaska and British Columbia (abstract); Geological Society of America, Abstracts with Programs, v. 23, p. A434.

McClelland, W.C., Gehrels, G.E., Samson, S.D., and Patchett, P.J.

in press: The Gravina belt and Yukon-Tanana terrane in central southeastern Alaska: protolith relations of metamorphic rocks along the western flank of the Coast Mountains batholith; *Journal of Geology*.

Monger, J.W.H.

1977: Upper Paleozoic rocks of the western Canadian Cordillera and their bearing on Cordilleran evolution; Canadian Journal of Earth Sciences, v. 14, p. 1832-1859.

Rubin, C.M. and Saleeby, J.B.

1991: Tectonic framework of the upper Paleozoic and lower Mesozoic Alava sequence: a revised view of the polygenetic Taku terrane in southern Alaska; *in* Contributions to the Geology and Geophysics of Northwestern British Columbia and Southeastern Alaska, (ed.) R.G. Anderson; Canadian Journal of Earth Sciences, v. 28, p. 881-893.

Samson, S.D., Patchett, P.J., McClelland, W.C., and Gehrels, G.E.

1991: Nd isotopic characterization of metamorphic rocks in the Coast Mountains, Alaskan and Canadian Cordillera: ancient crust bounded by juvenile terranes; *Tectonics*, v. 10, p. 770-780.

Souther, J.G.

1972: Telegraph Creek map area, British Columbia; Geological Survey of Canada, Paper 71-44, 38 p.

Wheeler, J.O. and McFeely, P.

1987: Tectonic assemblage map of the Canadian Cordillera; Geological Survey of Canada, Open File 1565.

Geological Survey of Canada Project 840046

Elbow Mountain crystalline complex, Iskut River map area, northwestern British Columbia

S. Porter¹
Cordilleran Division, Vancouver

Porter, S., 1992: Elbow Mountain crystalline complex, Iskut River map area, northwestern British Columbia; in *Current Research, Part A; Geological Survey of Canada, Paper 92-1A*, p. 309-313.

Abstract

The Elbow Mountain crystalline complex comprises amphibolite facies, polydeformed, metasedimentary rocks which were intruded by Early Jurassic and Eocene plutons. Protolith assemblages include garnet-bearing metapelite, metaconglomerate, metabasite, marble, quartzite, and calc-silicate rocks. Metamorphic rocks on Elbow Mountain range from low grade to lower amphibolite facies and possess primary cleavage (S_1) that was folded into north-northwest trending folds (D_2) that are overturned to the east-northeast. Farther north, gneissic metasediments underlie Glacier Mountain and are folded into northwest-trending isoclinal folds. Granoblastic mineral development is confined to S_1 cleavage and apparently syntectonic to D_1 . Late syn- to post-kinematic, Early Jurassic, foliated quartz monzodiorite crosscuts S_1 cleavage, but apophyses and dykes are subparallel to cleavage. Eocene plutons consist of at least two phases and crosscut Glacier Mountain gneiss.

Résumé

Le complexe cristallin d'Elbow Mountain comprend des roches métasédimentaires polydéformées à faciès des amphibolites qui ont été recoupées par intrusion par des plutons du Jurassique inférieur et de l'Éocène. Les assemblages de roche originelle contiennent de la métapélite grenatifère, du métaconglomérat, des roches ignées basiques métamorphisées, du marbre, du quartzite et des roches à silicates calciques. Les roches métamorphiques sur le mont Elbow dont le faciès varie d'un métamorphisme faible à un métamorphisme inférieur aux amphibolites possèdent un clivage primaire (S_1) qui a été déformé en plis à direction nord-nord-ouest (D_2) déversés vers l'est-nord-est. Plus au nord, les métasédiments gneissiques reposent au-dessous du mont Glacier et ont été déformés en plis isoclinaux à direction nord-ouest. La minéralisation granoblastique se limite au clivage S_1 et est apparemment syntectonique à D_1 . Une monzodiorite quartzique feuilletée tardive de syncinématique à post-cinématique du Jurassique inférieur recoupe le clivage S_1 , mais les apophyses et les dykes sont quasi parallèles au clivage. Les plutons éocènes sont composés d'au moins deux phases et recoupent le gneiss du mont Glacier.

¹ Department of Geology and Geophysics, University of Calgary, 2500 University Drive, N.W., Calgary, Alberta T2N 1N4

INTRODUCTION

Metamorphic and associated plutonic rocks along the west coast of British Columbia are commonly considered part of the Coast Plutonic Complex of the Coast Belt. Between 56-57° latitude in Canada, metamorphic rocks are restricted to the extreme northwest corner of the Iskut River map area (Geological Survey of Canada, 1957). The Elbow Mountain crystalline complex (EBCC) was mapped during August 6-15, 1991 as part of the regional mapping of the Iskut River map sheet (104B) under Project 840046. Field mapping and collection of oriented samples for further petrographic, geochemical, and geochronological work were focused in two areas, Elbow Mountain and Glacier Mountain. They are located southwest of the Stikine-Iskut rivers confluence and east of the Alaska-B.C. border (Fig. 1).

The study was undertaken as a baccalaureate thesis with the objectives of: 1) ascertaining the protolith assemblage; 2) defining the structural style and its relation to metamorphism; 3) assessing possible pressure and temperature conditions from the metamorphosed pelites; and 4) comparison of structural and metamorphic evolution of the EBCC with similar complexes along the eastern margin of the Coast Plutonic Complex.

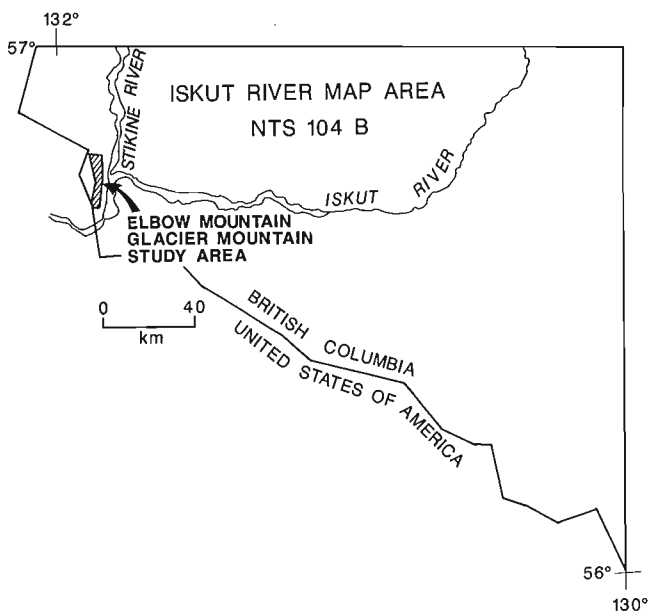


Figure 1. Study area location in northwest corner of Iskut River map sheet, British Columbia.

Figure 2. Geological map of Glacier Mountain and Elbow Mountain study areas. Abbreviations are: Jqmd = Early Jurassic quartz monzodiorite, Tqm = Tertiary (Eocene) quartz monzonite.

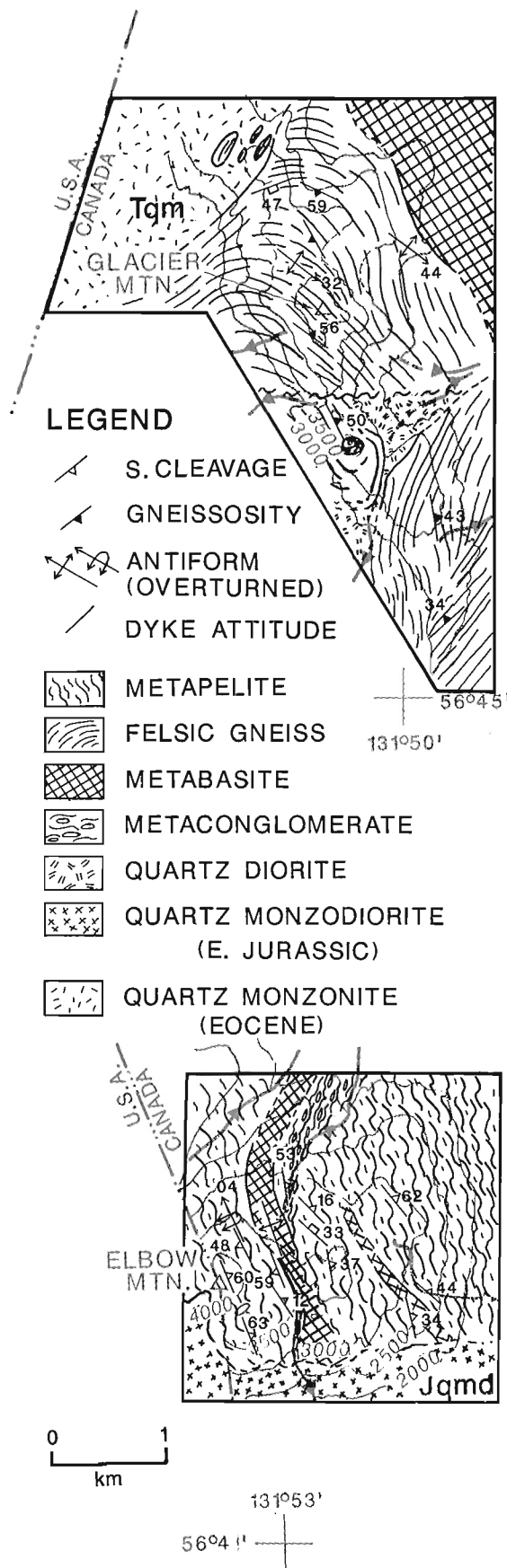


Table 1. Mineral assemblages in 24 thin-sections of metasediments from Elbow Mountain

SAMPLE #	Plg	Epd	Chl	Bt	Hbl	Gt	Str	Als	Crd	Trm	Msc	Cct	Sph	Opq
AT85-195-1				X										X
AT85-195-2				X										X
AT85-196-1				X				And	X					X
AT85-196-2	X			X						X				X
AT85-196-3	X			X	X	X			X					X
AT85-196-4				X							X		X	
AT85-196-5		X			X							X		X
AT85-196-6				X		X		And	X	X				
AT85-197-1	X			X	X								X	
AT85-197-2				X										Pyr
AT85-197-3	X		X	X							X			
AT85-198-1	X			X	X								X	
AT85-198-2	X			X	X							X	Rut	
AT85-198-3	X			X									X	
AT89-115-2												X	X	
AT89-115-3				X										Hem
AT89-115-4	X			X			X	And + Sil			X			X
AT89-115-5	X			X							X			X
AT89-115-6	X			X				And						X
AT89-115-7	X			X										
AT89-115-8	X			X									X	

GEOLOGY OF ELBOW MOUNTAIN CRYSTALLINE COMPLEX

The Elbow Mountain crystalline complex is best exposed at two localities, Glacier Mountain to the north and Elbow Mountain to the south (Fig. 2). To the north, along the north-trending ridge of Glacier Mountain, at least two phases of Tertiary quartz monzonite intrudes well-developed gneissic metasediments. Large xenoliths of country rock, up to 250 m in length, exist well within the intrusion. The country rocks are felsic gneiss comprising hornblende-bearing layers (1-2 cm thick) interlayered with chlorite-rich layers (<1 mm thick). Just south of Glacier Mountain summit there are numerous marble pods (about 1 m x 5-10 m) within the intensely folded felsic gneiss. The felsic gneiss underlies most of Glacier Mountain, and is folded into a series of northwest-trending, isoclinal folds at map to hand sample scales.

South of Glacier Mountain, a fault zone juxtaposes a 500 m thick panel of quartzite, metabasite, gneiss, and metaconglomerate against the typical felsic gneiss to the north and south. Structurally beneath this panel is a quartz diorite intrusion that contains radial, star-shaped aggregates of hornblende. This intrusion grades into a migmatitic zone that delineates the margin of the pluton with the metasediments above. In detail, the heterogeneous block of metasediments contains poorly preserved, metamorphosed conglomerate (of volcanic origin?), which consists of

heterolithic, angular-subangular, lapilli fragments in an altered, mafic matrix. This is structurally overlain by about 20 m of felsic gneiss, and 5 m of ultramafic metabasite that contains prolate, strained, epidotized relict (feldspar) phenocrysts. This sequence is capped by a thin quartzite containing 1-2 cm beds that are chaotically folded. Samples from this unit are currently being processed for detrital zircon geochronometry by W.C. McClelland.

The southern part of map area at Elbow Mountain contains low to medium grade metamorphic rocks and possesses somewhat similar protoliths and structural style as the Glacier Mountain area. Elbow Mountain metamorphic rocks consist of garnet-bearing metapelite, mafic-metavolcanic, metaconglomerate, marble, calc-silicate, and quartzite. The metaconglomerate is structurally overlain by the metavolcanic rocks and a 1-2 m thick quartzite, whose detrital zircons are also currently being dated by W.C. McClelland (McClelland and Mattinson, 1991). Metapelite and marble structurally overlie this succession and exhibit folded primary cleavage. The dominant cleavage is folded into north-northwest-trending folds and to the west and south is commonly crosscut at low angles by an Early Jurassic (M.L. Bevier, unpub. data) quartz monzodiorite intrusion (Fig. 4). The Early Jurassic pluton is locally well foliated, and the fabric is subparallel to the cleavage in the metamorphic rocks and the margins of dykes and apophyses. Plutonism is late synkinematic or post-kinematic with respect to development of S_1 cleavage.

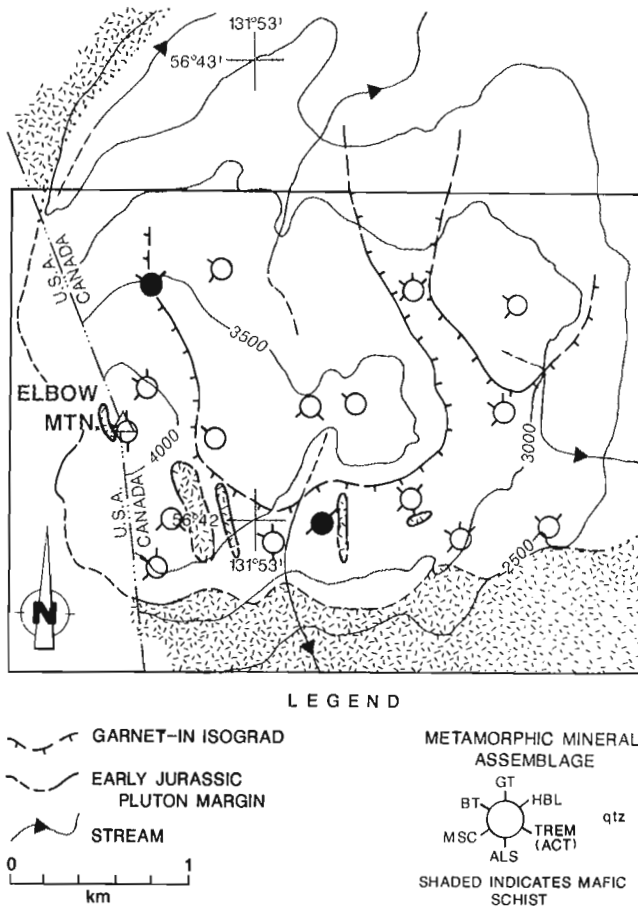


Figure 3. Early Jurassic plutonic margin and distribution of garnet-in isograd with respect to Elbow Mountain. Note narrow deviation of central part of isograd to the north.

Structure

The north-northwest-trending, east-dipping panel of metasediments in Elbow Mountain crystalline complex possesses at least two phases of deformation. The first phase, D_1 , is defined by the primary, northwest-trending, east dipping cleavage, schistosity, and compositional layering (S_1). The second phase of deformation, D_2 , deforms the S_1 cleavage into northwest-trending folds overturned to the northeast. Most overturned antiforms are characterized by classic S, M, and Z folds and commonly contain lenticular pods of marble aligned parallel to the southwest dipping axial planes.

Folding increases in intensity eastward from summit of Elbow Mountain but east of this folded area (at 1030 m elevation) the cleavage consistently dips to the northeast. This suggests the presence of a fault associated with D_2 that may be manifest by minor quartz veining and pyritized metasediments along a north-trending lineament (Fig. 2). An east-trending fault, described above, occurs south of Glacier Mountain summit and juxtaposes the metasedimentary and felsic gneiss.

Metamorphism

Table 1 shows mineral assemblages in 24 thin-sections from samples collected previously on Elbow Mountain in 1985 and 1989 (R.G. Anderson, unpub. data). Most metapelites have combinations of garnet, hornblende, and andalusite, although sample AT89-115-4 shows staurolite, andalusite, sillimanite, biotite, and quartz typical of lower amphibolite facies grade and temperatures greater than 500°C (Turner, 1981; p. 156,157). Other assemblages include tremolite, garnet, diopside, and biotite in calc-silicate rocks and biotite, hornblende (or chlorite), muscovite, and plagioclase in the mafic schist.

During 1991 field season, closely spaced samples were collected from the study area, providing good control on the distribution of metamorphic mineral assemblages. Figure 4 shows that the Early Jurassic pluton margin is subparallel with the garnet-in isograd. To the north, where small quartz diorite dykes outcrop, the garnet isograd diverges from subparallelism with the plutonic contact (Fig. 3).

Porphyroblast development in metapelite, marble, and metavolcanic rocks apparently occurred during D_1 because garnet and hornblende are commonly found within the S_1 cleavage. Alternatively, the subparallelism of pluton to garnet-in isograd plus the crosscutting of primary cleavage by pluton would suggest metamorphism is post- D_1 and associated with Early Jurassic plutonism. This agrees with U-Pb data from similar metasediments around Bradfield river, which indicate metamorphism is Early to Middle Jurassic (McClelland and Mattinson, 1991). However, porphyroblast development within S_1 cleavage indicates that metamorphism was synkinematic to D_1 and Early Jurassic plutonism was late-synkinematic to post-kinematic to D_1 . Parallelism of the garnet-in isograd to the plutonic margin is therefore interpreted to be a function of regional doming produced by pluton emplacement. The subparallel nature of the pluton to S_1 cleavage is likely a result of anisotropic, S_1 fabric guiding pluton emplacement.

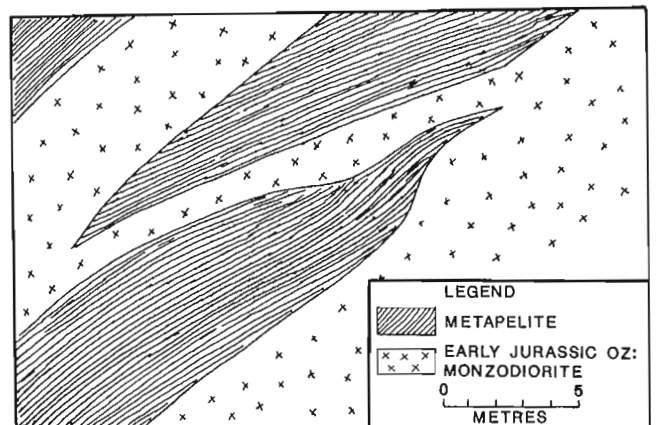


Figure 4. Outcrop sketch of quartz monzodiorite apophysis crosscutting primary, S_1 cleavage in metapelite.

CONCLUSION

Geological relationships among metamorphism, deformation, and plutonism suggest a complex history for the Elbow Mountain crystalline complex (EBCC). Intrusive relations, structural style of the metamorphic rocks, and the distribution of the garnet-in isograd suggest a close, but probably late synkinematic relationship among development of S_1 fabrics, lower amphibolite grade metamorphism and intrusion of the Early Jurassic quartz monzodiorite. The effects of contact metamorphism will be ascertained during further petrographic study. Additional petrographic, mineralogical, and geochronometric work currently underway will further constrain metamorphic conditions, timing of events and protolith correlations.

ACKNOWLEDGMENTS

Many thanks go out to Bob Anderson who, with infinite patience and resourcefulness, provided both an excellent baccalaureate thesis project and a most educational field season. Bill McClelland is thanked for providing initial

support and insight to the geology at Elbow Mountain and for his bizarre sense of humour, which lightened up the rainiest of days. Justin VandenBrink is thanked for his field assistance, his unique sense of humour, and also his 'GQ' poses for scale. Tonia Oliveric is thanked for her meticulous drafting of the figures.

REFERENCES

Geological Survey of Canada

1957: Stikine River area, Cassiar District, British Columbia; Geological Survey of Canada, Map 9-1957.

McClelland, W.M. and Mattinson, J.M.

1991: U-Pb (zircon) constraints on the age of the Yukon-Tanana terrane in the Coast Mountains, central southeast Alaska and British Columbia (abstract); Geological Society of America, Abstracts with Programs, v. 23, no. 5, p. A434.

Turner, F.J.

1981: *Metamorphic Petrology – Mineralogical, Field, and Tectonic Aspects*, Second Edition (text); Hemisphere Publishing Corporation.

Geological Survey of Canada Project 840046

Carboniferous limestone, Iskut River region, northwest British Columbia

M.H. Gunning¹
Cordilleran Division, Vancouver

Gunning, M.H., 1992: Carboniferous limestone, Iskut River region, northwest British Columbia; in *Current Research, Part A*; Geological Survey of Canada, Paper 92-1A, p. 315-322.

Abstract

Carboniferous limestone of the Stikine assemblage was studied in three areas along the eastern edge of the Iskut Icefield. Deformation precludes stratigraphic analyses at Round Lake and Newmont Lake, but 32 m of undeformed, fossiliferous strata are preserved north of Forest Kerr Glacier.

Micritic, echinoderm-rich, graded and massive wackestone to rudstone beds predominate. Faunal diversity is low, and small cerioid colonial rugose are the most abundant identifiable macrofossils. Limestone accumulated in shallow, open marine settings on gentle carbonate ramps devoid of carbonate buildups. Periodic disruption of partially lithified sediment, probably by storm events, produced well bedded successions dominated by proximal, graded, discontinuous beds.

Thick, regionally extensive Permian limestone successions in the Stikine River region are distinguished from Carboniferous limestone sequences by stratigraphic context, thickness, lateral extent, faunal aspects, and individual bed fabrics. Broadly similar facies in Permian and Carboniferous sequences indicate formation in analogous depositional environments.

Résumé

Le calcaire carbonifère de l'assemblage de Stikine a été étudié dans trois zones longeant la bordure orientale du champ de glace Iskut. La déformation a empêché la réalisation d'analyses stratigraphiques au lac Round et au lac Newmont, mais 32 m de couches fossilifères non déformées ont été conservées au nord du glacier Forest Kerr.

Les couches dominantes sont des couches de wackestone à rudstone micritiques, riches en échinodermes, granoclassées et massives. La faune est peu diversifiée et les macrofossiles les plus abondants identifiables sont les rugosas coloniaux cérioïdés. Le calcaire accumulé dans les milieux ouverts peu profonds sur des rampes carbonatées à pente douce ne comporte pas de complexes carbonatés. L'élimination périodique de sédiments partiellement lithifiés, probablement au cours de tempêtes, a produit des successions bien stratifiées dominées par des couches discontinues granoclassées proximales.

Les épaisses successions de calcaire permien d'échelle régionale dans la région de la rivière Stikine se distinguent des séquences de calcaire carbonifères par leur contexte stratigraphique, leur épaisseur, leur étendue latérale, leurs aspects fauniques et la fabrication de chacune des couches. La présence de faciès généralement semblables dans les séquences permien et carbonifères indique une mise en place dans des milieux sédimentaires analogues.

¹ Department of Geology, University of Western Ontario, London, Ontario N6A 5B7

INTRODUCTION

This is a preliminary report on the nature and distribution of Carboniferous limestone of the Stikine assemblage in the Iskut River region in northwest British Columbia. Stratigraphy of limestone at Forest Kerr Glacier is emphasized, supplemented by accounts of structural character and stratigraphic context of Carboniferous limestone at Newmont Lake and Round Lake.

Three summers of field work, beginning in 1991, will form the basis for a Ph.D. thesis to evaluate the character and evolution of the upper Paleozoic Stikine assemblage in the Iskut River region. The project is supported by R.G. Anderson who is currently conducting a 1:250 000 mapping study of the Iskut River map area.

The study area is located along the western margin of the Coast Mountains, in a rugged and isolated region of northwest British Columbia (Fig. 1). Strata examined are north of the Iskut River, near the headwaters of Forest Kerr Creek, and Sphaler Creek (Fig. 2). Descriptions in this report are from a nine-day field trip with E.W. Bamber of the Institute of Sedimentary and Petroleum Geology during which known Carboniferous limestone sequences were mapped in detail, stratigraphic sections were measured, and biostratigraphic samples were systematically collected at measured intervals.

DISTRIBUTION

Distribution of Upper Paleozoic rocks in the Stikine River region was first outlined from mapping by Forest Kerr from 1927 to 1931 (Kerr, 1948), and more detailed mapping was done in 1956 for Operation Stikine (Geological Survey of Canada, 1957). Lower Carboniferous limestone was first identified in the Round Lake area by the Pan American Petroleum Corporation (now Amoco) during a regional exploration program in 1959 and 1960 to assess hydrocarbon potential of the Bowser Basin. Measured stratigraphic

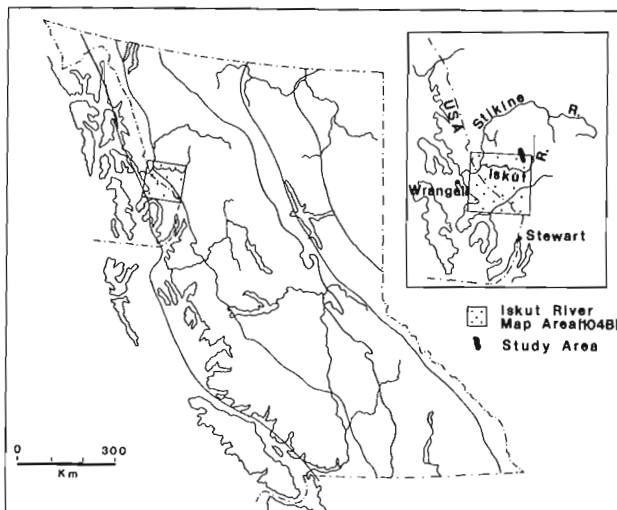


Figure 1. Location map of study area.

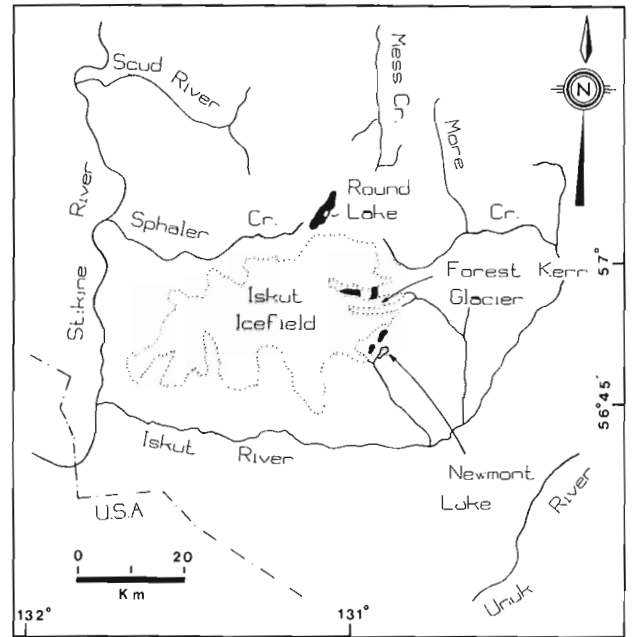


Figure 2. Location of main Carboniferous limestone occurrences, shown in black, in the Iskut River region.

sections and comprehensive biostratigraphic sampling were completed and a Middle Mississippian age was assigned to fauna from the Round Lake area (Fitzgerald, 1960; Rigby, 1961). More detailed mapping by Monger (1970) and Souther (1972) outlined the extent of limestone at Round Lake, and a Late Mississippian age was assigned on the basis of foraminifers, corals, bryozoans, and brachiopods (Mamet, 1976; Monger, 1977).

Ongoing 1:250 000 (Anderson, 1989) and 1:50 000 (Logan and Koyanagi, 1989a,b; Logan et al., 1990a,b) scale geological mapping have identified three different areas where Carboniferous limestone outcrops. The exposures are north of the Iskut River, located near Newmont Lake, Forest Kerr Glacier, and Round Lake (Fig. 2).

All three occurrences of Carboniferous limestone consist of thin, laterally discontinuous, variably deformed limestone bodies within thick, heterogeneous volcanic successions; conformable contacts are preserved at Newmont Lake and Forest Kerr Glacier. There are no isotopic dates from volcanic rocks (see time scale in Fig. 3).

FOREST KERR GLACIER

Little deformed Carboniferous limestone is well exposed on a ridge north of Forest Kerr Glacier, located at the headwaters of Forest Kerr Creek (Fig. 2). Two northwest-trending belts of limestone occur within a succession of volcanic conglomerate, lapilli tuff, felsic to mafic flows, and lesser epiclastic rocks. The relationship between the two limestone belts is equivocal; the less deformed eastern body was studied in detail and is described here.

Stratigraphy

Volcanic strata that host Carboniferous limestone constitute a heterogeneous succession dominated by volcanic conglomerate with subordinate amygdaloidal, porphyritic andesite flows (Fig. 4). Conformably underlying the limestone is dark purple and green, massive volcanic conglomerate with subordinate pale grey to white weathering, planar laminated crystal tuff and hyaloclastite, and irregular dark green andesite flows and lesser flow breccia and welded ash flows. Amygdaloidal andesitic flows are plagioclase and/or plagioclase-hornblende porphyritic and have irregular undulating bases over planar northwest-facing tuffaceous strata.

Volcanic conglomerate is dark purple to green, friable, with vesicular, feldspar-crystal rich tuffaceous groundmass. Beds are massive and developed on scoured surfaces of underlying strata. Fragments are predominantly scoria and amygdaloidal, pale green, feldspar and/or hornblende and rarely pyroxene porphyritic andesite. Intermediate, rounded, irregular shaped granitoid cobbles are also present, and there are no limestone cobbles.

Thin beds of bioclastic wackestone occur about 250 m below the main limestone succession, within volcanic conglomerate and planar laminated ash tuff and welded ash flows. There are three medium grey weathered limestone beds, from 1 to 7 m thick, with 20-40% modal white echinoderm columnals up to 1.7 cm in diameter.

The main limestone sequence is crosscut by several northwest-southeast trending, subvertical faults. Its base is exposed in at least three adjacent fault blocks, with graded wackestone and packstone conformably over dark green, planar laminated, siliceous siltstone. Siltstone exposures are

PERIOD	SUB-PERIOD	EPOCH	STAGE	ma	N. AMERICAN SUCCESSION		
				245			
PERMIAN		ZECHSTEIN	CHANGXINIAN	245	OOHOAN		
			LONGTANIAN				
			CAPITANIAN				
			WORDIAN				
			UFIMIAN				
		ROTILIEGENDES	KUNGURIAN	245	LEONARDIAN		
			ARTINSKIAN				
			SAKHARIAN				
			ASSELIAN				
						242	WOLFCAMPAN
CARBONIFEROUS	PENNSYLVANIAN	GZELIAN	240	VIRGLIAN			
		KASIMOVIAN					
		MUSCOVIAN					
		BUSHKIRIAN					
		SERPUKHOVIAN					
	MISSISSIPPIAN	VISEAN	303	MISSOURIAN			
	311	ATOKAN					
	323	MORROWAN					
	333	CHESTERIAN					
	350	MERAMECIAN					
	363	OSAGEAN					
		KINDERHOOKIAN					

Figure 3. Late Paleozoic time scale (from Harland et al., 1990).

minimized by abundant scree and moraine cover. Dark green volcanic conglomerate occurs from 40 to 50 m below the limestone. The total strike length of the carbonate body is about 2 km. Beds are northwest facing, and normal grading throughout the sequence indicates upright strata.

The limestone succession has a broad threefold division which is consistent along strike. The lower division is about 4 m of fossil-poor, thin-bedded wackestone and very minor

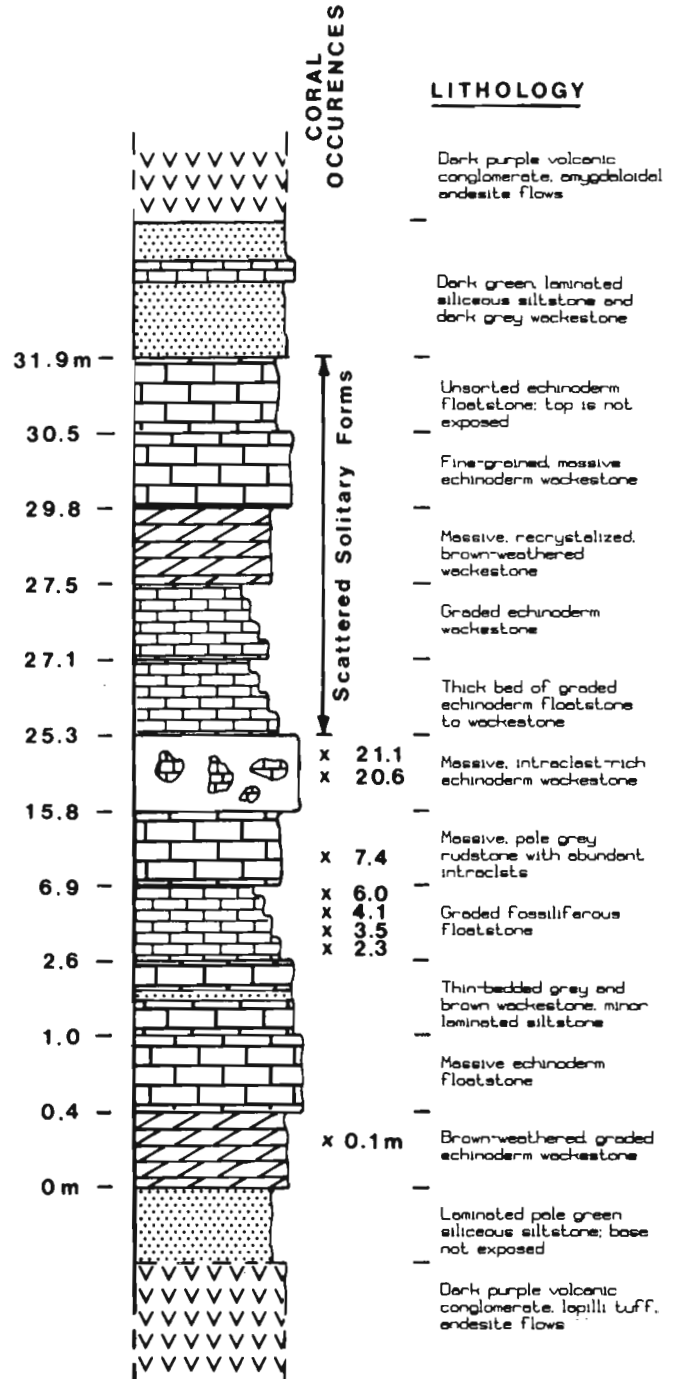


Figure 4. Stratigraphy of Carboniferous limestone north of Forest Kerr Glacier. Unit thicknesses not drawn to scale. Numbers to right of "x" give height above base for coral occurrence.

siltstone; the middle division is over 20 m of coral-bearing, intraclast-rich graded rudstone; the upper interval is less than 6 m of thin-bedded wackestone and packstone.

The lower division comprises thin-bedded brown and grey bioclastic wackestone to packstone, with subordinate coarse floatstone and thinly laminated siltstone. Graded beds are discontinuous, and contacts between graded units are planar to wavy, and sharp. Thickness of this interval in 3 different fault blocks ranges from 0.75 to 4.6 m. Echinoderm columnals (?) are from 3.5 cm in diameter at the bases of beds to less than 2 mm at the tops; a few scattered, small rugose corals were identified. Thin, dark green siliceous siltstone interbeds in the middle of the lower division are the only non-carbonate strata in the succession. Planar to crossbedded laminae indicate brief shallowing conditions, and continuity of the siltstone indicates lateral persistence of clastic sediment influx.

The middle division is over 20 m thick and is characterized by thick, discontinuous, graded packstone and rudstone beds and a laterally persistent intraclast-rich deposit at the top (Fig. 4, 5). Corals are abundant in the lower 5 m and are in four discrete horizons from 30 cm to 1 m thick (Fig. 4). Most solitary forms are less than 4 cm in diameter, and orientation of corals is random. Bioclasts are predominantly coarse echinoderm ossicles 2 to 5 cm in diameter, and randomly orientated echinoderm stem fragments up to 10 cm long. A thick, massive, intraclast-rich bed of floatstone was present in all outcrops examined. Maximum dimension of clasts ranges from 2 to 65 cm, and boundaries are sharp and irregular. Clasts are light grey, fine-grained echinoderm wackestone in a somewhat darker, finer-grained wackestone matrix. The only identified tabulate corals in the succession occur as isolated specimens in the upper 5 m of the unit.

The upper division comprises relatively thin units of graded and massive bioclastic wackestone and minor rudstone. The only macrofossils in the interval are scattered, small, solitary rugose corals. Bioclasts are predominantly small, fragmented echinoderm ossicles that are generally less

than 2 cm in diameter. Basal and upper contacts of graded and massive beds are sharp; undulating, scoured bases indicate some degree of turbulent sediment transport.

The upper contact of the limestone is not exposed. About 15 m stratigraphically above the limestone is thin-bedded, dark green, laminated siliceous siltstone with 1 to 3 m thick interbeds of bioclastic limestone. Wackestone beds have brown, dolomitic, bryozoan-echinoderm rudstone intervals less than 5 cm thick. These rocks are poorly exposed and overlain by dark purple volcanic conglomerate and green andesite flows. Conglomerate is dark purple to green, and limestone cobbles increase in abundance upwards.

Volcanic rocks above the Carboniferous limestone are overlain by a veneer of well-bedded Permian limestone that contains probable Early Leonardian fusulinids (Brown et al., 1991). Limestone cobbles are abundant in volcanic conglomerate below the Permian limestone and contain Serpukhovian or Bashkirian cerioid rugose corals (Logan et al., 1990a,b) and Bashkirian foraminifers (Brown et al., 1991). The Permian strata are characterized by medium to light grey, echinoderm wackestone with 10- to 30-cm alternating beds of tan to black, bedded and nodular chert (Fig. 1). Large solitary and fasciculate rugose corals and abundant fenestrate and ramose bryozoans are in fossil-rich rudstone beds. Greater apparent thickness of volcanic strata below the limestone indicates that carbonate was deposited toward the end of an Early to early Late Carboniferous volcanic event.

Age and nature of limestone

Ages assigned to the eastern belt of limestone range from Visean to Bashkirian based on colonial rugose corals (Logan et al., 1990b), Visean to Namurian based on conodonts (Anderson, 1989; Logan et al., 1990b), and Bashkirian based on foraminifers (Brown et al., 1991). Similar age ranges were obtained from fauna in the more deformed limestone body farther west (Logan et al., 1990a,b). Systematic sampling at measured intervals was done in 1991 for conodonts, foraminifera, and corals, and collections will be used to more closely define the age range of these limestone bodies.

Immature textures, including random orientation of coarse bioclasts in micritic matrix, indicate minimal reworking. Grading, and abundance of intraclasts are the result of periodic, short-lived disturbances, probably storm events, agitating and reworking bottom sediment, but involving resedimentation in a similar depositional environment. Homogeneity of intraclasts and matrix, absence of exotic fauna, the length of some echinoderm stem fragments and rarity of well-developed scour features indicate minimal transport. Abundance of echinoderm fragments throughout the succession indicates deposition proximal to growth sites. Opportunistic echinoderm growth may have contributed to low diversity of the faunal communities. There are no carbonate build-up facies, and limestone accumulated in a topographically subdued carbonate ramp setting.

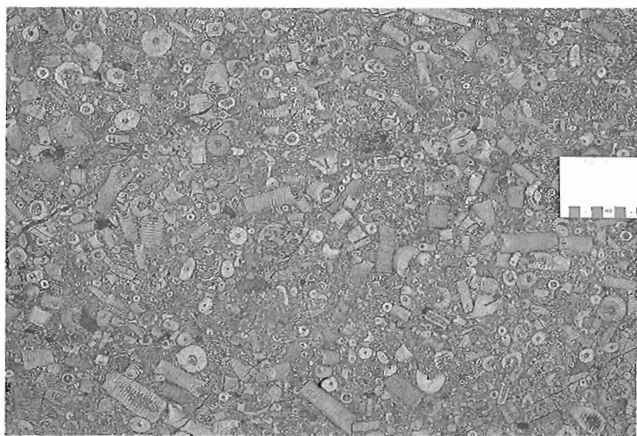


Figure 5. Coarse-grained echinoderm rudstone forms the bases of graded beds in Carboniferous limestone north of Forest Kerr Glacier.

NEWMONT LAKE

Carboniferous limestone is mainly in two localities west and northwest of Newmont Lake, about 11 km south of Forest Kerr Glacier (Fig. 2). Large scale folds are visible on cliff faces south of the section measured; facies changes and structure account for discontinuity of limestone bodies along strike.

Stratigraphy

Upper and lower contacts of the 56 m thick succession measured west of Newmont Lake are locally conformable (Fig. 6). Isolated outcrops of volcanic rocks within 100 m of the base of the limestone are well bedded to laminated, friable dark green to purple crystal lithic tuff and lesser calcite-amygdaloidal basalt flows. Immediately below the limestone is a 4 m thick unit of interbedded dark green to brown lithic tuff, poorly sorted volcanic sandstone, and dark grey to pale brown bioclastic wackestone and floatstone.

The limestone succession is characterized by intercalated echinoderm fragment-rich limestone beds and dark purple and green volcanic sandstone and limy litharenites (Fig. 6). The limestone is typically light grey and massive, and beds are separated by 0.2 to 2 m wavy fracture partings. Graded wackestone to rudstone beds are thin and far-spaced, and irregular-shaped intraclasts compositionally similar to matrix are common. Corals occur only in thin wackestone beds within volcanic rocks above the main limestone formation. Poorly preserved brachiopods are present near the base of the section. Clastic rocks have dark volcanic grains, quartz and feldspar crystal fragments, and echinoderm debris in a poorly sorted, planar laminated, limy matrix.

The limestone is immediately overlain by a homogeneous succession of dark purple and green volcanic sandstone. Decimetre- to metre-thick beds have limy matrices and distinctive centimetre-thick echinoderm concentrations. About 20 m above the main limestone sequence, there are several bioclastic packstone beds which contain abundant small solitary rugose corals.

A poorly exposed, rounded outcrop of light grey weathered intraclast-rich floatstone lies within volcanic rocks well above the main limestone sequence; its stratigraphic relation to the main Carboniferous limestone succession is uncertain. Intraclasts and matrix are medium to light grey wackestone with abundant white echinoderm fragments. There are abundant small cerioid rugose corals, and subordinate small solitary forms.

The limestone body northwest of Newmont Lake is characterized by massive and graded, thick bedded echinodermal floatstone and rudstone deposits with a paucity of identifiable macrofossils. The limestone is bounded by subvertical, north to northeast trending faults characterized by buff to orange weathering, limonitic, recrystallized limestone and orange ankeritic limestone breccia zones; alteration zones peripheral to faults are irregular.

Age and nature of limestone

The limestone body west of Newmont Lake has been dated as Early to Middle Mississippian based on conodonts (Logan et al., 1990b). A limestone cobble from polymictic volcanic conglomerate southwest of, and probably well above, the main limestone formation west of the lake (Fig. 2) contains small solitary corals of probable middle Carboniferous age (Logan et al., 1990b), and Bashkirian foraminifers (Brown et al., 1991).

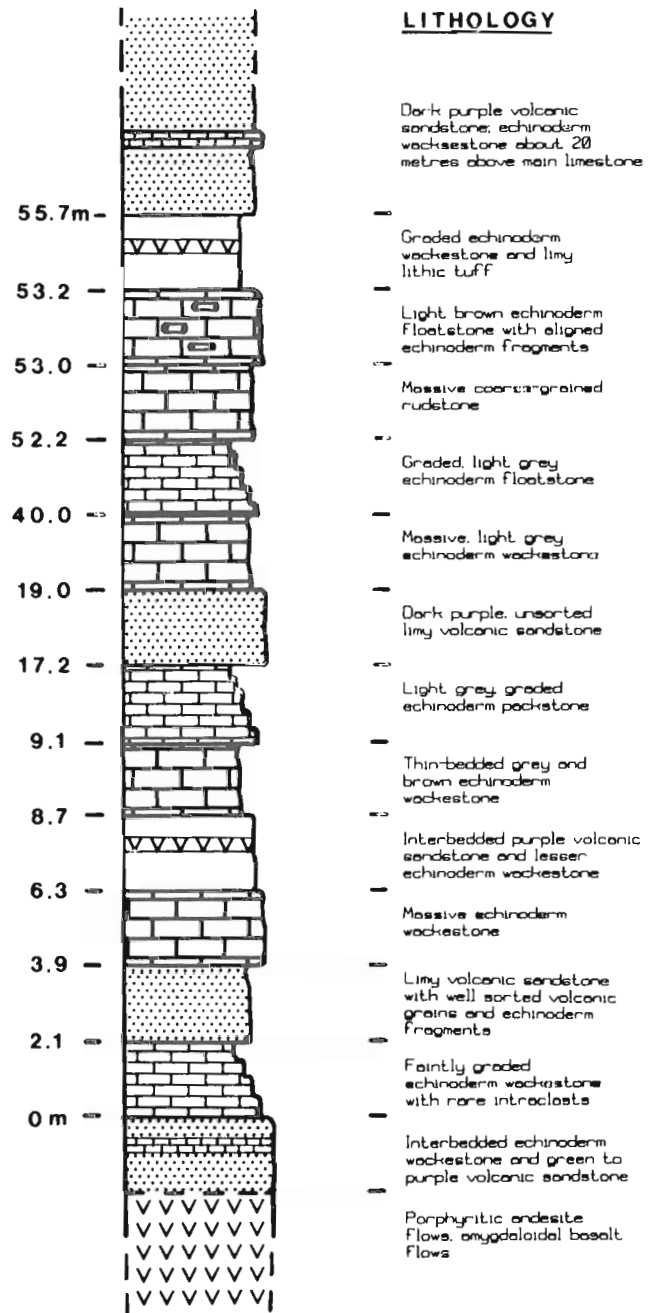


Figure 6. Stratigraphy of Carboniferous limestone west of Newmont Lake. Unit thicknesses not drawn to scale.

Large echinoderm stem fragments up to 10 cm long, and abundant ossicles up to 5 cm in diameter indicate prolific growth and near in-situ sedimentation. Planar bed forms, limy matrices, and echinoderm lag deposits in clastic facies indicate sporadic influx of non-carbonate detritus in a shallow marine setting. Carbonate sediment accumulated in an open marine, gentle carbonate ramp environment. Unsorted, coarse echinoderm debris, monomictic intraclasts, and immature textures indicate proximal depositional sites following sediment disturbance and intraclast formation.

There are several important differences between the Carboniferous limestone at Forest Kerr Glacier and that at Newmont Lake. Fewer corals were identified at Newmont Lake, but correlating biostratigraphy is tenuous because the number of preserved fauna could reflect degree of deformation and not original populations. Intercalation of reworked volcanic material at Newmont Lake differs from homogeneous nature of the limestone sequence at Forest Kerr Glacier, and indicates deposition in environments proximal to uplifted, actively eroding volcanic terranes.

Similarities between Carboniferous limestone successions at Forest Kerr Glacier and Newmont Lake include the locally conformable nature of upper and lower contacts with volcanic rocks. Limestone beds occur throughout a significant stratigraphic interval of volcanic rocks in both areas, indicating extensive submarine volcanism. The limited thickness of limestone deposits in both areas indicates periods of volcanic quiescence in the region were short-lived.

ROUND LAKE

Structural setting

Very deformed limestone outcrops in the Round Lake area about 18 km north-northwest of Forest Kerr Glacier. The sequence is characterized by open to tight, southeast-verging minor folds (Fig. 7), and associated moderate to steep, northwest dipping reverse faults. Limestone exposed on cliff faces north of Round Lake is light grey weathered and thick-bedded, except near faults where it is orange weathering, recrystallized, and brecciated. Asymmetric, southwest- and southeast-verging minor folds plunge shallowly to the northwest and northeast respectively. There is a pervasive fracture cleavage in limestone along faults which juxtapose bordering volcanic rocks.

General geology

Massive, pale grey, mottled, recrystallized wackestone is the dominant carbonate rock type. Nodular to bedded, tan to black chert is present throughout, and abundant structurally higher in the section. Texturally amorphous chert forms 5- to 20-cm thick beds with sharp, irregular boundaries. Where chert is absent, bedding is poorly defined by wavy metre-scale parting. Poorly preserved corals occur throughout but are not abundant. Non-carbonate intervals are rare, structurally disrupted and laterally discontinuous.

South of Round Lake, extensive limestone occurs in an open, northeast-trending antiform. At one locality, a 40 m panel of limestone forms a steeply dipping, northwest-facing fold limb. Contacts with bounding volcanic rocks are structurally conformable, and limestone pods are in crystal tuffs structurally above the limestone. Solitary, and rare, poorly preserved cerioid rugose corals, are present in a thin (<2 m), interval near the southeast margin of the limestone. This section may approximate true stratigraphic thickness of the deformed succession north of Round Lake. Thick, graded and massive bioclastic rudstone beds have abundant, randomly orientated echinoderm stem fragments up to 8 cm long, and chert nodules are absent in most exposures.

Volcanic rocks immediately above the limestone northwest of Round Lake are layered, crystal-rich lapilli tuff with up to 30% pumiceous and aphanitic andesite fragments. The contact is faulted and the limestone cleaved and tightly folded. Fasciculate rugose corals, rare at other Carboniferous limestone localities, are abundant about 10 m below the contact. The tuff is over 75 m thick and contains distinctive light grey to white weathering, discontinuous beds and pods of thin-bedded bioclastic wackestone. Echinoderm debris is abundant, and there are deformed solitary rugose corals and tabulate colonies in some pods. The tuff is overlain by a thick pile of dark green volcanic conglomerate with vesicular, porphyritic and lesser aphanitic, green volcanic fragments in a dark purple and green, feldspar crystal-rich groundmass.

Age and regional correlation

The limestone has been assigned a Late Mississippian age based on foraminifers, corals, bryozoans and brachiopods (Fitzgerald, 1960; Monger, 1970, 1977; Mamet, 1976). A single occurrence of the solitary rugosan coral *Solenodendron* sp. cf. *S. furcatum* (Smith) in limestone north of the lake was dated as late Visean (Logan et al., 1990b). Early Carboniferous conodonts are reported from pale grey limestone southwest of Round Lake (Logan et al., 1990b; Brown et al., 1991). Phyllite and metamorphosed volcanic rocks below the main limestone north of the lake contain rare



Figure 7. Asymmetric minor folds are throughout structurally thickened Carboniferous limestone at Round Lake.

limestone lenses with probable Mississippian corals, bryozoans, and echinoderm fragments (Monger, 1970). Laterally restricted, upper Lower Carboniferous pods of limestone are present in coarse-grained volcanic conglomerate structurally above the main limestone succession north of Round Lake (Monger, 1977).

Preserved carbonate textures and bed forms at Round Lake are similar to Carboniferous limestone near Forest Kerr Glacier and Newmont Lake, however there are several features unique to the succession at Round Lake. No known Bashkirian fauna have been identified at Round Lake. Chert nodules, abundant in limestone north of Round Lake, are absent in Carboniferous limestone elsewhere in the region. Distinctive limestone pods in volcanic conglomerate structurally above the limestone at Round Lake are not present at other localities.

COMPARISON OF CARBONIFEROUS AND PERMIAN LIMESTONE

Thick, regionally extensive Permian limestone successions characterize the Stikine assemblage from Terrace to the Tulsequah River region. The character of Permian limestone is given in preliminary descriptions from the Scud River (Brown and Gunning, 1989a,b; Gunning, 1990, 1991; Brown et al., 1991) and Sphaler Creek (Pitcher, 1960; Logan and Koyanagi, 1989a,b) areas. There are four main criteria to distinguish Permian from Carboniferous successions: regional extent and thickness; stratigraphic context; faunal aspects; and carbonate facies.

The thickness, and regional extent, of Permian limestone formations is the most obvious criterion. Thick, blanket-like exposures are nearly continuous for over 60 km from Round Lake to north of the Scud River (Brown and Gunning, 1989b; Logan and Koyanagi, 1989b). Stratigraphic thickness of the limestone in this belt consistently exceeds 500 m. In contrast, Carboniferous limestone formations are less than 50 m thick, and discontinuous along strike.



Figure 8. Light grey, fine-grained echinoderm wackestone and bedded to nodular chert is typical of Permian limestone in the Stikine River region. Photo is of limestone exposed north of Forest Kerr Glacier.

Stratigraphy of the two successions is different. In the Scud River area, a thick sequence of Permian limestone is underlain by sericitic ash tuffs and overlain by maroon crystal tuffs and radiolarian chert; carbonate production was uninterrupted throughout almost all of Permian time. There is no known limestone of Permian age in volcanic strata above or below the main Permian successions, and there are no non-carbonate facies within the limestone formations. In contrast, Carboniferous limestone is medial within a thick, heterogeneous pile of mafic to felsic flows and pyroclastic rocks. Carbonate accumulated in sporadic pulses over an extended interval of submarine volcanism which produced many widely spaced limestone deposits within a thick succession of tuff, flows, and volcanic conglomerate.

General differences between the Carboniferous and Permian faunas also permit distinction between the two carbonate formations in the field. Fusulinids occur throughout the Permian limestone in the Scud River and Sphaler Creek areas (Pitcher, 1960; Brown et al., 1991; Gunning, 1991). The younger Permian species are distinctive, large elliptical forms from 2 to 5 cm long. Bryozoan-fusulinid rudstone beds are common, many with distinctive giant solitary bothrophyllid rugose corals up to 40 cm long. Large fasciculate rugose colonies are also abundant in most Permian sequences. There are no large fusulinids in Carboniferous limestone, and bryozoans are restricted to limited numbers of ramose forms. The most abundant macrofauna in Carboniferous limestone, excepting coarse echinoderm fragments, are small cerioid and solitary rugose corals that are well preserved in lower intervals of Carboniferous limestone at Forest Kerr Glacier.

Carbonate fabrics in Permian and Carboniferous limestone indicate deposition in broadly analogous depositional environments. Micritic, bioclastic, echinoderm-rich limestone is predominant in both successions, indicating deposition in shallow, warm, open marine settings characterized by subdued carbonate ramp depositional environments. Periodic disruption of sediment, probably by storms, produced well-bedded limestone characteristic of both successions. Laterally discontinuous, graded grain-supported rudstone deposits with abundant echinoderm stem fragments from 6 to 10 cm long are unique to Carboniferous strata. Permian sequences are characterized by fine-grained echinoderm wackestone and chert which forms well-bedded, laterally continuous deposits (Fig. 8).

ACKNOWLEDGMENTS

Support from R.G. Anderson (Project 840046) has made the field component of research possible, and his ongoing encouragement is greatly appreciated. Direction from Wayne Bamber provided the foundation for a detailed study of Carboniferous limestone, and his continued enthusiastic support is appreciated. Joint funding from Energy, Mines and Resources Canada (Grant No. 343491) and NSERC (Grant No. CRD 117589) through the Research Agreement Program of EMR has been instrumental in making fieldwork in remote areas possible. Lab-orientated research costs are generously supported by R.W. Hodder, thesis supervisor, and the

University of Western Ontario. This article has been much improved by comments from Bob Anderson, Wayne Bamber, and Keith Dewing. I also thank Barry Larson for assistance in completing figures.

REFERENCES

Anderson, R.G.

1989: A stratigraphic, plutonic, and structural framework for the Iskut River map area; in *Current Research, Part E*; Geological Survey of Canada, Paper 89-1E, p. 143-151.

Brown, D.A. and Gunning, M.H.

1989a: Geology of the Scud River area; in *Geological Fieldwork 1988*, British Columbia Ministry of Energy, Mines and Petroleum Resources, Paper 1989-1, p. 251-268.

1989b: Geology and geochemistry of the Scud River and Scud Glacier map sheets; British Columbia Ministry of Energy, Mines and Petroleum Resources, Open File Map 1989-7.

Brown, D.A., Logan, J.M., Gunning, M.H., Orchard, M.J., and Bamber, W.E.

1991: Stratigraphic evolution of the Paleozoic Stikine assemblage in the Stikine and Iskut rivers area, northwestern British Columbia (NTS 104G and 104B); in *Contributions to the Geology and Geophysics of Northwestern British Columbia and Southeastern Alaska*, (ed.) R.G. Anderson; *Canadian Journal of Earth Sciences*, v. 28, no. 6, p. 958-972.

Fitzgerald, E.L.

1960: Geological evaluation of the Stikine River area, British Columbia; British Columbia Ministry of Energy, Mines and Petroleum Resources, Petroleum Resources Branch, Assessment Report 870, 4 p.

Geological Survey of Canada

1957: Operation Stikine; Geological Survey of Canada, Map 9-1957.

Gunning, M.H.

1990: Stratigraphy of the Stikine assemblage, Scud River area, northwestern British Columbia; in *Geological Fieldwork 1989*, British Columbia Ministry of Energy, Mines and Petroleum Resources, Paper 1990-1, p. 153-161.

1991: Permian carbonate stratigraphy of the Stikine assemblage, Scud River region, northwestern British Columbia (abstract); *Geological Association of Canada/Mineralogical Association of Canada, Program with Abstracts*, v. 16, p. A49.

Harland, W.B., Armstrong, R.L., Cox, A.V., Craig, L.E., Smith, A.G., and Smith, P.G.

1990: *A geologic time scale 1989*; Cambridge University Press, Cambridge, 263 p.

Kerr, F.A.

1948: Lower Stikine and western Iskut River areas, British Columbia; Geological Survey of Canada, Memoir 246, 95 p.

Logan, J.M. and Koyanagi, V.M.

1989a: Geology and mineral deposits of the Galore Creek area, northwestern British Columbia; in *Geological Fieldwork 1988*, British Columbia Ministry of Energy, Mines and Petroleum Resources, Paper 1989-1, p. 269-284.

1989b: Geology and mineral occurrences of the Galore Creek area (104G/3 and 104G/4); British Columbia Ministry of Energy, Mines and Petroleum Resources, Open File 1989-8.

Logan, J.M., Koyanagi, V.M., and Drobe, J.R.

1990a: Geology of the Forest Kerr Creek area, northwestern British Columbia (104G/15); in *Geological Fieldwork 1989*, British Columbia Ministry of Energy, Mines and Petroleum Resources, Paper 1990-1, p. 127-140.

1990b: Geology and mineral occurrences of the Forest Kerr-Iskut River area, northwestern British Columbia (104G/15); British Columbia Ministry of Energy, Mines and Petroleum Resources, Open File 1990-2.

Mamet, B.L.

1976: An atlas of microfacies in Carboniferous carbonates of the Canadian Cordillera; Geological Survey of Canada, Bulletin 255, 131 p.

Monger, J.W.H.

1970: Upper Paleozoic rocks of the Stikine Arch, British Columbia; in *Report of Activities*, Geological Survey of Canada, Paper 70-1, Part A, p. 41-43.

1977: Upper Paleozoic rocks of the western Cordillera and their bearing on Cordilleran evolution; *Canadian Journal of Earth Sciences*, v. 14, p. 1832-1859.

Pitcher, M.G.

1960: Fusulinids of the Cache Creek Group, Stikine River area, Cassiar District, British Columbia; M.Sc. thesis, Brigham Young University, Provo, Utah, 64 p.

Rigby, J.K.

1961: Upper Paleozoic rocks of central and northern British Columbia (abstract); in *Abstracts for 1961*, Geological Society of America, p. 253.

Souther, J.G.

1972: Telegraph Creek map area, British Columbia; Geological Survey of Canada, Paper 71-44, 68 p.

Geological Survey of Canada Project 840046

Stratigraphy and structure of the Sulphurets area, British Columbia

J.R. Henderson¹, R.V. Kirkham², M.N. Henderson², J.G. Payne³,
T.O. Wright⁴, and R.L. Wright³

Henderson, J.R., Kirkham, R.V., Henderson, M.N., Payne, J.G., Wright, T.O., and Wright, R.L., 1992: Stratigraphy and structure of the Sulphurets area, British Columbia; in *Current Research, Part A; Geological Survey of Canada, Paper 92-1A*, p. 323-332.

Abstract

Folded Upper Triassic Stuhini Group rocks were truncated by erosion prior to deposition of Lower Jurassic rocks. Fossiliferous limy sandstone and siltstone of the Jack formation (new name) occur above the unconformity. Mainly volcanic Lower Jurassic Hazelton Group overlies the Jack formation. An unconformity to disconformity also occurs at the base of the Mount Dilworth Formation near the top of the Hazelton Group. Middle and Upper Jurassic Bowser Lake Group conformably to disconformably overlies Hazelton Group. Dark mudstones and volcanogenic rocks of the Salmon River Formation occur at the base of Bowser Lake Group.

Structure of Triassic rocks is characterized by the broad north plunging McTagg anticlinorium between the Unuk River and Knipple Glacier. The breached core of the anticlinorium contains upright folds in Stuhini Group rocks. Jurassic Hazelton and Bowser Lake Group rocks exhibit overturned folds and thrusts that are west vergent on the west side, and southeast vergent on the east side of the study area.

Résumé

Les roches plissées du groupe triasique supérieur de Stuhini ont été tronquées par l'érosion avant la mise en place des roches du Jurassique inférieur. Le grès calcaire fossilifère et le siltstone de la formation de Jack (nouveau nom) du Jurassique inférieur sont situés au-dessus de la discordance. Les roches principalement volcaniques du groupe de Hazelton Jurassique inférieur, du reposent sur la formation de Jack. Une discordance ou discordance stratigraphique est aussi observée à la base de la formation de Mount Dilworth vers le sommet du groupe de Hazelton. Le groupe de Bowser Lake, Jurassique moyen et supérieur, du est en concordance ou discordance stratigraphique au-dessus du groupe de Hazelton. Des mudstones charbonneux et roches volcanogéniques de la formation de Salmon River sont observés à la base du groupe de Bowser Lake.

La géométrie structurale des roches triasiques est caractérisée par le large anticlinorium de McTagg, plongeant vers le nord, situé entre la rivière Unuk et le glacier Knipple. Le coeur érodé de l'anticlinorium contient les plis droits affectant les roches du groupe de Stuhini. Les roches des groupes de Hazelton et de Bowser Lake montrent des plis déversés et failles de charriage à symétrie orientée vers l'ouest du côté ouest et de symétrie vers le sud-est du côté est de la région étudiée.

¹ Continental Geoscience Division, Ottawa

² Mineral Resources Division, Ottawa

³ Granges Inc., Vancouver

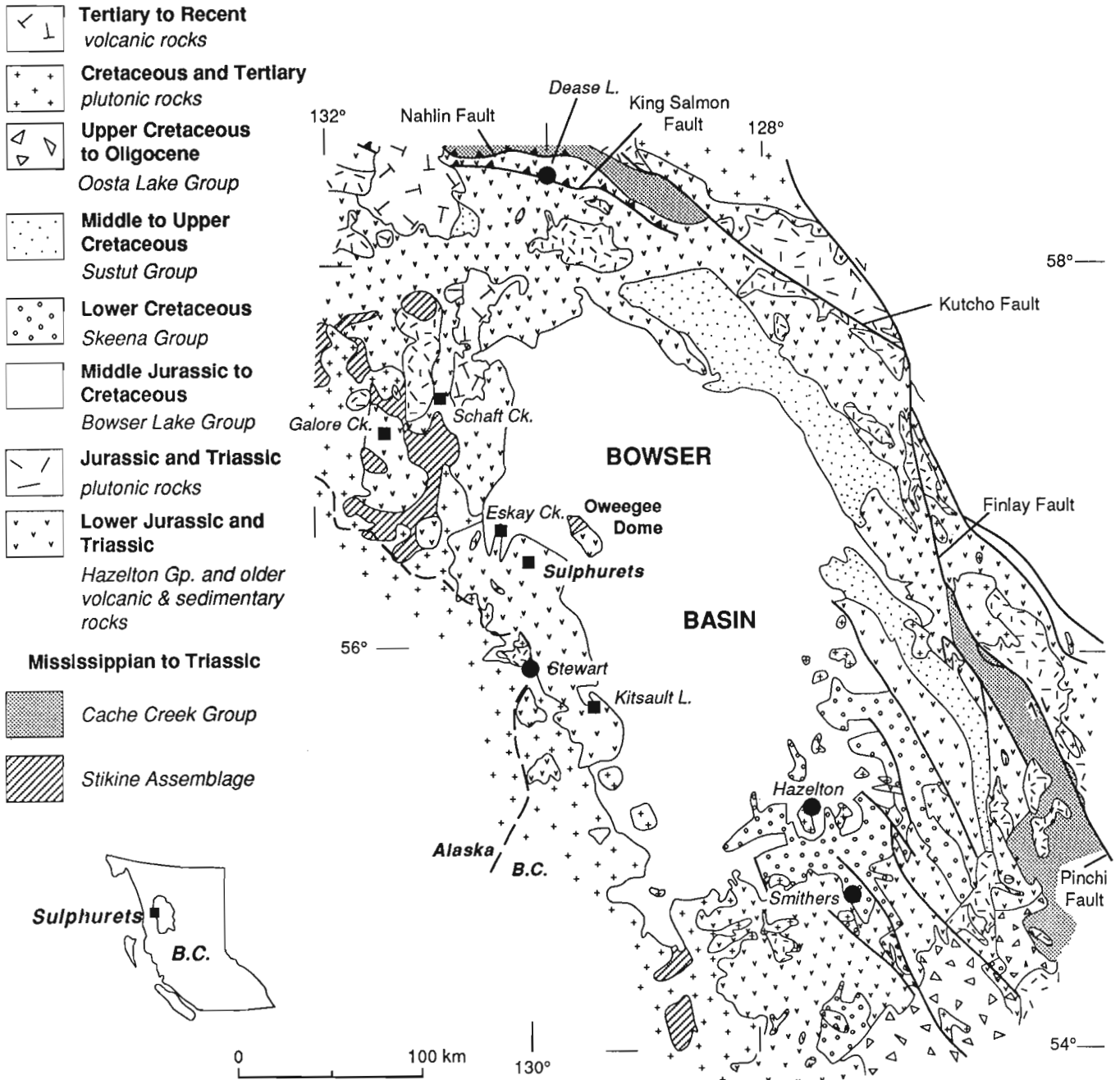
⁴ U.S. National Science Foundation.

INTRODUCTION

The purpose of this study was to document stratigraphic and structural relations in the Sulphurets region (104B/8,9; Fig. 1). Currently the area is being explored for precious and base metals. The stratiform, high-grade polymetallic deposit hosted in Hazelton group rocks at Eskay Creek is located a few kilometres west of the study area (Fig. 2). Within the area, abundant gossans are targets of current surface sampling

and exploration drilling. This report summarizes results of fieldwork in 1990 by RVK, JRH and MNH, and in 1991 by the former, and TOW, JGP and RW.

The Sulphurets area has a local relief of about 2 kilometres. The region above treeline provides rugged but excellent quality bedrock exposure; below treeline, outcrop is generally good, but mapping is difficult and slow due to dense vegetation and steep topography. Broad expanses of ice and snow conceal bedrock in much of the area.



RVK 1991

Figure 1. Regional geological map with location of Sulphurets area.

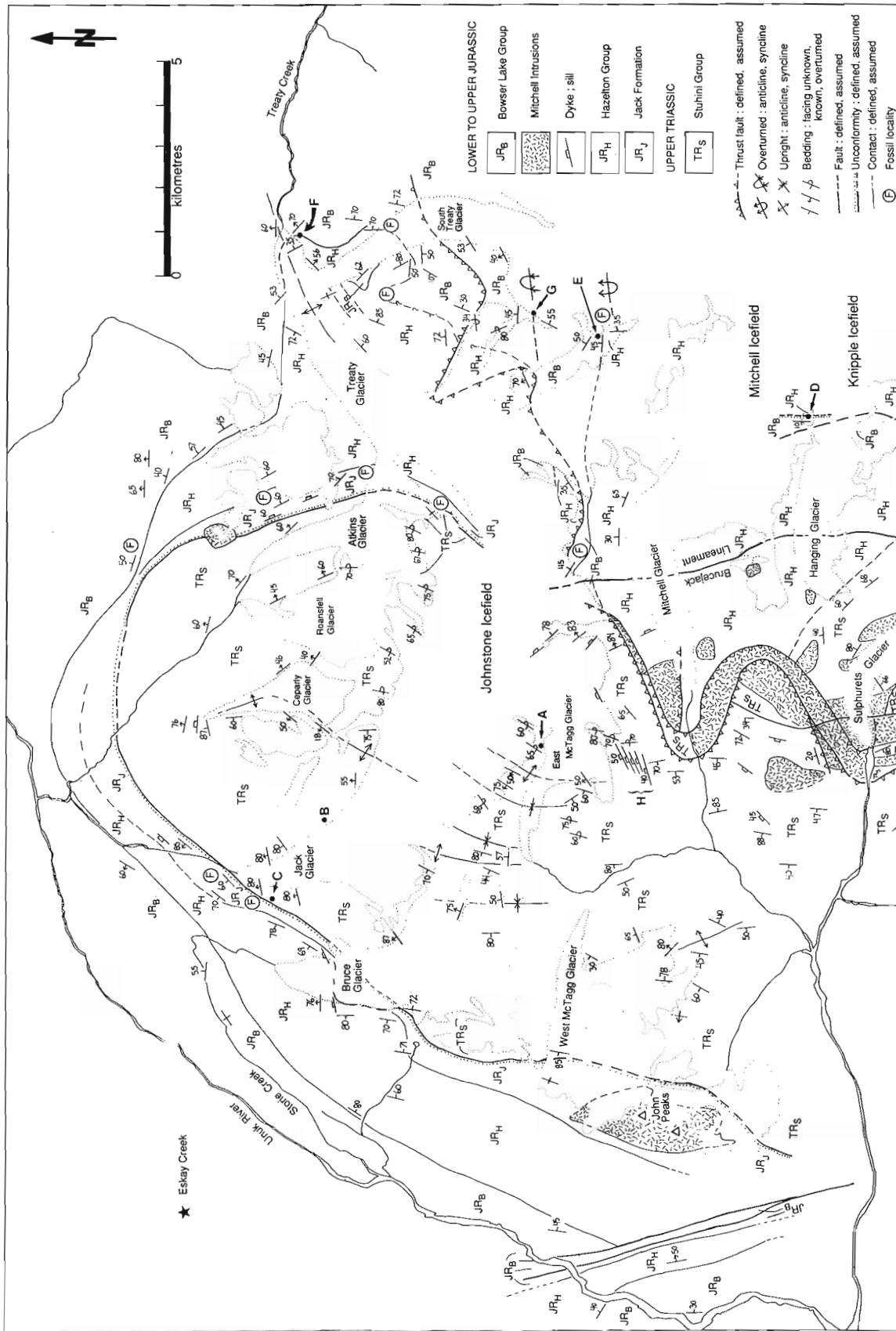


Figure 2. Geological map of the Sulphurets area. Localities mentioned in the text are shown by letters: A (lower Stuhini Group, Figure 3), B (volcanic part of Stuhini Group), C (upper Stuhini Group at Jack Glacier, Figure 5), D (sub-Mount Diiworth unconformity to disconformity in Figure 6), E (Salmon River Formation "pajama beds"), F (Salmon River Formation-lower Bowser Lake Group transition), G (overturned folds in Figure 8), H (dyke swarm cutting Stuhini Group sedimentary rocks).

PREVIOUS AND CURRENT WORK

Prospecting and exploration have been carried out in the area since the late 1800s (Wright, 1907; Mandy, 1936). Newmont Mining Corporation mapped extensively in the region in 1960 and 1961; the results of which were incorporated into Grove's studies in the mid-1960s (1986). Alldrick (1985) established the stratigraphy in the Stewart area and in the course of their mapping of the Sulphurets and Unuk River areas Alldrick and Britton (1988) and Alldrick et al. (1989) applied the previously established stratigraphy. In a summary report of their mapping results, Britton and Alldrick (1988) provided a bibliography of unpublished reports and theses done within the Sulphurets area. Anderson (1989) and Anderson and Thorkelson (1990) described the Mesozoic stratigraphic framework of the Iskut River area including the Sulphurets region. Kirkham (1991) published a 1:20 000 scale geological map of the Sulphurets area showing mineral occurrences.

Currently, R.G. Anderson is mapping, compiling and correlating work done in the Iskut River sheet (NTS 104 B, 1:250 000) which includes the study area. Between 1986 and 1991, the Geological Survey of Canada, has carried out a multi-disciplinary project, under the coordination of R.V. Kirkham, emphasizing geological, metal and mineral zoning, lithochemical, mineralogical and ore genesis studies in the Sulphurets and Treaty Glacier areas. Topical studies in the Sulphurets region are also being conducted by geologists with the University of British Columbia Mineral Deposits Research Unit (P. Lewis, D. Bridge, J. MacDonald, J. Thompson), and the Department of Geological Sciences, University of Oregon (J. Margolis). Much geological work is also being carried out by exploration companies active in the area.

REGIONAL GEOLOGY

The Sulphurets area lies near the west boundary of the Middle Jurassic to Cretaceous Bowser Basin, and overlies Paleozoic Stikine Assemblage rocks exposed to the east in the Oweege dome and to the west (Anderson and Thorkelson, 1990; Greig, 1991). The Sulphurets area includes rocks comprising the Upper Triassic Stuhini, Lower Jurassic Jack formation (new name), Lower Jurassic Hazelton and Lower to Upper Jurassic Bowser Lake groups (Fig. 2).

Submarine and lesser amounts of subaerial sedimentary and volcanic supracrustal rocks dominate the region. Intrusions are not extensive and comprise mainly abundant dykes, sills, plugs and small stocks in the Mitchell and Sulphurets glaciers area. Significantly, the intrusive rocks extend only as high in the stratigraphy as the volcanic units in the lower part of the Bowser Lake Group.

Stuhini Group rocks are exposed in the breached core of a north-plunging anticlinorium, named here the McTagg anticlinorium, which forms the major structural element in

the region. Stuhini Group rocks in the centre of the anticlinorium, located in the Johnstone Icefield, contain upright cusped anticlines and lobate synclines. These folds were eroded before deposition of Lower Jurassic rocks. Overlying Jurassic rocks exhibit west-vergent folds and thrusts in the Unuk River-Storie Creek area, and southeast vergent folds and thrusts in the Sulphurets-Treaty-Knipple glaciers area (Fig. 2). The regional structure is further complicated by local north-south and east-west-trending zones of steeply-dipping flattening fabrics, as well as numerous late brittle faults, probably mostly of minor throw.

STRATIGRAPHY

Britton and Alldrick (1988) assigned all of the supracrustal rocks exposed in the Sulphurets area to the Hazelton and Bowser Lake groups, which they considered to range in age from Upper Triassic (Norian) to Middle Jurassic (Bajocian). Anderson and Thorkelson (1990) recognized the Upper Triassic Stuhini Group, a conformably overlying transitional sedimentary unit of Triassic-Jurassic age, the Lower and Middle Jurassic Hazelton Group, and the Middle and Upper Jurassic Bowser Lake Group in the Sulphurets area. They divided the Hazelton Group into three heterogeneous volcanogenic units: basal Unuk River, middle Betty Creek and upper Mount Dilworth formations. The Salmon River Formation was distinguished as a largely sedimentary unit at the top of the Hazelton Group, passing conformably into Bowser Lake Group turbidites.

However, unconformities and erosional intervals recognized in this study suggest that modifications of stratigraphic assignments are desirable. Earlier work by Grove (1986) suffers from lack of fossil age control in critical areas such as the folded Triassic rocks in the core of the



Figure 3. Photograph of overturned ball-and-pillow structure in Stuhini Group turbidite beds (Fig. 2, locality A). GSC 1991-575B

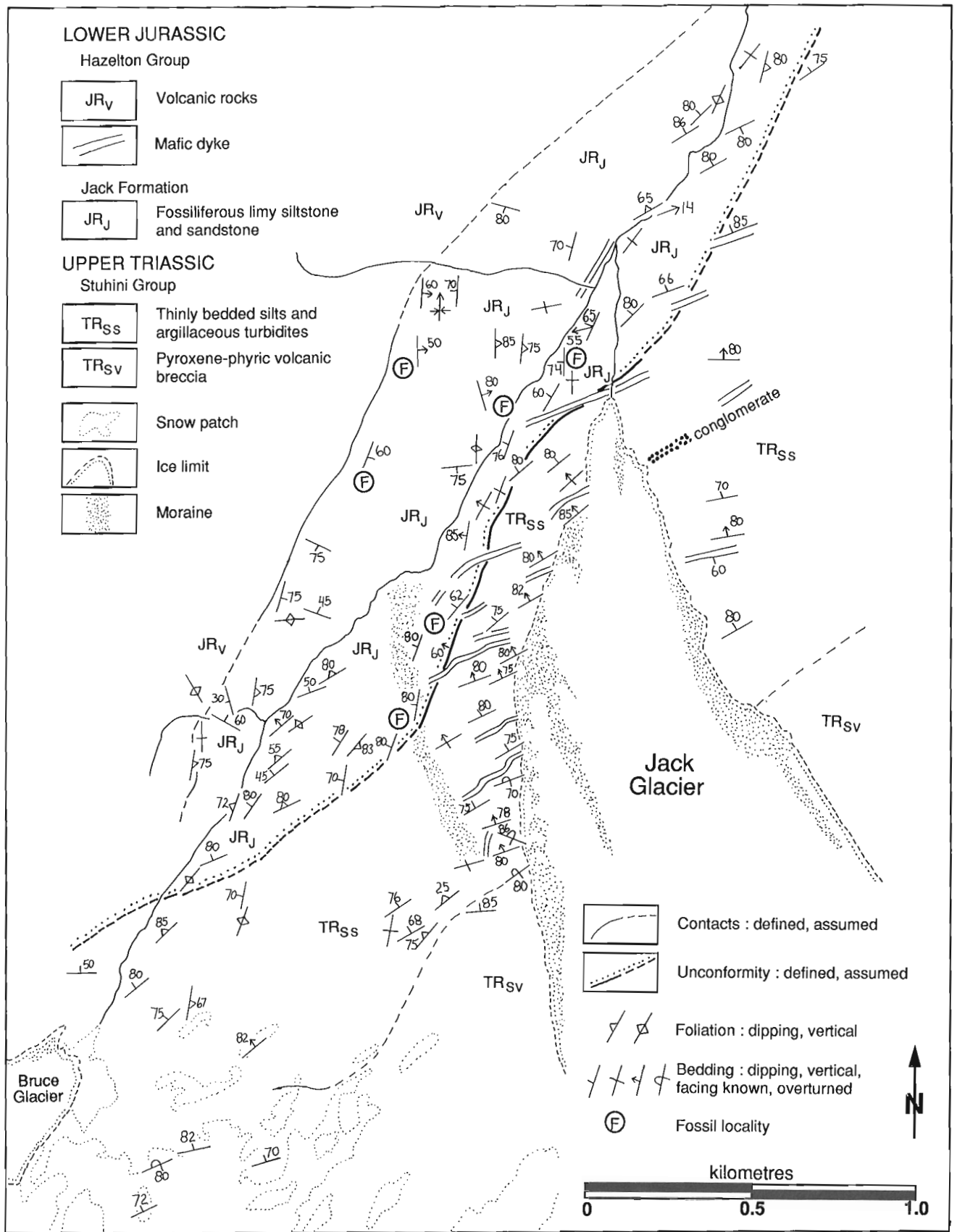


Figure 4. Geologic map of the area near the toe of Jack Glacier.

McTagg anticlinorium and from lack of recognition of thrust repetitions in reference sections (e.g. north of Mitchell Glacier).

Stuhini Group

The base of the Stuhini Group is not exposed in the area. The lowest Stuhini Group rocks are believed to occur in the breached core of the McTagg anticlinorium on ridges north and south of East McTagg Glacier (Fig. 2, locality A) where the rocks are mainly thin-bedded, argillaceous, turbiditic, fine-grained sandstone (Fig. 3) and thick-bedded, medium-grained sandstone. Rare granule conglomerate beds with quartz and chert granules dispersed in a silt matrix occur in this part of the section. Several hundred metres of pyroxene-phyric lava flows, breccia, tuff and conglomerate with lenses of sandy to silty, graded turbidite beds occur above the lower turbidite sequence. The Stuhini volcanics include flows, pyroclastic and epiclastic rocks. Good exposures of volcanic-rock dominated Stuhini Group, including pillow lava, occur along the ridge east of Unuk River and Storie Creek from John Peaks to Bruce Glacier, on the arête between Bruce and Jack glaciers and along the west side of Jack Glacier (Fig. 2, locality B) and eastward to the axis of the McTagg anticlinorium. A kilometre-thick



Figure 5. Photograph of the unconformity at the base of the Jack formation, located near the toe of Jack Glacier (Fig. 4). The Jack formation basal conglomerate overlies Stuhini Group thin-bedded siltstone-mudstone turbidites. GSC 1991-575C

turbidite sequence, similar to the lowermost Stuhini Group rocks, overlies the volcanic-rock dominated succession. The upper Stuhini Group turbidites are graded thin-bedded siltstone and mudstone with thicker sandstone interbeds and, locally (e. g., east of the toe of the Jack Glacier, Fig. 4), lenses of granitoid boulder conglomerate. The upper turbidite sequence is well exposed on the northeast valley wall near the head of Atkins Glacier. However, excellent exposures of this part of the Stuhini succession also occur near the toe of the Jack Glacier (Fig. 2, locality C; Fig. 4) where the Stuhini Group turbidite beds are overlain with angular unconformity by Lower Jurassic conglomerate (Fig. 5) and richly fossiliferous, limy siltstone and sandstone.

Thick sequences of very immature sandy conglomerate, breccia and minor interbedded sandstone with volcanic, sedimentary and a few granitoid clasts occur above gossanous rocks on the high ridge north of the Mitchell Glacier and on the west end of the Mitchell-Sulphurets ridge. In places, these rocks are intensely deformed with well-developed flattening fabrics. The precise stratigraphic position of these units is unknown but the geographical and structural locations suggest that they are probably part of the Stuhini Group, or possibly Lower Jurassic Jack formation.

Brown-weathering carbonate alteration of Stuhini Group rocks is widespread. High K-feldspar content of sedimentary rocks, and high K_2O content (about 5%) of mafic volcanic rocks in conjunction with the occurrence of pyroxene phenocrysts, may be stratigraphically distinctive.

Norian *Monotis* and Carnian *Halobia* found in the lower turbidite sequence indicate a Norian age for the Stuhini Group (T. Tozer, personal communication, 1991). Northwest of the Sulphurets area, Anderson and Thorkelson (1990) collected conodonts which also indicated an Upper Triassic age for the Stuhini Group.

Sandstone dykes, soft-sediment folds and slump units are common throughout the Stuhini Group, and ball-and-pillow structure (Fig. 3) is ubiquitous in silt-argillite turbidites, signifying a seismically-active depositional environment with a rapid recurrence rate of turbidity currents.

Jack formation (new name)

Lower Jurassic sedimentary rocks unconformably overlie the Stuhini Group in the study area. Basal Jack formation is varied; west of Bruce Glacier, the base is drawn below a distinctive cobble to boulder conglomerate containing granodiorite and dark limestone clasts. At the toe of the Jack Glacier (Fig. 4), a strongly discordant thin conglomerate unit containing clasts of subjacent Stuhini siltstone and mudstone beds (Fig. 5), with several exposures of *terra rossa*, occurs immediately above the unconformity. Interbedded, very fossiliferous, limy sandstone and siltstone occur above the basal conglomerate. Fossils include bottom-dwelling organisms (gastropods, pelecypods, bryozoans, corals, ?crinoids) and nektonic organisms (ammonites and belemnites). The fossil beds are more than a hundred metres thick at the Jack Glacier locality. Above the fossiliferous

beds are tens to more than a hundred metres of dark carbonaceous mudstone and lesser interbedded grey turbiditic sandstone.

The unconformity above the Stuhini Group has been traced from the Jack to the Treaty Glacier, where ammonites collected by W. Raven from the Jack formation have been dated tentatively as Sinemurian (P.L. Smith, personal communication to W. Raven, 1991). Between the Jack and Treaty glaciers, the Jack formation is overlain with apparent conformity by Hazelton Group volcanic rocks. To the south, near Sulphurets Creek, these characteristic fossil-bearing beds have been recognized discontinuously to John Peaks. Along the western contact of the Stuhini Group, in most places, a conglomerate containing granodiorite and limestone boulders separates the Stuhini Group and Jack formation rocks. A similar conglomerate is concordant within upper Stuhini Group rocks east of the Jack Glacier (Fig. 4), the unconformity should therefore be traced carefully, as conglomerate containing granitoid and limestone boulders is not necessarily distinctive of the basal Jack formation.

Hazelton Group

The Hazelton Group represents part of a terrane of andesitic flows and breccias with considerable paleotopographic relief, probably part of a volcanic chain.

Between the Jack and Treaty glaciers, Hazelton Group volcanic rocks are relatively thin, but are underlain by the Jack formation, and are overlain locally by Toarcian fossil-bearing beds (Fig. 2, locality F). The majority of Hazelton Group rocks are volcanic. In most areas the succession comprises from bottom to top, andesitic flows and coarse breccia (Unuk River Formation), epiclastic and pyroclastic rocks (Betty Creek Formation), rhyodacitic welded tuff, lapilli and ash tuff, breccia and flows (Mount Dilworth Formation). The volcanic sequence with less

abundant interbedded sedimentary units varies from several tens to several kilometres thick. Although thickness variations due to structural repetition or omission are common, the nature of the units indicates that considerable local topographic relief existed during Hazelton Group volcanism. The Sulphurets-Knipple Icefield was probably a volcanic centre with high local relief. The Hazelton volcanic sequence is probably thickest in this part of the area and thinnest in the northwestern parts of the study area (Fig. 2).

West of the Jack and Bruce Glaciers, the Jack formation is stratigraphically overlain by felsic welded tuff very similar to the Mount Dilworth Formation found elsewhere in the region, and it is in turn overlain by breccia, lapilli tuff and minor flows or well-bedded, dark, carbonaceous mudstone near Jack Creek. Opinions vary as to the stratigraphic position of those units; RVK interprets the felsic tuff as Mount Dilworth Formation overlain by the Salmon River Formation. JGP considers the felsic unit to be an unusual felsic volcanic member at the base of the Betty Creek Formation.

East of Hanging Glacier, felsic tuffs of the Mount Dilworth Formation overlie an erosional surface within the Hazelton volcanic sequence. In a nunatak in the icefield, an 18 metres-wide mafic dyke cuts Betty Creek epiclastic and pyroclastic rocks and is truncated at the Mount Dilworth contact (Fig. 2, locality D; Fig. 6). This relationship indicates significant erosion at the top of the Betty Creek Formation before deposition of the Mount Dilworth Formation.

Salmon River Formation (Bowser Lake Group)

The base of the Salmon River Formation is placed at the base of buff-weathering fossiliferous, limy sandstone unit (Fig. 2, locality F) that occurs locally above and interbedded with the Mount Dilworth Formation. Toarcian age fossils have been

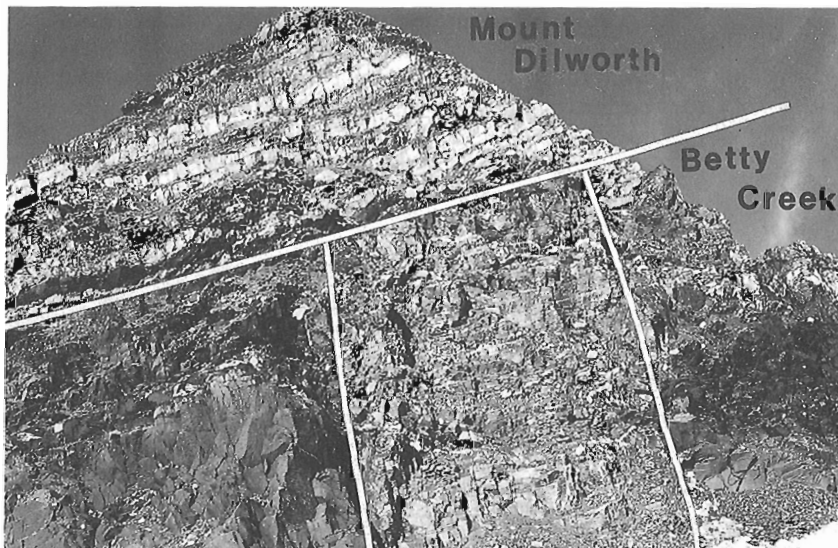


Figure 6. Photograph of the unconformity to disconformity at the base of Mount Dilworth Formation (Fig. 2, locality D). Maroon, well-bedded epiclastic and pyroclastic rocks of the Betty Creek Formation are cut by an 18m-wide phaneritic mafic dyke that is truncated at an erosional surface below pale, well-bedded felsic volcanic rocks of the Mount Dilworth Formation. Probably Toarcian limy fossiliferous sandstone and conglomerate at the base of the Salmon River Formation occur on top of the outcrop. GSC 1991-575E

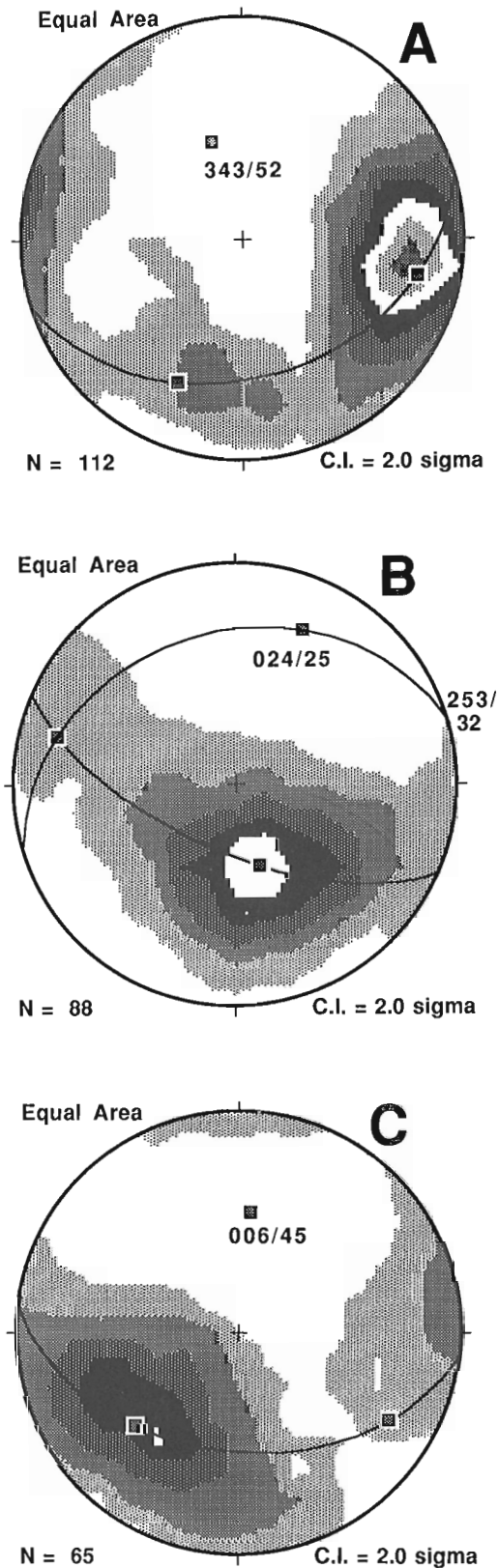


Figure 7. Stereoplots of bedding: **A.** Stuhini Group in McTagg anticlinorium; **B.** Hazelton and Bowser Lake groups east of McTagg anticlinorium in the Knipple Icefield area, and **C.** Hazelton and Bowser Lake groups north of McTagg anticlinorium.

collected from these limy beds (Anderson and Thorkelson, 1990). The fossiliferous beds are less than ten metres thick but are found locally over an area thousands of square kilometres (R.G. Anderson, personal communication, 1991).

Thin dark-, light- and rusty-weathering mudstone and tuffaceous siltstone occur in places above the Toarcian fossil beds, such as on the ridge north of South Treaty Glacier and on nunataks in the Knipple Icefield (Fig. 2, locality E). Similar rocks in the same stratigraphic position occur on Troy Ridge and form the distinctive "pajama beds" of the Salmon River Formation (Anderson and Thorkelson, 1990). Locally, thick units of pillowed- and columnar-jointed, amygdaloidal basalt and heterolithic breccia with mafic and felsic volcanic and sedimentary clasts occur in the Salmon River Formation.

Distinction between the Salmon River Formation and the rest of the Bowser Lake Group is based on the disappearance of submarine volcanic components characterizing the former, as well as a general increase upwards of the sandy component in the succession. Salmon River Formation thinly-bedded mudstone and tuffaceous siltstone beds pass gradually upward into interbedded grey sandstone and carbonaceous siltstone and mudstone locally containing plant-fossil debris. The transition between Salmon River Formation and the rest of the Bowser Lake Group is well exposed along Treaty Creek below Treaty Glacier (Fig. 2, locality F).

STRUCTURE

The geometry of bedding in the Sulphurets area is summarized in Figure 7. Stuhini Group sedimentary rocks form tight, upright folds plunging 52° towards 343° (Fig. 7A). In contrast, Jurassic rocks in the Knipple Icefield region, form strongly overturned, southeast-vergent reclined folds that plunge 25° towards 024° on axial surfaces trending about 253° and dipping 32° (Fig. 7B). In the northern part of the study area, north of the icefields, folds in Jurassic rocks are open, and plunge 45° towards 006° (Fig. 7C). A photograph of overturned folds in Jurassic rocks is shown in Figure 8.

In the McTagg Creek area and north of Jack Glacier near the core of the McTagg anticlinorium, upright folds are overprinted by subhorizontal macroscopic folds that are probably correlative with the folds in the overlying Jurassic rocks, but this relationship needs additional study. The opposing vergence of the overturned folds in Jurassic rocks west and east of the McTagg anticlinorium is puzzling, and also needs further study.

Cleavage is variably developed in rocks in the study area. It is a pressure solution cleavage in the cores of upright isoclinal anticlines in Stuhini Group beds. Cleavage in Jurassic rocks is developed in zones of apparent thrusting, and locally in cores of overturned folds. It is particularly well developed in sericitic, hydrothermally altered rocks. Mylonitic fabrics occur in Stuhini Group rocks in the McTagg Creek area, and extend south of the study area along ridges between the Ted Morris and Sulphurets glaciers.

Numerous faults that locally disrupt the stratigraphy are difficult to interpret kinematically.



Figure 8. View, looking west, of overturned folds in Bowser Lake Group (Fig. 2, locality G). The folds verge north (right on the photo) on the lower limb of a larger south-east vergent anticline. GSC 1991-575G

DISCUSSION AND CONCLUSIONS

An important conclusion resulting from this study is that folding and erosion affected Upper Triassic Stuhini Group rocks, prior to deposition of Lower Jurassic sediments and eruption of Hazelton Group volcanic rocks. Three main lines of evidence support this conclusion. One is the marked depositional angular discordance between the Stuhini Group and the overlying beds exposed near the toe of the Jack Glacier, noted above. The second derives from a swarm of north-dipping dykes south of the East McTagg Glacier (Fig. 2, locality H) cutting folded steeply-dipping, north-striking Stuhini Group turbidites. These dykes are interpreted to feed the overlying Hazelton Group. The third argument in support of a regional angular unconformity between Triassic Stuhini Group and younger rocks is their contrasting structural style: upright folds in the Stuhini Group and overturned folds in the Hazelton Group. Brown and Greig (1990) documented similar stratigraphic and structural relationships in the Stikine River-Yeheniko Lake area, about 100 km to the northwest, suggesting that post-Stuhini Group, pre-Lower Jurassic deformation was widespread.

There is some controversy on stratigraphic assignation of units above the Stuhini Group in the area west of the Jack and Bruce glaciers: if the felsic welded tuff is interpreted as Mount Dilworth Formation overlain by the Salmon River Formation (RVK), then the Betty Creek Formation is missing at this locality. If, on the other hand, the felsic unit is part of the Betty Creek Formation (JGP), overlying breccias are also Betty Creek and are stratigraphically overlain by poorly exposed Mount Dilworth Formation.

ACKNOWLEDGMENTS

R.G. Anderson is gratefully acknowledged for logistical support, geological discussion and an enjoyable, fruitful guided tour of the excellent exposures of Hazelton and Bowser Lake groups on Troy Ridge north of Stewart. Gerry McArthur (formerly with Calpine Resources Inc.) is thanked

for describing the stratigraphy at Eskay Creek, as well permitting us to visit the underground workings in 1990. We are indebted to Granges Inc., Newhawk Gold Mines Ltd., Corona Corporation, Calpine Resources Inc., Orequest Consultants Ltd. and Placer Dome Inc. for generous logistical support, access to their properties and geological information. Financial support for fieldwork by RVK, MNH and JRH was provided by the Geological Survey of Canada; TOW was supported by the US National Science Foundation and fieldwork by JGP and RLW was funded by Granges Inc. We thank D. Lindsay and K. Nguyen for drafting the figures. R.G. Anderson's critical review has improved this manuscript and is much appreciated.

REFERENCES

- Alldrick, D.J.**
1985: Stratigraphy and petrology of the Stewart mining camp (104B/1); in Geological Fieldwork, 1984, British Columbia, Ministry of Energy, Mines and Petroleum Resources, Paper 1985-1, p. 316-341.
- Alldrick, D.J. and Britton, J.M.**
1988: Geology and mineral deposits of the Sulphurets area (NTS 104 A/5, 104A/12, 104B/8 and 104B/9); British Columbia Ministry of Energy, Mines and Petroleum Resources, Geological Survey Branch, Open File Map 1988-4.
- Alldrick, D.J., Britton, J.M., Webster, I.C.L., and Russell, C.W.P.**
1989: Geology and Mineral deposits of the Unuk area; British Columbia Ministry of Energy, Mines and Petroleum Resources, Geological Survey Branch, Open File Map 1989-10.
- Anderson, R.G.**
1989: A stratigraphic, plutonic, and structural framework for the Iskut River map area, northwestern British Columbia; in Current Research, Part E, Geological Survey of Canada, Paper 89-1E, p. 145-154.
- Anderson, R.G. and Thorkelson, D.J.**
1990: Mesozoic stratigraphy and setting for some mineral deposits in Iskut River map area, northwestern British Columbia; in Current Research, Part E, Geological Survey of Canada, Paper 90-1F, p. 131-139.
- Britton, J.M. and Alldrick, D.J.**
1988: Sulphurets map area; British Columbia Ministry of Energy, Mines and Petroleum Resources, Geological Fieldwork, 1987, Paper 1988-1, p. 199-209.

Brown, D.A. and Greig, C.I.

1990: Geology of the Stikine River-Yehiniko Lake area, northwestern British Columbia (104G/11W and 12E); in Geological Fieldwork 1989, British Columbia Ministry of Energy, Mines and Petroleum Resources, Paper 1990-1, p. 141-151.

Greig, C.J.

1991: Stratigraphic and structural relations along the west-central margin of the Bowser Basin, Oweegee and Kinskuch areas, northwestern British Columbia; in Current Research, Part A, Geological Survey of Canada, Paper 91-1A, p. 197-205.

Grove, E.W.

1986: Geology and mineral deposits of the Unuk River-Salmon River-Anyox area; British Columbia Ministry of Energy, Mines and Petroleum Resources, Bulletin 63, 434 p.

Kirkham, R.V.

1991: Provisional geology of the Mitchell-Sulphurets region, northwestern British Columbia (104B/8, 9); Geological Survey of Canada, Open File 2416 (1:20 000).

Mandy, J.T.

1936: Unuk River area; in Annual Report of the Minister of Mines of the Province of British Columbia, 1935, p. B7-12.

Wright, F.E.

1907: The Unuk River mining region of British Columbia; in Report of the Minister of Mines of the Province of British Columbia, 1906, p. H68-74.

Geological Survey of Canada Projects 890021 and 700059

Jurassic biochronology in the Iskut River map area, British Columbia: a progress report

G. Nadaraju¹ and P.L. Smith¹
Cordilleran Division, Vancouver

Nadaraju, G. and Smith, P.L., 1992: *Jurassic biochronology in the Iskut River map area, British Columbia: a progress report*; in *Current Research, Part A*; Geological Survey of Canada, Paper 92-1A, p. 333-335.

Abstract

Jurassic biochronology is seen as both essential to understanding the regional geology and as a potential aid to mineral exploration in the Iskut River map area. At Eskay Creek, uppermost Pliensbachian ammonites were collected stratigraphically below the mineralization. Above the mineralization, Bajocian ammonites were collected and a single carbonate sample yielded radiolarians of Middle Toarcian to Early Bajocian affinities. From a core sample within the ore zone, a similar but less well preserved and less diverse radiolarian fauna was retrieved. New and extensive sampling from core offers the prospect of refining these age constraints.

On a regional scale, three suites of Jurassic faunas are distinguished: a benthonic fauna consisting of bivalves, sponges, corals and gastropods; a planktonic fauna of radiolarians; and a nektonic fauna of coleoids and ammonites.

Résumé

La biochronologie jurassique est considérée essentielle à la compréhension de la géologie régionale et potentiellement utile à l'exploration minérale dans la zone cartographique de la rivière Iskut. Au ruisseau Eskay, des ammonites sommitales du Pliensbachien ont été prélevées stratigraphiquement au-dessous de la minéralisation. Au-dessus de la minéralisation, on a prélevé des ammonites bajociennes, et un seul échantillon de roches carbonatées contenait des radiolaires ayant des affinités relevant du Toarcien moyen au Bajocien inférieur. D'un échantillon de carotte provenant de la zone minéralisée, on a extrait des radiolaires semblables mais moins bien conservés et moins diversifiés. Un nouvel échantillonnage par carottage plus étendu permettra d'affiner ces âges.

À l'échelle régionale, on distingue trois suites de faunes jurassiques : une faune benthonique composée de bivalves, d'éponges, de coraux et de gastropodes; une faune planctonique de radiolaires; et une faune nectonique de coléidés et d'ammonites.

¹ Department of Geological Sciences, University of British Columbia, 6339 Stores Road, Vancouver, B.C. V6T 2B4

INTRODUCTION

Jurassic rocks in the Iskut River map area have been the focus of recent attention because they host what appear to be stratabound mineral deposits such as Eskay Creek (Blackwell, 1990 and Britton et al., 1990). Lithostratigraphic refinements and correlations have proven difficult because of rapid lateral and vertical variations in facies that are compounded by structural complications. Biochronology is therefore important as an aid to geological mapping but, in addition, it has the potential to constrain the age of mineralization at specific sites and delimit temporal patterns of mineralization on a regional scale.

During the field season of 1991, Nadaraju began work on her Master's thesis research by systematically sampling drill core at the Eskay Creek camp. The aim is to increase the number and stratigraphic frequency of samples yielding radiolaria which offer the best prospect for refining the present age constraints on the mineralization. The processing of these samples should be completed by early 1992. Large collections of macrofossils from Eskay Creek, east of Snippaker Creek, north of Mitchell Glacier and south of Atkins and Treaty glaciers have been made by the authors, other investigators and mineral exploration geologists and are currently being studied (Fig. 1).

The Jurassic stratigraphy of the Iskut River map area is divisible into the Hazelton Group, a succession of Lower to Middle Jurassic volcanic, epiclastic, and sedimentary rocks, and the Bowser Lake Group, a Middle to Upper Jurassic succession of marine sedimentary rocks. In the eastern half of the map area Grove (1986) divided the Hazelton Group rocks of the Unuk River map area into three formations, in ascending order the Unuk River, Betty Creek, and Salmon River. He described the Unuk River Formation as a thick succession of volcanic, volcanoclastic, and sedimentary rocks thought to range in age from Hettangian to Toarcian based on fossil collections made east of the Unuk River (Fig. 1).

The Betty Creek Formation which occurs mostly east of the Unuk River, consists of red and green volcanic conglomerate and sandstone which yielded Lower and Middle Bajocian faunas. The Salmon River Formation was defined by Grove (1986) as colour banded siltstone and lithic wackes which contained moderately abundant Bajocian (or Bathonian?) to Upper Callovian and Early Oxfordian fossils.

Subsequent detailed mapping in the Iskut River map area by the B.C. Geological Survey Branch (Alldrick and Britton, 1988; Alldrick et al., 1989), distinguished the Mount Dilworth Formation between the Salmon River and Betty Creek formations. The Mount Dilworth Formation is a sequence of felsic pyroclastic rocks and welded tuff which represents the terminal stage of widespread volcanism. It hosts base and precious metal mineralization and is thought to be Toarcian in age based on fossil evidence elsewhere within the Stewart area (Alldrick, 1987; Brown, 1987). Anderson and Thorkelson (1990) divided the Salmon River Formation into 2 members. A lower member of Toarcian age is commonly a coarse, pyritiferous, calcareous wacke that is locally fossil-bearing (belemnites and *Weyla*). The upper member is divided into three different facies due to rapid lateral changes from the east to west within the map area. The eastern Troy Ridge facies is a radiolarian-bearing siliceous shale and white tuffaceous turbidite. The Eskay Creek facies which hosts the Eskay Creek deposit, is a sequence of pillow lavas overlying limy siliceous shale. The Snippaker Mountain facies which consists of andesitic volcanics, occurs to the west.

BIOSTRATIGRAPHY

During the summer of 1989, Smith visited localities in the upper drainage of the Unuk River. Macrofossils and samples for microfossil analysis were collected and faunal assemblages ranging in age from Late Pliensbachian to possibly Oxfordian were identified (Smith and Carter, 1990).

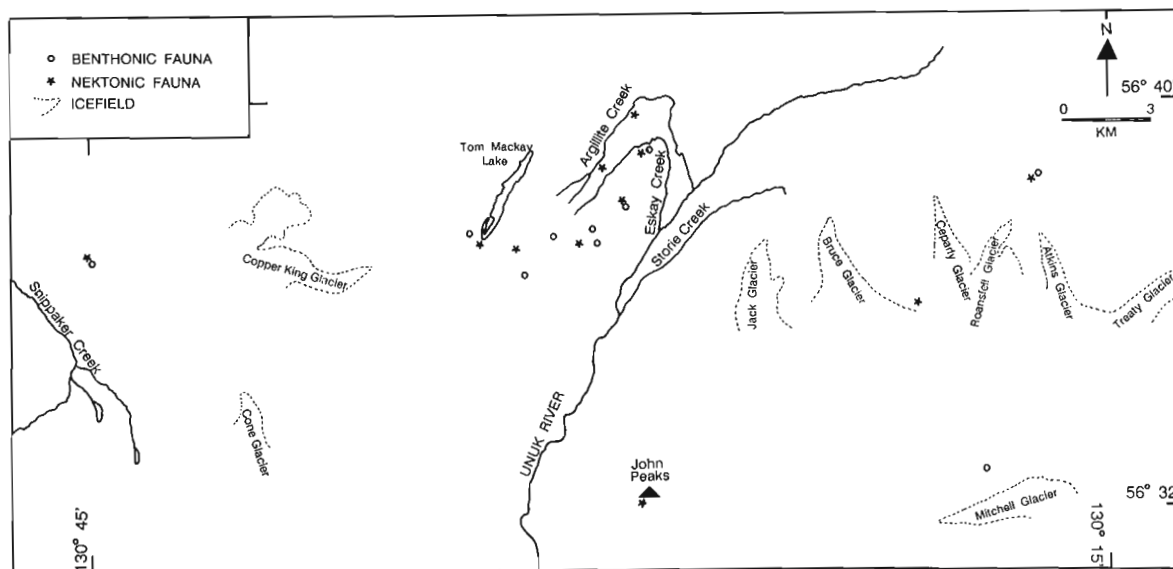


Figure 1. Location map of study area.

Stratigraphically below the Eskay Creek mineralized horizon, ammonites characteristic of the uppermost Pliensbachian Carlottense Zone were collected including *Tiloniceras propinquum* (Whiteaves), *Protogrammoceras* spp., and *Lioceratoides?* sp.. Stratigraphically above the mineralized horizon, the Bajocian ammonite *Stephanoceras* sp. was found (Donnelly, 1976) and a single float carbonate sample yielded the radiolarian species *Elodium* cf. *nadaensis* Carter, *Emiluvia acantha* Carter, *Napora* sp., *Paronaella variabilis* Carter, *Parvicingula* sp., *Perispyridium* spp., *Protoperispyridium hippaensis* Carter, *Pseudocrucella sanfilippoe* (Pessagno), and *Stichocapsa* cf. *convexa* Yao, broadly indicating a Middle Toarcian to Early Bajocian age. A similar but less well preserved and less diverse radiolarian assemblage has subsequently been retrieved from a core sample within the ore zone itself. The stratigraphic sequence of macro and microfossils is therefore consistent but at the present time only provides a Toarcian to Early Bajocian age constraint for the mineralization.

NEW FAUNA

Three suites of Jurassic faunas from the Iskut River map area are recognized from existing collections:

a) **Benthonic faunas:** Diverse benthonic communities in coarse clastic rocks are more widespread in time and space than initially believed. Abundant individuals of certain forms indicate a Tethyan influence particularly the calcareous sponges. The endemic east Pacific bivalve genus *Weyla* can also be common and the local abundance of gastropods, about which little is known at present, is remarkable. Compound and solitary scleractinian corals are widespread but not abundant. The evaluation of the relative age of these sporadically occurring benthonic communities is an important aim of the research.

b) **Planktonic faunas:** Many horizons in the map area have been sampled for carbonates and calcareous shale which are currently being processed for radiolaria.

c) **Nektonic faunas:** Many coleoids have been found especially within the ore zone at Eskay Creek but their biochronological significance is minimal. Of significance are the numerous ammonite localities that have been discovered during the summer of 1991 by the authors and geologists mapping the areas between Eskay Creek and Tom Mackay Lake, north of John Peaks, north of Atkins Glacier, and east of Snippaker Creek (Fig. 1).

ACKNOWLEDGMENTS

This work is being funded by Energy, Mines and Resources and the Natural Science and Engineering Research Council of Canada. Special thanks to Bob Anderson of the Geological Survey of Canada for logistical support, samples and

encouragement. Jack Henderson (Geological Survey Canada) gave us collections from the Sulphurets area. We thank James Stewart, Don Lewis, Carl Edmunds, Ken Rhye, Andy Onley, John Bellamy, and Jake Margolis of the Corona Corporation for logistical support, access to core samples and their warm hospitality at the Eskay Creek camp. Samples have kindly been collected by James McDonald, Art Ettliger, Peter Lewis, Tina Roth, Roland Bartsch, and Bruce Miller of the Mineral Deposit Research Unit at UBC. We thank Mark Rebagliati of Rebagliati Geological Consulting Ltd. for permission to sample on the SIB property and Wes Raven of Orequest for information on new fossil finds on the Tantalus property. We appreciate the field assistance of Peter Daubeny.

REFERENCES

- Alldrick, D.J.**
1987: Geology and mineral deposits of the Salmon River Valley, Stewart area (104A, 104B); British Columbia Ministry of Energy, Mines and Petroleum Resources, Geological Survey Branch, Open File 1984-22.
- Alldrick, D.J. and Britton, J.M.**
1988: Geology and mineral deposits of the Sulphurets area (NTS 104A/5, 104A/12, 104B/8 and 104B/9); British Columbia Ministry of Energy, Mines and Petroleum Resources, Geological Survey Branch, Open File Map 1988-4.
- Alldrick, D.J., Britton, J.M., Webster, I.C.I., and Russell, C.W.P.**
1989: Geology and mineral deposits of the Unuk area; British Columbia Ministry of Energy, Mines and Petroleum Resources, Geological Survey Branch, Open File Map 1989-10.
- Anderson, R.G. and Thorkelson, D.J.**
1990: Mesozoic stratigraphy and setting for some mineral deposits in Iskut River map area, northwestern British Columbia; in Current Research, Part E; Geological Survey of Canada, Paper 90-1E, p. 131-139.
- Blackwell, J.D.**
1990: Geology of the Eskay Creek #21 Deposits; Mineral Deposits Division, Geological Association of Canada, The Gangue, Number 31, April, 1990, p. 1-4.
- Britton, J.M., Fletcher, B.A., and Alldrick, D.J.**
1990: Snippaker map area (104B/6E, 7W, 10W, 11E); in Geological Fieldwork 1988, British Columbia Ministry of Energy, Mines and Petroleum Resources, Paper 1989-1, p. 241-250.
- Brown, D.A.**
1987: Geologic setting of the volcanic-hosted Silbak Premier Mine, northwestern British Columbia (104 A/4, 104 B/1); M.Sc thesis, The University of British Columbia, Vancouver, 219 p.
- Donnelly, D.A.**
1976: Study of the volcanic stratigraphy and volcanogenic mineralization on the Kay claim group, northwestern British Columbia; B.Sc. thesis, University of British Columbia, Vancouver, 61 p.
- Grove, E.W.**
1986: Geology and mineral deposits of the Unuk River-Salmon River-Anyox area; British Columbia Ministry of Energy, Mines and Petroleum Resources, Bulletin 63, 434 p.
- Smith, P.L. and Carter, E.S.**
1990: Jurassic correlations in the Iskut River map area, British Columbia, and the age of the Eskay Creek deposit; in Current Research, Part E; Geological Survey of Canada, Paper 90-1E, p. 149-151.

Highlights of the 1991 geological field program, Queen Charlotte Islands, British Columbia

Points saillants du programme de travaux géologiques sur le terrain dans les îles de la Reine-Charlotte en Colombie-Britannique

James W. Haggart
Cordilleran Division, Vancouver

James W. Haggart
Division de la Cordillère, Vancouver

Haggart, J.W., 1992: Highlights of the 1991 geological field program, Queen Charlotte Islands, British Columbia; in Current Research, Part A; Geological Survey of Canada, Paper 92-1A, p. 337-341.

Haggart, J.W., 1992 : Points saillants du programme de travaux géologiques sur le terrain dans les îles de la Reine-Charlotte en Colombie-Britannique; dans Recherches en cours, Partie A, Commission géologique du Canada, Étude 92-1A, p. 337-341.

INTRODUCTION

The 1991 field program in the Queen Charlotte Islands (103B, F, G, K) maintained the tradition of geological excitement established in previous seasons. Although 1:50 000-scale mapping of the islands is almost complete (Fig. 1), with only the spine of the San Christoval Range and a few adjacent areas remaining, new finds of macrofossils have proven the existence of several previously unrecognized Upper Jurassic stratigraphic horizons in the islands and complex new structures have been identified locally. The synthesis of these new data with the existing base will be challenging; however, the result enhances understanding of the geological evolution of the Queen Charlotte Islands and adjacent regions.

FIELD MAPPING PROGRAM

Geological mapping was undertaken at several different localities in the southern islands in 1991 (Fig. 1). This mapping was designed to complement the 1990 program and extend detailed coverage through the principal structural province recognized in the southern part of the islands, the Louscoone Inlet fault system (LIFS). Recent detailed mapping indicates that transcurrent faulting and extensional structures characterize the southern parts of the Louscoone Inlet fault system; however, earlier mapping under the Queen Charlotte Program in 1987-88 ruled out significant transcurrent movement at the northern end of the Louscoone Inlet fault system, and its northwestern extension, the Rennell Sound deformation zone (RSDZ). The 1991 program examined geology and structures in the northern part of the Louscoone Inlet fault

INTRODUCTION

Les travaux de terrain effectués dans les îles de la Reine-Charlotte (103 B, F, G, K) en 1991 ont permis de maintenir le climat géologique de fébrilité qui prévalait au cours des saisons précédentes. La cartographie à l'échelle de 1/50 000 des îles est presque complète (fig. 1); il ne reste que les sommets du chaînon San Christoval et quelques régions adjacentes à couvrir. Toutefois, la découverte de nouveaux macrofossiles a prouvé l'existence de plusieurs horizons stratigraphiques du Jurassique supérieur jamais identifiés auparavant dans les îles; de nouvelles entités structurales complexes ont aussi été décrites par endroits. L'intégration de ces données récentes avec les anciennes sera un défi de taille, mais les résultats obtenus devraient améliorer la compréhension de l'évolution géologique des îles de la Reine-Charlotte et des régions adjacentes.

PROGRAMME DE CARTOGRAPHIE SUR LE TERRAIN

En 1991, plusieurs endroits distincts de la partie sud des îles ont fait l'objet de cartographie géologique (fig. 1). Ces travaux ont été planifiés de façon à compléter le programme de 1990 et à couvrir en détail un peu plus de territoire de la principale province structurale identifiée dans la partie sud des îles, à savoir le système de failles de l'inlet Louscoone (LIFS). La cartographie de détail récente révèle que la section méridionale du LIFS est caractérisée par des failles de coulissage et des structures d'extension; à noter que les travaux de cartographie menés dans les îles de la Reine-Charlotte en 1987-1988 ont permis d'écarter la possibilité qu'il se soit produit des mouvements de coulissage importants à l'extrémité nord du LIFS et au niveau de son prolongement vers le nord-ouest, la zone de déformation de la baie Rennell (RSDZ). Le programme de 1991 a porté sur le contexte géologique et les éléments

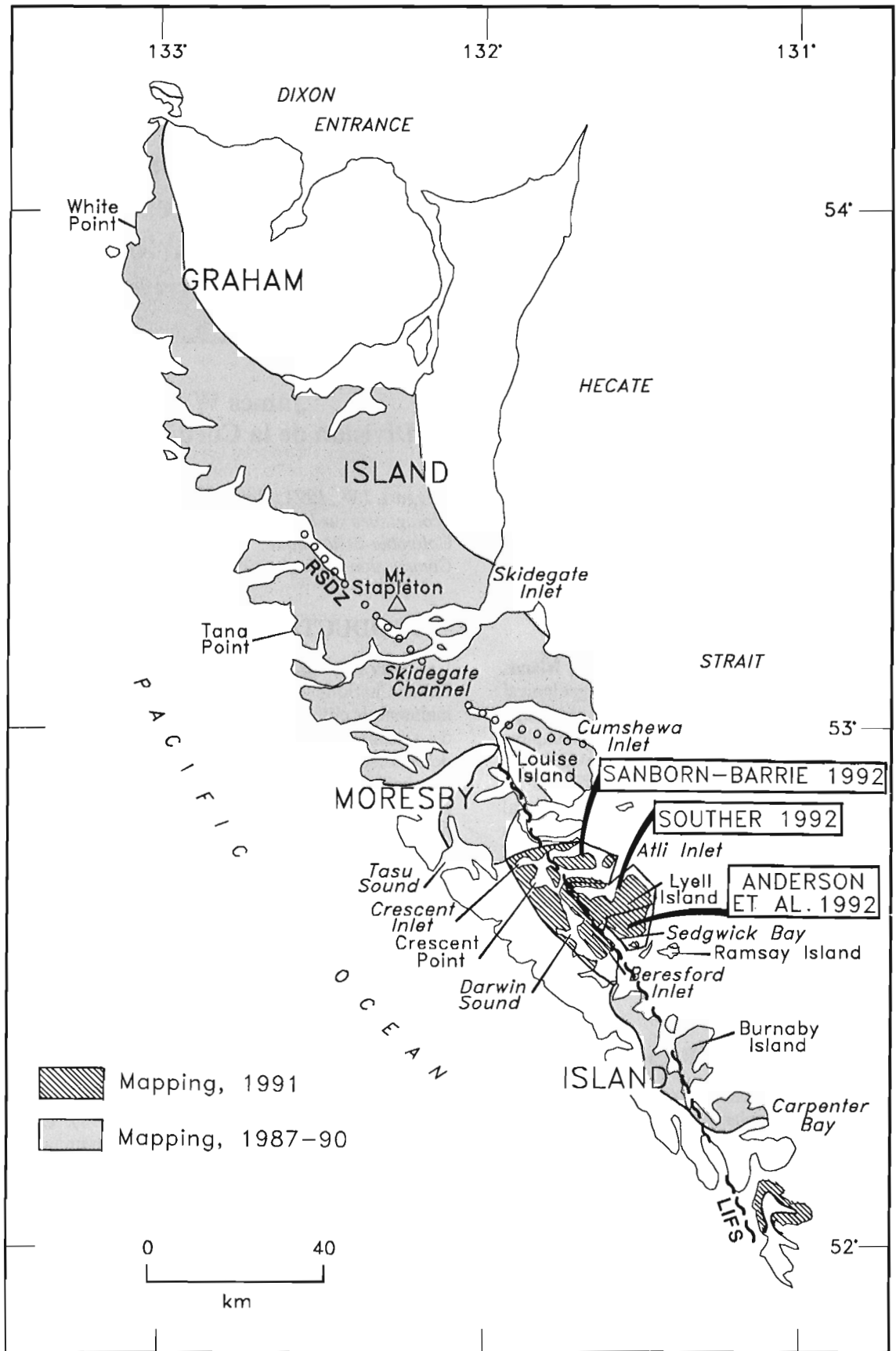


Figure 1. Map of Queen Charlotte Islands showing areas of 1991 mapping.
Figure 1. Carte des îles de la Reine-Charlotte montrant les régions qui ont fait l'objet de travaux cartographiques en 1991.

system, to compare them with those in the Rennell Sound deformation zone to the north and in the Louscoone Inlet fault system to the south.

The Lyell Island/Darwin Sound region was selected as the focus of this effort, in part because of proximity to major structural zones, and also because the extensive logging road network on Lyell Island is slated for rehabilitation over the 1991-93 period, as part of the development program for the new South Moresby Park Reserve. Papers by Anderson et al. (1992), Sanborn-Barrie (1992), and Souther (1992) detail the geology of this complex region of the Queen Charlotte Islands. The following are highlights of that work.

New exposures of the Middle Jurassic Yakoun Group were recognized on northern Lyell Island by Souther (1992). These strata include sedimentary and volcanic facies and were previously included in the Masset Formation. Macrofossils allow a firm determination of their Bajocian age.

Widely-separated exposures of mudstone identified at several localities in the region are now recognized as correlative by Haggart (1992). On Lyell Island the mudstone underlies conglomerate tentatively correlated by Souther (1992) with the Lower Cretaceous Longarm Formation and Sanborn-Barrie (1992) has suggested that, in the Crescent/Anna inlets area, the unit may overlies debris-flow conglomerate and breccia containing clasts with Bajocian age fossils. Haggart (1992) has also recognized the unit elsewhere in the southern part of the archipelago, including Burnaby Island. Macrofossils from the mudstone indicate a likely Middle Jurassic to Early Cretaceous age. Interestingly, the unit is less deformed than older strata and may postdate late Middle Jurassic deformation, heretofore unrecognized in this area but characteristic of the more northerly part of the islands.

The stratigraphy and rock types of the Lyell Island volcanic/plutonic assemblage have been addressed by Souther (1992) and Anderson et al. (1992). The plutonic complex on southeastern Lyell was found by these workers to be much more extensive than previously recognized and the volcanic rocks are considered to be the extrusive equivalents of the shallow plutonic rocks.

An important splay of the Louscoone Inlet fault system appears to trend through Sedgwick Bay on central Lyell Island, rather than through Beresford Inlet as previously interpreted. Sanborn-Barrie (1992) studied structures in Beresford Inlet, and has attributed them to competency contrasts between plutonic rocks and the country rocks. Souther (1992) has established that the fault zone in Sedgwick Bay shows evidence of transcurrent movement, at least locally, although magnitude and direction of offset are unknown. According to Souther, the fault zone separates highly deformed Triassic and Lower Jurassic rocks on the west from less deformed Middle Jurassic through Tertiary rocks on the east. Deformation along the fault zone affected Middle Jurassic Yakoun Group rocks

structuraux de la section septentrionale du LIFS; il visait à les comparer avec ceux de la RSDZ au nord et de la section méridionale du LIFS.

Cette année, l'attention s'est tournée vers la région de l'île Lyell et du chenal Darwin, partiellement en raison de sa proximité des principales zones structurales, mais aussi parce que l'important réseau de routes utilisées pour la coupe forestière dans l'île Lyell a été désigné pour être rénové entre 1991 et 1993, dans le cadre du programme d'établissement de la Réserve de parc national Moresby-Sud. Les articles d'Anderson et al. (1992), de Sanborn-Barrie (1992) et de Souther (1992) décrivent en détail la géologie de cette région complexe des îles de la Reine-Charlotte. Les paragraphes qui suivent présentent les faits saillants de ces travaux.

Dans la partie nord de l'île Lyell, de nouveaux affleurements du groupe de Yakoun du Jurassique moyen ont été décrits par Souther (1992). Ces strates à faciès volcaniques et sédimentaires étaient auparavant associées à la formation de Masset. Les macrofossiles permettent de déterminer avec précision qu'elles datent du Bajocien.

Des affleurements de mudstone très distants l'un de l'autre ont été décrits à plusieurs endroits dans la région; selon Haggart (1992), il s'agit d'unités correspondantes. Sur l'île Lyell, les mudstones sont sous-jacents à des conglomérats que Souther (1992) a tenté de corréler avec la formation de Longarm du Crétacé inférieur. Sanborn-Barrie (1992) a plutôt suggéré que dans la région des inlets Crescent et Anna, l'unité puisse reposer sur des conglomérats et des brèches de coulée de débris dont les clastes contiennent des fossiles bajociens. Haggart (1992) a également observé ces roches dans la partie sud de l'archipel, y compris dans l'île Burnaby. Les macrofossiles des mudstones indiquent un âge possible allant du Jurassique moyen au Crétacé précoce. Fait intéressant, cette unité est moins déformée que les strates plus anciennes; il se peut donc qu'elle soit postérieure à la déformation de la fin du Jurassique moyen, qui jusqu'ici n'a jamais été identifiée dans la présente région, mais qui est caractéristique des zones plus septentrionales de l'archipel.

La stratigraphie et les lithologies de la succession volcanique-plutonique de l'île Lyell ont été étudiées par Souther (1992) ainsi que Anderson et al. (1992). Ils ont établi que le complexe plutonique de la partie sud-est de l'île est beaucoup plus important que ce qui avait été déterminé auparavant et que les roches volcaniques constituent des équivalents extrusifs des roches plutoniques de faible profondeur.

Une importante divergence du LIFS semble s'orienter dans la baie Sedgwick du centre de l'île Lyell, et non dans l'inlet Beresford tel qu'on l'avait auparavant interprété. Sanborn-Barrie (1992) a étudié les structures de l'inlet Beresford et les a expliqué par des différences de compétence entre les roches plutoniques et leurs encaissants. Souther (1992) a établi que dans la zone de failles de la baie Sedgwick, il y avait des indications de mouvements de coulissage, du moins par endroits, bien que l'importance et l'orientation du rejet transversal n'aient pas été déterminées. Selon Souther, la zone de failles sépare les roches très déformées du Trias et du Jurassique inférieur, à l'ouest, des roches moins déformées du Jurassique moyen au Tertiaire, à l'est. La déformation le long de la zone de failles a affecté les roches du groupe jurassique de Yakoun et Souther

and Souther has recognized that the zone is overlapped on northern Lyell Island by volcanics of possible Miocene age. The timing of movement is therefore likely pre-Miocene.

Sanborn-Barrie (1992) identified a large, previously unrecognized structure in the Darwin Sound area. Mesoscopic fabric data indicate that low-angle, reverse shear characterizes several outcrops and older Triassic strata may have been transposed over younger rocks on the east. Continuity of this feature, running through the central part of the sound, with the Louscoone Inlet fault system is unlikely, given the different structural histories of the two features. The Darwin Sound structure may reflect an older deformation event.

In addition to the Lyell Island/Darwin Sound area, detailed mapping and stratigraphic studies were continued in the central Queen Charlotte Islands to verify interpreted geological relations. Mapping on northern Moresby Island and southern Graham Island by Haggart (1992) focused on the Jurassic and Cretaceous outcrop belts to address the structural controls on Cretaceous sedimentation. This work has determined that block faulting was not extensive in this part of the islands during most of Cretaceous time and indeed, likely did not continue after the Late Jurassic/earliest Cretaceous.

STRATIGRAPHY AND SEDIMENTOLOGY

Fieldwork continues to improve understanding of the later Mesozoic stratigraphic succession of the islands. Macrofossil collections indicate that several stratigraphic horizons are locally present in the Upper Jurassic of the northern part of the islands, including Callovian/Oxfordian and Oxfordian/Kimmeridgian (Haggart, 1992). These strata are coarse clastics associated with volcanic rocks and are partly coeval with the extensive Middle-Late Jurassic plutonism recognized in the islands. The presence of these Upper Jurassic horizons indicates that the Late Jurassic hiatus in the islands is less extensive than previously considered. The mudstone unit widely distributed across the Lyell Island/Burnaby Island region described above may be a southerly equivalent of these Late Jurassic sequences.

Gamba (1992) has continued sedimentological investigations of the Cretaceous Queen Charlotte Group succession, characterizing the facies associations which comprise the group. The assemblages indicate that the bulk of the group represents deposition in relatively shallow water. Gamba was able to further recognize several cycles of sea level fluctuation within the well-preserved Albian part of the succession. This work promises fine-scale future correlation of the Cretaceous rocks of the islands.

signale que dans le nord de l'île Lyell, la zone est recouverte de volcanites datant peut-être du Miocène. Ainsi, il est vraisemblable que ce mouvement soit antérieur au Miocène.

Sanborn-Barrie (1992) a décrit pour la première fois une grande structure dans la région du chenal Darwin. Les données sur la fabrique mésoscopique font ressortir que plusieurs affleurements présentent un cisaillement inverse à pendage faible et qu'il se peut que des strates plus anciennes du Trias aient été transportées sur des roches plus jeunes, à l'est. Il est invraisemblable que le prolongement de cette structure, qui traverse la partie centrale du chenal, soit le LIFS, étant données les différences dans l'évolution structurale de ces deux entités. La structure du chenal Darwin peut correspondre à un épisode de déformation plus ancien.

Outre la région de l'île Lyell et du chenal Darwin, il y a la partie centrale des îles de la Reine-Charlotte qui a fait l'objet de cartographie détaillée et d'études stratigraphiques, afin de vérifier les liens géologiques établis par interprétation. Les travaux de cartographie dans la partie nord de l'île Moresby et la partie sud de l'île Graham (Haggart, 1992) ont été effectués surtout dans les zones d'affleurement du Jurassique et du Crétacé et visaient à identifier le contrôle structural de la sédimentation crétacée. Ainsi, il a été établi que le morcellement par failles n'avait pas été important dans cette partie de l'archipel pendant la presque totalité du Crétacé et qu'en réalité, il était vraisemblable qu'il se soit terminé au Jurassique tardif ou tout début du Crétacé.

STRATIGRAPHIE ET SÉDIMENTOLOGIE

Les travaux de terrain continuent d'aider à mieux comprendre la succession stratigraphique de la fin du Mésozoïque de l'archipel. Les échantillons de macrofossiles indiquent que de nombreux horizons stratigraphiques s'observent localement dans le Jurassique supérieur de la partie nord des îles, qui englobe le Callovien-Oxfordien et l'Oxfordien-Kimmeridgien (Haggart, 1992). Ces strates se composent de roches clastiques à grain grossier associées à des roches volcaniques et sont contemporaines de l'important épisode de plutonisme qui s'est produit dans les îles du Jurassique moyen à tardif. La présence de ces horizons du Jurassique supérieur témoigne du fait que l'hiatus du Jurassique tardif qui a eu lieu dans les îles est moins important que ce qui avait été estimé. Il se peut que l'unité de mudstone très répandue dans la région de l'île Lyell et de l'île Burnaby qui a été décrite auparavant soit un équivalent méridional des ces séquences du Jurassique tardif.

Gamba (1992) a poursuivi les études sédimentologiques de la succession crétacée du groupe de Queen Charlotte en décrivant les associations de faciès dans lesquelles le groupe se trouve. Celles-ci montrent que la plupart des lithologies correspondent à une sédimentation en eau relativement peu profonde. Gamba a aussi réussi à mieux détailler de nombreux cycles de fluctuation du niveau marin dans la section bien conservée de la succession, associée à l'Albien. Ces travaux devraient aboutir à une corrélation à petite échelle des roches crétacées des îles.

REFERENCES

- Anderson, R.G., Gunning, M.H., and Porter, S.**
1992: Progress in mapping of Jurassic and Tertiary plutonic styles, Queen Charlotte Islands; *in* Current Research, Part A; Geological Survey of Canada, Paper 92-1A.
- Gamba, C.A.**
1992: Lithofacies of the late Early to early Late Cretaceous Queen Charlotte Group, Queen Charlotte Islands, British Columbia; *in* Current Research, Part A; Geological Survey of Canada, Paper 92-1A.
- Haggart, J.W.**
1992: Progress in Jurassic and Cretaceous stratigraphy, Queen Charlotte Islands, British Columbia; *in* Current Research, Part A; Geological Survey of Canada, Paper 92-1A.
- Sanborn-Barrie, M.**
1992: Geology of the Darwin Sound area, Queen Charlotte Islands, British Columbia; *in* Current Research, Part A; Geological Survey of Canada, Paper 92-1A.
- Souther, J.G.**
1992: Geology of central Lyell Island, Queen Charlotte Islands, British Columbia; *in* Current Research, Part A; Geological Survey of Canada, Paper 92-1A.

Geological Survey of Canada Projects 870070, 880038

BIBLIOGRAPHIE

- Anderson, R.G., Gunning, M.H., and Porter, S.**
1992: Progress in mapping of Jurassic and Tertiary plutonic styles, Queen Charlotte Islands; *in* Current Research, Part A; Geological Survey of Canada, Paper 92-1A.
- Gamba, C.A.**
1992: Lithofacies of the late Early to early Late Cretaceous Queen Charlotte Group, Queen Charlotte Islands, British Columbia; *in* Current Research, Part A; Geological Survey of Canada, Paper 92-1A.
- Haggart, J.W.**
1992: Progress in Jurassic and Cretaceous stratigraphy, Queen Charlotte Islands, British Columbia; *in* Current Research, Part A; Geological Survey of Canada, Paper 92-1A.
- Sanborn-Barrie, M.**
1992: Geology of the Darwin Sound area, Queen Charlotte Islands, British Columbia; *in* Current Research, Part A; Geological Survey of Canada, Paper 92-1A.
- Souther, J.G.**
1992: Geology of central Lyell Island, Queen Charlotte Islands, British Columbia; *in* Current Research, Part A; Geological Survey of Canada, Paper 92-1A.

Projets 870070 et 880038 de la Commission géologique du Canada

Geology of central Lyell Island, Queen Charlotte Islands, British Columbia

J.G. Souther
Cordilleran Division, Vancouver

Souther, J.G., 1992: Geology of central Lyell Island, Queen Charlotte Islands, British Columbia; in Current Research, Part A; Geological Survey of Canada, Paper 92-1A, p. 343-350.

Abstract

Lyell Island is underlain by rocks ranging in age from Late Triassic to Tertiary. Triassic volcanic rocks of the Karmutsen Formation and Late Triassic to Early Jurassic sedimentary rocks of the Kunga Group were deformed prior to intrusion of Middle to Late Jurassic plutons. A broad northwest-trending fault zone through central Lyell Island separates these older rocks from less deformed Middle Jurassic Yakoun Group and younger strata to the northeast. The latter are cut by north- to northwest-trending normal faults that may be related to extension accompanying Tertiary igneous activity. Tertiary volcanics which form a thick overlap succession on northwestern Lyell Island are believed to be the eruptive equivalents of a large subvolcanic complex in the east.

Résumé

L'île Lyell repose sur des roches dont l'âge varie du Trias supérieur au Tertiaire. Les roches volcaniques triasiques de la formation de Karmutsen et les roches sédimentaires du Trias supérieur au Jurassique inférieur du groupe de Kunga ont été déformées avant l'intrusion des plutons du Jurassique moyen à supérieur. Une large zone faillée à direction nord-ouest traversant le centre de l'île Lyell sépare ces anciennes roches des couches moins déformées du groupe de Yakoun du Jurassique moyen et des couches plus récentes au nord-est. Ces dernières sont découpées par des failles normales à direction de nord à nord-ouest qui pourraient être liées à une distension accompagnant une activité ignée tertiaire. Les roches volcaniques tertiaires qui forment une épaisse succession de recouvrement dans le nord-ouest de l'île Lyell sont considérées être équivalentes à un large complexe hypabyssal dans l'est.

PREVIOUS WORK

The first systematic mapping of Lyell Island was done in conjunction with a regional reconnaissance of the Queen Charlotte Islands in the 1950s and early 1960s (Sutherland Brown, 1968). Sutherland Brown identified Lyell Island as a major centre of Tertiary igneous activity. This was later confirmed by the study of regional dyke swarms (Souther and Jessop, 1991) and the detailed examination of plutons (Anderson and Greig, 1989; Anderson and Reichenbach, 1991). Reinterpretation of Sutherland Brown's stratigraphy on Lyell Island by Cameron and Hamilton (1988) raised several unresolved problems regarding the Jurassic/Cretaceous succession and emphasized the need for further paleontological work.

PRESENT STUDY

In 1988 Lyell Island (103B) was incorporated into the South Moresby National Park Reserve. Prior to that time large segments of the island had been logged. On becoming part of the park reserve logging was halted on the island and in 1991 a decision was made by Parks Canada to restore the logged areas as nearly as possible to their natural state. Because the restoration involves the virtual destruction of all roads, bridges, and culverts the present mapping was undertaken to record the geology exposed in roadcuts before access was lost. Work along the roads was supplemented by boat traverses of the adjacent shoreline.

GENERAL GEOLOGY

The geology of Lyell Island encompasses rocks ranging in age from Triassic to Late Tertiary and includes most of the stratigraphic units present in the southern Queen Charlotte Islands (Fig. 1). Good exposures are present along much of the coastline and in roadcuts and quarries along the many logging roads. Elsewhere the island is largely mantled by thick colluvium and dense forest that covers even the uppermost ridges.

Karmutsen Formation

Fine grained mafic volcanics at the extreme western end of Atli Inlet are the only Karmutsen rocks exposed within the mapped area. They have been moderately sheared, chloritized, and veined with irregular quartz-epidote stringers but some of the outcrops exhibit spheroidal structures. Pillow lavas are characteristic of the less deformed Karmutsen farther west and the structures in Atli Inlet are probably pillows that have been moderately deformed. The contact between Karmutsen rocks and adjacent Tertiary volcanics was not observed.

Kunga Group

Rocks assigned to the Triassic/Jurassic Kunga Group are exposed in a broad northwest-trending belt between Sedgwick and Beljay bays. They are bounded on the

northeast by the Sedgwick Bay fault and, farther west, intruded by Jurassic plutons of the Beresford complex. Stratigraphic contacts with underlying and overlying strata were not observed.

The belt is structurally complex. Intense folding is overprinted by pervasive fracturing and shearing that increases toward the Sedgwick Bay fault zone, where mylonite is well developed along several parallel fault strands. Although the stratigraphy is structurally disrupted, the varied lithology of the belt suggests that most Kunga Group strata are present. Good exposures of Sadler Limestone and thin-bedded Sandilands Formation clastic sediments are widespread; however, Peril Formation limestone is known at only a few isolated outcrops and its true extent is unknown.

Sadler Limestone

Massive, light grey limestone is intermittently exposed along the axis of the belt of Kunga Group rocks. It appears to form the cores of anticlinal structures flanked by highly deformed, thin-bedded strata of the Peril? and Sandilands formations.

Peril Formation?

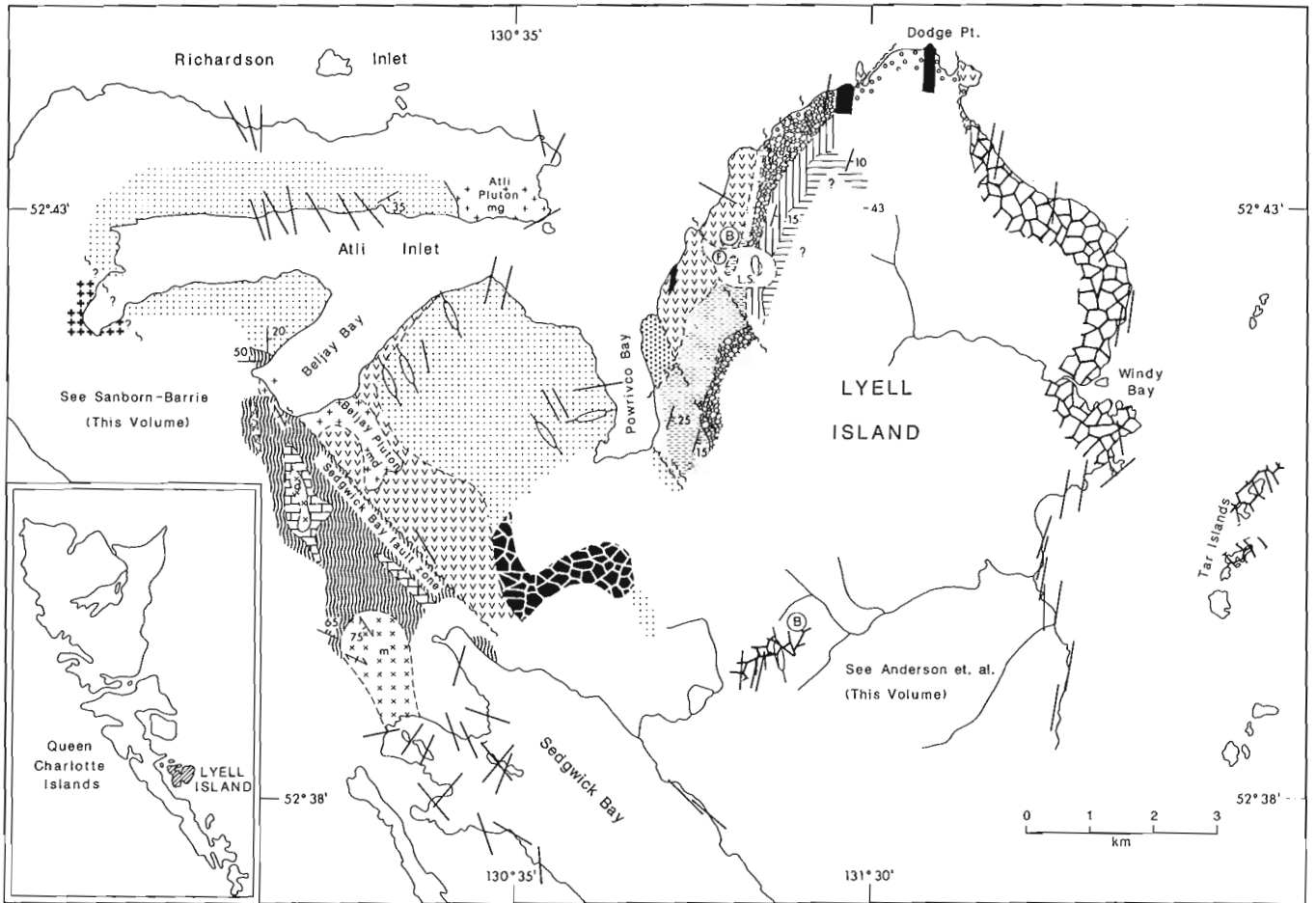
Dark grey, thin-bedded limestone and calcareous siltstone are exposed in roadcuts west of Beljay Bay. Primary sedimentary layering is preserved in some beds which have suffered less deformation than the surrounding, highly sheared rock. Although the lithology is typical of Peril limestone the beds may not be in their original stratigraphic context. Considering the structural complexity of the zone, the thin-bedded limestone may represent fault-bounded slices of slightly more competent rock surrounded by highly tectonized Sandilands Formation siltstone and shale.

Sandilands Formation

The bulk of the Kunga Group rocks on Lyell Island comprise thin-bedded shale, siltstone, and minor sandstone. These rocks structurally overlie the Sadler Limestone south of Beljay Bay and are believed to be correlative with the Sandilands Formation. Many of the beds have distinctive light and dark grey laminar banding due to sorting and grading of the fine sandstone interbeds. However, complex folding and faulting and intrusion of numerous fine grained diorite dykes and sills preclude any estimate of thickness or internal stratigraphic succession.

Maude Group

Medium-bedded sandstone on the east side of Powrivco Bay was originally assigned to the Maude Group by Sutherland Brown (1968). A Toarcian age for these rocks was favoured by Cameron and Tipper (1985: p. 25) based on subsequent study of fossil collections; however, the stratigraphic relationship of these rocks to underlying and overlying strata is still unresolved. The sandstone beds are separated from Yakoun Group volcanics and unnamed Jura-Cretaceous shale



TERTIARY VOLCANIC ROCKS

- Murrelet facies:** (a) Feldspar-phyric andesite breccia, minor tuff, lava flows and lahar deposits. (b) Basalt.
- Beljay facies:** Mainly subaerial dacite? and basalt? breccia, minor tuff, flows and related intrusions.

INTRUSIVE ROCKS
KANO PLUTONIC SUITE

- (mg) Monzogranite; (md) Monzodiorite, feldspar porphyry.

DYKES

- >30 m, <30 m: Basalt, hornblende-feldspar-phyric andesite.

MIXED VOLCANIC-INTRUSIVE COMPLEXES

- Eastern facies:** Subvolcanic intrusions, minor breccia and flow remnants. Basalt, hornblende-feldspar porphyry, feldspar-phyric andesite, dacite and minor rhyolite.
- Western facies:** Mainly dacite? and andesite volcanic breccia cut by numerous dykes and subvolcanic intrusions.

JURASSIC AND/OR CRETACEOUS

- Longarm? Formation:** Thick-bedded, conglomerate, interbedded sandstone.
- Powivco facies:** Thin-bedded siltstone, mudstone, minor sandstone and grit.

- Bedding (tops known, unknown)
Gneissosity, foliation
Fault (defined, assumed)
Stockwork of epithermal veins

JURASSIC

BURNABY ISLAND PLUTONIC SUITE:

- Beresford complex: (m) Monzodiorite; (d) diorite.

YAKOUN GROUP

- Upper unit:** Volcanic breccia, aquagene tuff, minor pillow lava, flows and subvolcanic intrusions.
- Lower unit:** Sandstone, conglomerate, tuff, volcanic sandstone and grit.

MAUDE GROUP

- Sandstone.

TRIASSIC AND/OR JURASSIC

KUNGA GROUP

- Sandilands Formation:** Thin-bedded siltstone, minor sandstone.
- Peril? Formation:** Thin-bedded dark grey limestone.
- Sadler Limestone:** Massive light grey limestone.

TRIASSIC

- Karmutsen Formation:** Chloritized basalt, greenstone, and derived mylonite.

- L.S. Landslide
(F) Fossil locality
(B) Bitumen occurrence

Figure 1. Geological map of central Lyell Island.

by narrow drift-filled valleys. The presence of extensive Fe-Mn cement in the colluvium in these valleys suggests the deep circulation of groundwater along faults.

Yakoun Group

The Middle Jurassic Yakoun Group is the most lithologically diverse stratigraphic succession within the mapped area. It includes volcanic flows and primary pyroclastic rocks as well as volcanoclastic sandstone, grit, conglomerate, and minor tuffaceous shale. Although the various lithologies are locally interstratified, sedimentary rocks predominate in the lower part of the succession and volcanic rocks in the upper part. Unlike the underlying Kunga Group, Yakoun Group rocks are relatively undeformed and exhibit little evidence of internal strain.

Lower unit

Steeply dipping but relatively undeformed sediments of the lower unit of the Yakoun Group are well exposed on wave-cut benches west of Dodge Point where Haggart (1991a) reported Early Bajocian ammonites. Sandstones discovered east of Dodge Point during the present study yielded a similar fauna (J.W. Haggart, pers. comm., 1991) and are probably correlative with the Early Bajocian beds farther west.

The newly discovered sediments east of Dodge Point are similar to those described in detail by Haggart (1991a) farther west. They mainly comprise medium- to thick-bedded, fine- to coarse-grained sandstone interlayered with thin beds of varicoloured tuff and thick beds of conglomerate and grit. The sandstones are commonly well sorted and form light grey-weathering beds up to 2 m thick. Many contain shell fragments and some contain carbonized wood. The conglomerate is found in beds up to a few metres thick, or as lenses less than a metre thick within the sandstone succession. Many of the latter are matrix-supported and some of the sandstone beds contain isolated layers of pebbles and cobbles, suggesting rapid shifts in the energy level of the depositional environment.



Figure 2. Andesite sills and dykes enclosing remnants of Powrivco facies mudstone.

Upper unit

East of Dodge Point steeply eastward-dipping sandstone of the lower unit of the Yakoun Group is in fault contact with massive volcanic breccia of the upper unit (Fig. 2). The sandstone succession is also exposed east of the fault (Fig. 1) where it appears to underlie the breccia stratigraphically. Lithologically similar volcanic breccia is the predominant lithology of upper Yakoun Group rocks exposed to the west and south, between Dodge Point and Powrivco Bay. The breccia and associated flows include both aphyric basalt and feldsparphyric rocks of intermediate composition. In most exposures the textures and structures are consistent with a subaerial eruptive environment. However, aquagene tuff breccia and pillow lava are present locally.

The upper Yakoun rocks south of Beljay Bay are more highly altered and comprise a greater proportion of massive flows than correlative, mainly pyroclastic rocks farther east. Widespread fracturing and local development of foliation in the more westerly volcanic facies reflect their proximity to the Sedgwick Bay fault zone and the pervasive quartz-epidote alteration observed in these rocks was probably associated with emplacement of the Beljay Bay pluton.

Burnaby Island plutonic suite

The Jurassic Burnaby Island plutonic suite includes several discrete plutons on southern Lyell Island which Anderson and Reichenbach (1991) referred to collectively as the Beresford complex. Farther north, in central Lyell Island, two plutons which cut Kunga Group strata west of the Sedgwick Bay fault zone are believed to be part of the same Jurassic complex. The more southerly body consists of medium- to coarse-grained hornblende monzodiorite. Contacts with intensely folded Kunga Group sediments are sharp and well exposed. Lenticular xenoliths and mafic schlieren in a broad contact zone give the adjacent monzodiorite a gneissic fabric that is roughly concordant with the contacts. In contrast the central part of the body has a uniform, unfoliated texture.

The smaller, more northerly body consists of fine-grained mafic diorite which cuts massive Sadler Limestone in the core of an anticlinal structure.

Jurassic and/or Cretaceous sediments

Two structurally concordant but lithologically distinct sedimentary assemblages are extensively exposed along logging roads northeast of Powrivco Bay. The lower, unnamed succession consists almost entirely of thin-bedded, friable siltstone and mudstone whereas the upper unit is primarily massive conglomerate interbedded with lesser amounts of sandstone. The conglomerate was originally assigned to the Cretaceous Longarm Formation (Sutherland Brown, 1968). Cameron and Hamilton (1988) argued, however, that the lithology is more consistent with Middle Jurassic Yakoun Group rocks. The Jurassic correlation has been questioned by Haggart (1991b) but in the absence of good fossil control the age remains unresolved. Large inoceramid bivalves in the lower, shale succession could be

either Jurassic or Cretaceous in age (J.W. Haggart, pers. comm., 1991). For the purposes of this report the conglomerate succession is tentatively correlated with the Longarm Formation and the underlying mudstone succession is referred to informally as the Powrivco facies.

Powrivco facies

The stratigraphy of the Powrivco facies is complicated by the presence of massive sills and dykes of fine-grained andesite which locally form stockworks comprising up to 80% of the rock volume (Fig. 3). However, at least 150 m of thin-bedded siltstone are exposed in a continuous section east of Powrivco Bay. Despite the paucity of uninterrupted sections the overall map pattern suggests a dramatic northeasterly thinning of the Powrivco facies between underlying Yakoun Group volcanics and overlying Longarm? Formation conglomerate.

The basal contact of the Powrivco facies was not observed. However, Yakoun volcanics exposed in a quarry 5 km northeast of Powrivco are separated from overlying inoceramid-bearing mudstone by a 3 m sill of Tertiary rhyolite with obsidian selvages. Neither the underlying Yakoun volcanics nor the overlying mudstone show evidence of strain, suggesting that the sill was injected along a stratigraphic, rather than a tectonic, contact. The upper contact of the Powrivco facies with overlying Longarm? conglomerate was observed at several places and appears conformable in outcrop. The apparent northeastward thinning of the mudstone succession, however, may reflect an erosional unconformity at the base of the conglomerate.

Longarm? Formation

The Longarm? Formation conglomerate forms prominent cliffs that extend along the ridge east of Powrivco Bay almost to Dodge Point. Individual beds of well-rounded, clast-supported boulders and cobbles often reach tens of metres in thickness and are locally interbedded with sandstone. Unlike the underlying Powrivco mudstone the

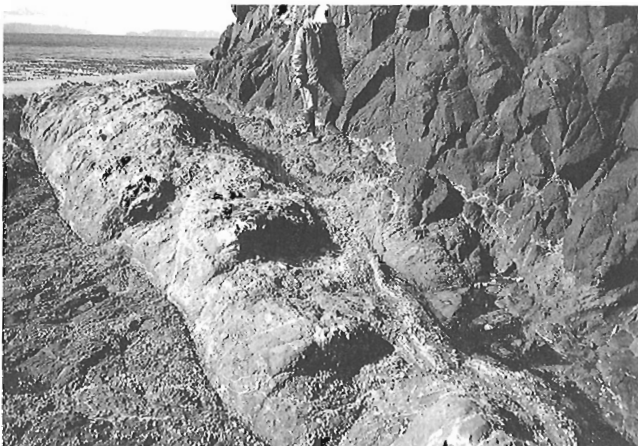


Figure 3. Fault between lower Yakoun Group sandstone (left) and volcanic breccia (right). East of Dodge Point looking north.

Longarm? strata are cut by relatively few dykes and sills. This is probably not related to the age of dyke emplacement but rather to the difference in competency and anisotropy of the two units. The conglomerate is structurally conformable with overlying southeast-dipping Tertiary volcanics.

Tertiary igneous rocks

The Masset Formation as originally defined by Sutherland Brown (1968) encompassed all of the Tertiary volcanic and subvolcanic rocks on Queen Charlotte Islands, including the Dana Facies developed on Lyell and adjacent islands. The formation was redefined by Hickson (1991) who specifically excluded the Dana Facies on the basis of lithological differences and on evidence that it was older (early Tertiary and Cretaceous) than the Late Oligocene to Pliocene Masset Formation rocks on Graham Island. However, the age of the Tertiary volcanic rocks on Lyell Island is based primarily on correlation of the eruptive rocks with nearby plutonic and subvolcanic bodies (Atli Inlet and Sedgwick Bay plutons) which have yielded dates ranging from 25.4 to 35.7 Ma (Anderson and Reichenbach, 1991), as well as with dykes in southern Moresby Island which have yielded dates as old as 54.5 Ma (Souther and Jessop, 1991). While this correlation is probably valid for most of the volcanics the dating of hornblende porphyry on Talunkwan Island (13.0 ± 5.7 Ma) suggests that at least some of Sutherland Brown's Dana Facies is post-Oligocene in age (Irving and Souther, in prep.).

In this work an attempt was made to discriminate in field mapping between volcanic, subvolcanic, and plutonic phases of the Lyell Island Tertiary igneous assemblage. However, in the central and western part of the island the volcanic and subvolcanic rocks are too intimately mixed to show on the map and they are therefore represented schematically as mixed phases on the map (Fig. 1).

Volcanic rocks

The Tertiary volcanic rocks of Lyell Island comprise two lithologically and geographically distinct assemblages. The Murrelet facies forms the high ridges northeast of Powrivco Bay while rocks of the Beljay facies extend northwest from Powrivco Bay to the north side of Atli Inlet and beyond.

On the east, rocks of the Murrelet facies overlie Longarm? Formation strata with little or no angular discordance. Two distinct units can be recognized within the Murrelet facies. The lower unit includes a thick basal sequence of poorly consolidated debris flow and/or rock avalanche deposits and is overlain by 100 to 150 m of varicoloured, feldsparphyric andesite breccia interlayered with minor andesite flows and tuff.

Breccias of the lower unit of the Murrelet facies are overlain conformably by at least 100 m of aphyric, columnar-jointed basalt flows which form the upper unit of the facies. The Murrelet facies rocks show only minor evidence of hydrothermal alteration or veining.

The predominant lithology of the Beljay facies is light green aphyric or slightly feldsparphyric breccia. Although clast size varies from about half a metre in some areas to

lapilli sized material in others the entire pile is remarkably lacking in primary bedding features. No systematic textural or lithological variation was observed between exposures at sea level and those at elevations of more than 300 m. Within a single outcrop clasts vary, from angular, to subrounded, to irregular primary ejecta with quenched selvages and interlocking boundaries.

The Beljay facies corresponds with Sutherland Brown's (1968; Fig. 17) "mixed breccia" which he described as breccia containing both basalt and rhyolite clasts. On the basis of field and preliminary petrographic study of the Beljay facies rocks the writer was not able to confirm this wide range of compositions. However, the clasts noted exhibit a wide range of textures, from aphanitic to microphyric, and many of them have microscopic amygdules filled with chlorite, quartz, and zeolites?. The matrix of highly comminuted rock contains an abundance of blocky shards bounded by fractures that cut across vesicles. Both clasts and matrix contain secondary chlorite, zeolites, silica, and uranalite? formed during diagenesis and hydrothermal alteration of the pile.

Unlike rocks of the Murrelet facies, much of the Beljay pile is cut by a pervasive stockwork of hydrothermal veins. These are particularly abundant in the area between Powriwco and Beljay bays where numerous zones from tens to hundreds of metres wide are permeated with a network of anastomosing silica veins and veinlets ranging from a few centimetres to less than a millimetre thick. The absence of similar veining in the underlying Mesozoic rocks suggests that it is the product of a shallow hydrothermal system associated with cooling and degassing of the Tertiary volcanic pile.

Origin

Sutherland Brown (1968) recognized the distinctive character of the Dana Facies which he attributed in part to a submarine eruptive environment as opposed to the subaerial origin which characterizes most Tertiary volcanic rocks of the Queen Charlotte Islands. The present work is in general agreement with Sutherland Brown's interpretation. The breccias of the Beljay facies are typical of the unwelded subaqueous pyroclastic flow deposits described by Fisher and Schmincke (1984, p. 287) whereas the Murrelet lower facies appears to represent a transition to the columnar-jointed subaerial flows which comprise the upper part of the Murrelet facies. This difference in eruptive environment would also explain the relative abundance of hydrothermal alteration and veining in the Beljay facies rocks.

Intrusive rocks

At least two, and possibly three, plutons of the Tertiary Kano plutonic suite are present on Lyell Island. The largest of these - the Sedgwick Bay pluton on southwestern Lyell Island - yielded a U-Pb date of 35.7 ± 0.3 Ma (Anderson and Reichenbach, 1991). It forms the core zone of the Lyell Island plutonic complex which is believed to be coeval and coextensive with the subvolcanic intrusions in the central and western part of the island (Anderson et al., 1992).

The Atli pluton is well exposed on the northwest side of Atli Inlet where its steep western contact cuts sharply across dacite? breccia of the Tertiary Beljay volcanics. The narrow contact zone is not associated with veining or shearing and appears to be intrusive; however, the possibility of a tectonic contact cannot be ruled out. The plutonic rock is pinkish brown, medium-grained monzogranite, characterized by numerous small quartz/feldspar-lined miarolitic cavities which reflect its shallow depth of emplacement and correspondingly low confining pressure. Young (1981) reported a whole rock K-Ar date of 25 ± 4 Ma for the pluton.

A third Tertiary pluton was originally identified by Sutherland Brown (1968) on the south side of Beljay Bay. Based on new roadcuts the body is now known to be much larger than originally mapped. Also, it is more lithologically diverse than most of the other Tertiary plutons, ranging from diorite to quartz-feldspar porphyry. The southwestern part of the body is highly fractured, silicified, and veined. However, it lacks the prominent foliation characteristic of pre-Tertiary rocks close to the Sedgwick Bay fault zone. This suggests that major fault movement predates the pluton's emplacement although it may have been affected by subsequent reactivation along the fault.

Tertiary dykes within the mapped area are commonly subvertical and reflect the regional northerly trend described by Souther and Jessop (1991) for most of the southern Moresby archipelago. Dykes less than 30 m thick are shown schematically on the map (Fig. 1). The very thick (>100 m) north-trending composite dykes in the vicinity of Dodge Point are lithologically similar to, and probably coextensive with, basalt and hornblende-feldspar andesite porphyry in the sheeted subvolcanic complex farther south and west. Their relationship to the Murrelet volcanic facies is unknown.

Mixed volcanic-subvolcanic complexes

The large composite porphyry intrusions of central and eastern Lyell Island were originally described by Sutherland Brown (1968) who correctly interpreted them as subvolcanic equivalents of the Tertiary volcanic rocks. In this report the subvolcanic intrusions and associated plutons are referred to informally as the Lyell Island plutonic complex (Souther and Jessop, 1991).

The eastern facies of the complex is exposed along most of the east shore of Lyell Island. Similar rocks outcrop farther east on the Tar Islands, as well as in the interior of Lyell Island along logging roads between Windy Bay and Sedgwick Bay. The predominant lithologies are feldsparphyric basalt, feldspar- and feldspar/hornblende-phyric andesite, pyritic dacite, and minor rhyolite. Most of the rock occurs as sheeted, vertical, north-trending tabular intrusions from a few metres to hundreds of metres thick. Contacts between adjacent bodies are commonly difficult to distinguish from pervasive north-trending vertical joints. However, the local presence of remnant screens of volcanic breccia supports the concept of a relatively shallow composite intrusive complex.



Figure 4. Landslide on ridge northeast of Powrivco Bay. Note recent slumps caused by slope failure where logging roads cross thick colluvium along the margins of the landslide.

The western facies of the Lyell Island plutonic complex comprises a similar assemblage of intrusive rocks. However, it includes a higher proportion of relatively fresh volcanic rock, some of which resembles breccia of the Beljay volcanic pile.

STRUCTURAL GEOLOGY

Tight folds in Kunga Group rocks south of Beljay Bay are truncated by unfoliated plutons of the Beresford complex and by northwest-trending mylonitic fabric in the Sedgwick Bay fault zone. The late Triassic/early Jurassic rocks thus appear to have been severely folded prior to intrusion of the Burnaby Island plutonic suite and prior to major movement on the Sedgwick Bay fault zone. The latter comprises a northwest-trending zone up to half a kilometre wide in which slices of Kunga and Yakoun rocks are intensely fractured, slickensided and locally reduced to mylonite. The orientation of slickensides on near vertical fault surfaces is commonly subhorizontal, suggesting transcurrent movement. No similar fabrics were observed in Tertiary rocks on the north side of Beljay Bay where the blocky basal breccia of the lowest Tertiary flow rests unconformably on Kunga Group sediments. This relationship, plus the absence of shearing in the Beljay rocks, suggests that they are an overlap succession that postdates significant movement on the Sedgwick Bay fault zone.

East of Powrivco Bay Yakoun Group and younger rocks have been tilted and faulted but they show no evidence of the intense folding and shearing that characterizes the Jurassic and older rocks farther west. Between Powrivco Bay and Dodge Point the entire Jurassic to Tertiary succession is broadly conformable and dips moderately toward the southeast. However, complex intraformational structures are locally developed, particularly where the thin-bedded Powrivco facies has been invaded by a large volume of sills and dykes. Also, the succession is cut by north- to north-northwest-trending normal faults, with offsets of a few tens to a few hundreds of metres. The fault zones are

commonly less than a metre wide and comprise a stockwork of veins and silicified gouge (Fig. 3). Rocks adjacent to the faults are unstrained, suggesting a relatively shallow origin. Although the faults clearly cut Tertiary strata their common association with hydrothermal veining suggests that some of them may have been coeval with the igneous activity. In fact both the normal faults and the Tertiary igneous activity may be manifestations of the same episode of regional extension.

BITUMEN OCCURRENCES

Two new occurrences of bitumen were discovered within the mapped area. The first is in aquagene tuff-breccia and pillow lava near the top of the Yakoun succession northeast of Powrivco Bay. The bitumen occurs as brittle, vitreous black globules in a vuggy stockwork of zeolite?-lined fractures and is clearly of natural origin. The second occurrence is in a quarry south of Powrivco Bay where granular black bitumen fills open joints in andesite porphyry. The possibility that the latter material was introduced during road construction cannot be ruled out. However, natural bitumen showings in similar rock have long been known in the Tar Islands off the east coast of Lyell Island. Samples from both of the new occurrences are being submitted for Rock-Eval/TOC analysis.

LANDSLIDES

A landslide almost a kilometre wide and more than a kilometre long extends from an elevation of 550 m on the ridge northeast of Powrivco Bay almost to sea level (Fig. 4). The slide has been logged and roads built across both margins have subsequently collapsed; apparently, the unstable nature of the landslide deposits was not recognized during road construction. This strongly emphasizes the need for careful evaluation of bedrock and surficial geology before new road construction is undertaken on similar terrane in the Queen Charlotte Islands.

ACKNOWLEDGMENTS

M.E.K. Souther provided able assistance with the field work and logistics. Both she and the author wish to thank Gerry Johnson, Judy Hadley and Kayoko Daugert of Resource Management Services for their hospitality and help in the field. The author gratefully acknowledges the support of Jim Haggart whose thoughtful discussion and careful review of the manuscript contributed substantially to this work.

REFERENCES

- Anderson, R.G. and Greig, C.J.
1989: Jurassic and Tertiary plutonism in the Queen Charlotte Islands, British Columbia; in *Current Research, Part H*; Geological Survey of Canada, Paper 89-1H, p. 95-104.
- Anderson, R.G. and Reichenbach, I.
1991: U-Pb and K-Ar framework for Middle to Late Jurassic (172-2158 Ma) and Tertiary (46-27 Ma) plutons in Queen Charlotte Islands, British Columbia; in *Evolution and Hydrocarbon Potential of the Queen Charlotte Basin, British Columbia*, (ed.) G.J. Woodsworth; Geological Survey of Canada, Paper 90-10, p. 59-87.

Anderson, R.G., Gunning, M.H., and Porter, S.

1992: Progress in mapping of Jurassic and Tertiary plutonic styles, Queen Charlotte Islands, British Columbia; *in* Current Research, Part A; Geological Survey of Canada, Paper 92-1A.

Cameron, B.E.B. and Hamilton, T.S.

1988: Contributions to the stratigraphy and tectonics of the Queen Charlotte Basin, British Columbia; *in* Current Research, Part E; Geological Survey of Canada, Paper 88-1E, p. 221-227.

Cameron B.E.B. and Tipper, H.W.

1985: Jurassic stratigraphy of the Queen Charlotte Islands, British Columbia; Geological Survey of Canada, Bulletin 365.

Fisher, R.V. and Schmincke, H.U.

1984: Pyroclastic Rocks; Springer-Verlag, Berlin. Heidelberg, New York, Tokyo.

Haggart, J.W.

1991a: New sections of Yakoun Group (Middle Jurassic) strata, Queen Charlotte Islands, British Columbia; *in* Current Research, Part A; Geological Survey of Canada, Paper 91-1A, p. 359-366.

1991b: A synthesis of Cretaceous stratigraphy, Queen Charlotte Islands, British Columbia; *in* Evolution and Hydrocarbon Potential of the Queen Charlotte Basin, British Columbia, (ed.) G.J. Woodsworth; Geological Survey of Canada, Paper 90-10, p. 253-277.

Hickson, C.J.

1991: The Masset Formation on Graham Island, Queen Charlotte Islands, British Columbia; *in* Evolution and Hydrocarbon Potential of the Queen Charlotte Basin, British Columbia, (ed.) G.J. Woodsworth; Geological Survey of Canada, Paper 90-10, p. 305-324.

Souther J.G. and Jessop, A.M.

1991: Dyke swarms in the Queen Charlotte Islands, British Columbia, and implications for hydrocarbon exploration; *in* Evolution and Hydrocarbon Potential of the Queen Charlotte Basin, British Columbia, (ed.) G.J. Woodsworth; Geological Survey of Canada, Paper 90-10, p. 465-487.

Sutherland Brown, A.

1968: Geology of the Queen Charlotte Islands, British Columbia; British Columbia Department of Energy, Mines and Petroleum Resources, Bulletin 54, 226 p.

Young, I.F.

1981: Structure of the western margin of the Queen Charlotte Basin, British Columbia; M.Sc. thesis, University of British Columbia, Vancouver, 380 p.

Geological Survey of Canada Project 870070

Geology of the Darwin Sound area, Queen Charlotte Islands, British Columbia

Mary Sanborn-Barrie
Cordilleran Division, Vancouver

Sanborn-Barrie, M., 1992: Geology of the Darwin Sound area, Queen Charlotte Islands, British Columbia; in Current Research, Part A; Geological Survey of Canada, Paper 92-1A, p. 351-360.

Abstract

The Darwin Sound area is underlain by Upper Triassic mafic volcanic rocks and Upper Triassic-Lower Jurassic carbonate and siliciclastic rocks with Wrangellian affinities. These are disconformably overlain by coarse clastic breccia of probable later Jurassic age which, in turn, is overlain by turbiditic mudstone and wacke. Minor Cretaceous sedimentary rocks and extensive Tertiary volcanic rocks are present. Jurassic plutonic rocks dominate central parts of the map area and Tertiary intrusive rocks are minor but widespread.

A structural discontinuity along the west side of Darwin Sound juxtaposes west-facing, undeformed strata to the west, with east-facing panels of Triassic-Jurassic strata to the east. Ductile shear zones occur across the breadth of Darwin Sound in Triassic-Lower Jurassic strata. These are dominantly low-angle, reverse structures, although some have normal and transcurrent displacement. Relatively unstrained Tertiary dykes cut the shear zones.

Résumé

Le sous-sol de la région du détroit de Darwin contient des roches volcaniques mafiques du Trias supérieur et des roches carbonatées et silicoclastiques du Trias supérieur et du Jurassique inférieur, qui présentent des affinités avec les roches de la Wrangellia. Ces roches sont recouvertes en disconformité par une brèche clastique grossière qui date probablement du Jurassique supérieur et qui elle-même est recouverte par un mudstone et une grauwacke turbiditiques. On rencontre des quantités mineures de roches crétacées et de vastes étendues de roches volcaniques tertiaires. Les roches plutoniques d'âge jurassique prédominent dans les portions centrales de la région cartographiée, et les roches intrusives d'âge tertiaire sont d'importance mineure mais couvrent de grandes étendues.

Une discontinuité structurale bordant le côté ouest du détroit de Darwin juxtapose des strates non déformées orientées vers l'ouest et à l'est des panneaux de strates triasiques-jurassiques orientés vers l'est. Des zones de cisaillement ductile apparaissent sur la largeur du détroit de Darwin dans des strates du Trias et du Jurassique inférieur. Ce sont surtout des structures inverses faiblement pentées, mais qui parfois présentent un déplacement normal et un coulissement. Des dykes relativement peu déformés, d'âge tertiaire, traversent les zones de cisaillement.

INTRODUCTION

The Darwin Sound area near east-central Moresby Island, Queen Charlotte Islands (QCI) is one of the most recent areas studied as part of the GSC's QCI Program (QCIP) initiated in 1987 to evaluate the evolution and hydrocarbon potential of the Queen Charlotte Basin (Woodsworth, 1991). Fundamental to that program are onshore stratigraphic and structural studies which help constrain the understanding of the offshore basin. Geological mapping near Darwin Sound (Fig. 1) complements earlier studies and links the Tasu Sound studies of Taite (1990, 1991a, b) with those of Burnaby Island (Lewis, 1991a, b). These areas differ lithologically and structurally.

Previous mapping of Darwin Sound was conducted in 1960 by Sutherland Brown (1968) in a comprehensive geological investigation of the QCI. Subsequent detailed studies of the Mesozoic litho- and biostratigraphy of the islands have resulted in refinement of Sutherland Brown's (1968) stratigraphic nomenclature (Cameron and Tipper, 1985; Desrochers and Orchard, 1991; Orchard, 1991; Poulton et al., 1991; Tipper et al., 1991; and Haggart, 1991a). A recent synthesis of the structural evolution of the QCI was presented by Lewis et al. (1991) and a comprehensive study of plutonic rocks was undertaken by Anderson and Reichenbach (1991). Stratigraphic nomenclature presently in use is shown in Haggart (1992).

Geological data relating to this project was collected and stored in the field using the Atari Portfolio¹ handheld computer, as described by Struik et al. (1991). The data are readily transferable to a database linked with AutoCAD² through the FIELDLOG³ program to allow efficient production of the geological map, at a variety of scales; manipulation of structural data; and integration of data with that of adjacent regions.

LITHOLOGIC UNITS

Roughly 70% of the map area is underlain by supracrustal rocks and the remainder by plutonic rocks. Supracrustal rocks are dominated by mafic volcanic rocks of the Triassic Karmutsen Formation and Tertiary volcanic rocks, but also include sedimentary rocks of the Triassic-Jurassic Kunga Group and Cretaceous Queen Charlotte Group, and probable Middle to Upper Jurassic sedimentary and volcanic rocks. Not recognized in the map area are sedimentary rocks of the Lower Jurassic (Pliensbachian to Aalenian) Maude Group or the Lower Cretaceous (Berriasian? to Aptian) Longarm Formation. Plutonic rocks include diorite and quartz diorite of Middle to Late Jurassic age, felsic intrusions of Cretaceous age, and pervasive Tertiary dykes and sills.

The general geology of the Darwin Sound area is shown in Figure 2. Localities referred to in the text are shown in Figure 1.

Supracrustal rocks

Karmutsen Formation

Mafic volcanic rocks of the Upper Triassic (Carnian) Karmutsen Formation dominate the western part of the area (Fig. 2) and include massive and amygdaloidal flows, pillowed flows, pillow fragment breccia, flow top breccia, and minor tuff. These are fine-grained, equigranular, tholeiitic (Barker et al., 1989) basalt with a colour index (CI) of 35-45. They may be weakly to moderately magnetic, and contain secondary calcite and minor disseminated pyrite. Amygdaloidal flows of intermediate composition (CI=20-25), exposed near Raven Bay, may represent a compositionally distinct horizon within the upper Karmutsen Formation.

In contrast to the western part of the area, mafic volcanic rocks exposed within and east of Darwin Sound form narrow, discontinuous units and are massive, fine grained, and locally amygdaloidal. Mafic volcanic breccia is exposed on the central south shore of Kunga Island.

Limestone layers and lenses (20 cm to 2 m wide) occur with mafic volcanic rocks on Shuttle Island, the Topping Islands, the west shore of Lyell Island, and eastern Richardson Island. Limestone interbeds are described by Sutherland Brown (1968) in the upper and lower parts of the Karmutsen Formation.

Kunga Group

The Upper Triassic to Lower Jurassic (Norian to Sinemurian) Kunga Group comprises the Sadler Limestone, argillaceous limestone of the Peril Formation, and siliciclastic rocks of the Sandilands Formation (Sutherland Brown, 1968; Cameron and Tipper, 1985).

Sadler Limestone is exposed in the Crescent Inlet-Anna Inlet area, on Kunga Island (including Titul Island and Kalo Rocks), and along the west sides of Richardson and Lyell islands (Fig. 2). A conformable contact between Karmutsen Formation volcanics and Sadler Limestone is observed on Titul Island and Kalo Rocks, although this contact is generally faulted. Characteristically, the Sadler Limestone is massive and weathers light grey. Locally, thick to very thick beds are defined by thin laminations of oolitic calcarenite or thin cherty (siliciclastic?) interbeds.

Limestone at the north and south ends of Shuttle Island (Fig. 2) differs from the Sadler Limestone, in having well-defined, millimetre- to centimetre-scale layering; rare, thin chert beds; and minor clastic interbeds. These rocks resemble carbonate units exposed at Hutton Point (Fig. 1) which may be of Carboniferous to Permian age (Sutherland Brown, 1968; Hesthammer et al., 1991). Alternatively, they may simply be tectonized limestone of the Sadler or Karmutsen formations.

Argillaceous limestone of the Peril Formation conformably overlies the Sadler Limestone. The transition between the two is marked by an increase in clay and graphite and a corresponding darkening in weathering. Thin-shelled

¹ Atari Portfolio is the registered trademark of Atari Corporation.

² AutoCAD is the registered trademark of AutoDesk Inc.

³ FIELDLOG is a program of the Ontario Geological Survey.

Halobia bivalves occur in the lower and middle parts of the formation, and *Monotis* occurs in the upper part (Desrochers and Orchard, 1991). In the map area, Peril Formation may be well-bedded and comprise thickly laminated to thinly bedded, graphitic, argillaceous limestone with interstratified beds or discontinuous layers (4-20 cm wide) of light grey-weathering carbonate. Beds are generally ungraded and sedimentary structures are absent. Commonly the rocks are strongly foliated, graphitic, and beds are thoroughly disrupted.

Siliciclastic rocks of the Upper Triassic to lowermost Jurassic (Hettangian and Sinemurian) Sandilands Formation are conformable and transitional with the underlying Peril Formation. The base of the Sandilands Formation is placed at the top of the highest *Monotis* coquina bed (Desrochers and

Orchard, 1991). Exposures of the Sandilands Formation near Darwin Sound are limited. The exposed section on eastern Kunga Island (Fig. 2) consists of dark black/grey-weathering, thickly laminated to thinly bedded, weak- to noncalcareous, silt-size, siliciclastic rocks with minor thin interbeds of buff-weathering, fine to coarse sand-size feldspathic wacke. Wacke units can contain moderate amounts of secondary calcite. Micritic concretions are common and Sinemurian ammonites (Palfy et al., 1990) are locally abundant. On the northwest shore of Crescent Inlet, thinly bedded siliciclastic rocks are interstratified with dark brown-weathering, pyritic, carbonate beds up to 35 cm thick. These are interpreted as fine to medium sand-size wacke beds replaced by carbonate, and may correlate with massive sandstones observed at the base of the formation elsewhere (Hesthammer, 1990; Taite, 1990). Strongly foliated to massive, noncalcareous, black

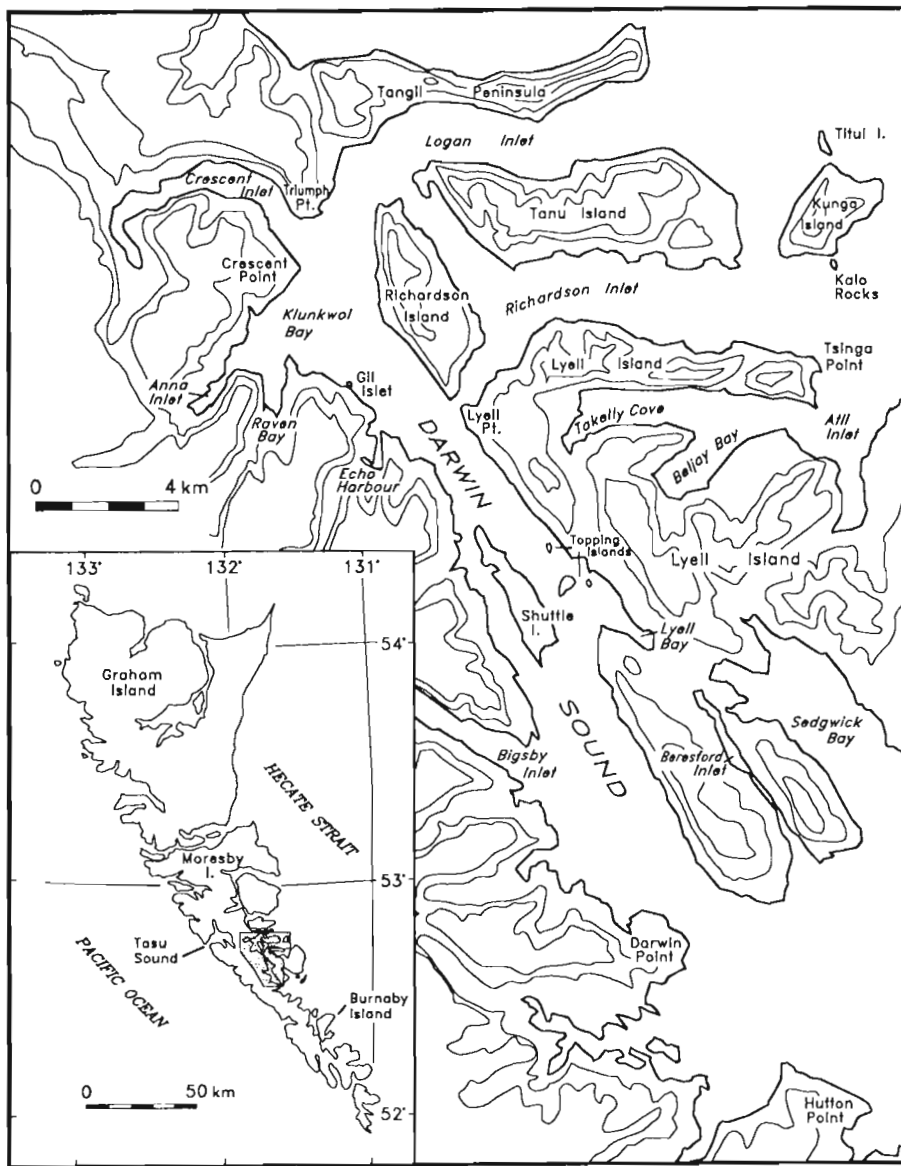


Figure 1. Location map of the Darwin Sound area, east-central Moresby Island, Queen Charlotte Islands. Contour lines at 500 and 1000 feet.

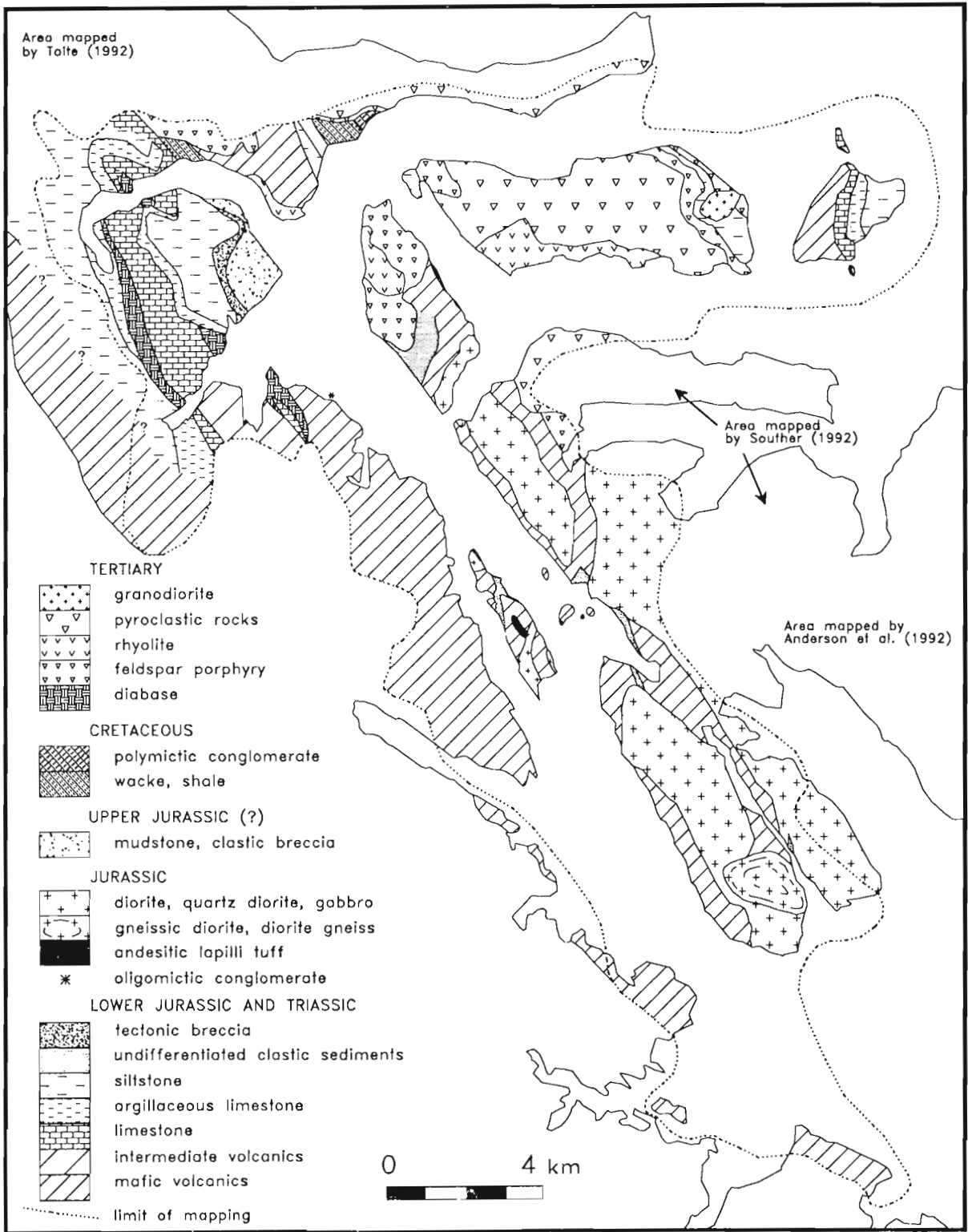


Figure 2. General geology of the Darwin Sound area.

siltstone of the Sandilands Formation is exposed along eastern Richardson Island, eastern Shuttle Island, and northeast of Triumph Point. Thermal metamorphism of the formation results in a bleached appearance, commonly to pale pink, pale grey or whitish weathering. This is well displayed in narrow exposures on western Tanu Island and near Tsinga Point on northern Lyell Island.

Breccia units dominated by tabular, pebble- to boulder-size clasts of Peril and Sandilands formations are exposed from near Crescent Point to Gil Islet at the north end of Darwin Sound (Fig. 2, 3). This poorly sorted, massive unit

is spatially associated with a disconformity between upper Kunga Group strata and possible Middle to Late Jurassic sedimentary rocks (discussed below).

Yakoun Group

The Yakoun Group is a diverse assemblage of Middle Jurassic (Bajocian) volcanic flows, pyroclastic rocks, shale, siltstone, sandstone and conglomerate (Sutherland Brown, 1968; Cameron and Tipper, 1985; Hesthammer, 1991; Haggart, 1991b). Two isolated occurrences may be part of

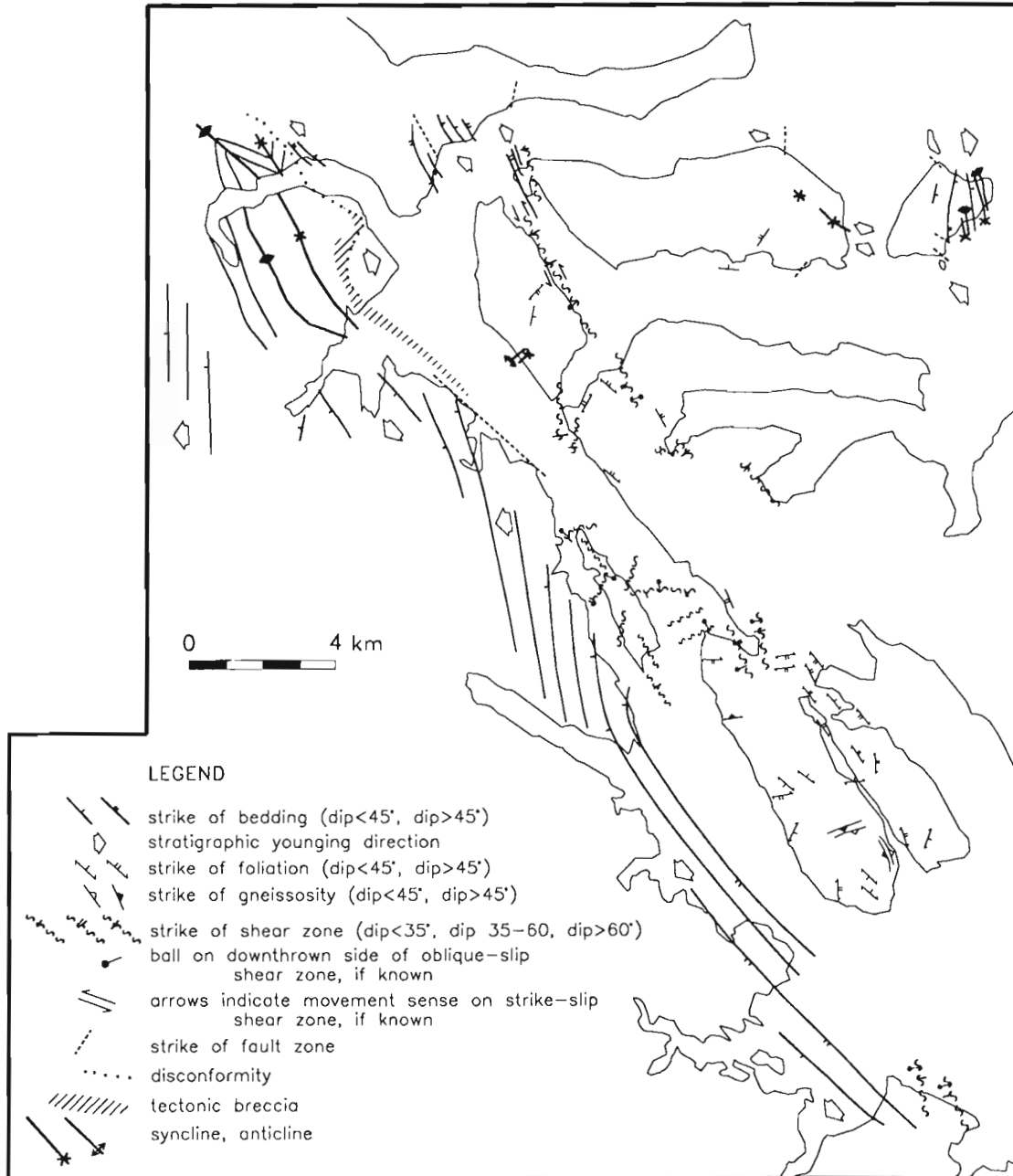


Figure 3. Major structural elements of the Darwin Sound area.

this group. Distinctive float in a valley on the east side of Shuttle Island is dominated by andesitic lapilli tuff cemented by white-weathering calcite. This distinctive unit is considered to be diagnostic of the basal Yakoun Group elsewhere on the QCI (Sutherland Brown, 1968).

The second locality of possible Yakoun strata is near Gil Islet in northwest Darwin Sound. Cobble conglomerate with well-rounded, spherical, dark green-weathering gabbroic clasts in a mafic-derived, fine sand-size matrix forms a small (2 m by 1.5 m) exposure. Grey limestone, volcanic rocks, and dykes and sills also occur at this locality. The relationship of the conglomerate to the other supracrustal units is not clear.

Middle to Upper Jurassic sedimentary rocks

Clastic sedimentary rocks near Crescent Point (Fig. 2) disconformably overlie upper Kunga Group strata. The basal part of the succession consists of an unsorted and unbedded sedimentary breccia of tabular, pebble- to boulder-size clasts (maximum 2 m by 4 m) of Sandilands Formation siltstone,



Figure 4. Sedimentary breccia near Crescent Point. (A) Unsorted nature of coarse sedimentary breccia. (B) Boulder-size clast of fossiliferous wacke within breccia unit.

argillaceous limestone of the Peril Formation, fossiliferous wacke and grit conglomerate, and minor volcanic/plutonic clasts (Fig. 4). A clast of wacke contains fossils of probable Middle Jurassic (Bajocian) age (H. Tipper, pers. comm., 1991). Clasts are supported in coarse sand- to pebble-size, dark grey-weathering, lithic wacke. The basal unit is overlain locally by poorly bedded, poorly graded breccia composed predominantly of plagioclase-phyric volcanic clasts and minor Sandilands Formation siltstone clasts in a mudstone matrix. These rocks appear to grade upward into dark brown-weathering, friable, noncalcareous mudstone and fine sand-size lithic wacke with turbidite characteristics. Entire coarse-ribbed inoceramid bivalves and associated shell debris occur within the mudstone/wacke facies.

On eastern Lyell Island, dark brown-weathering, friable mudstone containing coarse-ribbed inoceramids, similar to that near Crescent Point (J. Haggart, pers. comm., 1991) is informally designated the Powrivco facies (Souther, 1992).

Queen Charlotte Group

Cretaceous strata are represented by two laterally restricted sections of clastic sedimentary rocks in the northern part of the map area (Fig. 2). On the north shore of Crescent Inlet, poorly-bedded, ungraded, blue/grey-weathering shale with minor thin interbeds of light grey-weathering, ungraded, fine sand-size feldspathic wacke form the lower part of the exposed section. Quartz forms a significant component (up to 50%) of the wacke. Upsection, increasingly well-bedded lithic wacke and feldspathic wacke are exposed which contain preferentially weathered calcareous concretions (to 40 cm long) and rare blue/black-weathering nodules (to 6 cm long). A 2 m thick bed of polymictic cobble conglomerate of the Honna Formation occurs approximately in the middle of the exposed section. The conglomerate is discordant with the underlying wacke, which is interpreted to reflect local scouring.

The Cretaceous section on the north shore of Logan Inlet is more complete than that on Crescent Inlet. The lower part is dominated by massive to very thinly bedded, blue/grey-weathering, noncalcareous shale with minor thin interbeds of very fine sand-size feldspathic wacke. The wacke may be graded, parallel laminated or cross-stratified and displays load and scour structures. These rocks grade upward to turbidites, designated the Skidegate Formation elsewhere in the QCI (Gamba et al., 1990; Haggart, 1991a). Within the turbidite sequence, rare 2 m wide interbeds of intraformational cobble conglomerate are composed dominantly of cream-weathering calcareous clasts which may represent mudstone intraclasts replaced by diagenetic carbonate (C. Gamba, pers. comm., 1991). Polymictic conglomerate of the Honna Formation overlies the turbidite succession. Elsewhere on the QCI, a conformable and locally interstratified relationship exists between the Cretaceous turbidite or sandstone/shale facies and the Honna conglomerate (Gamba et al., 1990; Gamba, 1991; Haggart, 1991a).

Tertiary volcanic rocks

Volcanic and volcanoclastic rocks of Tertiary age are exposed in the north-central part of the area (Fig. 2; see also Souther, 1992). These are pale green- to buff-weathering rocks which, on fresh surfaces, are a distinctive pale green to aquamarine. Intermediate lapilli tuff and tuff breccia dominate, and are exposed on the Tangil Peninsula, Tanu Island, and the north shore of Lyell Island. These are poorly sorted rocks in which bedding and grading are seldom recognized. Fragments are dominantly intermediate to felsic in composition, with slightly plagioclase-phyric rhyolite fragments comprising a significant (10-15%) component. These rocks were designated the Dana facies of the Masset Formation by Sutherland Brown (1968); however, in contrast to Sutherland Brown's (1968) observations elsewhere, pyroclastic rocks in the map area rarely contain fragments of mafic composition.

Blue/grey-weathering dacitic ash, tuff, and lapilli tuff occur north of Crescent Inlet and appear to unconformably overlie Cretaceous shales (Fig. 2).

Fine grained, homogeneous, intermediate to felsic volcanic rocks are exposed on northern Richardson Island. Massive, fine grained to aphanitic rhyolite predominates and a sequence of dacitic to rhyodacitic flows is also noted.

Subvolcanic rocks

Massive, unfoliated, feldspar-phyric rocks of intermediate composition are minor but widespread in the Logan Inlet area (Fig. 2). They contain 5-30% euhedral to subhedral feldspar (0.5-3 mm long) in a light grey/green-weathering, fine grained, equigranular (<0.5 mm) groundmass with CI=18-25. Locally these rocks are strongly fractured and veined. They appear to underlie Tertiary volcanic rocks and may represent their subvolcanic equivalent.

Coarse grained intrusive rocks with well developed diabasic texture form tabular units up to 250 m wide within Karmutsen Formation and Kunga Group strata in the Crescent Inlet-Anna Inlet area. They contain 15-80% plagioclase phenocrysts in a pale green-weathering, medium grained groundmass with CI=15-25. Plagioclase occurs as euhedral, lath-shaped crystals (to 2 cm long) and subhedral, equidimensional crystals (average 5 mm by 8 mm). Vesicles (1-2%) filled with quartz or chlorite occur locally. These rocks are spatially associated with (and appear to grade into) vesicular andesitic rocks that intrude Kunga Group strata. The diabasic rocks are interpreted to be Middle Jurassic or Tertiary in age and are considered to be distinct from the diabasic, comagmatic, hypabyssal rocks of the Karmutsen Formation that have higher CI (approximately 50) and subophitic texture (Barker et al., 1989).

Intrusive rocks

Studies of plutonic rocks in the QCI (Sutherland Brown, 1968; Anderson and Reichenbach, 1991) reveal two suites of Middle to Late Jurassic plutons and a Tertiary suite. The San Christoval plutonic suite (SCPS) comprises ~172-171 Ma, homogeneous, massive to foliated diorite and quartz diorite

and generally occurs on the west coast of the QCI (Anderson and Reichenbach, 1991). The Burnaby Island plutonic suite (BIPS) comprises slightly younger (~168-158 Ma), unfoliated gabbro, diorite, quartz monzodiorite, quartz monzonite, and leucodiorite. The Kano plutonic suite (KPS) spans ~46-27 Ma and comprises relatively small monzodioritic to granitic plutons (Anderson and Reichenbach, 1991).

Mapping near Darwin Sound has revealed significantly more plutonic rocks than previously recognized. Diorite and quartz diorite are prevalent throughout western Lyell Island, southern Richardson Island, and Shuttle Island (Fig. 2). Where unstrained, these rocks are medium grained, equigranular, pale green-weathering with CI=12-25. Mafic minerals are amphibole ± chlorite. Locally these rocks may contain up to 10% interstitial quartz. Strongly tectonized diorite and quartz diorite is fine grained, light grey weathering, strongly foliated to phyllonitic. Gabbro, leucodiorite, hornblende porphyritic diorite, and quartz monzodiorite are minor phases throughout western Lyell Island and Darwin Sound. Gneissic diorite and diorite gneiss occur on southwest Lyell Island (Fig. 2).

Intermediate to felsic plutonic rocks are sporadically exposed throughout central Lyell Island and generally intrude diorite and quartz diorite. Granodiorite to quartz monzodiorite occur on northern Lyell Island west of Tsinga Point and on eastern Tanu Island (Fig. 2), and intrude Sandilands Formation. Fine grained, equigranular, biotite-bearing rocks of dioritic composition are prevalent in the Crescent Point area but are not shown on Figure 2.

STRUCTURAL GEOLOGY

Bedding, folds

Volcanic rocks of the Karmutsen Formation in the western part of the map area strike north-northwest, dip moderately (25-50°) to the west and young to the west (Fig. 3). As such, an oblique section through the formation is observed along the west shore of Darwin Sound, from spectacularly exposed pillowed basalt in Bigsby Inlet to vesicular flows of intermediate composition within the upper part of the formation in the Raven Bay area. Kunga Group beds above the Karmutsen Formation near Crescent and Anna inlets similarly strike northwest, but are folded about a northwest-striking anticline and syncline (Fig. 3). Minor folds in this vicinity plunge moderately (10-30°) northwest.

In the eastern part of the map area, Kunga Group strata strike northerly, dip moderately to steeply (40-70°) east, and are similarly folded about north-northwest-striking anticline/syncline pairs (Fig. 3). These rocks, however, young to the east, as do discontinuous panels of Kunga Group exposed throughout Darwin Sound. Triassic/Jurassic strata therefore face in opposite directions across western Darwin Sound.

Middle to Late Jurassic (?) clastic rocks young to the east (Fig. 3). Well-bedded mudstone and wacke in the upper part of the exposed section are folded, possibly by two generations

of folds. First generation folds strike north and are refolded about an east-striking syncline. These folds may be related to intrusion of fine grained dioritic rocks of the KPS in the Crescent Point area (not shown).

Cretaceous strata strike northwest, dip moderately (40-70°) to the northwest, and young to the northeast. Rarely observed beds in Tertiary volcanic rocks strike southwest and dip 45-50°.

Foliation

Penetrative planar mineral fabrics appear to be more prevalent in the Darwin Sound area than in adjacent areas (Thompson and Lewis, 1990; Lewis, 1991b; Taite, 1991b). Most notable are strongly foliated to mylonitic rocks within Darwin Sound and along the east side of Richardson Island. These rocks display evidence of differential displacement and are discussed further below (see shear zones).

Mafic volcanic rocks east of Darwin Sound possess a moderately-developed, penetrative foliation which strikes east and dips steeply (60-85°) south (Fig. 3). A strongly- to intensely-developed, northwest-striking schistosity overprints the east-striking foliation in northern Beresford Inlet. Mineral lineations are rarely observed on these fabrics.

Diorite and quartz diorite on southern Lyell Island exhibit a moderately-developed foliation, and locally, gneissosity. Foliations are generally north- and northwest-striking, and dip moderately to steeply to the northeast and southwest (Fig. 3). Gneissosity attitudes in southwest Lyell Island appear to define a discrete intrusion (Fig. 3). Plutonic rocks exposed on central and northwest Lyell Island and southern Richardson Island are generally massive.

Shear zones

Ductile deformation zones with strongly- to intensely-developed, planar fabric, a conspicuous mineral lineation, and centimetre-scale kink folds transect Triassic and Jurassic supracrustal and plutonic rocks (Fig. 5). Locally, millimetre-scale rodding may parallel the mineral lineation. Determination of kinematics is generally based on asymmetries of composite S/C or C/C' fabrics (Simpson and Schmidt, 1983) in planes subparallel to the observed mineral lineation. In plutonic rocks, relict phenocrysts may show asymmetries that reflect the sense of displacement. Preliminary observations are reported below.

Attitudes of shear fabrics vary (Fig. 3), although three dominant attitudes are observed. 1) East-striking deformation zones dip shallowly to moderately (20-55°) to the south, possess strongly developed mineral lineations which plunge moderately (20-45°) to the southeast, and display kinematic evidence of oblique-reverse displacement (i.e., north side down and to the east). 2) North-northwest-striking deformation zones generally dip moderately (30-66°) to the east and west, and possess mineral lineations that plunge moderately (15-50°) to the southeast and southwest, respectively. These zones generally display reverse displacement, but locally show evidence of normal

movement (i.e., Lyell Bay area). 3) Northwest-striking, steeply dipping (75-89°) shear zones possess shallowly plunging (2-15°) mineral lineations and display dextral, transcurrent shear.

Faults

Although minor faults are pervasive, few large faults are recognized. Brittle structures are observed between Gil Islet and the west shore of Darwin Sound (Fig. 3) where west-facing volcanic rocks are juxtaposed against east-facing sedimentary rocks of the Peril Formation. Strongly fractured and veined outcrops of Tertiary volcanic rocks occur on Tangil Peninsula north of Richardson Island, and on southeast Tanu Island.

Stratigraphic discontinuities and repeated stratigraphic sequences revealed by map patterns (Fig. 2) imply the presence of faults at several localities (i.e., between Tanu and Kunga islands; through Klunkwoi Bay?).

DISCUSSION AND CONCLUSIONS

New interpretations of the geology of the Darwin Sound area resulting from this work are as follows. 1) Considerably more plutonic rocks are recognized. These form an elongate, northwest-trending belt through western Lyell Island. Fabric development (foliation and gneissosity) in diorite and quartz diorite on southwest Lyell Island suggests these rocks may be part of the SCPS. Massive diorite, quartz diorite, leucodiorite, quartz monzodiorite, and granodiorite on northwest Lyell Island and southern Richardson Island may be part of the BIPS. 2) Panels of Kunga Group strata occur on Richardson Island, Shuttle Island, the Topping Islands, and western Lyell Island; areas previously mapped as Karmutsen Formation. 3) Thermally altered siliciclastic rocks of the Sandilands Formation are recognized on eastern Tanu Island, rather than Yakoun Group strata. 4) Clastic sedimentary rocks disconformably (unconformably?) overlie upper Kunga Group strata near Crescent Point. Fossils from this sedimentary succession should more precisely constrain the depositional age; however, sedimentary clasts bearing Bajocian ammonites and plagioclase-phyric volcanic clasts (probable Yakoun Group) in the lower part of this sedimentary succession suggest that these rocks postdate the Yakoun Group, and may be temporally equivalent to late Middle Jurassic (late Bathonian to early Callovian) Moresby Group strata (Cameron and Tipper, 1985; Poulton et al., 1991) or younger Jurassic strata recently identified (Haggart, 1992).

Structurally, the map area is transected by shear zones that juxtapose and repeat Triassic-Lower Jurassic strata. A major zone of ductile deformation through Darwin Sound consists of low-angle, reverse shear zones, although normal and transcurrent structures are observed locally. This zone may be part of the Louscoone Inlet fault system (Sutherland Brown, 1968; Lewis, 1991a, b, c) although structures throughout Darwin Sound appear to reflect mainly earlier, oblique-slip movement, rather than later dextral, transcurrent movement as reported by Lewis (1991c). High strain fabrics

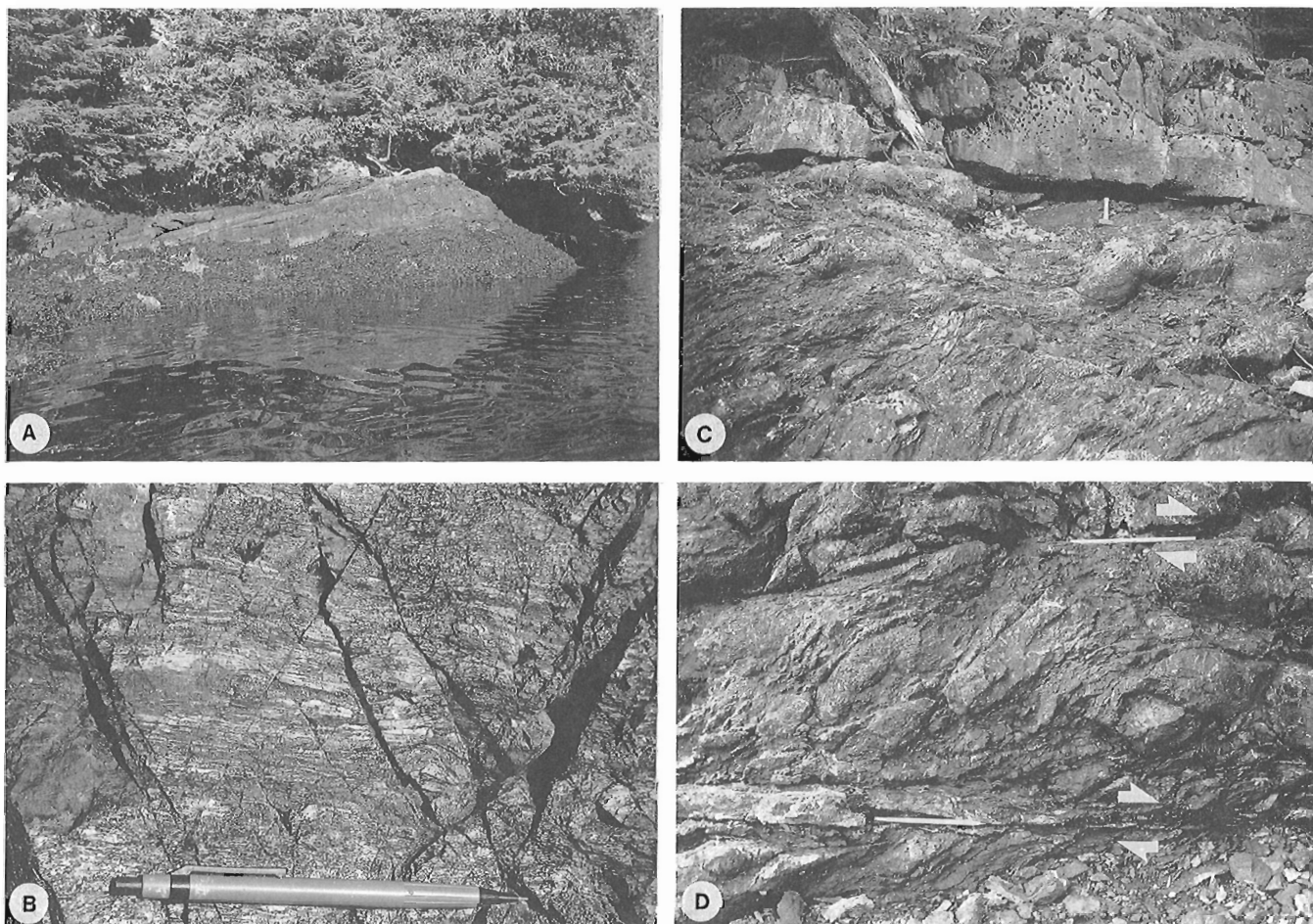


Figure 5. Tectonized Triassic-Jurassic strata in Darwin Sound. (A) Shallow, west-dipping tectonic layering in plutonic rocks on the east side of Shuttle Island. (B) Detail of (A) showing strongly-developed, down-dip mineral lineations on shear foliation. Kinematic indicators reveal reverse (west-side-up) displacement. (C) Sadler limestone (above hammer) structurally overlying tectonized siltstone and limestone of the Peril and Sandilands formations on the west side of Shuttle Island. (D) Detail of tectonized siltstone in (C) taken perpendicular to the lamination showing the sigmoidal nature of the shallow-dipping fabric which reveals a minor component of dextral displacement accompanied west-side-up thrusting.

in Beresford Inlet, and the conspicuous topographic lineament that coincides with the inlet, are attributed to competency contrasts between a narrow belt of mafic volcanic rocks and the enclosing intrusive rocks. Fabrics in northern Beresford Inlet are to be investigated by Ian Foreman as part of a B.Sc. project at Queens University. Mylonitic rocks exposed near Beljay Bay are on strike with strongly fractured and veined rocks which extend from central Lyell Island to southeast Sedgwick Bay (see Anderson et al., 1992; Souther, 1992). These may define a regional structural zone parallel to the Darwin Sound deformation zone.

ACKNOWLEDGMENTS

Assistance in the field was provided by Ian Foreman and Mark Hamilton. In addition, Ian Foreman conducted independent mapping of northern Beresford Inlet and Mark Hamilton mapped Karmutsen volcanics in the western

part of the map area. I thank them both for their hard work and good cheer. Audrey and Dave Putterill provided superb expediting services and cheerful contact throughout the field season. This work benefitted from discussions with J. Haggart, R. Anderson, J. Souther, S. Taite, P. Lewis, H. Tipper, and D. Tempelman-Kluit.

REFERENCES

- Anderson, R.G. and Reichenbach, I.
1991: U-Pb and K-Ar framework for Middle to Late Jurassic (172-2158 Ma) and Tertiary (46-27 Ma) plutons in Queen Charlotte Islands, British Columbia; in *Evolution and Hydrocarbon Potential of the Queen Charlotte Basin, British Columbia*, (ed.) G.J. Woodsworth; Geological Survey of Canada, Paper 90-10, p. 59-87.
- Anderson, R.G., Gunning, M.H., and Porter, S.
1992: Progress in mapping of Jurassic and Tertiary plutonic styles, Queen Charlotte Islands; in *Current Research, Part A*; Geological Survey of Canada, Paper 92-1A.

- Barker, F., Sutherland Brown, A., Budahn, J.R., and Plafker, G.**
1989: Back-arc with frontal-arc component origin of Triassic Karmutsen basalt, British Columbia; *Chemical Geology*, v. 75, p. 81-102.
- Cameron, B.E.B. and Tipper, H.W.**
1985: Jurassic stratigraphy of the Queen Charlotte Islands, British Columbia; *Geological Survey of Canada, Bulletin* 365, 49 p.
- Desrochers, A. and Orchard, M.J.**
1991: Stratigraphic revisions and carbonate sedimentology of the Kunga Group (Upper Triassic-Lower Jurassic), Queen Charlotte Islands, British Columbia; in *Evolution and Hydrocarbon Potential of the Queen Charlotte Basin, British Columbia*, (ed.) G.J. Woodsworth; Geological Survey of Canada, Paper 90-10, p. 163-172.
- Gamba, C.A.**
1991: An update on the Cretaceous sedimentology of the Queen Charlotte Islands, British Columbia; in *Current Research, Part A; Geological Survey of Canada, Paper* 91-1A, p. 373-382.
- Gamba, C.A., Indrelid, J., and Taite, S.**
1990: Sedimentology of the Upper Cretaceous Queen Charlotte Group, with special reference to the Honna Formation, Queen Charlotte Islands, British Columbia; in *Current Research, Part F; Geological Survey of Canada, Paper* 90-1F, p. 67-73.
- Haggart, J.W.**
1991a: A synthesis of Cretaceous stratigraphy, Queen Charlotte Islands, British Columbia; in *Evolution and Hydrocarbon Potential of the Queen Charlotte Basin, British Columbia*, (ed.) G.J. Woodsworth; Geological Survey of Canada, Paper 90-10, p. 253-277.
1991b: New sections of Yakoun Group (Middle Jurassic) strata, Queen Charlotte Islands, British Columbia; in *Current Research, Part A; Geological Survey of Canada, Paper* 91-1A, p. 359-366.
1992: Progress in Jurassic and Cretaceous stratigraphy, Queen Charlotte Islands, British Columbia; in *Current Research, Part A; Geological Survey of Canada, Paper* 92-1A.
- Hesthammer, J.**
1990: Structural interpretation of Upper Triassic and Jurassic units exposed on central Graham Island, Queen Charlotte Islands, British Columbia; in *Current Research, Part F; Geological Survey of Canada, Paper* 90-1F, p. 11-18.
1991: Lithologies of the Middle Jurassic Yakoun Group in the central Graham Island area, Queen Charlotte Islands, British Columbia; in *Current Research, Part A; Geological Survey of Canada, Paper* 91-1A, p. 353-358.
- Hesthammer, J., Indrelid, J., Lewis, P.D., and Orchard, M.J.**
1991: Permian strata on the Queen Charlotte Islands, British Columbia; in *Current Research, Part A; Geological Survey of Canada, Paper* 91-1A, p. 321-329.
- Lewis, P.D.**
1991a: Dextral strike-slip faulting and associated extension along the southern portion of the Louscoone Inlet fault system, southern Queen Charlotte Islands, British Columbia; in *Current Research, Part A; Geological Survey of Canada, Paper* 91-1A, p. 383-391.
1991b: Geology of the Burnaby Island/Ramsay Island map area, Queen Charlotte Islands, British Columbia; Geological Survey of Canada, Open File 2316.
1991c: Structural geology and processes of deformation in the Mesozoic and Cenozoic evolution of the Queen Charlotte Islands; Ph.D. thesis, University of British Columbia, Vancouver, 323 p.
- Lewis, P.D., Haggart, J.W., Anderson, R.G., Hickson, C.J., Thompson, R.I., Dietrich, J.R., and Rohr, K.M.M.**
1991: Triassic to Neogene geologic evolution of the Queen Charlotte region; *Canadian Journal of Earth Sciences*, v. 28, p. 854-869.
- Orchard, M.J.**
1991: Late Triassic conodont biochronology and biostratigraphy of the Kunga Group, Queen Charlotte Islands, British Columbia; in *Evolution and Hydrocarbon Potential of the Queen Charlotte Basin, British Columbia*, (ed.) G.J. Woodsworth; Geological Survey of Canada, Paper 90-10, p. 173-193.
- Palfy, J., McFarlane, R.B., Smith, P.L., and Tipper, H.W.**
1990: Potential for ammonite biostratigraphy of the Sinemurian part of the Sandilands Formation, Queen Charlotte Islands, British Columbia; in *Current Research, Part F; Geological Survey of Canada, Paper* 90-1F, p. 47-50.
- Poulton, T.P., Hall, R.L., Tipper, H.W., Cameron, B.E.B., and Carter, E.S.**
1991: Current status of Middle Jurassic biostratigraphy of the Queen Charlotte Islands, British Columbia; in *Evolution and Hydrocarbon Potential of the Queen Charlotte Basin, British Columbia*, (ed.) G.J. Woodsworth; Geological Survey of Canada, Paper 90-10, p. 237-252.
- Simpson, C. and Schmidt, S.M.**
1983: An evaluation of criteria to deduce the sense of movement in sheared rocks; *Geological Society of America Bulletin*, v. 94, p. 1281-1288.
- Souther, J.G.**
1992: Geology of central Lyell Island, Queen Charlotte Islands, British Columbia; in *Current Research, Part A; Geological Survey of Canada, Paper* 92-1A.
- Struik, L.C., Atrens, A., and Haynes, A.**
1991: Handheld computer as a field notebook, and its integration with the Ontario Geological Survey's "FIELDLOG" program; in *Current Research, Part A; Geological Survey of Canada, Paper* 91-1A, p. 279-284.
- Sutherland Brown, A.**
1968: Geology of the Queen Charlotte Islands, British Columbia; British Columbia Department of Mines and Petroleum Resources, *Bulletin* 54.
- Taite, S.P.**
1990: Observations on structure and stratigraphy of the Sewell Inlet-Tasu Sound area, Queen Charlotte Islands, British Columbia; in *Current Research, Part F; Geological Survey of Canada, Paper* 90-1F, p. 19-22.
1991a: Geology of the Sewell Inlet-Tasu Sound area, Queen Charlotte Islands, British Columbia; in *Current Research, Part A; Geological Survey of Canada, Paper* 91-1A, p. 393-399.
1991b: Geology of the Sewell Inlet-Tasu Sound area, Queen Charlotte Islands, British Columbia; Geological Survey of Canada, Open File 2317.
- Thompson, R.I. and Lewis, P.D.**
1990: Geology, Louise Island, British Columbia; Geological Survey of Canada, Map 2-1990, scale 1:50 000.
- Tipper, H.W., Smith, P.L., Cameron, B.E.B., Carter, E.S., Jakobs, G.K., and Johns, M.J.**
1991: Biostratigraphy of the Lower Jurassic formations of the Queen Charlotte Islands, British Columbia; in *Evolution and Hydrocarbon Potential of the Queen Charlotte Basin, British Columbia*, (ed.) G.J. Woodsworth; Geological Survey of Canada, Paper 90-10, p. 203-235.
- Woodsworth, G.J. (ed.)**
1991: *Evolution and Hydrocarbon Potential of the Queen Charlotte Basin, British Columbia*, Geological Survey of Canada, Paper 90-10, 569 p.

Progress in Jurassic and Cretaceous stratigraphy, Queen Charlotte Islands, British Columbia

James W. Haggart
Cordilleran Division, Vancouver

Haggart, J.W., 1992: *Progress in Jurassic and Cretaceous stratigraphy, Queen Charlotte Islands, British Columbia*; in *Current Research, Part A*; Geological Survey of Canada, Paper 92-1A, p. 361-365.

Abstract

Detailed mapping and paleontological studies of Jurassic and Cretaceous rocks of the Queen Charlotte Islands have identified several new stratigraphic levels and provided details of the Cretaceous history of the region. New macrofossil finds indicate that Upper Jurassic rocks of Callovian/Oxfordian and Oxfordian/Kimmeridgian age are locally present. These are coarse clastic lithologies, spatially associated with intermediate volcanics. The new finds indicate that the Late Jurassic hiatus in the Queen Charlotte Islands is substantially shorter and/or less widespread than previously interpreted. A section spanning the Jurassic/Cretaceous boundary appears to be present in the northwestern part of the islands.

New mapping and revised paleontological age dating of Cretaceous rocks indicate that there is no evidence for post-Hauterivian block faulting in the islands.

Résumé

La cartographie détaillée et les études paléontologiques des roches jurassiques et crétacées des îles de la Reine-Charlotte ont permis de reconnaître plusieurs nouveaux étages stratigraphiques et nous ont fourni des détails sur l'évolution de la région au Crétacé. Les découvertes de nouveaux macrofossiles indiquent que localement, existent des roches du Jurassique supérieur, datées du Callovien/Oxfordien et de l'Oxfordien/Kimméridgien. Ces roches ont une lithologie clastique grossière, et sont spatialement associées à des roches volcaniques intermédiaires. Les nouvelles découvertes indiquent que dans les îles de la Reine-Charlotte, le hiatus du Jurassique supérieur est beaucoup plus bref ou moins étendu, ou les deux à la fois, qu'on ne l'estimait auparavant. Une coupe stratigraphique englobant la limite entre le Jurassique et le Crétacé semble exister dans la portion nord-ouest des îles.

Les nouveaux travaux de cartographie et la révision des datations paléontologiques des roches crétacées n'indiquent pas dans les îles de la Reine-Charlotte la formation post-hauterivienne de blocs faillés.

INTRODUCTION

Detailed geological mapping and stratigraphic study in the Jurassic and Cretaceous outcrop belt of the central and northern parts of the Queen Charlotte Islands (103B, F, G) have been carried out for several seasons (Fig. 1). This mapping has been undertaken to provide a firm stratigraphic basis for latest Jurassic and Cretaceous biostratigraphic studies and to help infer the geological history of the islands during this part of the later Mesozoic.

Several new discoveries have resulted from this work over the past two field seasons. Of great importance is the recognition that further Upper Jurassic stratigraphic intervals are present in the islands than previously assumed (Fig. 2). As well, a detailed analysis of Cretaceous stratigraphic sequences has provided new details of the Cretaceous geological history of the islands.

NEW STRATIGRAPHIC HORIZONS

Recent macrofossil collections have established the presence of several new stratigraphic intervals in the archipelago.

Oxfordian strata

Skidegate Channel

Exposures of rocks in the Skidegate Channel area have recently provided several macrofossil collections indicating the presence of Oxfordian strata. The collections come from outcrops within the strongly deformed northwest-southeast trending zone transecting the central part of the archipelago (Thompson et al., 1991) and consequently, stratigraphic sections and continuity are mostly lacking. Enclosing lithologies consist of coarse clastics, rich in volcanic detritus, and the outcrops are geographically associated with extensive exposures of volcanic rocks, typically of intermediate composition.

Fossils collected from sandstones and siltstones exposed at GSC loc.C-187412 include several examples of the ammonite *Cardioceras* (*Scarburgiceras*) and probably represent the Cordatum Zone, or uppermost zone of the European Lower Oxfordian (H.W. Tipper, pers. comm., 1991; Frebald and Tipper, 1975). An additional, poorly located collection from this general area includes a large ammonite tentatively referred to the genus *Procerites*, also suggesting the possibility of lower Oxfordian to upper Callovian strata (H.W. Tipper, pers. comm., 1991).

Both these collections represent a somewhat younger faunal horizon than previously identified in this part of the Jurassic section of the Queen Charlotte Islands. They postdate slightly the youngest faunas recovered to date from the Moresby Group, Late Bathonian to Early Callovian (Cameron and Tipper, 1985; Poulton et al., 1991). Earlier workers have postulated a major unconformity at the top of the Moresby Group, essentially spanning later Callovian to Tithonian time (Cameron and Tipper, 1985; Poulton et al., 1991). Although it is uncertain whether the Oxfordian strata represent a separate cycle of sedimentation from the Moresby

Group, their lithologies are similar to those found in the group, and they might thus reflect still younger horizons of this poorly-known sequence. Further stratigraphic studies are necessary to determine the degree of conformity of the Oxfordian strata with the older, Moresby Group package.

Recent mapping in the Skidegate Channel area has determined that many rocks previously considered part of the Cretaceous outcrop belt in this area are more likely Jurassic in age. These include volcanic assemblages of intermediate composition and very immature, volcanically derived sedimentary strata. Additional fossil collecting is required to determine the relative extent of Yakoun Group (Bajocian), Moresby Group, and younger Jurassic strata in this area.

White Point

Strata exposed south of White Point, on the northwest coast of Graham Island (Fig. 1), have produced new macrofossil collections which indicate the presence of Late Jurassic rocks. At GSC loc.C-185036 the author collected bivalves referable to *Buchia concentrica* (*sensu lato*), of Late Oxfordian to Early Kimmeridgian age (Frebald, 1964), from conglomeratic strata near the base of the section described by

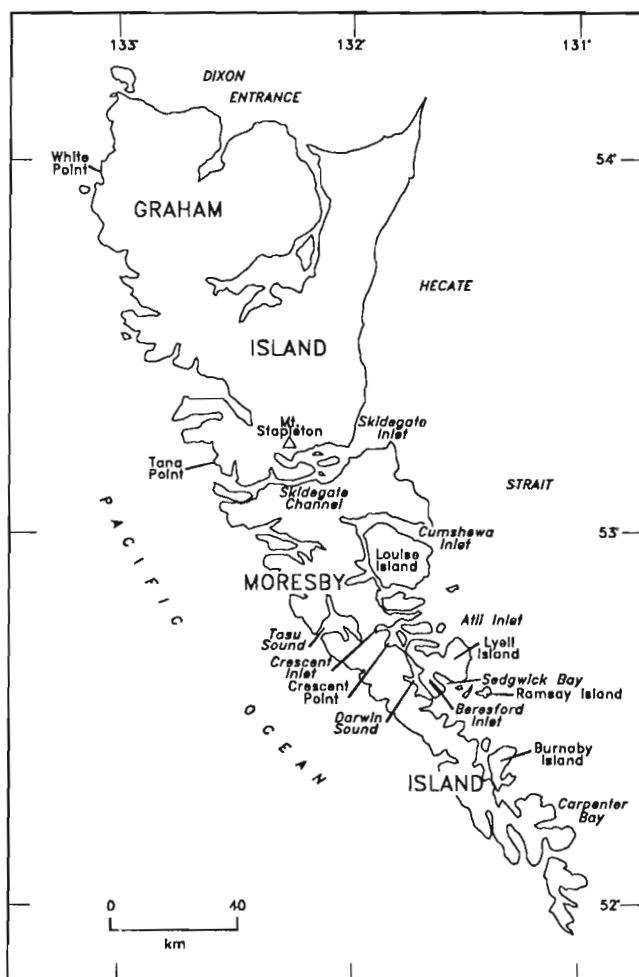


Figure 1. Location map.

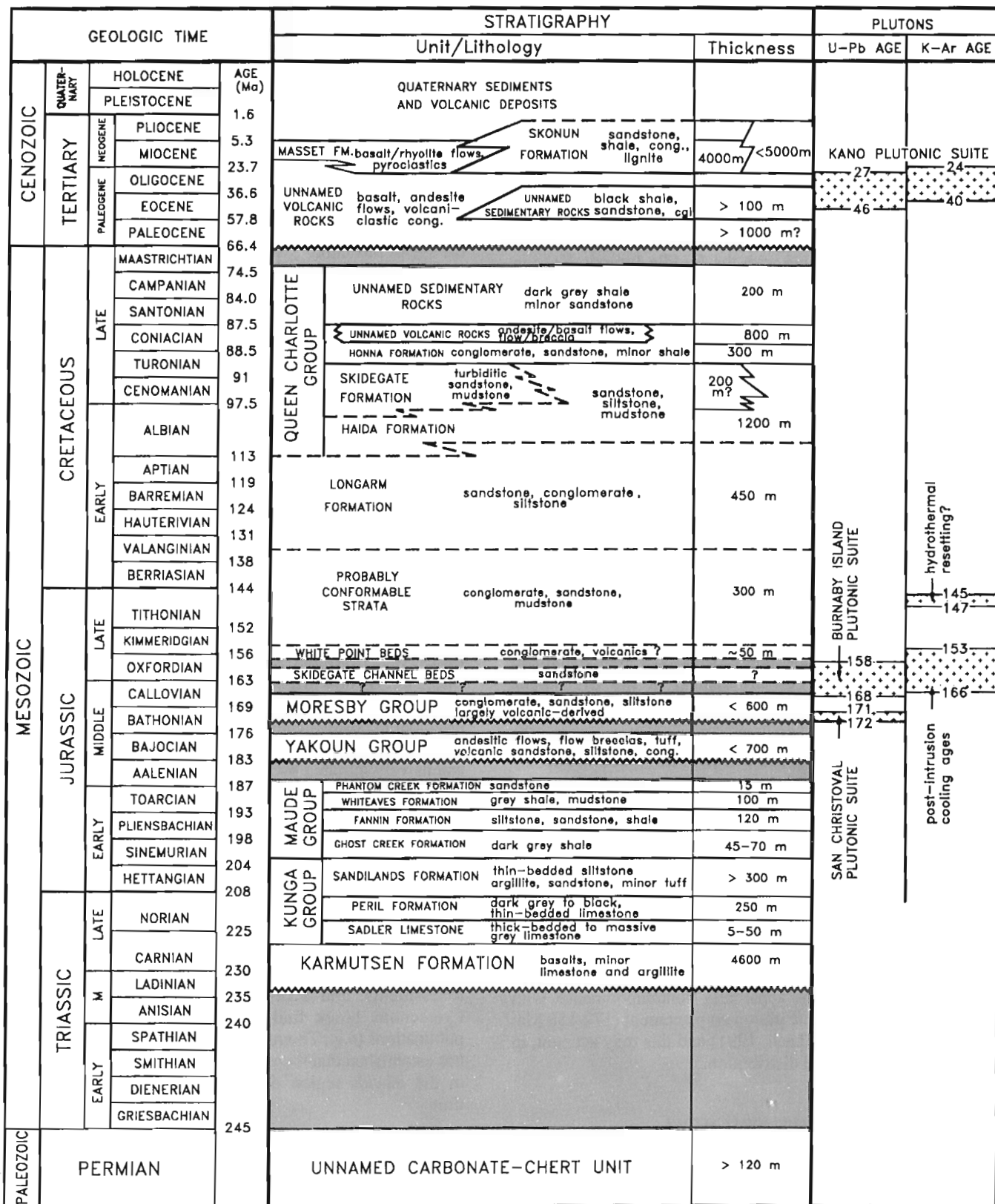


Figure 2. Summary of stratigraphic and plutonic history for the Queen Charlotte Islands showing newly recognized late Jurassic stratigraphic horizons (modified after Lewis et al., 1991).

Haggart (1989) and Gamba (1991). A likely late Tithonian age for nearby exposures of conglomeratic strata was previously determined by Jeletzky (1984), based on analysis of submitted fossil collections (see Cameron and Tipper, 1985, p. 42); the presence and age of the Tithonian beds have subsequently been confirmed by the author.

The new collections were made at several tens of metres above the base of a thick sedimentary succession which overlies approximately 55 m of volcanic strata of intermediate composition. The author described these volcanic rocks previously (Haggart, 1991) and suggested that they might be correlative with the Middle Jurassic Yakoun Group. However, the degree of unconformity between the volcanic rocks and the overlying sedimentary strata appears to be small and the revised age interpretation for the sedimentary succession raises the possibility that the volcanic package is significantly younger than the Yakoun Group, or of possible Oxfordian-Kimmeridgian age. The presence of a Late Jurassic volcanic/sedimentary package in the Queen Charlotte Islands augments the similarity of the later Mesozoic succession in this region with that of sequences in southeastern Alaska.

Strata overlying the beds with *Buchia concentrica* in the section south of White Point are poorly macrofossiliferous but consist of a thick sequence of additional conglomerate, succeeded by mudstone (Haggart, 1989). The section appears to be continuous and conformable, although it is cut by several large faults. No volcanic strata are present in this section. Overlying these rocks, again with apparent conformity, are sandstones and siltstones of Late Valanginian to Barremian age which are typical of the Cretaceous Longarm Formation and are correlated with that unit (Haggart, 1989).

The entire succession in the White Point area thus appears to represent a continuous section spanning the Jurassic-Cretaceous boundary. Given that early Late Jurassic-age strata are preserved at the base of this section, apparently conformable beneath Early Cretaceous strata, the length of time inferred for the Late Jurassic unconformity in the Queen Charlotte Islands (Poulton et al., 1991) should be reduced considerably. Indeed, given the new finds of Callovian-Oxfordian rocks described above, the Upper Jurassic section of the islands may prove to be rather complete, if poorly represented. Deposition of these Upper Jurassic sediments was apparently contemporaneous with Middle and Late Jurassic pluton emplacement (172-158 Ma: Anderson and Reichenbach, 1991) and this may account, in part, for their restricted distribution.

Jurassic? and/or Cretaceous? strata

Exposures of a succession of mudstone, siltstone, fine sandstone, and shale, locally of significant thickness (~150-180 m), were identified in the southern part of the islands in 1990-91. Although sparsely represented, these rocks are widespread over a large part of the eastern side of the archipelago, including Atli Inlet on Lyell Island, Crescent Point, and the northwestern and western part of Burnaby Island. The unit also appears to underlie sections typical of

the Cretaceous Longarm Formation at several localities. Turbiditic facies are developed in the unit at Crescent Point (see Sanborn-Barrie, 1992) and Ramsay Island (see Gamba, 1991). Locally, as at Lyell Island, the mudstones are spatially associated with Yakoun Group volcanic and sedimentary strata (see Souther, 1992), and they contain possible Bajocian bivalves as well. It is thus possible that they are part of the Yakoun Group succession, or of slightly younger age, perhaps equivalents of the Moresby Group or the younger Late Jurassic deposits described above. Paleontological investigations in progress should more precisely determine the age of this unit.

NEW CRETACEOUS SECTIONS

New sections of Cretaceous strata were identified and studied in 1990-91. The westernmost occurrence of Longarm Formation deposits in the central islands was identified by float occurrences at Tana Point, north of Skidegate Channel on the west coast of Graham Island. This exposure had previously been noted by Sutherland Brown (1968: Fig. 11) but not described. The exposures rest above steep cliffs of likely Yakoun volcanic and sedimentary strata and lithologies present in the float blocks at the base of the scarp include shallow water sandstone with buchiid bivalves, a facies previously identified at several localities in the islands (Haggart, 1989, 1991; Gamba, 1991).

Additional exposures of likely Cretaceous rocks were studied briefly in the alpine regions at the head of Lagins Creek, west of Mount Stapleton on southern Graham Island. These strata were originally correlated with the Cretaceous Longarm Formation by Sutherland Brown (1968). The principal exposures consist of interbedded argillite and fine sandstone, locally showing turbiditic features, and are extensively intruded by Tertiary Kano Pluton rocks, as well as dykes of intermediate composition. Lithologically, the argillites and sandstones appear similar to the turbiditic facies of the shale member of the Haida Formation (*sensu* Haggart et al., 1989, 1991). Unfortunately, no macrofossils have been recovered from these beds.

CRETACEOUS BLOCK FAULTING

New detailed mapping, revised paleontological age assessments, and a re-examination of the evidence for Cretaceous block faulting presented in several earlier publications (e.g., Thompson et al., 1991; Lewis et al., 1991) has established that there is little likelihood of block faulting in the islands region during post-Hauterivian Cretaceous time.

The evidence for block-faulting of this age presented by earlier workers included: 1) the observation that coarse clastics of the Honna Formation, typically interstratified *within* the Cretaceous succession, locally rest unconformably on older units of Triassic-Cretaceous age; 2) the presence of geographically juxtaposed stratal blocks showing different Cretaceous ages.

A detailed analysis of the factors mitigating against a block faulting interpretation is in preparation. In brief these include:

1) Little, if any, sedimentological evidence indicative of syndepositional block faulting is seen. Adjacent to inferred zones of active block-faulting one would expect to find chaotic and highly diverse lithological assemblages, where cannibalized debris from the elevated block was rapidly deposited on the downdropped one. Instead, these areas are characterized by widespread, laterally continuous belts of shallow marine Cretaceous strata (see Haggart, 1991) which cross the inferred fault traces.

2) Detailed study of the stratigraphic succession of the Honna and Haida formations on northeastern Moresby Island has shown that the lower part of the Honna Formation in this area is locally interstratified with very shallow water deposits of the Haida Formation. The Honna Formation in this region is thus a shallow water deposit and does indeed locally rest on older, Triassic and Jurassic rock units. The observed unconformities are best explained, however, as resulting from the initiation of Cretaceous shallow-marine sedimentation at these locales, rather than by the removal of older Cretaceous strata during Cretaceous time. Haggart (1991) previously suggested that such a relationship might be invoked to explain local sub-Honna unconformities. The shallow-water interpretation for the Honna Formation in the northeastern Moresby Island area complements the sedimentological model of Gamba (1991) for a relatively shallow-water, shelf origin for part of the Honna Formation exposed at the type section some 18 km to westward.

Other areas where the Honna Formation was earlier inferred to rest on older Cretaceous units, such as in Skidegate Channel where it has been mapped resting on the Longarm Formation, are now known to include more complete Cretaceous sequences than previously thought, or represent juxtapositions of Cretaceous and older strata along previously unnoted faults.

3) Revised paleontological age assessments indicate that some geographically-adjacent localities showing Cretaceous strata of quite different inferred ages are actually less diachronous than previously considered. Thus, local uplift of blocks containing older Cretaceous stratigraphies is not required to explain the observed distribution of rock ages. This reassessment underscores the importance of continued biostratigraphic studies in analysis of Cordilleran stratigraphy.

ACKNOWLEDGMENTS

The author thanks H.W. Tipper who identified the Jurassic ammonites and provided valuable discussions of Jurassic stratigraphy and biochronology. J.G. Souther and H.W. Tipper are thanked for reviews of the manuscript.

REFERENCES

- Anderson, R.G. and Reichenbach, I.**
1991: U-Pb and K-Ar framework for Middle to Late Jurassic (172- \geq 158 Ma) and Tertiary (46-27 Ma) plutons in Queen Charlotte Islands, British Columbia; in *Evolution and Hydrocarbon Potential of the Queen Charlotte Basin, British Columbia*, (ed.) G.J. Woodsworth; Geological Survey of Canada, Paper 90-10, p. 59-87.
- Cameron, B.E.B. and Tipper, H.W.**
1985: Jurassic stratigraphy of the Queen Charlotte Islands, British Columbia; Geological Survey of Canada, Bulletin 365, 49 p.
- Frebold, H.**
1964: Illustrations of Canadian fossils. Jurassic of western and Arctic Canada; Geological Survey of Canada, Paper 63-4, 107 p., 51 pls.
- Frebold, H. and Tipper, H.W.**
1975: Upper Callovian and Lower Oxfordian ammonites from southeastern Bowser Basin, British Columbia; *Canadian Journal of Earth Sciences*, v. 12, no. 2, p. 145-157.
- Gamba, C.A.**
1991: An update on the Cretaceous sedimentology of the Queen Charlotte Islands, British Columbia; in *Current Research, Part A*; Geological Survey of Canada, Paper 91-1A, p. 373-382.
- Haggart, J.W.**
1989: Reconnaissance lithostratigraphy and biochronology of the Lower Cretaceous Longarm Formation, Queen Charlotte Islands, British Columbia; in *Current Research, Part H*; Geological Survey of Canada, Paper 89-1H, p. 39-46.
1991: A synthesis of Cretaceous stratigraphy, Queen Charlotte Islands, British Columbia; in *Evolution and Hydrocarbon Potential of the Queen Charlotte Basin, British Columbia*, (ed.) G.J. Woodsworth; Geological Survey of Canada, Paper 90-10, p. 253-277.
- Haggart, J.W., Lewis, P.D., and Hickson, C.J.**
1989: Stratigraphy and structure of Cretaceous strata, Long Inlet, Queen Charlotte Islands, British Columbia; in *Current Research, Part H*; Geological Survey of Canada, Paper 89-1H, p. 65-72.
- Haggart, J.W., Taite, S., Indrelid, J., Hesthammer, J., and Lewis, P.D.**
1991: A revision of stratigraphic nomenclature for the Cretaceous sedimentary rocks of the Queen Charlotte Islands, British Columbia; in *Current Research, Part A*; Geological Survey of Canada, Paper 91-1A, p. 367-371.
- Jeletzky, J.A.**
1984: Jurassic-Cretaceous boundary beds of western and Arctic Canada and the problem of the Tithonian-Berriasian stages in the Boreal Realm; in *Jurassic-Cretaceous Biochronology and Paleogeography of North America*, (ed.) G.E.G. Westermann; Geological Association of Canada, Special Paper 27, p. 175-255.
- Lewis, P.D., Haggart, J.W., Anderson, R.G., Hickson, C.J., Thompson, R.I., Dietrich, J.R., and Rohr, K.M.M.**
1991: Triassic to Neogene geologic evolution of the Queen Charlotte region; *Canadian Journal of Earth Sciences*, v. 28, p. 854-869.
- Poulton, T.P., Hall, R.L., Tipper, H.W., Cameron, B.E.B., and Carter, E.S.**
1991: Current status of Middle Jurassic biostratigraphy of the Queen Charlotte Islands, British Columbia; in *Evolution and Hydrocarbon Potential of the Queen Charlotte Basin, British Columbia*, (ed.) G.J. Woodsworth; Geological Survey of Canada, Paper 90-10, p. 237-252.
- Sanborn-Barrie, M.**
1992: Geology of the Darwin Sound area, Queen Charlotte Islands, British Columbia; in *Current Research, Part A*; Geological Survey of Canada, Paper 92-1A.
- Souther, J.G.**
1992: Geology of central Lyell Island, Queen Charlotte Islands, British Columbia; in *Current Research, Part A*; Geological Survey of Canada, Paper 92-1A.
- Sutherland Brown, A.**
1968: Geology of the Queen Charlotte Islands, British Columbia; British Columbia Department of Mines and Petroleum Resources, Bulletin 54, 226 p., 18 pls.
- Thompson, R.I., Haggart, J.W., and Lewis, P.D.**
1991: Late Triassic through early Tertiary evolution of the Queen Charlotte Basin, British Columbia, with a perspective on hydrocarbon potential; in *Evolution and Hydrocarbon Potential of the Queen Charlotte Basin, British Columbia*, (ed.) G.J. Woodsworth; Geological Survey of Canada, Paper 90-10, p. 3-29.

Lithofacies of the late Early to early Late Cretaceous Queen Charlotte Group, Queen Charlotte Islands, British Columbia¹

Charle A. Gamba²
Cordilleran Division, Vancouver

Gamba, C.A., 1992: *Lithofacies of the late Early to early Late Cretaceous Queen Charlotte Group, Queen Charlotte Islands, British Columbia*; in *Current Research, Part A; Geological Survey of Canada, Paper 92-1A*, p. 367-376.

Abstract

The Queen Charlotte Group is divisible into five lithofacies assemblages: sandy shelf, muddy ramp, sandy submarine fan, conglomeratic submarine fan, and muddy shelf. Each assemblage is characterized by a suite of facies deposited in shallow shelf to submarine fan environments. From Albian to Early Turonian time the sandy shelf, muddy ramp, and sandy submarine fan assemblages were deposited along the eastern margin of a westwards deepening forearc basin. At least three episodes of relative sea-level fluctuation, recorded by sharp-based transgressive cyclic successions preserved in the deposits of the sandy shelf assemblage, affected deposition basinwide during the Albian. During Middle to Late Turonian time, shelf conditions were abruptly terminated by the westward progradation of conglomeratic submarine fans. This event was likely a response to subduction-related tectonic activity which led to the unroofing of the magmatic-arc situated to the east, dramatically accelerating subsidence rates in the forearc basin.

Résumé

Le groupe de Queen Charlotte peut se diviser en cinq assemblages de lithofaciès : plate-forme sableuse, rampe boueuse, cône sous-marin sableux, cône sous-marin conglomératique et plate-forme boueuse. Chaque assemblage est caractérisé par une suite de faciès déposés dans des milieux allant de plate-forme peu profonde à cône sous-marin. De l'Albien au Turonien inférieur, les assemblages de plate-forme sableuse, de rampe boueuse et de cône sous-marin sableux ont été déposés le long de la marge orientale d'un bassin d'avant-arc s'approfondissant vers l'ouest. Au moins trois épisodes de fluctuation du niveau de la mer relatif, attestés par des successions cycliques transgressives, à base bien définies, conservées dans les dépôts de l'assemblage de la plate-forme sableuse, ont affecté la sédimentation dans tout le bassin durant l'Albien. Entre le Turonien moyen et supérieur, les conditions de plate-forme ont été abruptement interrompues par la progradation vers l'ouest des cônes sous-marins conglomératiques. Cet événement a probablement été causé par une activité tectonique de subduction qui est à l'origine du décapage de l'arc magmatique situé à l'est, accélérant considérablement les vitesses de subsidence dans le bassin d'avant-arc.

¹ Contribution to Frontier Geoscience Program

² Department of Geology, McMaster University, Hamilton, Ontario L8S 4M1

CRETACEOUS LITHOSTRATIGRAPHY

The Queen Charlotte Group is composed of marine sediments deposited in shallow shelf to basinal environments along the western margin of a forearc basin during Albian to Maastrichtian time. Each environment is represented by an assemblage of facies. These assemblages include the sandy shelf, muddy ramp, sandy submarine fan, conglomeratic submarine fan, and muddy shelf assemblages.

Previous sedimentological studies of the Queen Charlotte Group have tended to concentrate upon specific formations rather than the group as a whole. Yagishita (1985) focused primarily upon the provenance of the Haida and Honna formations rather than on their sedimentology. Although Yagishita (1985) identified five facies within these two formations, the facies are so inadequately described as to preclude a reliable sedimentological interpretation. Higgs (1990) recognized three lithofacies within the Honna Formation, which, with the addition of three new facies, are incorporated and described in this paper.

Haggart et al. (1991) provided the most comprehensive lithostratigraphic scheme for the group, dividing it into three broad lithological units (Table 1). This concept forms the basis of the lithostratigraphic framework outlined in this paper.

This paper divides the Queen Charlotte Group into five facies assemblages, provides detailed facies descriptions of these assemblages, and presents a regional facies interpretation.

SANDY SHELF ASSEMBLAGE (SSA)

Basal cross-stratified facies

This facies consists of grouped cosets of trough cross-stratified medium-grained to granular pebbly arkose and feldspathic arenite. Interbedded units of swaley

cross-stratified medium- to coarse-grained pebbly sandstone up to 4.5 m thick also occur. The facies is best developed in Skidegate Inlet, reaching a thickness of 8 m, and to the east of McClellan Island in Cumshewa Inlet where it is 18.8 m thick. Rare oyster fragments have been found. Common trace fossils include *Ophiomorpha*, *Macronichnus* and *Skolithos*.

Sandy and gravelly storm deposit facies

The remainder of the assemblage is divisible into cyclic successions, each composed of two facies: a lower, sharp based sequence of sandy and gravelly storm deposits and a gradationally overlying upper sequence of massive, bioturbated sandstone (Fig. 1).

The lower storm deposit facies is composed of amalgamated units of swaley cross-stratified (SCS) and hummocky cross-stratified (HCS) fine- to medium-grained lithic arenite and arkose. At Onward Point, swaley cross-stratified sandstone is interbedded with broadly lenticular units of polymictic pebble conglomerate up to 60 cm thick. The conglomerates are composed primarily of rounded Yakoun Group andesitic clasts with lesser argillite and plutonic clasts. Thick-shelled articulated and disarticulated trioniid bivalves are common in this facies. Common trace fossils include *Ophiomorpha*, *Thalassinoides*, and *Skolithos*. This facies reaches a thickness of 12 m in Skidegate Inlet.

Massive bioturbated sandstone facies

The storm deposit facies is gradationally overlain by massive, bioturbated buff to dark green weathering fine-grained poorly sorted lithic arenite and wacke. This facies forms monotonous massive intervals up to 544 m thick containing abundant buff weathering dolomitic concretions. In roadcut exposures large scale tabular bedding is observed.

Table 1. Comparison of Cretaceous lithostratigraphic schemes

Cretaceous Stratigraphy	Lithologic Units of Haggart et al (1991)	Assemblages of this paper	Age ¹	Thickness
Unnamed Shales	Deep water shales	Muddy shelf	Late Santonian to Maastrichtian	>43.5 m
Honna Fm	Honna	Conglomeratic submarine fan	Early Coniacian to Early Santonian	1600 ² m
Skidegate Fm	Deep water shales	Sandy submarine fan	Cenomanian to Early Turonian	630 ³ m
Haida Mudstone		Muddy ramp	Cenomanian to Early Turonian	>428 m
Haida Sandstone	Shallow water sandstones	Sandy shelf	Albian	1046 m
Longarm Fm		Longarm Fm	Valanginian to Aptian	

¹ from Haggart (1991)

² from Gamba (1991)

³ from Sutherland Brown (1968)

BEARSKIN BAY

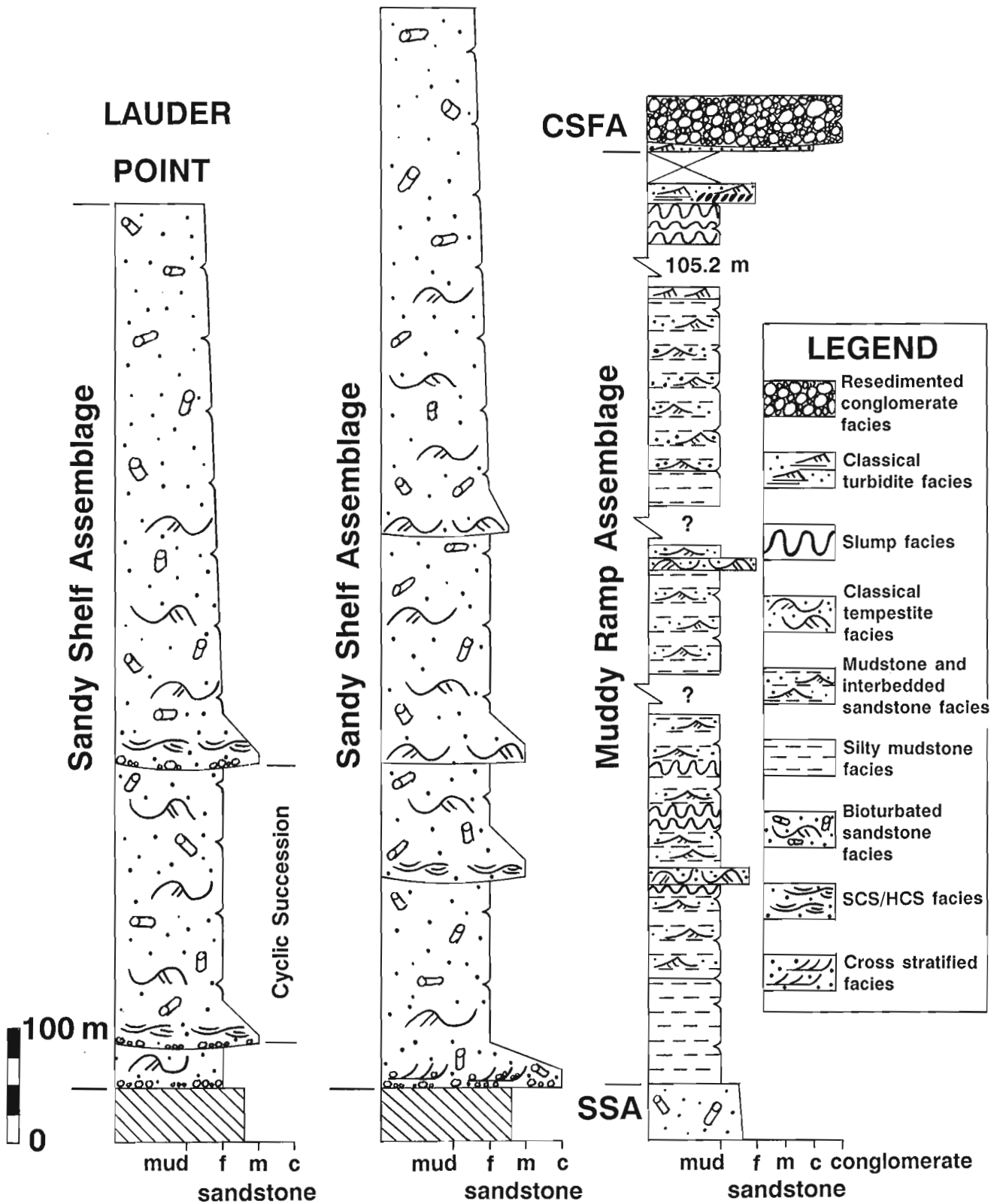


Figure 1. Schematic stratigraphic sections of the sandy shelf and muddy ramp assemblages exposed at Bearskin Bay, Skidegate Inlet, and Lauder Point, northwestern Graham Island. Bearskin Bay section is approximately 50% covered.

Unbioturbated lenticular units of hummocky cross-stratified fine-grained sandstone are occasionally observed (Fig. 2). This facies is richly fossiliferous and contains abundant ammonites, thin shelled articulated and disarticulated bivalves, gastropods, shark teeth, and rare reptiles. Abundant plant debris and wood fragments including tree trunks up to 3 m long are also common. Trace fossils include: *Ophiomorpha*, *Thalassinoides*, *Teredolites*, *Planolites*, *Paleophycus* and *Diplocraterion*.

Four cyclic successions composed of the above two facies are preserved within the assemblage at Bearskin Bay, whereas three are preserved at Lauder Point (Fig. 1). The uppermost succession at each of these localities reaches thicknesses of 544 m and 508 m respectively. Both successions grade upwards into very fine grained silty sandstones, suggesting that they, and the thinner cyclic successions beneath them, may be correlative.

MUDDY RAMP ASSEMBLAGE (MRA)

Black silty mudstone facies

This facies consists of thinly interbedded massive black mudstone and grey siltstone forming couplets up to 2 cm thick. These resemble Bouma T_{ac} turbidites. Rare, tabular beds of massive to current rippled fine- to very-fine grained glauconitic sandstone, generally less than 2 cm thick, also occur. This facies forms sequences up to 23 m thick.

Common in-situ *Mytiloides* and thin discontinuous winnowed shell lags were observed. Large buff to grey weathering carbonate concretions, locally with septarian development, commonly form distinct horizons. Ammonites and other macrofossils are rare.

Black mudstone and interbedded sandstone facies

This is the most common facies within the assemblage, forming sequences up to 52 m thick. It consists of interbedded black silty mudstone and very fine- to fine-grained massive to wave rippled glauconitic arkose and feldspathic arenite. The ratio of mudstone to sandstone varies between 95:5 and 50:50. The buff weathering sandstone units are sharp-based, tabular, less than 5 cm in thickness, and are commonly heavily bioturbated. The sandstones are sharply interbedded with, or grade upwards into, heavily bioturbated black silty mudstone. Rare interbedded units of hummocky cross-stratified sandstone up to 10 cm thick and thin intraclast breccia lags were observed. Flattened buff- and grey-weathering dolomite and limestone concretions, small black-coloured spherical concretions, coprolites, and plant fragments are common.

Trace fossils are abundant and include *Muensteria*, *Helminthopsis*, *Planolites*, *Rhizocorallium*, *Paleophycus*, *Chondrites*, *Teichichnus*, *Cosmoraphae* and several unidentified forms. Macrofossils are generally sparse, and include in-situ *Mytiloides*, snails, and rare ammonites.

Chaotic facies

Chaotic deposits are commonly interbedded with the black mudstone and interbedded sandstone facies described above. Three distinct varieties were observed: 1) homogenized, 2) coherent, and 3) debris flows. The first two varieties are composed of the interbedded black mudstone and sandstone facies. In the homogenized facies, primary stratification is absent. The most recognizable features are randomly oriented early diagenetic concretions which were rotated during transport. Homogenized deposits reach thicknesses of up to 10.2 m.

Coherent deposits are composed of highly deformed strata containing large, coherent rotated intraformational blocks. Coherent deposits vary in thickness between 0.2 and 17.2 m. A continuum exists between the homogenized- and coherent-type deposits.

Debris flow deposits are rare and contain large rounded to angular buff weathering carbonate concretions, angular intraformational cobbles and boulders of the interbedded mudstone and sandstone facies, smaller chloritized intraformational pebble- to cobble-sized clasts of siltstone and mudstone, coprolites, and rare rounded extraformational pebbles and cobbles, all resting within a silty mudstone matrix (Fig. 3). The deposits are framework- to matrix-supported and very poorly sorted, with large clasts often protruding from the top of the flow into the overlying deposits. These deposits contain ammonites, shark teeth, and reptilian bones transported from shallower depths. The debris flows are broadly lenticular and reach thicknesses of 2.5 m in Cumsheewa Inlet.

Tempestite facies

Tempestites exhibit sharp, scoured basal contacts overlain by well-developed fine-grained hummocky cross-stratified glauconitic sandstone which grades upwards into bioturbated sandstone and silty mudstone (Fig. 4). Tabular hummocky

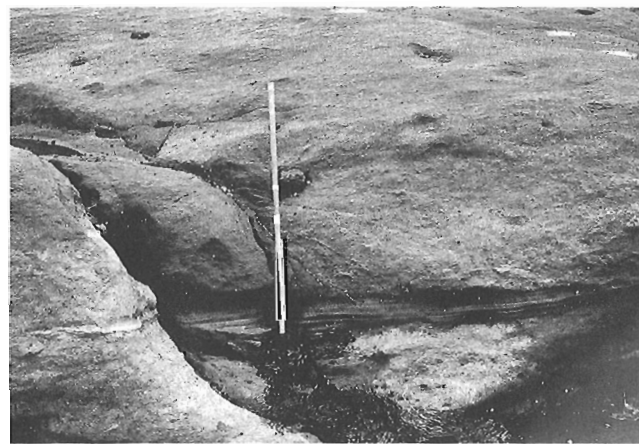


Figure 2. Massive bioturbated sandstone facies of the sandy shelf assemblage. Note the unbioturbated lens of hummocky cross-stratified sandstone. Pogo stick 1.5 m in length.

cross-stratified units 1.05 m thick were observed. The tempestites alternate with sequences of interbedded black silty mudstone and wave rippled sandstone up to 2 m thick.

At Kagan Bay, amalgamated tempestites infill channels incised in coherent and homogenized deposits. Channels up to 3.5 m deep and 40 m wide infilled with fine grained amalgamated tempestites were observed in the Bearskin Bay section exposed at Queen Charlotte City.

Trace fossils in this facies are essentially identical to those observed within the black silty mudstone and interbedded sandstone facies, with the exception of *Zoophycus*, which appears to be distinct to this facies. Macrofossils are rare and include in-situ *Mytiloides*.

SANDY SUBMARINE FAN ASSEMBLAGE (SSFA)

Classical turbidite facies

Thin- to thick-bedded classical turbidites are found within this assemblage. Classical turbidites exhibit parallel bedding, monotonous interbedding of sandstones and mudstones, a consistent set of sedimentary structures which can be described by the Bouma sequence, and an absence of scouring. Thin- to medium-bedded turbidites are generally less than 20 cm thick, are fine grained lithic arenites, and exhibit mudstone to sandstone ratios of 95-50:5-50. Thick-bedded classical turbidites are generally fine- to medium-grained, reach thicknesses of 2 m, and exhibit mudstone to sandstone ratios of 50:50.

Macrofossils are rare. Common trace fossils include *Muensteria*, *Chondrites*, *Rhizocorallium*, *Teichichnus*, *Planolites*, and *Helminthopsis*, as well as a variety of as yet unidentified grazing traces.



Figure 3. Debris flow facies of the muddy ramp assemblage.



Figure 4. Classical tempestite facies of the muddy ramp assemblage.

CCC-type turbidite facies

This facies is a variety of the thinly-bedded classical turbidite facies. CCC-type turbidites are fine-grained, generally less than 10 cm thick, and feature well developed Bouma sequences exhibiting convolutions, climbing ripples, and abundant intraclasts (hence CCC-type). Interbedded units composed of the homogenized facies are common. Sequences of CCC-type turbidites underlie or are interbedded with sequences of Honna Formation conglomerate, as observed in central Graham Island (Indrelid, 1990) and Sewell Inlet (Taite, 1991). Macrofossils are rare, and include ammonites and articulated inoceramid bivalves. Trace fossils include *Cosmoraphae*.

Sandy turbidite facies

Sandy turbidites exhibit well-developed Bouma sequences, are fine- to medium-grained lithic arenites, occur in units up to 2 m thick, exhibit scoured bases, are commonly amalgamated, and exhibit mudstone to sandstone ratios of 0-10:100-90. Sequences of this facies feature prominent channelized basal contacts with up to 2.5 m of relief, usually scouring into underlying sequences of thinly-bedded classical turbidites.

Single units of massive, medium- to coarse-grained T_a -type turbidites forming channelized units up to 3.2 m thick are commonly interbedded with the sandy turbidite facies.

Intraformational conglomerate facies

This facies is composed of channelized and amalgamated units of poorly sorted intraformational conglomerate up to 1.7 m thick interbedded with thin units of sandy,

predominantly T_b fine-grained turbidites. The conglomerates are framework-supported and are composed of rounded to subangular platy mudstone clasts and rare extraformational pebbles resting in a moderately sorted matrix of fine- to medium-grained sandstone. The clasts exhibit a poorly developed imbrication.

CONGLOMERATIC SUBMARINE FAN ASSEMBLAGE (CSFA)

Conglomerate facies

This facies forms the bulk of the assemblage, forming sequences up to 700 m thick at Pillar Bay. The conglomerates are polymictic, framework-supported and poorly sorted, and occur in broadly lenticular sharp-based units up to 4 m thick. Conglomerates may be interbedded with thinner, medium- to coarse-grained, well sorted pebbly to sandy channelized T_a and T_{ab} turbidites. Higgs (1990) recognized five distinct types of conglomerate: ungraded, inverse graded, normally graded, inverse to normally graded, and parallel stratified. To these can be added a lateral accretion type composed of low-angle inclined gravelly foresets interfingering laterally with massive medium- to coarse-grained sandstone (Fig. 5). This facies forms broadly lenticular units up to 3 m thick which are interpreted as the deposits of gravelly submarine bars (Hein, 1984). Macrofossils, including ammonites and bivalves, are rare.

Classical and sandy turbidite facies

These facies are indistinguishable from the classical and sandy turbidites facies of the sandy submarine fan assemblage, although they occur interbedded with thick sequences of conglomerate. The sandy turbidite facies of this assemblage commonly often contain abundant extraformational pebbles, a feature never observed within the sandy turbidite facies of the sandy submarine fan assemblage.



Figure 5. Inclined lateral accretion sets of the conglomerate facies, conglomeratic submarine fan assemblage. Ruler at bottom left is parallel to bedding, 15 cm in length.



Figure 6. Massive turbiditic sandstone facies of the conglomeratic submarine fan assemblage. Pogo stick 1.5 m in length.

These facies form sequences up to 125 m thick which are interbedded with sequences of the conglomerate facies at Pillar Bay and South Bay. Macrofossils are scarce. Common trace fossils include *Planolites*, *Paleophycus*, *Muensteria*, *Helminthopsis*, *Paleodictyon* and *Chondrites*.

Massive turbiditic sandstone facies

This facies is composed of thick channelized units of medium- to very coarse-grained massive lithic arenitic T_a and T_{ae} turbidites up to 4.6 m thick (Fig. 6). Units are typically amalgamated and may contain abundant intra- and extraformational clasts. The facies is usually interbedded with thick-bedded classical turbidites forming sequences up to 63 m thick in western Skidegate Inlet. Macrofossils are absent. One example of *Thalassinoides* was observed within the facies at Gust Island.

Stratified pebble conglomerate and sandstone facies

This facies is unique to a 13.7 m-thick succession exposed on western Gust Island (see Haggart et al., 1989 for a discussion of the stratigraphy in this area). The facies is composed of interbedded, matrix- to clast-supported poorly sorted pebble conglomerate and massive, poorly sorted medium-grained sandstone. The conglomerate units are lenticular to wavy, up to 20 cm thick, and generally exhibit sharp, erosive bases. Conglomerates are observed to grade normally into the medium-grained sandstone. The sandstones are generally thinner, and in some cases tuffaceous. The succession is interbedded with thick massive porphyry mafic volcanic flows. Macrofossils and trace fossils are absent.

Fine-grained symmetrically rippled and swaley cross-stratified facies

This facies is composed of interbedded symmetrically rippled fine-grained sandstone and silty mudstone, and medium- to coarse-grained swaley cross-stratified sandstone. The facies

is best exposed at Dyer Point on northwest Lina Island, where 6.8 m of symmetrically rippled sandstone and interbedded silty mudstone is abruptly overlain by 7.5 m of swaley cross-stratified sandstone. This succession is sandwiched between two sequences composed of the conglomerate facies, and is described further by Gamba (1991). Macrofossils are absent. Common trace fossils include *Rhizocorallium*, and *Paleophycus*.

MUDDY SHELF ASSEMBLAGE (MSA)

Shale facies

Deposits of this assemblage conformably overlie conglomerates of the Honna Formation at Pillar Bay, Langara Island, and the Slatechuck Mountain area (Haggart and Higgs, 1989; Haggart, 1991). The facies is composed of friable, black mudstone containing abundant carbonate concretions. Haggart and Higgs (1989) noted medium- to coarse-grained sandstone dykes within a 30 m thick succession exposed at Slatechuck Mountain. Macrofossils include in-situ inoceramids and common ammonites.

Interbedded silty mudstone and sandstone facies

A 43.5 m thick sequence of this facies is exposed in Pillar Bay, northwestern Graham Island. The facies is composed of interbedded friable black silty mudstone and thin, lenticular to tabular units of massive bioturbated to rippled very fine- to fine-grained sandstone. The ratio of mudstone to sandstone does not exceed 80:20. No well developed Bouma sequences were observed. Macrofossils include ammonites and thin-shelled bivalves. Common trace fossils include *Rhizocorallium* and *Cosmoraphe*.

FACIES INTERPRETATION

The basal cross-stratified facies of the sandy shelf assemblage was deposited in a shallow shoreface environment under fairweather wave conditions. Based on textural maturity and the apparent absence of marine macrofossils and trace fossils, Fogarassy and Barnes (1991) suggested that the facies was deposited in a braided fluvial environment. Recent finds of marine macrofossils and marine trace fossils within this facies negate this interpretation. The textural maturity of the facies can instead be attributed to prolonged reworking by fairweather wave processes.

The cyclic successions were deposited in a slightly deeper shelf environment under storm wave conditions. The sandy and gravelly storm deposit facies is clearly of storm origin. Rare patches of hummocky cross-stratified sandstone within the massive bioturbated sandstone facies also confirm its storm-related origin. Between storms events, the deposits of this facies were pervasively reworked by marine organisms, completely destroying stratification. The absence of interbedded mudstone is attributed to intense winnowing during storm events. The cyclicity of the successions, comprising a sharp based unit of swaley cross-stratified to hummocky cross-stratified sandstone overlain by a relatively

thicker unit of massive bioturbated sandstone, can be attributed to relative sea level fluctuations. Each succession represents a sharp drop in relative sea level followed by slow transgression. The basal portion of each succession, composed of the swaley cross-stratified and hummocky cross-stratified sandstone facies, was deposited in relatively shallower water under highly energetic storm conditions. The gradationally overlying massive bioturbated sandstone succession was deposited as sea level rose. The relatively lower energy conditions afforded marine organisms an opportunity to recolonize the substrate, allowing intense biological reworking of the storm deposits between storm events. The great thickness of these successions suggests that the rate of sedimentation closely matched that of subsidence. At least four such fluctuations in sea level are recorded in the Queen Charlotte City section whereas three are recorded at Lauder Point.

The presence of wave formed sedimentary structures within sandstones of the black mudstone and interbedded sandstone facies and the tempestite facies of the muddy ramp assemblage, together with bioturbation including *Rhizocorallium*, *Muensteria* and *Teichichnus*, suggests deposition at shelf depths (Frey and Pemberton, 1984). The chaotic facies are interpreted as slump deposits, and their association with deposits of the tempestite and interbedded mudstone and sandstone facies suggests that the ramp possessed an appreciable slope. The silty black mudstone facies of this assemblage was likely deposited in a relatively quieter, low energy setting on the ramp. The occurrence of channelized units of the tempestite facies immediately above some of the slumped units in the Skidegate Inlet area suggests that slumps may have been triggered by particularly intense storm events, by seismic activity, or by a drop in base level.

The well-developed Bouma sequences observed within the classical, CCC-type, and sandy turbidite facies of the sandy submarine fan assemblage confirm their turbiditic origin. The channelized and amalgamated nature of the sandy turbidite facies is indicative of deposition within submarine channels while classical turbidites are generally interpreted as lower to middle fan deposits (Walker, 1990). The massive silty mudstone facies was probably deposited in low energy environments adjacent to the fan. The occurrence of such trace fossils as *Rhizocorallium* and *Muensteria* argues against deep-water basinal deposition and suggests that both the muddy ramp assemblage and sandy submarine fan assemblage were deposited at similar paleodepths. A sequence of tempestites interbedded with classical turbidites of the submarine fan assemblage in western Kagan Bay would seem to confirm this.

The conglomerate, massive sandstone facies, and stratified pebble conglomerate facies of the conglomeratic submarine fan assemblage compare favourably with channelized turbidite deposits described by Walker (1990). The symmetrically rippled and interbedded swaley cross-stratified facies are interpreted as shallow shelf deposits, as suggested by Gamba (1991). The thinly-bedded classical turbidite facies is interpreted as lower to middle submarine fan deposits. The eastern provenance of the assemblage has been documented by Yagishita (1985), Higgs

(1990), Gamba et al. (1990), and Gamba (1991). Yagishita (1985) interpreted the Honna Formation, represented here by the conglomeratic submarine fan assemblage, as the deposits of a canyon-fed submarine fan. Points in favour of a submarine fan interpretation include: the resedimented nature of the conglomerates, the occurrence of interbedded sandy turbidites, and the interfingering of CCC-type turbidite and conglomerate. The CCC-type turbidite facies were interpreted as levee-deposits by Gamba et al. (1990) and Gamba (1991).

In contrast, Higgs (1990) and Gamba (1991) interpreted the Honna as fan delta deposits. The lack of associated subaerial and deltaic deposits appears to be incompatible with this interpretation.

The storm deposits and bioturbation of the tempestite facies of the muddy shelf assemblage reflect deposition at relatively shallow shelf depths. The absence of interbedded slump deposits suggests that deposition occurred upon a gently inclined shelf rather than upon a ramp. Haggart and Higgs (1989) suggested that the shale facies was deposited within a muddy shelf environment.

REGIONAL FACIES INTERPRETATION

Two large-scale depositional systems are observed within the Queen Charlotte Group. The sandy shelf, muddy ramp, and sandy submarine fan facies assemblages occupied the eastern margin of a westwards-deepening basin exhibiting a northwest-southeast trending strandline (Fig. 7) (Gamba, 1991; Haggart, 1991). Sediment was delivered to the basin via deltas, as illustrated by the localized nature of the basal crossbedded facies (deposited proximally to deltaic sources) and by thickness variations of the sandy shelf assemblage. The thick sandy shelf succession exposed at the Bearskin Bay section was probably deposited proximal to a deltaic source, in contrast to the thinner successions interbedded with deposits of the muddy ramp assemblage exposed in Cumshewa Inlet, which were probably deposited in a relatively more distal setting.

The shallow sandy shelf graded westwards into a deeper ramp environment. The predominance of storm deposits within both of these assemblages indicates that paleodepths did not exceed 200 m. The interfingering of muddy ramp deposits and sandy submarine fan deposits in western Kagan

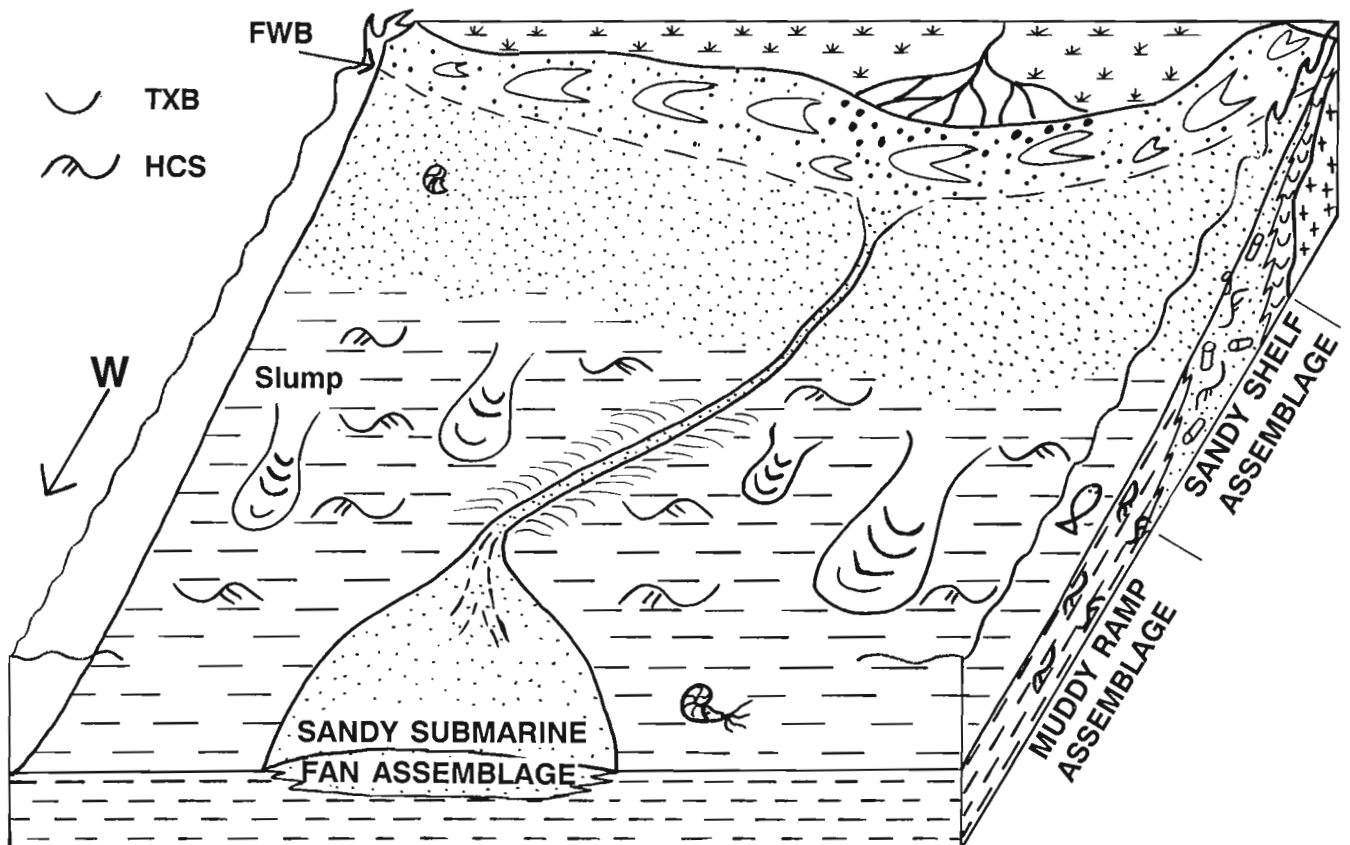


Figure 7. Albian to Early Turonian schematic model of the Queen Charlotte Basin (modified after Haggart, 1991: Fig. 7). FWB – fairweather wave base, HCS – hummocky cross-stratification, TXB – trough crossbedding.

Bay suggests that a sandy submarine fan was located at the foot of the ramp in the west. The absence of deep water trace fossils in all facies of the SSFA suggests that paleodepths did not greatly exceed that of the ramp. The abundance of slump deposits within the muddy ramp and sandy submarine fan assemblages may be attributed to frequent seismic disturbances along a tectonically active margin, or to slope instability due to rapid rates of sedimentation.

The broad geographical distribution of the three assemblages suggests that deposition did not occur within a series of small, fault-controlled basins, as suggested by Lewis et al. (1991). Instead, changes in relative sea level, which affected deposition basinwide (ie. the cyclic successions of the sandy shelf assemblage), are likely attributed to subduction-related tectonism affecting the Coast Plutonic Complex.

Sandy shelf and muddy ramp deposition was abruptly terminated by the onset of conglomeratic submarine fan deposition in Early Coniacian time (Haggart, 1991). A hiatus spanning approximately 2 Ma separates the deposits of the Cenomanian to Early Turonian sandy submarine fan assemblage and Early Coniacian to Early Santonian conglomeratic submarine fan assemblage. The similarities however between facies of the sandy and conglomerate submarine fan assemblages, their interfingering relationship and the petrological similarities exhibited by sandstones of both assemblages (documented by Fogarassy and Barnes, 1991), suggests that the transition within deeper parts of the basin was more gradational than on the shelf.

The Honna Formation forms a narrow northwest trending belt in the Lina Narrows/central Graham Island area. This belt may represent an exhumed paleocanyon, an interpretation supported by several observations. First, paleocurrents measured from pebble imbrication in this area exhibit a strong northerly directed paleoflow which parallels the trend of the belt (Gamba et al., 1990; Higgs, 1990). Second, an exposure of the shallow water symmetrically rippled and interbedded swaley cross-stratified facies occurs at the southeastern (canyon-head) termination of this belt on northwestern Lina Island (Gamba, 1991). Third, conglomerates of the Honna Formation are absent to the west of this belt, where the Skidegate Formation apparently grades upwards into Santonian shales in the Slatechuck Mountain area (J.W. Haggart, pers. comm., 1991).

The average sedimentation rate of the conglomerate submarine fan assemblage is approximately 1.066 mm/a, a figure which greatly exceeds the approximately 0.092 mm/a rate of the sandy shelf and muddy ramp assemblages. This suggests relatively rapid rates of basin subsidence coupled with rapid uplift and unroofing of the Coast Plutonic Complex to the east during deposition of the conglomeratic submarine fan assemblage.

From Early Santonian to Maastrichtian time muddy shelf conditions prevailed within the basin (Haggart, 1991). This likely marks an end to the tectonism responsible for deposition of the conglomeratic submarine fan assemblage.

ACKNOWLEDGMENTS

Jim Haggart is thanked for useful discussions concerning Cretaceous litho- and biostratigraphy both in and out of the field, and also for a thoughtful review of an earlier version of this manuscript. Thanks also to Peter Mustard for comments concerning an earlier draft of this manuscript. Bob Anderson, Mary Sanborn-Barrie, Jack Souther, Roger Walker, and Glenn Woodsworth are thanked for useful discussions in the field. Thanks also to Audrey and Dave Putterill for their speedy and hospitable expediting. Jim Haggart and the Frontier Geoscience Program are acknowledged for logistical support during the 1991 field season.

REFERENCES

- Fogarassy, J.A.S. and Barnes, W.C.**
1991: Stratigraphy and diagenesis of the Middle to Upper Cretaceous Queen Charlotte Group, Queen Charlotte Islands, British Columbia; in *Evolution and Hydrocarbon Potential of the Queen Charlotte Basin, British Columbia*, (ed.) G.J. Woodsworth; Geological Survey of Canada, Paper 90-10, p. 279-294.
- Frey, R.W. and Pemberton, S.G.**
1984: Trace fossil facies models; in *Facies Models*, 2nd edition, (ed.) R.G. Walker; Geoscience Canada Reprint Series 1, p. 189-208.
- Gamba, C.A.**
1991: An update on the Cretaceous sedimentology of the Queen Charlotte Islands, British Columbia; in *Current Research, Part A*; Geological Survey of Canada, Paper 91-1A, p. 373-382.
- Gamba, C.A., Indrelid, J., and Taite, S.**
1990: Sedimentology of the Upper Cretaceous Queen Charlotte Group, with special reference to the Honna Formation, Queen Charlotte Islands, British Columbia; in *Current Research, Part F*; Geological Survey of Canada, Paper 90-1F, p. 67-73.
- Haggart, J.W.**
1991: A synthesis of Cretaceous stratigraphy, Queen Charlotte Islands, British Columbia; in *Evolution and Hydrocarbon Potential of the Queen Charlotte Basin, British Columbia*, (ed.) G.J. Woodsworth; Geological Survey of Canada, Paper 90-10, p. 253-277.
- Haggart, J.W. and Higgs, R.**
1989: A new Late Cretaceous mollusc fauna from the Queen Charlotte Islands, British Columbia; in *Current Research, Part H*; Geological Survey of Canada, Paper 89-1H, p. 59-64.
- Haggart, J.W., Lewis, P.D., and Hickson, C.J.**
1989: Stratigraphy and structure of Cretaceous strata, Long Inlet, Queen Charlotte Islands, British Columbia; in *Current Research, Part H*; Geological Survey of Canada, Paper 89-1H, p. 65-72.
- Haggart, J.W., Taite, S., Indrelid, J., Hesthammer, J., and Lewis, P.D.**
1991: A revision of stratigraphic nomenclature for the Cretaceous sedimentary rocks of the Queen Charlotte Islands, British Columbia; in *Current Research, Part A*; Geological Survey of Canada, Paper 91-1A, p. 367-371.
- Hein, F.J.**
1984: Deep-sea and fluvial braided channel conglomerates: a comparison of two case studies; in *Sedimentology of Gravels and Conglomerates*, (ed.) E.H. Koster and R.J. Steel; Canadian Society of Petroleum Geologists, Memoir 10, p. 33-50.
- Higgs, R.**
1990: Sedimentology and tectonic implications of Cretaceous fan delta conglomerates, Queen Charlotte Islands, Canada; *Sedimentology*, v. 37, p. 83-104.
- Indrelid, J.**
1990: Stratigraphy and structures of Cretaceous units, central Graham Island, Queen Charlotte Islands, British Columbia; in *Current Research, Part F*; Geological Survey of Canada, Paper 90-1F, p. 5-10.
- Lewis, P.D., Haggart, J.W., Anderson, R.G., Hickson, C.J., Thompson, R.I., Dietrich, J.R., and Rohr, K.M.M.**
1991: Triassic to Neogene geologic evolution of the Queen Charlotte region; *Canadian Journal of Earth Sciences*, v. 28, p. 854-869.

Sutherland Brown, A.

1968: Geology of the Queen Charlotte Islands, British Columbia; British Columbia Department of Mines and Petroleum Resources, Bulletin 54, 226 p.

Taite, S.

1991: Geology of the Sewell Inlet-Tasu Sound area, Queen Charlotte Islands, British Columbia; in Current Research, Part A; Geological Survey of Canada, Paper 91-1A, p. 393-399.

Walker, R.G.

1990: Turbidites and turbidity currents: introduction, facies sequence and models; American Association of Petroleum Geologists Deep Water Clastic Reservoirs School, June 7-11, Ventura, California.

Yagishita, K.

1985: Mid- to Late Cretaceous sedimentation in the Queen Charlotte Islands, British Columbia: lithofacies, paleocurrent and petrographic analyses of sediments; Ph.D. thesis, University of Toronto, Ontario.

AUTHOR INDEX

Blais, A.	195	Mahoney, J.B.	243, 249
Bond, L.	179	McClay, K.	121
Broster, B.E.	237	McClelland, W.C.	303
Brown, D.	121	Metcalfe, S.	113
Brown, R.L.	63	Monger, J.W.H.	209
Carrière, J.J.	47	Mudroch, A.	1
Clague, J.J.	185	Murphy, D.C.	163
Coish, R.A.	95	Mustard, P.S.	13
Colpron, M.	157	Nadaraju, G.	333
Crowley, J.L.	63	Northcote, B.R.	215
Crowley, S.E.	63	O'Brien, J.A.	209
Currie, L.D.	199	Payne, J.G.	323
Dawson, K.M.	173, 179	Percival, J.B.	1
Dunn, C.E.	1	Plouffe, A.	189
Evans, S.G.	185	Porter, S.	309
Evenchick, C.A.	77, 85	Price, R.A.	157
Friedman, R.M.	137, 261	Read, P.B.	105
Gamba, C.A.	367	Roots, C.F.	163
Gareau, S.A.	267	Ross, K.V.	179
Gehrels, G.E.	209	Rouse, G.E.	13
Godwin, C.I.	179	Sanborn-Barrie, M.	351
Gordey, S.P.279		Sanders, C.	225
Greig, C.J.	145	Sangster, D.F.	47
Gunning, M.H.	315	Seemann, D.	85
Haggart, J.W.	337, 361	Simony, P.S.	71
Hall, G.E.M.	1	Smith, P.L.	333
Harms, T.A.	297	Souther, J.G.	343
Hart, B.S.	55	Stevens, R.A.	287
Henderson, J.R.	323	Stevens, W.	33
Henderson, M.N.	323	Struik, L.C.	25
Hickson, C.J.	129, 249	Thompson, P.H.	41
Hunt, J.A.	249	Tyson, T.M.	261
Huntley, D.H.	237	van der Heyden, P.	113, 137, 249
Jackson, L.E. Jr.	33	Van-Konijnenburg, J.-H.	225
Jaasma, M.	225	Vogl, J.J.	71
Journeay, J.M.	95, 215, 225, 261	Wright, R.L.	323
Kirkham, R.V.	323	Wright, T.O.	323
Lowe, C.	85		

NOTE TO CONTRIBUTORS

Submissions to the Discussion section of Current Research are welcome from both the staff of the Geological Survey of Canada and from the public. Discussions are limited to 6 double-spaced typewritten pages (about 1500 words) and are subject to review by the Chief Scientific Editor. Discussions are restricted to the scientific content of Geological Survey reports. General discussions concerning sector or government policy will not be accepted. All manuscripts must be computer word-processed on an IBM compatible system and must be submitted with a diskette using WordPerfect 5.0 or 5.1. Illustrations will be accepted only if, in the opinion of the editor, they are considered essential. In any case no redrafting will be undertaken and reproducible copy must accompany the original submissions. Discussion is limited to recent reports (not more than 2 years old) and may be in either English or French. Every effort is made to include both Discussion and Reply in the same issue. Current Research is published in January and July. Submissions should be sent to the Chief Scientific Editor, Geological Survey of Canada, 601 Booth Street, Ottawa, Canada, K1A 0E8.

AVIS AUX AUTEURS D'ARTICLES

Nous encourageons tant le personnel de la Commission géologique que le grand public à nous faire parvenir des articles destinés à la section discussion de la publication Recherches en cours. Le texte doit comprendre au plus six pages dactylographiées à double interligne (environ 1500 mots), texte qui peut faire l'objet d'un réexamen par le rédacteur scientifique en chef. Les discussions doivent se limiter au contenu scientifique des rapports de la Commission géologique. Les discussions générales sur le Secteur ou les politiques gouvernementales ne seront pas acceptées. Le texte doit être soumis à un traitement de texte informatisé par un système IBM compatible et enregistré sur disquette WordPerfect 5.0 ou 5.1. Les illustrations ne seront acceptées que dans la mesure où, selon l'opinion du rédacteur, elles seront considérées comme essentielles. Aucune retouche ne sera faite au texte et dans tous les cas, une copie qui puisse être reproduite doit accompagner le texte original. Les discussions en français ou en anglais doivent se limiter aux rapports récents (au plus de 2 ans). On s'efforcera de faire coïncider les articles destinés aux rubriques discussions et réponses dans le même numéro. La publication Recherches en cours paraît en janvier et en juillet. Les articles doivent être envoyés au rédacteur en chef scientifique, Commission géologique du Canada, 601, rue Booth, Ottawa, Canada, K1A 0E8.

Geological Survey of Canada Current Research, is now released twice a year, in January and in July. The four parts published in January 1992 (Paper 92-1, parts A to D) are listed below and can be purchased separately.

Recherches en cours, une publication de la Commission géologique du Canada, est publiée maintenant deux fois par année, en janvier et en juillet. Les quatre parties publiées en janvier 1992 (Étude 92-1, parties A à D) sont énumérées ci-dessous et vendues séparément.

Part A, Cordillera and Pacific Margin
Partie A, Cordillère et marge du Pacifique

Part B, Interior Plains and Arctic Canada
Partie B, Plaines intérieures et région arctique du Canada

Part C, Canadian Shield
Partie C, Bouclier canadien

Part D, Eastern Canada and national and general programs
Partie D, Est du Canada et programmes nationaux et généraux

Part E (this volume)
Partie E (ce volume)